# The Impact of Climate Change on Historic Interiors

# Paul Lankester

Thesis submitted in fulfilment of the requirements for the degree of
Doctor of Philosophy

# University of East Anglia

School of Environmental Sciences

In collaboration with

# English Heritage

January 2013

# Abstract

It is widely understood that the environment is critical for the preservation of historic collections and interiors, if the environment is unsuitable it can create an increased risk of damage. In historic houses collections are usually on open display, and the room environment often has little control thus it is vulnerable to changes in the outdoor environment. The future outdoor environment is projected to change so the aim of this work has been to develop a widely applicable model to investigate the potential impact of climate change on historic interiors.

A simple transfer function has been used to predict indoor temperature and relative humidity. The method is widely applicable and easily transferable between unheated buildings. It has been shown that it is important to assess each location and room on an individual basis. The method has been coupled with future climate output, from both the UKCP09 weather generator and the Hadley model, where data has been downscaled.

The high resolution climate output allows for projections of future indoor environment. Future temperature is projected to increase in unheated historic houses around the UK and across Europe, although less than outdoors. Annual average relative humidity is largely unchanged in the future.

Damage functions are used to determine the impact of the future indoor environment on materials. Typically temperature driven damage such as chemical degradation of paper and silk and insect pest activity increase in the future, whereas damage driven by relative humidity, such as salt transitions, depends upon the location assessed. In general risk of mould growth increases, and dimensional changes to wood decrease. The significance of future changes is an important consideration, requiring some further work.

Annual averages are shown to hide seasonal changes, thus it is important to assess these, which can impact upon management strategies. At Knole it is projected that the summer humidity will decrease and the winter humidity increase slightly, which raises the risk of mould growth. The application of conservation heating has been shown to be less effective in future, but is still an effective strategy, although dehumidification may become more appropriate in some locations. The future energy use of conservation heating has a negligible change.

There are a number of inherent uncertainties associated with the models used here. Specifically with climate modelling, future emissions are unknown and the physical processes of the climate are not fully understood. There is a statistical error associated with the transfer function, and the damage functions also have a number of related uncertainties. It is important to consider these when assessing future indoor projections.

The results allow for long term planning by collection managers, to prepare for the impact of climate change, thus preserving heritage for future generations.

# Contents

**Appendices**

Appendix A – Climate

Appendix B – Building simulation

Appendix C – Europe results

Appendix D – UKCP09 results

Appendix E – AWK programs

Appendix F – Publications

# List of Figures

Figure 3.6: Monthly average temperature over the period 2006-8, outdoors at Brodsworth Hall and indoors in the Library.

Figure 3.7: Monthly average relative humidity over the period 2006-8, outdoors at Brodsworth Hall and indoors in the Library.

Figure 3.8: First prediction of temperature indoors for the library at Brodsworth Hall, determined by applying monthly differences to the outdoor temperature.

Figure 3.9: Initial prediction of relative humidity indoors for the library at Brodsworth Hall, determined by applying monthly ratios to the outdoor relative humidity.

Figure 3.10: Smoothing of the outdoor relative humidity at Brodsworth Hall using the lagged function.

Figure 3.11: Comparison of predicted relative humidity, using a smoothing technique. Plotted as a 5 day moving average, over the period 01/2006-12/2008.

Figure 3.12: Comparison of observed and predicted relative humidity in the Library at Brodsworth Hall, using the triangular smoothing technique. Plotted as a 5 day moving average, over the period 01/2006-12/2008.

Figure 3.13: Comparison of monthly average predicted and observed temperature, over the period 2006-8, at Brodsworth Hall.

Figure 3.14: Comparison of monthly average predicted and observed relative humidity, over the period 2006-8, at Brodsworth Hall.

Figure 3.15: Daily average specific humidity indoors and outdoors at Brodsworth Hall.

Figure 3.16: Outdoor specific humidity plotted against indoor specific humidity at Brodsworth Hall, for the period 01/2006-12/2008.

Figure 3.17: Daily average predicted and observed indoor specific humidity in the Library at Brodsworth Hall, over the period 2006-8.

Figure 3.18: Predicted indoor relative humidity calculated from the predicted temperature and specific humidity, compared to the observed relative humidity in the Library at Brodsworth Hall. The relative humidity is plotted as a 5 day moving average.

Figure 3.19: Comparison of outdoor temperature observed at Gatwick weather station, to the observed indoor temperature from the Cartoon Gallery. For the period 01/2001-06/2009.

Figure 5.2: Projected indoor temperature of the idealised room across the seven locations, for the period 1860-2100. The data is plotted as a 5 year smoothed average, to help visualise the long term trend.

Figure 5.3: Projected indoor relative humidity of the idealised room across the seven locations, for the period 1860-2100. The data is plotted as a 5 year smoothed average.

Figure 5.4: The projected number of days, per year, where the average daily temperature indoors exceeds 20°C, across the seven locations. Results are plotted as a five year smoothed average.

Figure 5.5: The projected number of days, per year, where the average daily temperature indoors exceeds 25°C, for the seven idealised rooms across Europe. Results are plotted as a five year smoothed average.

Figure 5.6: The projected chemical degradation rate of bleached bisulfite pulp paper, using the Zou damage function, for the period 1860 to 2100, across the seven locations. Results are plotted as a five year smoothed average. The baseline period medians of all locations are significantly different to those of the corresponding far future period.

Figure 5.7: The projected relative degradation rate of paper using the Pretzel damage function, from 1860 through to 2100 across the seven locations. The rate is shown as a 5 year smoothed average.

Figure 5.8: The projected effect of climate change on the degradation of silk. The rate is plotted as a smoothed five year average. The baseline period medians of all locations are significantly different to those of the corresponding far future period.

Figure 5.9: The projected impact of climate change on mould growth, as described by Isaksson et al. Results for the seven European locations, from 1860 to 2100. Results are plotted as a five year smoothed average.

Figure 5.10 a and b: Projected number of days per year where the critical relative humidity is exceeded, resulting in risk of mould growth. (a) four of the European locations and (b) the other three, which have been split for clarity. Results are plotted as a five year smoothed average. The baseline period medians of all locations are significantly different to those of the corresponding far future period.

Figure 5.11 a and b: Projected number of days, per year, where mould is expected to grow, for the years 1860-2100. (a) includes four of the seven European locations and (b) the other three, they have been split for clarity. With the exception of Leon and Prague the

baseline median of the other locations is significantly different to that of the far future median.

Figure 5.12: The projected impact of climate change on the number of degree days (base 15°C) indoors. Results are presented as five year smoothed averages, from 1860 to 2100, for seven European locations. The baseline period medians of all locations are significantly different to those of the corresponding far future period.

Figure 5.13 a and b: The projected number of transitions exceeding 10 MPa of thenardite to mirabilite. Results are plotted as five year smoothed averages, from 1860 to 2100. (a) includes three of a total seven European locations, and (b) the remaining four, these have been split for clarity. The baseline period medians of all locations are significantly different to those of the corresponding far future period.

Figure 5.14 a and b: The projected number of halite transitions at a critical humidity of 75.3%. (a) presents three of seven locations and (b) the other four. Results are presented as five year smoothed averages. The baseline period medians of all locations are significantly different to those of the corresponding far future period.

Figure 5.15 a and b: Projected yearly number of 5% humidity fluctuations, from one day to another, as described for the Michalski damage function for dimensional change. Seven locations are shown across the period 1860-2100, with (a) having four of the seven and (b) three, they have been split for clarity. Results are plotted as five year smoothed averages. The baseline period medians of all locations are significantly different to those of the corresponding far future period.

Figure 5.16: The projected yearly number of 30% day to day humidity fluctuations, for the 30% humidity shock damage function. Seven European locations are shown, for the period 1860-2100. The baseline period medians of all locations except Leon and Oviedo are not significantly different to those of the corresponding far future period.

Figure 5.17: Projected number of damaging events to cotton wood per year, due to adsorption of moisture as described by the Mecklenburg damage function. Results for seven locations for the period 1860-2100, plotted as five year smoothed averages. The baseline period medians of all locations are significantly different to those of the corresponding far future period.

Figure 5.18 a and b: The projected impact of climate change on the number of damaging events indoors to cotton wood, caused by desorption of moisture. (a) presents four of seven European locations and (b) the remaining three. Results are plotted as five year

smoothed averages. The baseline period medians of all locations are significantly different to those of the corresponding far future period.

Figure 5.19: The projected number of damaging events to cotton wood from both adsorption and desorption events. Results for seven locations are shown from 1860 to 2100. Results are plotted as five year smoothed averages. The baseline period medians of all locations are significantly different to those of the corresponding far future period.

Figure 5.20: The projected impact of climate change on the number of damaging events per year to white oak by moisture adsorption, as described in the damage function by Mecklenburg. Results for seven locations are presented from 1860 to 2100. Results are plotted as five year smoothed averages. The baseline period medians of all locations are significantly different to those of the corresponding far future period.

Figure 5.21: The projected number of damaging events per year for white oak, caused by moisture desorption. Seven European locations are presented, with results from 1860 to 2100. Results are plotted as five year smoothed averages. The baseline period medians of all locations are significantly different to those of the corresponding far future period.

Figure 5.22: the projected number of damaging events per year to white oak, from both adsorption and desorption of moisture. Results from 1860-2100 for seven European locations are shown. Results are plotted as five year smoothed averages. The baseline period medians of all locations are significantly different to those of the corresponding far future period.

Figure 5.23 a and b: The projected impact of climate change on the yearly number of damaging events to white oak that will cause failure of the material. (a) presents four of seven locations and (b) the remaining three. Results are plotted as five year smoothed averages. The baseline period medians of all locations are significantly different to those of the corresponding far future period.

Figure 6.1: The impact of climate change on the annual average temperature at Knole, outdoors and in the two galleries. The error bars represent the interquartile range, with the data point the median value.

Figure 6.2: The impact of climate change on the annual average relative humidity at Knole, outdoors and in the two galleries. The error bars represent the interquartile range, with the data point the median value.

Figure 6.3: The projected rise in specific humidity in the Cartoon Gallery across the coming century. Error bars represent the interquartile range.

Figure 6.4: The seasonal temperature in the Cartoon Gallery, for the baseline and far future periods. The enclosed region represents the interquartile range of the weather generator outputs.

Figure 6.5: The seasonal relative humidity in the Cartoon Gallery, for the baseline and far future periods. The enclosed region represents the interquartile range of the weather generator outputs.

Figure 6.6: The number of days projected per year with an average temperature exceeding 20°C in the Cartoon and Leicester Galleries at Knole. Error bars represent the interquartile range.

Figure 6.7: The percentage of time projected per month with an average daily temperature exceeding 20°C in the Cartoon Gallery at Knole. Error bars represent the interquartile range.

Figure 6.8: The annual average projected degradation rate of paper derived from the Zou damage function in the Cartoon and Leicester Galleries at Knole. Error bars represent the interquartile range.

Figure 6.9: The monthly average projected degradation rate of paper derived from the Zou damage function in the Cartoon Gallery at Knole. Error bars represent the interquartile range.

Figure 6.10: The annual average projected degradation rate of paper derived from the Pretzel damage function in the Cartoon and Leicester Galleries at Knole. Error bars represent the interquartile range.

Figure 6.11: The monthly average projected degradation rate of paper derived from the Zou damage function in the Cartoon Gallery at Knole. Error bars represent the interquartile range.

Figure 6.12: The annual average projected degradation rate of silk derived from the silk isoperm damage function in the Cartoon and Leicester Galleries at Knole. Error bars represent the interquartile range.

Figure 6.13: The monthly average projected degradation rate of silk derived from the silk isoperm damage function in the Cartoon Gallery at Knole. Error bars represent the interquartile range.

Figure 6.14: The annual average projected number of mould risk days derived from the Isaksson damage function in the Cartoon and Leicester Galleries at Knole. Error bars represent the interquartile range.

Figure 6.15: The monthly average projected number of mould risk days derived from the Isaksson damage function in the Cartoon Gallery at Knole. All future time periods show the increase over time.

Figure 6.16: The annual average projected number of mould risk days derived from the critical relative humidity damage function in the Cartoon and Leicester Galleries at Knole. Error bars represent the interquartile range.

Figure 6.17: The monthly average projected number of mould risk days derived from the critical relative humidity damage function in the Cartoon and Leicester Galleries at Knole. Error bars represent the interquartile range.

Figure 6.18: The annual average projected number of degree days in the Cartoon and Leicester Galleries at Knole. Error bars represent the interquartile range.

Figure 6.19: The cumulative monthly average projected number of degree days in the Cartoon Gallery at Knole. Error bars represent the interquartile range.

Figure 6.20: The annual average projected number of thenardite mirabilite salt transitions in the Cartoon and Leicester Galleries at Knole. Error bars represent the interquartile range.

Figure 6.21: The monthly average projected number of thenardite mirabilite salt transitions in the Cartoon Gallery at Knole. Error bars represent the interquartile range.

Figure 6.22: The annual average projected number of 75.3% salt transitions in the Cartoon and Leicester Galleries at Knole. Error bars represent the interquartile range.

Figure 6.23: The monthly average projected number of 75.3% salt transitions in the Cartoon Gallery at Knole. Error bars represent the interquartile range.

Figure 6.24: The annual average projected number of 85% salt transitions in the Cartoon and Leicester Galleries at Knole. Error bars represent the interquartile range.

Figure 6.25: The monthly average projected number of 85% salt transitions in the Cartoon Gallery at Knole. Error bars represent the interquartile range.

Figure 6.26: The annual average projected number of damaging events arising from a 5% humidity change in the Cartoon and Leicester Galleries at Knole. Error bars represent the interquartile range.

Figure 6.27: The monthly average projected number of damaging events arising from a 5% humidity change in the Cartoon Gallery at Knole. Error bars represent the interquartile range.

Figure 6.28: The annual average projected number of damaging events arising from a 30% humidity change in the Cartoon and Leicester Galleries at Knole. Error bars represent the interquartile range.

Figure 6.29: The monthly average projected number of damaging events arising from a 30% humidity change in the Cartoon Gallery at Knole. Error bars represent the interquartile range.

Figure 6.30: The annual average projected number of damaging events arising from a 40% humidity change in the Cartoon and Leicester Galleries at Knole. Error bars represent the interquartile range.

Figure 6.31: The monthly average projected number of damaging events arising from a 40% humidity change in the Cartoon Gallery at Knole. Error bars represent the interquartile range.

Figure 6.32: The annual average projected number of damaging events arising from adsorption of moisture in the Cartoon and Leicester Galleries at Knole. Error bars represent the interquartile range.

Figure 6.33: The monthly average projected number of damaging events arising from adsorption of moisture in the Cartoon Gallery at Knole. Error bars represent the interquartile range.

Figure 6.34: The annual average projected number of damaging events arising from desorption of moisture in the Cartoon and Leicester Galleries at Knole. Error bars represent the interquartile range.

Figure 6.35: The monthly average projected number of damaging events arising from desorption of moisture in the Cartoon Gallery at Knole. Error bars represent the interquartile range.

Figure 6.36: The annual average projected number of failure events in the Cartoon and Leicester Galleries at Knole. Error bars represent the interquartile range.

Figure 6.37: The monthly average projected number of failure events in the Cartoon Gallery at Knole. Error bars represent the interquartile range.

Figure 6.38: The annual average projected temperature in the Library at Brodsworth Hall, and outdoors at Brodsworth. Error bars represent the interquartile range.

Figure 6.39: The annual average projected % relative humidity in the Library at Brodsworth Hall, and outdoors at Brodsworth. Error bars represent the interquartile range.

Figure 6.40: The monthly average projected temperature in the Library at Brodsworth Hall, for the baseline and far future periods. The enclosed region represents the interquartile range.

Figure 6.41: The monthly average projected % relative humidity in the Library at Brodsworth Hall, for the baseline and far future periods. The enclosed region represents the interquartile range.

Figure 6.42: The annual average projected number of days where the daily average temperature exceeds 25°C in the Library at Brodsworth Hall. Error bars represent the interquartile range.

Figure 6.43: The monthly average projected number of days where the daily average temperature exceeds 25°C in the Library at Brodsworth Hall. Error bars represent the interquartile range.

Figure 6.44: The annual average projected degradation rate of paper in the Library at Brodsworth Hall. Error bars represent the interquartile range.

Figure 6.45: The monthly average projected degradation rate of paper in the Library at Brodsworth Hall. Error bars represent the interquartile range.

Figure 6.46: The annual average projected number of degree days in the Library at Brodsworth Hall. Error bars represent the interquartile range.

# List of Tables

# Accompanying Material

Appendices A through F can be found on the accompanying CD

# Acknowledgements

I would like to sincerely thank Peter Brimblecombe, thank you for the guidance, support and knowledge, all of which have been second to none. Through the difficult times you have always given me the motivation to continue.

Secondly thank you to Dave Thickett, your expertise and support has helped me continually throughout this work, but particularly in the final stages of writing up.

I have been fortunate to have two excellent supervisors in Peter and Dave who are highly respected across the field of conservation science. Thank you both again for the opportunity to learn from the best, for which I am extremely grateful.

Thanks also go to Carlota Grossi Sampedro who has always been on hand to provide assistance when required. Particular thanks also go to Helen Lloyd, of the National Trust, for your support of this work, helpful discussions and access to data.

I also thank everybody that has helped from English Heritage, the National Trust and Historic Royal Palaces, without your support this work would not have been possible.

Thank you to all my friends who have always been on hand to provide relief from work, I am very fortunate to have such a great group of friends.

Thanks also to my family, particularly my Mum, Dad and Brother Martin. Thank you for your unequivocal support and commitment to everything that I do, it wouldn't be possible without you.

# CHAPTER 1

# INTRODUCTION

The environment within a historic house is critical for the preservation of historic collections and interiors. Unsuitable indoor environments can lead to an increased risk of damage. Typically the indoor environment is thought of as more stable than the outdoor environment, but often the most significant and sensitive collections are displayed indoors. Historic houses can be quite different to museums, with objects usually on open display, and the environments less controlled than air conditioned museum spaces. Such collections are vulnerable to changes in the outdoor environment.

Future outdoor environmental conditions are projected to change, due to anthropogenic climate change. This will result in a number of serious effects, from rising sea levels to increasing temperatures (Solomon et al., 2007). The impact of climate change on cultural heritage outdoors has been studied previously (Sabbioni et al., 2010); however there has been little work on the impacts that climate change may have on historic interiors, and the collections displayed within them.

Using building simulation techniques it is possible to predict the indoor environment using the outdoor environment. These are often complex models that require specific information relating to the physics of a building, and produce results beyond that of the indoor environment, such as energy usage, and outcomes from various alternate scenarios.

Typically building simulation is beyond the reach of those who manage heritage sites. The first aim of this research is to develop a simple building simulation model, to predict the indoor temperature and relative humidity of unheated historic rooms. Ideally the technique developed will be simple enough to allow those within heritage organisations to predict the indoor environment in their historic houses.

This building simulation model will then be coupled with future climate projections outdoors to allow for projections of future indoor environments. The second aim is to determine how the future indoor projections may have an impact on damage to historic collections. Damage functions will be used to relate temperature and relative humidity to the risk of material damage. Future climate projections are an estimate of the possibilities in the future; they are not certain predictions or forecasts. The overall aim of this work is to develop a method for projecting future indoor environment and damage, allowing for

collection managers to prepare for the impact of climate change, taking into account specific projections for their own collection.

## 1.1 Building simulation

This research focuses upon the impact of climate change indoors, future climate output is available outdoors, thus a method is required to transfer this indoors, projecting future indoor climate, and allow for an assessment of the impacts of climate change on collections and historic interiors.

One purpose of a building is that it acts as a buffer to the external environment. The environment within a building has external drivers, for example solar radiation, air exchange and heat conduction across walls. The extent of these external drivers depends upon the construction materials chosen, for example thin or conductive walls are sensitive to the apparent daily course of the sun. In addition the location of a room can be important, inner rooms are shielded from the external drivers, smoothing out their impact (Camuffo, 1998). To determine the relationship between the external and internal environment the building climate must be observed, such that modelling of the building can take place.

There are a variety of building simulation programmes available (Crawley et al., 2005a); they are typically advanced computer models which predict the transfer of heat and moisture through buildings. In general building simulation programmes have a number of different categories by which they can be assessed, for example zone loads, building envelope and day lighting, infiltration and ventilation, electrical systems and equipment, and HVAC systems among others. Some models operate similarly, while others do not, for example in determining the simulation solution most calculate loads simultaneously, but some only do so sequentially (DOE-2, BLAST and TRACE). Most models include a full geometric description of the walls/roofs/floors/windows/doors and external shading, but some do not, for example Energy-10 and HAP (Crawley et al., 2005b). Under the zone loads category some of the underpinning fundamental calculations can be found. Again different models adopt different approaches. Most use a heat balance calculation, and some include building material moisture adsorption or desorption (a combined building envelope heat and mass transfer), BSim, EnergyPlus, ESP-r and Tas are some examples of programmes that include both (Crawley et al., 2005b). There are other important calculations, with different methods for solving these, some models give the user an option of which to choose, and others make this choice for the user. In some models some aspects are not included, potentially where it is not important for the specific use of

that model, for example solar analysis is absent from both Energy-10 and HAP, other models only include some aspects of this and others a more comprehensive assessment. The same is true with other aspects also, such as with calculations involving windows (Crawley et al., 2005b).

Building simulation software is more often used in the design process of buildings (Augenbroe, 2002), but is beginning to be used to simulate the historic environment (Cassar and Taylor, 2004).These programs can be used to predict temperature, relative humidity and energy consumption before buildings are constructed, most of these programs however are concerned with human comfort, and therefore model temperature rather than relative humidity. However effective humidity prediction is important because a historic house can contain a considerable amount of hygrothermal material that will exchange moisture with the air, affecting the ambient relative humidity (Taylor et al., 2005).

One such program has been identified as the most reliable model for the simulation of the hygrothermal environment of historic buildings, this is EnergyPlus (Sabbioni et al., 2006). This software is appropriate because it accounts for hygrothermal properties of the building fabric and contents, which is essential for attaining an accurate simulation of relative humidity (Taylor et al., 2005).

The decision was made that this research would attempt to determine an alternative solution to using a complex building simulation model. While these can be excellent, with very good accuracy, they go above and beyond what is required here, with respect to the model outputs, this work only requires the temperature and relative humidity, whereas complex models allow for much more, such as energy usage, and analysis of alternate scenarios. Additionally estimating some inputs can be problematic, for example you cannot drill into a historic wall to determine its cross section construction. Here an attempt at a simple transfer equation will be made, that predicts indoor temperature and relative humidity rapidly by assessing the mathematical relationship between the indoor and outdoor climate.

The topics introduced here are discussed in greater detail in chapter 3, building simulation.

Temperature and relative humidity have been mentioned a number of times already, the opportunity will be taken here at this early stage to define these terms, as they are used on numerous occasions throughout this work, and they form a central part of the research. According to Camuffo (1998) temperature is defined as:

"The condition which determines the direction of the net flow of heat between two bodies"

Temperature is understood by most, but the concept of relative humidity may not be, its definition is:

"The ratio between the mass of vapour ($m_v$) actually present in whatever volume of atmosphere, to the greatest amount possible at the same temperature ($m_{v,sat}$)"

Another term related to these and used later in this work is that of specific humidity, this can be defined as:

"The ratio of the mass of water vapour ($m_v$) to the mass of moist air ($m_a + m_v$)"

Both the relative humidity and specific humidity definitions are from Camuffo (1998). A psychrometric chart plots several thermohygrometric parameters, including the temperature and relative humidity, as shown in figure 1.1. A number of relationships are plotted on a psychrometric chart, the vertical lines (isotherms) represent the humidity ratio, similar to the specific humidity, but with respect to dry air not moist air, the humidity ratio increases as the line ascends. The horizontal lines are constant in terms of humidity ratio, a shift in either direction along these lines indicates a change in temperature, without a change in humidity ratio, however the relative humidity will change. Relative humidity is shown by the curved red lines, along which the relative humidity is constant. The 100% relative humidity curve is also the saturation curve, the point at which the atmosphere can hold the greatest mass of vapour. The blue lines represent the wet bulb temperature, ascending these the temperature decreases and the humidity ratio increases. A number of other properties can also be included, the psychrometric chart allows for each point on the chart to fully describe the complete thermodynamic state of the air parcel (Camuffo, 1998). In addition to the relationships shown in figure 1.1, it is also possible to define the dew point, this is defined by following the horizontal line to the saturation curve, for example at 25°C and 50% RH the dew point is 14°C.
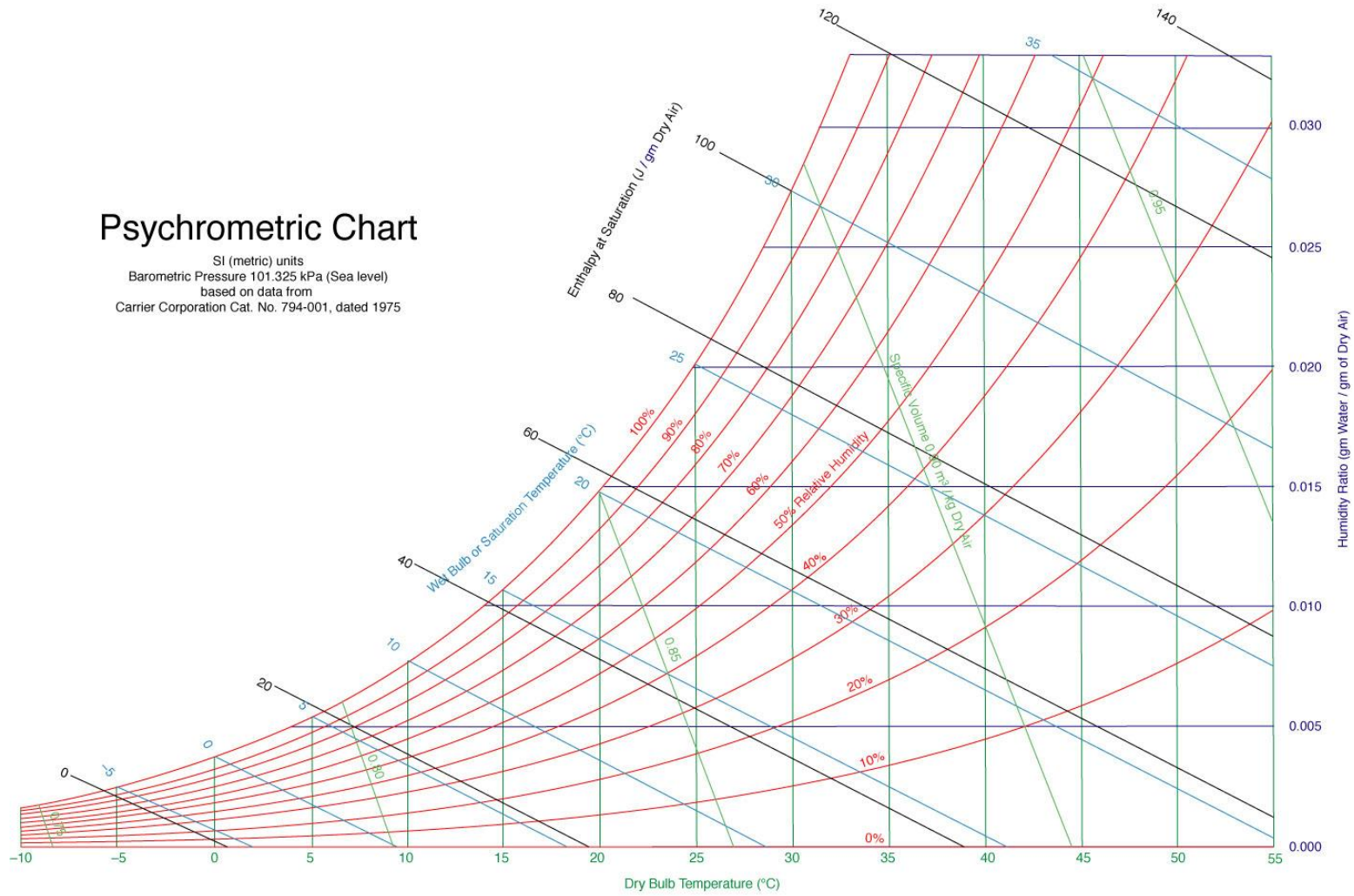
Figure 1.1: A standard psychrometric chart.

## 1.2 Damage

It is important that historic collections are preserved for future generations; an obstacle to this preservation is damage. Damage appears in many different forms, and is often referred to by different names, such as deterioration, decay, and change. The word change introduces a very important concept, damage is often thought as bad, whereas change is not always, this highlights that not all change is negative (Bell, 2008, Brimblecombe, 2008). An example is the change of copper from a bronze colour to green, this is technically deterioration, but is often intended and not seen as a negative change. Evidence also suggests that not all soiling of stone (aesthetic damage) is unacceptable (Grossi and Brimblecombe, 2004, Brimblecombe and Grossi, 2005), this is because of how it is perceived, and because it doesn't imply physical damage.

There are many causes of damage; these are often broken down into categories of damage (Brimblecombe, 1994, Brimblecombe, 2008, The National Trust, 2006). One example is the separation into catastrophic, severe and cumulative damage (The National Trust, 2006). Catastrophic damage could include fire, flood or earthquake which can destroy entire collections, but are relatively infrequent. Severe damage is classed as catastrophic for an object, but with limited impact on the collection, for example breaking a piece of china. Cumulative damage builds up as time passes, for example the fading of colour as it is exposed to light, the longer the exposure the greater the damage (The National Trust, 2006).

Other examples of grouping different damage types are available (Brimblecombe, 1994, Brimblecombe, 2008), where damage is separated by the mode. The first mode is cumulative change (or dose law/deposition velocity), as discussed above where the damage is proportional to the dose or deposition. The second mode of damage is cyclic change or fluctuations, for example the cycling of temperature around zero can cause frost damage. The final mode of damage defined is impulsive processes, such as earthquakes or dropping a fragile object; in this category the probability of an event occurring is significant. Little can be done to prepare for catastrophic event, which is likely to be a rare occurrence, whereas precautions can be taken when handling objects to prevent damage, which may occur frequently (Brimblecombe, 2008).

The different categories of damage are often important in understanding the processes; they imply how damage is caused, however they do not explicitly describe the process causing damage. The National trust (2006) identify nine agents of deterioration, somewhat similar to those introduced by Michalski (1990), that cause damage to collections:

- Fire
- Loss
- Water
- Physical
- Chemical
- Biological
- Light
- Wrong relative humidity
- Wrong temperature

Again other approaches of describing the agents of deterioration are available, for example Brimblecombe (2008) describes some slightly differently, but generally they fall into the broad categories above, but with descriptions that are more scientific, which is to be expected as the two publications are for different audiences. Michalski (2007) subdivides two of these categories further providing more information, three types of wrong, or incorrect temperature are defined: too high, too low and fluctuations about a mean. Four subdivisions of incorrect relative humidity are provided: damp, above and below a critical value, above 0% and fluctuations about a mean (Michalski, 2007).

Some of the agents of deterioration are directly influenced by environmental conditions or climate, and others have no direct relationship to the environment, for example dropping and breaking an object. In this work only damage which is caused by the environment is included, where it is likely that climate change may have a direct impact. Specifically the focus is upon the temperature and relative humidity in indoor environments, this is quite important as the factors affecting damage indoors and outdoors can be different.

The environmental conditions that collections and historic interiors encounter can cause damage in three ways, chemically, biologically and physically/mechanically (Koestler et al., 1994, Sebera, 1994, Pretzel, 2005, The National Trust, 2006, Taylor et al., 2005, Brimblecombe, 1994, Grossi et al., 2007, Sabbioni et al., 2008, Reilly et al., 1995, Ginell, 1994, ASHRAE, 2003). The conditions that are important in causing damage indoors and affect the rate of deterioration are: temperature, relative humidity, light (and UV radiation), air pollutants and dust (La Gennusa et al., 2008, Image Permanence Institute, 2005, Reilly et al., 1995, Brimblecombe, 1994, Bionda, 2006, Taylor et al., 2005, Thickett et al., 2007, Bell, 2008, Sebera, 1994, Koestler et al., 1994, Erhardt et al., 1995, Pavlogeorgatos, 2003, ASHRAE, 2003, PAS 198, 2012). Along with these, additional factors are important for outdoor collections, such as rainfall and wind speed (Sabbioni et al., 2010). In addition to these environmental issues there are also extreme events that are caused by the

environment and can be catastrophic, such as flooding, hurricanes or landslides, although the impact of climate change upon these is not considered in this work.

These environmental factors can be separated by an important issue; temperature and relative humidity are usually present, whereas for example exposure to light can be prevented. Other factors are important when present; however temperature and RH are usually the most significant aspects to consider when assessing damage by the environment to indoor collections. Outdoors, rain or moisture has great significance. While they are always present and have significant effects, they also act as enablers (or inhibitors) of damage by other factors such as light or pollutants (Reilly, 2005). In addition higher temperatures speed up the reaction rate for deterioration (PAS 198, 2012) and higher RH will generally facilitate decay reaction, particularly hydrolysis (Taylor et al., 2005, PAS 198, 2012).

## 1.3 Climate change

Climate change is one of the most important problems facing the world today. Climate change implies that the environmental conditions will be different in the future, and thus shift the external factors important to cultural heritage. The impact of environmental conditions upon historic collections has been discussed already with respect to the damage. Effective management of this change requires knowledge of the impact climate will have on historic collections.

### 1.3.1 Background

Climate change is not new; the Earth's climate has changed continually throughout history. However this is attributable to natural factors (English Heritage, 2008), whereas contemporary climate change is largely caused by anthropogenic factors. This indicates that the definition of climate change is important, one such definition is:

> "Any change in climate over time, whether due to natural variability or as a result of human activity." (IPCC, 2007a)

Therefore the cause of climate change is significant, there is a growing expectation that increases in the concentrations of greenhouse gases arising from human activity will lead to substantial changes in climate in the twenty first century (Johns et al., 2003).

There is already evidence that anthropogenic emissions of greenhouse gases (GHGs) have altered the large-scale patterns of temperature over the twentieth century, although natural factors have also contributed (Johns et al., 2003). However, greenhouse gas

forcing has very likely (>90%) caused most of the observed global warming over the last 50 years (IPCC, 2007a).

The global atmospheric concentration of GHGs such as carbon dioxide, methane and nitrous oxide have increased markedly as a result of human activities since 1750 and now far exceed pre-industrial values determined from ice cores spanning many thousands of years. The global increases in carbon dioxide concentration are due primarily to fossil fuel use and land use change, while those of methane and nitrous oxide are primarily due to agriculture (IPCC, 2007a).

Future climate change will probably be dominated by the response to anthropogenic forcing factors (GHGs), however large uncertainties remain (Johns et al., 2003).

The climate system is modelled in order to project the future climate, by looking at the physical processes of the climate and the expected levels of emissions, or GHGs, these are known as emission scenarios and lead to some of the uncertainties of future projections. These model outputs indicate the effects of climate change.

### 1.3.2 Modelling future climate change

The future climate is modelled in order to project how it will behave, and what affect climate change will have. There are two significant parts to the process of projecting the future climate, first the emission scenario and secondly the actual model. The emissions help define the model initially and in the future drive the model (Johns et al., 2003).

*Emission Scenarios*

As discussed, GHG emissions cause climate change; these emissions are the product of very complex dynamic systems, determined by driving forces such as demographic development, socio-economic development and technological change. The future evolution of emissions is highly uncertain (Goodess et al., 2007), different scenarios show alternative images of how the future might unfold; as such they can be used to assist climate change projections (IPCC, 2000). These scenarios are used in order to drive the climate models.

The scenarios cover a wide range of the main driving forces of future emissions, they are based upon extensive assessment of the literature, six different modelling approaches and feedback from individuals (IPCC, 2000). From this four different narrative storylines were developed to describe the relationships between emission driving forces and their evolution and to add context for the scenario quantification. Each storyline represents

different demographic, social, economic, technological and environmental developments (IPCC, 2000).

Each scenario represents a specific quantitative interpretation of the respective storyline, there are more scenarios than storylines as different modelling approaches were used for the same storyline, giving different scenarios (IPCC, 2000). The four storylines are A1, A2, B1 and B2, which are then separated into six scenario groups, A1F1, A1T, A1B, A2, B1 and B2. In all there are 40 scenarios, they arise from exploring uncertainties in driving forces (IPCC, 2000). The specific scenarios and their descriptions will be discussed later (section 2.5).

*Physical model*

The primary tool for understanding and attributing past variations and future projections of climate is a group of models called the atmosphere-ocean general circulation models (AOGCMs) (IPCC, 2007a). These models are based upon well-established physical principles and have been demonstrated to reproduce observed features of recent climate and past climate changes. There is confidence that these models provide credible estimates of future climate change, particularly at continental scales. Some climatic variables have a greater level of confidence than others, specifically temperature and precipitation respectively (IPCC, 2007a).

These models are mathematical representations of the actual climate system, expressed as computer codes and run on powerful computers. The models are extensively tested by comparing their simulations to observations of the atmosphere, ocean, cryosphere and land surface. This places confidence in the models, so that when different emission scenarios are used with the models, for future projections, the predictions can be relied upon (IPCC, 2007a).

There is a great deal more information that could be discussed about climate models, as this topic is very complex, however the exact ways in which the models work is not within the scope of this thesis.

The IPCC (2007a) describe 23 different models from around the world, but this project will use data from the UK developed model, developed by the Hadley centre for Climate prediction and research, and the Meteorological office. However, using more than one model can place greater confidence within results, as has been shown with the ENSEMBLES project (Van der Linden and Mitchell, 2009).

The Hadley centre global model is called the HadCM3; it was developed from the earlier HadCM2 model, with various improvements applied (Johns et al., 2003). The full description is available in Johns et al. (2003), however some of the more basic aspects of the model are that it consists of 19 atmospheric levels with a horizontal resolution of 2.5° latitude by 3.75° longitude. This equates to roughly 265 km by 300 km over the UK (Hulme et al., 2002a). The oceanic component has 20 levels with a horizontal resolution of 1.25° x 1.25°, this greater resolution is required to represent important details in oceanic current structures (Johns et al., 2003).

The atmosphere spatial resolution is important in this project, as this is the area for which the future data will be relevant for. This is a very large area, and to make the projections relevant to specific collections within buildings at a much smaller scale will prove a challenge. Another problem with the model could be the temporal resolution. Data is available as a daily value, but this may not be useful for some damage processes. Some materials have a slow response time, and daily data will be acceptable, but if the response time is faster this could pose a problem.

The HadCM3 model is run from 1860 through to 2100, the period 1960-90 is the baseline period, where the model matches the measured conditions, and then the period 1990-2100 is projected climate, this differs depending upon the emission scenario used (Johns et al., 2003).

The United Kingdom Climate Projections (UKCP) weather generator (Jones et al., 2009) is also used here, this provides downscaled climate output, using the HadRM3 model, thus overcoming the limitations described above. It also allows for probabilistic projections, as some modelling uncertainties are taken into account. The weather generator is described in more detail in section 2.1.

*Uncertainties*

The difficulty of projecting the future is because of inherent uncertainties; these can arise from a number of sources. Firstly there are emissions uncertainties; hence different emission scenarios exist to cover possible outcomes. We do not know however which emission scenario will turn out to be closest to reality and the actual emissions may lie outside even these limits (Hulme et al., 2002b, Goodess et al., 2007).

The second source of uncertainty comes from science (Goodess et al., 2007); there are some factors which are not fully understood, such as how important is the cooling effect of aerosols and the warming effect of soot particles (Hulme et al., 2002b). Different climate

models work in slightly different ways, because of the interpretation of these scientific uncertainties, thus different models will give different results at a local scale (Hulme et al., 2002b).There are further more complex sources of uncertainties; these will not be discussed here as they are not of direct relevance to the research here. Further discussion of these can be found in Hulme et al. (2002a) and Goodess et al. (2007). It is important to understand the relation of these uncertainties to results projected from just one emission scenario and one model. Provided these are taken into account, and stated with the results then this is a valid approach (Grossi et al., 2007).

### 1.3.3 Effects of future climate change

Modelling provides climate projections. Often a range of possible values are given, in order to accommodate the uncertainties associated with the emission scenarios.

*Temperature*

A warming of 0.2°C per decade for the next two decades is projected for a range of emission scenarios. Even if the concentrations of all GHGs and aerosols had been kept constant at year 2000 levels, a further warming of about 0.1°C per decade would be expected (IPCC, 2007a). This indicates an important point; even if we reduce our emissions the concentrations of GHGs take some time to decrease, due mainly to the slow response of the oceans (IPCC, 2007a).

Looking at overall global warming (global mean temperature increase), relative to 1900 it is projected that the increase in the year 2050 will be 1.5 to 2.5 K and this will rise to 2.6 to 5.3 K by the year 2100. Land and sea temperatures mirror the rise in global means, but with a fairly consistent land-sea contrast, with a ratio of about 1.7 (Johns et al., 2003).

In contrast to the above figures, although very similar, the IPCC (2007a), which takes data from multiple climate models, as opposed to the one model which the work by Johns et al. (2003) is focussed, gives the following figures. The best estimate of warming is between 1.8°C for the low scenario (B1) and 4.0°C for the high scenario (A1F1), however when all uncertainties are taken into account the full range could be from 1.1°C to 6.4°C (IPCC, 2007a).

These climate projections are for global changes, however more specific projections are available for the United Kingdom, where this research is based, and case studies will be carried out for UK collections. In principle the techniques can be applied to other locations. It is projected, using the medium emission scenario, that by the 2080's the annual temperature across the UK may rise by between 2°C and 4°C, for winter and summer

periods respectively, although there are pronounced differences between the north and south of the UK (Jenkins et al., 2009).

Along with increases in temperature the frequency of extreme temperatures will change, in the UK high summer temperatures will become more frequent and very cold winters will become increasingly rare (Hulme et al., 2002b). Another effect is caused directly because of global warming, the melting of sea ice (Johns et al., 2003). It is projected to shrink in both the Arctic and Antarctic under all emission scenarios (IPCC, 2007a).

*Sea level rise*

Another important effect of climate change is sea level rise, the largest contribution to the projected rise in future global-mean sea level during the period 1900 to 2100 is from the thermal expansion of the ocean, this ranges from 21 to 34 cm. When additional contributions of sea level rise are added, for example melting of land ice, the overall increase in mean sea level ranges from 30 to 48 cm (Johns et al., 2003). Other figures for sea level rise can be found: a range of 18 to 59 cm is given by the IPCC (2007a), and the reason for the difference is again because of more climate model projections being used.

Some important points need to be highlighted here. Firstly if the concentrations of atmospheric carbon dioxide were stabilized by the year 2100, the sea level would continue to rise for several centuries (Johns et al., 2003). The second point is that there is considerable spatial variation of the projected sea level rise, some regions show the rise as slightly negative or close to zero, where others indicate a rise of up to twice the global mean (Johns et al., 2003).

*Precipitation*

The third important effect of climate change is the increase in global-mean annual precipitation, with a sensitivity of around 1%/K (Johns et al., 2003). However, again the change is dominated by the location with some locations having increases in precipitation, and some decreases (Johns et al., 2003). Along with location differences there are seasonal differences, so summer rain may increase, but winter rain may decrease (e.g., in Southeast Asia) (Johns et al., 2003). Specifically increases in the amount of precipitation are very likely (>90%) in high latitudes, while decreases are likely (>66%) in most subtropical land regions, possibly by as much as 20% by 2100 (IPCC, 2007a).

Another effect of climate change is linked to changes in precipitation, the level of soil moisture, for northern extra-tropical continents the soil is wetter in winter, but becomes drier over much of North America and Europe in summer (Johns et al., 2003).

Looking at the projections for the UK, using the medium emission scenario, it is expected that winters will become wetter and summers drier everywhere, the largest change may be a decrease by almost 40% of summer precipitation in SW England by the 2080's and an increase in winter precipitation by 30% (Jenkins et al., 2009).

*Other effects*

Three main areas of climate change effects have been covered, there are more however, such as changes of cloud cover and solar radiation. In the UK climate may become sunnier than at present, with an increase in solar radiation and a decrease in cloud cover in the summer. This will be significant in the south where by the 2080's there may be a reduction of 18% of cloud cover. Again there is seasonal variation, along with geographical differences with the north seeing smaller changes (Jenkins et al., 2009).

Finally climate change may affect relative humidity, an important factor for historic collections. It is projected using the medium emission scenario that relative humidity may decrease in summer in southern England by as much as 10%, with smaller changes moving north. In the winter changes are only a few percent in either direction, across the whole of the UK (Jenkins et al., 2009).

*Amplification*

All of the discussed effects of climate change may appear to be small changes, and it can be difficult to imagine this causing serious damage to durable materials. However some damage mechanisms can be particularly sensitive to such small changes and as a result the damage caused can be amplified (Sabbioni et al., 2006, Brimblecombe et al., 2006b).

A typical example of a mechanism that is affected by this small change is freeze-thaw damage. There can be a significant change in the number of freeze-thaw cycles when the temperature changes only by a few degrees, this can have a large effect on the material, considering the original small change (Brimblecombe et al., 2006a).

It would appear that this sensitivity is especially significant when there are phase changes, such as freezing and the crystallisation/dissolution of salts (Grossi et al., 2008b, Brimblecombe, 2010). They are sensitive to the small changes because the damage caused is related to the phase change, which occurs at discrete values of temperature and relative humidity, thus a change in conditions allows for the crossing of the phase boundary more or less frequently, in turn causing more or less damage (Benavente et al., 2008).

## 1.4 Chapter plan

In the following chapters three methods chapters are presented, chapter two is based on the climate data, which can be separated into two sections. The first introduces three case study locations. The second relates to climate models, and presents work to overcome some of the limitations, along with an analysis of emission scenarios. Additionally the UKCP09 weather generator output is assessed, and the two baseline periods of each climate model are compared.

Research into a simple building simulation model is presented in chapter three. This is compared with a typical building simulation model, and the possibility of using the simple transfer function for short term predictions is investigated.

Chapter four focuses upon damage functions, and where necessary the adaptation required allowing for their use in this work. Damage functions presented include chemical degradation of paper and silk, the risk of mould growth, the number of salt weathering events and the risk of dimensional change events on wood.

The results chapters begin with chapter five, where the impact of climate change to historic interiors across Europe is projected, using the Hadley model. This uses the concept of an idealised room to estimate the future environment and the impact this will have on damage.

In chapter six the UKCP09 weather generator output is used to project the impact of climate change on the indoor environment and the risk this poses to damage, across three UK case study locations. The seasonality of these results is also assessed. Initially results are presented by location, followed by comparison between locations. The significance of the projections of change is assessed here.

The application of conservation heating as a tool to manage the environment and prevent damage is assessed under a changing climate in chapter seven. This is assessed in a number of ways, as previously with relation to the environment and damage, but additionally with respect to energy usage. The conclusions and further work are presented in chapter eight.

# CHAPTER 2

# CLIMATE DATA

## 2.1 Introduction

Climate modelling and the projections of climate change outdoors have been discussed in depth previously (section 1.3). Here greater detail of the climate output used is discussed, along with the limitations, and techniques used to overcome these.

Two different climate models will be used, but the second model is a derivation of the first model. The primary model is the Hadley centre, HadCM3, and the future climate output from this will be used directly, with some additional techniques utilised to overcome limitations. The second model is that of the United Kingdom Climate Projections 2009 (UKCP09) work. This applies a weather generator (dynamical downscaling with HadRM3) to output from the HadCM3 model, thus overcoming some of the limitations of the model when used alone. Additionally information from other climate models, with different but plausible representations of climate processes, is used to take into account some of the uncertainties associated with climate modelling. From this probability density functions (PDFs) are generated, the weather generator is run multiple times, sampling the PDFs, which brings in the notion of the probability of outcomes (Jenkins et al., 2009).

The two types of climate output are used, but for separate investigations. The Hadley model is used to estimate the impact of climate change on heritage throughout Europe, and the UKCP09 weather generator is used to estimate future damage at the case study locations around the UK. Although they are different the two techniques are compared to each other as they could both be used in the UK. However the UKCP09 weather generator is not available across Europe, it is constrained to the United Kingdom. The two sets of climate outputs are not compared in the future as here they do not use the same emission scenarios.

Also discussed are the current observations of climate at the case study locations, where the process of projecting future indoor damage will be applied.

## 2.2 Current climate observations

Often the environment is monitored at historic houses, using data loggers. Temperature and relative humidity are routinely recorded and occasionally additional environmental parameters are also measured, such as light and pollution levels (The National Trust,

2006, Thomson, 1999, Knell, 1994). Recent research also allows for dust levels to be monitored (Bowden and Brimblecombe, 2005). The data recorded at each of the case study locations that will be used to implement the process of projecting future damage will be discussed. In these cases the environment is also monitored outdoors at close proximity to the property. The opportunity will also be taken here to describe the locations used in detail.

### *2.2.1 Brodsworth Hall*

*Background*

Brodsworth Hall is run by English Heritage, it was donated to them in 1990, before being opened to the public in 1995, during these five years a major programme of restoration and conservation was undertaken (English Heritage, 2007). The house is Victorian, being built and furnished between 1861-3, many of the original contents have survived, but by 1990 both the house and its collections were is a state of decay. Serious damage was caused by mining subsidence, water penetration and eroding stonework, this was extensively repaired before opening to the public. The interiors of Brodsworth Hall were conserved as they were found, rather than restored. The exterior of Brodsworth Hall is built of soft pale magnesian limestone, some of which is from the estate (English Heritage, 2007). The front elevation of Brodsworth hall is shown in Figure 2.1.

This research focuses upon one room at Brodsworth Hall, the Library, which is quite small in terms of what some may imagine when a room is called a library. It contains over 1000 leather bound books, which are located on one wall (Thickett et al., 2007)(see Figure 2.2). Other decorations include a carpeted floor, of multiple layers, and wallpaper. A number of paintings hang on the walls and furnishings include a rosewood table and cabinet dating from the early 19th century (English Heritage, 2007). A number of upholstered chairs, and tables also furnish the room. The room has two floor to ceiling windows, which have a south-westerly aspect. These features can be seen in Figure 2.3, which shows the other side of the room as seen in Figure 2.2.

Figure 2.1: The front elevation of Brodsworth Hall. Copyright: The Author.



Figure 2.2: The collection of leather bound books in the Library at Brodsworth Hall.
Copyright: The Author.

Figure 2.3: Further objects of the collection in the Library at Brodsworth Hall. Copyright: The Author.

*Observations*

The environment at Brodsworth is monitored both indoors and out. The period of observations runs from January 2006 to March 2011, for which the temperature and relative humidity is recorded on a half hourly basis. To avoid duplication the observed temperature and humidity are shown in figures 3.1 and 3.3 in chapter 3, where they are more relevant. There are many problems with the data, the most significant is missing data. This is most likely to occur when the radio telemetry signals fail to reach the base unit, and therefore no observations are recorded, on occasions this leads to very little data being recorded for long periods. Where this data is utilised daily averages and monthly averages are calculated, with all of the gaps that are present in the data the decision was made that if less than half of the daily measurements were recorded then no daily average would be calculated. Also accordingly with the monthly average, if less than half the days have an average then the monthly average will not be calculated. Unfortunately this occurs on multiple occasions, and is problematic (see section 3.2). The data available for the Library is summarised in table 2.1.

Table 2.1: Summary of available data for the Library at Brodsworth Hall, indicating months where insufficient data is available. The column *count of days* indicates the number of days where 50% or more of data is available (24 of 48 readings are available).

| Year | Month | Count of days | Average T | Average RH | % of days | Less than 50% |
|------|-------|------|-----------|------------|-----------|------|
| 2006 | 1 | 25 | 9.36 | 57.9 | 80.6 | |
| | 2 | 8 | 8.73 | 48.5 | 28.6 | XXX |
| | 3 | 8 | 9.80 | 52.9 | 25.8 | XXX |
| | 4 | 21 | 15.97 | 42.4 | 70.0 | |
| | 5 | 26 | 17.30 | 48.9 | 83.9 | |
| | 6 | 26 | 19.75 | 52.0 | 86.7 | |
| | 7 | 17 | 22.15 | 52.5 | 54.8 | |
| | 8 | 5 | 21.44 | 54.3 | 16.1 | XXX |
| | 9 | 4 | 21.41 | 63.3 | 13.3 | XXX |
| | 10 | 17 | 17.98 | 59.4 | 54.8 | |
| | 11 | 14 | 13.71 | 54.7 | 46.7 | XXX |
| | 12 | 4 | 11.50 | 48.4 | 12.9 | XXX |
| 2007 | 1 | 23 | 11.32 | 51.3 | 74.2 | |
| | 2 | 5 | 10.89 | 48.0 | 17.9 | XXX |
| | 3 | 20 | 11.97 | 49.7 | 64.5 | |
| | 4 | 28 | 17.10 | 48.8 | 93.3 | |
| | 5 | 31 | 17.27 | 48.4 | 100.0 | |
| | 6 | 28 | 19.71 | 56.8 | 93.3 | |
| | 7 | 26 | 19.58 | 56.6 | 83.9 | |
| | 8 | 30 | 20.72 | 51.5 | 96.8 | |
| | 9 | 30 | 19.45 | 52.2 | 100.0 | |
| | 10 | 28 | 16.84 | 55.3 | 90.3 | |
| | 11 | 18 | 11.80 | 51.0 | 60.0 | |
| | 12 | 24 | 10.74 | 48.9 | 77.4 | |
| 2008 | 1 | 24 | 12.59 | 52.3 | 77.4 | |
| | 2 | 14 | 11.50 | 50.1 | 48.3 | XXX |
| | 3 | 5 | 12.35 | 46.4 | 16.1 | XXX |
| | 4 | 27 | 13.58 | 47.8 | 90.0 | |
| | 5 | 28 | 17.66 | 50.2 | 90.3 | |

| | | | | | |
|---|---|---|---|---|---|
| | 6 | 26 | 18.79 | 51.3 | 86.7 |
| | 7 | 29 | 19.98 | 57.6 | 93.5 |
| | 8 | 27 | 20.47 | 58.9 | 87.1 |
| | 9 | 30 | 18.75 | 58.3 | 100.0 |
| | 10 | 31 | 16.24 | 49.6 | 100.0 |
| | 11 | 30 | 13.88 | 46.5 | 100.0 |
| | 12 | 31 | 10.39 | 50.0 | 100.0 |
| 2009 | 1 | 30 | 8.80 | 51.2 | 96.8 |
| | 2 | 27 | 8.83 | 52.9 | 96.4 |
| | 3 | 29 | 11.39 | 49.2 | 93.5 |
| | 4 | 30 | 14.92 | 49.9 | 100.0 |
| | 5 | 31 | 16.21 | 50.2 | 100.0 |
| | 6 | 30 | 19.26 | 51.8 | 100.0 |
| | 7 | 31 | 20.39 | 54.6 | 100.0 |
| | 8 | 31 | 20.58 | 55.4 | 100.0 |
| | 9 | 30 | 19.15 | 53.3 | 100.0 |
| | 10 | 31 | 17.08 | 52.7 | 100.0 |
| | 11 | 30 | 13.72 | 51.5 | 100.0 |
| | 12 | 31 | 10.44 | 48.5 | 100.0 |
| 2010 | 1 | 31 | 8.76 | 47.8 | 100.0 |
| | 2 | 28 | 8.56 | 48.5 | 100.0 |
| | 3 | 29 | 10.90 | 48.1 | 93.5 |
| | 4 | 28 | 14.69 | 44.7 | 93.3 |
| | 5 | 31 | 16.69 | 45.4 | 100.0 |
| | 6 | 30 | 20.12 | 50.1 | 100.0 |
| | 7 | 28 | 21.15 | 52.6 | 90.3 |
| | 8 | 31 | 19.73 | 54.2 | 100.0 |
| | 9 | 30 | 18.90 | 54.5 | 100.0 |
| | 10 | 31 | 16.68 | 51.2 | 100.0 |
| | 11 | 30 | 12.90 | 48.2 | 100.0 |
| | 12 | 31 | 7.40 | 43.6 | 100.0 |
| 2011 | 1 | 31 | 10.67 | 48.2 | 100.0 |
| | 2 | 28 | 12.38 | 53.1 | 100.0 |
| | 3 | 29 | 11.85 | 48.4 | 93.5 |

Table 2.1 indicates that for the first three years of data (2006-8) there is only one occasion that sufficient data is available for two of the months, February and March. This is a serious issue, an average of three years gives a balanced estimate of the climate over these three years, should one year have a very cold winter the other two years may balance this out. Fortunately as the research progressed more data became available, and the problem of gaps reduced significantly. At the start of the research only the first three years of data were available, and not having acceptable data for February and March was a major problem, however once the recent data was available this was no longer a significant concern as there is now reliable data for a number of these months.

The February 2008 data was used, even though there is less than 50% of the data. It is very close to this boundary, at 48%, and had this not been a leap year would have been accepted, this helps to balance the total number of February's in comparison to the other months. It is likely that if one more day were available to bring the value above 50% that the average of the data is unlikely to be significantly different. Looking at the other months, there are six months where 4 years of monthly averages are available, a further five months have 5 years of data, and January has all six years of data available.

Ideally more than five years and three months of data would be used, but this is all that is available for this location. It is likely that the greater the number of years available the more representative the average will be of the climate. The accepted norm is 30 years of data in climate science, but it is unlikely that there are records of this length of indoor environments in historic buildings.

The gaps in the data are frustrating especially for long periods where the loggers fail to send the data to the base unit. The gaps can be filled with a place marker to identify the gap, which a program can read to interpret the value as a gap in the data. Even doing this within the same dataset can be complex as occasionally no timestamp is associated with the data gaps. These must be added manually to complete the time series. Significant amounts of time have been spent normalising data to account for gaps and getting the values in a similar format. Data loggers manufactured by different companies tend to structure the recordings differently.

The relative humidity is controlled by conservation heating (Thickett et al., 2007). Conservation heating is the control of a space by the relative humidity rather than the temperature, a humidistat is used instead of a thermostat. A specification will be set, stating the upper relative humidity level, if this is exceeded the temperature is raised to reduce the relative humidity. For a full and further explanation of conservation heating see section 7.1.

### 2.2.2 Knole

*Background*

Knole is a historic house close to Sevenoaks in England, owned and run by The National Trust. Although the Sackville-West family still reside in various private apartments throughout the house, for which they hold a 200 year lease that was granted when they donated the house to the trust in 1946 (Sackville-West, 1998). The house is surrounded by a large park, still owned by the Sackville-West family; they also own many of the collections of the house. Knole can be seen in Figure 2.4.



Figure 2.4: The front elevation, and entrance at Knole, Sevenoaks. Copyright: The National Trust.

Parts of Knole data back to the mid-15th-century, and has seen alterations since. In the early 17th century the building was an archbishop's palace and was transformed into a renaissance mansion, and by the end of the 17th century Knole had acquired a unique collection of Stuart furniture and textiles (Sackville-West, 1998). Little has changed at Knole since the late 18th century, when old master and contemporary English paintings were bought.

This research focuses on two rooms at Knole, the Cartoon and Leicester Galleries (Figures 2.5 and 2.6). The Leicester Gallery is named after the Earl of Leicester who was

granted Knole by Queen Elizabeth before its acquisition by Thomas Sackville (Sackville-West, 1998). The Leicester Gallery is surrounded by rooms on most sides, with 3 areas of fenestration, one at the end of the gallery with a north-easterly aspect, another which is technically within the billiard room, however there is no physical barrier between these rooms; this has a south-easterly aspect. The final windows face into a courtyard, with a north-westerly aspect. The long gallery is decorated with oak panelling dating from 1605-8, and there is a stone chimneypiece dating from the 15th century. Furnishings include a remarkable collection of early 17th century furniture with objects such as two 'Armada' chests with elaborate locks and a chair with original upholstery of crimson silk damask. Various other furnishings are also present including settees, chairs and stools, and candle stands, a number of paintings also adorn the walls in the Leicester Gallery (Sackville-West, 1998).

The second of the two rooms focussed on at Knole is the Cartoon Gallery, named after the set of six large copies of Raphael's cartoons that decorate the room. These are thought to date from 1624, a cartoon in this and the original sense described a full scale design of a tapestry or painting (Sackville-West, 1998). The Cartoon Gallery is a long gallery with windows along an outer wall, with a south-westerly aspect (Lankester and Brimblecombe, 2012a).  Further decorations include a plasterwork ceiling and wooden floor; the walls are hung with crimson stamped woollen velvet known as caffoy. Furniture in the long gallery includes a gilt table and pair of candle stands along with various chairs and stools, made from woods including oak and walnut (Sackville-West, 1998).

No heating is used in these two rooms at Knole, so the indoor temperature and humidity are driven largely by the outdoor environment.

Figure 2.5: The Cartoon Gallery at Knole. Copyright: The National Trust.

Figure 2.6: The Leicester Gallery at Knole. Copyright: The National Trust.

*Observations*

At Knole both the indoor and outdoor climates are monitored. Indoors the data held for the Cartoon and Leicester Galleries spans from March 2000 to June 2009, and June 2003 to December 2008 respectively, and is recorded on an hourly basis. Again there are gaps in this data, so it requires normalising, also removing any obvious anomalies, such as temperatures stepping up ten degrees between each observation up to 80°C in a clear pattern. The observed temperature and relative humidity are shown in figures 2.7 and 2.8 for the Cartoon Gallery, and 2.9 and 2.10 for the Leicester Gallery.
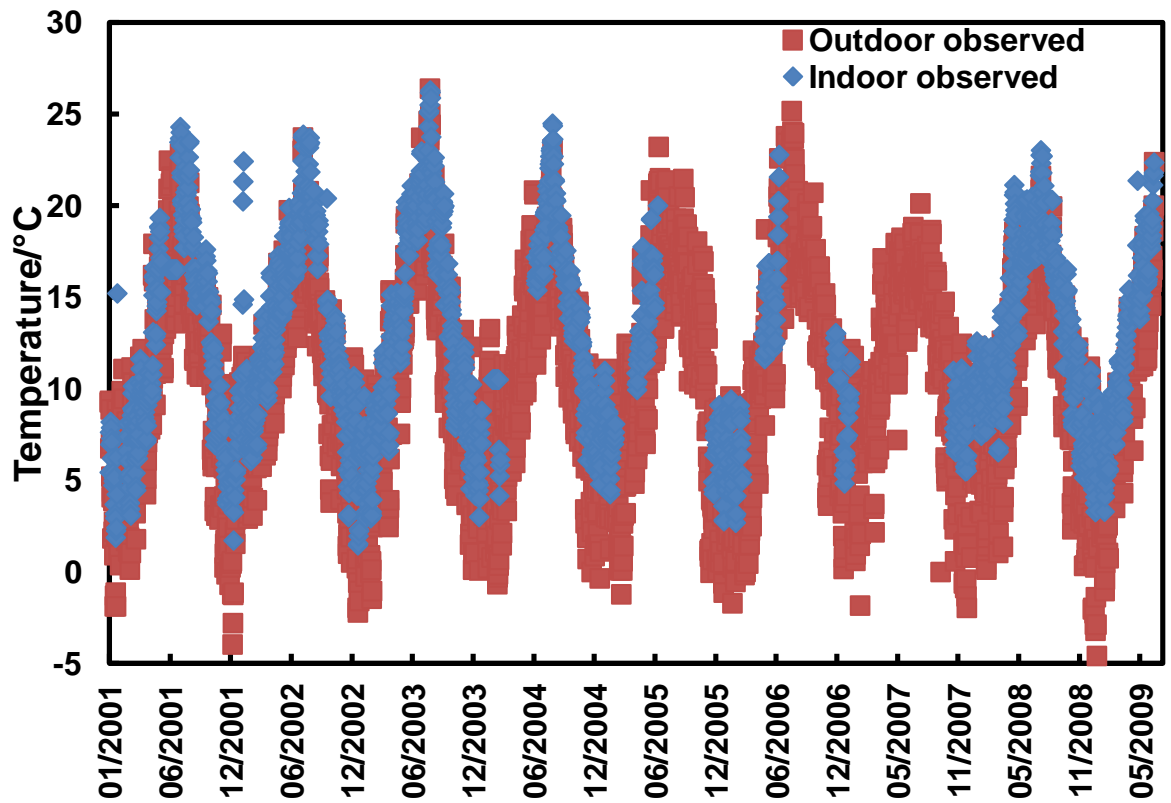
Figure 2.7: Observed indoor temperature in the Cartoon Gallery at Knole over the period 01/2001-06/2009. Observed outdoor temperature for Gatwick.
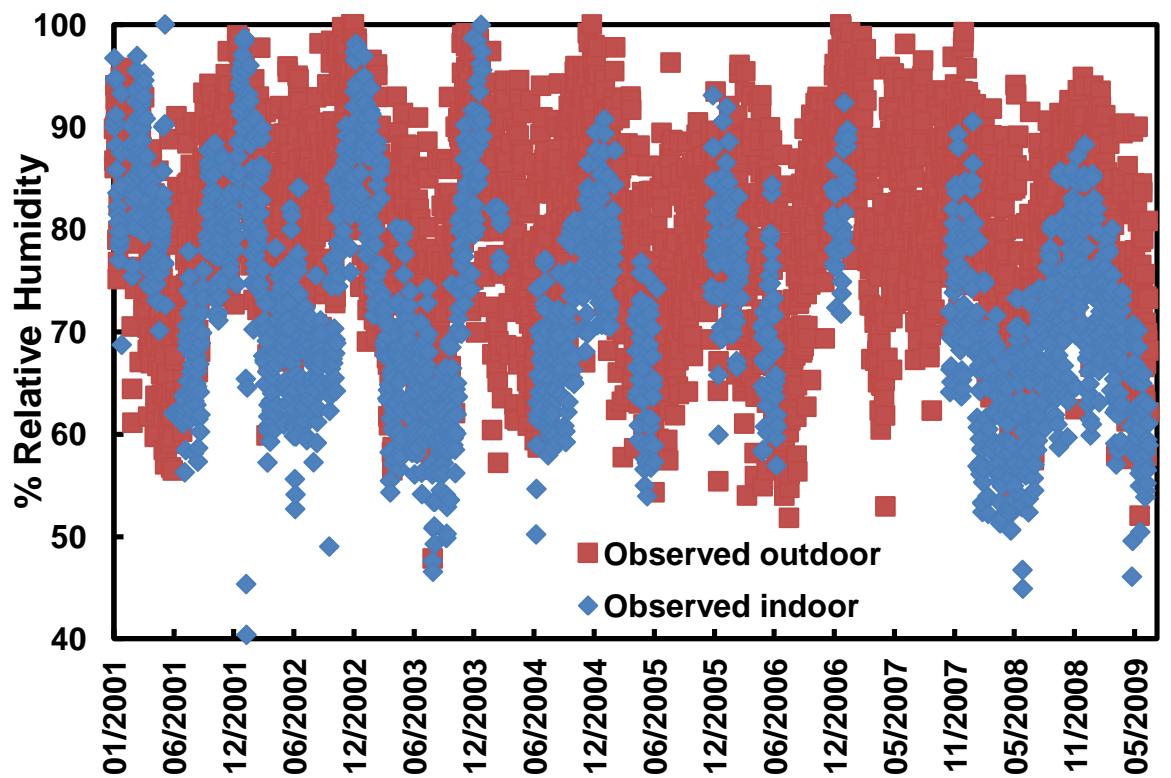


Figure 2.8: Observed indoor relative humidity in the Cartoon Gallery at Knole over the period 01/2001-06/2009. Observed outdoor relative humidity for Gatwick.
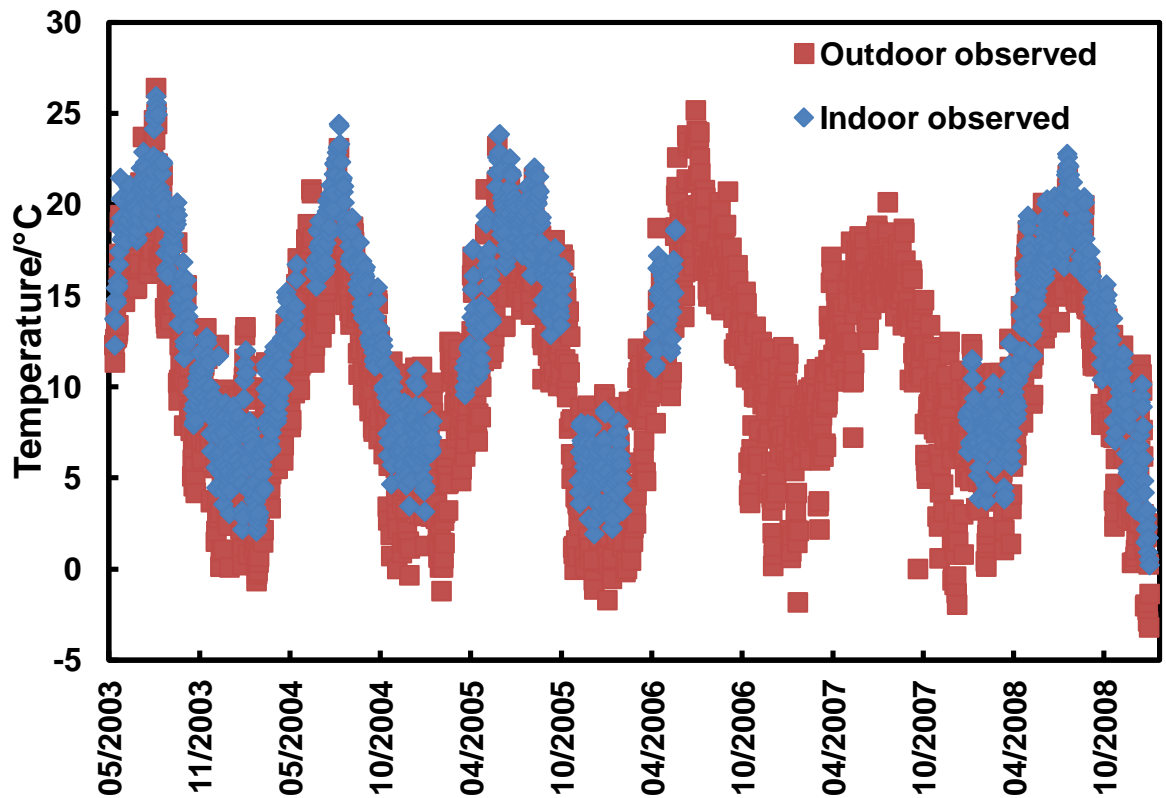
Figure 2.9: Observed indoor temperature in the Leicester Gallery at Knole over the period 06/2003-12/2008. Observed outdoor temperature for Gatwick.
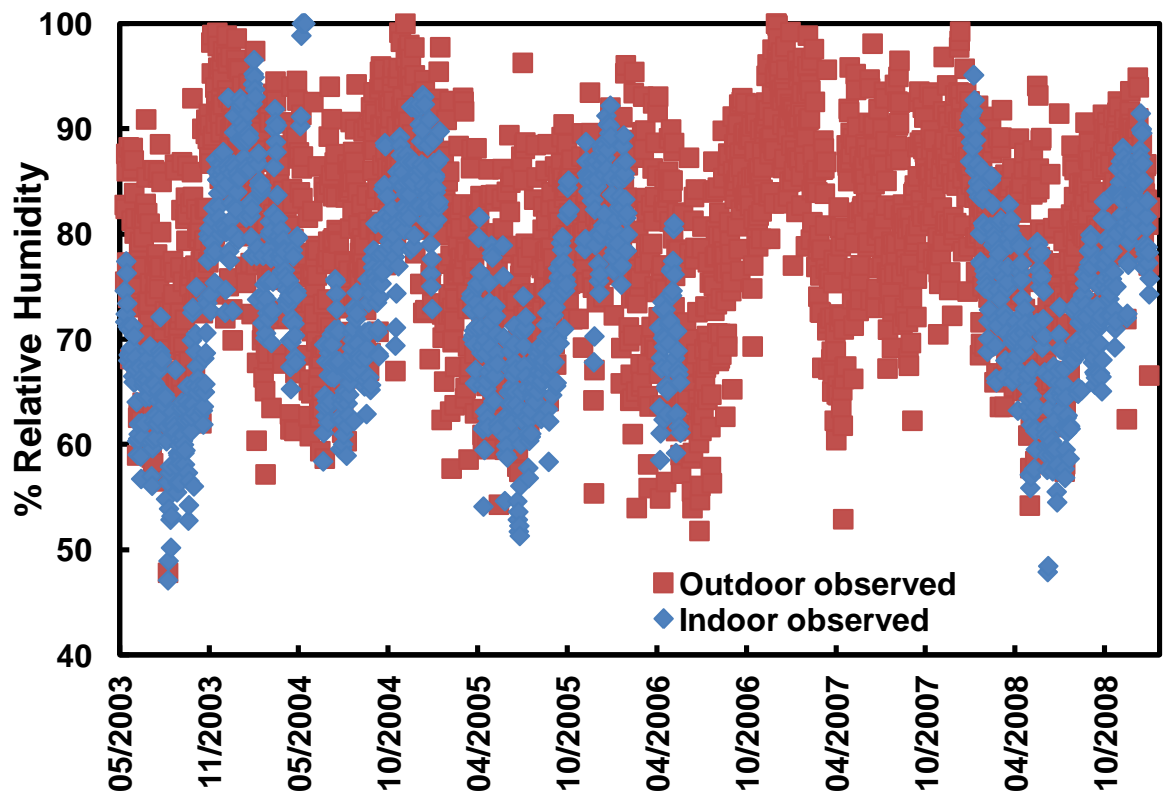


Figure 2.10: Observed indoor relative humidity in the Leicester Gallery at Knole over the period 06/2003-12/2008. Observed outdoor relative humidity for Gatwick.

Outdoors the observed data has significant gaps, while it is recorded from 2001 to the end of 2002 and 2008 to mid 2009; no data is available for the interim period of 2003-2007. The decision was made that this data consisting of about 3 and a half years in total, but split by 5 years was not adequate. Various nearby weather stations were explored to find a data set that spanned the time period required, March 2000 to June 2009 with the required observations of temperature and relative humidity, and with minimal gaps in observations. It was also necessary that the data served as proxy data for the outdoor climate at Knole, so it was important that there was good correlation between the outdoor observations that are available for Knole and the weather station observations.

The weather station chosen was at Gatwick airport, approximately 30 km away. The available data from the weather station, accessible through the British Atmospheric Data Centre (BADC) MIDAS land surface stations database (UK Meteorological Office, 2006), fulfilled the requirements discussed to act as proxy data for the exterior climate at Knole.

This is significant because some historic houses may only record indoor climate, but no outdoor climate, or only have short records of outdoor climate. If it is possible to use proxy data from nearby stations it allows future projections of climate at these properties.

The analyses carried out to determine the suitability of the Gatwick weather station are shown in figures 2.11 and 2.12. The monthly average of the temperature observations available outdoors at Knole are compared to those from Gatwick in figure 2.11. The large gap in the data, is seen in the middle of figure 2.11. The temperatures, with occasional exceptions compare well, indicating that the two locations share a similar temperature. The exceptions tend to be in summer, where Knole gets slightly warmer. The correlation coefficient for this comparison is $R^2 = 0.973$, with an equation of the best fit close to a 1:1 relationship, but not quite, because of the summer difference.
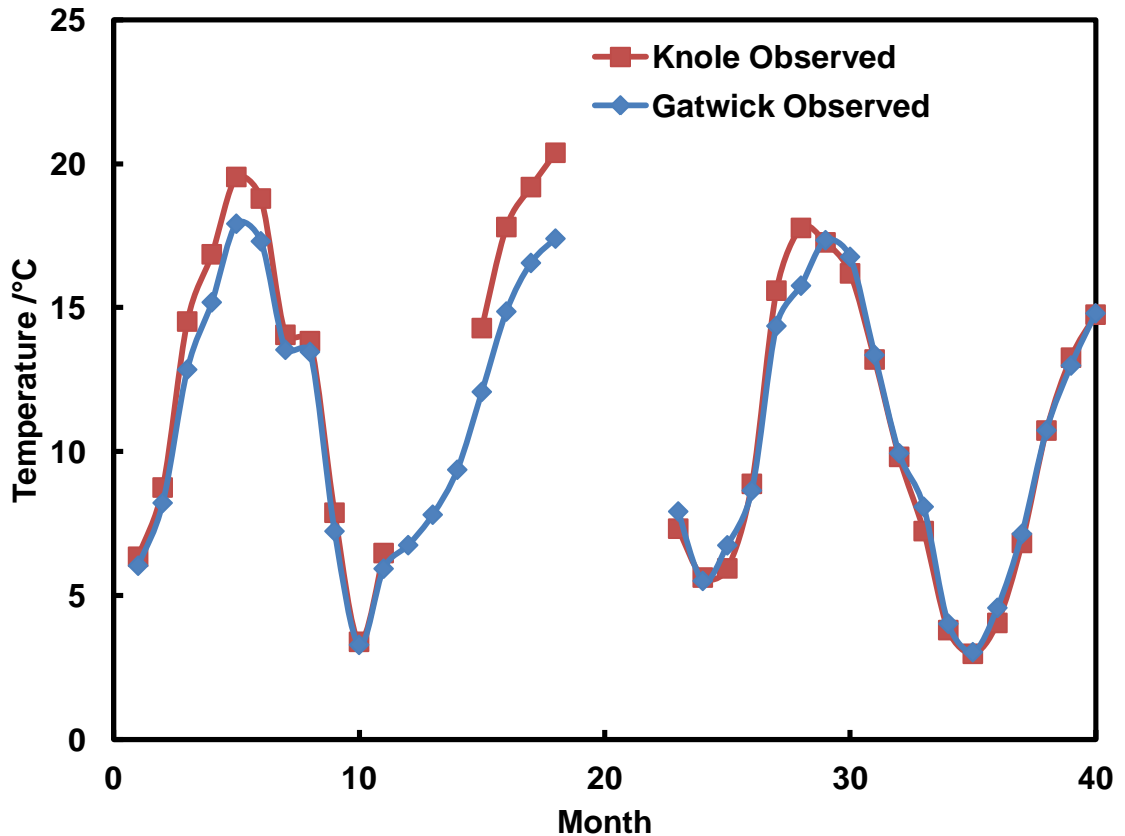
Figure 2.11: Monthly Average observed temperature at Knole and Gatwick. Month 1 corresponds to 03/2001, which follows through to month 18 which is 08/2002. The large gap in the data is represented by the break in all of the data. Then month 23 corresponds to 01/2008, continuing through until 06/2009.

The monthly average observed relative humidity for Knole and Gatwick is shown in figure 2.12. The comparison of the humidity is not as favourable as for temperature, but it is representative. The humidity at Knole tends to increase more than that at Gatwick, when it is high, and also decreases more when humidity is low. Some of the errors were larger, therefore the averages of all the data of each month was compared, for example all Knole January data was compared to all Gatwick January data, and a calibration determined. This was carried out for both temperature and humidity for the observed Gatwick data, so it represented outdoors at Knole. Temperature was calibrated using the difference, and relative humidity a ratio.
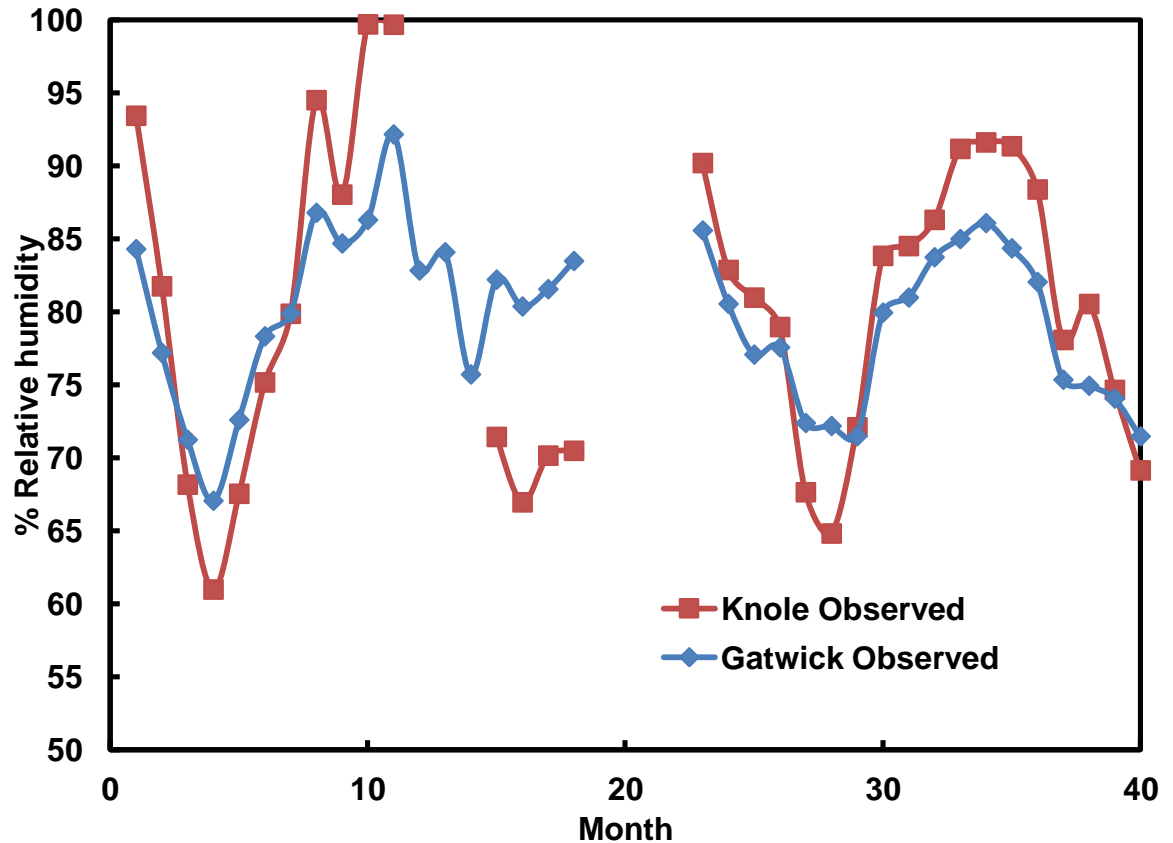
Figure 2.12: Monthly Average observed relative humidity at Knole and Gatwick. Month 1 corresponds to 03/2001, which follows through to month 18 which is 08/2002. The large gap in the data is represented by the break in all of the data. Then month 23 corresponds to 01/2008, continuing through until 06/2009.

### *2.2.3 Swiss Cottage at Osborne*

*Background*

The Swiss Cottage at Osborne, on the Isle of Wight was previously the private possession of Queen Victoria, and is now managed by English Heritage. The cottage is constructed of timber and imitates a traditional Swiss farmhouse; it was built between 1853-54. Prince Albert intended the cottage to be a place that his children could learn housekeeping and cookery and somewhere to entertain their parents (Howatson, 2007). The Swiss cottage museum can be seen in Figure 2.13.

Currently the Swiss cottage is presented as a museum, housing objects that the royal family received. The collection is vast is its origin, ranging from carved ivory balls, to natural history specimens to ancient Egyptian objects, the majority of these are stored in wooden showcases, as seen in Figures 2.14 and 2.15. The museum is relatively small,

comprising of six areas, two of which are those shown in Figures 2.14 and 2.15. When the museum is open the doors are constantly open, resulting in the indoor environment being largely dependent on the outdoor environment. The museum is dehumidified all year round, however during the open season the doors tend to be left open, and the indoor environment is dominated by that of outdoors. In the winter two small plug in radiators are used, to prevent damage from frost, they are not used for human comfort. Both of these effects can be seen in figures 2.16 and 2.17.



Figure 2.13: The Swiss Cottage Museum at Osborne. Copyright Dave Thickett.

Figure 2.14: Example of the collections and showcases in the Swiss Cottage Museum.



Figure 2.15: Further example of the collections and showcases in the Swiss Cottage Museum.

*Observations*

Both the indoor and outdoor climate is monitored half hourly at the Swiss Cottage over the period October 2008 to December 2010. The observed data is shown in figures 2.16 and 2.17, there are significant gaps in both the indoor and outdoor observed temperature and relative humidity for the initial period from 10/2008-07/2009. Therefore for the majority of the months there is only one year of observations. This is quite critical, as the data does not describe an average climate, it just describes one year which could have data that is extreme and doesn't represent the typical climate.
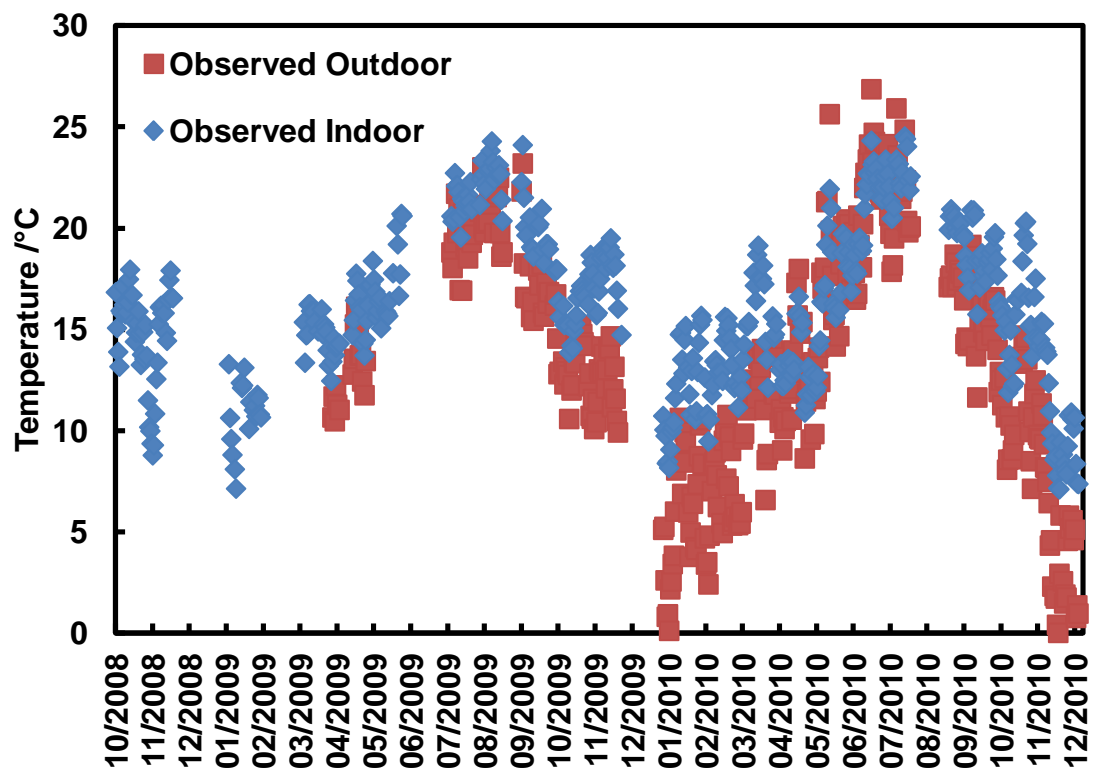


Figure 2.16: Observed indoor and outdoor temperature of the Swiss Cottage over the period 10/2008-12/2010.
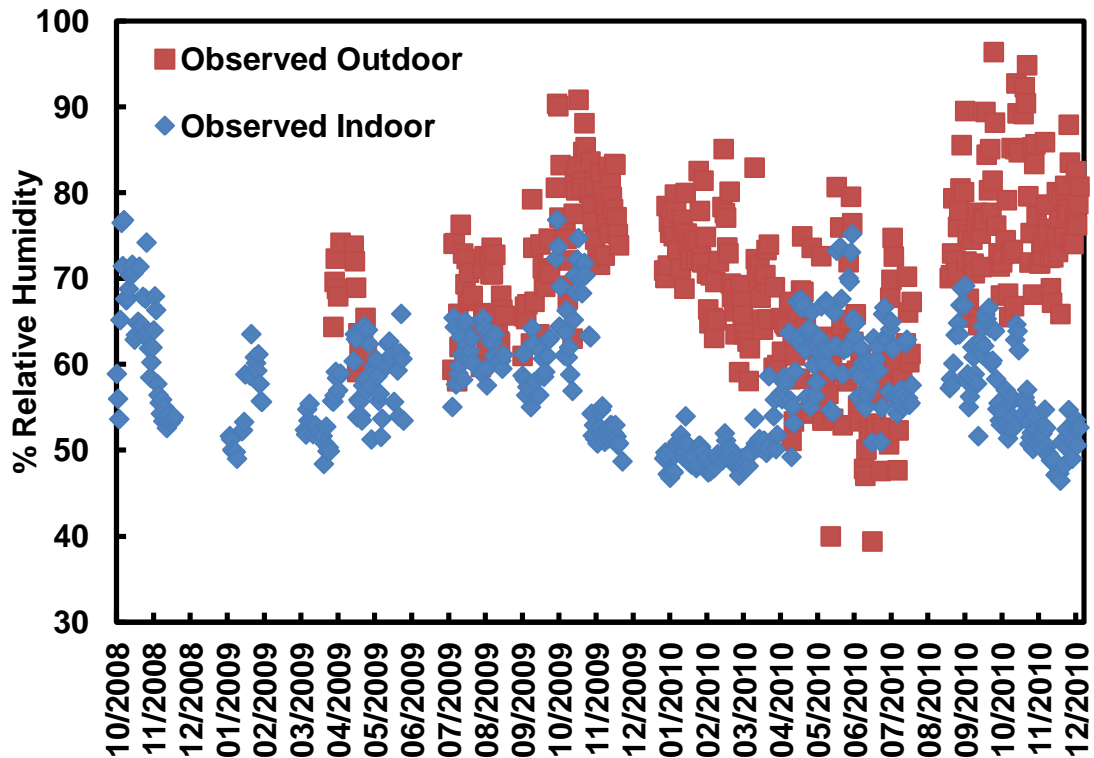
Figure 2.17: Observed indoor and outdoor Relative humidity of the Swiss Cottage over the period 10/2008-12/2010.

## 2.3 Hadley model

The Hadley model, HadCM3 has been discussed in the introductory chapter (section 1.3.2). The output from the model is specific to each grid square that covers a wide area, 2.5 × 3.75 degrees, which relates to 295 × 278 km at 45°N latitude (Grossi et al., 2008a). This is one limitation in applying the Hadley model, to specific historic houses; the future climate output needs to be downscaled. Without downscaling there can be differences between modelled and observed climate due to the size of the grid (Grossi et al., 2008a), topographical features such as mountain ranges produce variations in local climate. The importance of downscaling for the two geographically close locations (87 km) of Leon and Oviedo, in Spain, has been shown, because of the Cantabrian mountains that separate the two locations (Lankester and Brimblecombe, 2012a).

Output from HadCM3 is available as daily averages for the period 1961-2099, which could present itself as a problem. The response time of materials to the environment can vary from hours to months depending upon the object (ASHRAE, 2003). Therefore damage can occur at intervals of less than a day; if only daily averages are used some damage could be under predicted. Techniques have been developed to partially overcome the

spatial and temporal limitations, however they are still constrained by the model performance.

### 2.3.1 Spatial downscaling

The fairly simple bias adjustment used here originates from Grossi et al. (2008a) where the model output is calibrated by taking between 10 and 30 years of observed temperature and relative humidity and comparing this to the corresponding model output. The calibration is dependent upon the month, to allow for seasonal variation, therefore different correction factors are derived for each month. For temperature the difference between observed data and modelled output was calculated and used as the correction factor. With relative humidity the ratio between the observed data and modelled output is used. The correction factors derived for the bias adjustment are assumed to remain the same over the next century (Grossi et al., 2008a). In this work the method is referred to as downscaling, whereas it is simpler than downscaling typically used in climate research, and would not fall under this definition.

This method was applied at seven locations, for the work undertaken in chapter 5. These locations are Sevenoaks and Doncaster in the UK; Paris; Prague; Almeria, Oviedo and Leon, all in Spain. Localised outdoor observations were available for these locations, and downscaling of the Hadley model was required to project the outdoor environment into the future.

*Sevenoaks*

The total monthly average of the outdoor observations of temperature and relative humidity at Gatwick were determined. Thus the data for the January of each year was averaged, and so on for each month, over the period 01/2001-11/2009. The same was also carried out for the available Hadley output for the corresponding area, over the same period. These averages were compared and the difference or ratio determined for the calibration of the Hadley output. Figure 2.18 shows the comparison of the observed data, Hadley output and downscaled Hadley output temperature, and table 2.2 the calibration difference and ratio. The downscaled Hadley output monthly average temperatures match the observed temperature exactly, with the $R^2$=1, this is also true for the relative humidity. This is not surprising as the calibration was carried out with this data, at monthly averages, at lower temporal resolution it is expected that the correlation will reduce.
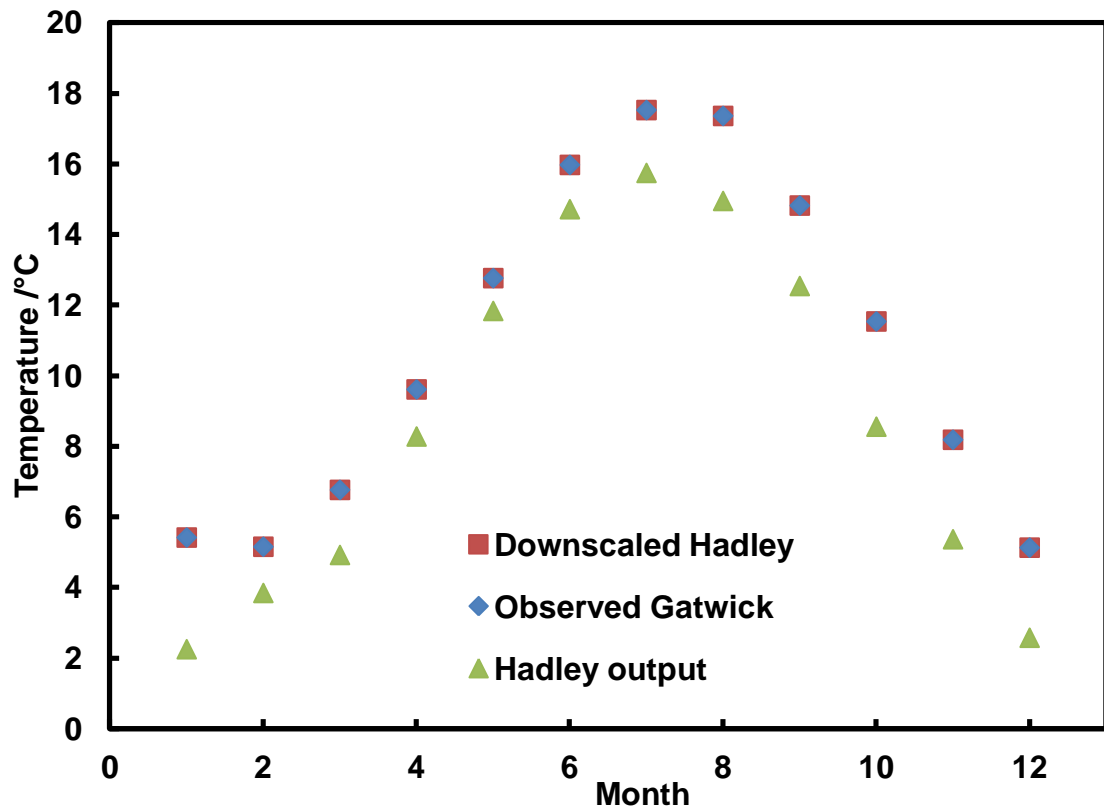
Figure 2.18: Comparison of the overall monthly average temperatures, for Sevenoaks, over the period 01/2001-11/2009.

Table 2.2: The observed and Hadley output overall monthly average temperature and relative humidity at Sevenoaks, used to calculate the calibration.

| | Temperature | | | Relative Humidity | | |
|---|---|---|---|---|---|---|
| Month | Observed | Hadley | Difference | Observed | Hadley | Ratio |
| Jan | 5.42 | 2.25 | 3.16 | 86.5 | 96.0 | 0.90 |
| Feb | 5.16 | 3.85 | 1.31 | 83.0 | 93.7 | 0.89 |
| Mar | 6.77 | 4.92 | 1.84 | 79.8 | 87.7 | 0.91 |
| Apr | 9.61 | 8.28 | 1.33 | 75.2 | 86.5 | 0.87 |
| May | 12.76 | 11.83 | 0.93 | 76.0 | 83.8 | 0.91 |
| Jun | 15.97 | 14.72 | 1.25 | 73.9 | 83.6 | 0.88 |
| Jul | 17.52 | 15.74 | 1.78 | 75.6 | 84.0 | 0.90 |
| Aug | 17.36 | 14.95 | 2.41 | 77.3 | 84.4 | 0.92 |
| Sep | 14.82 | 12.54 | 2.28 | 78.5 | 86.3 | 0.91 |
| Oct | 11.54 | 8.56 | 2.98 | 84.5 | 92.3 | 0.92 |
| Nov | 8.19 | 5.37 | 2.82 | 86.2 | 96.0 | 0.90 |
| Dec | 5.13 | 2.58 | 2.55 | 87.8 | 96.4 | 0.91 |

The total monthly average of the observed and downscaled Hadley temperature would be expected to match, but it is important to look at the downscaled data at a lower temporal scale to see how this represents the observed data. Figure 2.19 shows the monthly averages of the observed and downscaled Hadley output temperature. These compare quite favourably, with a correlation coefficient of $R^2=0.89$. It is when there are unusually warm or cold months that the calibration is not as effective, thus weather extremes are not dealt with very well. Some error in the calibration is expected, as the method attempts to calibrate to the mean temperature, but obviously observed temperatures vary around the mean. Initially it was also stated that this should be carried out for at least 10 years of data, here there are only 9, which is likely to have little impact. However other locations have significantly less data, which will decrease the effectiveness of the downscaling. The more data available the better prediction that is likely, as the average should be representative. However there is an interesting point to raise here, the more data available, the increased likelihood that climate change has had an effect upon the observed data, thus impacting the calibration, and possibly introducing error, this will become increasingly important in the future.
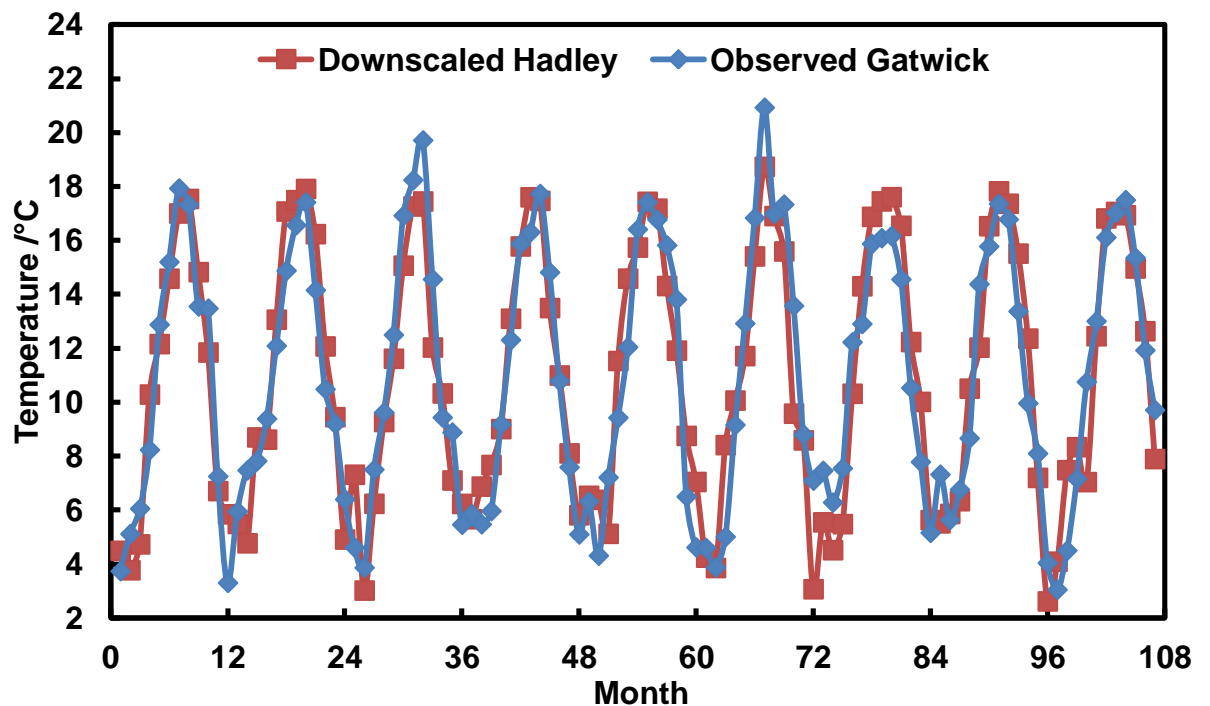


Figure 2.19: Comparison of the monthly average temperatures for the observed and downscaled data at Sevenoaks over the period 01/2001-11/2009.

The observed and downscaled Hadley output monthly relative humidity averages are shown in figure 2.20. The calibration doesn't appear to have worked as well as for the temperature; the observed humidity is more variable, thus making the calibration less effective. Therefore the comparison is not as good, with a correlation of $R^2=0.53$. In other applications this may not be such an issue, as overall the observed and downscaled data have the same total monthly averages. However in this work this may be significant, specific thresholds of humidity, around 70% are important, and higher humidity can cause greater damage. Thus the slight errors, although they may even out with respect to humidity, may not with respect to the estimated damage, there could be an overestimate of mould growth, or an underestimate of paper degradation.

In hindsight, of work in following chapters, it may have been more appropriate to downscale the temperature and specific humidity, rather than the relative humidity. Relative humidity is not an absolute measurement; it is dependent upon the temperature, whereas specific humidity is not. This is described in full in section 3.2.3. This presents further work that could be carried out in an attempt to improve this downscaling technique.
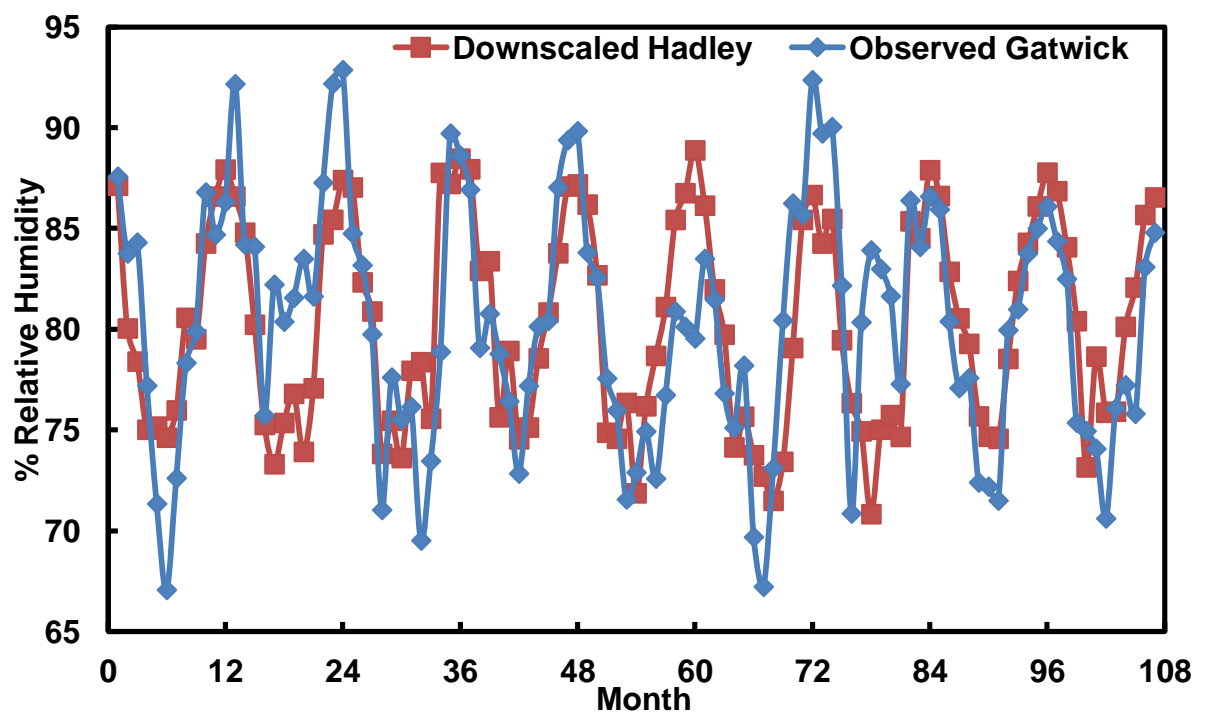


Figure 2.20: Comparison of the monthly average relative humidity for the observed and downscaled data at Gatwick over the period 01/2001-11/2009.

*Doncaster*

The same technique as applied at Sevenoaks was applied at Doncaster, over the period 01/2006-12/2008. The calibration values determined are shown in table 2.3. It was decided that only 3 years of data was insufficient, therefore the comparison of the data was carried out with 10 years of the downscaled data, from 2002-2011, with 2006-8 being the midpoint of this range. This comparison resulted in very similar graphs as shown previously in figure 2.20, with the correlation coefficient for both the temperature and relative humidity comparisons, as $R^2$=1. Some of the differences in temperature are quite large, but this is not unusual when the Hadley output covers such a large area, and the observed data is from one specific site.

Table 2.3: The observed and Hadley output overall monthly average temperature and relative humidity at Doncaster, used to calculate the calibration.

| Month | Temperature | | | Relative Humidity | | |
|---|---|---|---|---|---|---|
| | Observed | Hadley | Difference | Observed | Hadley | Ratio |
| Jan | 5.90 | 1.92 | 3.98 | 82.2 | 95.0 | 0.86 |
| Feb | 5.00 | 3.42 | 1.58 | 80.9 | 94.1 | 0.86 |
| Mar | 5.56 | 4.88 | 0.67 | 76.0 | 87.9 | 0.86 |
| Apr | 9.12 | 8.95 | 0.17 | 74.2 | 88.1 | 0.84 |
| May | 11.82 | 11.74 | 0.09 | 74.9 | 83.1 | 0.90 |
| Jun | 14.67 | 15.00 | -0.33 | 74.7 | 82.7 | 0.90 |
| Jul | 16.46 | 16.21 | 0.25 | 75.2 | 82.3 | 0.91 |
| Aug | 15.94 | 14.87 | 1.08 | 76.5 | 82.2 | 0.93 |
| Sep | 13.74 | 13.59 | 0.15 | 78.1 | 84.5 | 0.92 |
| Oct | 11.18 | 8.40 | 2.79 | 82.2 | 90.5 | 0.91 |
| Nov | 6.45 | 5.77 | 0.68 | 82.3 | 95.1 | 0.87 |
| Dec | 5.13 | 1.20 | 3.92 | 84.3 | 96.0 | 0.88 |

The monthly average temperatures of the observed and downscaled Hadley output are shown in figure 2.21. There is good agreement here, but again occasionally there is some error, which is more evident here because of the lack of data available to calibrate the downscaling. For this comparison the correlation coefficient is $R^2=0.88$. The humidity comparison is also similar to that previously, on this occasion the correlation is better, with an $R^2=0.61$.
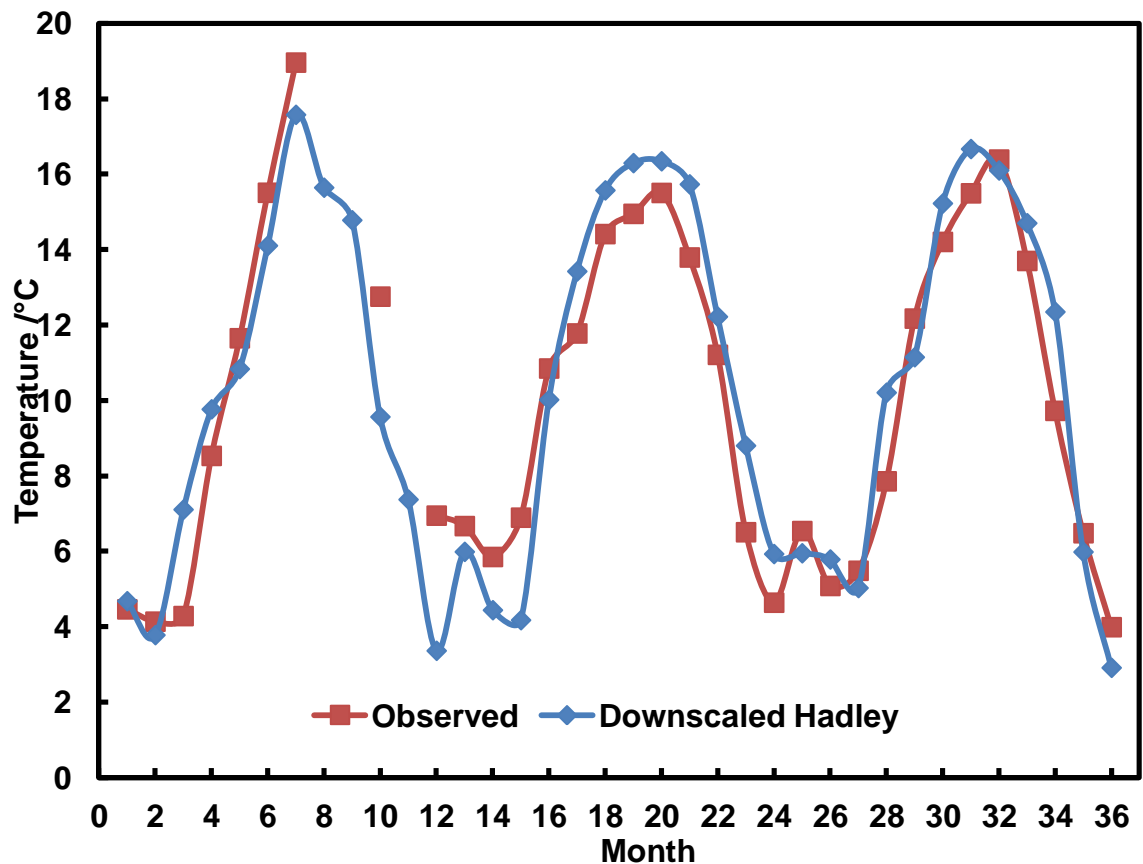


Figure 2.21: Comparison of the monthly average temperatures for the observed and downscaled data at Doncaster over the period 01/2006-12/2008.

*Paris, Prague, Almeria, Oviedo and Leon*

Downscaling was also carried out for: Paris, with data over the period 1981-2004 used; Prague, with data over the period 1981-2003; Almeria, with data over the period 1971-2000; Oviedo and Leon, both with data over the period 1971-2000. For each location downscaling was carried out for the corresponding Hadley model cell of the specific location. The differences and ratios determined can be found in tables 1-5 in appendix A. The graphs comparing the data for each of these locations are very similar to those that have been shown for the previous locations.

The data for Almeria, Oviedo and Leon was available from Instituto Nacional De Meteorologia (2004), a publication of monthly 30 year averages of climate observations across Spain. The data for Paris and Prague was available from the website www.tutiempo.net and have previously been used by Grossi et al. (2008a), with the same Oviedo data also.

It is important to state that due to the lack of data it has not been possible to work with independent calibration and validation periods. Ideally data would be calibrated with one period of data, and then validated with a separate period. As the validation is carried out with the calibration data it is likely that the validation results are over confident. Additionally it is important to note that the validation carried is at a monthly resolution, however the work uses daily data.

This concludes the spatial downscaling work that was carried out, the downscaled Hadley output for each of the locations is used to estimate the impact of climate change throughout Europe in chapter 5.

### 2.3.2 Temporal downscaling

It would be advantageous in understanding future damage, in some circumstances to have data at smaller intervals than the daily averages available from the model output. e.g. some materials respond to changes in the environment in short timescales, an example of this would be paper or textiles on display, as opposed to paper stored in a box, this provides a buffer to the environment, and means that the environment inside the box takes time to react to changes of the environment (The National Trust, 2006).

Here the average diurnal cycle of temperature and specific humidity for the observed data was determined for the room in question. This average diurnal cycle, in terms of difference from the daily average can then be applied to a set of daily averages predicting the hourly averages. It would be possible that the average cycle could be broken down into time steps less than an hour, to downscale to sub-hourly if desired.

Throughout this work this is referred to as temporal downscaling, however it is more accurately described as a disaggregation of daily averages. This method makes the assumption that in the future climate change will not affect the shape of the diurnal cycle determined here.

Determination of this method was carried out with the data available in the Cartoon Gallery at Knole, which is observed hourly. Initially the temperature was assessed, and the daily averages calculated, followed by the deviation from the daily average for each hour. The deviation from the daily average for each time period was averaged for each month, to allow for seasonal variations. The cycle determined for January is shown in figure 2.22.
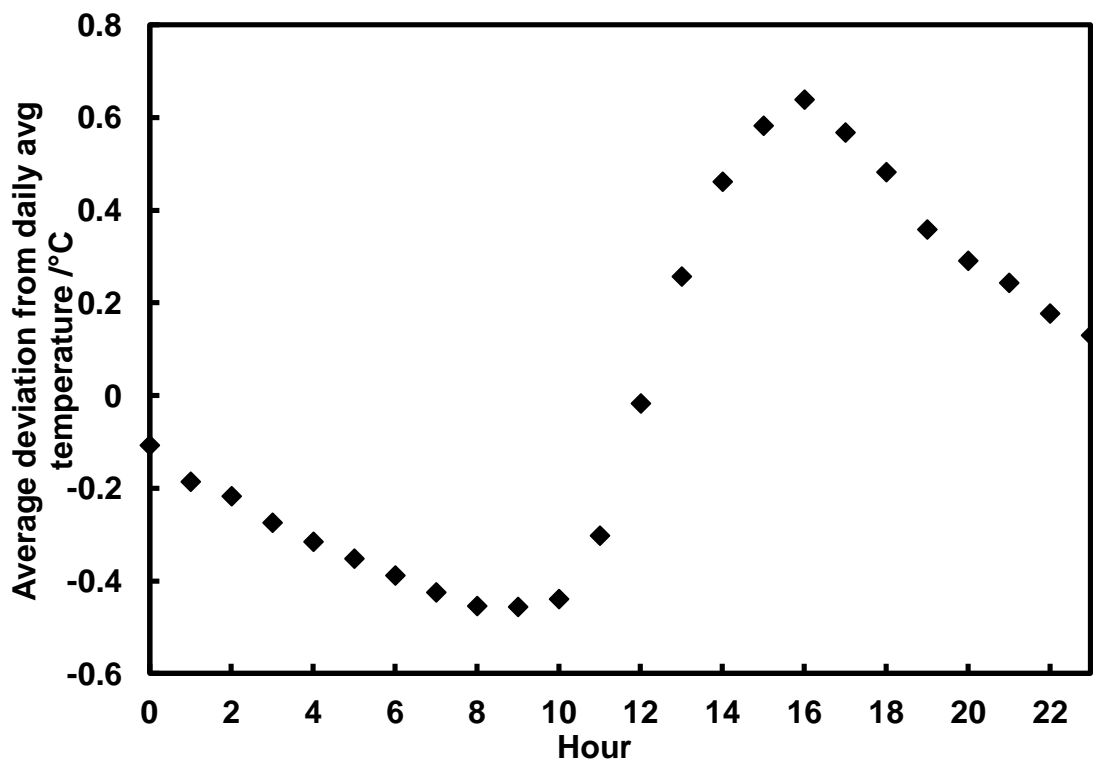


Figure 2.22: The average deviation from the daily average temperature of the Cartoon Gallery at Knole, for the month of January. This allows for estimates of the average diurnal variation around the mean.

Figure 2.23 compares the cycle for each month and shows that monthly calibration is necessary. This allows for a daily average from the Hadley output to be downscaled to hourly averages, or another period of time. The same method was also applied to the specific humidity in the Cartoon Gallery.  The cycle determined for the month of May is shown in figure 2.24. The specific humidity was chosen as the relative humidity had no apparent daily cycle, whereas the specific humidity did. This is likely to be because relative humidity is not an absolute measure of moisture content; it is dependent on the temperature, where specific humidity is an absolute measure. The relative humidity can subsequently be calculated from the temperature and specific humidity (for equations see section 3.2.3).
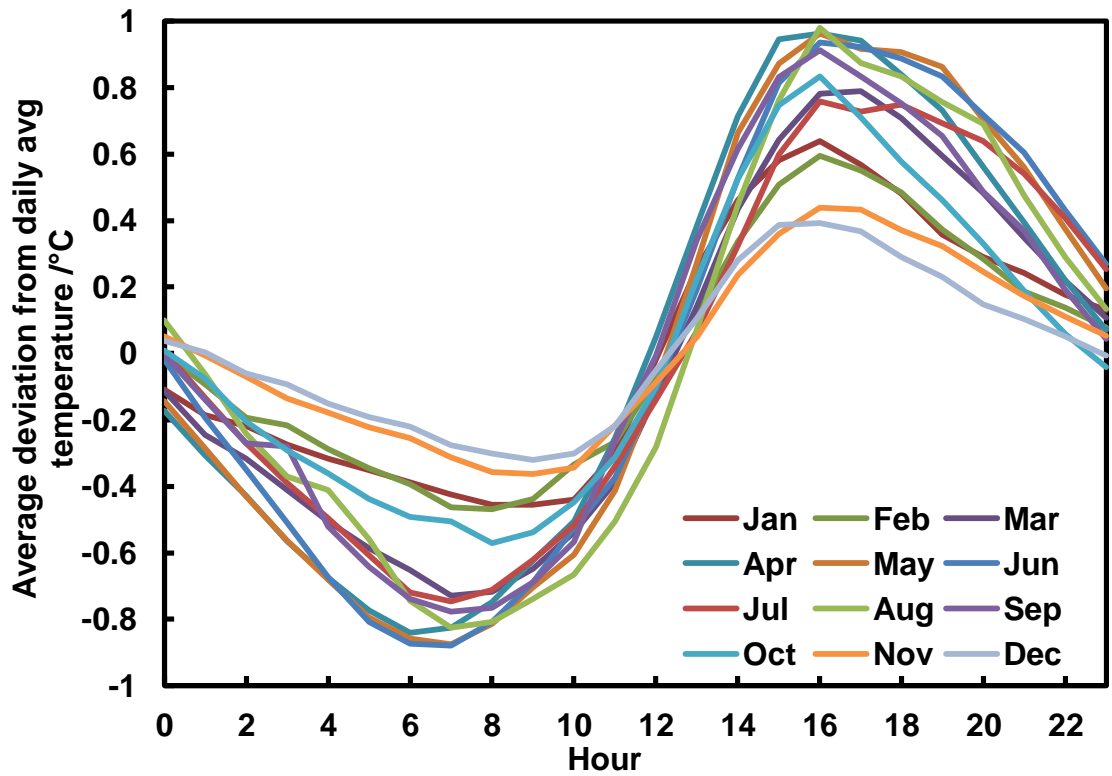
Figure 2.23: The average deviation from the daily average temperature of the Cartoon Gallery at Knole, for all months, showing the seasonal variation.
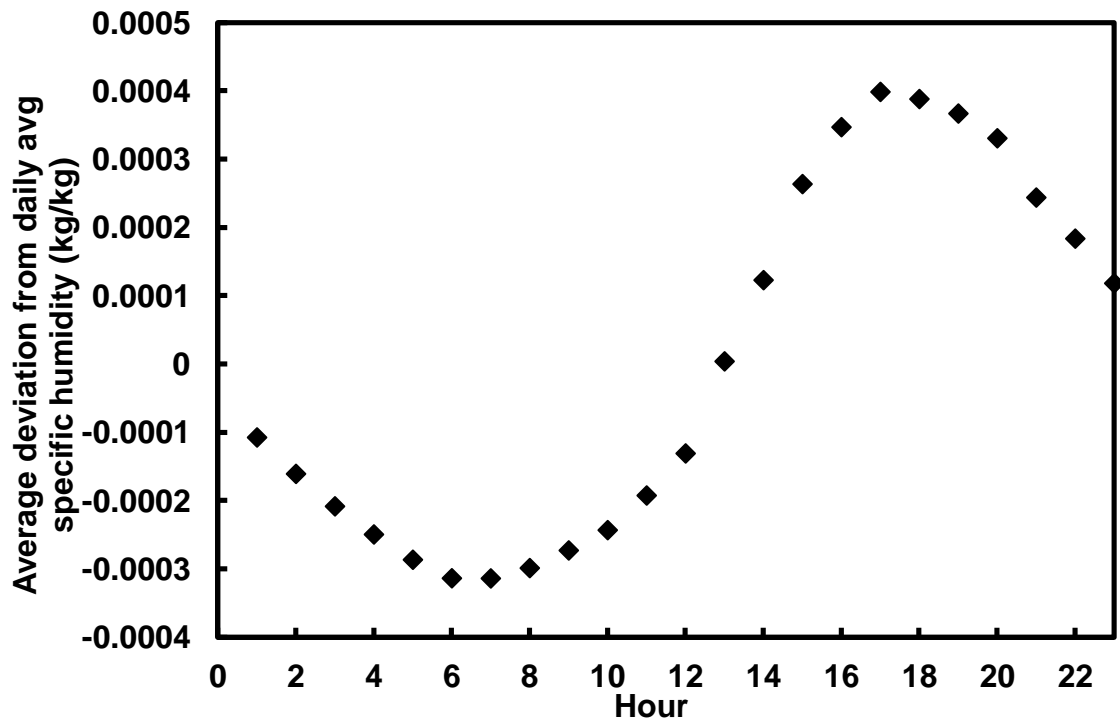


Figure 2.24: The average deviation from the daily average specific humidity of the Cartoon Gallery at Knole, for the month of May. This allows for estimates of the average diurnal variation of the specific humidity around the mean.

It is important to validate the temporal downscaling technique, so it was tested against the observed data (for the 8 day-period from the 20/6/2009). The observed and downscaled data is shown in figure 2.25. This shows that the downscaling is a good estimate of the observed data, as expected there are some errors, as the technique determines the average, and the observed data varies around this. However the correlation coefficient is very good, $R^2$=0.95. The observed data is only recorded with accuracy of half a degree, but the downscaled data is not limited to this, which could also introduce some of the error found. The technique also doesn't allow for a totally continuous data set, each day is viewed individually; therefore the first and last readings could be somewhat different, leading to a large jump in the data.
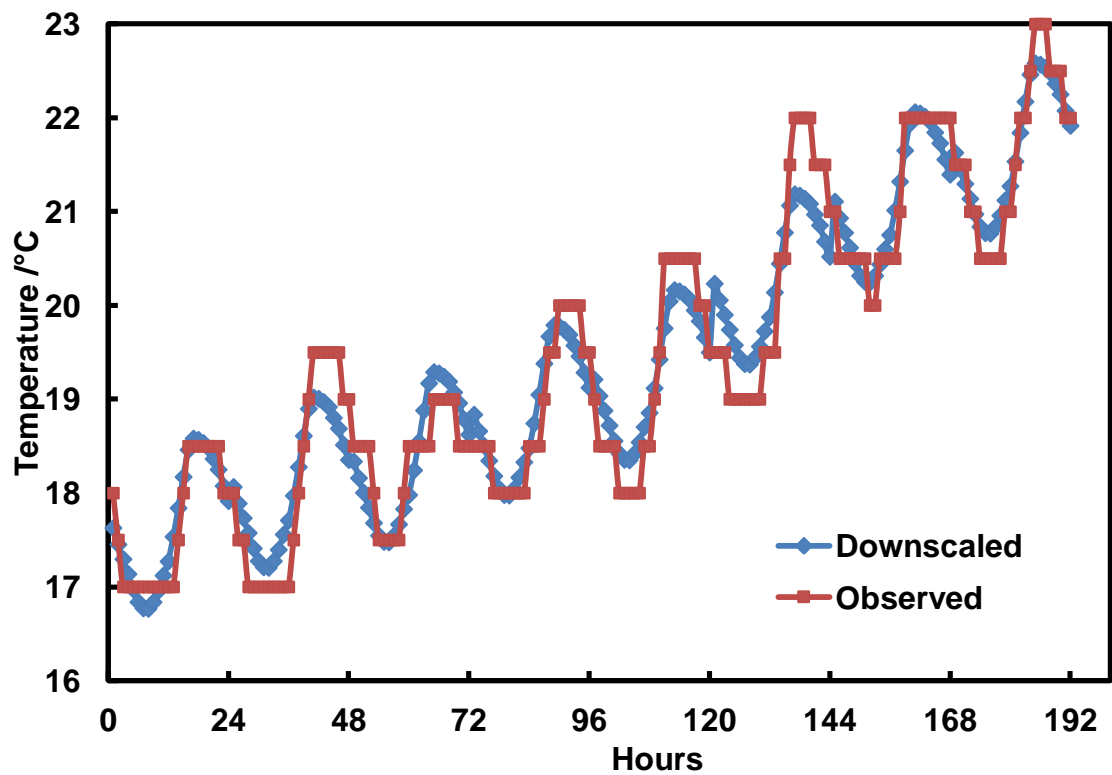


Figure 2.25: Comparison of the observed and temporally downscaled Hadley output temperature for a period of 8 days from 20/6/2009. This is for the Cartoon Gallery at Knole, the Hadley data has been transferred indoors.

Additionally the full datasets were compared, all of the observed and downscaled temperatures, specific humidity and the calculated relative humidity. The correlation of the temperatures was very good, with an $R^2 = 0.99$, this is shown in figure 2.26, with a few areas of outliers, this is a very small percentage of the data, and the odd pattern is because the observed temperature only has accuracy of 0.5°C. The specific humidity comparison is also good, with an $R^2 = 0.96$. As discussed previously it would be ideal to validate this with data from a different time period, therefore it is possible that the validation results of this method over state the confidence.

There was one problem with the relative humidity calibration; occasionally the combined temperature and specific humidity resulted in a relative humidity of over 100%. This occurred on 45 occasions, out of a possible 81684, a total of 0.055% of the time. It was decided that these would be corrected to a relative humidity of 100%. The comparison of the observed and downscaled relative humidity is acceptable, with a correlation coefficient of $R^2 = 0.92$. The downscaling predictions of the three measures, temperature, specific humidity, and relative humidity all perform well, providing representative estimates of the hourly observations.
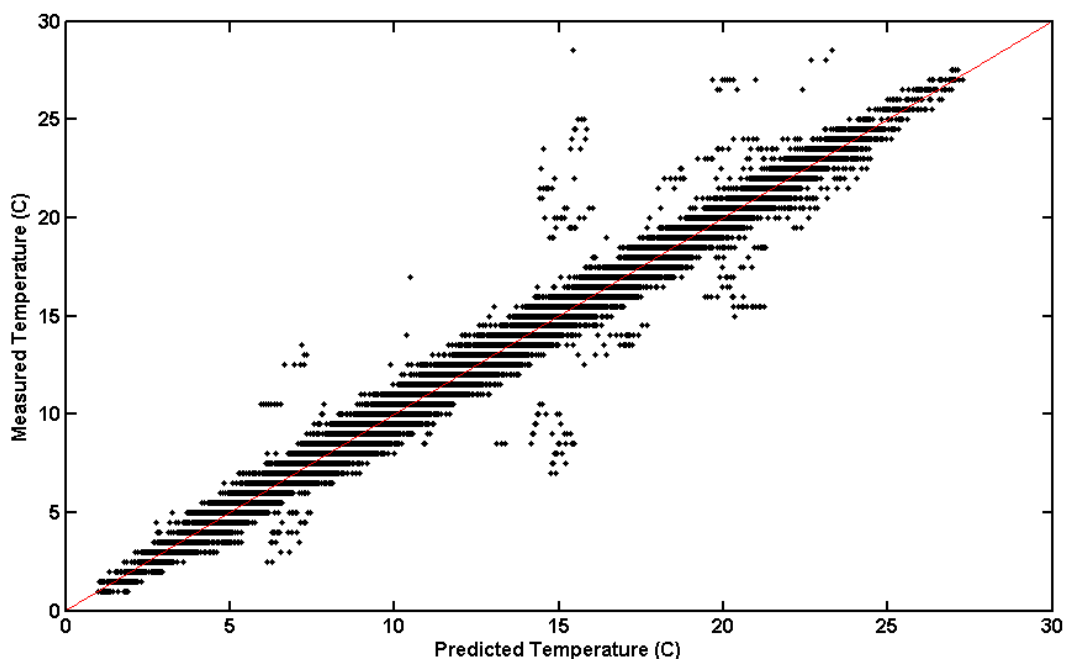


Figure 2.26: The observed data and downscaled output for the Cartoon Gallery (after transferring indoors) compared to one another. The red line is the line of best fit.

This concludes the introduction of this method, which could also be applied at other locations. The technique is useful for downscaling daily averages from the Hadley output,

or alternative data. When this is applied it makes computational sense to apply it after the indoor data has been predicted, but before the damage analysis is carried out, rather than before the indoor prediction. This would reduce the computational effort required for the indoor prediction, as currently there is one daily value, but if downscaling was carried out before this would increase to 24 daily values, creating 24 times more calculations to predict the indoor values. It is important to note that the defined temperature and specific humidity cycle is dependent upon the room and property in question, and will require recalibration for each location.

## *2.4 UKCP09 weather generator*

The second climate model is the United Kingdom climate projections 2009 (UKCP09) weather generator. The principal aim of the weather generator is to provide sufficient temporal and spatial detail for the user's needs (Jones et al., 2009), thus overcoming the limitations of the lone Hadley model as discussed previously. It was felt there was a requirement for a standardised procedure of downscaling methods so that there was consistency across the range of impact sectors (Jones et al., 2009).

Where possible the UKCP09 weather generator model will be used, in preference to the Hadley model, to standardise the downscaling method, with one that is more robust. The UKCP09 weather generator only covers the United Kingdom, thus research here that falls outside of the United Kingdom will continue to use the original HadCM3 output and the associated downscaling methods described previously.

Output from the weather generator is available either on a daily or hourly basis for a grid square 5 × 5 km, a very high spatial resolution compared to that of the Hadley model. The output does not correspond to specific days in the future; it is not a weather forecast for the 30th of August 2086, for example. The output is statistically representative of the climate which may occur in the future, it has statistical representations of real observed weather variables, combined with the climate signal in the UK climate projections, additionally the output is contiguous, thus the output on day 2 is related to that of day 1 and 3 (Jones et al., 2009).

The output is available as eight different time periods, the first being the baseline period 1961-1990, and for seven future periods. These overlap by 10 years, beginning with 2010-2039 and ending with 2070-2099. For each of these periods there are 100 runs of the weather generator, producing 100 different time series, with each having a 30 year output of data. The 100 runs of the generator allow for the variation of the future climate output to be included, as there is inherent uncertainty associated with these, which increases

further into the future. The weather generator takes into account information from other global climate models about the uncertainty associated with the physical processes of the climate. Probabilistic projections are determined from these, in the form of probability density functions, which are sampled in each run of the weather generator, therefore the 100 runs take into account some of the associated uncertainties. Temperature output is as a daily minimum and maximum value; here these are averaged to get the daily average temperature.

The weather generator is based upon a stochastic rainfall model that simulates future rainfall, other variables are then determined according to the rainfall, being defined by predetermined statistical relationships. These are termed inter-variable relationships (IVRs) and maintain the consistency between and within each of the variables, such as temperature (Jones et al., 2009). The IVRs are calculated from the baseline climate, and at least 30 years of data is required to fit the weather generator. In addition to IVRs, change factors are determined that define the change in variables from the modelled baseline period to each of the future time periods as described by the UKCP09 probabilistic projections (Jones et al., 2009). The weather generator performance has been tested, and shown to correspond to the observed baseline climate (Jones et al., 2009).

As yet temporal downscaling has not been discussed; effectively a daily average is disaggregated, based on observed data, such that the average of the hourly variables equals the daily average, whilst taking into account the diurnal cycle. This assumes that the daily behaviour of the climate variables will stay the same in the future (Jones et al., 2009). This method is somewhat similar to that developed previously (section 2.3.2), which also maintains the daily average as the same, while taking into account the average diurnal cycle.

Some limitations are still associated with the UKCP09 weather generator, it assumes that observed relationships between weather variables will stay the same in the future (Jones et al., 2009), as does the spatial downscaling method presented for the Hadley model (Grossi et al., 2008a). It also has no physical basis, it learns from the behaviour of observed data, but there is no basis in physics or meteorology (Jones et al., 2009).

This explanation of the UKCP09 weather generator is simplified significantly the full explanation can be found it the weather generator report (Jones et al., 2009).

### 2.4.1 Case study locations UKCP09 weather generator output

The UKCP09 weather generator output for each of the locations described earlier was downloaded from the user interface website, http://ukclimateprojections-ui.defra.gov.uk. There are a number of choices that have to be made to download the data; the general steps taken to download the data for each location will be described here, with the specific information required for each site. Firstly a new request is started, selecting by data source. This gives the option to choose the weather generator simulations, as used here, with the mandatory option of standard weather generator variables. The next selection required is the emission scenario, these are discussed elsewhere (section 2.5), and any of the three options, low medium and high, can be chosen, but only one at a time.

The time period of the output is the next requirement, there are options for each of the seven future periods, again only one can be chosen, therefore for this work this process has been completed for each time period, to give the full set.

Selection of the location is the next decision; the UK is divided into a number of cells, each with its own unique identification (ID) number. The cell ID numbers of each location assessed are shown in table 2.4.

Table 2.4: Cell identification numbers for the case study locations. *Knole is the case study location, however the cell ID is for Gatwick, the proxy outdoor location for Knole.

| Location | Cell ID no. |
|---|---|
| Knole* | 5300145 |
| Brodsworth Hall | 4550410 |
| Swiss Cottage | 4550095 |

Following the location selection the sampling method is chosen, here random sampling of the model variants was chosen, with 100 samples. The time frequency is chosen next, at either the daily average or hourly average. The duration of each weather generator run was set as 30 years, and the option to set the random seed was chosen. This was done so if required the same output could be reproduced, and to allow for the corresponding hourly data to be generated if required later. The random seed to start off the generator was always set to 86. The only output type available was chosen, raw data, as a CSV file. The output was given a unique description, to allow for identification.

### 2.4.2 Distribution of UKCP09 weather generator output

When assessing results of the weather generator in the weather generator report the median and percentiles are used (Jones et al., 2009). This brings about an assumption that the results are not normally distributed, rather than assume this the nature of the output has been investigated. At Knole the UKCP09 weather generator output of temperature and relative humidity was analysed. All of the data (all 100 runs of the 30 years) for the baseline period and the 2080 period individually was separated into 'bins', for the temperature this was done for each degree. This allowed the data to be plotted as a distribution. Figure 2.27 shows the baseline temperature distribution of the data from Knole. The data does not follow a normal distribution, thus non-parametric statistics should be used. The same is true for the 2080s period also, which has a similar distribution to the baseline. For relative humidity the data was separated into 'bins' of each humidity percentage. The resulting distribution for the 2080 period is shown in figure 2.28. This also is not normally distributed, the graph takes an unusual form because of the nature of relative humidity, and there is a maximum value that the humidity can be. Because of this it was decided that the specific humidity would also be investigated.
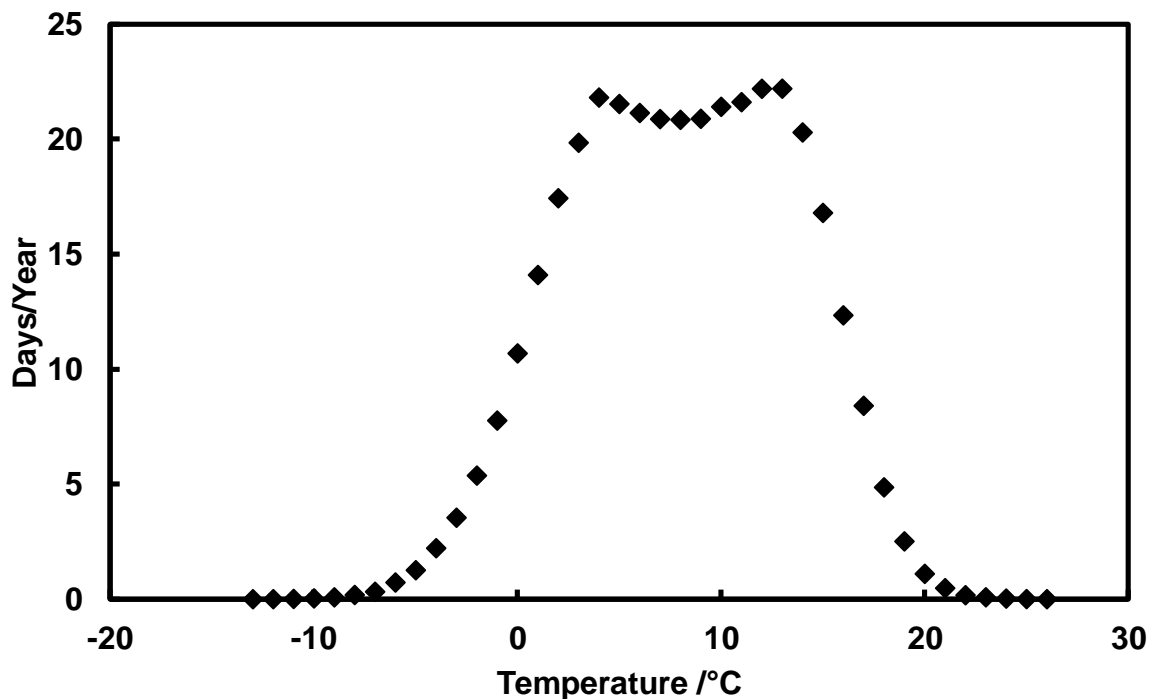
Figure 2.27: Distribution of the temperature from the baseline period of the UKCP09 weather generator data, at Knole. The average number of days per year of each °C is shown.

The distribution of the specific humidity for the baseline period is shown in figure 2.29. This also does not follow a normal distribution, and this does not change in the future. Therefore care must be taken in the application of statistical tests to these results.
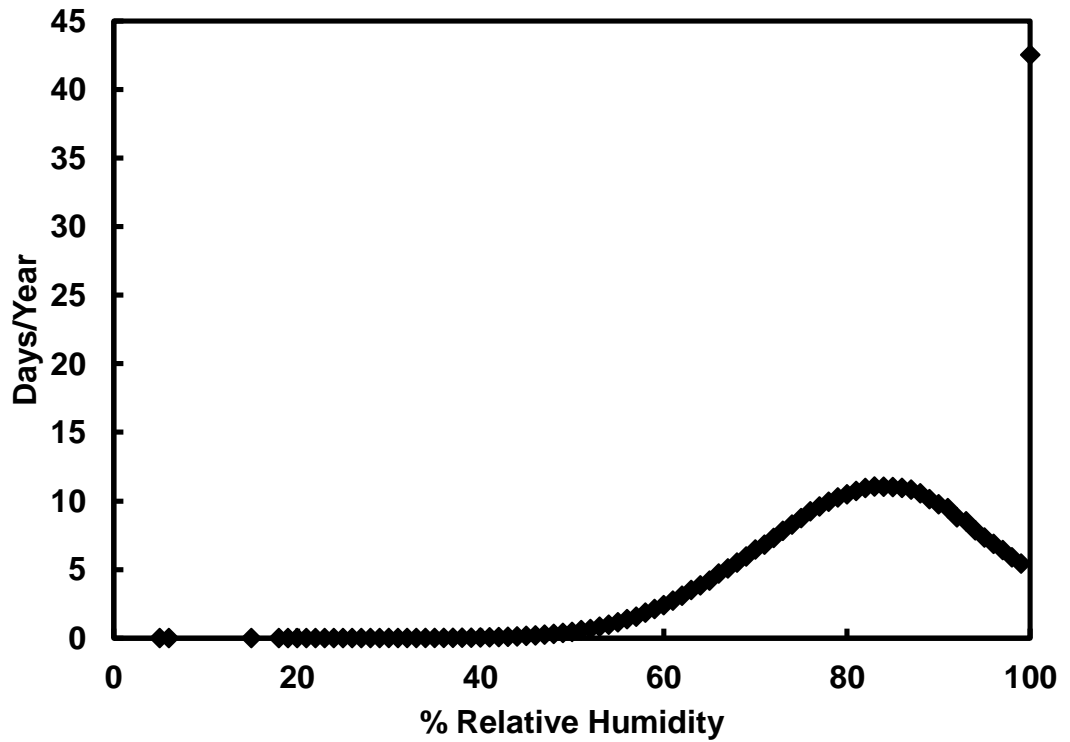


Figure 2.28: Distribution of the relative humidity from the UKCP09 weather generator data, at Knole. The average number of days per year of % relative humidity is shown.
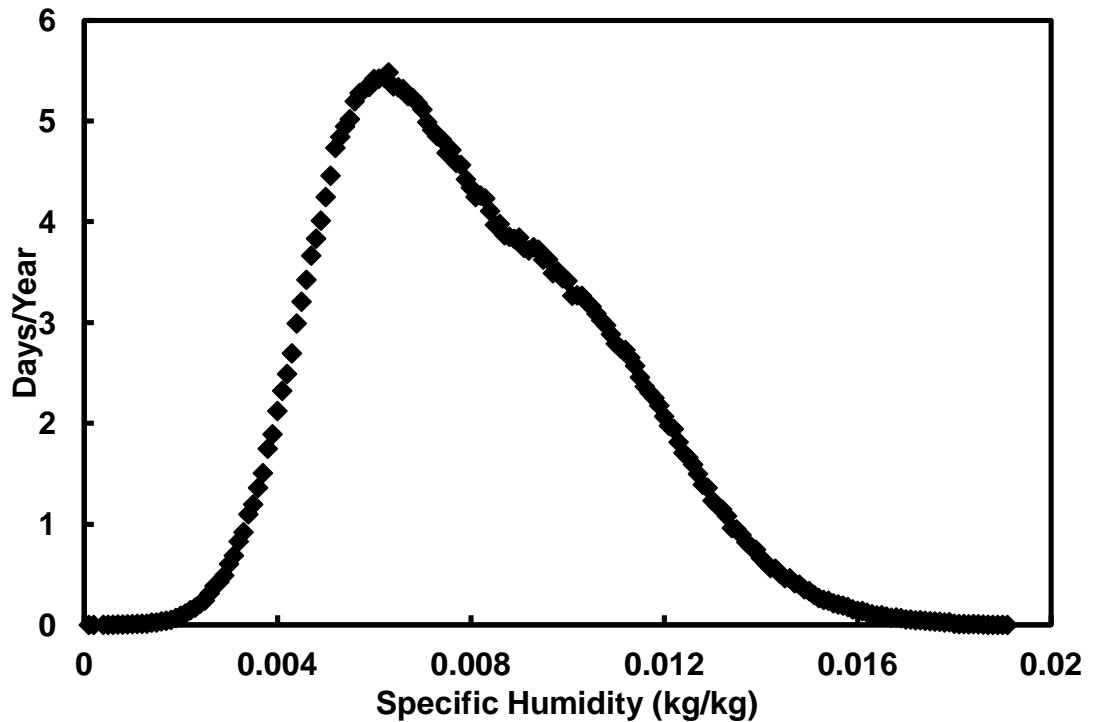
Figure 2.29: Distribution of the specific humidity from the UKCP09 weather generator data, at Knole. The average number of days per year of each increment in 0.0001 kg/kg specific humidity is shown. Note that the days per year values are significantly smaller than those in previous figures, this is because there are a greater number of 'bins' in this figure, reducing the amount within each one.

## 2.5 Emission scenarios

As mentioned previously the emission scenarios drive the climate models. They describe different storylines of future emissions, from various driving forces (IPCC, 2000).

In this research the A2 scenario will be used with the Hadley model, and the B1, A1B and A1F1 scenarios will be used with the UKCP09 weather generator, which relates to the low, medium and high scenarios available to use with the weather generator.

Each storyline has a description attributed to it, the A2 storyline and scenario describes a very heterogeneous world. The underlying theme is of self-reliance and preservation of local identities. Fertility patterns across regions converge very slowly, which results in continuously increasing global population. Economic development is primarily regionally orientated and per capita economic growth and technological change are more fragmented and slower than in other storylines (IPCC, 2000).

The reason that the A2 scenario has been chosen with the Hadley model is because it gives pronounced changes in future climate (Brimblecombe et al., 2006b), so it should result in strong signals in terms of future pressures, identifying the problems most likely to be critical (Brimblecombe et al., 2006a, Grossi et al., 2007). When management of climate change is investigated, with respect to historic collections, this will give the worst case scenario of impacts (Brimblecombe et al., 2007).

This particular scenario sees high energy and carbon use, giving rise to high GHG emissions (Brimblecombe et al., 2006b), no one emission scenario has a greater probability of occurrence than another, and the probability of one occurring exactly as described is highly unlikely (IPCC, 2000). It is possible that the projections determined for this scenario are an overestimate, but also they could be an underestimate, as it is difficult to predict the future, so no probability can be placed on the projections of one individual scenario (Hulme et al., 2002a).

With the UKCP09 weather generator all three of the available scenarios are used initially, the B1 scenario describes a convergent world with the same global population that peaks in mid-century and declines after, with rapid changes in economic structures toward a service and information economy, with reductions in material intensity, and the introduction of clean and resource-efficient technologies. The emphasis is on global solutions to economic, social and environment sustainability, including improved equity, but without additional climate initiatives (IPCC, 2000).

The A1 scenario describes a future world of very rapid economic growth, global population that peaks in mid-century and declines thereafter, and the rapid introduction of new and more efficient technologies. Major underlying themes are convergence among regions, capacity building, and increased cultural and social interactions, with a substantial reduction in regional differences in per capita income. The A1 scenario splits in different ways that describe alternative directions of technological change in the energy system. A1B describes a balance across all energy sources, and A1F1 describes an emphasis on fossil intensive energy sources, the final A1 scenario A1T, not used in this work, focuses upon non-fossil energy sources (IPCC, 2000).

As discussed there are three emission scenarios that can be used with the UKCP09 weather generator, a low (B1), medium (A1B) and high (A1F1) emission scenario. The impact that each scenario has on projected indoor temperature in the Cartoon Gallery at Knole has been assessed. The results are shown in figure 2.30, where as expected they follow the order from low to high for the impact they have in the far future on the increase in temperature. It is also apparent that until the 2045 time period the impact on

temperature is similar for all three scenarios. The emissions that drive the models, and climate change, are 'locked in' until 2045. No matter how we change our usage of fossil fuels, amongst other things, the warming until 2045 will occur (Solomon et al., 2007).  It is beyond 2045, towards the far future where the different scenarios affect the projected temperature.
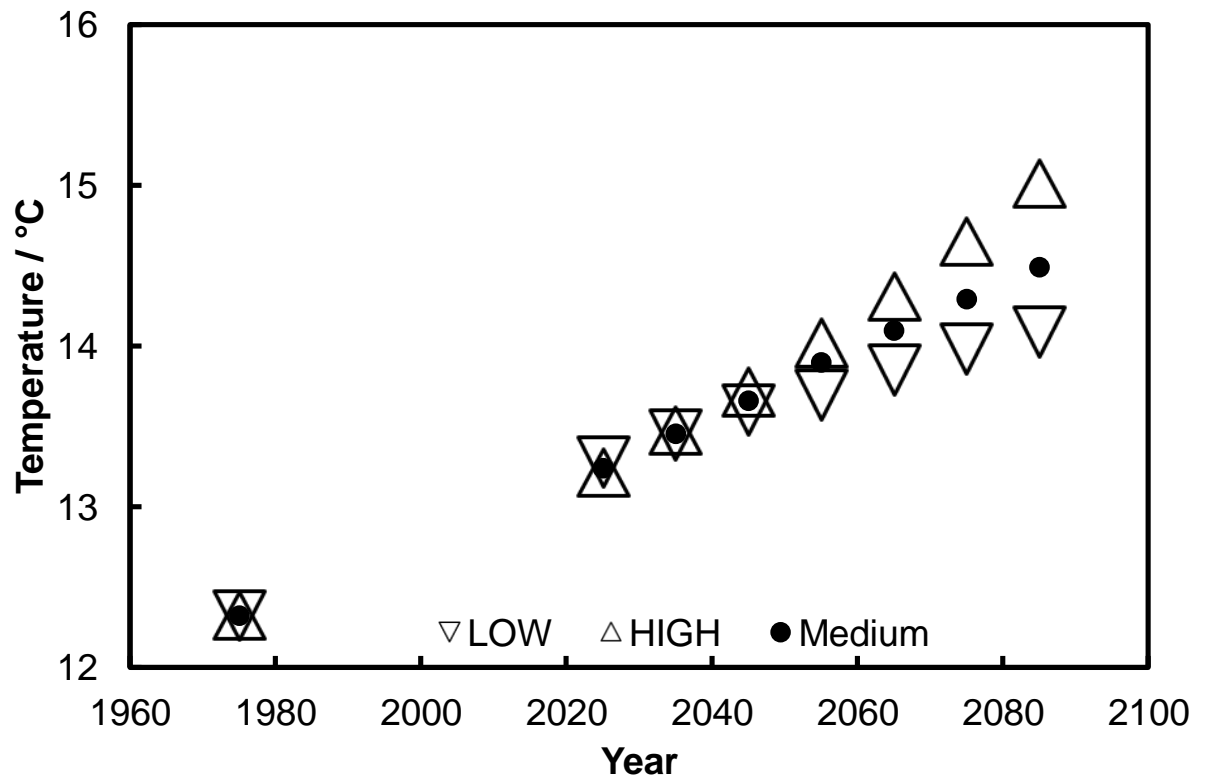


Figure 2.30: Comparison of the effect of each emission scenario on the projected indoor temperature within the Cartoon Gallery at Knole.

It is likely to be the near to mid-term future that is of greatest importance to collection managers when they assess the risk towards collections if they are attempting to adapt to mitigate the risk to collections posed by climate change. Thus the use of only the high emission scenario for the rest of this work is a reasonable choice, it also presents the worst case scenario in the far future (Brimblecombe and Grossi, 2008, Sabbioni et al., 2010, Grossi et al., 2008b).

## 2.6 Comparison of Hadley and UKCP09 weather generator baselines

Two different methods are used for obtaining future climate output in this work. It was necessary to compare these two techniques, both in terms of the actual data and the methodology used. The Hadley output used here is downscaled, temporally and spatially, although the most significant of these is the spatial downscaling. The method applied for

this downscaling is quite simplistic, a calibration between observed and Hadley output is determined, and applied to downscale the data. The UKCP09 weather generator is a more complex method. The weather generator was also introduced in order to provide a uniform technique that everybody can use, rather than many different downscaling techniques being used. For this reason it has been decided that here, where possible, the UKCP09 weather generator output will be used over the downscaled Hadley output. However outside of the UK this is not possible, and in chapter 5, where locations around Europe are investigated, along with UK locations, all use the downscaled Hadley data, for consistency.

Although the two techniques will not be used together in the same aspects of this research it was sensible to compare the data. The downscaled Hadley data and the UKCP09 weather generator output for the baseline period at Brodsworth Hall are shown in figures 2.31 and 2.32. These use the yearly averages, for the UKCP09 weather generator output there are a total of 3000 years (100 runs of 30 years), and for the downscaled Hadley output there are 30 years of data (1961-1990). The temperature output of the two models is very similar. The medians are 9.45°C and 9.53°C for UKCP09 weather generator and Hadley respectively, and both have similar interquartile ranges, 9.20-9.71°C and 9.29-9.81°C respectively. Therefore there is good agreement between the two model temperature outputs.
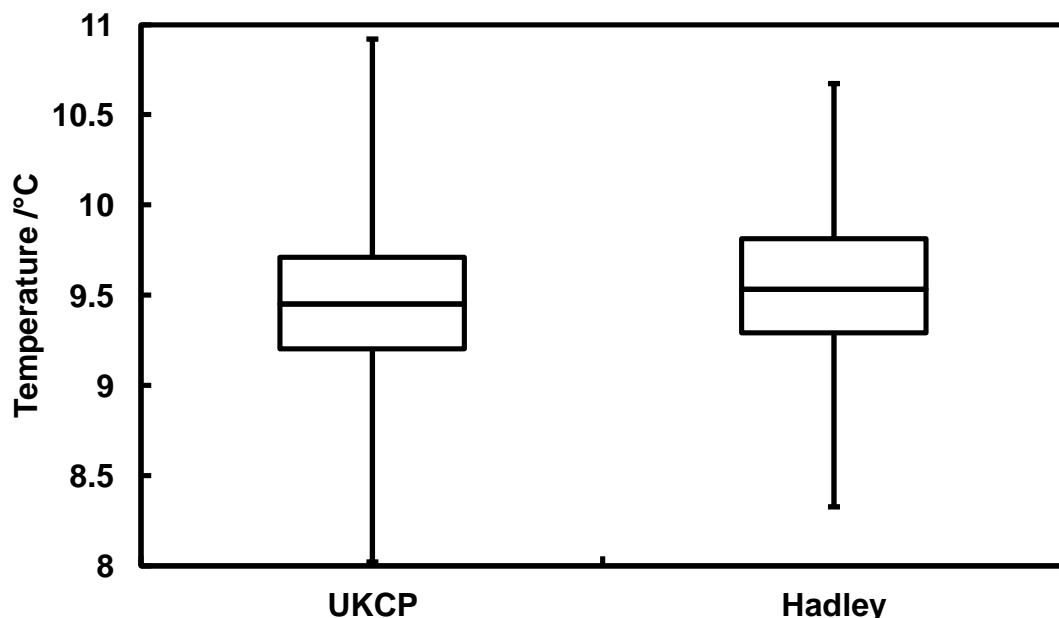


Figure 2.31: Comparison of the distribution of annual average baseline temperature for the two climate model outputs downscaled to Brodsworth Hall. The error bars plot the minimum and maximum values, with the box showing the interquartile range and the median.

Figure 2.32 shows the comparison of the relative humidity output, these are quite similar, but not exactly the same, the median values are 81.7% and 80.0% for the UKCP09 weather generator and Hadley output respectively. Therefore there is slight disagreement, although this may be expected, the downscaled Hadley output is only calibrated with 3 years of data, whereas the UKCP09 weather generator output uses an ideal 30 years, giving it greater reliability. This is another reason to use UKCP09 weather generator output where possible because the calibrations are carried out with 30 years of data, making them more reliable than those using shorter records.
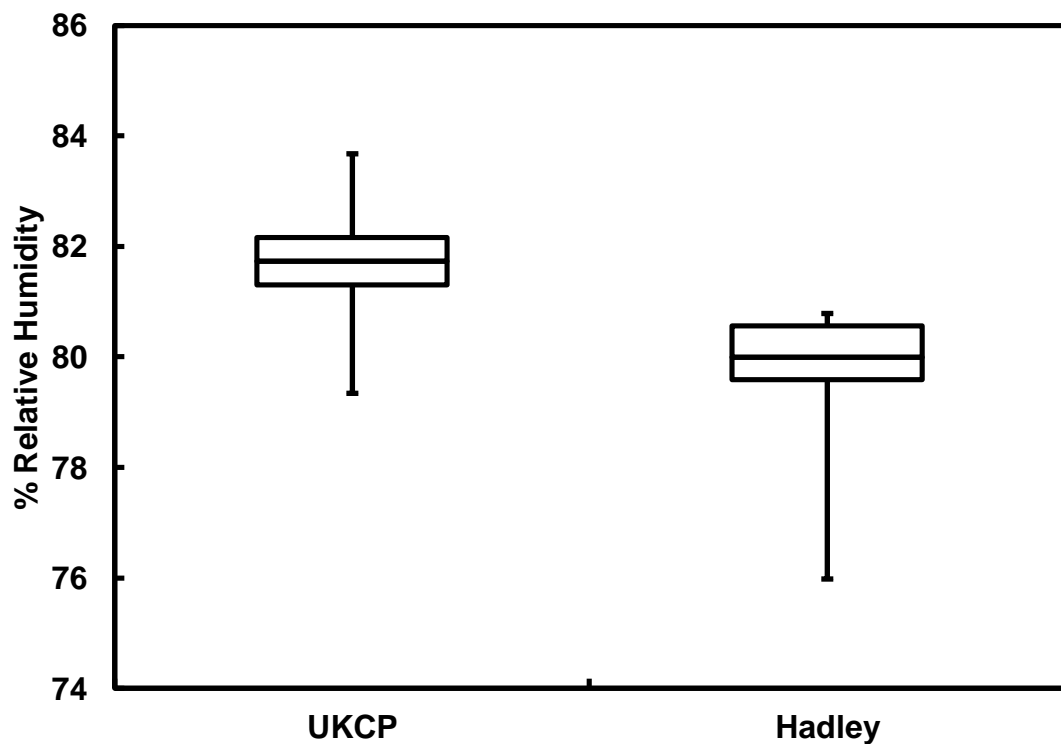


Figure 2.32: Comparison of the distribution of annual average relative humidity for the two climate model outputs downscaled to Brodsworth Hall. The error bars plot the minimum and maximum values, with the box showing the interquartile range and the median.

## 2.7 Conclusions

Various sets of observations will be used in this work, problems with some of these datasets were found upon examination. Initially at Brodsworth Hall there was very little data available for the months of February and March. However, further data, available once the project was underway, helped relieve some of these limitations. Some problems arose because of the way in which data from different organisations is recorded, occasionally within the same data set the method changed. As an aside, it would benefit all users of data from various sources if a standard format was followed, with missing data recorded in the same way, this would save significant amounts of time spent standardising data.

For each of the historic houses in question there are less than an ideal number of observations. Typically in climate science periods of 30 years are analysed. However, in historic properties it is rare that observations of temperature and humidity are available for such long time periods, thus any of the research carried out is with less than optimal data. Electronic data logging is a relatively recent technique, and where the environment was recorded previously this is unlikely to have been digitalised. There can also be problems with loss of data from electronic loggers that send the data to a central computer via radio signals, these can become blocked, or weakened, and large portions of time can pass before the logger is effective again, creating large gaps in data.

Gatwick weather has been used to represent the outdoor data at Knole, after some calibration. This is important as it is possible that local weather stations can be used elsewhere as approximation of outdoor data where it is not recorded at the property, or only partially recorded. However, comparison to observed data is advisable, allowing for calibration between the two datasets and greater reliability. If this is possible it would allow for future climate projections at a wider number of properties.

Two climate models are used to provide future output of temperature and relative humidity. The Hadley model has some limitations, the spatial and temporal resolution. Downscaling was carried out to improve the spatial resolution, thus providing data that is relevant to specific locations. Due to the nature of the spatial downscaling weather extremes are not dealt with effectively. There is also an assumption that the relationship will stay constant in the future.

The downscaled relative humidity at Knole is not ideal, because of a larger variability in the observed data. When assessing climate directly this may not be problematic, however it becomes a problem here when assessing damage. Specific thresholds of humidity are

important, and higher humidity can cause greater damage. Thus the slight errors, although they may even out with respect to humidity, may not with respect to the estimated damage. It is possible that there could be an overestimate of mould growth, or an underestimate of paper degradation, for example.

Temporal downscaling was also implemented for the Hadley output. This produces a realistic diurnal cycle from the daily average, allowing damage with a fast response time to be assessed.

Both the spatial and temporal resolution problems are dealt with in the other climate model used, the UKCP09 weather generator. Consistent techniques are employed to carry out this downscaling, that results in output that has a high spatial resolution, and data at hourly intervals.

The distribution of data from the UKCP09 weather generator did not show a normal distribution; therefore non-parametric statistics will be used. The baselines of the two climate models were found to have a similar temperature average, and the relative humidity was slightly different. It is expected that the UKCP09 weather generator output is more reliable, this is because the data is fitted over the ideal time period of 30 years, whereas the downscaled Hadley data is only calibrated using a fraction of this. Thus where possible the UKCP09 weather generator will be used in this work, however this is limited to the UK.

The three UKCP09 weather generator emission scenarios have been investigated, until 2045 there is little difference, the high scenario has been chosen as the sole scenario where the weather generator is used. It must be stressed that it is of the greatest importance to consider the uncertainties associated with future climate projections, and associated impact projections.

# CHAPTER 3

# BUILDING SIMULATION

## 3.1 Introduction to building simulation

Building simulation has been briefly discussed in the introduction, it allows for predictions of the indoor environment, when given the outdoor environment, and is typically used before constructing new buildings, to determine energy loads among other building performance indicators (Crawley et al., 2005a). More recently building simulation has been used with historic buildings, where the program EnergyPlus has been used in the investigation of the drying out of wooden walls after a flood (Blades et al., 2008) and reviewing past heating regimes (Taylor et al., 2005).

### 3.1.1 EnergyPlus

EnergyPlus is developed by the American government energy department (Crawley et al., 2000), and is a state-of-the-art building energy analysis program, featuring the best capabilities of the DOE and BLAST programs. It was first released in 2001, with several versions since, that have added features and improved simulation results (Monfet et al., 2007, Crawley et al., 2000).

The inputs that are required by EnergyPlus to construct a model and simulate the building are comprehensive. Firstly the physical properties of the building are required along with a weather file with the local climate conditions (Sabbioni et al., 2006). Specifically some of the inputs required are the size, shape, construction materials and orientation, in relation to the building itself. From the inside of the building the room surface area, thermal conductivity of walls, air exchange rate, volume of space and internal sources of heat are all required (Taylor et al., 2005).

In addition to this the external climate data is required, this contains some data which can be problematic to acquire, and are not always routinely measured. Some requirements are temperature, humidity, wind speed and direction, atmospheric pressure, solar radiation and cloud cover (Crawley et al., 1999). Solar radiation consists of three parts, global, horizontal and diffuse radiation (Crawley et al., 1999), In the UK some parts of solar radiation are routinely measured, but others are not, and are not available to complete the weather file. Further to this it is very unlikely that all these measurements have been made at the location of a historic house, occasionally temperature and relative

humidity are measured, with rare occurrences of some of the other parameters, but these are far from routine measurements. The combination of these factors makes it problematic to complete a representative weather file. Energy Plus and other programs also typically include internal heat sources such as electrical systems and equipment, along with heating, ventilation and air conditioning (HVAC) systems (Crawley et al., 2005a).

The large amount of data required is evident, and collection of this can be time consuming and problematic, for example in some cases it is not possible to determine the interior structure of a historic wall by taking a sample, therefore the model cannot be said to be 100% accurate. While the model may not have all the information about the cross section of the wall the approximation can be validated with observed data, to show that it is a valid assumption. With relative humidity for example it is often only the initial surface layer of a material that moisture exchanges with, and thus the full cross-section is not required. For spruce wood there is evidence that this surface layer is 1-2cm (Sabbioni et al. 2010).

Often in a model a number of assumptions need to be made, such as heating and moisture inputs. As a result there are inherent uncertainties attributed to the predictions of a model (Taylor et al., 2005).

It is not EnergyPlus alone that requires such inputs, hygrothermal simulations are discussed by Hall (2010), where the inputs required are described, split into four categories: (i) assembly, orientation and inclination of building component, (ii) hygrothermal material parameters and functions, (iii) boundary condition surface transfer (indoor and outdoor climate), (iv) initial condition, calculation period and numerical control parameters. Further information is given on these four categories, for example building material parameters should include: bulk density, specific heat capacity, thermal conductivity, porosity, moisture storage, vapour permeability and liquid diffusivity (Hall, 2010).

From these inputs the model simulates the building's indoor environment, which is a result of the interaction of the external climate and the buildings physical properties (Sabbioni et al., 2006). An important part of developing a model for an existing building is calibrating/validating it, this is essential to ensure the model is correct, to within certain limits (Monfet et al., 2007). Validation of a model is possible by comparing the model output with observed temperature and relative humidity (Sabbioni et al., 2006, Blades et al., 2008, Cassar and Taylor, 2004). This all contributes to making the modelling process very complex, and a specialist subject itself, requiring the expertise of a building scientist to make the appropriate decisions (Taylor et al., 2005).

EnergyPlus has been briefly described, a full in depth description is presented by Crawley et al. (2000). In addition to EnergyPlus a multitude of building simulation models exist, such as BLAST, BSim, ECOTECT, Energy Express, eQUEST and HEED, among others, which are all compared to one another and Energy Plus by Crawley et al. (2005a). Another possible program that can be used is HAMBASE (Neuhaus and Schellen, 2007), which has been used in heritage research. The programs HELIOS and HYGRO have also been used (Bionda, 2004), HELIOS models the air and surface temperatures, and HYGRO the air humidity. However both require significant characterisation, as with EnergyPlus, for example the dynamic water sorption capacity of materials in the building is required, these were determined experimentally (Bionda, 2004). It is likely that this is not an option in a large number of historic houses, and again adds significant time to the process of predicting the indoor environment. Another program has also been used for heritage research, WUFI (Kilian et al., 2010), in this instance it models the heat and moisture transport through materials, although full building simulation modelling is also possible.

### 3.1.2 Transfer Function

As mentioned in the introduction, instead of using a complex building simulation model to predict the indoor conditions it has been decided that a simpler solution will be determined allowing for rapid and easy prediction of indoor conditions. One of the important aspects of this simple model is that it is easily portable, allowing for multiple rooms and properties to be individually assessed, to determine the impact of climate change on damage to collections and interiors. This is not possible on such a scale with the complex simulation models, as they require considerable parameterisation to calibrate and validate them.

While it is recognised that it is unlikely that the accuracy of the transfer equation will be as good as that attainable with a complex building simulation program, it is possible that the level of accuracy will be acceptable, allowing for projection of future pressures on collections. This may be the trade off required to allow the simpler solution to be easily and rapidly applicable to a variety of historic houses. In terms of cost this method will be readily accessible to heritage organisations, taking little time and money, in comparison to extensive investigations into building parameters and the expertise of a building scientist.

There are additional limitations of a simplified mathematical model, for example it is not possible to carry out research into hypothetical alternative uses of each room. Using a mathematical model assumes that the room use stays constant in the future, with similar occupancy levels, changes to these in the future cannot be estimated, whereas this would be possible with a program such as Energy Plus. There are examples of the investigation

of different uses, examining possible heating scenarios from the past (Taylor et al., 2005), or drying out strategies for flooded buildings in the future (Blades et al., 2008).

One of the reasons that it was felt a simplified transfer model may be applicable is that typically the climate of unheated rooms are largely dependent upon the outdoor climate (Lankester and Brimblecombe, 2012a). Initially investigations will begin with unheated rooms, but ideally this will progress onto rooms heated by other methods. Since the start of this work some research has been published that provides additional evidence that a simplified relationship may exist and that exploring this possibility is worthwhile. This found that the relationship between indoors and outdoors appears to be linear for a number of building types, including houses and offices (Coley and Kershaw, 2010).

This has given an introduction to building simulation and its uses, along with some of the programs available. The limitations and advantages of the complex model and a simplified mathematical model have been discussed. Next the investigation into determining a simple model is discussed.

## 3.2 Research into a simplified model

Research into a simplified building simulation model began with comparing observed data that is available from the Library at Brodsworth Hall to the outdoor data (section 2.2.1). Measurements are taken both in the Library and locally outdoors by English Heritage. Initially three years of temperature and relative humidity data was available, covering the period 2006-08, and there are significant problems with this data. As mentioned previously there was very little data available for the months of February and March, when comparing the indoor environment to that outdoors it leaves a significant gap in the comparisons. Fortunately later into the project two additional years (2009-10) of data was added to the dataset, and this solved the issue surrounding these months. While considerable time was taken analysing the three year data set, the following analysis will focus on the full data set, which simplified some of the research significantly.

### 3.2.1 Data comparison

The first approach taken was to plot the data available, as it may be expected in unheated buildings that there is a relationship between indoor and outdoor temperature. On the first occasion this highlighted the significant issues surrounding the gaps in the data, and anomalous observations that stood out. The anomalies were simple to identify, for example the temperature jumping up to 40°C in March, when previously averaging around 8°C, this is an extremely high temperature, and it is very unlikely that it is a true reading.

Comparing this to the maximum temperature, with this removed, justifies the removal of the data. The maximum daily average temperature is almost 24°C, considerably lower than 40°C, and this occurred in mid August, as opposed to March. Other anomalies similar to this were also removed, another involved the hourly reading jumping up precisely 10°C each hour, up to around 80°C, clearly this is an anomaly. When anomalies were found with the observed data both the temperature and relative humidity observations were removed. Typically these are replaced with a place marker, to identify that no value exists for this time period, as occasionally it is important that the gaps are acknowledged. In this work the place marker used was 'XXX'; it is possible to construct the AWK programs to identify if the current line is a gap in the data.

Once the data sets were 'cleaned up' daily averages were calculated from the half hourly observations available. The AWK program that was used to calculate the daily average can be found in appendix E. This made the datasets more manageable, reducing 91,968 unique half hourly time periods to 1,916 daily time periods, for which there are observations of temperature and relative humidity, both indoors and outdoors, so effectively four times the values above. At this stage data at the daily temporal scale is acceptable. Finally after this preparation work the data was ready for plotting, as shown in figures 3.1 and 3.3.

Figure 3.1: Daily average temperature indoors in the Library and outdoors at Brodsworth Hall for the period 01/2006-03/2011.
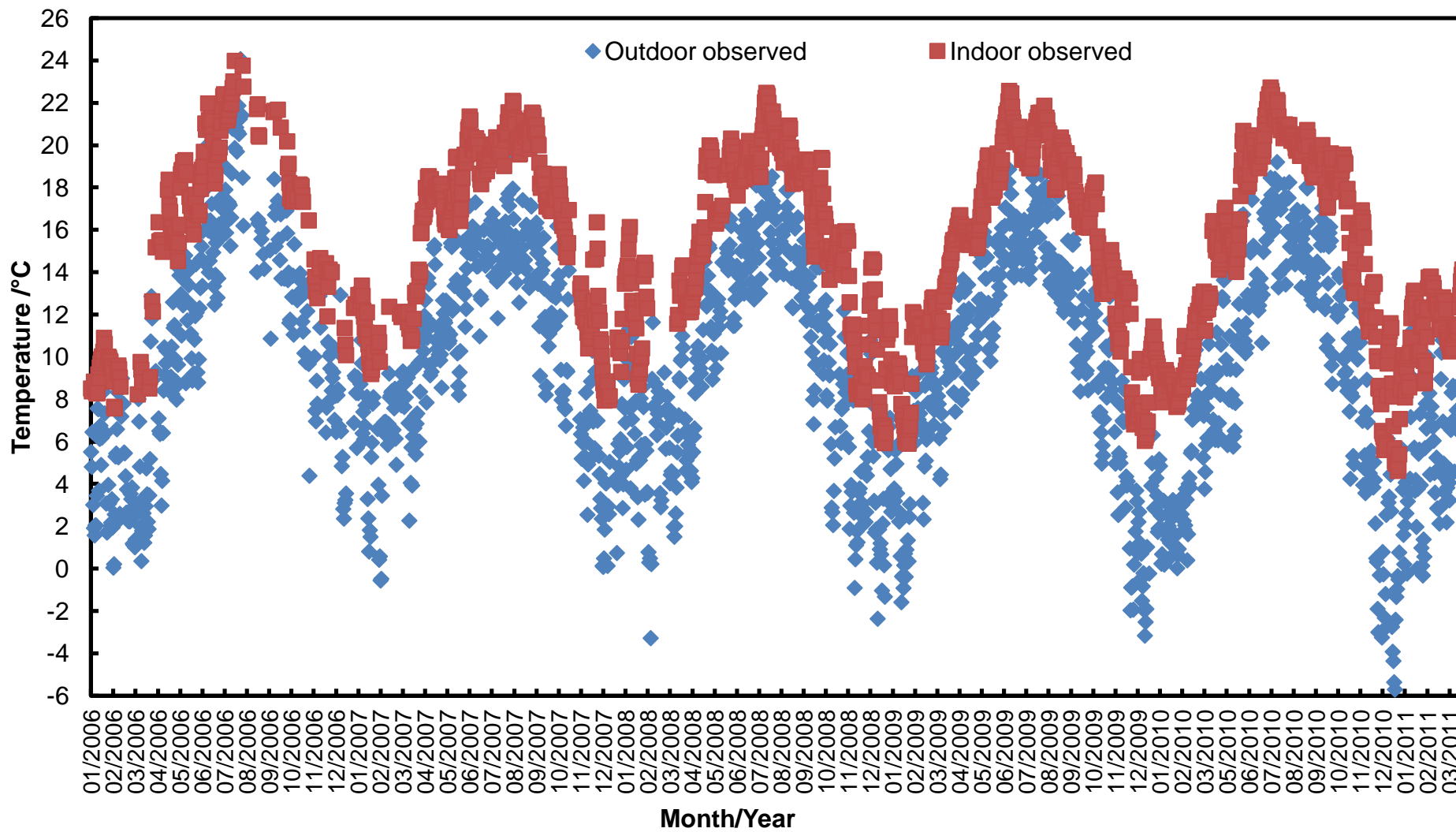
Figure 3.1 plots the indoor and outdoor daily average temperature, the annual temperature cycle is immediately apparent, with colder temperatures in the winter and warmer temperatures in the summer, both indoors and out. The temperature range outdoors is larger than that indoors, as would be expected, as the building provides some buffering. In the winter the indoor temperature is significantly higher than that outdoors, the minimum value over the five years indoors is 4.6°C compared to -5.7°C outdoors. Typically the indoor temperature is warmer than the outside temperature, even though it is dependent upon it; this can arise from a number of sources, the main one is likely to be solar gain.

Factors that affect the temperature and humidity of the air within a building are the heating, ventilation and air conditioning systems (HVAC), people, lighting, solar radiation, air exchange, heat and moisture transport across surfaces, and buffering capacity of materials. In historic buildings buffering capacity (or moisture diffusion) can be important; there can often be a significant amount of hygroscopic material, which allows for buffering of the relative humidity (Camuffo, 1998).

The solar radiation, heat and moisture transport across walls and other surfaces, and the air exchange through openings are factors driven by external forces. The extent that these external forces affect the temperature and humidity depends upon the material construction. Walls that are either conductive or thin are sensitive to solar radiation, and windows may allow for penetration of solar beams. Alternatively thick walls, typical of some historic buildings are effective at buffering daily temperature cycles. The quality of construction of the building fabric can have an effect on the air exchange rate. Further to this the location, or exposure of the room in relation the external environment can have an impact on the internal temperature and humidity. Rooms which are towards the centre of a building are more shielded and external forcing is smoothed out (Camuffo, 1998).

From figure 3.1 it appears that the indoor and outdoor temperatures are related; they both follow a similar pattern. In figure 3.2 the indoor and outdoor temperature are plotted against each another on separate axes. This indicates that there is a good correlation ($R^2$=0.84) between the two sets of temperature. It is possible that this relationship could be used as part of a transfer function; this may have potential and will be investigated further.
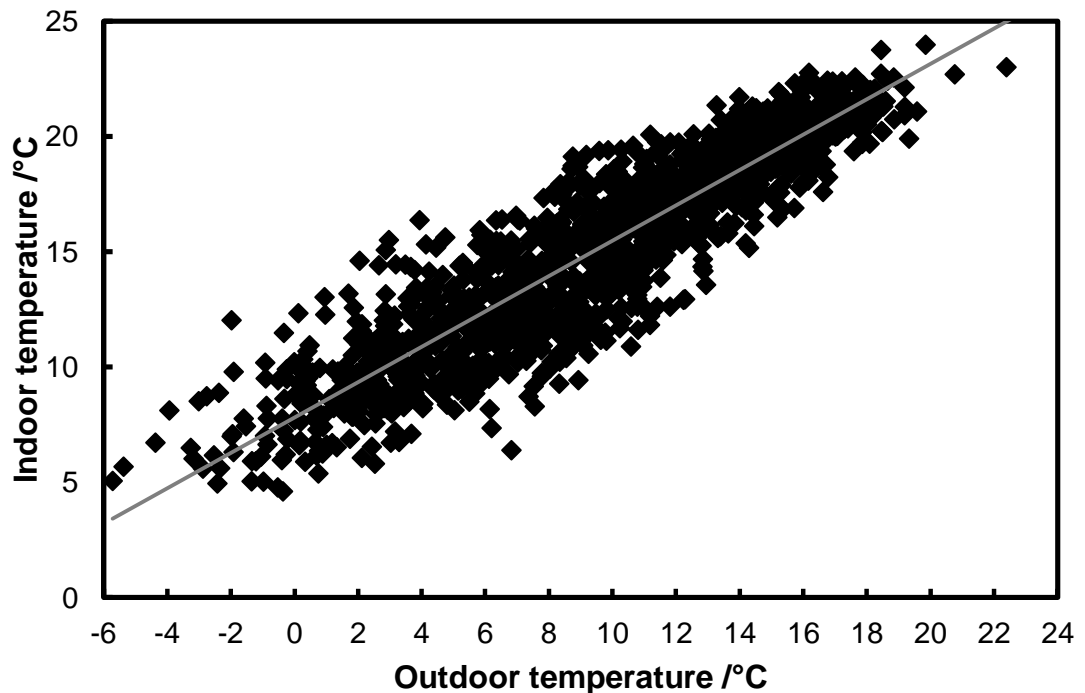
Figure 3.2: Outdoor temperature plotted against indoor temperature, daily averages from 01/2006-03/2011 at Brodsworth Hall.

Figure 3.3 plots the indoor and outdoor daily average relative humidity; the first thing that is apparent is that the indoor and outdoor relative humidity is quite different from one another. It was quite obvious that the two temperature datasets were related, but this is not initially apparent here. The indoor relative humidity stays within a band of about 35-70% RH, lower than the outdoor RH, which typically occupies the range 60-95% RH. After the initial comparisons, a closer look at the data reveals some trends, the annual trend is just visible, with higher relative humidity in the winter, and lower in the summer. It is quite difficult to find any other information in this figure, in order to show other information the moving average is plotted to remove some of the numerous data points.

The 7 day moving average of the two relative humidity data sets is plotted in figure 3.4. Even after applying this technique it is quite difficult to see any areas where the two data sets correspond to one another, there are a few areas, for example May to July 2007 and August to October 2010. These are in the minority however, and more often than not there is no obvious relationship between the two sets of relative humidity values. The correlation coefficient ($R^2$=0.11) confirms that there is no significant correlation between the indoor and outdoor relative humidity; this plot can be seen in Figure 3.5. As no obvious correlation exists for relative humidity attempts at various models will be made to try and predict the indoor relative humidity.

Figure 3.3: Daily average relative humidity indoors in the Library and outdoors at Brodsworth Hall for the period 01/2006-03/2011.
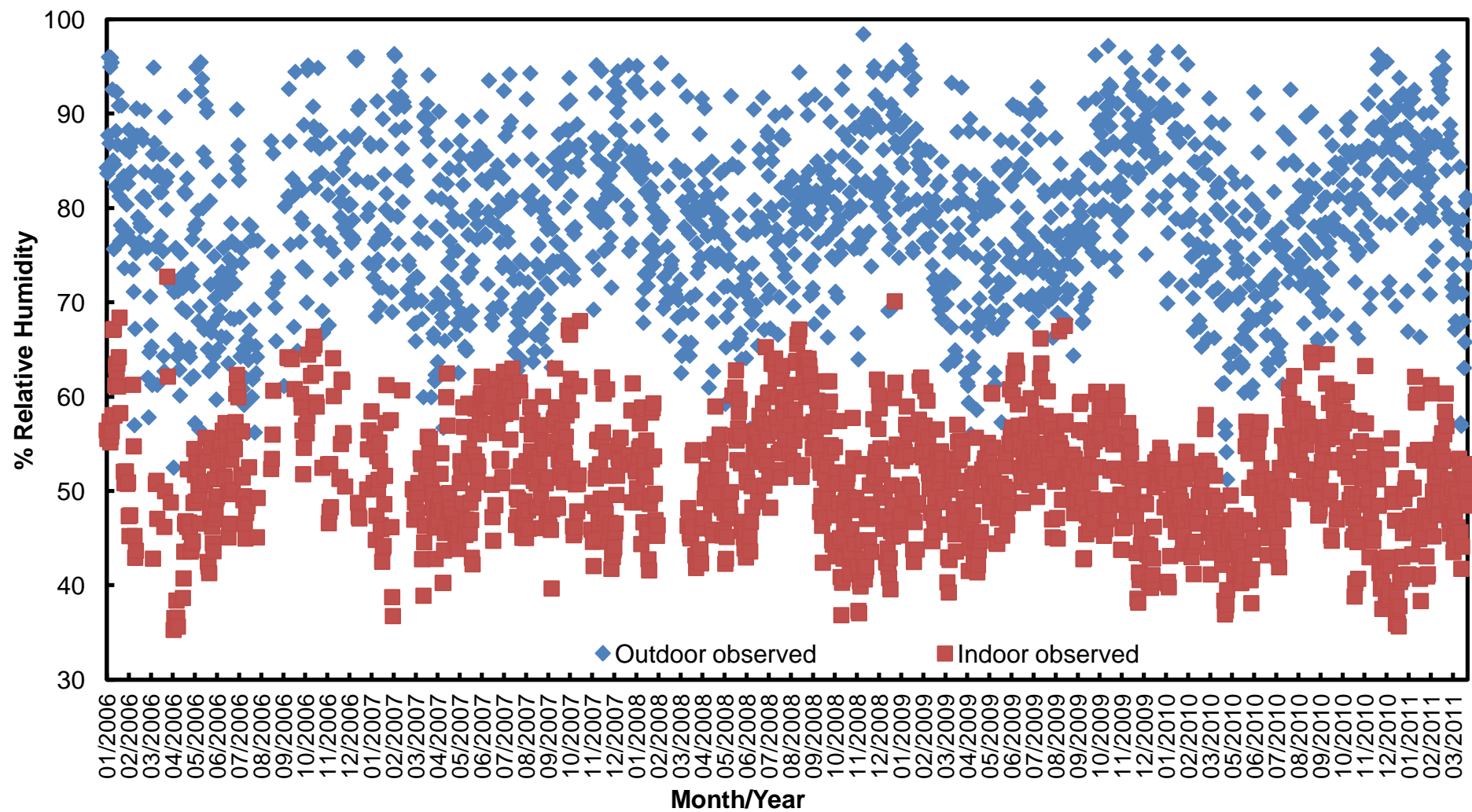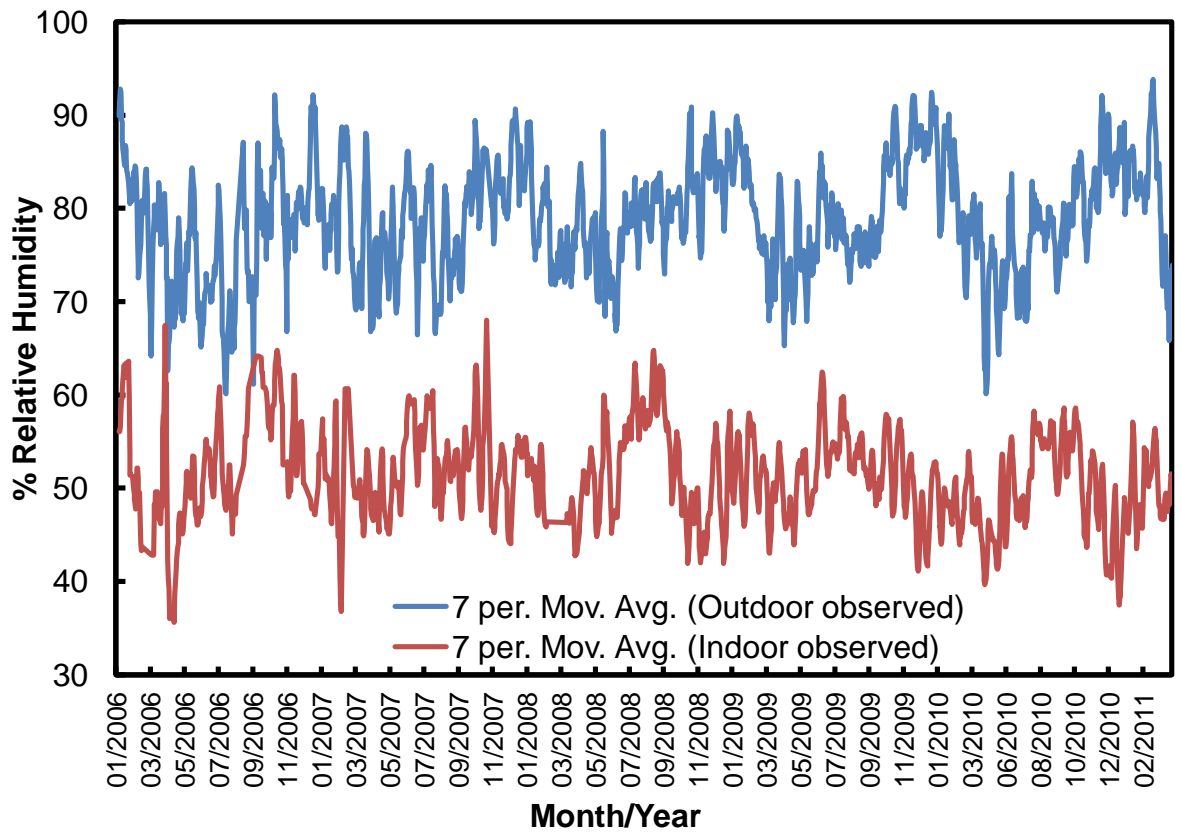
Figure 3.4: Seven period moving average trend lines for the indoor and outdoor observed relative humidity, as plotted in figure 3.3.
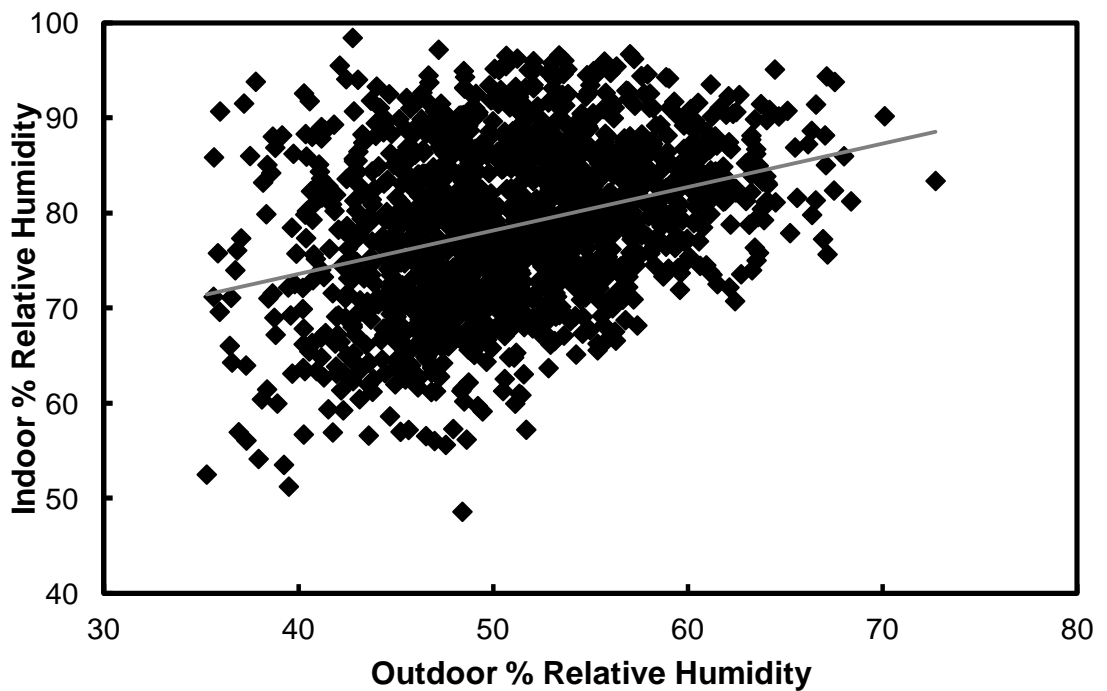


Figure 3.5: Outdoor relative humidity plotted against indoor relative humidity, daily averages from 01/2006-03/2011.

### 3.2.2 Initial model

Initial attempts of a model were made; this involved using the monthly relationships of the indoor and outdoor data, similar to that presented in figures 3.6 and 3.7. The idea of monthly comparison rather than yearly was borrowed from the downscaling technique described in section 2.3.1, (Grossi et al., 2008b). The transfer of temperature and humidity from outdoors to indoors also borrowed from this technique. The relationship between indoor and outdoor temperature on a monthly basis was determined, and calibration coefficients calculated based on the difference between the monthly averages. Relative humidity used the ratio between the two monthly averages. Figure 3.6 plots the monthly averages of temperature over the period 2006-2009 indoors and out at Brodsworth Hall, the annual temperature trend, as seen previously is apparent. The corresponding relative humidity monthly averages are plotted in figure 3.7. The ratios derived from the monthly averages are presented in table 3.1.
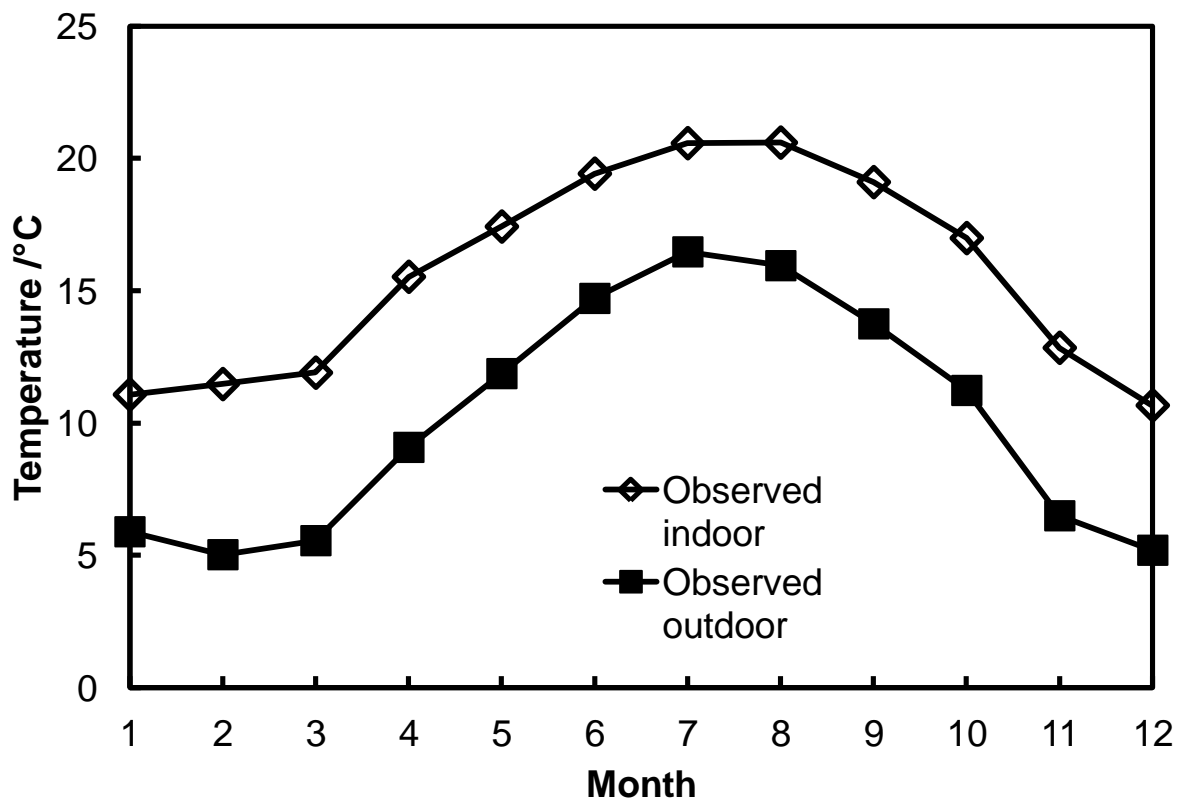


Figure 3.6: Monthly average temperature over the period 2006-8, outdoors at Brodsworth Hall and indoors in the Library.
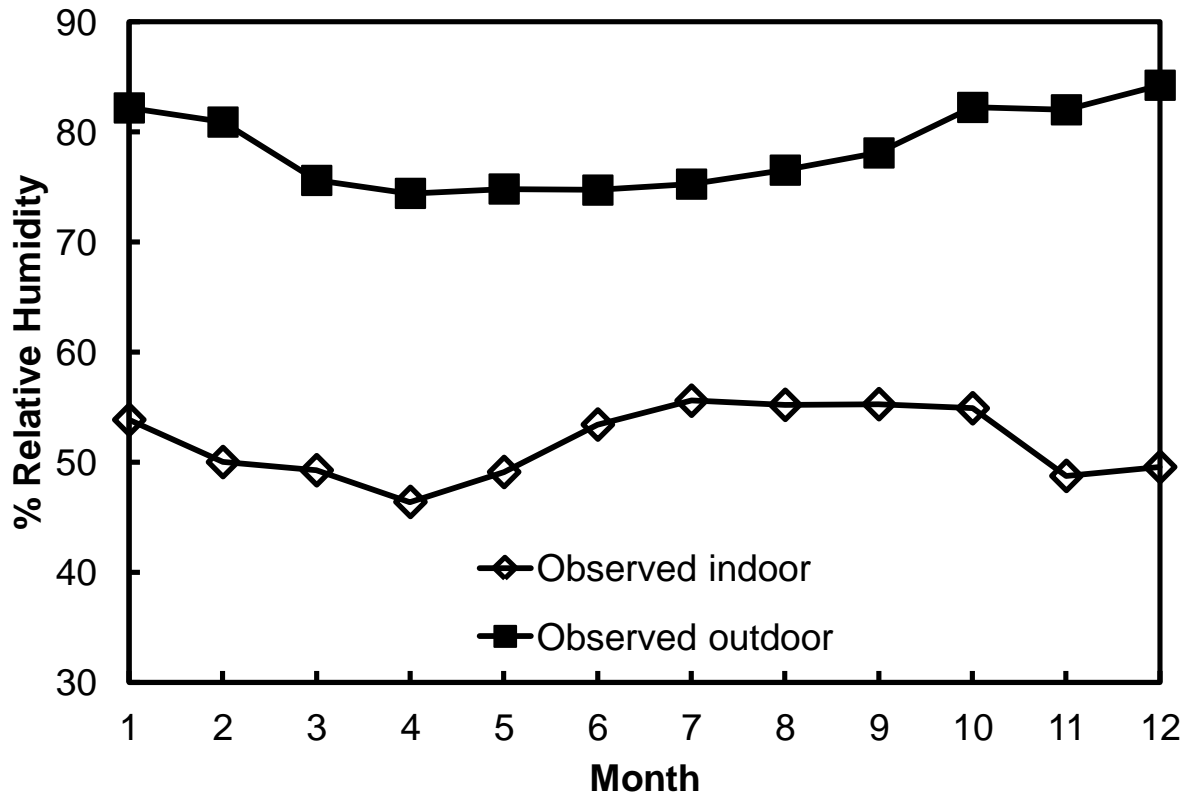
Figure 3.7: Monthly average relative humidity over the period 2006-8, outdoors at Brodsworth Hall and indoors in the Library.

Table 3.1: Difference in temperature and the ratio of relative humidity between outdoors and indoors at Brodsworth Hall.

| Month | Difference in temperature indoors | Ratio of outdoor to indoor relative humidity |
|---|---|---|
| 1 | 5.19 | 0.66 |
| 2 | 6.45 | 0.62 |
| 3 | 6.35 | 0.65 |
| 4 | 6.45 | 0.62 |
| 5 | 5.56 | 0.66 |
| 6 | 4.71 | 0.71 |
| 7 | 4.11 | 0.74 |
| 8 | 4.66 | 0.72 |
| 9 | 5.36 | 0.71 |
| 10 | 5.76 | 0.67 |
| 11 | 6.35 | 0.59 |
| 12 | 5.47 | 0.59 |

The predictions of indoor temperature derived by applying the temperature difference values to the outdoor observed data is compared to the observed indoor data in figure 3.8, for the period 2006-8. While the comparison of the observed indoor and outdoor data is for the complete 5 year data set, the predictions that follow were completed with the initial 3 year data set. The results of the prediction look promising, the pattern of the predicted data follows that of the observed data well, and the correlation coefficient is quite good with an $R^2$ value of 0.81. For a first attempt this is excellent, with room for improvement. For example the predicted data has greater variability than the observed data; it is too warm in the summer, and too cold in the winter months.
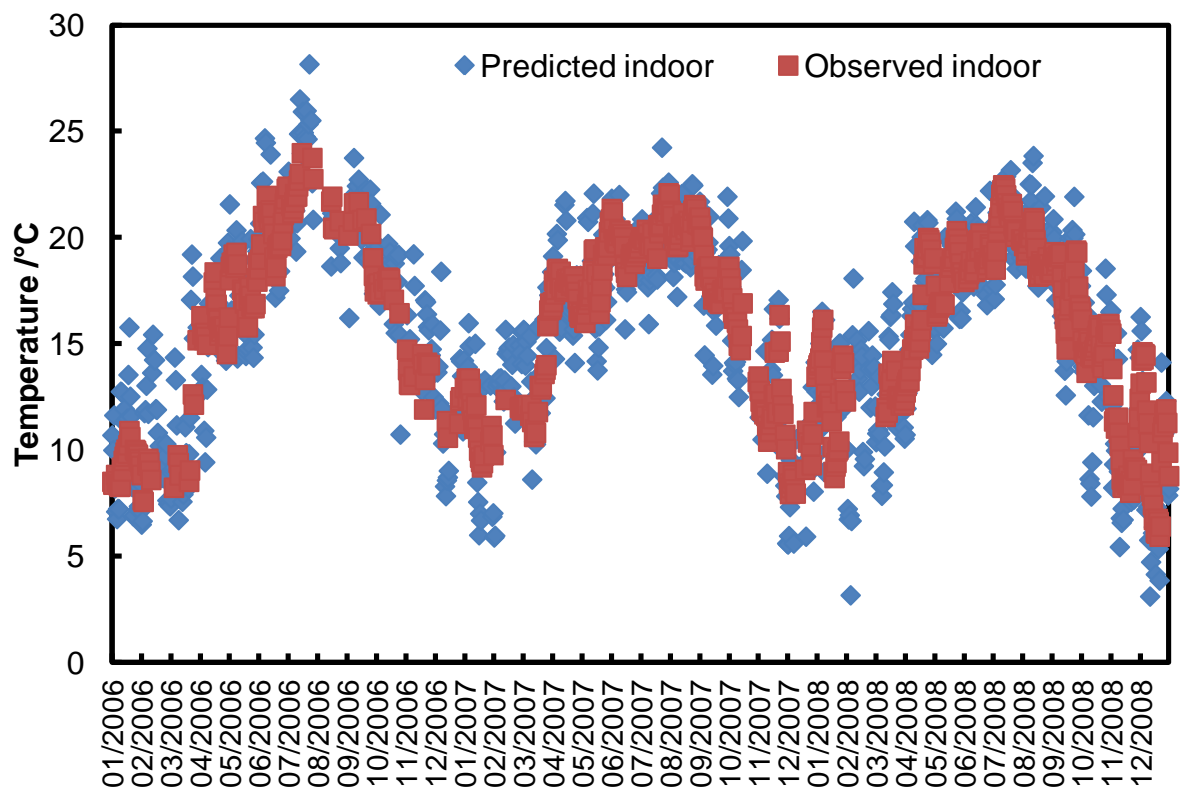


Figure 3.8: First prediction of temperature indoors for the library at Brodsworth Hall, determined by applying monthly differences to the outdoor temperature.

The prediction of relative humidity indoors at Brodsworth Hall is compared to the observed indoor climate in figure 3.9. It is not obvious from the figure how well the prediction compares to the observed climate, it is however in the right vicinity, between about 40-65% relative humidity, although it does vary from this occasionally. The correlation coefficient helps provide evidence as to whether the data compares favourably, here the $R^2$ value equals 0.33. This is quite poor, and further work is needed on relative humidity prediction.

It appears as though with a little further work the temperature prediction is possible, however it is quite good currently, but significant work is required to predict the relative humidity effectively.
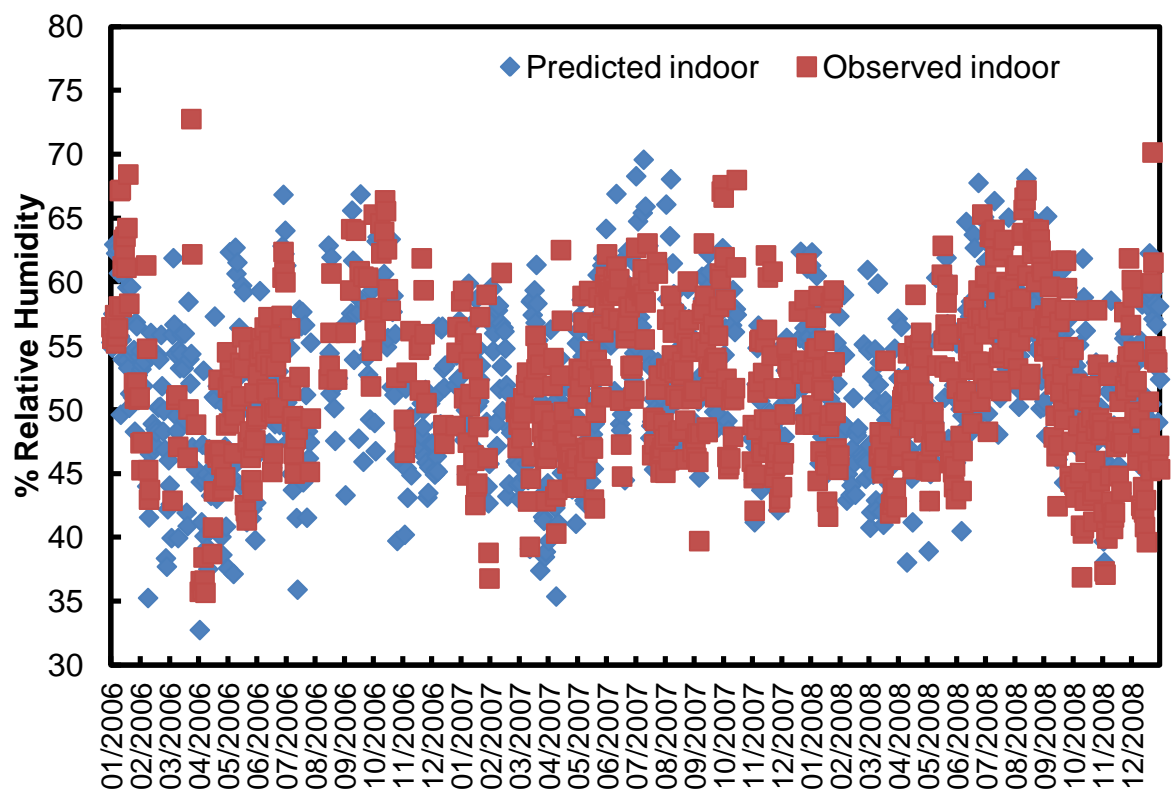


Figure 3.9: Initial prediction of relative humidity indoors for the library at Brodsworth Hall, determined by applying monthly ratios to the outdoor relative humidity.

It was decided that a different approach would be investigated to see how this would predict the indoor relative humidity. These predictions of indoor humidity rely upon the outdoor humidity initially, it is apparent from figure 3.9 that occasionally the predictions are too extreme. The decision was taken to smooth the outdoor data before attempting to transfer the data indoors to see if this may help improve the predictions.

Therefore the process of predicting indoor temperature and relative humidity would become: smooth the outdoor humidity; calculate the specific humidity; predict the indoor temperature using the monthly differences; recalculate the relative humidity, from the specific humidity now that the temperature has changed; apply the monthly ratios to predict indoor relative humidity. The smoothing is applied to the relative humidity because it has been observed that there is greater variation in RH outdoors than indoors, implementation of a smoothing technique is an attempt to replicate the indoor variation and improve the prediction.

### 3.2.3 Specific Humidity

In addition to the temperature and relative humidity the specific humidity needs to be calculated. The reason for this is because relative humidity is not an absolute measure of moisture content; it is dependent upon the temperature, as the capacity of the air to hold moisture alters with temperature. Specific humidity is an absolute measure, after the temperature has changed it can then be used in conjunction with the specific humidity to calculate the relative humidity. Therefore when heat and moisture is transferred from outdoors to indoors, or vice versa, it is the absolute humidity, not the relative humidity that is transferred, and the initial moisture, wherever it is transferred to is conserved, whereas this is not true of relative humidity.

The direction in which moisture transport occurs firstly depends on whether the moisture is in liquid or vapour form. Here it is both the vapour and liquid transport of water that is important. Water vapour diffusion is driven by differences in vapour pressure (specifically the partial pressure of water vapour), with movement from high to low. When considering water vapour diffusion through porous materials the effect that the material has on the process is taken into account by the water vapour diffusion resistance factor, which is characteristic for each material. For liquid transport (surface diffusion) the direction of movement is driven by the relative humidity (Kunzel, 1995).

The specific humidity was calculated from the temperature and relative humidity pairings of each time period. The calculation of specific humidity used the equations presented in the ASAE (American Society of Agricultural Engineers) standards (1998), this quotes two other sources of the equations used, Brooker (1967) and Keenan and Keyes (1936). The equations used are presented here:

$$RH = \frac{P_v}{P_s}$$

**(Eq. 3.1)**

$$SH = \frac{0.6219\ P_v}{P_{atm} - P_v}$$

**(Eq. 3.2)**

$$\ln P_s = 31.9602 - \frac{6270.3605}{T} - 0.46057\ \ln T$$

**Where** $255.38 \leq T \leq 273.16$ **(Eq. 3.3)**

$$\ln\left(\frac{P_s}{R}\right) = \frac{A + BT + CT^2 + DT^3 + ET^4}{FT - GT^2}$$

**Where** $273.16 \leq T \leq 533.16$ **(Eq. 3.4)**

Initially the temperature and relative humidity are known, here temperature is in Kelvin and relative humidity in the decimal form (RH/100). From the temperature the saturation vapour pressure, $P_s$, can be calculated using either equation 3.3 or 3.4. This allows the vapour pressure, $P_v$, to be calculated from equation 3.1. The vapour pressure can then be used to calculate the specific humidity, using the atmospheric pressure, $P_{atm}$, in equation 3.2. The standard atmospheric pressure of 101,325 Pa is used. The equations can also be used in reverse to calculate relative humidity, when given temperature and specific humidity. The constants in equation 3.4 are defined as:

$A$ = -27,405.526        $E$ = -0.48502 $\times 10^{-7}$

$B$ = 97.5413        $F$ = 4.34903

$C$ = -0.146244        $G$ = 0.39381 $\times 10^{-2}$

$D$ = 0.12558 $\times 10^{-3}$        $R$ = 22,105,649.25

The AWK program used to calculate specific humidity is available in appendix E.

### 3.2.4 Smoothing function

The first smoothing function attempted was that of a lagged function, following the form displayed in equation 3.5. It was decided for now to continue using relative humidity in order to predict the indoor environment.

$$\sum_{l=1}^{n} \left( \frac{1}{Z} \times (Z) \times RH \right) \qquad \textbf{(Eq. 3.5)}$$

$$Z = \exp - \left( \frac{kl}{n} \right) \qquad \textbf{(Eq. 3.6)}$$

Where: $k$ is a variable constant between 0 and 1. $n$ is the total number of readings in the current time period used for the smoothing, for example data from over 48 periods would use one days data, were there half hourly readings, to calculate the current reading. $l$ is the current time period from 1 to $n$. This was carried out using an AWK program, which can be found in appendix E.

Initially the model was used with $k=1$ and $n=96$. This smoothed the outdoor data slightly, as was desired; this can be seen in figure 3.10, reducing the higher values slightly and increasing the lower values slightly.
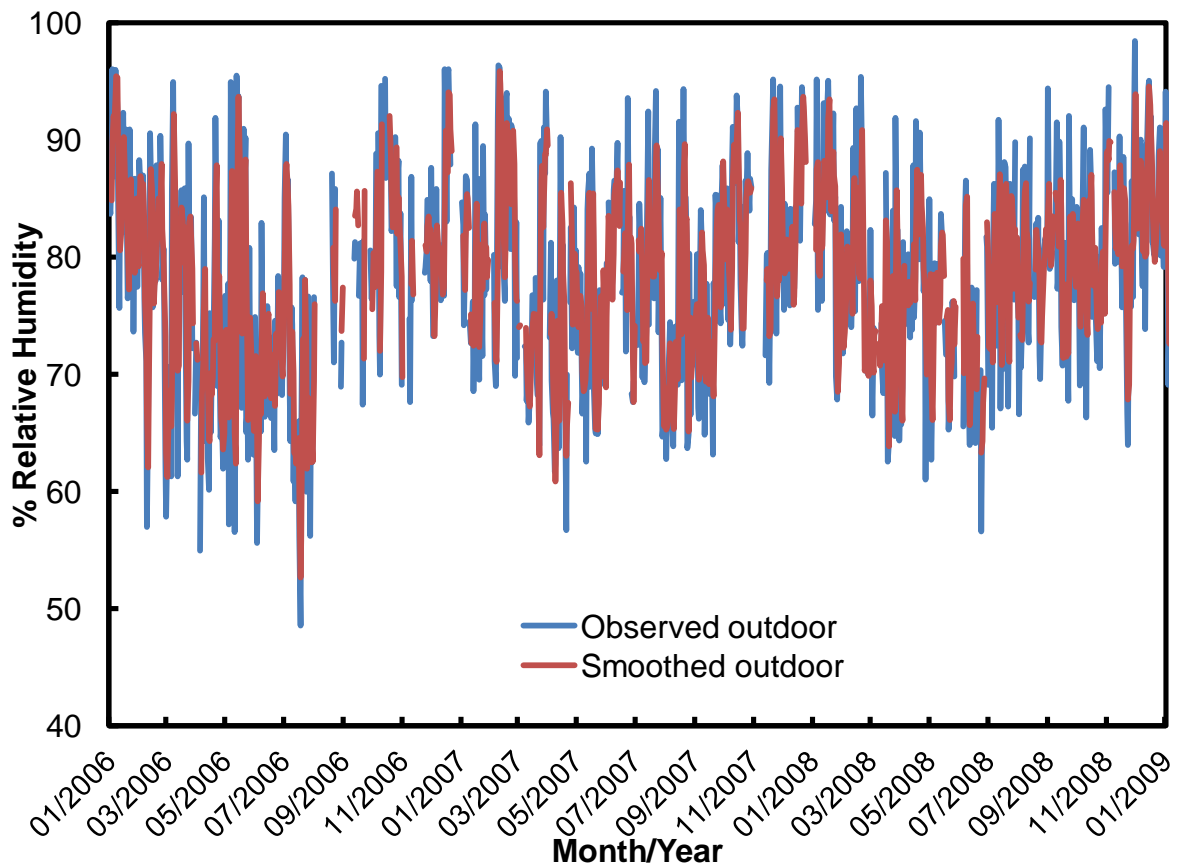


Figure 3.10: Smoothing of the outdoor relative humidity at Brodsworth Hall using the lagged function.

Once the data was smoothed the rest of the process of predicting the indoor relative humidity was completed. This was carried out numerous times in an attempt to determine the optimal values of $k$ and $n$. It was determined that the optimal prediction of relative

humidity was when $k = 2.5$ and $n = 24$, a smoothing window length of 12 hours. While this was the optimal prediction it only improved on the original prediction slightly. Figure 3.11 compares the improved prediction to the real data. The $R^2$ value increased from 0.33 to 0.35, still quite poor correlation. The 5 day moving average was plotted, as plotting a daily average makes comparison difficult. Visually assessing the comparison also confirms the poor prediction of relative humidity, there is significant deviation from the observed relative humidity over certain periods, such as November-December 2006 and June-August 2007. The prediction of relative humidity was completed using an AWK program; this consisted of multiple smaller programs merged into one, to speed up the process, so the smoothing took place, followed by calculating the specific humidity along with each other stage of the prediction.
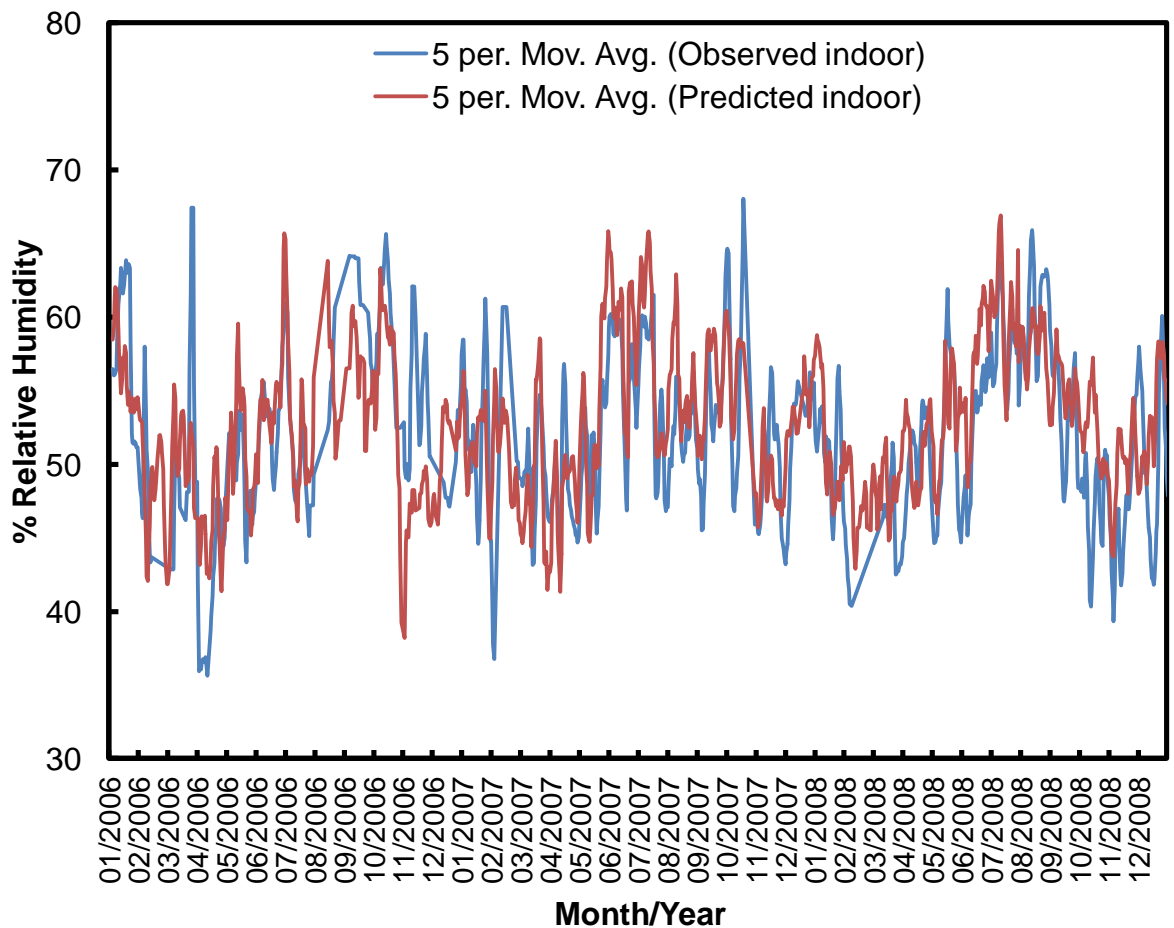


Figure 3.11: Comparison of predicted relative humidity, using a smoothing technique. Plotted as a 5 day moving average, over the period 01/2006-12/2008.

It was apparent that this method of smoothing has not helped improve the prediction of relative humidity significantly. Other methods of smoothing will now be investigated to try and improve further upon this prediction. A Pascal filter was attempted initially, however it

was apparent from the outset that it was not appropriate, being too heavily weighted towards the recent values, with the majority of the smoothed value coming from the first five values, only 2 and a half hours of readings. Next a triangular filter for smoothing the data was attempted.

*Triangular filter*

This smoothing technique applies weighting that forms the shape of a triangle, with the weights gradually becoming smaller, following a constant gradient (figure B2, in appendix B). Various lengths of the smoothing window were investigated, with 48 periods, or 1 day, being determined as the best. Using this window length sets the function up as follows: the first period is determined by multiplying the observed RH by 48/1176, where 1176 is the sum of 48+47+46.....+1=1176. The next period is determined using 47/1176, and so on until 1/1176, and the value of each period is summed to determine the smoothed value. Again this is the first step of the full process of predicting the relative humidity. The AWK program used to implement this filter can be found in appendix E.

Figure 3.12 compares the observed relative humidity to that predicted using this smoothing technique. There is very little difference between how this performs compared to the original smoothing method, some areas compare well, July-August 2007, and some do not, November 2006 to January 2007. The correlation coefficient for this prediction gives an $R^2$ value of 0.31, quite similar to the first method. The smoothing functions do not appear to be improving the prediction of relative humidity. It was decided that next a simpler filter would be applied.
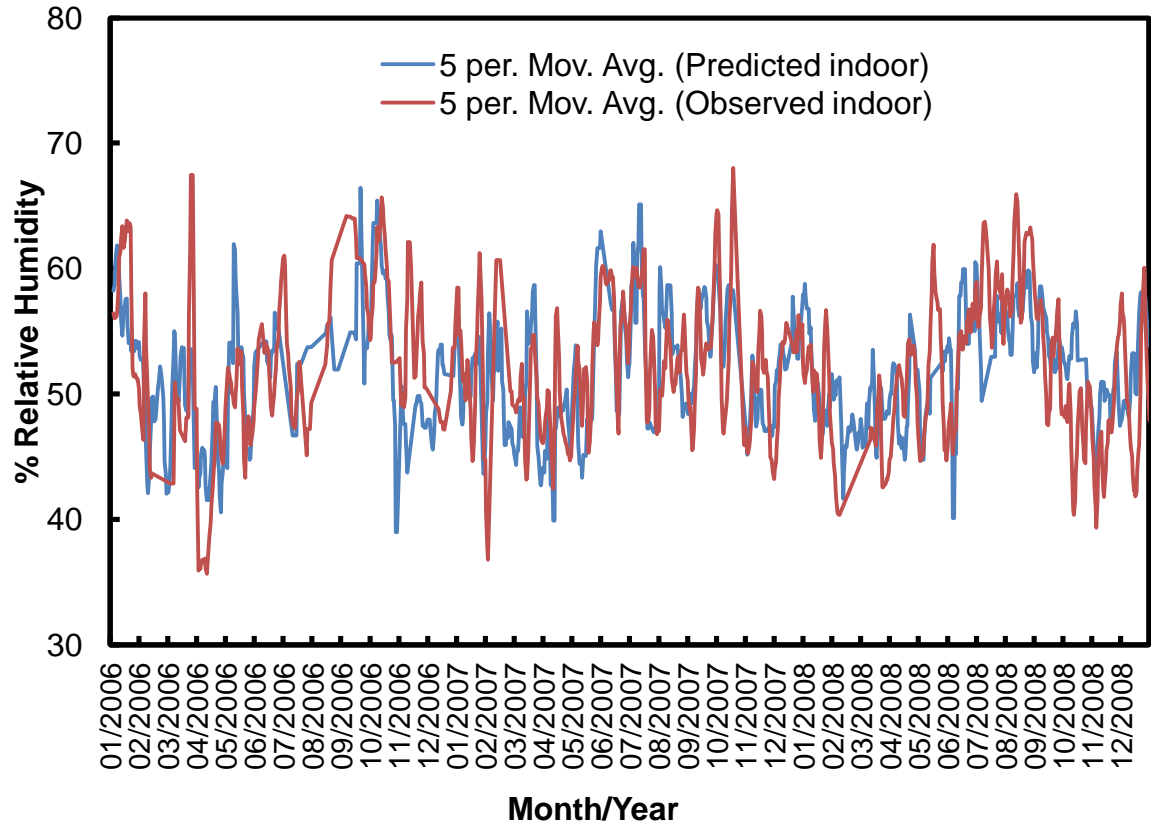
Figure 3.12: Comparison of observed and predicted relative humidity in the Library at Brodsworth Hall, using the triangular smoothing technique. Plotted as a 5 day moving average, over the period 01/2006-12/2008.

*Further filters*

In addition to the triangular filter further filters were attempted, a square filter, square root filter and cube root filter. While these were investigated they did not move forward the prediction of indoor environment. Therefore the results of these additional filters and discussion of these can be found in appendix B.

The smoothing techniques have so far failed to improve the prediction of relative humidity. Looking instead at the monthly averages, rather than the daily averages used so far and the ideal level at which good prediction is required, there are some positives. Figure 3.13 and 3.14 show the predicted monthly average temperature and relative humidity respectively, and compare it to the observed data. Figure 3.13 shows good comparison, for the temperature, as observed previously, with slight variations from the observed data, especially during the three February months. The correlation coefficient for this data is good with an $R^2$ value of 0.96, and the equation of the line of best fit is close to observing a 1:1 ratio ($y$=1.02$x$-0.4).
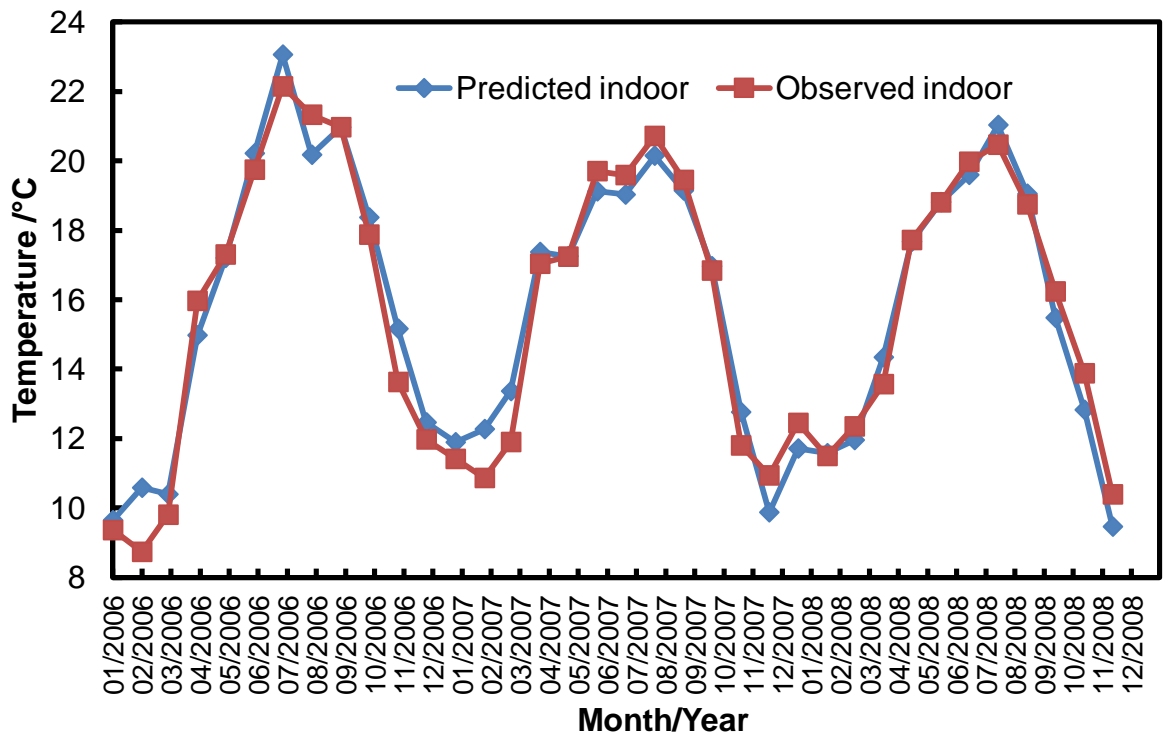
Figure 3.13: Comparison of monthly average predicted and observed temperature, over the period 2006-8, at Brodsworth Hall.

However again the relative humidity prediction is not as good, see figure 3.14. Sometimes the prediction is not too bad, but at other points, such as September and October 2006 the prediction is approximately 5% different, which at the scale here is too large an error. The correlation coefficient here has an $R^2$ value of 0.71, a great improvement on that seen at the daily average scale, but that is the scale that is important, the monthly average helps give an overview.
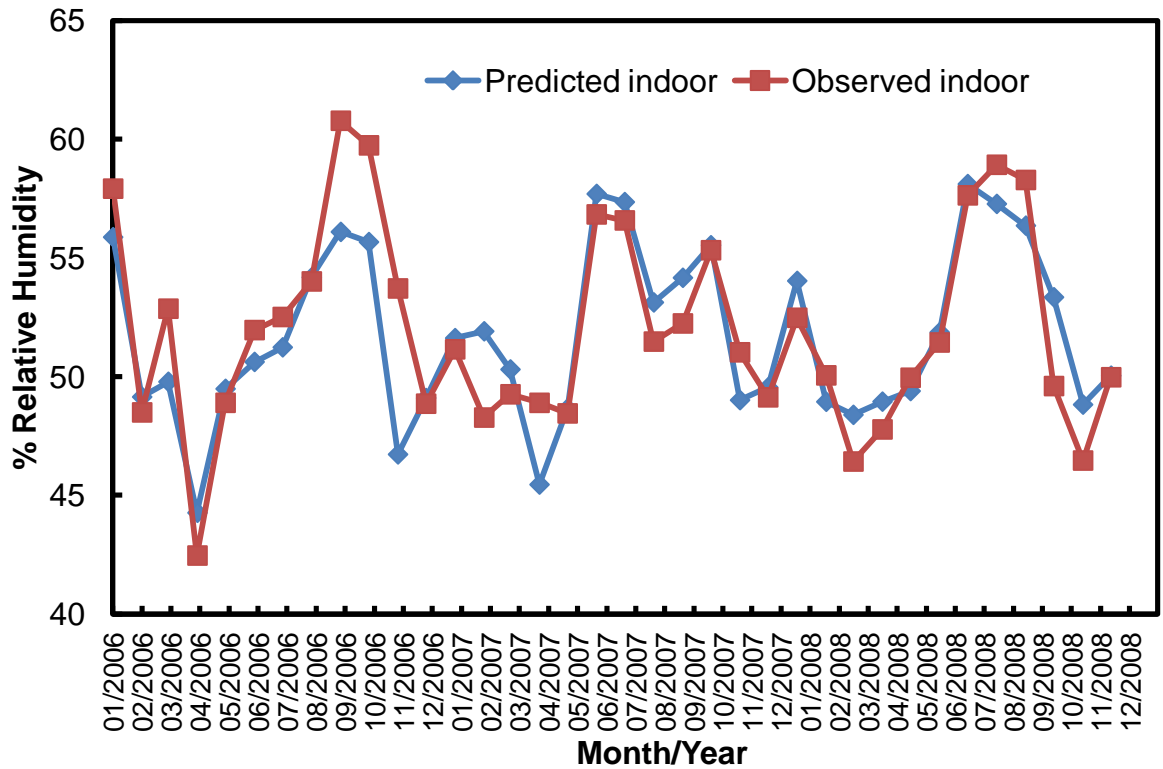
Figure 3.14: Comparison of monthly average predicted and observed relative humidity, over the period 2006-8, at Brodsworth Hall.

However, none of the smoothing functions implemented thus far have improved on the original function, which itself was poor ($R^2$=0.35). Therefore efforts moved from trying to use the relative humidity onto another method, which uses the specific humidity.

### 3.2.5 Specific humidity transfer

Specific humidity has been discussed earlier (section 3.2.3), and as mentioned, the moisture content or specific humidity is actually the property that is transferred from outdoors to indoors. Relative humidity alone is not an absolute measure of the moisture content of the air; at different temperatures the same relative humidity describes different values of actual moisture content.

Firstly the relationship between indoor and outdoor specific humidity will be investigated, as was carried out previously for temperature and relative humidity. The comparison of outdoor to indoor specific humidity at Brodsworth Hall over the period 2006-March 2011 is plotted in figure 3.15. There is quite clearly a relationship between the two observations, they follow the same yearly trend, and have quite similar values, with the indoors slightly lower.

Figure 3.15: Daily average specific humidity indoors and outdoors at Brodsworth Hall.
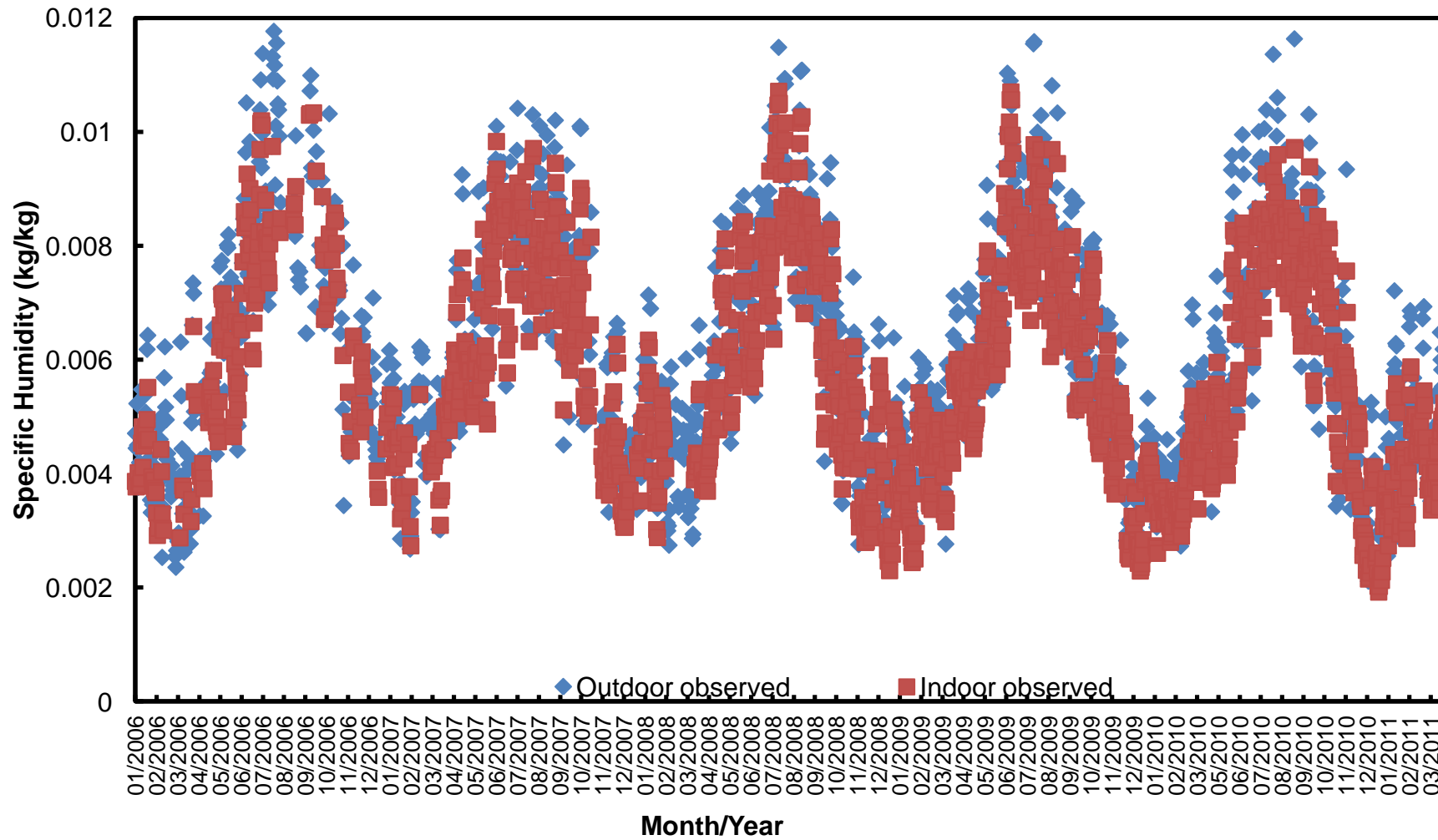
The plot of indoor and outdoor specific humidity in figure 3.16, shows that there is strong correlation ($R^2$ =0.91) between the outdoor and indoor specific humidity. This strong correlation along with the correlation of the temperature indoors and out is promising, and may provide the answer to predicting the indoor environment.
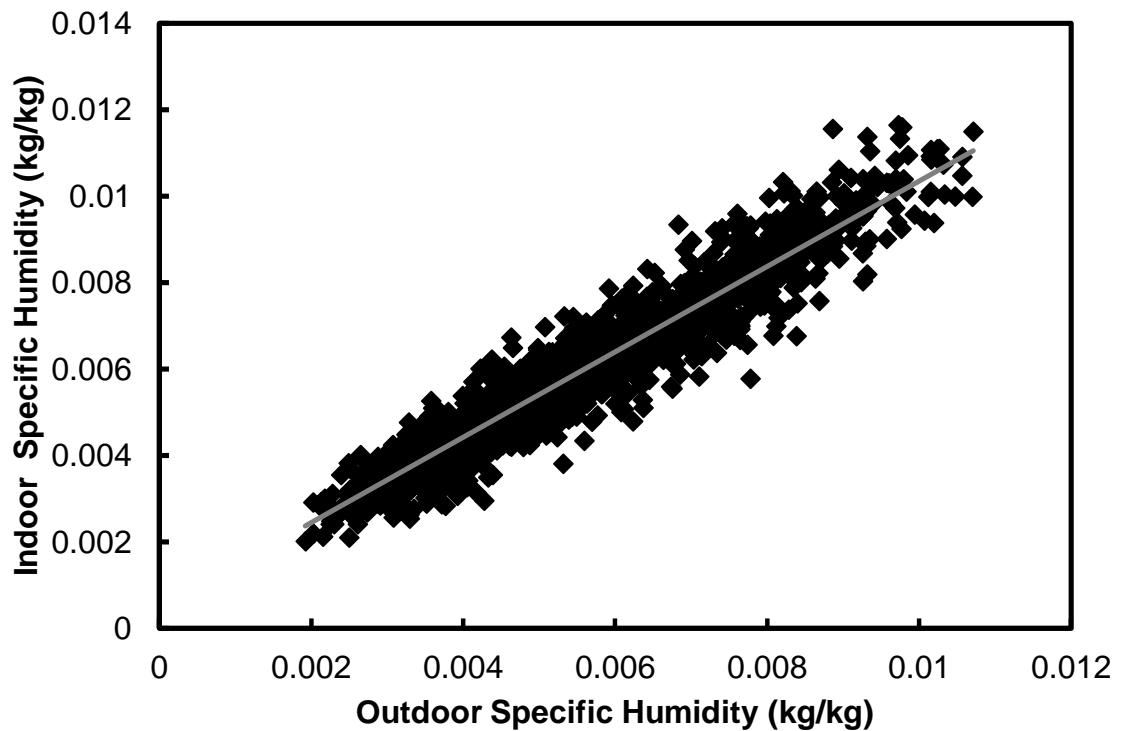


Figure 3.16: Outdoor specific humidity plotted against indoor specific humidity at Brodsworth Hall, for the period 01/2006-12/2008.

Similar to the previous method, a ratio would be applied to the outdoor specific humidity to predict the indoor specific humidity. The ratio was determined by calculating the monthly average over the three year period, and comparing between indoors and out. The prediction of specific humidity using this technique is compared to the observed indoor specific humidity in figure 3.17. The prediction is initially promising, and the correlation coefficient provides evidence of this, with an $R^2$ value of 0.92. The equation of the line of best fit also indicates that this is close to being a 1:1 relationship ($y=0.96x+0.29$). However to compare this to the other methods the predicted relative humidity needs to be calculated from the predicted temperature (section 3.2.2) and this predicted specific humidity.
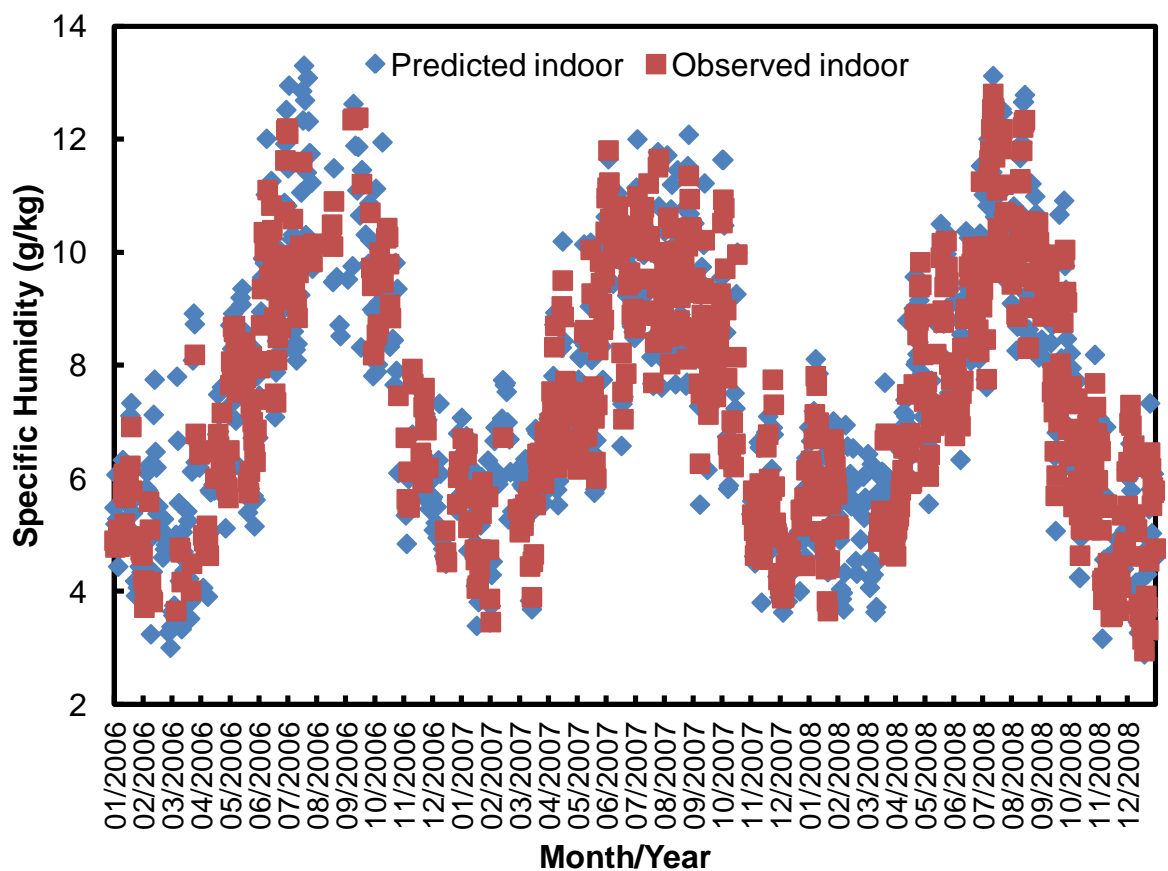


Figure 3.17: Daily average predicted and observed indoor specific humidity in the Library at Brodsworth Hall, over the period 2006-8.

The relative humidity calculated from the predicted temperature and specific humidity is compared to the observed data in figure 3.18. Unfortunately this returns to the poor predictions of relative humidity that was seen with the previous methods. There are still periods where the humidity prediction is poor, and the correlation coefficient has a value of $R^2$=0.34, similar to that of previous predictions.
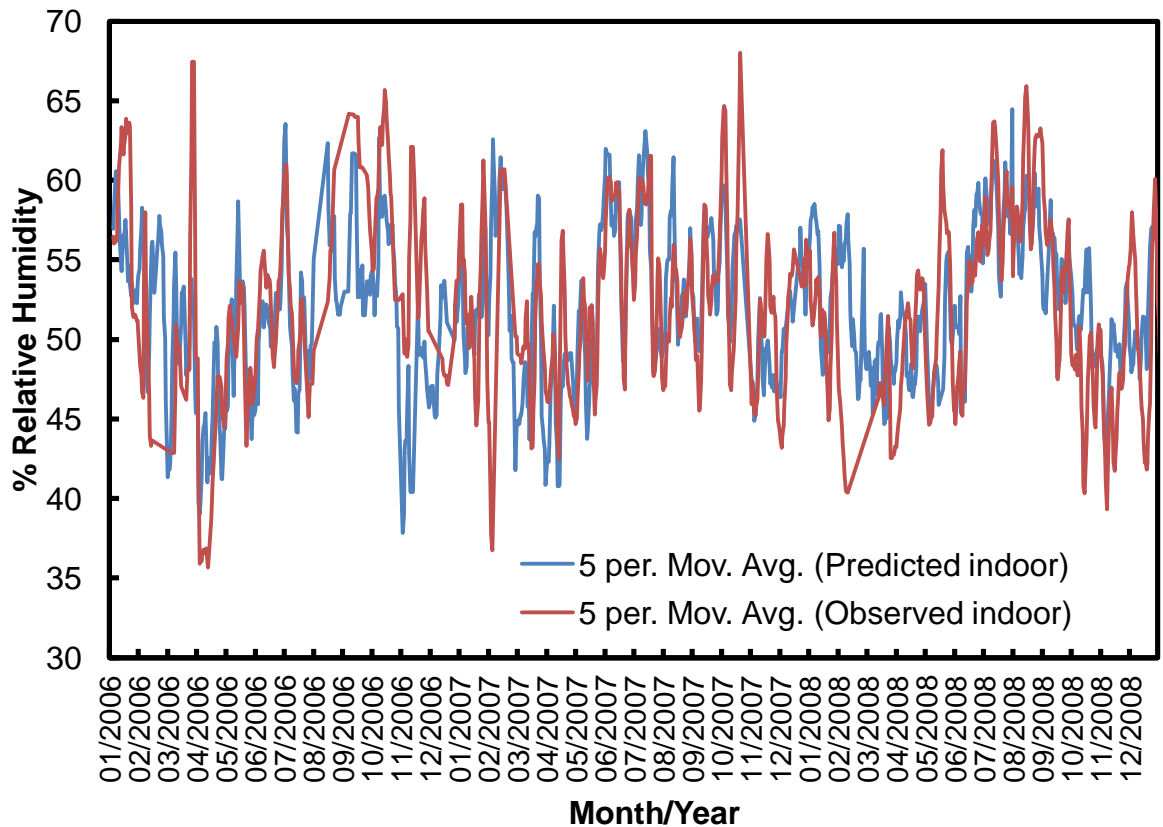


Figure 3.18: Predicted indoor relative humidity calculated from the predicted temperature and specific humidity, compared to the observed relative humidity in the Library at Brodsworth Hall. The relative humidity is plotted as a 5 day moving average.

The observed indoor temperature was used with the predicted specific humidity to calculate the relative humidity, instead of using the predicted temperature. This was done to try and identify problems causing the poor prediction of relative humidity. The result was a greatly improved correlation coefficient (0.66) for the relative humidity prediction, and the equation of the line of best fit was close to being a 1:1 relationship ($y$=1.03$x$-1.18). This is obviously expected somewhat when using the observed temperature, but it helped to identify that the temperature prediction may be an important factor contributing towards the poor relative humidity prediction. Even though the temperature prediction was thought to be acceptable, it may be that a better prediction is required to improve the relative humidity prediction.

It was found that the specific humidity calculation is sensitive to temperature; therefore a small temperature error would propagate to larger relative humidity errors. Therefore further investigation into the temperature prediction was required.

Comparing again the predicted temperature and observed temperature seen previously in figure 3.8 it is apparent that there is error at the extremes, in the summer the temperature is over predicted, and in the winter temperature in under predicted. It was determined that a method was required that would introduce a similar amount of variation to the data, in comparison to the indoor data.

### 3.2.6 Quadratic regression

The first attempt at introducing a similar amount of variation was to apply quadratic regression. Here the quadratic equation that best fitted the outdoor and indoor data when plotted over one year (using the average of the three available values of day 1 and so on), was defined. It was then thought that transformations of the outdoor equation could be implemented until it was an approximation of the indoor quadratic equation. This transformed equation could then be used with the outdoor data to predict the indoor data.

The quadratic equations were described, and some transformations applied to begin the process of transforming the equation. From this investigation, another line of research was determined. The relationship between two similar datasets following a similar pattern may be described with linear regression, as has been used to judge whether previous predictions have been acceptable. So applying an equation in the form $y=ax+b$ to the outdoor data might predict the indoor data, should the two follow a similar form. Where $y$ is the indoor temperature or specific humidity, $x$ is the outdoor temperature or specific humidity, and $a$ and $b$ are the regression coefficients.

### 3.2.7 Linear Regression

Initially simple investigations were carried out to determine the suitability of the technique. Firstly the data was plotted against one another, and the linear equation of best fit determined (see figure 3.19). This included the whole dataset, which was for the Cartoon Gallery at Knole (section 2.2.2) as this had recently been acquired, so the initial investigations used this dataset, spanning from 01/2001-06/2009. Applying the linear equation to the whole of the outdoor data predicted the indoor temperature, which gave a correlation coefficient of $R^2= 0.88$, an improvement upon the previous technique. The line of best fit ($y=0.91x+3.12$) is also close to 1:1, but with the indoor temperature typically warmer than outdoors.

However, the correlation coefficients are not directly comparable as they are from different datasets, but this indicated that it may be an improved transfer process. This was also evidenced from a visual analysis of the prediction (figure 3.20), which appears to reduce the error seen previously early in the dataset, where there was an over estimate of temperature in the summer and an under estimate in winter. However later in the dataset it is difficult to judge, as there are large periods of missing data, where no outdoor data was recorded.
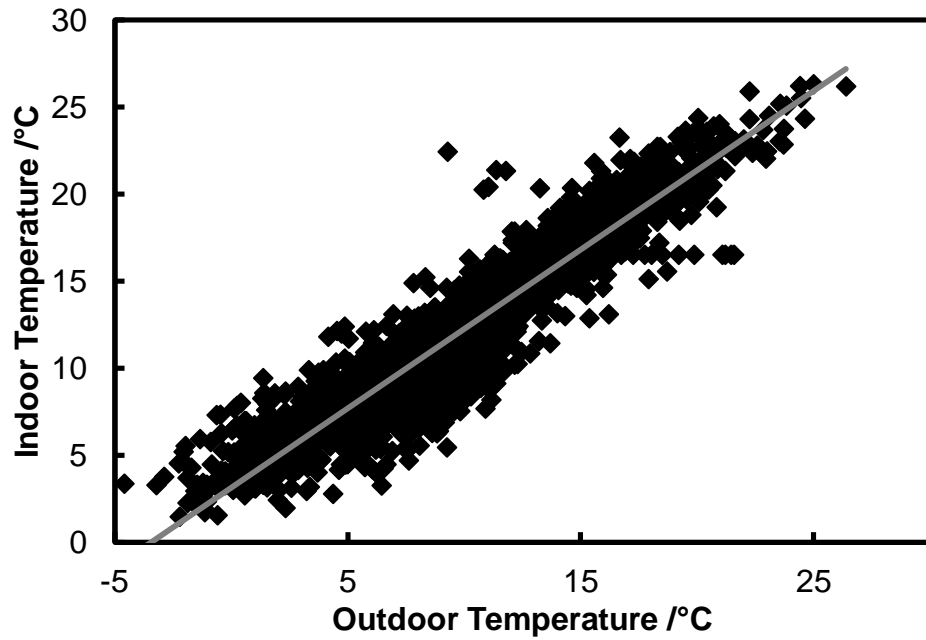


Figure 3.19: Comparison of outdoor temperature observed at Gatwick weather station, to the observed indoor temperature from the Cartoon Gallery. For the period 01/2001-06/2009.
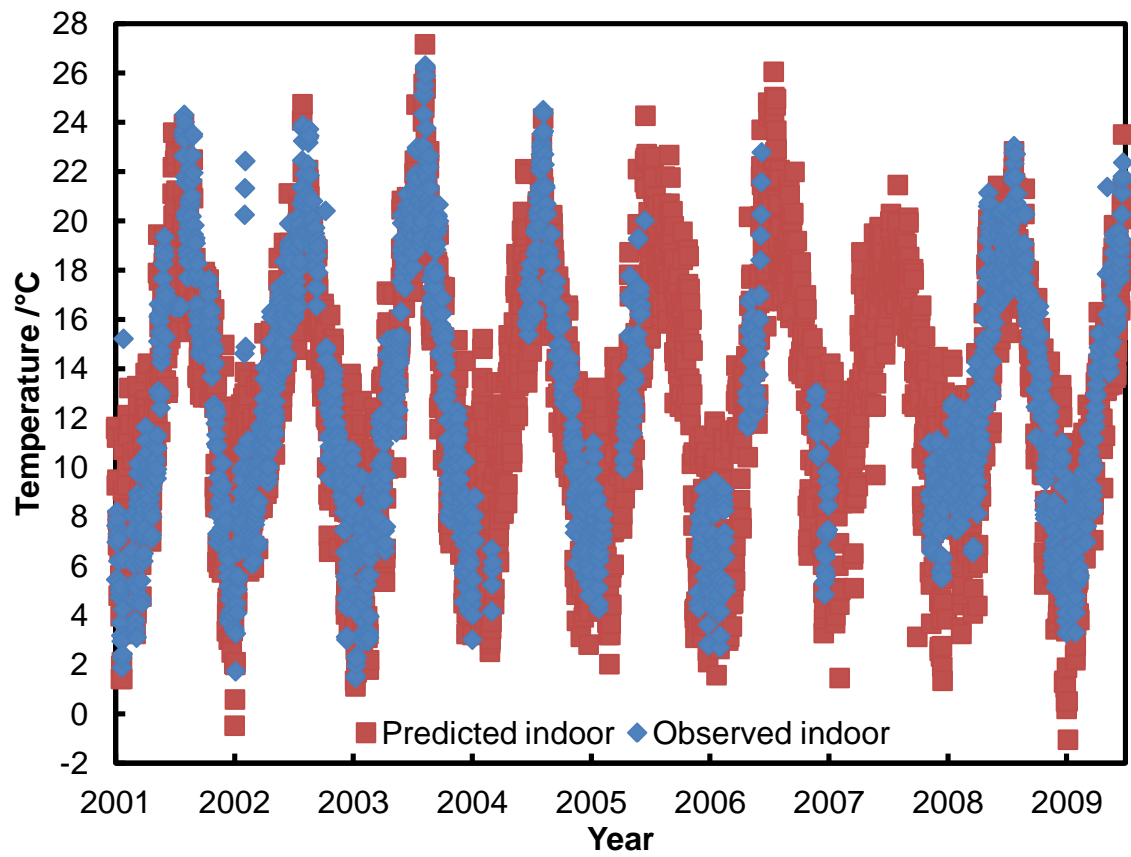
Figure 3.20: Comparison of observed indoor environment at the Cartoon Gallery to initial investigations of predicted indoor data, using a linear regression equation for the whole year. The predictions cover the period 01/2001-06/2009.

Rather than a yearly calibration a monthly one was applied, as used in previous techniques, to see if this improved the temperature prediction further. The monthly calibrations were determined, using the same technique as above, plotting all the data from each month from indoors against outdoors. The different monthly equations were applied to the outdoor data, to predict the indoor environment. This improved upon the previous prediction, with a linear correlation of $R^2 = 0.94$. Figure 3.21 plots the comparison of the observed indoor environment to the predicted environment. This shows an improvement in the areas where there were errors previously, giving an improved prediction of extreme temperatures. The AWK program, to determine the regression coefficients can be found in appendix E.
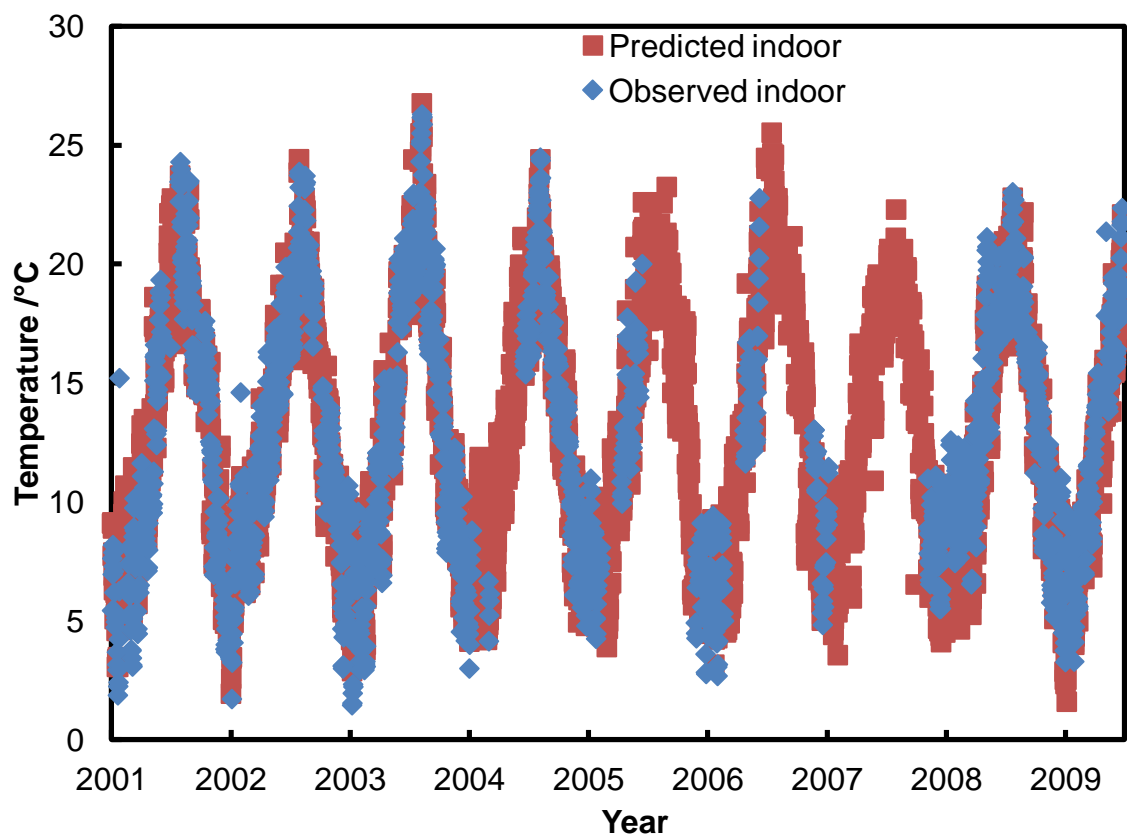


Figure 3.21: Comparison of predicted indoor temperature, using a monthly calibration, to the observed indoor temperature at the Cartoon Gallery. The predictions cover the period 01/2001-06/2009.

With the improvement in temperature prediction it was decided that this technique would also be applied to the specific humidity transfer, and consequently the indoor relative humidity calculated to see how the prediction performed using the new method.

The indoor specific humidity was predicted by applying monthly calibrations to the outdoor specific humidity, in the form of $y=ax+b$. This resulted in the prediction shown in figure

3.22, that has a correlation coefficient of $R^2$=0.93, similar to the result of the previous prediction using the former method, although again not directly comparable as they are different datasets. Again this was close to a 1:1 correlation, with the equation being $y$=0.93$x$+0.0005. This stresses that there is a lower sensitivity, compared to the temperature correlation; the specific humidity is very similar, whether indoors or out. Visually the predictions appear to compare well with the observed data, where there are measurements.
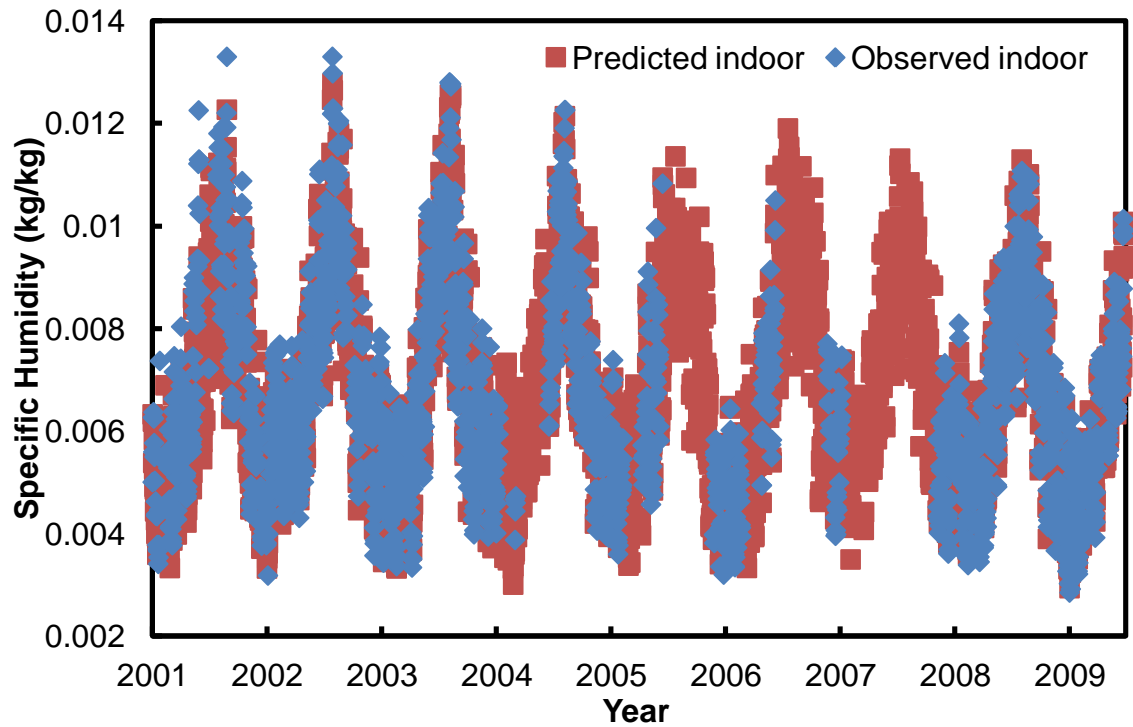


Figure 3.22: Comparison of observed specific humidity in the Cartoon Gallery, to the predicted specific humidity, using a monthly calibration technique of linear equations. The daily averages over the period 01/2001-06/2009 are plotted.

The predicted temperature and specific humidity are used to calculate the predicted relative humidity, and compared to the observed relative humidity, to evaluate this technique. Figure 3.23 compares the two relative humidity datasets. Good correlation is observed between the two datasets, although it is not perfect. The correlation coefficient here has a value of $R^2=0.60$, a significant improvement on the previous best of 0.35, although again not directly comparable as discussed earlier because of the two different datasets used, however comparable data is assessed later.
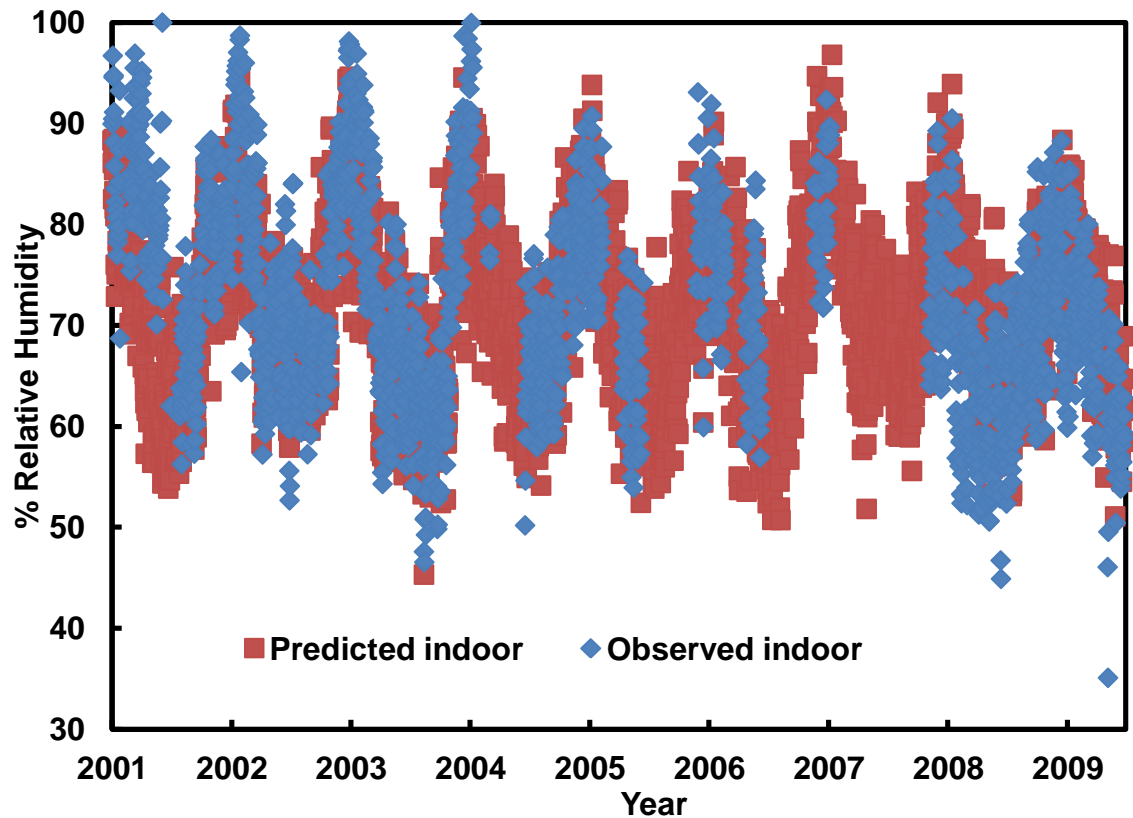


Figure 3.23: Comparison of observed relative humidity of the Cartoon Gallery to the predicted relative humidity, calculated from the predictions of temperature and specific humidity.

In addition to the plots used in the figures presented so far the predicted and observed climates can also be compared using a psychrometric chart, typically used by heating engineers, but previously used in the heritage field (Camuffo, 1998). These plot both the temperature and specific humidity, with additional gridlines of relative humidity also plotted. These are a useful tool in assessing the prediction of indoor climate, for example allowing a quick assessment of climate, to identify potential damage issues.

The predicted indoor temperature and specific humidity of the Cartoon Gallery are shown on a psychrometric chart in figure 3.24. This compares the observed indoor climate, which the prediction is an estimate of, and the observed outdoor climate, which the predictions originate from. The predicted climate exhibits similar characteristics in comparison to the observed indoor climate, although at low temperatures there is some deviation from the observed climate.
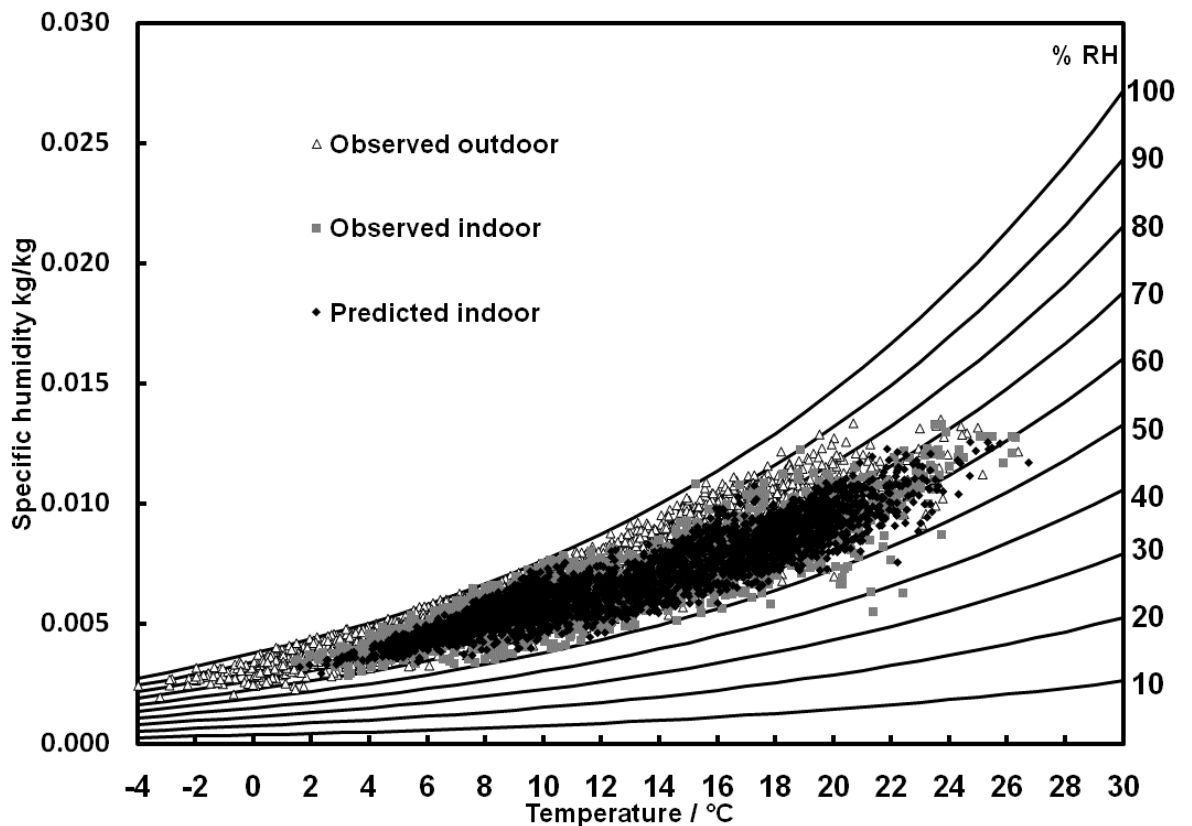


Figure 3.24: Comparison of the observed outdoor climate to the observed indoor climate along with the predicted indoor climate, plotted on a psychrometric chart over the period 01/2001-06/2009.

Assessing the prediction of the environment in general there are some problems, firstly any technique will use an average climate to determine the calibration, therefore when this is applied to one specific year there will immediately be error introduced. This is because the climate will undoubtedly be different from the average, thus to get the most reliable predictions a representative average climate is required. Typically 30 year averages are used, but as discussed previously it is very difficult to get near 30 years of data of indoor measurements from a historic house. Therefore some error must be accepted, and this will be true for both the temperature and specific humidity prediction. So the error will be two fold, and when these are used to calculate the relative humidity this error is introduced

into the prediction of relative humidity. Even though there are inherent errors with the predictions of the indoor climate it is possible to get realistic projections.

*Brodsworth Hall*

The transfer function has been initially developed using the data from the Cartoon Gallery at Knole, it is important to also test the technique at the Library of Brodsworth Hall, to allow for a like for like comparison of the techniques. Figure 3.25 compares the observed indoor temperature of the Library at Brodsworth Hall, to the indoor prediction using the transfer function, with monthly coefficients calibrated for this location. Good correlation between these are observed, and the correlation coefficient is also good, $R^2$=0.88, with the equation of best fit observing a 1:1 relationship ($y=x$-0.05). This improves on the previous technique, which had an $R^2$=0.81, also visually it appears to be a better prediction of the observed temperature, with less variation around the observed values.
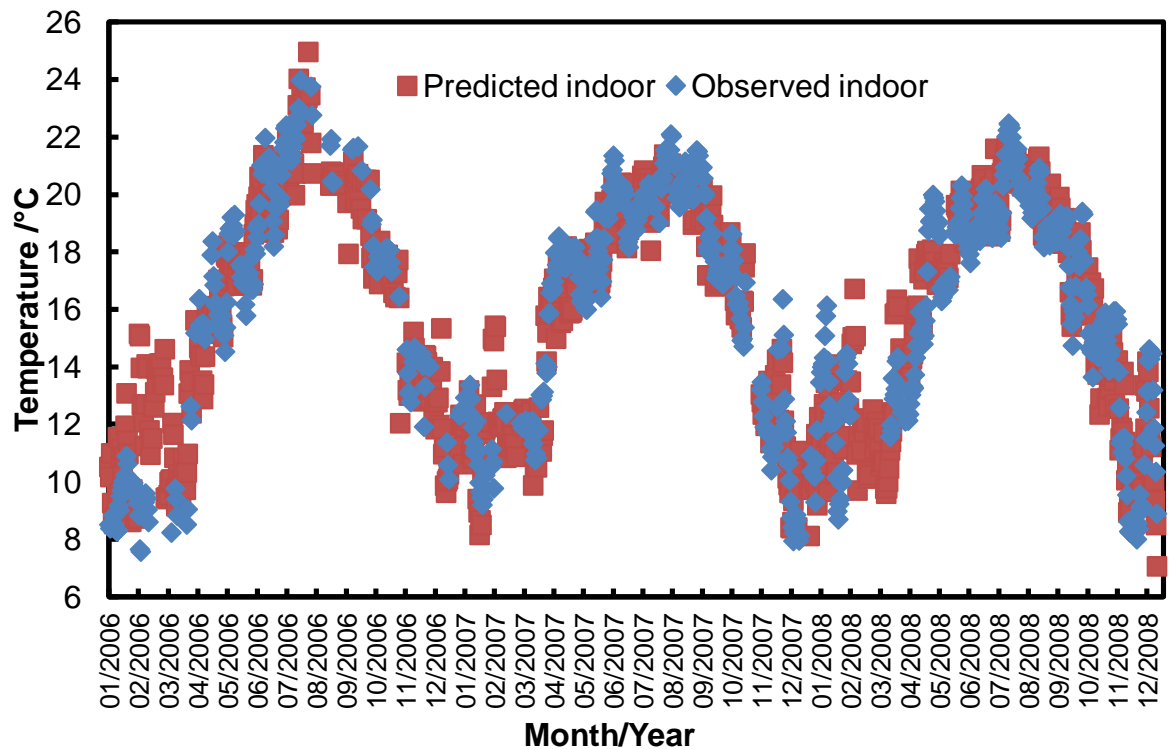


Figure 3.25: The observed temperature of the Library at Brodsworth Hall compared to the predicted temperature over the period 01/2006-12/2008.

The prediction of specific humidity is shown in figure 3.26, again good correlation is observed, $R^2$=0.91. This is very similar to the previous prediction ($R^2$=0.92) that used a ratio to predict the specific humidity at Brodsworth Hall. However here the equation of best fit ($y=x$-0.0005) is closer to a 1:1 fit than the previous method (specific humidity ratio transfer section 3.2.5). Both the temperature and specific humidity predictions are

acceptable, however it is the relative humidity prediction that has previously been
challenging.
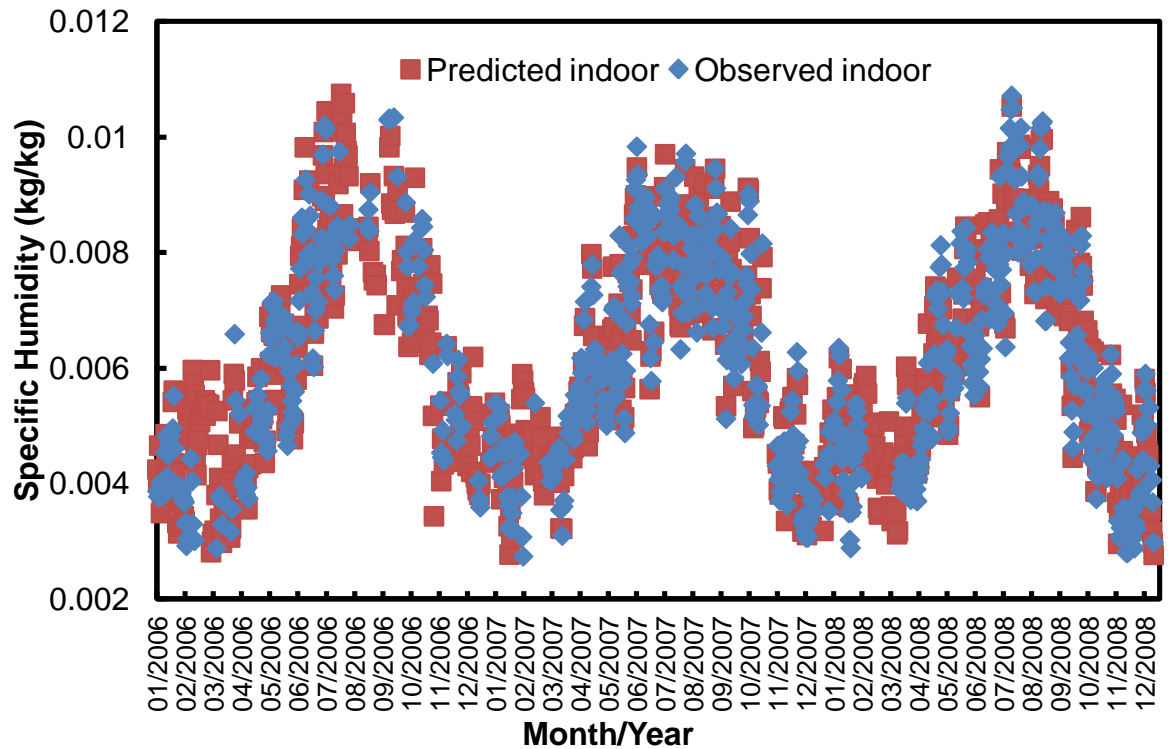


Figure 3.26: Comparison of the observed and predicted indoor specific humidity at
Brodsworth Hall, from 01/2006-12/2008.

The prediction of indoor relative humidity, calculated from the predicted temperature and
specific humidity is compared to the observed relative humidity in figure 3.27, using a five
day moving average as the daily averages are difficult to interpret. Good correlation is
observed for some periods, but occasionally the prediction deviates from the observed.
Some of these deviations appear to be during the February and March periods, which
have been highlighted previously as problematic. Other areas where there appears to be
no correlation is occasionally where there are no observations, and are therefore are not
significant. One such area is August to September 2006.

The correlation coefficient for this prediction of relative humidity is $R^2=0.65$, again a
significant improvement on the previous prediction for the Library ($R^2=0.35$). If February
and March are excluded from the comparisons, because of the problems with these
months, this improves the correlation coefficient for the relative humidity prediction to
$R^2=0.72$.
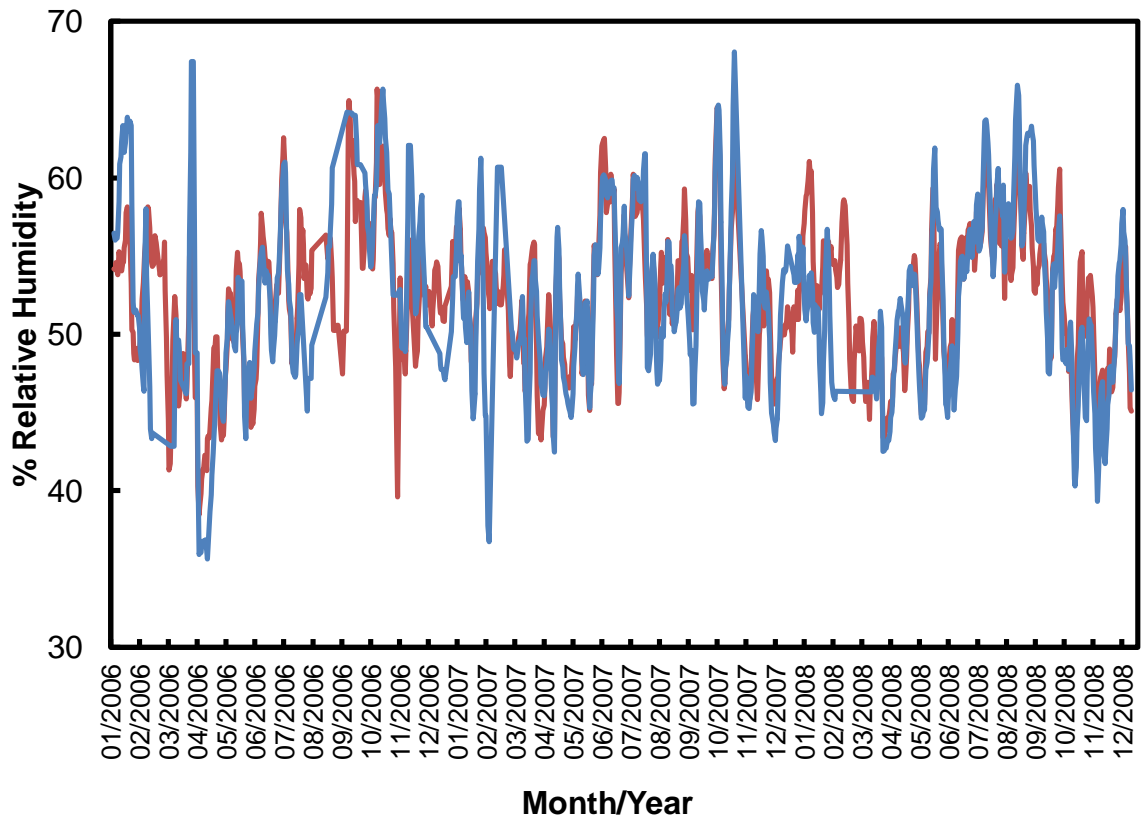
Figure 3.27: Comparison of the predicted and observed relative humidity in the Library at Brodsworth Hall, over the period 01/2006-12/2008. The relative humidity is plotted as a five day moving average, to help visualise the trends of each dataset.

The comparison of the transfer function for predicting the indoor environment to the previous best technique, the lagged function (section 3.2.5), shows large improvements, particularly in the relative humidity predictions. The predictions are not ideal, and some reasons for better predictions being unattainable have been discussed.

It may be possible that the current technique, from here on called the transfer function, could be improved upon. Applying techniques such as already investigated, or alternatives may improve the technique further. However the current method predicts the indoor environment effectively, so this approach was adopted. Improvements to the technique could present future work. Additionally it is possible to determine the range of observed values from a given predicted value, as discussed next.

It is important to remember that the transfer function must be calibrated for each individual room, to account for variables in the building construction, and that it is calibrated on a monthly basis to allow for the variation in climate and use of the building. While the transfer function has been validated with observed data, future climate projections may fall outside this range, particularly at the higher temperatures. Therefore the relationship

under such conditions is not fully understood and may not be well represented by the transfer function. It is unlikely to be the norm that the temperature exceeds the calibration range throughout the year. Even so it does not appear that the system is particularly non-linear, thus serious problems with extrapolation would not be expected. It is believed that the transfer function will work well in a changed climate.

### 3.2.8 Confidence assessment

An assessment has been carried out for three of the locations described previously, to determine the range that the observed values falls in, for a given predicted value. The Leicester Gallery was assessed first, the regression line of best fit was determined, along with the 95% confidence intervals. The coefficients of the upper and lower confidence intervals allow for the range of expected observed values to be determined for a given predicted value. Figure 3.28 shows the observed and predicted temperature in the Leicester Gallery, for the period 05/2003-12/2008, with the line of best fit plotted, along with the confidence intervals. The ranges of possible observed values for various predicted temperatures are shown in table 3.2.  The equations that fit the confidence intervals are shown in figure 3.28, allowing for other ranges to be established.
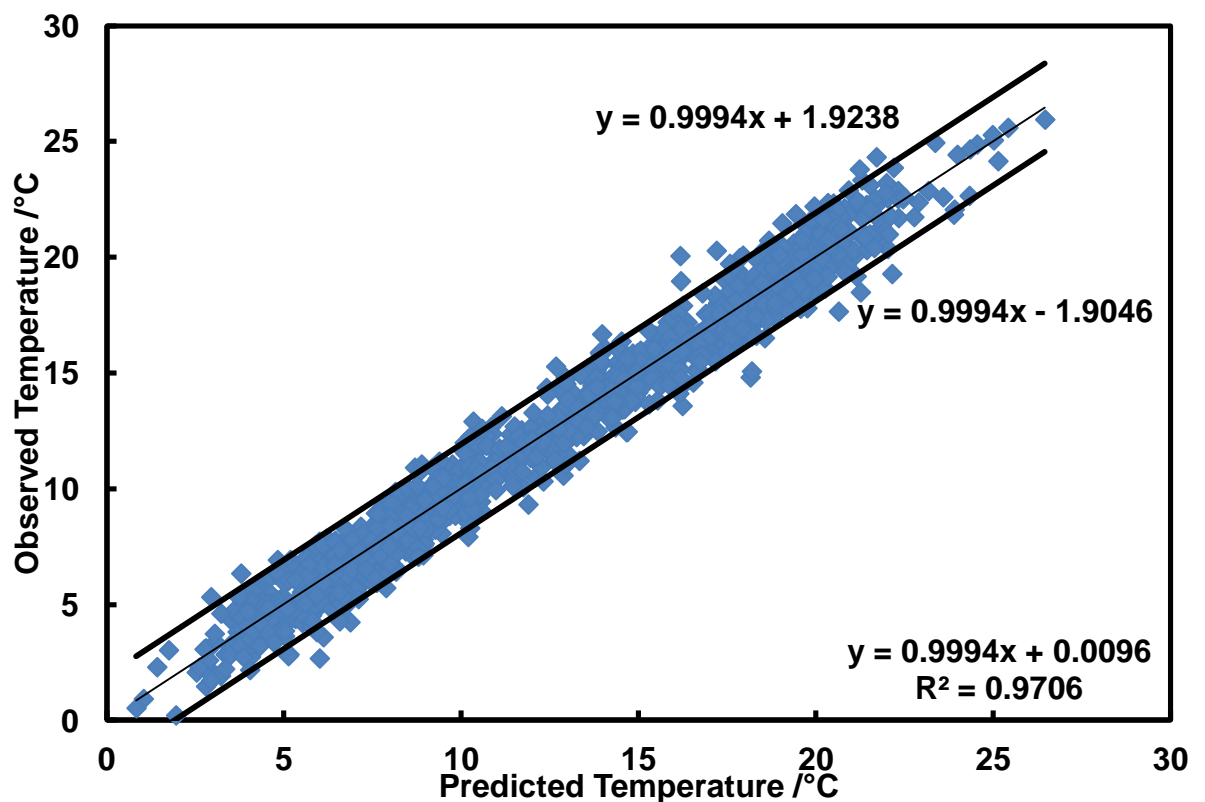


Figure 3.28: Comparison of the predicted and observed temperature in the Leicester Gallery at Knole. The 95% confidence interval lines are shown, each with the associated

equation. The line of best fit is also shown, with the equation and correlation coefficient, in the bottom right corner.

Table 3.2: 95% confidence interval ranges of temperature for the predicted temperature, in the Leicester Gallery at Knole.

| Predicted Temperature | Lower 95% CI | Upper 95% CI | Predicted Temperature | Lower 95% CI | Upper 95% CI |
|---|---|---|---|---|---|
| 1 | -0.91 | 2.92 | 16 | 14.09 | 17.83 |
| 2 | 0.09 | 3.91 | 17 | 15.09 | 18.82 |
| 3 | 1.09 | 4.91 | 18 | 16.08 | 19.82 |
| 4 | 2.09 | 5.90 | 19 | 17.08 | 20.81 |
| 5 | 3.09 | 6.89 | 20 | 18.08 | 21.80 |
| 6 | 4.09 | 7.89 | 21 | 19.08 | 22.80 |
| 7 | 5.09 | 8.88 | 22 | 20.08 | 23.79 |
| 8 | 6.09 | 9.88 | 23 | 21.08 | 24.79 |
| 9 | 7.09 | 10.87 | 24 | 22.08 | 25.78 |
| 10 | 8.09 | 11.86 | 25 | 23.08 | 26.77 |
| 11 | 9.09 | 12.86 | 26 | 24.08 | 27.77 |
| 12 | 10.09 | 13.85 | 27 | 25.08 | 28.76 |
| 13 | 11.09 | 14.85 | 28 | 26.08 | 29.76 |
| 14 | 12.09 | 15.84 | 29 | 27.08 | 30.75 |
| 15 | 13.09 | 16.83 | 30 | 28.08 | 31.74 |

The 95% confidence ranges shown in table 3.2 indicate where the actual observed value may lie. Therefore this can be used to determine the likely range that the true value would lie within, which can also be used with future predictions. Considering that the majority of the data is taken into account with the 95% confidence intervals, a range of the approximately ±2°C, at the daily average scale shows good reliability of the transfer function.

The confidence intervals were also determined for the relative humidity in the Leicester Gallery; the range of observed values for each predicted value is shown in table 3.3. The equation for the lower 95% confidence interval is $y=0.85x+0.52$, and $y=0.85x+20.72$, for the upper 95% confidence interval. The possible error here is quite large, but this is due to

the problem discussed previously, that the errors from the temperature and specific humidity predictions are combined.

Table 3.3: 95% confidence interval ranges of relative humidity for the predicted relative humidity, in the Leicester Gallery at Knole.

| Predicted Relative Humidity | Lower 95% CI | Upper 95% CI | Predicted Relative Humidity | Lower 95% CI | Upper 95% CI |
|---|---|---|---|---|---|
| 5 | 4.8 | 25.0 | 55 | 47.5 | 67.7 |
| 10 | 9.1 | 29.3 | 60 | 51.8 | 72.0 |
| 15 | 13.3 | 33.5 | 65 | 56.1 | 76.3 |
| 20 | 17.6 | 37.8 | 70 | 60.4 | 80.6 |
| 25 | 21.9 | 42.1 | 75 | 64.6 | 84.8 |
| 30 | 26.2 | 46.4 | 80 | 68.9 | 89.1 |
| 35 | 30.4 | 50.6 | 85 | 73.2 | 93.4 |
| 40 | 34.7 | 54.9 | 90 | 77.5 | 97.7 |
| 45 | 39.0 | 59.2 | 95 | 81.7 | 101.9 |
| 50 | 43.3 | 63.5 | 100 | 86.0 | 106.2 |

In table 3.3 where the humidity range is shown to exceed 100% this would be set to 100% rather than state an impossible value.

The other two locations, the Cartoon Gallery at Knole and the Great Hall at Canons Ashby were also assessed, and the 95% confidence intervals determined, the principle is the same as described for the Leicester Gallery, with different ranges, which are shown in tables 1-4 in appendix B . These tables show that each location behaves differently, and that some predictions are more effective than others, this is likely to depend on the quality and length of the original data available.

Again it is important to note that ideally validation would be carried out with an independent time period. Due to data constraints this has not been possible. Therefore it is possible that this assessment is an overstatement of the reliability of the model when used with a different time period.

Subsequently Coley and Kershaw (2010) have provided evidence that the transfer function adopted here is a viable method for predicting indoor climate from the outdoor climate. They found that the relationship between external and internal temperature

increases, due to climate change, are linear. This supports the approach used here for the temperature prediction. Coley and Kershaw (2010) apply their method to various types of buildings, such as offices, schools, apartments and houses, with the amplification coefficient varying between buildings. This provides some scope for applying the transfer function to other types of buildings, not historic houses alone. It may also be suggested that this will allow for assessment of buildings with alternative heating scenarios, rather than those currently assessed, which have no heating.

## 3.3 Comparison of the transfer function and EnergyPlus

While the purpose of the research was to determine a simplified model, rather than use an available building simulation program, it is useful to compare the results of the two methods. The EnergyPlus model used in the work by Taylor et al. (2005) is used here to predict the environment within the Library at Brodsworth Hall, and subsequently the two techniques will be evaluated.

### 3.3.1 EnergyPlus

EnergyPlus requires an input file which includes all of the architectural, mechanical and electrical data, such as the geometry and HVAC descriptions, this is known as the IDF file (Monfet et al., 2007). In previous research an EnergyPlus model has been developed for the Library at Brodsworth Hall (Taylor et al., 2005), this is one of the case study locations used in this research (section 2.2.1). This EnergyPlus model will be used to predict the indoor environment, for comparison with the transfer function.

The Brodsworth Hall EnergyPlus model was designed with an older version of EnergyPlus, therefore it required updating to use with the version available at the time of the research. This involved no adjustment of the actual model that describes the Library, just a rearrangement of parameters that were in different locations in the newer version of the software. A detailed description of the EnergyPlus model for Brodsworth Hall can be found in appendix B. One of the important parameters is the air exchange rate, this was measured using a SF6 tracer gas decay method, and found to be 0.56 air changes per hour, somewhat lower than expected.

In addition to the IDF file describing the building a weather file is also required as discussed previously. EnergyPlus was developed to model buildings before their construction, so weather files represent a typical year. This allows the building behaviour to be understood over a range of typical conditions for the specific location (Crawley et al., 2000, Crawley et al., 1999). The weather file can be a continuous file of real weather data,

but with a maximum length of one year. In this work three separate weather files were assembled for the years 2006-8, the period that measured outdoor data was available at Brodsworth Hall.

The weather files consist of a number of elements, for each hour there are values of: temperature, dew point temperature, relative humidity, atmospheric pressure, wind speed, wind direction, global solar irradiation and direct irradiation amount. The temperature and relative humidity are available from the observations at Brodsworth. The dew point can be calculated from temperature and relative humidity using equation 3.7, available from Lawrence (2005).

$$t_d = \frac{B_1 \left[ \ln \left( \frac{RH}{100} \right) + \frac{A_1 t}{B_1 + t} \right]}{A_1 - \ln \left( \frac{RH}{100} \right) - \frac{A_1 t}{B_1 + t}}$$

**(Eq. 3.7)**

In equation 3.7, $t_d$ = dew point temperature, $A_1$ = 17.625, $B_1$ = 243.04 and $t$ = temperature in °C. The AWK program for this calculation can be found in appendix E.

The other parameters are slightly more difficult to obtain, the British Atmospheric Database Centre (BADC) (UK Meteorological Office, 2006) have a database called MIDAS land surface stations data that contains historic and recent weather data. Fortunately there was a local weather station nearby to Brodsworth Hall, at Church Fenton that measured the required data. This is approximately 5km away from Brodsworth, and the station identification number from the database is 533. This is the closest approximation to the actual data at Brodsworth Hall, and without measuring these at the site it is not possible to validate the accuracy of these measurements.

Initially the weather files were tested with EnergyPlus, to ensure they worked. However with the correct gap place marker for the temperature and relative humidity observations, here -999, the model terminated before completion, because there were too many gaps. So the decision was made to remove the -999 gap markers to allow the model to run without terminating prematurely.

This allowed the model to run fully, with each weather file, predicting the indoor temperature and relative humidity for the period 2006-08, this is shown in figures 3.29 and 3.30, in comparison to the observed data of the Library.

Figure 3.29 shows the pattern of the predicted temperature that appears to follow the observed data, where there are peaks and troughs these are generally replicated. This

agreement is reflected in the correlation coefficient, $R^2$=0.865. If it was not for one other problem the $R^2$ value while not being excellent, would be acceptable and within the expected accuracy. However, it is immediately obvious when looking at the graph that the predicted temperature is consistently lower indoors, throughout the whole three years, than the observed values by a number of degrees. This difference is quite significant; the equation of the line of best fit helps provides evidence of this. The equation is $y$=0.96$x$+4.09, indicating that the predicted temperature is roughly four degrees out, this obviously varies, but gives a guide to the error.
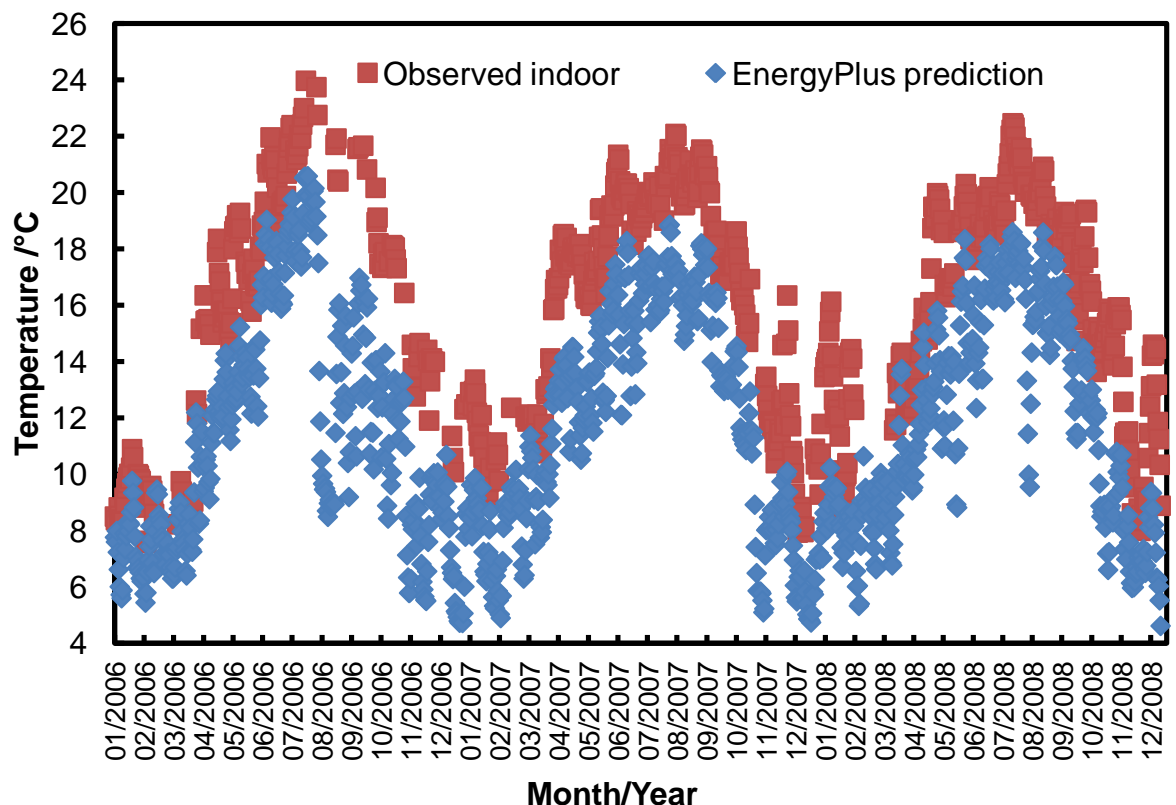


Figure 3.29: Predicted indoor temperature from EnergyPlus, compared to the observed temperature in the Library at Brodsworth Hall over the period 01/2006-12/2008.

The EnergyPlus relative humidity prediction for the years 2006-08 at the Library of Brodsworth Hall is shown in figure 3.30. Firstly there are a lot of data points that have a very low relative humidity, even some at zero, which is very unlikely. It would appear that these arise when gaps in the outdoor data exist, and that EnergyPlus fails to deal with this effectively when the gap markers are removed, this is a serious issue. Neglecting this for the moment, the main bulk of the data would appear to be between 40/45% RH and approximately 90% RH. The lower band is not too different from the observed data; however the upper limit is considerably higher than the maximum of the observed data, at

about 65% RH. Effectively the relative humidity prediction is unusable, as it has no useful relationship to the observed data; this is evidenced by a poor $R^2$ value of 0.115.
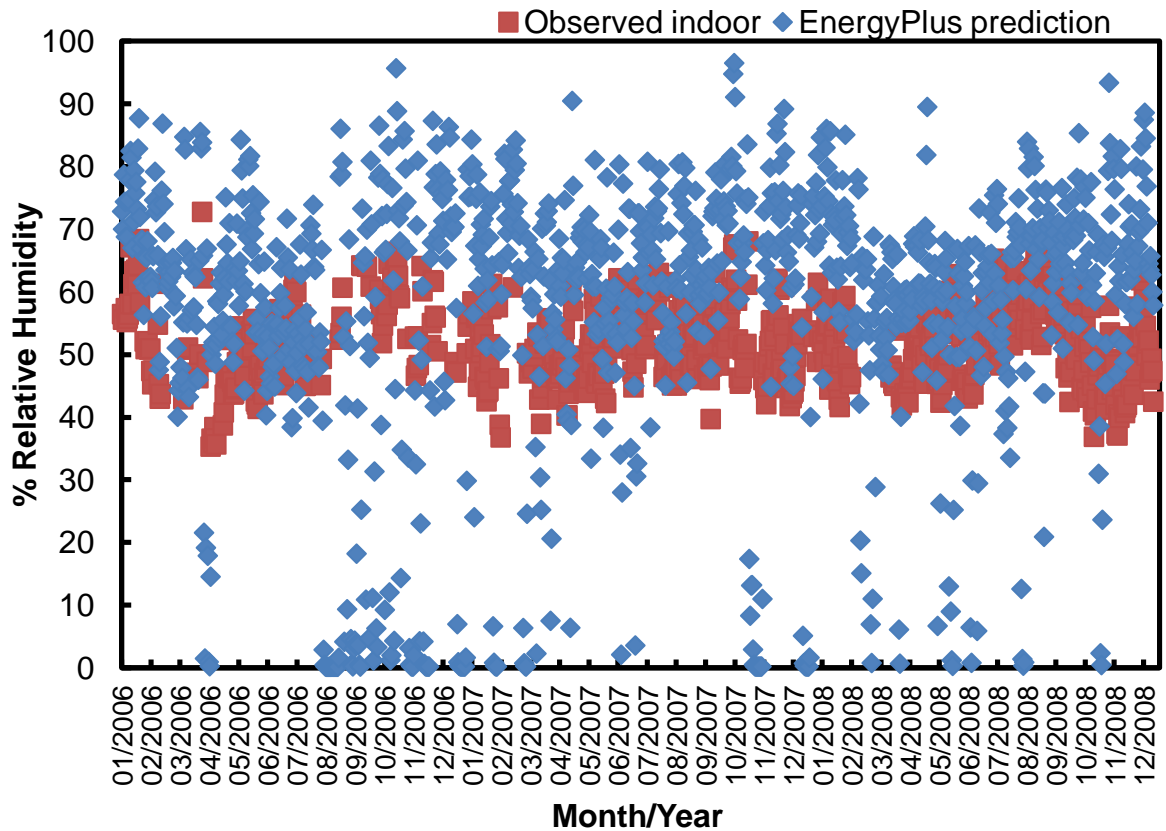


Figure 3.30: Predicted indoor relative humidity from EnergyPlus, compared to the observed relative humidity indoors in the Library at Brodsworth Hall over the period 01/2006-12/2008.

The poor predictions of relative humidity probably arise from the gaps in the data outdoors, where there are no observations. It appears that the gaps are taken to be 0% relative humidity, therefore the indoor prediction quickly moves towards this. It was decided that the last observations of temperature and relative humidity before a gap would be used for each following missing observation. This is a simple gap filling method that allows the model to run to completion, this was deemed adequate as most gaps were only a few hours, overall more than 95% of the data is available. There are alternative solutions to filling gaps in data, but these were not implemented here. One alternate solution could be to produce a reference year weather file, as typically used with EnergyPlus. However this would not allow for direct comparison to observed indoor data.

The prediction of temperature and relative humidity following the application of the technique above is compared to the observed data in figures 3.31 and 3.32.
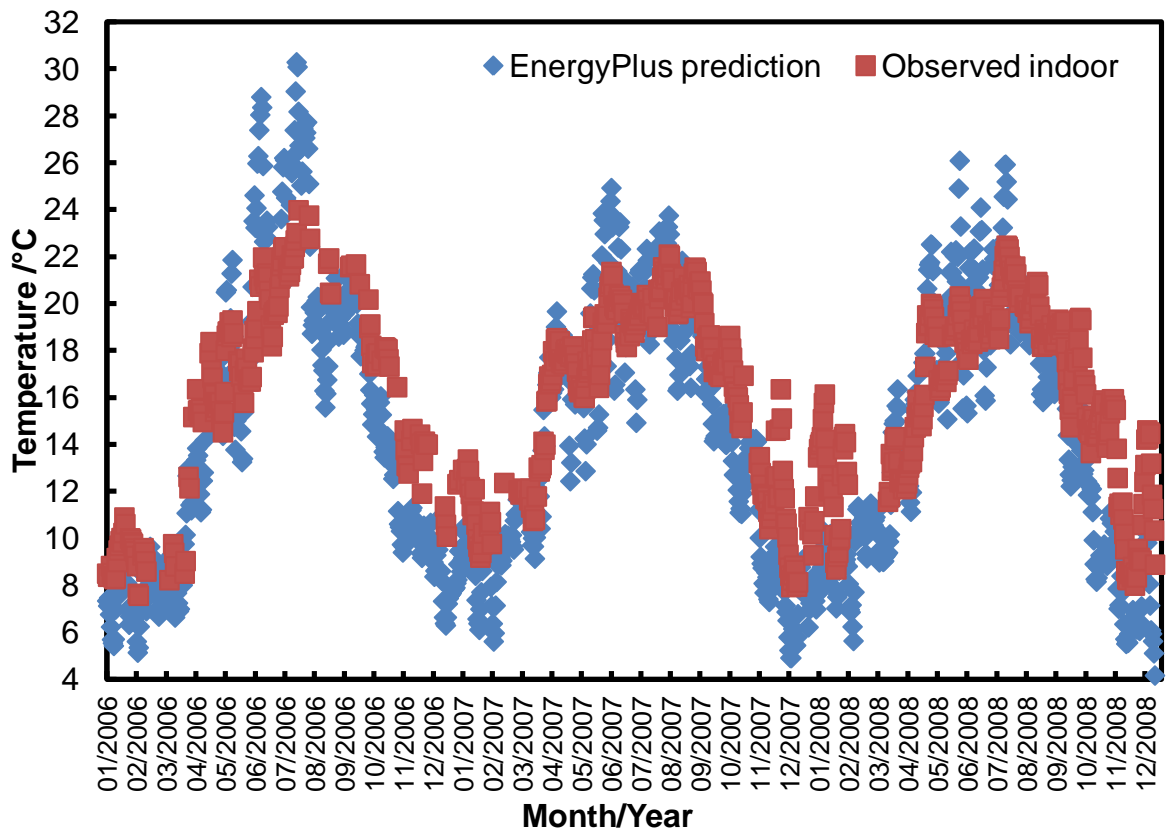
Figure 3.31: Predicted indoor temperature from EnergyPlus, compared to the observed temperature indoors in the Library at Brodsworth Hall over the period 01/2006-12/2008.

The predicted temperature from EnergyPlus, with gaps filled is plotted in figure 3.31. The temperature no longer follows the annual trend as well as previously, for example the summer temperature exceeds the observed by some way. However the prediction for most of the year now appears to have a better relationship than previously, before it was about 4 degrees low for the majority of the time, although the prediction is still not ideal. The correlation coefficient is quite good ($R^2$=0.84), but the equation of the line ($y$=1.28$x$-5.75) means the relationship is not 1:1.

Poor predictions of relative humidity improves after filling the gaps in the data, but as seen in figure 3.32 shows the prediction is still poor ($R^2$=0.25). The relative humidity prediction is consistently too high, as it was previously, so it is unlikely that the method used to fill the gaps has caused this.
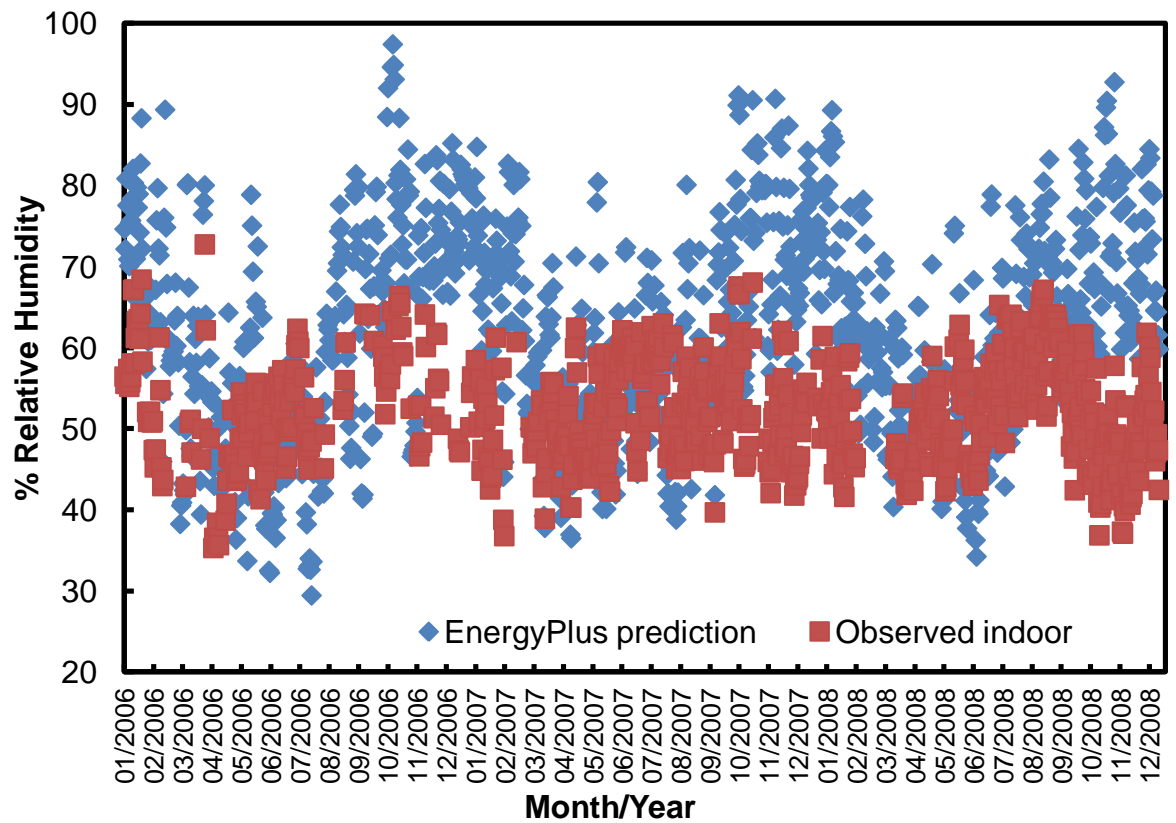
Figure 3.32: Predicted indoor relative humidity from EnergyPlus, compared to the observed temperature indoors in the Library at Brodsworth Hall over the period 01/2006-12/2008.

This simple method of gap filling was initially used as an attempt to get the model working. It succeeded, and highlighted that the EnergyPlus model still doesn't predict the environment satisfactorily. Other techniques are available to fill gaps in data sets, which might help, but were not explored.

Predictions from the EnergyPlus model of temperature and relative humidity are not acceptable. The main problem is with the relative humidity. An EnergyPlus specialist may be able to recalibrate the model so that it works effectively, however this has been carried out in the past, so there is no reason why the model shouldn't work effectively.

### 3.3.2 Comparison of EnergyPlus and the Transfer Function

The EnergyPlus model for the Library at Brodsworth Hall was compared to the observed data. It is also necessary to compare it to the transfer function derived previously (section 3.2.7). Figure 3.33 and 3.34 show the predictions of temperature and relative humidity respectively, from both the transfer function and the EnergyPlus model, in comparison to

the observed environment over the period 01/2006-12/2008 for which the EnergyPlus predictions are available.
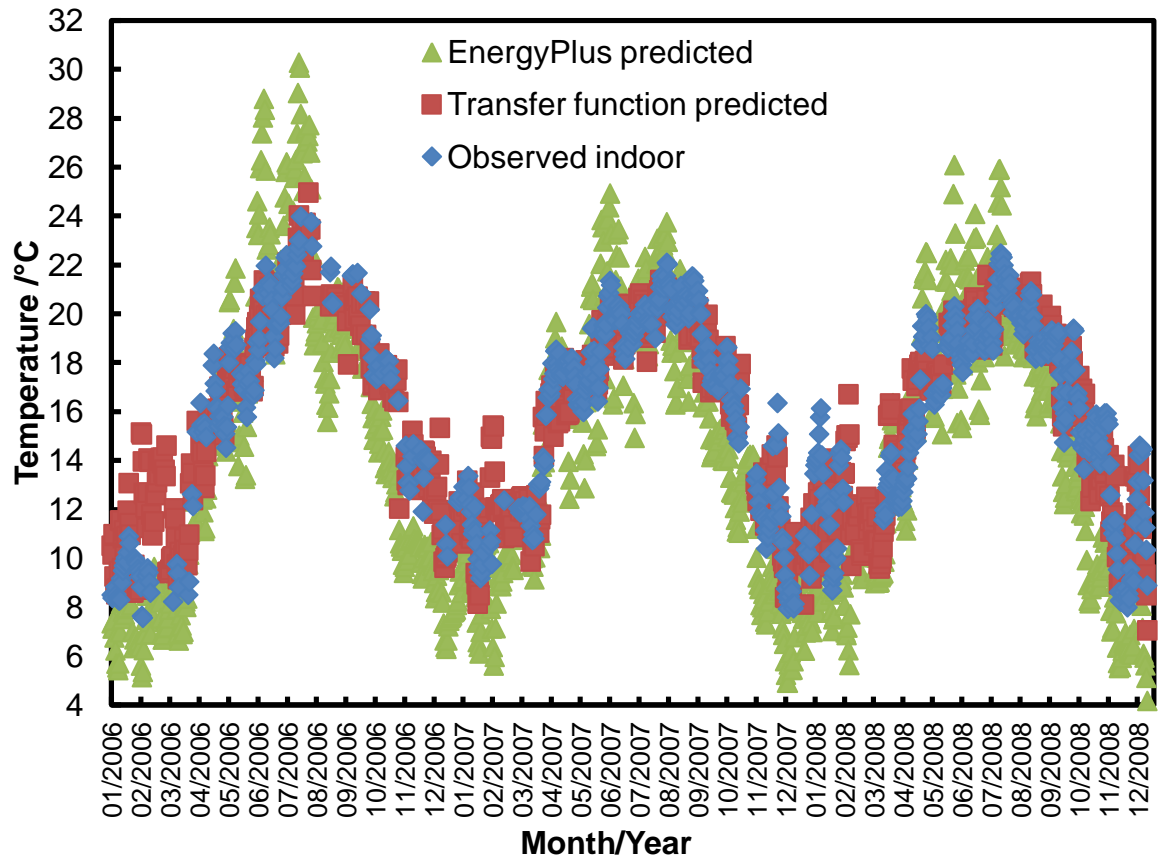


Figure 3.33: Comparison of temperature predictions indoors for the Library at Brodsworth Hall for the period 01/2006-12/2008. The transfer function is compared to the EnergyPlus model, and to the observed data.

It is immediately apparent from figure 3.33 that the predicted temperatures from the transfer function are more closely matched than the predictions from EnergyPlus. While the $R^2$ value for the transfer function to observed data comparison is only slightly better than that of the EnergyPlus (0.88 and 0.84 respectively), the equations of the lines of best fit tell another story. The regression equation for the transfer function comparison is $y=1.01x-0.25$, indicating an almost 1:1 relationship. The equation for the EnergyPlus comparison is $y=1.28x-5.75$, indicating a significantly worse agreement.
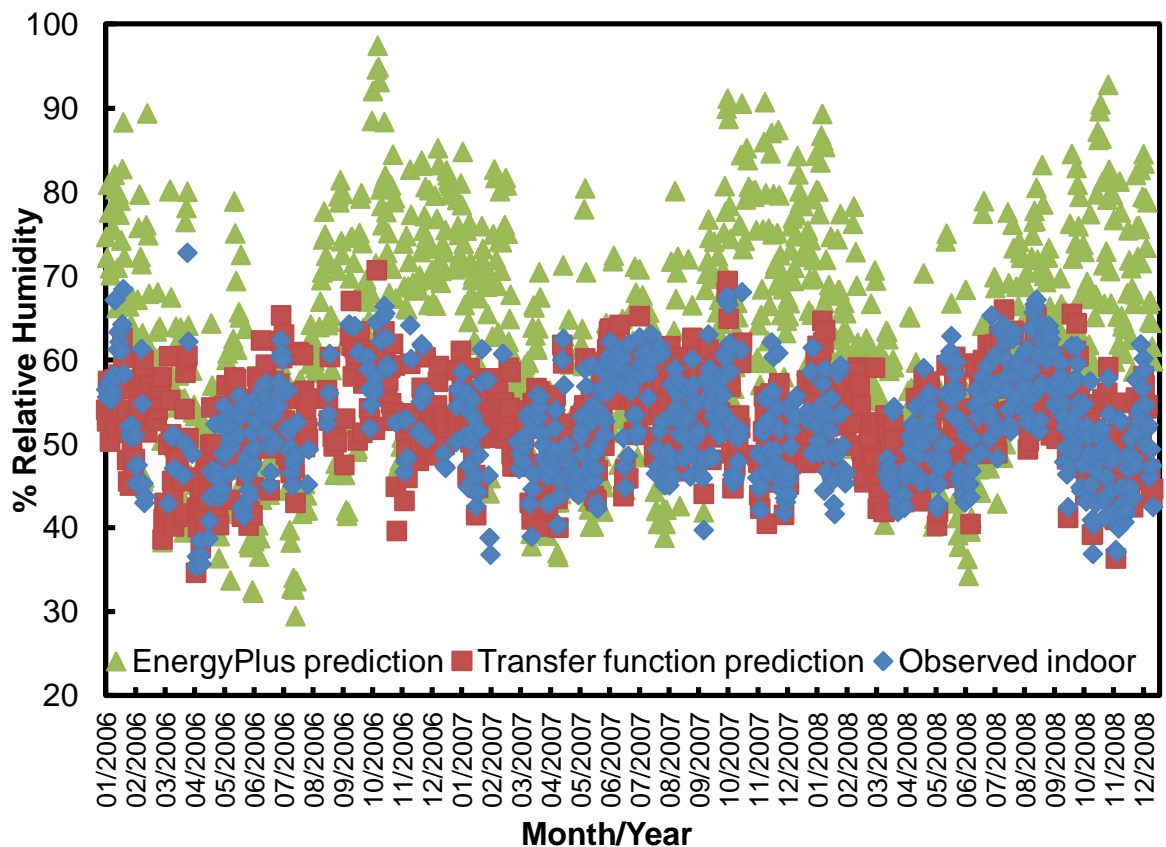
Figure 3.34: Comparison of relative humidity predictions indoors for the Library at Brodsworth Hall for the period 01/2006-12/2008. The transfer function is compared to the EnergyPlus model, and to the observed data.

The comparison of predicted relative humidity is shown in figure 3.34. Again it is immediately apparent which method performs best. The prediction from the transfer function appears to follow the general pattern of the observed relative humidity, staying roughly within the same boundaries of the observed data. The $R^2$ value for the transfer function to observed data here is 0.65, compared to 0.25 for the EnergyPlus comparison. The quoted $R^2$ values for the transfer function also include the months of February and March, where there is insufficient data to correctly apply the transfer function for the three year data set, as described previously. Thus it will underperform and may reduce the effectiveness of the prediction for these months, resulting in a lower $R^2$ value.

From the analysis of the two prediction models it can be concluded that the transfer function outperforms the EnergyPlus model available, providing reliable predictions that are an acceptable reproduction of the observed environment.

The EnergyPlus model has been previously used in other research (Taylor et al., 2005), and was built by a building scientist. In the published research it is difficult to determine

how good the prediction of temperature and relative humidity was, as there is no discussion of this. Also the graph that presents the results plots both temperature and humidity, thus the scale is quite small so differences in temperature are difficult to see. However the relative humidity is somewhat easier to see, and there are some differences, the most notable in the summer.

It appears likely that there is a significant problem with this EnergyPlus model, as it is expected that this should work better, however without the expertise of a building scientist it is not possible to improve this further. An investigation into the model indicates that the option for a humidistat, as used in conservation heating is not selected, and could be the reason why the relative humidity prediction is poor, as it is not limited as seen in the observations. Modification of the model could present further work. However if it was improved it is possible that the transfer function may still out perform EnergyPlus. Additionally EnergyPlus is not rapidly applicable in the way that the transfer function is, which is a disadvantage.

## 3.4 Conservation Heating Issue

The transfer function may not be applicable where conservation heating is implemented, this is used in the Library at Brodsworth Hall. Fitting coefficients from the transfer function may vary when conservation heating is used under different climate regimes. Currently the coefficients are established from the mathematical relationship between indoor and outdoor data. Conservation heating controls humidity by increasing the temperature (section 7.1), so if humidity changes in the future then the temperature will also change. The current relationship between indoor and outdoor temperature will alter, having an effect on the regression coefficients, which will change. Thus the current transfer function cannot be used where conservation heating is applied.

This raises some problems, as the Library at Brodsworth has been used in determining the transfer function. However it has been shown that the transfer function is applicable at other locations, where there is no heating. Additionally the transfer function is valid at Brodsworth Library currently, as it is calibrated for this period, but it may not be in the long term future if the relative humidity changes. Thus the comparison to EnergyPlus is also still valid, as it is carried out over the period for which the transfer function is calibrated.

The possibility of the transfer function not being applicable in the future poses a problem. It was decided that a work around of the problem would be attempted so that projections of future damage could be undertaken for rooms with conservation heating.

Further data was gathered from two properties, Canons Ashby and Chasleton. At both locations there are instances of rooms with conservation heating and rooms that are unheated. Additionally at Brodsworth Hall data from the Dining Room was collected, which is unheated currently, due to a fault with the heating system. This further data allowed for comparison between outdoor data, and data for rooms with and without conservation heating. It became apparent that the conservation heating in the Library at Brodsworth does not appear to be working as effectively/efficiently compared with other locations (Figure 3.35). The range of data at Brodsworth is greater than the other two locations, with a considerable amount of the data well below the set point value (RH≈60%), and the variation in the data is higher. Chasleton has very little variation day to day while Brodsworth shows larger variation. The three sets of data compared in figure 3.35 are not over the same time period; hence the axis is presented in days rather than a specific time frame.
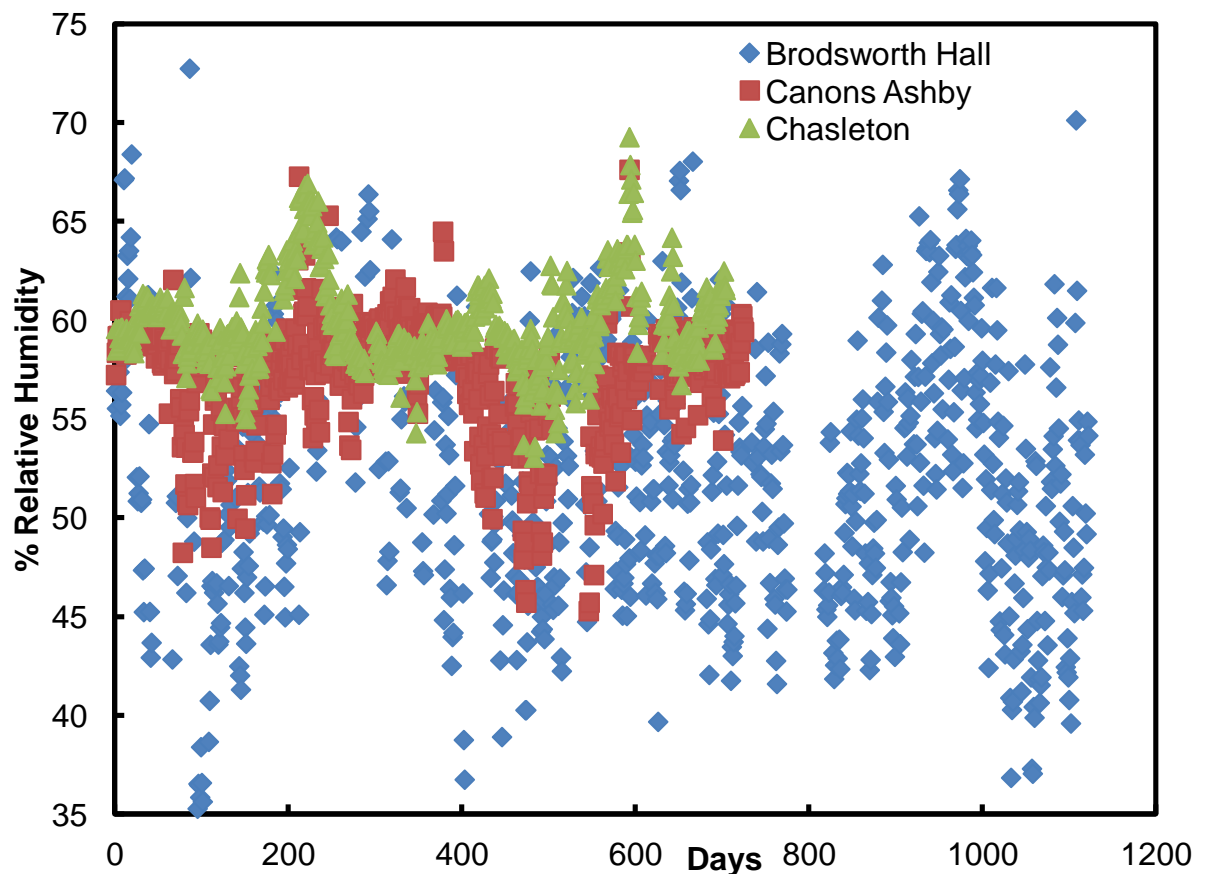


Figure 3.35: Comparison of the relative humidity in three rooms with conservation heating at Brodsworth Hall, Canons Ashby and Chasleton. The data at Brodsworth Hall covers three years, and the other two locations two years. Each location covers a different time period; however they all begin at the start of January.

If the conservation heating is not working effectively, this may be improved at some point, making the projections of future indoor climate incorrect.

Considerable effort was taken (with additional help from Carlota Grossi, UEA) to investigate how the data from rooms with conservation heating compares to the unheated rooms and outdoors. For example determining what the temperature or humidity is outdoors when the relative humidity is below the specific set points of conservation heating. This was in an attempt to describe when conservation heating may be applied, this helped understand when conservation heating tends to be switched on, but did not help towards formulation of a different model. This required an alternative method as described below.

### 3.4.1 Conservation Heating Transfer Function

The original transfer function remains applicable to unheated rooms, so the relationship between the unheated rooms and those with conservation heating was investigated.

*Brodsworth Hall*

Figure 3.36 compares the relative humidity in the Library (with conservation heating) and the Dining Room (no heating) at Brodsworth Hall. Unfortunately there is only valid data for the Dining Room over the period of April 2010 – February 2011, a total of 11 months. There is no data for March, so further years would give a better understanding of the relationship. There is a close relationship between the relative humidity of the two rooms, with both having a similar pattern of peaks and troughs of the humidity. Further evidence is also provided by the correlation coefficient, $R^2=0.60$, this is not as high as may be expected when looking at the plot of the room data, but it is acceptable. The relationship changes across the year, in summer the humidity of each room is more similar to each other than over the winter periods. This is likely to be because conservation heating is often switched off in summer months, to prevent unacceptably high temperatures. Therefore if a monthly calibration is applied, as used previously, to account for the seasonal variation this should help improve any predictions, as evidenced when first investigating the transfer function.
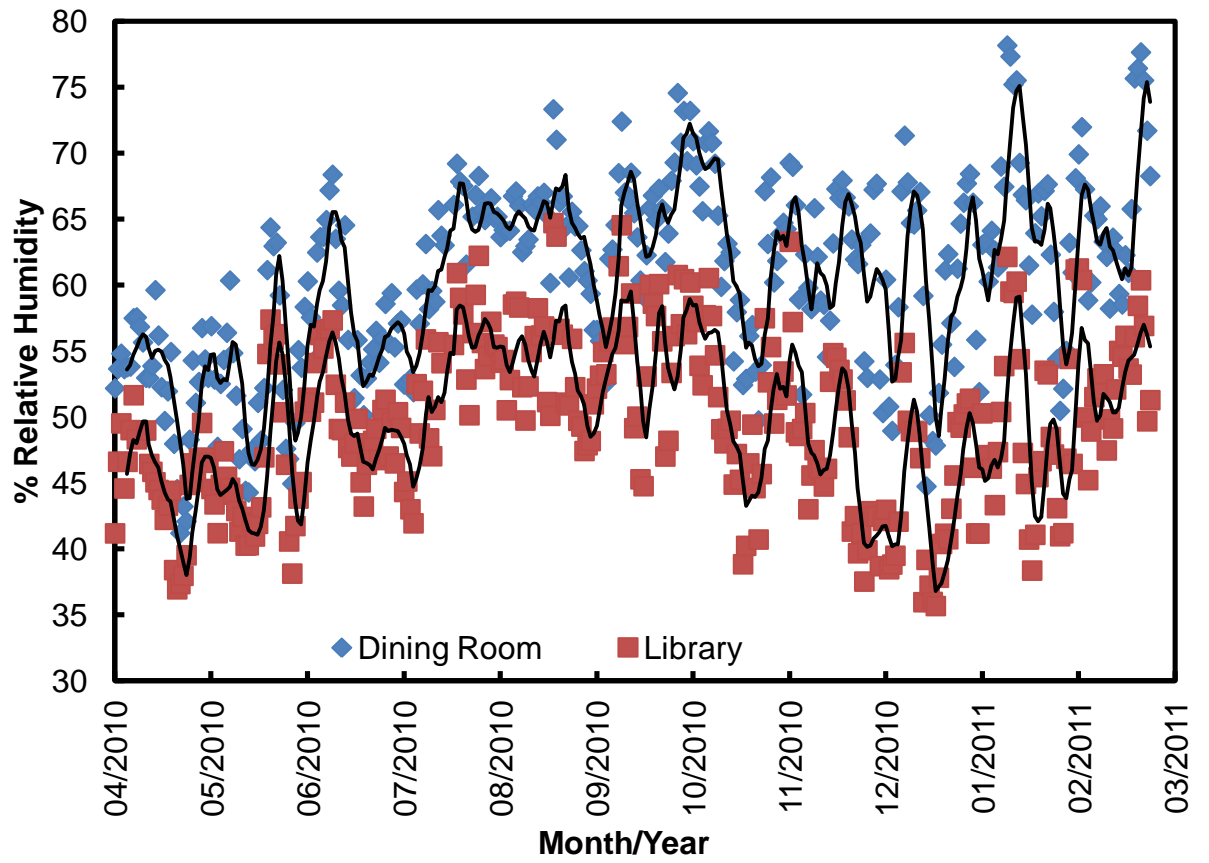
Figure 3.36: Comparison of the relative humidity indoors in the unheated Dining Room and the controlled Library at Brodsworth Hall, for the 11 month period 04/2010-02/2011.

The indoor relative humidity was calibrated, using monthly ratios to predict the relative humidity in the Library using the Dining Room humidity. The predicted relative humidity is compared to the observed relative humidity of the Library in figure 3.37. This shows a good agreement ($R^2$=0.76), with correlation in most periods. The AWK program for this can be found in appendix E.

The temperature can be calculated from the predicted relative humidity and the specific humidity, using the equations discussed previously in Section 3.2.3. The specific humidity is predicted using the original transfer function, from outdoors to indoors in the Library. The specific humidity prediction will be valid in the future as it is the temperature that alters if the patterns in the usage of conservation heating change. This provides a workable solution, but it is not ideal, as not all locations will have an unheated room to compare to a room that applies conservation heating.
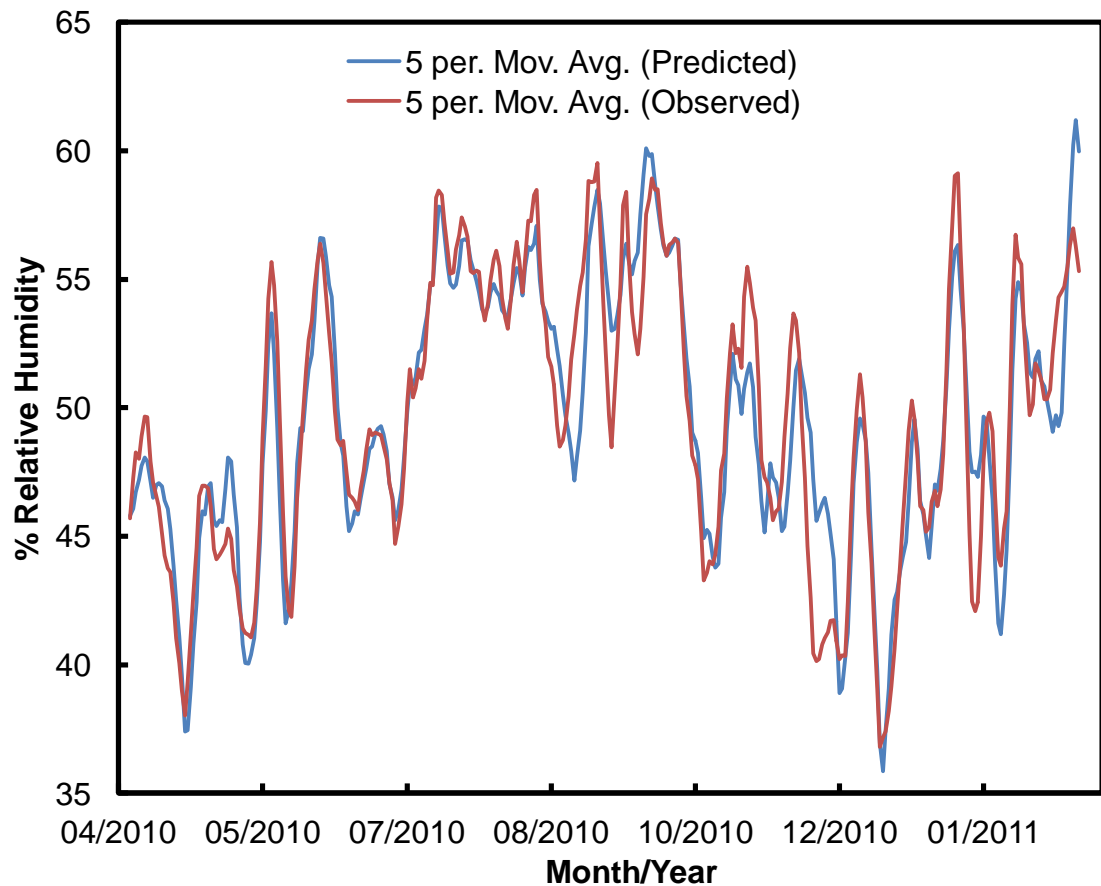


Figure 3.37: Comparison of the observed and predicted relative humidity for the Library, using the dining room.

The predicted temperature is shown in figure 3.38. The errors probably arise because this prediction is itself a product of two previous predictions, so errors get amplified, as discussed before. The variation around the observed temperature is quite big ($R^2$=0.76), which in comparison to previous temperature predictions is not as good.
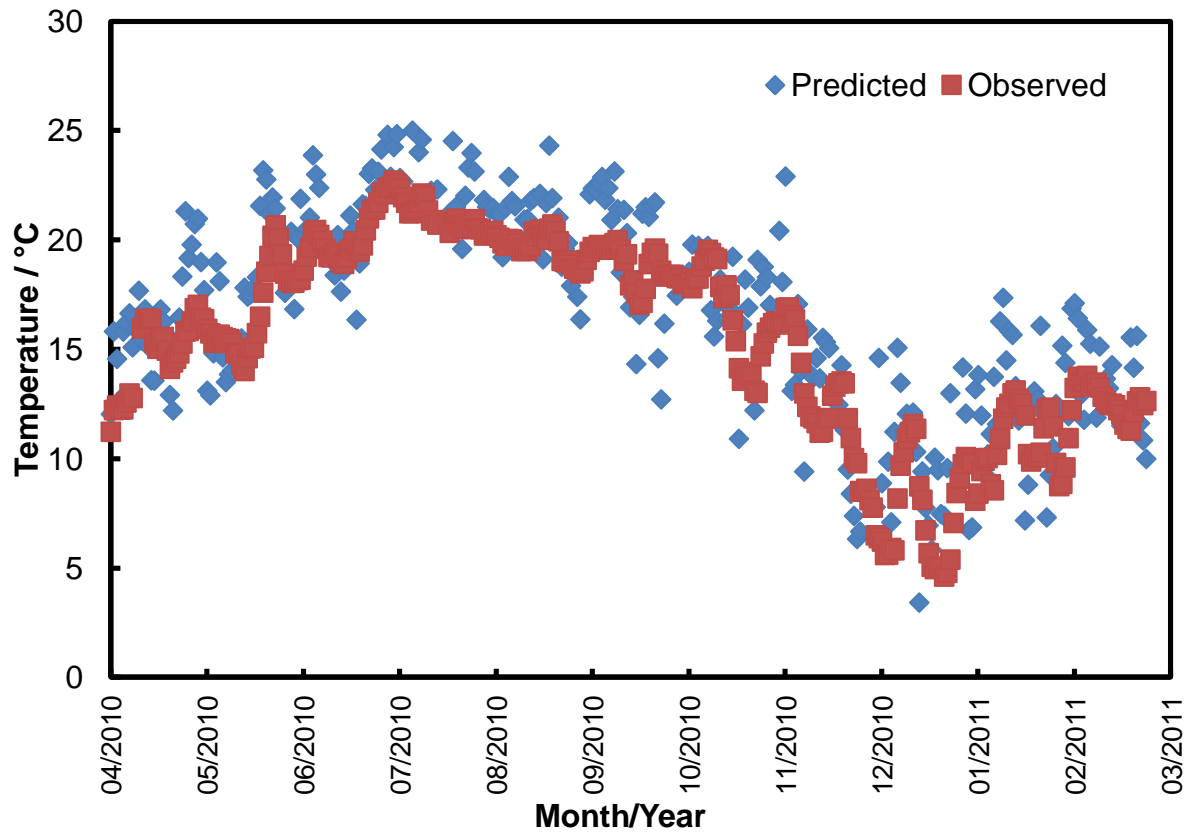


Figure 3.38: Comparison of the observed and predicted temperature for the Library. Calculated from the predicted relative humidity and the predicted specific humidity using the, dining room and outdoor data respectively.

*Canons Ashby and Chasleton*

In an attempt to solve this problem, two other properties were investigated. While there is little data available for the Dining Room at Brodsworth more data is available for the rooms at Canons Ashby and Chasleton, both spanning January 2009 – December 2010, two full years. It would obviously be better if more data was available, but 2 complete years is significantly better than 11 months. Additionally it is important to see how the controlled rooms compare to the uncontrolled rooms, as the conservation heating at Brodsworth has been identified as not working as effectively as it could.

Figures 3.39 and 3.41 compare the unheated rooms to those controlled by conservation heating at the two properties. At Canons Ashby the Great Hall is unheated, and the

Drawing Room controlled, and at Chasleton the Long Gallery is unheated, and the Great Chamber controlled. At Canons Ashby the relative humidity when not limited to the set point, which is rare and typically in the summer, has a similar pattern to the humidity of the Great Hall. It is not appropriate to state the linear correlation coefficient, as one dataset is limited to the set point for the majority of the time; however the plot of the humidity of each room against each other is useful to understand how the humidity is controlled.
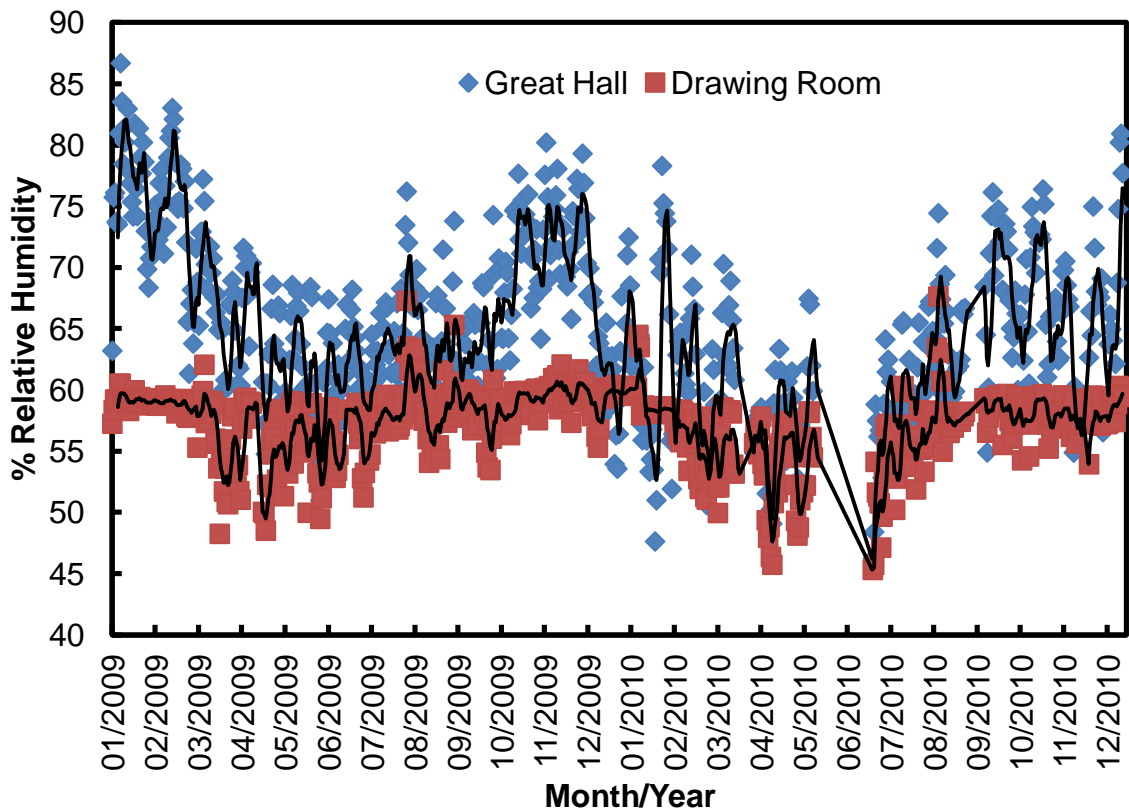


Figure 3.39: Comparison of the relative humidity in the unheated Great Hall and the controlled Drawing Room at Canons Ashby, for the period 01/2009-12/2010. The five day moving average is also plotted over the daily averages.

Figure 3.40 shows the humidity is low in the Great Hall, typically in spring/summer, the Drawing Room humidity is also low. Once the relative humidity in the Great Hall reaches about 60-65% the humidity in the Drawing Room is limited because of the application of conservation heating. Occasionally the humidity rises above the set point, which appears to be approximately 59% relative humidity. This is likely to be in late summer when humidity increases, but temperatures are still warm, preventing the application of conservation heating, because of the maximum temperature limit of 22°C. Figure 3.41 compares the humidity in the two rooms at Chasleton, again when the humidity is not limited, or cannot be applied there appears to be a close relationship between the two rooms.
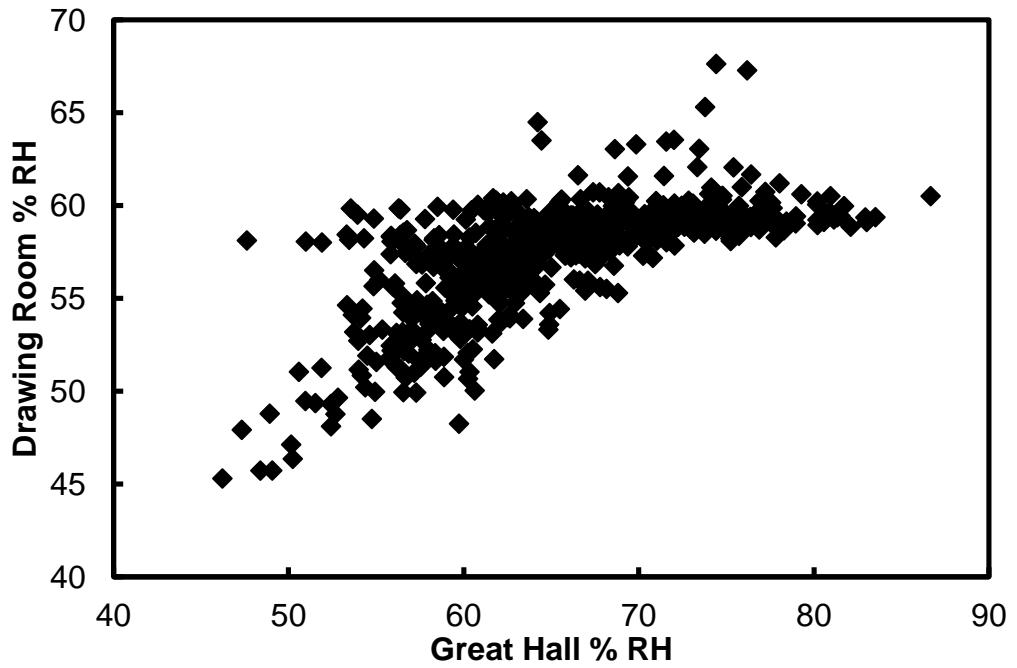
Figure 3.40: Relative humidity of the Great Hall plotted against the Drawing Room relative humidity for the period 01/2009-12/2010.
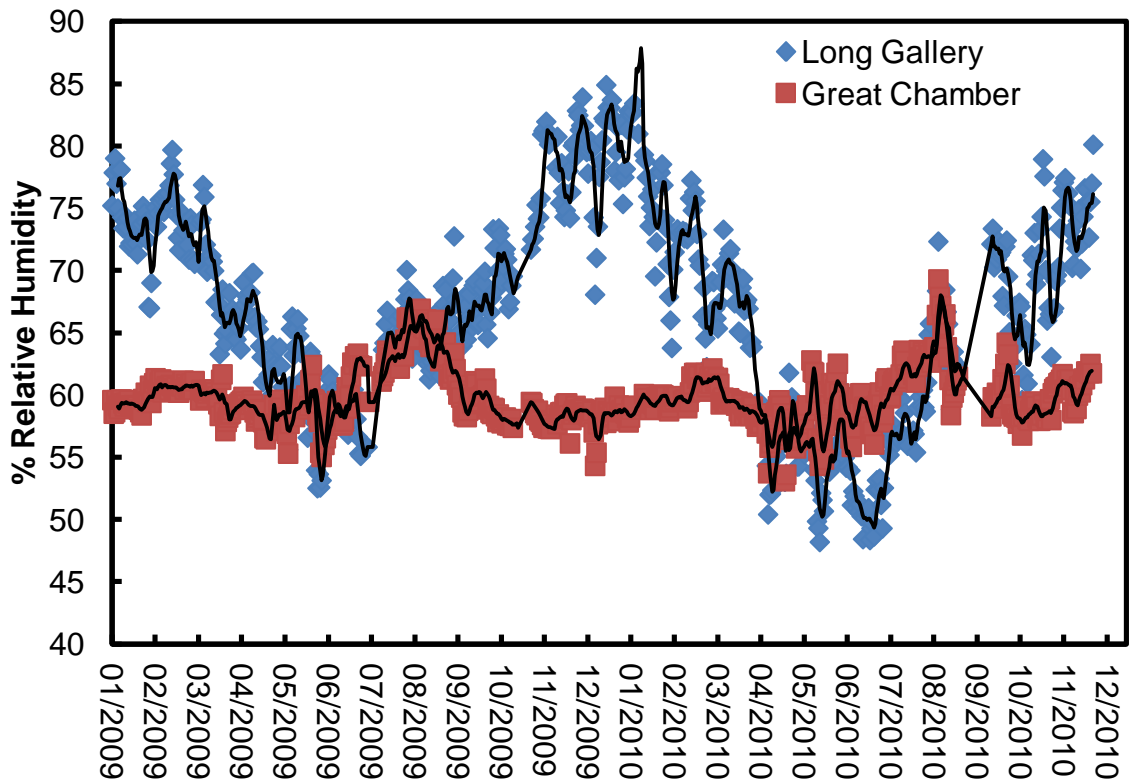


Figure 3.41: Comparison of the relative humidity in the unheated Long Gallery and the controlled Great Chamber at Chasleton, for the period 01/2009-12/2010. The five day moving average is also plotted over the daily averages.

The previous figures help define and understand conservation heating. A new technique, that didn't work previously at Brodsworth Hall, because of the less than optimal operation of the conservation heating system, may now work. This applies the set points of conservation heating to the data from the uncontrolled rooms, to predict the controlled room. This didn't work at Brodsworth because the relative humidity doesn't often stay constant, but at Canons Ashby and Chasleton this occurs more frequently, thus the effectiveness of the technique in replicating conservation heating should improve.

This technique, from here on called the conservation heating transfer function is described as follows. As previously the temperature and relative humidity of the unheated room is predicted, then the specific humidity is compared between the two rooms, often they are similar but if they are different a calibration is applied, as specific humidity is not affected by conservation heating. An optional step is the calibration of the temperature, these are compared in the summer and if they are different a calibration is applied to the whole of the data. This occurs in the summer because conservation heating is switched off, so no additional heating increases the temperature. Once the calibration has been made the relative humidity is recalculated as it will be different after calibration. Then conservation heating is applied to the data, following specific set points, which include a maximum relative humidity and a maximum temperature (22°C). The humidity set point is determined from analysis of the observed data; but usually the relative humidity is set to around 58% for conservation heating. An AWK program reads each temperature - relative humidity pair and if relative humidity is over the set point it is reduced to the set point, and the corresponding temperature increase calculated and applied, dependent upon the specific humidity. This mimics heating switching on to reduce the relative humidity when the humidity is over the limit. If the temperature increase required for the reduction of humidity to the set point raises the room temperature above 22°C then the temperature is set to this value, and the relative humidity recalculated correspondingly. There are occasions where some heating can be applied, reducing the humidity, but not fully, as the temperature reaches the set point.

This technique was applied at Chasleton as shown in Figure 3.42 where the initial predicted relative humidity in the Great Chamber was derived from specific humidity in the unheated Long Gallery. Both the temperature and the specific humidity were calibrated in the Great Chamber on this occasion. There were some successes and failures in this approach; firstly the initial approximation approaches the observed data, suggesting this approach is hopeful. The specific set point, 59% on this occasion, means that predicted relative humidity always is at that specific value, but in reality there is likely to be some variation around this, as can be seen. This is not likely to be a significant issue, as the variation averages around the set point. More important are the times when humidity falls below or exceeds the set point. The two occasions in spring where relative humidity drops below the set point are represented in the prediction, and in the correct places, but there are not enough occurrences compared to the observed relative humidity.
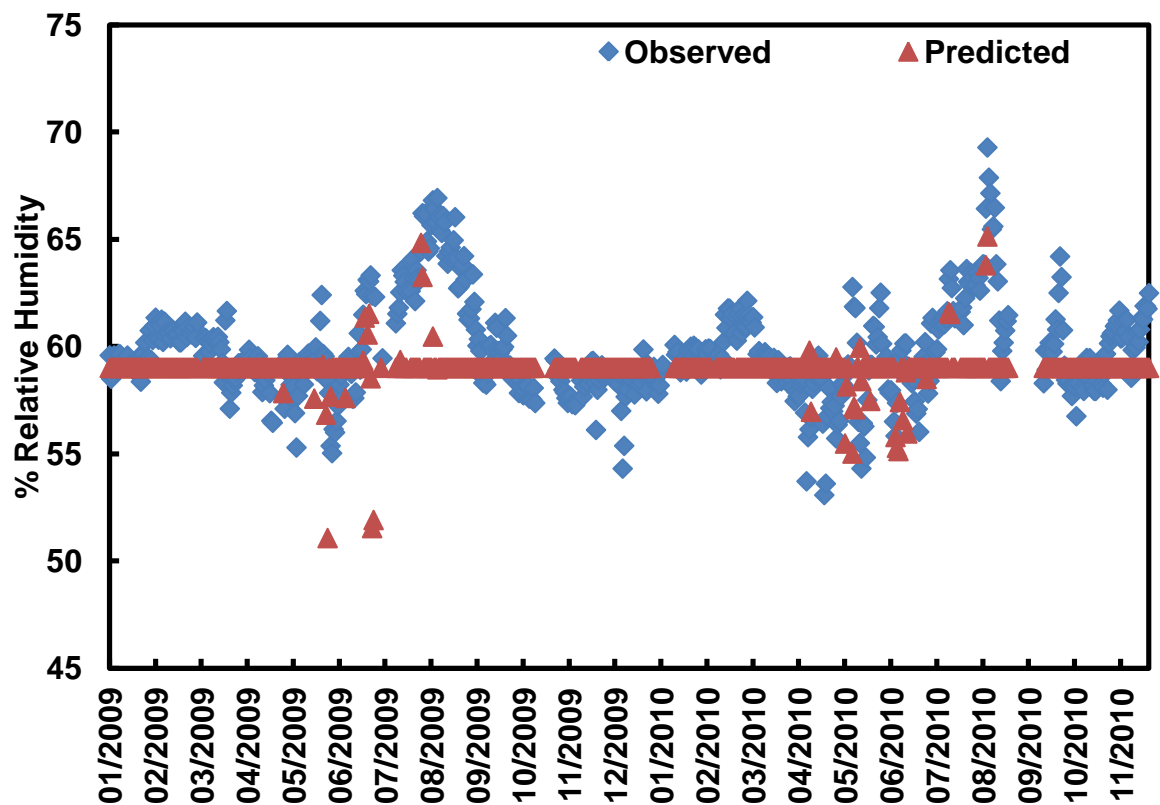


Figure 3.42: Comparison of the observed and predicted relative humidity for the Great Chamber at Chasleton, using an initial version of the conservation heating transfer function. Covering the period 01/2009-11/2010.

When the humidity control is lost, in the two summers represented the predicted humidity shows very little loss of control, so does not perform well. These initial calculations still applied the conservation heating set points in the summer, where in reality it is likely that the system was turned off, to save energy. Thus a second calculation was made where

the conservation heating was not applied for the warmer months of July and August. This results in the relative humidity from the unheated room being used for the prediction, after calibration was applied. The results are plotted in figure 3.43 and show the number of occasions where humidity control is lost is overestimated, as opposed to the previous under estimate. However they occur at the correct times. In August 2009 conservation heating appears to be switched back on and the humidity slowly decreases to the set point. Unfortunately this is not possible in the current model, as switching on the conservation heating for August would bring the humidity back to 59% immediately. It would be necessary to adjust the model further to allow for a gradual return to the set point.
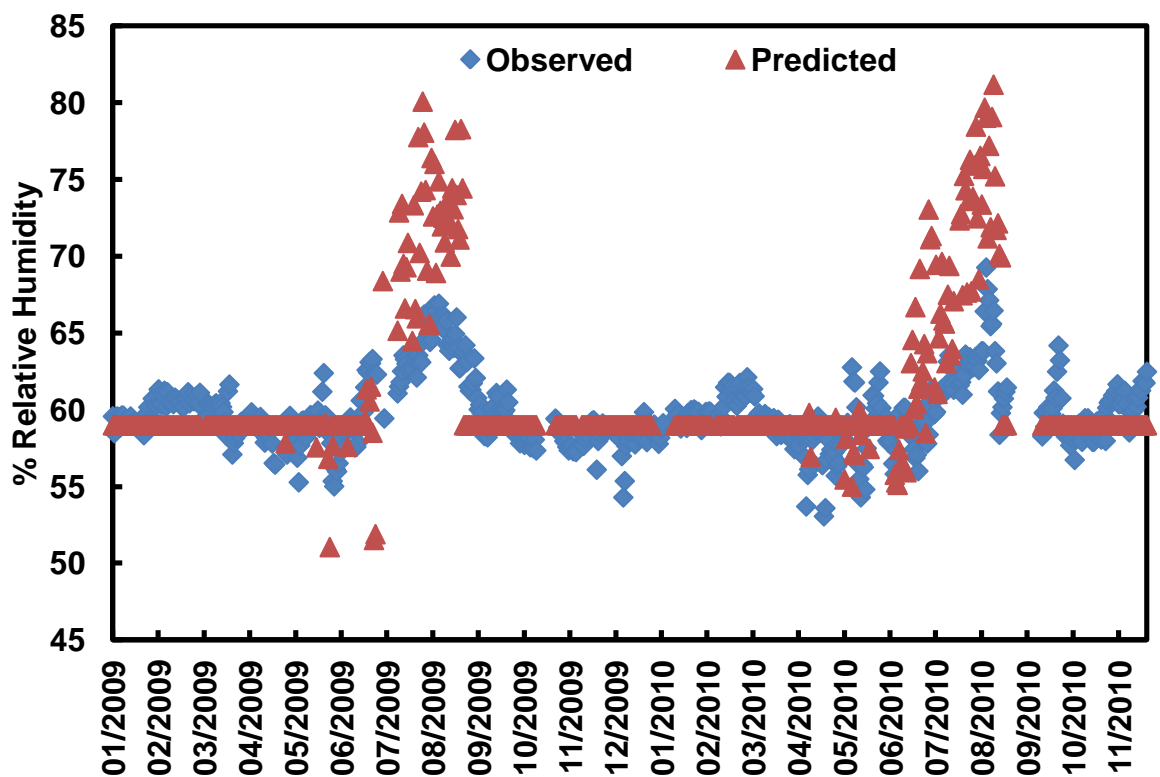


Figure 3.43: Comparison of the observed and predicted relative humidity for the Great Chamber at Chasleton, using an improved conservation heating transfer function. Covering the period 01/2009-11/2010.

The conservation heating transfer function was also applied at Canons Ashby, and the relative humidity prediction is shown in figure 3.44. The periods where humidity drop below the set point (59%) appear to correspond well here, although not exactly at the right time, but generally the two sets of values are similar. In the summer periods where humidity control is lost the prediction also appears to emulate this effectively, although with slight error. There appears to be one problem though, for the period of September 2009 to December 2009 the observed humidity drops below the set point occasionally, however the predictions don't show this. It is possible that initially in September the temperature is high; driving down the humidity, but this is an unlikely explanation for December.
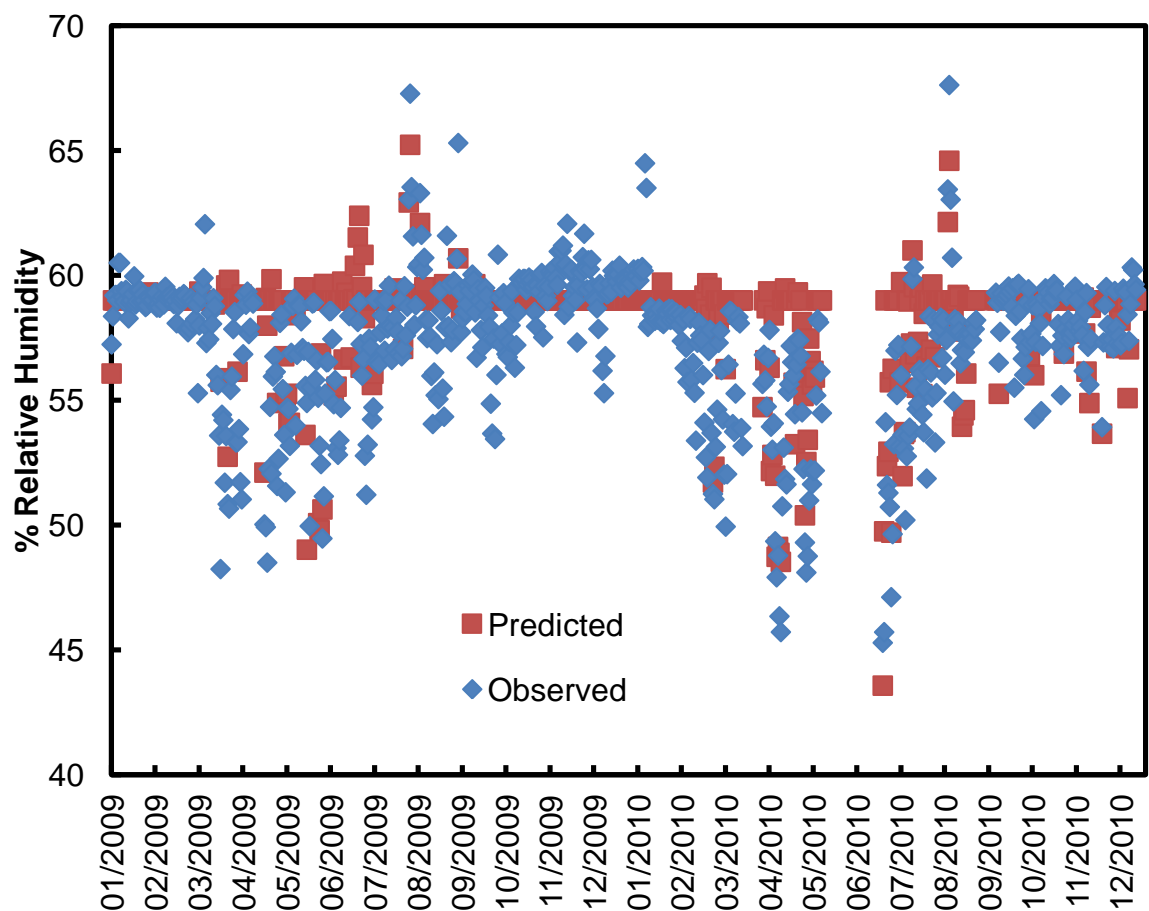


Figure 3.44: Comparison of the observed and predicted relative humidity for the Drawing Room at Canons Ashby, using the conservation heating transfer function. Covering the period 01/2009-12/2010.

In addition to the relative humidity prediction the temperature prediction is also important, to see if the increase in temperature from heating corresponds to the observed data. Figure 3.45 compares the observed and predicted temperature in the Drawing Room at Canons Ashby. The predicted temperature is slightly lower for most of the year, but the greater spread of data that is observed in the winter months, because of heating is replicated in the prediction.
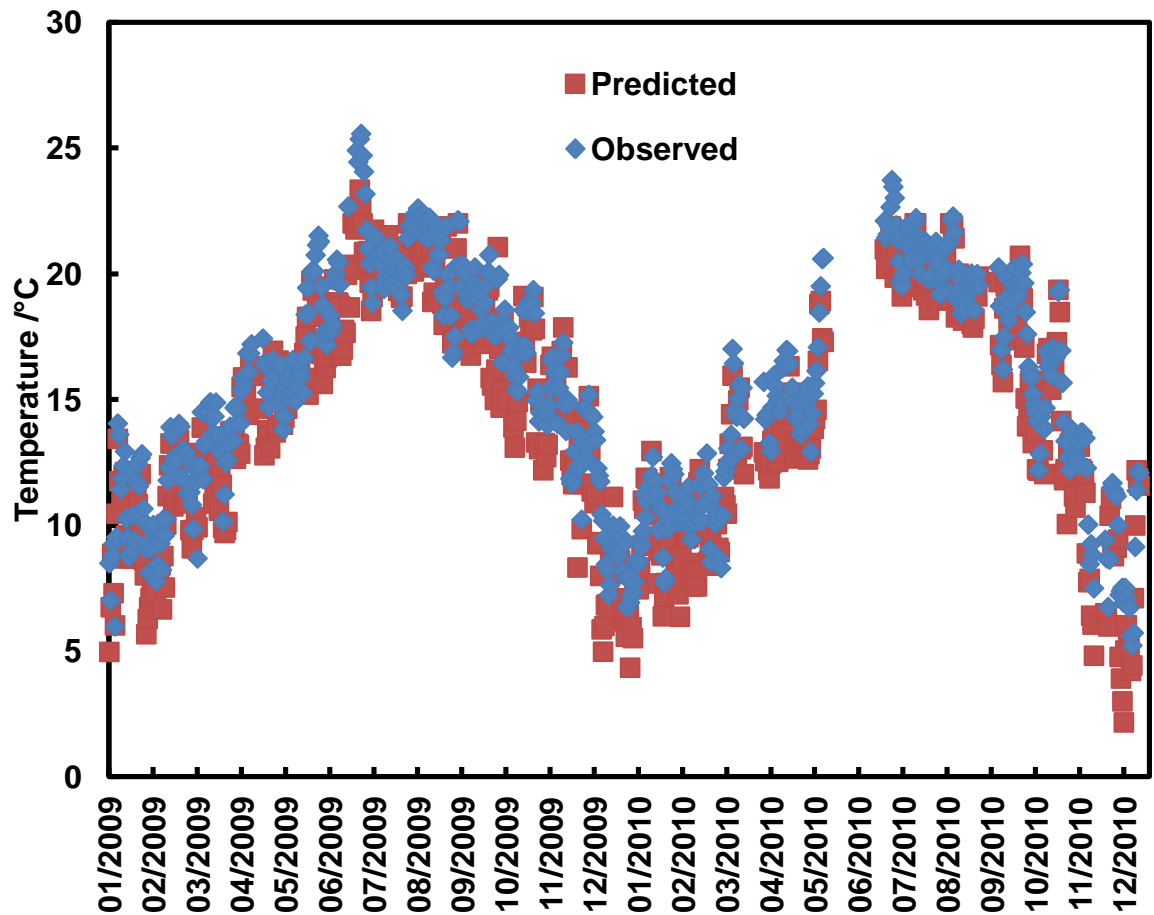


Figure 3.45: Comparison of the observed and predicted temperature for the Drawing Room at Canons Ashby, using the conservation heating transfer function. Covering the period 01/2009-12/2010.

The predicted temperature for the Great Chamber at Chasleton is shown in figure 3.46. This corresponds well to the observed data, although with higher variation, but again the winter prediction appears to have worked, replicating conservation heating well.
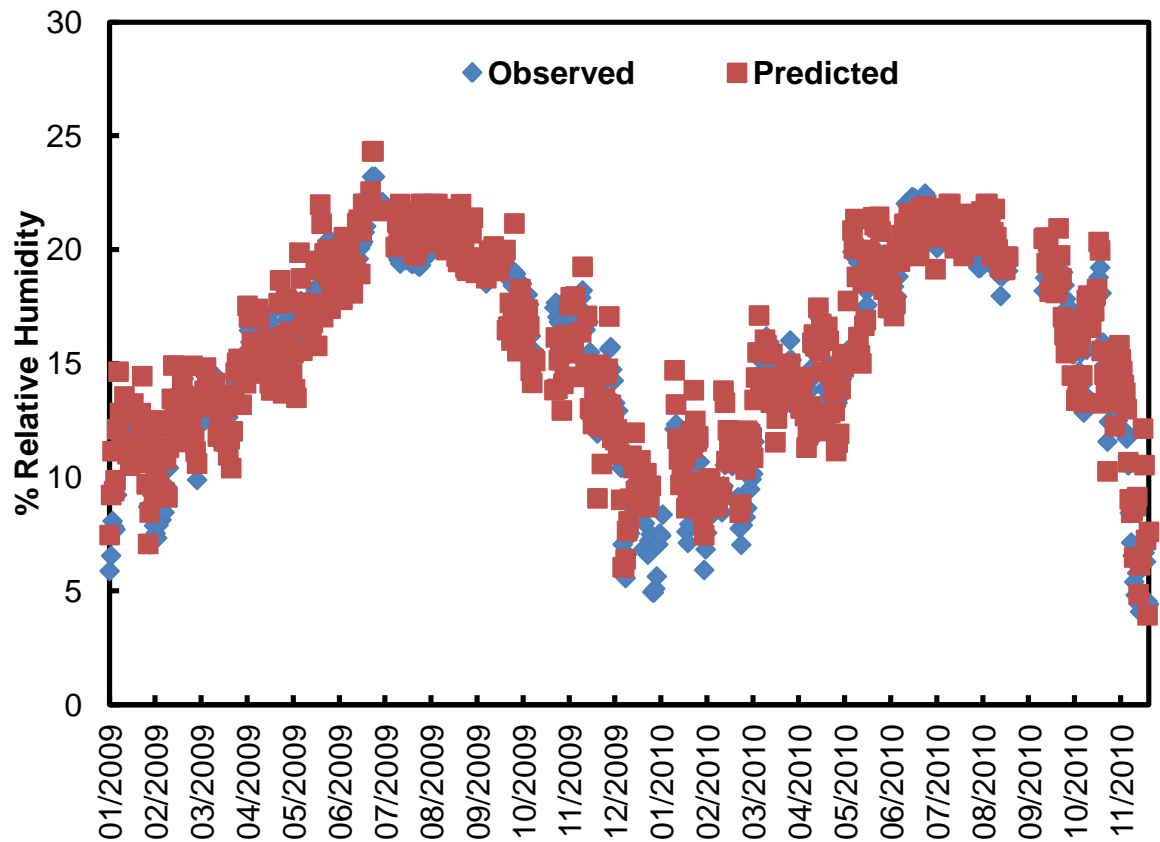


Figure 3.46: Comparison of the observed and predicted temperature for the Great Chamber at Chasleton, using the conservation heating transfer function. Covering the period 01/2009-11/2010.

This provides a technique that is a first approximation of predicting the indoor environment of a room with conservation heating, which supplements the traditional transfer function for unheated rooms.

This technique is not an ideal solution for predicting the indoor environment in rooms with conservation heating. If time had allowed, further investigations of a relationship between the outdoor environment and indoor rooms with conservation heating would have been undertaken, so this presents possible work in the future. Additionally work would need to investigate the absence of conservation heating in the summer.

Work with Canons Ashby and Chasleton data shows that the conservation heating in the library at Brodsworth Hall is not ideal. There are too few observations (11 months) in the unheated room to use the conservation heating transfer function. Had there been

sufficient observations for the unheated room it may have been possible to use the conservation heating transfer function, and assume that the conservation heating will run optimally. Alternatively the relative humidity relationship could have been used in this case, but again there is only 11 months of data, and this is not sufficient. Despite the existence of conservation heating the present study of the Library at Brodsworth Hall will use the standard transfer function alone, with the caveat that should relative humidity change significantly in the future it may not be valid. The AWK program for this can be found in appendix E.

## 3.5 Short term forecast

The use of building simulation or a transfer function is not limited to long term forecasts of the indoor environment; it can also be applied in the short term (Lankester and Brimblecombe, 2012a). The transfer equation, calibrated for each location, can be applied to standard weather forecasts of temperature and relative humidity. Such indoor forecasts could be used to determine the appropriate time to implement preventive conservation strategies. Covering collections for the winter closure would be an example. If these were covered during periods of high humidity, moisture can become trapped, leading to corrosion on objects such as candlestick holders. Indoor forecasts would allow conservators to foresee the optimal time to carry out conservation activities (Lankester and Brimblecombe, 2012a). Additional research has found that periods of high humidity can encourage the cementation of dust to surfaces (Brimblecombe et al., 2009), indoor forecasts could also be used to determine periods of special cleaning to prevent this damage (Lankester and Brimblecombe, 2012a).

### 3.5.1 Brodsworth indoor forecast

A weather forecast was used from Church Fenton, the closest weather station to Brodsworth Hall (≈35 km); this consisted of both temperature and relative humidity. The forecast spanned five days, with the first two days having a forecast for every three hours, beginning at 0700 hours on the first day through to 1600 hours on the second day. For the remaining three days there was a daily minimum and maximum temperature forecast, these were averaged to get the daily temperature forecast. Relative humidity was already as a daily average for these three days. The forecast used began on Saturday the 8th of May, 2010, and ran through until Wednesday the 12th of May. The forecast temperature and relative humidity are shown in table 3.4.

Table 3.4: The BBC weather 5 day forecast for Church Fenton

| Day | Date | Time | Temperature | Relative Humidity |
|---|---|---|---|---|
| SAT | 08/05/2010 | 0700 | 7 | 86 |
| SAT | 08/05/2010 | 1000 | 11 | 59 |
| SAT | 08/05/2010 | 1300 | 11 | 52 |
| SAT | 08/05/2010 | 1600 | 11 | 62 |
| SAT | 08/05/2010 | 1900 | 9 | 69 |
| SAT | 08/05/2010 | 2200 | 7 | 80 |
| SUN | 09/05/2010 | 0100 | 6 | 84 |
| SUN | 09/05/2010 | 0400 | 6 | 84 |
| SUN | 09/05/2010 | 0700 | 6 | 87 |
| SUN | 09/05/2010 | 1000 | 9 | 81 |
| SUN | 09/05/2010 | 1300 | 8 | 68 |
| SUN | 09/05/2010 | 1600 | 10 | 52 |
| MON | 10/05/2010 | 0000 | 5 | 61 |
| TUES | 11/05/2010 | 0000 | 6.5 | 53 |
| WEDS | 12/05/2010 | 0000 | 7 | 49 |

As the transfer function is derived for use with daily averages the forecast was adjusted to meet this requirement. A moving average was calculated over 6 periods, the number of readings per day, so that the average represented the previous 24 hour period. This delayed the start of the forecast, with the first period having a midpoint time of 1430; the adjusted forecast is available in table 3.5.

Table 3.5: The BBC weather 5 day forecast for Church Fenton, adjusted to present values that represent a 24 hour average.

| Date | Time | Temperature | Relative Humidity |
|---|---|---|---|
| 08/05/2010 | 1430 | 9.3 | 67.1 |
| 08/05/2010 | 1730 | 9.2 | 66.8 |
| 08/05/2010 | 2030 | 8.3 | 70.8 |
| 08/05/2010 | 2330 | 7.5 | 77.0 |
| 09/05/2010 | 0230 | 7.2 | 80.7 |
| 09/05/2010 | 0530 | 7.0 | 80.6 |
| 09/05/2010 | 0830 | 7.5 | 75.3 |
| 10/05/2010 | 1200 | 5.0 | 61.0 |
| 11/05/2010 | 1200 | 6.5 | 53.0 |
| 12/05/2010 | 1200 | 7.0 | 49.0 |

The forecast was used with the transfer function for May to forecast the temperature and relative humidity indoors. The result of the indoor temperature forecast is compared to the subsequently observed data (Fig. 3.47), and a further indoor prediction using the observed data. There is some error between the outdoor forecast and the values later observed, particularly for the first day of the forecast, but it improves after this. The indoor forecast shows some error also, on average just over a degree different from the observed data. Some of this error may be from the initial outdoor forecast error, but differences in the later days are unlikely to be from this. Additionally the prediction of the indoor temperature when using the observed data also has a similar error. It is important to remember that the transfer function is normally used to predict data that will fit a long term average, so some error when comparing to observed data is expected. This may be a contributing factor to the small error apparent here, in both the indoor predictions.
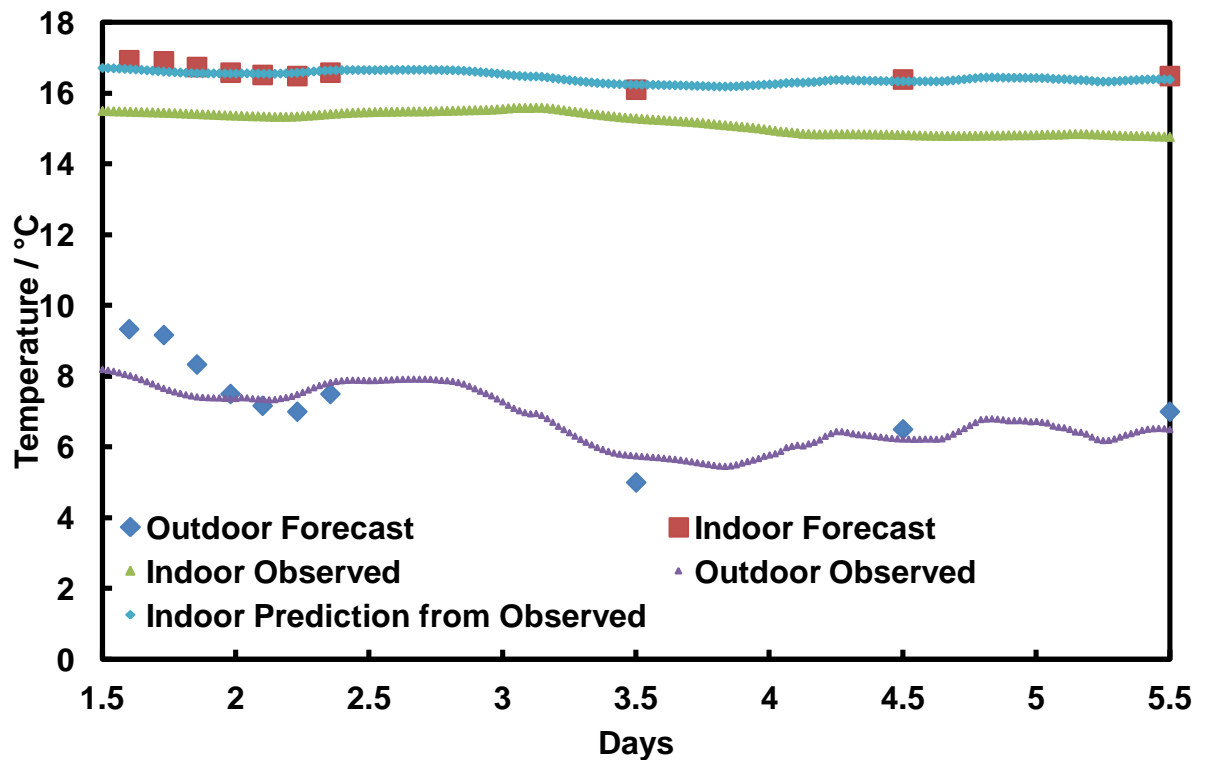


Figure 3.47: Comparison of the BBC weather forecast to the indoor temperature forecast for the Library at Brodsworth, and the subsequently obtained observations indoors and out. The indoor prediction using the observed temperature is also plotted.

The relative humidity indoor forecast is shown in figure 3.48, compared to the observed data indoors, and the prediction using the observed data. The outdoor forecast does not compare well with the observed humidity outdoors; initially there is error, of between 5-10%, which reduces into the second day. However the forecast on the subsequent three days is quite poor, initially just over 15% different, but increasing to over 20% different on the final two days, which is a very large error. This has an impact on the indoor forecast, with the final three days all around 7% different from the observed. Although there is error towards the end of the forecast, which is typical as the further in the future a forecast is the more uncertain it becomes, the first two days compare well. It is also satisfying that the observed indoor humidity is very similar to the prediction that uses the observed outdoor humidity. This implies that the error in the initial prediction of humidity is probably from the error in the forecast. Clearly accurate relative humidity forecasts are required.
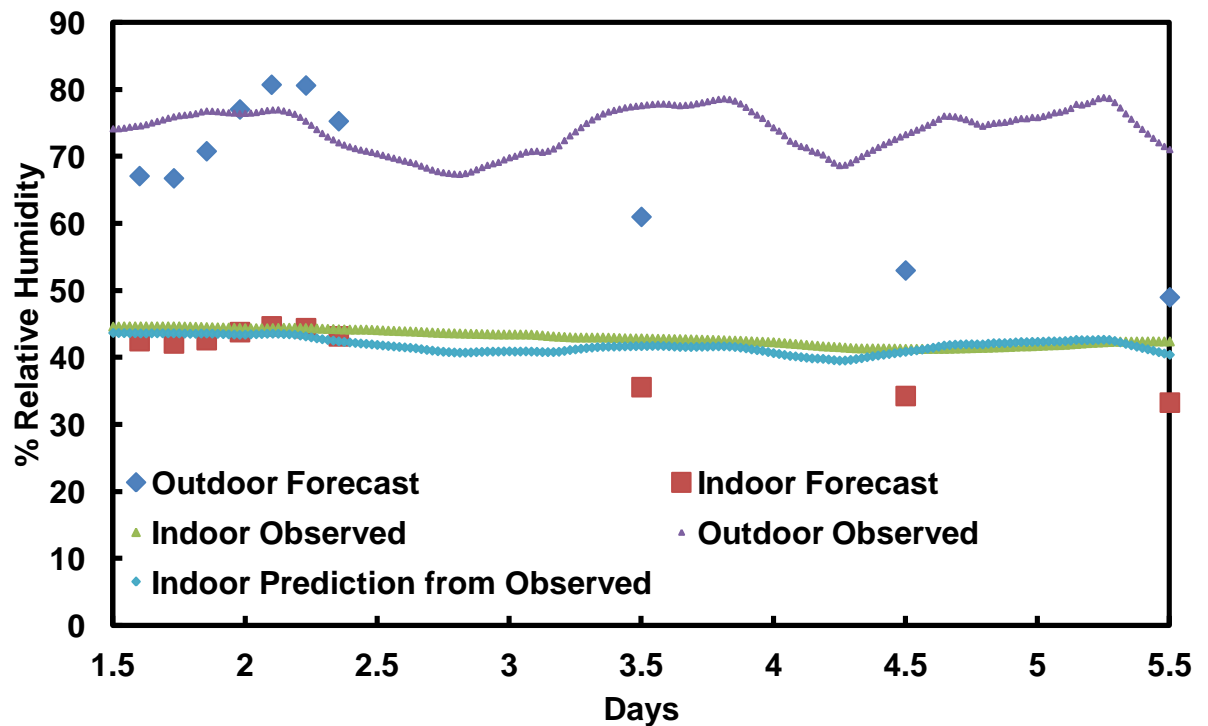


Figure 3.48: Comparison of the BBC weather forecast to the indoor relative humidity forecast for the Library at Brodsworth, and the subsequently obtained observations indoors and out. The indoor prediction using the observed relative humidity is also plotted.

### 3.5.2 Short term predictions

Forecasting error outdoors limits short term predictions, but the possible effectiveness of forecasts can be estimated by using observed outdoor data rather than outdoor forecasts. This was carried out at Knole (in two rooms) and at Canons Ashby.

A random number generator was used to pick a line of a file as the start point of the prediction. Both the indoor and outdoor observations were checked to see if they contained gaps, if so another number was generated. As previously the length of the 'forecast' will be five days.

At Knole both the Leicester Gallery and the Cartoon Gallery were investigated. In the Leicester Gallery the start was chosen to be the 11th November 2003, figure 3.49 compares the observed outdoor and indoor data to the predicted indoor temperature. The observed indoor and outdoor data have quite different trends, and this has an effect on the indoor prediction, as it is derived from the outdoor data, so it is not a surprise to see that the indoor prediction takes a similar form to the outdoor data. Comparing the predicted values of temperature to the observed sometimes they are quite good, on days 2 and 5 for example. However on days 1 and 4 there is an error of 0.8 and 0.5 of a degree respectively, and on day three even greater error, of 1.5 degrees.
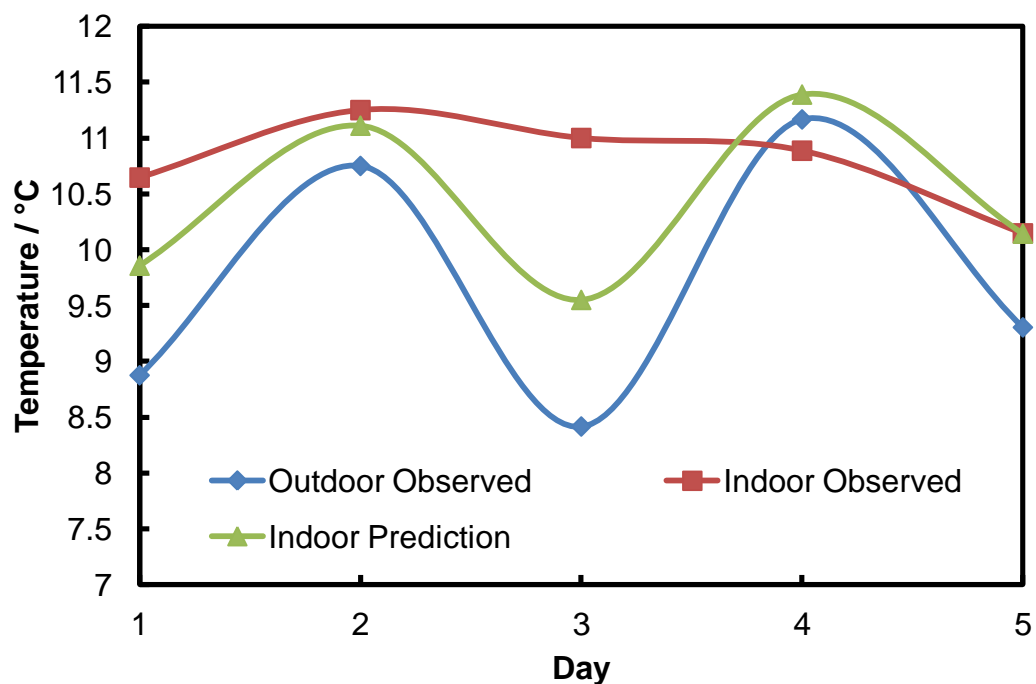


Figure 3.49: Comparison of the observed temperature indoors and outdoors to the indoor temperature forecast for the Leicester Gallery at Knole.

The predicted relative humidity for the Leicester Gallery is shown in figure 3.50, compared with the observed data. Again the indoor prediction has a similar trend to the observed outdoor data, which results in some error. The prediction for the first day is quite poor, but this is because of the unusually high outdoor humidity, after this the error is quite small, at approximately 2%, apart from day four, where the observed relative humidity drops below

the observed indoor humidity. When this occurs there can only be one result from this, the predicted humidity will be less than the observed outdoors, resulting in this error.
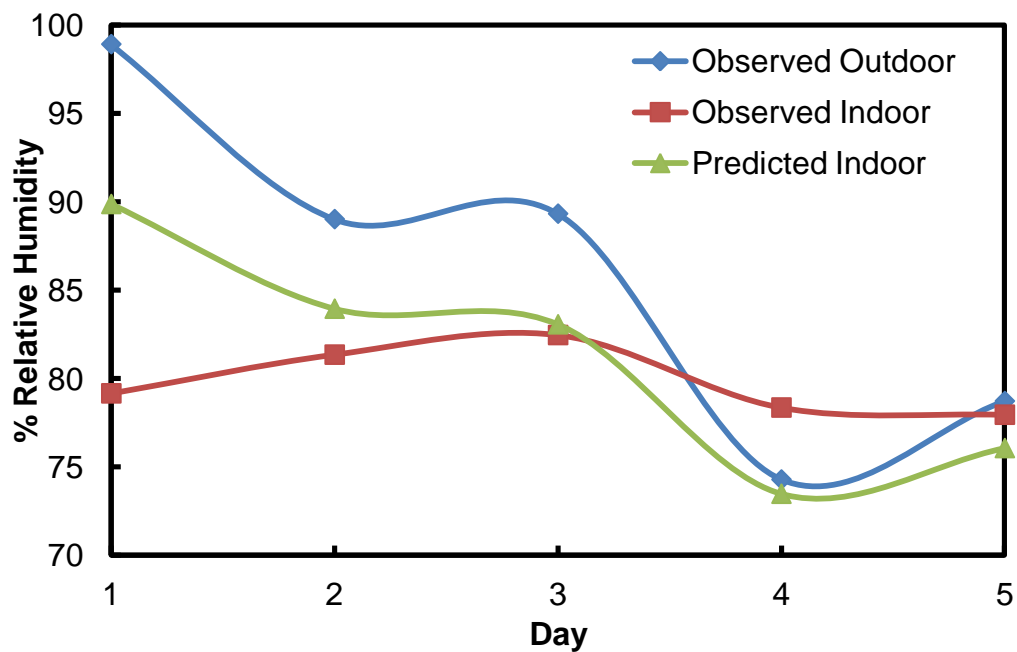


Figure 3.50: Comparison of the observed relative humidity indoors and outdoors to the indoor relative humidity forecast for the Leicester Gallery at Knole.

It would appear that in the short term the transfer function does not dampen the data as much as required. Overall there are some issues with the short term indoor forecasts, however it is important to look at other locations to see if these problems persist or are not apparent elsewhere.

A short term forecast was also determined for the Cartoon Gallery, again the start date was chosen at random, with the first day being the 9th of April 2002. Figure 3.51 shows the predicted indoor temperature and the observed indoor and outdoor temperature. On this occasion the predicted temperature compares favourably with the observed temperature, with very little error.
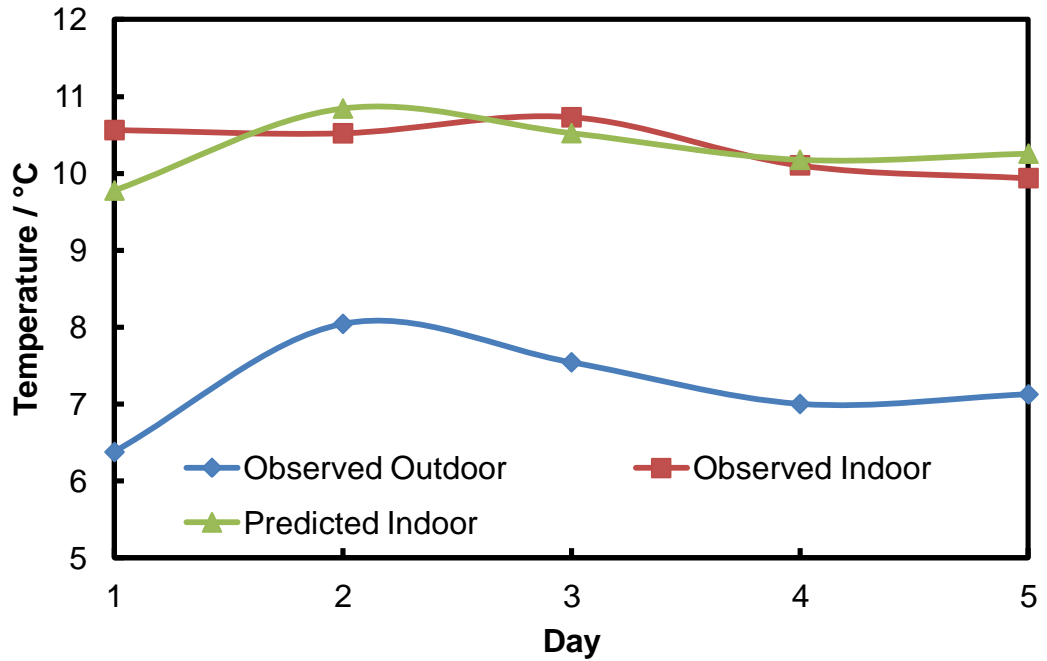
Figure 3.51: Comparison of the observed temperature indoors and outdoors to the indoor temperature forecast for the Cartoon Gallery at Knole.

The predicted relative humidity for the Cartoon Gallery is shown in figure 3.52, along with the observed indoor and outdoor humidity. Again the prediction compares well to the observed humidity, with the error 3% or less, except on one occasion (6%).
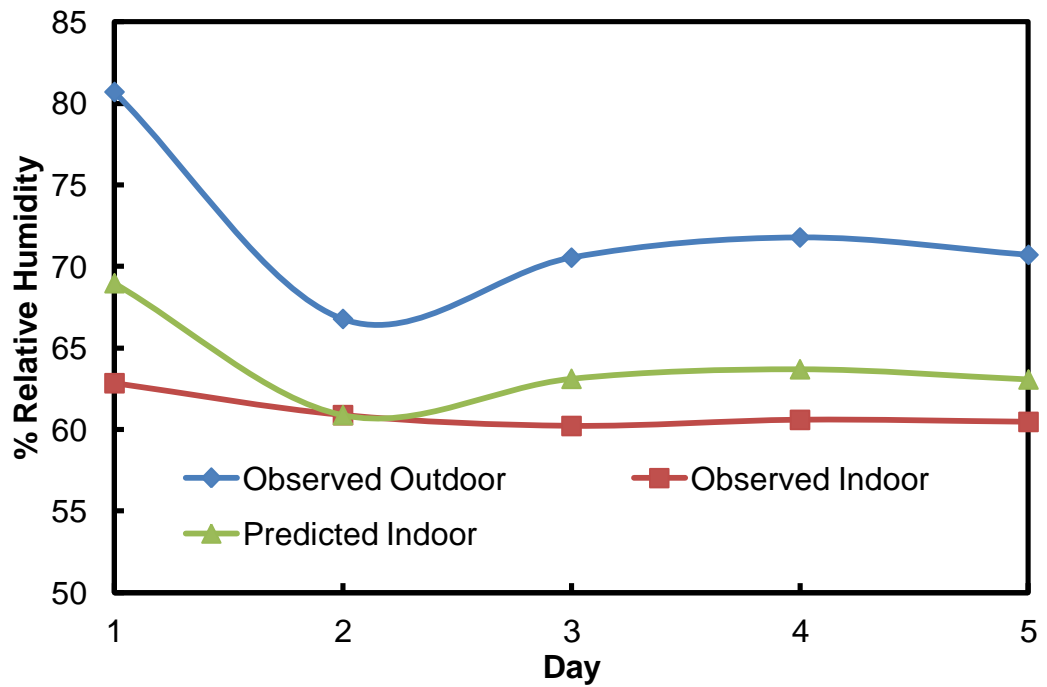


Figure 3.52: Comparison of the observed relative humidity indoors and outdoors to the indoor relative humidity forecast for the Cartoon Gallery at Knole.

The short term forecast method was also applied at Canons Ashby, for the Great Hall. Here the randomly chosen start date was the 13th March 2010. The predicted temperature is shown in figure 3.53, with the observed temperatures indoors and out also. The prediction is similar to previous ones, with good correlation of some points, and also some with error, the maximum at 1.5 degrees.
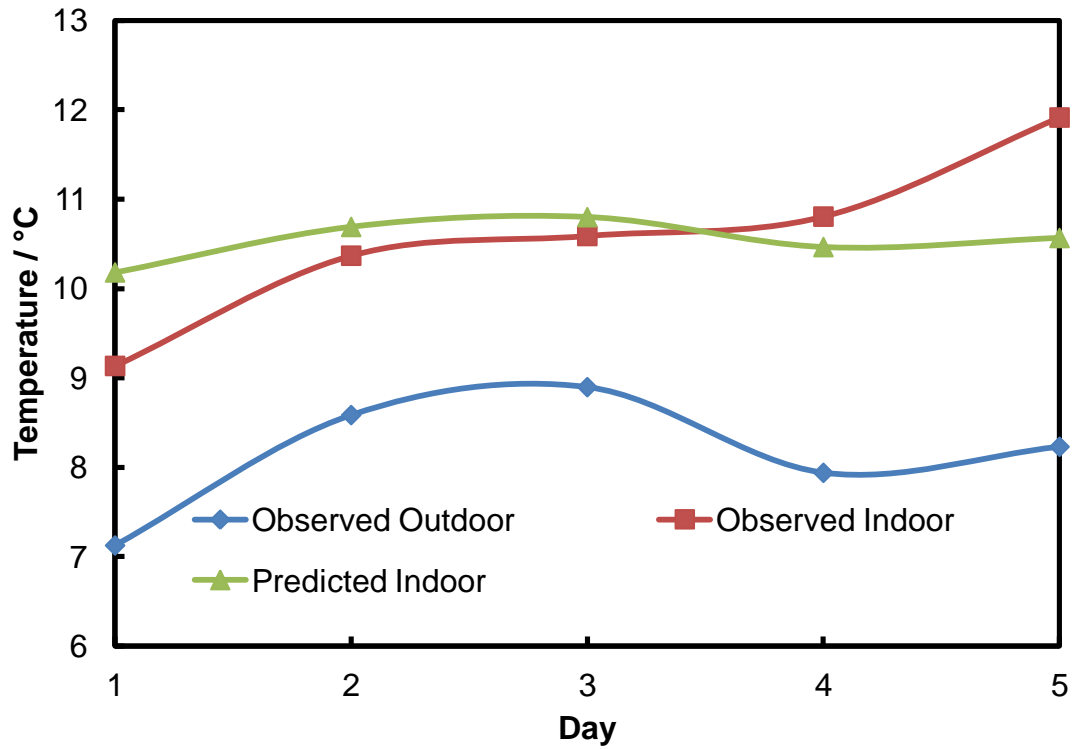


Figure 3.53: Comparison of the observed temperature indoors and outdoors to the indoor temperature forecast for the Great Hall at Canons Ashby.
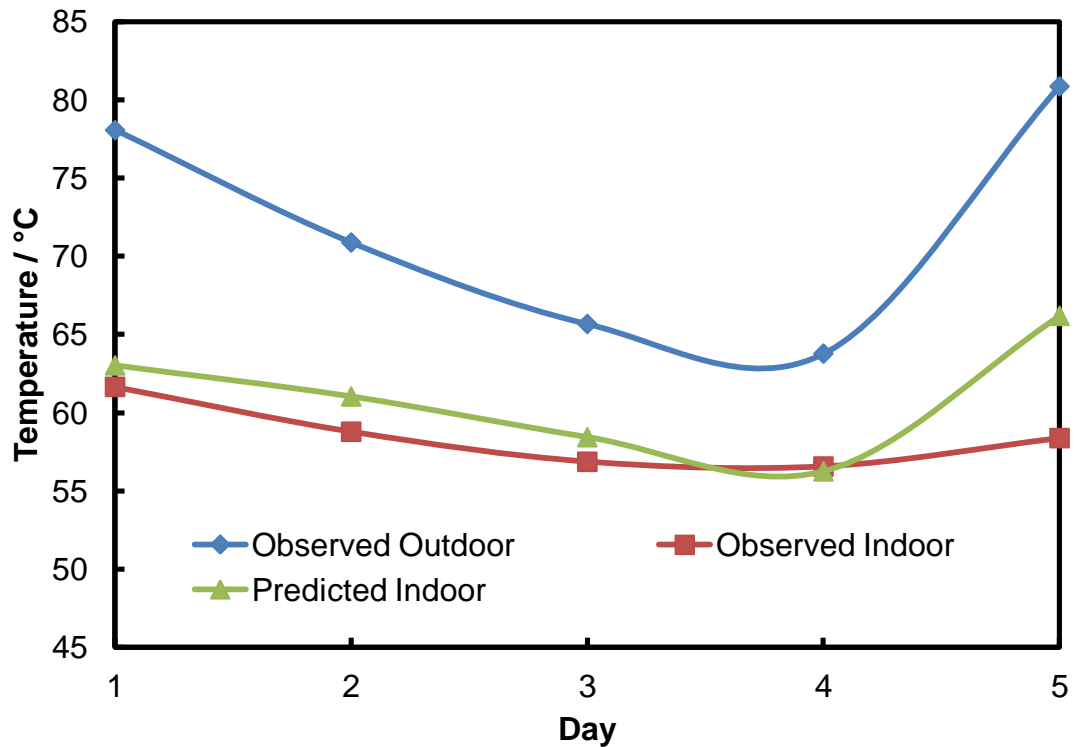
Figure 3.54: Comparison of the observed relative humidity indoors and outdoors to the indoor relative humidity forecast for the Great Hall at Canons Ashby.

Figure 3.54 shows the predicted relative humidity for the Great Hall at Canons Ashby, compared to the observed humidity. The prediction shows good correlation with the majority of the observed data, with less than 2.5% difference, apart for day 5 (8%).

The short term predictions are now appearing to be quite similar, so no more comparisons are necessary. Some points are raised from the analysis of the short term predictions. Firstly how much error is acceptable for a short term prediction, and secondly are these predictions useful. The answer to the first question is likely to be determined by the use of the forecast, and the accuracy required will be determined by this. If the end user is trying to determine the warmest day, or driest day, in order to carry out a task, then the error is unlikely to have an effect, and the forecast will be valid. However if a specific threshold is being determined then the error of the forecast will be important. If for example if the occurrence of humidity over 80% is being monitored, to look at dust cementation risk (Brimblecombe et al., 2009), then a lower value should be used, so that any error is taken into account, and also to provide an early warning system of sorts.

### 3.5.3 Confidence assessment

As previously undertaken in section 3.2.8 it is possible to determine the range that observed values fall in, for a given predicted value. This is particularly useful when using the short term forecasts as it is possible to determine when to set alarms to warn of possible damage, or that attention is required.

The 95% confidence ranges shown previously in table 3.2 indicate where the actual observed value may lie; therefore this can be used with the short term forecast to indicate the probability of the predictions. For instance if a temperature of 22°C was important, the upper temperature limit of conservation heating for example, in the Leicester Gallery a predicted temperature of 20°C would need to be set as the warning point, as the range of the observed values for this predicted value is between 18.1-21.8°C. While there is 95% chance that all observed values lie in this range, it is unlikely that a significant number of events lie close to the top limit, so setting 20°C as the warning point is likely to provide early warning, allowing for the implementation of management techniques as required. Again it is important to remember that the method has not been independently validated, therefore the limitations of this must be considered.

Compared to the temperature the range of possible relative humidity is quite large, however it is still possible that the short term forecast would indicate unfavourable conditions approaching. For example a critical value of 80% (dust cementation) would require an alert to be set when the humidity reached 70% (60.4-80.5%), the prediction is still likely to be useful, and warn that humidity is increasing, with the possibility that cleaning may be required to prevent dust cementation.

This doesn't take into account the weather forecast, an uncontrollable factor, which has been shown to include error. This would also have to be taken into account, but the error associated with this is unknown and requires further study. However it seems plausible that the short term forecast technique would be a useful tool for collection managers.

### 3.5.4 Back-casting

It is also possible that the transfer function could be used to predict interiors of the past. Where historic observations outdoors have been recorded the transfer function could be applied, determining the past indoor temperature and relative humidity. This possibility is discussed by Bionda (2004) with respect to the relationship that may be determined with historic damage. Previous work (Brimblecombe and Grossi, 2008) has applied damage functions to historical data to estimate damage, for the period 1100-2100. This is of

significance later, as knowing what damage has been caused by certain environmental conditions can aid with determining the significance of future damage projections.

## 3.6 Conclusions

In an attempt to simplify the traditional complex building simulation programs, various methods have been investigated to predict the temperature and relative humidity indoors.

It can be concluded that a successful transfer function has been determined that allows for the prediction of indoor temperature and relative humidity in unheated historic rooms. The method has advantages and disadvantages in comparison with the traditional approach. The main advantage is that the transfer function is quick and easy to implement for new rooms and locations, where it must be calibrated for each, making it accessible to heritage organisations.

The transfer function predicts indoor temperature and relative humidity from the corresponding outdoor conditions. It is calibrated across a period where the environment has been monitored, and can be applied into the future. There is good agreement between observations and predictions. While there is good agreement in the present, this is not a guide to whether there will be good agreement in the future under different conditions. This may be particularly important where temperatures rise, as the transfer function has not been calibrated with such temperatures, and there is always a risk when extrapolating data, that the relationship may not hold true. However it is unlikely that this will be the norm, even so the system does not appear to be non-linear, so serious problems with extrapolation would not be expected.

In comparison to EnergyPlus the model outperforms this for the Library at Brodsworth Hall. Two alternate methods have been presented for predicting the environment of rooms that employ conservation heating.

In addition to using the transfer function in the long term future it is useful in the short term, helping to inform conservation decisions. It would also be possible to use the method to predict into the past rather than the future.

# CHAPTER 4

# DAMAGE FUNCTIONS

## 4.1 Introduction

The three types of damage caused by environmental conditions have been mentioned, chemical, biological and physical damage. An example of chemical damage is the hydrolysis or oxidation of cellulose, from which 90% of paper deterioration can be attributed (Sebera, 1994). A classic example of biological damage is mould growth caused by high humidity (Erhardt et al., 1995), which can affect a variety of collections, usually organic in nature. Fluctuation of humidity can cause shrinking and swelling of hygroscopic materials, that results in dimensional change. This can cause physical damage (Pavlogeorgatos, 2003), particularly if the materials are restrained (Jakiela et al., 2008). A multitude of other examples exist for these damage categories, it is unnecessary to detail every one of these, as they are not all included in the research here. However each one is quite likely to be affected in the future as the climate changes, as they are dependent upon the environment.

Each type of damage can be described by a damage mechanism, although separate mechanisms can result in similar damage, for example the disintegration of stone could be caused by biological, chemical or physical mechanisms of damage (Ginell, 1994). Some mechanisms (or processes) are described by Brimblecombe (1994), including photo-degradation, freezing, crystallization stress and biodegradation. A number of mechanisms have associated damage functions, or dose – response functions. These mathematically relate environmental parameters, such as temperature and relative humidity, to the rate of deterioration of materials (Brimblecombe and Grossi, 2008, Lankester and Brimblecombe, 2012a).

There is occasionally some confusion over the two terms, damage function, and dose – response function, sometimes they are used interchangeably, but they have different meanings. A dose response function tends to have a discrete mathematical formula, and sometimes presents a relationship that extends to a maximum value of damage, with a linear or sigmoidal response, depending upon the function, however this is not always the case (Ashley-Smith, 1999). A damage function describes the necessary conditions for damage, but this may not be limited, for example salt transitions, which could occur numerous times. Here the term damage function alone will be used.

In this research a number of damage functions, covering various materials important to historic collections will be used with future indoor climate projections (Chapter 3) to assess potential damage to collections as a result of climate change. For each damage function utilised in this work the relevant mechanism causing damage will be described in the introduction to the function. The functions chosen cover a variety of aspects, there is at least one for each of the chemical, biological and physical types of damage, and they also cover two modes of damage, change by accumulation and by fluctuations.

As discussed temperature and relative humidity are usually the most significant aspects of the environment to consider when assessing damage to a variety of materials. The damage functions used only relate to these two environmental parameters. The projection of future climate indoors only has temperature and humidity data because they are the most significant for damage. This is not to say other environmental parameters are not important, but they are not the focus of this research.

The specific relationship between the rate of deterioration and the temperature and relative humidity for each damage mechanism will be explained for each function. It is widely accepted in science that an increase in temperature increases the reaction rate (Sebera, 1994), and thus causes increasing damage if related to a damage mechanism. Vice versa a reduction in temperature will slow the reaction rate and reduce damage in chemical reactions.

Controlling the environment is an important strategy to minimise damage, it is exceedingly unlikely that all damage can be prevented as over time small changes accumulate resulting in damage. However monitoring, assessing and controlling environments can significantly reduce damage, this relies upon our understanding of damage mechanisms. Environmental control, among other techniques, is currently used as a management strategy to reduce the risk of damage (The National Trust, 2006, Thomson, 1999). In the future it will still be useful, because the mechanisms that cause damage will not change, so they can still be controlled using traditional methods. However the effectiveness of these techniques may change in the future, or require differing levels of resources to continue to provide an effective solution. (Chapter 7)

It is important to understand damage when attempting to manage it; some environments will be stable for specific collections, but cause significant damage to others. This research will use the damage functions to determine how damage will change in the future with respect to indoor environments, providing vital information that can be used to decide how best to prevent this damage. This will allow planning to take place well in advance so adaptation measures can be introduced before damage occurs.

A final note before introducing the individual damage functions, they must be used with care, it is assumed that they hold true in the future. It is possible that constants used are relevant now, but may change in the future, as Brimblecombe and Grossi (2008) discovered. One constant of the Lipfert function describes the solubility of $CaCO_3$, which is a function of carbon dioxide partial pressure and temperature, both of which change in the future (IPCC, 2007b). Additionally some functions are derived empirically, using a given set of conditions, for example observed damage in the temperature range 0-20°C to a material. Thus the function would only be valid under these conditions, and extreme care must be taken outside of this range, it could be that a different reaction dominates, giving an increased level of damage. For these reasons caution must be exerted when using the damage functions.

In summary, to fully appreciate the impact that climate change could have on collections it is important to understand how changes to the indoor environment will manifest as damage. Damage (or dose response) functions will be used to relate the projected environmental conditions to material damage, indicating how the risk of damage may change in the future.

***Cumulative Damage***

## 4.2 Paper

Paper is usually made from cellulose, typically derived from wood, although it can be made from synthetic fibres (May and Jones, 2006). There are a number of processes that can be used to make paper, historically paper was made from cotton or linen rags, but this is rare today (May and Jones, 2006). Wood goes through the pulping process which separates the individual fibres; the pulp is then used to make paper. There are a number of pulping processes, from mechanical to chemical including the kraft and sulphite pulping processes, among others (Biermann, 1996).

Paper can be damaged by a number of mechanisms (Sebera, 1994, Menart et al., 2011), light can cause paper to turn yellow/brown and as a hygroscopic material, water from the environment can be absorbed and released causing swelling and shrinkage respectively, that can lead to damage (The National Trust, 2006). While these are important mechanisms the damage functions here focus upon the chemical deterioration of paper, a major cause of paper strength loss (Menart et al., 2011) which can be attributed to 90% of paper deterioration (Sebera, 1994). This chemical deterioration describes the hydrolysis and oxidation reactions of cellulose (Sebera, 1994), alternatively this is occasionally called natural ageing (Reilly, 2005, Taylor et al., 2005).

Temperature and moisture have a significant impact on the rate of the chemical deterioration. The influence of temperature on chemical reaction rates, and thus deterioration is explained by the Arrhenius equation, first derived in 1878, and developed in 1889 by SA Arrhenius (Pretzel, 2005). This principle is explained by a number of authors in relation to heritage (Zou et al., 1996a, Padfield, 2011, Pretzel, 2005, Menart et al., 2011). The equation describes the dependence of the reaction rate on temperature:

$$K = Ae^{(-\frac{E}{RT})} \quad \textbf{(Eq. 4.1)}$$

Where $T$ is temperature in Kelvin, $A$ the frequency factor, $E$ the activation energy in KJ mol$^{-1}$, and $R$ is the gas constant (8.314 J mol$^{-1}$ K$^{-1}$). The frequency factor is independent of temperature and involves several factors, correction of different units in expressing the rate, entropy change and the chance of correct orientation of molecules for reaction (Padfield, 2011, Michalski, 2002), it also represents other experimental parameters such as humidity, acidity, pollution, light and the physical structure (Menart et al., 2011).

Concerns have been raised over the use of the Arrhenius equation (Brimblecombe, 1994), it is possible that it underestimates damage. Typically the rate of degradation at high temperatures is determined, for example in experiments using accelerated ageing, and extrapolated to lower temperatures. It is possible in the case of complex objects that there is more than one reaction causing damage, with varying activation energies. Therefore at lower temperatures the second reaction could have a greater rate than the first reaction, which has a faster rate at high temperature. Thus just using the first degradation reaction will underestimate damage from the second reaction at low temperatures (Brimblecombe, 1994).Therefore this limitation must be kept in mind when using the Arrhenius equation. A representation of this is shown in figure 4.1, reproduced from Brimblecombe (1994).
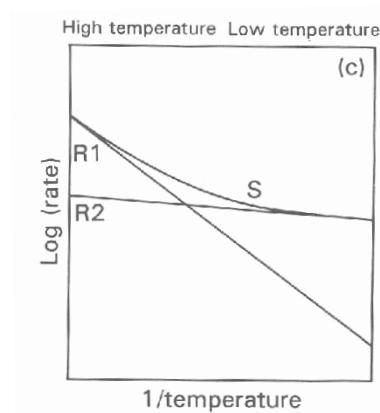


Figure 4.1: Reproduced from Brimblecombe (1994), highlighting the nonlinearity in the summation of two Arrhenius plots.

The moisture content of paper is important as it is directly related to the rate of deterioration of cellulose by acid hydrolysis (Sebera, 1994, Zou et al., 1996a, Strang and Grattan, 2009). Degradation of cellulose is caused by the scission of inter-monomer bonds (Menart et al., 2011), a full explanation of the degradation of cellulose is given by Zou et al. (1996a). The age of paper is also crucial to its degradation, after about 1850 acidic paper was produced that degrades much faster than paper produced before this date (Menart et al., 2011). It is crucial to mention that it is specifically the moisture content of the paper that controls the degradation rate, not the relative humidity of the environment. These two factors are related; however the damage functions deal with this in different ways, thus this will be explained in greater detail in the description of the individual functions.

Four damage functions are presented that predict the damage to paper collections by chemical deterioration, it is difficult to know whether comparison between the functions is possible. One is specifically for a certain type of paper, and the others are relative measures, so it is hard to determine whether there can be comparison between these. This will be discussed in the results section where it is possible to see how the results differentiate from each other.

One paper damage function has been used in previous work by the author, where the results were presented as degradation lifetimes (Lankester and Brimblecombe, 2012a), however it has been decided to use degradation rate instead. It was decided that degradation rates were more useful in a scientific context, scientists are familiar with rates, whereas many conservators (but not all) have very little background in science, and so converting a rate to a relative lifetime can help some people understand the research easier. The various functions that look at paper degradation tend to use lifetimes, so initially this was adopted. One immediate issue arises from this, it is possible that the predicted relative lifetime is actually shorter than the time span covered when looking at climate change, which may confuse some. This is actually arbitrary as the lifetime is often a relative lifetime, compared to standard conditions which have been assigned a lifetime, which may be realistic, but can be subjective depending on the definition of lifetime. This can range from the useable lifetime of an object, for example can you still read the book without causing damage, to the point where the paper is falling apart. Here it was decided to use the degradation rate to simplify this somewhat, and stay with the scientific consensus. However, it is very important to engage the people that are in everyday contact with collections, often the conservators, or those responsible for its management, so in the right context lifetimes would be appropriate, with careful consideration. Without

this engagement and dissemination of work to these people the work could have no impact on collection management, for future protection.

### 4.2.1 Method 1 – Zou et al.

The rate of chemical degradation of paper in absolute terms is estimated by this damage function, as described by Zou et al. (1996a, 1996b). The Arrhenius equation is the basis of this function, with a pre-exponential factor that is dependent upon moisture content and pH. This is important because other functions (*methods 2 and 3*) use relative humidity (Sebera, 1994, Reilly et al., 1995), but Zou et al. (1996a) show that the rate reaction is dependent upon moisture content. These other functions predict relative lifetime, however using parameters specific to one type of paper allows the approach used by Zou et al. (1996a) to estimate absolute lifetimes.

A moisture sorption curve (Dwan, 1987) is used to determine the moisture content from relative humidity, which can be used in the equations of Zou et al. (1996a), one of which is the Arrhenius equation:

$$(1/DP_{final} - 1/DP_{initial}) = k_1 t_{life} \quad \textbf{(Eq. 4.2)}$$

$$k_1 = A_a \exp(-E_a/RT) \quad \textbf{(Eq. 4.1)}$$

$$A_a = A_{a0} + A_{a2}\, cH_2O + A_{a5}\, aH + cH_2O \quad \textbf{(Eq. 4.3)}$$

Where: $DP_{final}$ = 200, $DP_{initial}$ = 1336, $t_{life}$ = time in days, $E_a$ = 104 kJ mol$^{-1}$, $R$ = 8.314 J mol$^{-1}$ K$^{-1}$ (gas constant), $T$ = temperature in K, $A_{a0}$ = 4.54 × 10$^9$ day$^{-1}$, $A_{a2}$ = 2.83 × 10$^{12}$ day$^{-1}$, $A_{a5}$ = 9.85 × 10$^{16}$ 1mol$^{-1}$ day$^{-1}$, $cH_2O$ = moisture content in %, $aH^+$ = molar hydrogen ion concentration (activity).

The function used in this work is specific to a bleached bisulfite pulp paper, with an initial pH of 4.85. This type of paper is relevant to historic collections as the sulphite process of manufacturing paper pulp was dominant from 1900 to 1940 (Biermann, 1996). The activation energy ($E_a$), and the initial and final degree of polymerization values ($DP_{final}$ and $DP_{initial}$) are other variables specific to this type of paper. The predicted lifetime is calculated ($t_{life}$) in days, but converted to yearly values for the comparisons later in this work. The deterioration rate will also be used rather than lifetime; this is equal to the reciprocal of the lifetime value. This damage function has been used to project future damage to paper indoors, and results deriving from this research have been published by the author (Lankester and Brimblecombe, 2012a).

In future chapters this damage function will be referred to as the Zou damage function. As described in previous chapters the AWK programming language is used throughout this research, and the AWK program for this function can be found in appendix E.

### 4.2.2 Method 2 – The Isoperm

This method also predicts damage, or strength loss, of paper from chemical reactions, specifically the hydrolysis and oxidation of cellulose (Sebera, 1994). The damage function quantifies the effect of varying temperature and relative humidity on the life expectancy of paper collections (Sebera, 1994). Whereas *method 1* allows for predictions in absolute terms this method uses relative rates of deterioration. This is important to remember as it is not possible to directly compare the two results. For example if a relative rate of 0.5 is given this indicates that the rate of deterioration has been halved, effectively doubling the useful lifetime. Sebera (1994) tends to use life expectancy values, so a relative rate of 0.5 would double the relative life from 45 to 90 years, or 100 to 200 years, this is used as it is described as 'a more useful term to describe the effect of the environment'. It is possibly also used to simplify the science for conservators with limited scientific background. However, here the relative deterioration rate will be used, this again is the inverse of the relative permanence.

As discussed previously temperature and relative humidity have an effect on the chemical reactions affecting paper, Sebera (1994) presents an equation (Eq. 4.4) that when evaluated allows for a quantitative measure of permanence changes.

$$\frac{P_2}{P_1} = \left(\frac{RH_1}{RH_2}\right)\left(\frac{T_1+460}{T_2+460}\right) \times 10^{394\Delta H\left(\frac{1}{T_2+460}-\frac{1}{T_1+460}\right)}$$

(Eq. 4.4)

The temperature in the above equation is degrees Fahrenheit. This equation requires two sets of temperature and relative humidity, $T_1$, $RH_1$ and $T_2$, $RH_2$, the first set is that of the reference conditions, here $T_1$=68 °F (20 °C) and $RH_1$=50%, which have a permanence ($P_1$) of 1. The second set of temperature and relative humidity is that of the environment at a given time, evaluating the equation gives a value of $P_2/P_1$ , the relative permanence rate, and thus the relative deterioration rate can be determined by taking the reciprocal of this value and ΔH is the enthalpy of activation which is recommended as 30-35 Kcal/mol (Sebera, 1994).

It is possible that two different combinations of temperature and relative humidity will result in the same permanence, the different changes in temperature and humidity can

exactly compensate for each other and result in the same permanence. There are an infinite set of these paired temperature and relative humidity's and when plotted on a graph generate a line with the same permanence, which can be defined as an isoperm (Sebera, 1994), hence the name of the function. Figure 4.2 shows an example of an isoperm.
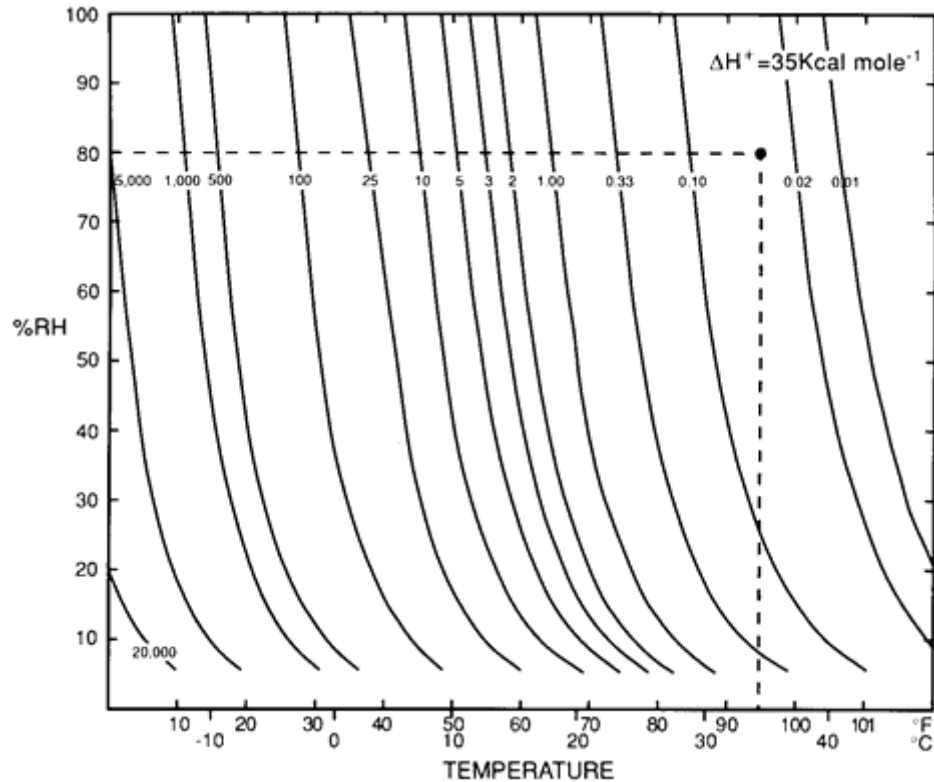


Figure 4.2: Reproduced from Sebera (1994). Percent relative humidity versus temperature Isoperm diagram. Permanence values are calculated for ΔH = 35 kcal relative to paper at 68 degrees F and 50% RH taken as comparison standard (permanence equal to 1.00). Relative permanence at 95 degrees F and 80% RH is 0.03.

The relative deterioration rate is calculated for each set of temperature and humidity, and averaged over a set time period, here a year is used. It is important to average over a complete year, or multiples, as incomplete years bias the result, slow winter deterioration can cause significant reduction on the overall rate, which is increased by faster summer rates of deterioration, thus both must be taken into account.

While Sebera (1994) introduced this technique Padfield (2012) presents an equation that is an approximation of Sebera's, this is used here as it reduces the computational time required. The equation of the relative rate of degradation is:

$$\text{Rate} = RH \times 1.34 \times 10^{16} \times \exp(-100000/(8.314 \times (t+273))) \qquad \textbf{(Eq. 4.5)}$$

The activation energy used here is 100 kJ/mol, which converts to 23.9 Kcal/mol, lower than that recommended by Sebera, but said to be typical (Padfield, 2012), and similar to the 104 kJ/mol used by Zou et al. (1996a). Michalski (2002) also states that the activation energy for most paper and film studies falls in the range of 80-120 kJ/mol.

While Padfield (2012) presents this equation as an approximation, no evidence is shown in support of this, therefore the two separate equations are evaluated below to provide evidence that use of the approximation is justified. The standard conditions of 20°C (68°F) and 50% relative humidity are first used, the original equation becomes:

$$\frac{P_2}{P_1} = \left(\frac{50}{50}\right)\left(\frac{68+460}{68+460}\right) \times 10^{394\Delta H\left(\frac{1}{68+460} - \frac{1}{68+460}\right)}$$

**(Eq. 4.4)**

This evaluates to $P_2/P_1 = 1$, the relative permanence, and taking the reciprocal gives a relative deterioration rate of 1. The approximation equation becomes:

Relative Rate = 50 × 1.34 ×10$^{16}$ × exp(-100000/(8.314 × (20+273)))     **(Eq. 4.5)**

This evaluates to a relative rate of 1, and thus is correct. A second set of data will be tested to check the approximation at another point, 24°C (75.2°F) and 70% relative humidity. The original equation evaluates to a relative rate of 2.46, and the approximation to 2.42. This indicates that the equation given by Padfield is an acceptable approximation, and therefore is used here.

The *isoperm method* has been challenged (Strang and Grattan, 2009) as evidence suggests that paper degradation has a direct relationship with moisture content, as opposed to relative humidity (Strang and Grattan, 2009, Zou et al., 1996a). The work by Sebera (1994) assumes that there is a linear relationship between moisture content and relative humidity, however this is inconsistent with the sorption isotherm, which describes the relationship as an S-shaped curve (Strang and Grattan, 2009). Sebera (1994) alludes to this stating that outside of the range of 30-65% humidity behaviour deviates from the linear relationship described. Therefore at the extremes of high and low relative humidity the relationship is not linear, and Sebera's (1994) isoperm is incorrect. A modified equation is proposed (Strang and Grattan, 2009), however currently some parameters are undefined for use with paper thus rendering the equation unusable until further work is carried out, at which point it appears sensible that this equation should supersede Sebera's (1994). Further revision is suggested by Menart et al. (2011) as there is

evidence that the degradation of acidic papers is also dependent upon pH differently to alkaline papers.

Therefore the *isoperm method* is used, while taking into consideration the limitations; it is possible that *method 1* is more realistic than the *isoperm method*, as it takes into account that it is the moisture content that is important. An example of this method in use is presented by Thickett (2005). The AWK program for this function, which will be referred to as the isoperm damage function in future chapters, can be found in appendix E.

### *4.2.3 Method 3 – TWPI*

The third method to estimate damage to paper is the time weighted preservation index (TWPI) developed by the Image Permanence Institute (IPI) and part of the Climate Notebook software. Again the function is based on the rate of chemical reactions, describing the quality of the environment with respect to preservation of organic materials (Reilly et al., 1995). A preservation index (PI) is calculated for each measurement of temperature and relative humidity, with the value in years, these measurements are then averaged correctly (by taking the reciprocal to determine the rate and converting back to a lifetime value at the end) to give the time weighted preservation index that takes into account the increased deterioration that occurs when temperature and humidity are high (Reilly, 2005). The PI or TWPI gives an idea of the time taken for significant deterioration to occur to organic materials, this is criticised by Padfield (2012) as there are limitations in applying one value across all organic materials. Paper and wood behave very differently, with wood having greater resistance to the chemical reactions relevant here, this is discussed in another paper after the initial one describing TWPI (Reilly, 2005).

In more recent work the scope of applicability is narrowed, mentioning vulnerable organic materials, with examples given such as acidic wood-pulp paper, colour photos and acetate film amongst others, which deteriorate significantly in about 50 years at room temperature and moderate relative humidity (Nishimura, 2009). But it is also stated that the life expectancy value can be used in a relative sense for all organic objects, while it can be used literally for short lived items, such as those described above (Nishimura, 2009).

As mentioned this measure is part of the commercial software *Climate Notebook*, thus the full description of how the method was derived has not been published (Strang and Grattan, 2009). It is known that it is based on a study of deterioration of cellulose acetate by hydrolysis (Reilly et al., 1995), and that each temperature and humidity pair has an associated PI value (Reilly et al., 1995).

Whilst the data determining the PI value of each set of environmental values hasn't been published an equation has been fitted to the data that Padfield (2012) attributes to IPI, but as mentioned has not yet been published by IPI. This equation takes the following form:

Lifetime = (($E$-134.9 × $RH$) / (8.314 × $T$) +0.0284 × $RH$-28.023)/365 **(Eq. 4.6)**

In this equation temperature is in Kelvin. Again the result is given as a lifetime value, in this work the rate of degradation will be used, as with the previous two methods, again this is the reciprocal of the lifetime value. It is possible to use the software Climate Notebook to determine the TWPI values, testing this with the equation above gives corresponding values. However realistically it is not viable to use the software in this project as it is extremely prohibitive with the large amounts of data that will be used, it would take a considerably long time. However it is possible to use the equation provided by Padfield (2012) with the AWK programming language and the results are available in a (very small) fraction of the time required to input the multiple data sets into Climate Notebook. The AWK program for this function can be found in appendix E. An example of this function, referred to in future chapters as the TWPI damage function, in use is also given by Thickett (2005) and Thickett et al. (2007).

### 4.2.4 Method 4 – Pretzel

This method is presented in full by Pretzel (2005), this applies the Arrhenius equation (equation 4.1), to take into account the effect of temperature, as the other methods do, with a power law relationship that describes the effect of relative humidity. This power law is described by Michalski (2002), it states that the rate of acid hydrolysis should follow a power law relationship when determining the effect of relative humidity. For cellulosic materials a power index of 1.3 is suggested as a best fit for the majority of the data (equation 4.7). The isoperm idea of Sebera (1994) is also applied by Pretzel (2005), to calculate relative lifetimes of deterioration (equation 4.8) instead of the true reaction rate. Relative rates will be determined as previously explained rather than lifetimes.

$$K \quad (\text{RH})^{1.3} \quad \textbf{(Eq. 4.7)}$$

$$L_r = \frac{(RH_1)^{1.3} \times \exp\left(\frac{-E_a}{(R \times T_1)}\right)}{(RH_2)^{1.3} \times \exp\left(\frac{-E_a}{(R \times T_2)}\right)} \quad \textbf{(Eq. 4.8)}$$

Where: $L_r$ =relative lifetime, $E_a$ = activation energy (kJ/mol), $R$ = gas constant, $T_1$, $T_2$, $RH_1$ and $RH_2$ are the reference and comparison temperature (in Kelvin, K) and relative

∝

humidity, respectively in both cases. The activation energy used here will be 100 kJ/mol, and the reference temperature and humidity as before, 20°C and 50%, so that comparison may be possible between the similar methods. The AWK program for this function, referred to in future chapters as the Pretzel damage function, can be found in appendix E.

## 4.3 Silk

Silk is a natural fibre produced by silkworms, which is processed and used as a textile with various uses, from curtains to furnishings, wall coverings and clothing (Luxford, 2009). Typically light has been regarded as the most damaging environmental factor to silk (Luxford, 2009). As a natural fibre silk is hygroscopic, until recently little research had been undertaken to investigate the effect of relative humidity on silk deterioration, but Luxford (2009) has highlighted the importance of relative humidity on silk damage, and developed a relevant damage function.

### *4.3.1 Silk Isoperm*

A single method is presented that estimates the damage caused by temperature and humidity on silk (Luxford, 2009). This is an adaptation of the isoperm function that describes damage to paper (Sebera, 1994), with experimental data of silk deterioration replacing the relevant aspects. Once again the method follows the Arrhenius principle; here the activation energy used is 50 kJ/mol, determined from a kinetics study by Luxford (2009). As previously the standard conditions of 20°C and 50% RH are used, at which relative permanence is 1, and in this case an approximate lifetime of 250 years.

The reaction rate for these standard values becomes:

$$\text{Rate} = \text{RH} \times \text{A} \times \exp(-50000/(8.314 \times (t+273))) \qquad \textbf{(Eq. 4.9)}$$

Where A is the pre-exponential factor $8.2 \times 10^6$, therefore:

$$\text{Rate} = 50 \times 8.2 \times 10^6 \times \exp(-50000/(8.314 \times (20+273))) \qquad \textbf{(Eq. 4.9)}$$

$$\text{Rate} = 5.02 \times 10^{-13}$$

If we divide the pre-exponential factor by this standard rate (when temperature is 20°C and 50% relative humidity) this replaces the pre-exponential factor in the Sebera equation, which determines the relative rate. So:

$$8.2 \times 10^6 / 5.02 \times 10^{-13} = 1.64 \times 10^7$$

Thus the Isoperm equation changes from:

$$\text{Relative Rate} = RH \times 1.34 \times 10^{16} \times \exp(-100000/(8.314 \times (t+273))) \qquad \textbf{(Eq. 4.5)}$$

To:

$$\text{Relative Rate} = RH \times 1.64 \times 10^{7} \times \exp(-50000/(8.314 \times (t+273))) \qquad \textbf{(Eq. 4.10)}$$

One limitation is the assumption that relative humidity has the same effects at all temperatures; however the experimental data is limited to results from 80°C across the range of relative humidity. As discussed previously it is possible that extrapolation of the Arrhenius equation is not always possible, as it can result in an underestimation of damage. Therefore this isoperm is a first approximation; further research is required to determine the effect of relative humidity at other temperatures, to increase the accuracy of deterioration predictions (Luxford, 2009). Thus care must be taken when using this function as the isoperm extrapolates to low temperatures. The set of silk isoperms determined by Luxford (2009) is reproduced in figure 4.3. The AWK program for this function, referred to in future chapters as the silk isoperm damage function, can be found in appendix E.
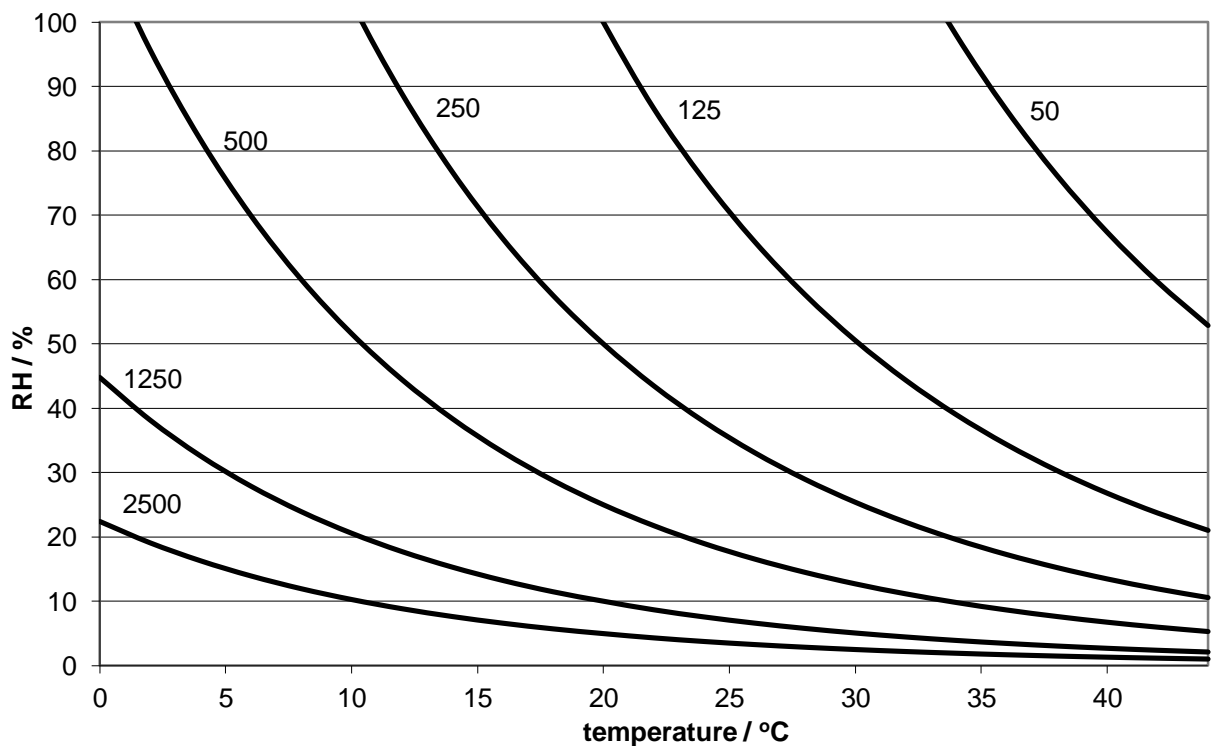


Figure 4.3: Isoperms for silk deterioration (predicted display lifetimes in years, are shown next to each isoperm). Reproduced from Luxford (2009).

## 4.4 Mould

The previous damage functions have focused upon specific materials, now though the focus turns to mechanisms that can affect a greater range of materials. Here mould is discussed which can be an issue for a number of materials, most frequently those that are organic in nature, such as wood and paper. Mould has been described as the single greatest risk worldwide arising from incorrect climate (Michalski, 2007).

Mould is a lay term for a fungus (The National Trust, 2006), there are four main genera of fungi that affect collections worldwide, being *Cladosporium, Alternaria, Aspergillus* and *Penicillium* (Florian, 2002). Mould growth occurs in two distinct stages, firstly germination of conidia (often incorrectly called spores (Florian, 2002)) must occur, after this mould begins to grow. Hyphae are produced which secrete enzymes at their tips that dissolve the substrate, thus causing damage; the substrate is used as a food source for further growth (The National Trust, 2006). Mould also causes damage in other ways such as discolouration, either from the fungal growth itself or through staining, caused by the secretion of fungal pigments into the substrate (Florian, 2002).

In order for mould growth to occur specific conditions must be met, occasionally called the favourable conditions (Brimblecombe, 2010, Hukka and Viitanen, 1999). This relates to temperature and relative humidity, and occasionally critical relative humidity's are quoted as minimum requirements of mould growth, for example 62% (ASHRAE, 2003), 65% (The National Trust, 2006), 70% (Florian, 2002) and 80% (Sedlbauer et al., 2003). These specific conditions can vary depending upon the circumstances, for example the species of mould and the substrate (Moon and Augenbroe, 2003). A critical humidity alone is often insufficient and could overestimate potential mould growth as other factors such as time and temperature are also important (Moon and Augenbroe, 2003, Ayerst, 1969, Isaksson et al., 2010, Hukka and Viitanen, 1999, ASHRAE, 2003, PAS 198, 2012). Specific requirements of these will be discussed for each damage function. A critical humidity value is included as part of one of the damage functions, this will be used alone in order to compare the prediction to the more complex model of mould growth risk.

In addition to critical humidity values other factors are occasionally taken into account using the isopleth system (Sedlbauer et al., 2003, Isaksson et al., 2010), reproduced in figure 4.4. This accounts for temperature, relative humidity, substrate and time. The lowest isopleth for mould (LIM) is a similar notion to the critical humidity, but accounts for other important factors. The humidity required for germination when temperature is high is similar to the values of critical humidity stated, but as temperature decreases the humidity

required for germination increases. There is also LIM data for growth after germination, which behaves differently to that required for germination; this is another advantage over a critical humidity value. Sometimes these are quoted as the conditions required for growth, but are also discussed with respect to preventing mould growth (The National Trust, 2006, Florian, 2002), these are two different things, if humidity is below the critical value then mould will not grow, but if it is above it indicates mould can grow, but doesn't mean that it will, other conditions must be met. Therefore using a simple critical humidity to predict mould growth simplifies the matter greatly.
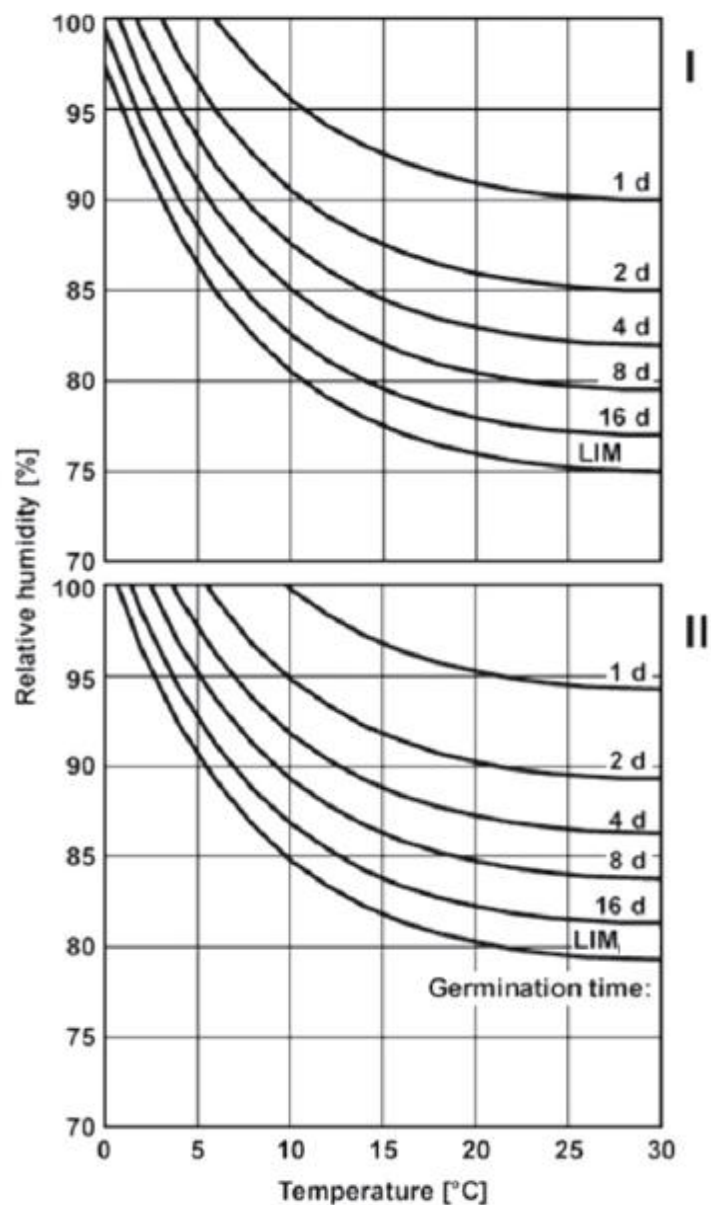


Figure 4.4: Generalised isopleth system for spore germination valid for all fungi of substrate categories I (bio-utilisable substrates) and II (substrates with porous structure), reproduced from Isaksson (2010).

This describes how temperature and humidity effect mould growth in general; each function deals with this in different ways, specific to each method. Sometimes these critical values are only relevant in an environment that doesn't change, this poses a challenge when environments with varying conditions are encountered. Fortunately this is taken into account in the damage functions described.

### 4.4.1 Method 1 – Isaksson et al.

This dose-response function predicts the onset of mould growth on spruce and pine sapwood. It is based on experimental data for mould growth on wood (Isaksson et al., 2010). It allows for variations in the environment over time, as required to estimate future damage in a changing environment.

This method can be calibrated to substrates other than pine and spruce sapwood; therefore it is particularly useful as the technique can be applied to different wood species, so that specific heritage materials can be considered. This work will use the pine sapwood reference example, under constant conditions of 20°C and 90% relative humidity this required 29 days ($N_{ref}$) for mould growth to initiate. Spruce sapwood required 38 days for mould to germinate at the reference conditions, if experiments are carried out under the reference conditions other substrates, such as heritage specific materials, could be used with the method allowing for prediction of mould risk (Isaksson et al., 2010). This simple experiment widens the scope of this method, and it is potentially very useful for further investigations into mould risk in historic collections, and is a source of further work.

A total daily dose ($D$) is calculated, being the product of two components dependent upon the daily average temperature ($T_d$) and relative humidity ($RH_d$). This is expressed in days, and is equal to 1 where the temperature and relative humidity are equal to that of the reference climate.

$$\text{Daily dose}(D) = T_d \times RH_d. \quad \textbf{(Eq. 4.11)}$$

The components $T_d$ and $RH_d$ are defined as:

$$T_d = \exp(0.74 \times \ln(T/20)) \qquad \textbf{when } 0.1 < T \leq 30°C \qquad \textbf{(Eq. 4.12)}$$

$$RH_d = \exp(15.53 \times \ln(RH/90)) \qquad \textbf{when } 75 < RH \leq 100\% \qquad \textbf{(Eq. 4.13)}$$

The daily dose ($D$) is summed to get a running total of the dose over multiple days, and can be compared to the reference, by the means of a relative dose ($D/N_{ref}$), a value of one indicates that favourable conditions have been met for mould germination. A value below

one indicates less than favourable conditions, and above one more than favourable, with two being twice as favourable.

Negative daily doses are possible when conditions are unfavourable, providing a setback for the germination process, however the accumulated daily dose can never be negative. The values of $T_d$ and $RH_d$ under unfavourable conditions are:

$$\boldsymbol{T_d} = -0.5 \qquad\qquad \textbf{when } T<0.1°C \qquad\qquad \textbf{(Eq. 4.14)}$$

$$\boldsymbol{RH_d} = -2.7 + (1.1 \times RH)/30 \qquad\qquad \textbf{when } 60<RH<75\% \qquad\qquad \textbf{(Eq. 4.15)}$$

$$\textbf{Or}$$

$$\boldsymbol{RH_d} = -0.5 \qquad\qquad \textbf{when } RH<60\% \qquad\qquad \textbf{(Eq. 4.16)}$$

The predicted indoor environment, from the transfer equation is coupled with this function, and the number of days reported when the cumulative relative dose is greater than 1, indicating germination is possible. This damage function has been used to project future mould growth risk indoors, and results deriving from this research have been published by the author (Lankester and Brimblecombe, 2012b).

The AWK program for this function, referred to in future chapters as the Isaksson damage function, can be found in appendix E.

### 4.4.2 Method 2a and b – Hukka and Viitanen

This model simulates mould growth on pine and spruce sapwood also; it is based on previous regression models for mould growth on said materials (Hukka and Viitanen, 1999). A number of equations combine to form this model, which takes into account fluctuating conditions when calculating possible mould growth. While this model is idealised for either spruce or pine wood the form of the model can be reasoned to be valid for other wooden materials (Hukka and Viitanen, 1999).

The model calculations cumulate in a prediction of mould growth, $M$, the mould index (no units). The value of $M$ is based upon an existing standard index of the visual appearance of the material being studied. A value of zero indicates no mould growth, 1: some growth detected, with microscopy, 2: moderate growth under microscopy (>10% coverage), 3: growth detected visually, 4: growth detected visually (>10% coverage), 5: growth detected visually (>50% coverage), 6: growth detected visually (100% coverage). Therefore a value of $M$=1 is critical and indicates initiation of mould growth (Hukka and Viitanen, 1999).

As discussed various equations combine to form this model, this first part describes the conditions favourable for initiation of mould growth. The moisture content of the wood is critical to mould growth and this is affected by ambient humidity (Jakiela et al., 2008). The following equations describe the critical relative humidity required for initiation of mould growth:

$$RH_{crit} = -0.00267 \times T^3 + 0.160 \times T^2 - 3.13 \times T + 100 \quad \textbf{when } T \leq 20 \quad \textbf{(Eq. 4.17)}$$

$$RH_{crit} = 80\% \quad \textbf{when } T > 20 \quad \textbf{(Eq. 4.18)}$$

As mentioned, occasionally a specific relative humidity is quoted as required to prevent mould growth. Therefore the above equations alone will form one damage function (2a), in order to see how the results of this compare to the more complex functions of mould growth prediction. The AWK program for this function, referred to in future chapters as the critical relative humidity damage function, can be found in appendix E.

The second part of the complete model addresses the maximum mould growth possible, as there can be a limit to this, depending upon the previous environmental conditions. $M_{max}$ (no units) is the value of maximum mould growth, calculated using the following formula:

$$M_{max} = 1 + 7(RH_{crit} - RH/RH_{crit} - 100) - 2(RH_{crit} - RH/RH_{crit} - 100)^2 \quad \textbf{(Eq. 4.19)}$$

The next part of the model addresses the growth of mould during favourable conditions, the basis of the equation is taken from Viitanen (1999) this presents a regression equation for the response time, in weeks, needed for the initiation of mould growth, under constant environmental conditions. Isaksson et al. (2010) interpret this equation as a differential relationship, allowing for varying environmental conditions to be assessed, as required in this work. This equation (Eq. 4.20) therefore represents the initiation response time, and such is only valid before germination occurs ($M<1$).

$$t_m = \exp(-0.68 \times \ln(T) - 13.9 \times \ln(RH) + 0.14W - 0.33SQ + 66.02) \quad \textbf{(Eq. 4.20)}$$

Once germination occurs and mould growth is initiated the above equation is no longer valid, and a second regression equation is required, again from Viitanen (1999), describing the time required for visual appearance of mould ($M=3$).

$$t_v = \exp(-0.74 \times \ln(T) - 12.72 \times \ln(RH) + 0.66W + 61.50) \quad \textbf{(Eq. 4.21)}$$

Equations 4.20 and 4.21 are combined into a correction coefficient, $K_1$, equation 4.22. Equation 4.22 forms part of the final equation (4.24) therefore when $M < 1$ no correction is applied, $K_1 = 1$, and the following correction is applied otherwise:

$$K_1 = 2/(t_v/t_m - 1) \qquad \textbf{when } M > 1 \quad \textbf{(Eq. 4.22)}$$

A second correction coefficient ($K_2$) also forms part of the final equation (4.24), this relates to the maximum mould growth attainable, equation 4.23, this correction is described below:

$$K_2 = 1 - \exp[2.3(M - M_{max})] \quad \textbf{(Eq. 4.23)}$$

Equations 4.20, 4.22 and 4.23 combine to make the final form of the model, which is interpreted as a differential relationship, where $M$ is assumed to increase linearly in time (measured in days) (Hukka and Viitanen, 1999). Equation 4.24 is valid when conditions are favourable for growth:

$$dM/dt = [1/7 \times \exp(-0.68 \times \ln(T) - 13.9 \times \ln(RH) + 0.14W - 0.33SQ + 66.02)]K_1K_2$$
$$\textbf{(Eq. 4.24)}$$

In the previous equations the variables $W$ and $SQ$ represent the species of wood and the sawn quality of the wood respectively. $W$ is either equal to 0, for pine, or 1, for spruce. $SQ$ also equals 0 or 1, for re-sawn and kiln dried wood respectively.

One final set of equations are required, to model the growth when the environmental conditions are not favourable, this causes a set back to the growth of mould. The degree of setback is dependent upon the time that unfavourable conditions exist for $(t - t_1)$, this is described below:

$$\textbf{\textit{dM/dt}} = \text{-0.032} \qquad \textbf{when } t - t_1 \leq 6\text{h} \qquad \textbf{(Eq. 4.25)}$$

$$\textbf{\textit{dM/dt}} = 0 \qquad \textbf{when } 6\text{h} \leq t - t_1 \leq 24\text{h} \qquad \textbf{(Eq. 4.26)}$$

$$\textbf{\textit{dM/dt}} = \text{-0.016} \qquad \textbf{when } t - t_1 > 24\text{h} \qquad \textbf{(Eq. 4.27)}$$

Thus for each pair of temperature and relative humidity a value of $dM/dt$ is determined, this is continually summed to give the value of $M$, when this exceeds a value of 1 germination is possible. Here the number of days where the mould index exceeds 1 is determined. This completes the model described by Hukka and Viitanen (1999), the AWK program for this can be found in appendix E. In future chapters this is referred to as the Hukka damage function.

### 4.4.3 Method 3 – Moon and Augenbroe

This model is based upon mould germination graphs, see figure 4.5, utilised with a mould growth analysis method (Moon and Augenbroe, 2003), to predict mould growth, with fluctuating conditions of temperature and relative humidity.
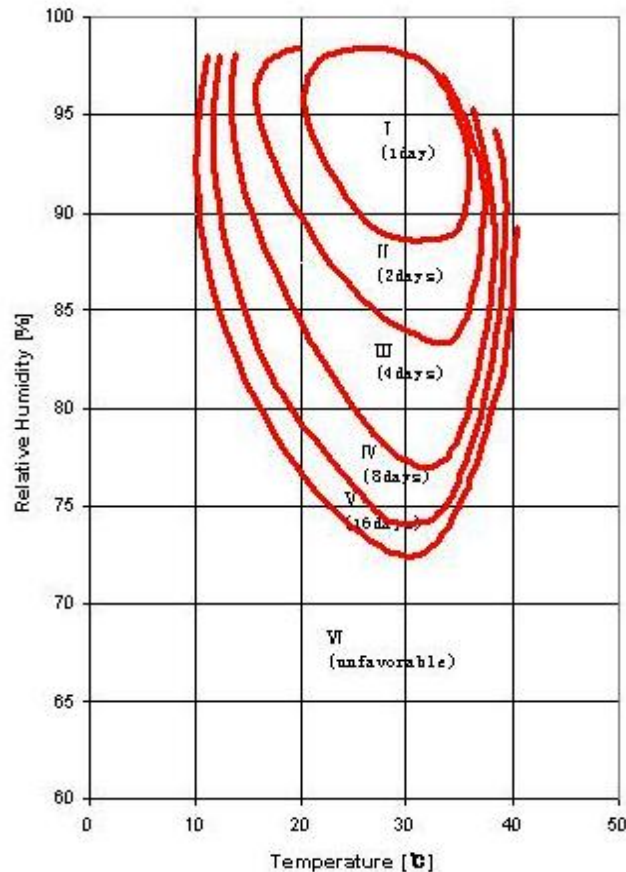


Figure 4.5 : Reproduced from Moon and Augenbroe (2003), Mould germination graph showing each group with temperature, relative humidity and required exposure time for the initiation of mould germination.

Figure 4.5 presents the mould germination graph for *Aspergillus restrictus*, used by Moon and Augenbroe (2003), this states the required time for mould growth to occur at various pairings of temperature and humidity. Group I takes only 1 day for growth to occur, the time required doubles between each groups, so 4 days for group III, and 16 days for group V, group VI contains the unfavourable conditions where no growth will occur.

No specific material is mentioned with regards to the mould growth predictions. However the effect of different substrates on mould growth is discussed; and a correction is in development for other building materials (Moon and Augenbroe, 2003).

This method records the accumulated exposure time of each group individually, and when the required exposure time for a specific group is reached this indicates that there is a risk of mould growth. The analysis is carried out with the daily averages of temperature and humidity. Where the data falls into a higher group (where group I is the highest) than the previous day the accumulated exposure of the lower groups are also increased, and compared to the required exposure. When the opposite occurs; i.e. the conditions are in a lower group than the previous day, the exposure time of higher groups are set to zero, as germination will not occur in the higher groups (Moon and Augenbroe, 2003). An example of the process is shown in the annotated table below:

Table 4.1: Reproduced from Moon and Augenbroe (2003), Example of the application of the germination graph method.

| Day | Temp. | RH | Group | Accu. Exposure time | Req. Exposure time | Mould Growth Risk | |
|-----|-------|-----|-------|---------------------|--------------------|-----|-----|
| 1 | 20 | 70 | VI | - | - | X | X |
| 2 | 25 | 80 | III | 1 | 4 | X | X |
| 3 | 23 | 85 | III | 2 | 4 | X | X |
| 4 | 26 | 90 | II | 1 | 2 | X | X |
| | | | III | 3 | 4 | X | |
| 5 | 30 | 95 | I | 1 | 1 | O | O |
| | | | II | 2 | 2 | O | |
| | | | III | 4 | 4 | O | |
| 6 | 22 | 85 | III | 5 | 4 | O | O |
| 7 | 18 | 97 | II | 1 | 2 | X | O |
| | | | III | 6 | 4 | O | |
| 8 | 25 | 80 | III | 7 | 4 | O | O |
| 9 | 18 | 97 | II | 1 | 2 | X | O |
| | | | III | 8 | 4 | O | |
| 10 | 20 | 70 | VI | - | - | X | X |
| 11 | 25 | 80 | III | 1 | 4 | X | X |
| 12 | 18 | 97 | II | 1 | 2 | X | X |
| | | | III | 2 | 4 | X | |

Annotations:
- Favourable in group III
- Favourable in group II, continue counting III.
- Favourable in group I, continue counting II + III. Required exposure time reached, risk of mould growth recorded.
- Group II count reset, as previous conditions unsuitable for group II.
- Mould risk ceases as conditions return to unfavourable.

It is simple to take a few predictions of temperature and relative humidity and determine the groups within which they fall, and thus mould growth risk. However in the work described in this thesis there will be significantly more than a few pairs of temperature and humidity values (365 days × 30 years × 100 runs × 8 time periods = 8.76 million pairs of values per room investigated). Therefore it is necessary to describe figure 4.4 as an algorithm so that a program can complete the calculations. In order to do this ellipsis were fitted as best as possible over the germination graph to give an equation that can be evaluated determining which group a pairing of temperature and relative humidity fall into. The equations of the fitted ellipsis can be found in the AWK program for this damage function, referred to in future chapters as the graph method damage function, the program can be found in appendix E.

## 4.5 Degree days

In other specialist areas such as agriculture various degree day levels are routinely specified for different pests. However it is also used in a variety of ways such as determining energy requirements from heating and cooling (Brimblecombe, 2010). This function is useful in relation to pest management, but has been used rarely.

The degree days measurement counts temperature above a threshold value (Brimblecombe, 2010), which here is set as 15°C, the lower boundary of temperature required for optimum growth of most insect species (The National Trust, 2006, Child, 2007). This is not a perfect measure, as pests require more than just an ideal temperature to be viable, such as moisture (Pinniger, 2001). However higher temperatures generally increase insect activity, and some pests, such as the biscuit beetle and webbing clothes moth do not require moisture from the environment (Child, 2007, Brimblecombe and Lankester, 2012).

It is known that changes to climate leads to distribution differences in flora and fauna (Ridout, 2000). Warmer temperatures in the future may allow the spread of Mediterranean or sub-tropical flora and fauna to the United Kingdom. One particular example that may pose a significant threat in the UK could be termites (Ridout, 2000). Termites feed on cellulosic materials, such as wood, paper and some textiles, all significant materials in the field of cultural heritage. Some termites require a moisture source, however dry wood termites do not, as their name suggests. They live in dry wood and are less dependent upon external moisture (Ridout, 2000). Should climate change have a significant effect upon the UK climate several species of termites would almost certainly become established (Ridout, 2000).

It is possible that the degree day method can be used as an indicator of future increases of temperature, and therefore the threat of damage arising from increased pest activity, assuming other factors are not limiting.

Examples of pests relevant to historic collections are the common furniture beetle *(Anobium punctatum)* and the death watch beetle *(Xestobium rufovillosum)*, both which are wood borers (The National Trust, 2006, Child, 2007, Pinniger, 2001). Two further examples are the webbing clothes moth (*Tineola bisselliella*) and booklice *(Liposcelis bostrychophylus* and *Lepinotus patruelis)* which tend to attack materials made of cellulose, such as paper and cotton (The National Trust, 2006, Child, 2007, Pinniger, 2001).

Recently Stengaard Hansen et al. (2011) have used a similar principle, counting degree days over 20°C to project the impact of climate change on one specific pest, the brown carpet beetle, *Attagenus smirnovi*. They project that damage to collections in Scandinavia will increase in the future, with a 30% rise in degree days over 20°C. In addition to this Brimblecombe and Lankester (2012) have subsequently projected damage from insect pests, and relate life cycle data to degree days, resulting in an approximation of 490 degree days required for one life cycle of the biscuit beetle, *Stegobium paniceum*. They also investigate the impact of climate change on the number of flying days, and the number of eggs produced (Brimblecombe and Lankester, 2012).[1]

Degree days are calculated based on a daily average of temperature, and summed over a period. The calculation used for each individual day is:

$$\text{Degree Day } (DD) = T_{da} - T_{sp} \textbf{ When } T_{da} > 15 \qquad \textbf{(Eq. 4.28)}$$

Where $T_{da}$ = daily average temperature, and $T_{sp}$ = set point temperature, here 15°C.

This measure can be useful in a number of ways, if damage is triggered when, for example, degree days exceed 200, then it is possible to project future periods of damage. This would be important for implementing strategies to manage the risk of damage. If data was available determining the required degree days for one life cycle of the pest then future projections can estimate increased damage through an increased pest population.

---

[1] This paper, while co-authored by the author of this thesis, does not form part of this thesis. Some work derives from that presented in the thesis, such as the indoor predictions and degree day predictions. However the novel work in the paper was undertaken mainly by P. Brimblecombe, thus is not presented in this work.

This damage function has been used to project the number of future degree days indoors, and results deriving from this research have been published by the author (Lankester and Brimblecombe, 2012b).The AWK program for this function, referred to as the degree day function in future chapters, can be found in appendix E.

*Damaging Events*

## 4.6 Salt Weathering

Salts can cause damage to porous materials, such as stone or ceramics. The source of salts in materials can arise from a number of mechanisms, sea-spray, groundwater or unsuitable building materials (The National Trust, 2006, Price, 2000). Salt weathering is largely associated with outdoor materials, however there are also examples of salt damage indoors.

Damage from salts can take two forms, aesthetic and physical damage (Benavente et al., 2008). Salts crystallise at specific conditions, which can occur either on the surface of the stone (efflorescence), causing aesthetic damage, or under the surface (sub-efflorescence) causing physical damage (Benavente et al., 2008).  Here the focus will be upon physical damage caused by sub-efflorescence. The environment controls crystallisation of salts, which can only occur when the relative humidity is below the equilibrium relative humidity. In the case of hydrated salts this can be dependent upon temperature also (Benavente et al., 2008), e.g. the equilibrium relative humidity for halite is 75.3% at 25°C (Grossi et al., 2011, Sabbioni et al., 2010). Fluctuation of humidity can allow salts to move into and out of solution (crystallise), this is a phase transition (Grossi et al., 2008b, Brimblecombe, 2010). These are particularly important, as only slight changes in environmental conditions are required for phase transitions to occur, such as those associated with climate change. This may lead to the amplification of damage, as discussed previously. Such crystallisation – dissolution cycling can lead to significant damage from multiple crystallisation events (Grossi et al., 2011, Sabbioni et al., 2010).

Powdering, delamination, flaking  and granular disaggregation of the surface are typical types of physical damage caused by salts, this leads to loss of the surface gradually, which is particularly significant if the stone is carved as this detail is lost (Price, 2000, Ginell, 1994).

Damage is caused by the salts crystallising within the pores of the material, if the pressure exerted exceeds the tensile strength of the stone then physical damage is caused (Grossi

et al., 2008b). The pressure exerted is dependent upon the pore structure; if pore size is large pressure is low. Many traditional building stones are vulnerable to salt decay, as they have low strength and high porosity, which made them easy to carve (Grossi et al., 2008b). The magnitude of the pressure is also dependent upon the salt, typically hydrated salts exert higher pressures (Benavente et al., 2008).

Whether salts cause efflorescence or sub-efflorescence depends upon the equilibrium between the rate of water evaporation at the surface and the rate at which this is replenished (Ginell, 1994). The speed of environmental change is important, gradual changes allow slow evaporation, and salts precipitate as efflorescence. Fast changes in the environment cause rapid evaporation and salts crystallise within the pores (Benavente et al., 2008).

Two specific damage functions are described, along with the generalisation of the method used, allowing any other salt to be assessed.

### 4.6.1 Method 1 – Thenardite/Mirabilite transitions

The number of damaging salt transitions is determined by this damage function. Specifically the transitions in the system of thenardite ($Na_2SO_4$) and mirabilite ($Na_2SO_4 \cdot 10H_2O$) are predicted, as described by Benavente et al. (2008). Pressures in excess of 10MPa can be exerted by a phase transition in this sulphate system, sufficient to disrupt porous building stone. Such pressures occur when the relative humidity increases across values described by:

$$RH_{crit} = 0.87549\,T + 59.11 \quad \text{where} \quad 0 < T < 22.5 \ ^{\circ}C \qquad \textbf{(Eq. 4.29)}$$

In this work each damaging transition is recorded and the yearly average reported. This function was used in the NOAH'S ARK project, projecting an increase in future transitions outside (Sabbioni et al., 2010). This method has also been used to project indoor salt damage in the future by the author (Lankester and Brimblecombe, 2012a).

The AWK program for this function can be found in appendix E. In future chapters this damage function is referred to as the salt transition – thenardite/mirabilite damage function.

### 4.6.2 Method 2 – Halite and generalisation

*Method 1* highlights the example of the thenardite/mirabilite system; other systems exist, with varying critical humidity's, halite (NaCl) for example has a critical humidity of 75.3% (at 25 °C) (Benavente et al., 2008, Grossi et al., 2008b, Benavente et al., 2011). Three

systems will be described here, following the form of *method 1*, but with critical humidity's of 60, 75.3 and 85%. These form two imaginary scenarios of mixtures of salts, which is known to alter the critical humidity (Price, 2000), thus showing the possible generalisation of this method, allowing for any critical humidity to be assessed, projecting future transitions assuming that the critical humidity will stay constant. The third system of 75.3% relative humidity describes the halite system, which is virtually independent of temperature (Grossi et al., 2008b, Benavente et al., 2008, Brimblecombe, 2010). The halite system has been used previously in the NOAH'S ARK project to project future changes, although outdoors (Sabbioni et al., 2010). Again each daily transition is recorded and presented as a yearly average. The generalisation of the salt transition method has been mentioned briefly previously (Lankester and Brimblecombe, 2012a), and the work here implements this.

The AWK programs for these functions can be found in appendix E. They are referred to as the salt transition damage functions, for either 60, 75.3 or 85%.

## 4.7 Dimensional change

When the relative humidity of the environment fluctuates it causes hygroscopic materials to either absorb or desorb moisture, from increases and decreases of relative humidity respectively. This causes the materials to change their dimensions which can lead to damage being caused. It is important for all hygroscopic materials, such as wood and paper.

Although not investigated here dimensional change is also important for composite materials, not necessarily organic in nature, for example metal railings inserted into stone, or metal pins used in sculptures, corrosion of the metal will cause it to expand possibly causing the encasing stone to crack (The National Trust, 2006). This specific example is an example of a cumulative process, rather than cyclic. Another example of damage by dimensional change is the deterioration of materials containing clay, when wet the material expands, and it contracts after drying, possibly leading to damage (Sabbioni et al., 2010).

The damage functions utilised in this work focus on dimensional change of wood. For dimensional change to cause damage it is usually, but not always, necessary for the material to be restrained in some way (Erhardt et al., 1995). Often wood has some restraint, from being part of a larger structure, such as furniture, damage is more readily caused when materials are restrained. Wood can also be seen as a special case with respect to dimensional change because each direction (longitudinal, tangential and radial)

responds at different rates to changes in humidity (the moisture coefficient of expansion) (Richard et al., 1995). Therefore if two pieces of wood meet in construction it may be that the opposing directions cause one piece of wood to restrain the other (Jakiela et al., 2008), especially as the tangential direction responds significantly more than the other directions. Restraint causes stress within the material and if this exceeds the yield point wood can be irreversibly damaged and cracks may form (Richard et al., 1995, Mecklenburg et al., 1998, Erhardt et al., 1995). Additionally different species of wood absorb moisture at different rates (Mecklenburg et al., 1998) and wood is occasionally painted, which can cause restraint, either to the wood, or the painted surface (Mecklenburg et al., 1998). Considerable effort has been put into determining the allowable fluctuations of relative humidity (Erhardt et al., 1995, Jakiela et al., 2008, Mecklenburg et al., 1998, Michalski, 1996).

This damage function explains the effect of humidity on dimensional change of wood, temperature has an effect, but it is small in comparison to the effect of humidity (Richard et al., 1995).  Thus it is largely ignored, for comparison the thermal coefficient of expansion is 0.0000385/°C compared to a moisture coefficient of expansion of 0.004 for tangentially cut white oak (Richard et al., 1995); a difference of two orders of magnitude.

Another important factor when considering dimensional change is the response time of the material, short fluctuations , of less than an hour, are unlikely to have an effect as there is insufficient time for the material to respond, unless the change in humidity is very large (ASHRAE, 2003). The actual response time can depend upon the size of the wood; naturally a large piece of wood takes longer to fully equilibrate in comparison to a smaller piece. Another important consideration is the covering applied to the wood, layers of varnish can slow down the response time, as can paint layers (ASHRAE, 2003).

Four damage functions that estimate dimensional change are presented here.

### 4.7.1 Method 1 – Mecklenburg et al.

This function is used to predict the frequency of instances where wood acts as its own restraint. This occurs where pieces of wood meet at a joint with different directions of the grain, which react at different rates to changes in moisture, therefore preventing the natural shrinking and swelling, causing restraint. It is also possible to use the function to look at restraint caused by design layers on wood and by the wood to the paint layer (Mecklenburg et al., 1998).

The function determines whether a change in relative humidity exerts sufficient strain to cause permanent deformation, in this instance to white oak and cotton wood, but other substrates can be investigated, such as Spruce. The level at which strain produces permanent deformation is defined as the yield point, and has been shown to be around 0.004 for wood (Richard et al., 1995). This assumes that the wood has not been strain-hardened, and thus is a worst case scenario. It is assumed that the restraint is in the tangential direction, but other directions can be examined. However, the tangential direction has the greatest dimensional response to changes in moisture, and is again a worst case scenario.

The amount of allowable stress is dependent upon the starting relative humidity. If this is between 40 and 60% then large fluctuations are required before permanent deformation occurs, for example a change from an initial RH of 60% to 40% would not cause damage. When the initial RH is outside this range the allowable humidity change reduces quite significantly, for example a change from 80% to about 75% is likely to cause damage.

Graphs indicating changes in RH that will cause permanent deformation are available from Mecklenburg *et al.* (1998) (an example is reproduced in figure 4.6). These were transformed to the set of ranges shown in tables 4.2 and 4.3 in order to allow an AWK program to determine whether the change in future RH is unacceptable. A critical value of RH, beyond which exceedance causes permanent deformation is calculated from the initial RH. Table 4.2 contains the set of ranges used to calculate the critical RH under adsorption and desorption for white oak, and table 4.3 the same for cotton wood. Each exceedance of the critical RH is summed and reported as a yearly average.

This damage function has been used to project future damage to wood indoors as described, and results deriving from this research have been published by the author (Lankester and Brimblecombe, 2012b). The AWK program for these functions can be found in appendix E. In future chapters these damage functions are referred to as either the cotton wood or white oak, adsorption, desorption or total damage functions.
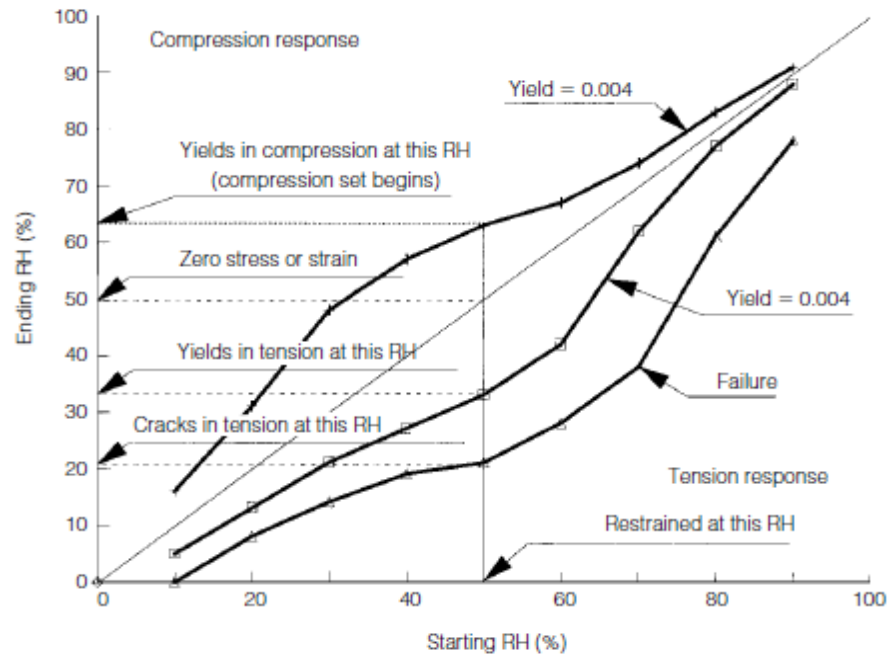
Figure 4.6: Calculated reversible RH range of fully restrained, tangentially cut white oak versus ambient RH. A yield value of 0.004 was used as the limiting criterion in both tension and compression. The values of the dotted lines are for stress-free wood that has been fully equilibrated to 50% RH. Reproduced from Richard et al. (1995).

Table 4.2: White oak critical RH ranges for deformation

| Adsorption | | Desorption | |
|---|---|---|---|
| **Initial RH** | **Critical RH** | **Initial RH** | **Critical RH** |
| $10 <= RH <= 30$ | $1.5 \times RH + 1$ | $10 <= RH <= 30$ | $0.8 \times RH - 3.33$ |
| $30 < RH <= 40$ | $1.0 \times RH + 18$ | $30 < RH <= 50$ | $0.6 \times RH + 3.33$ |
| $40 < RH <= 50$ | $0.5 \times RH + 38$ | $50 < RH <= 60$ | $0.9 \times RH - 12$ |
| $50 < RH <= 60$ | $0.4 \times RH + 43$ | $60 < RH <= 70$ | $2.0 \times RH - 78$ |
| $60 < RH <= 90$ | $0.8 \times RH + 19$ | $70 < RH <= 80$ | $1.6 \times RH - 50$ |
| | | $80 < RH <= 90$ | $1.05 \times RH - 6$ |

Table 4.3: Cotton wood critical RH ranges for deformation

| Adsorption | | Desorption | |
|---|---|---|---|
| Initial RH | Critical RH | Initial RH | Critical RH |
| 10<= *RH*<=20 | 1.3 × *RH*+4 | 10<= *RH*<=20 | 0.9 × *RH*-4 |
| 20< *RH*<=30 | 2.1 × *RH*-12 | 20< *RH*<=30 | 0.7 × *RH* |
| 30< *RH*<=40 | 1.3 × *RH*+12 | 30< *RH*<=40 | 0.5 × *RH*+6 |
| 40< *RH*<=50 | 0.3 × *RH*+52 | 40< *RH*<=50 | 0.5 × *RH*+6 |
| 50< *RH*<=60 | 0.4 × *RH*+47 | 50< *RH*<=60 | 0.4 × *RH*+11 |
| 60< *RH*<=70 | 0.2 × *RH*+59 | 60< *RH*<=70 | 1.5 × *RH*-55 |
| 70< *RH*<=80 | 0.8 × *RH*+17 | 70< *RH*<=80 | 2.5 × *RH*-125 |
| 80< *RH*<=90 | 1.1 × *RH*-7 | 80< *RH*<=90 | 1.3 × *RH*-29 |

The previous two tables detail conditions for permanent deformation. There is also a set of ranges to describe the stress required for failure of the material. Failure requires a yield point in excess of 0.009 (Richard et al., 1995). The graph in figure 4.6 was interpreted, producing the ranges in table 4.4 that relate to the failure of white oak wood. Again each event is counted and reported as a yearly average. The AWK program for this function, referred to in future chapters as the white oak failure damage function, can also be found in appendix E.

Table 4.4: White oak critical RH ranges for failure

| Failure | |
|---|---|
| Initial RH | Critical RH |
| 10<= *RH*<=20 | 0.8 × *RH*-8 |
| 20< *RH*<=30 | 0.5 × *RH*-2 |
| 30< *RH*<=40 | 0.6 × *RH*-5 |
| 40< *RH*<=50 | 0.2 × *RH*+11 |
| 50< *RH*<=60 | 0.7 × *RH*+14 |
| 60< *RH*<=70 | 1.0 × *RH*-32 |
| 70< *RH*<=80 | 2.4 × *RH*-130 |
| 80< *RH*<=90 | 1.6 × *RH*-66 |

### 4.7.2 Method 2 – Michalski

The damage that relative humidity can cause to wood has been discussed previously. Michalski (1996) presents a table titled 'Vulnerability of wooden artefacts to humidity fluctuations'. In the table the degree of vulnerability is the principal variable, with four categories ranging from very high vulnerability to low. Over the four categories there are four different values of humidity change, 5, 10, 20 and 40%, based on short term fluctuations. A combination of these values are assigned to the type of damage that they cause, which varies depending upon the vulnerability, for example a 10% RH change will cause gradual fatigue, or plastic deformation in objects of a high vulnerability, whereas a 40% RH change will cause a fracture on the first occurrence. The full table is reproduced in table 4.5, which also defines examples of artefacts, allowing for case study objects to be placed into a category, and the risk of humidity fluctuations determined.

Table 4.5: Reproduced from Michalski (1996)

**Table 2. Vulnerability of Wooden Artifacts to Humidity Fluctuations**

| Degree of Vulnerability | Artifact Examples |
|---|---|
| **Very High Vulnerability**<br><br>±5%RH: gradual fatigue fracture<br>±10%RH: fracture possible each cycle<br>±20%RH: fracture definite first cycle | (This class of wooden artifact breaks the rules of cautious woodworking, or else the fracture of these coatings has never been considered disfiguring, e.g. painted doors). Aged glue, lacquer, varnish, gesso or oil paint which bridges joints where wood grains meet at right angles (lap joints, mortise and tenon joints,etc., also, any knots in wood components). Aged glue, lacquer, varnish, gesso, or oil paint which bridges a crack formed by a check, knot, side-by-side butt joint, or mitre joint. Inlays of metal, horn, ivory, shell, (but not wood; marquetry is considered below as medium vulnerability, since it is much tougher and more resilient). The longer the inlay runs across the grain, the more vulnerable the piece. |
| **High Vulnerability**<br><br>±5%RH: zero fatigue fracture<br>±10%RH: gradual fatigue fracture, or plastic deformation<br>±20%RH: fracture possible each cycle<br>±40%RH: fracture definite first cycle<br><br>Much of this type of fracture has already occurred in old artifacts. Only artifacts from less fluctuating conditions, or from higher annual average conditions, or those recently re-attached by inflexible treatments will fall in this category. | Veneer over corner joints where wood grains meet at right angles (lap joints, mortise and tenon joints etc., also any knots in wood base components). Lacquer, oil paints, gilding, over single knot-free wood components, or over joints that use feathered inserts, fabric, tissue, etc. that are still sound. When new and fairly flexible, these layers may drop to only medium vulnerability. Fretwork, applied ornaments, especially if the wood grain follows the notch; assemblies with metal bands, bolts, nails, screws that restrain the wood unevenly. Checked timber or sculpture with a hard new fill; cracked panel or panel painting in a rebate or cradle that jams. Large pieces of recently seasoned wood such as folk art, also all knots and uneven grain in wood must be considered prestressed in this way. New plywood, newly steam-formed wood held by other components. Panels near intermittently damp walls; floorboards over damp crawlspace; glued veneer or joints where the glue bond has softened and readhered at the expanded component position. |
| **Medium Vulnerability**<br><br>±10%RH: zero fatigue fracture<br>±20%RH: gradual fatigue fracture, or plastic deformation<br>±40%RH: fracture possible each cycle | Most wood joinery, veneers, and marquetry over single, clear pieces of wood at crossed grain; any prestressed pieces from above that have stress-relaxed more than a decade. Any wood with little or no coating, subjected to an RH fluctuation shorter than its response time. This leads to warping or surface checking e.g. backs of picture frames; on exposed end grain it results in end-checks e.g. tenons, dovetails, feet of furniture, overhangs in carved totem poles. |
| **Low Vulnerability**<br><br>±40%RH: possible accumulation of fatigue fracture or plastic deformation if the freedom to move, or the coatings, or the slowness of the fluctuation are less than perfect | Aside from possible cracks in any varnish, and given either a slow enough change in humidity or good moisture barrier coatings, then: already loose joinery; floating panels; loose tabletops; tongue and groove or lapped planking nailed or bolted at one point only, e.g. wainscotting, boxes on farm machinery (unless jammed due to painting, warping), hollowed out totem poles, hollowed-out sculpture, most single component tool handles, veneer on wood with parallel grain, joined wood components with parallel grain. |

The data from table 4.5 is used as the basis of the damage function, the occurrence of the four different humidity change values (5, 10, 20 and 40) being calculated from future indoor climate projections, on a day to day basis and reported as a yearly average. They can be separated into the varying vulnerabilities as required for specific objects or collections.

The AWK program for this function can be found in appendix E. In future chapters each of the parts of the method presented here is referred to, as either the 5/10/20 or 40% humidity shock damage function.

### 4.7.3 Method 3 – Jakiela et al.

This function is similar to the previous, but arises from different work (Jakiela et al., 2008). Here a value of 30% RH change between consecutive days is said to have a considerable damaging potential for wooden objects, because of mechanical damage (Jakiela et al., 2008). This is based on modelling of the stresses caused as wooden objects respond dimensionally to changing humidity. When stress causes strain that exceeds the yield point of the wood (0.004) deformation will occur, as described previously. This assumes restraint of the wood, as the mechanism would not be important otherwise. The modelling was based on moisture diffusion in a cylindrical wood specimen (lime wood, *Tilia sp.*), thus simulating wooden sculptures. Allowable variations of relative humidity were derived from this, and are presented in figure 4.7, this indicates, as did Mecklenburg et al. (1998), that larger variations are tolerable in the region of approximately 30-70% RH. It is shown that a 20% RH change, independent of the starting RH, can cause irreversible damage. A value of 30% change instead of 20% appears to have been chosen because they have considerable potential to cause damage (Jakiela et al., 2008), whereas 20% is close to the boundary of reversible response in some regions.

There are limitations to this method as it neglects the curvature of growth rings and is thus is only valid for wood cut from positions away from the axis of the trunk (Jakiela et al., 2008). This function has previously been used to estimate the impact of climate change across Europe in the NOAH'S ARK project (Sabbioni et al., 2010), where much of the UK shows no increase for the near future, in comparison to the recent past. A small increase is projected in the far future (approximately 1 event per year). As with *method 2* the frequency of 30% change is summed and reported as a yearly average. The AWK program for this function can be found in appendix E. In future chapters this is referred to as the 30% humidity shock damage function.
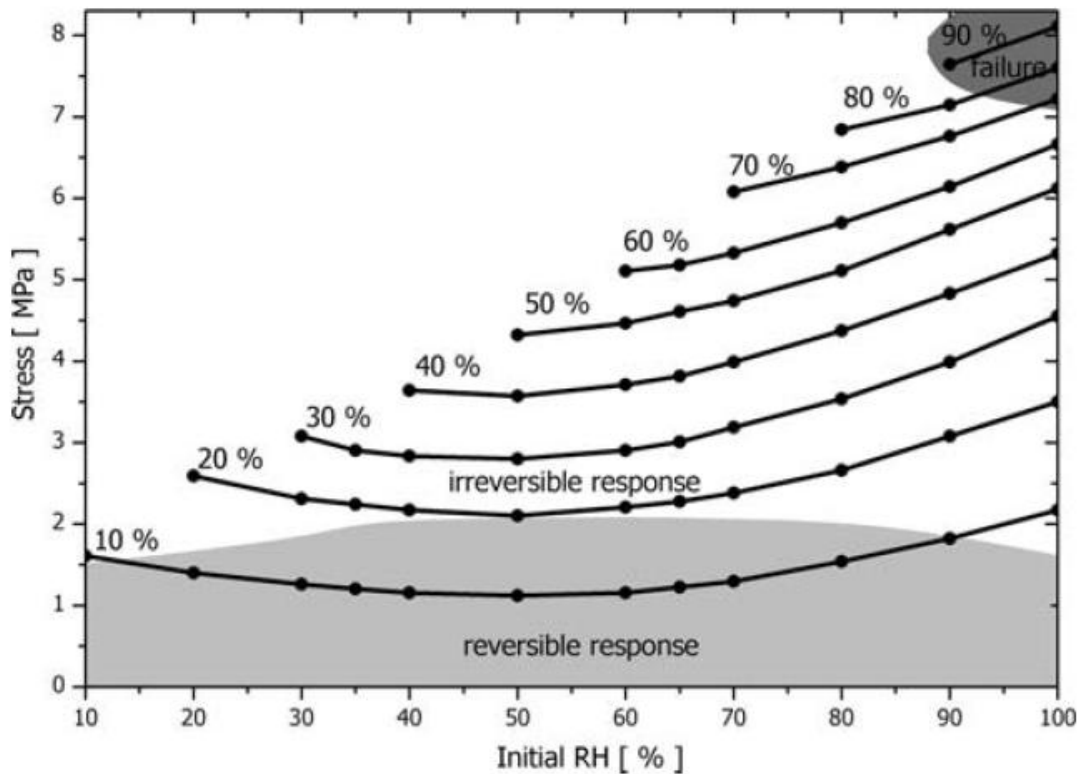
Figure 4.7: Maximum stress induced by RH variations between 10 and 90% occurring over the time period of 24 h plotted as a function of the initial RH level from which the variation starts. Domains of RH variations endangering the wood by irreversible response (deformation) or complete failure are marked together with the domain of tolerable variations producing safe, reversible response of the wood. Figure reproduced from Jakeila et al. (2008).

### 4.7.4 Method 4 – EMC

This method is part of the climate notebook software package. As with previous methods this also investigates the risk associated with adsorption and desorption of moisture under varying environmental conditions, leading to physical damage (Reilly, 2005, Nishimura, 2009). This is assessed by determining the equilibrium moisture content (EMC) of a wooden object and determining whether this falls outside of the stated boundary values. These are set as a minimum of 5% and a maximum of 12.5% EMC.

The equation that is used to determine EMC is from The U.S. Forest products Laboratory, this relates relative humidity and temperature of the surrounding air to the EMC for wood of average species (Simpson and TenWolde, 1999). The equation is shown below:

$$M = \frac{1800}{W}\left[\frac{Kh}{1-Kh} + \frac{K_1Kh + 2K_1K_2K^2h^2}{1 + K_1Kh + K_1K_2K^2h^2}\right] \text{ (Eq. 4.30)}$$

Where *M* is moisture content (%) and *h* is relative humidity (%/100). *W, K, K_1 and K_2* are defined below, with temperature in Celsius.

$$W = 349 + 1.29\,T + 0.0135\,T^2 \qquad \textbf{(Eq. 4.31)}$$

$$K = 0.791 + 0.000463\,T - 0.000000844\,T^2 \quad \textbf{(Eq. 4.32)}$$

$$K_1 = 6.34 + 0.000775\,T - 0.0000935\,T^2 \quad \textbf{(Eq. 4.33)}$$

$$K_2 = 1.09 + 0.0284\,T - 0.0000904\,T^2 \quad \textbf{(Eq. 4.34)}$$

The average EMC will be calculated. The AWK program for this function, referred to in future chapters as the equilibrium moisture content damage function, can be found in appendix E.

## 4.8 Alternative damage estimates

It is likely that other damage functions are available that are not discussed here, for example some outdoor methods may be suitably adapted for indoor use. Additionally alternative methods are available that define damage, for example various ideal temperatures are quoted with respect to pest activity (The National Trust, 2006, Pinniger, 2001). It would be possible to simply run a function that counts the number of days where the average temperature (or humidity) falls within specific boundaries. It would be futile to run every conceivable alternative method, as there are a large number. Additionally where similar limits are suggested determining one will give an indication of the others, for example the specific temperature at which a pest is said to become active, which can differ between each reference. Some examples will be investigated to show how alternative methods can be implemented.

Alternative methods could include the number of days where the temperature is low enough to increase the risk of burst pipes, 5°C is given as a good indicator (ASHRAE, 2003), however this seems to be quite high. Opposing this, the number of warm days can be counted; this will be carried out to assess how the environment will change in the future indoors, but with no connection to an associated risk, although it is likely to increase damage from a number of mechanisms such as pest activity. The number of days above 20°C and 25°C will be investigated. The AWK programs for these functions can be found

in appendix E. In future chapters these are referred to as the daily average temperature >20°C, or >25°C, damage functions.

# CHAPTER 5

# EUROPE

## 5.1 Introduction

In this chapter the impact of climate change across Europe will be investigated. This research has formed the main body of a publication (appendix F) the aim of which was to highlight the whole process of applying a building simulation model to future climate and estimating future damage from the indoor projections of climate (Lankester and Brimblecombe, 2012a).

There are a number of hurdles to overcome in to carry out this projection in comparison to the UKCP09 weather generator projections presented in the following chapter. Firstly it is not possible to use the UKCP09 weather generator, instead the Hadley model, HADCM3 (section 2.3), is used, with the downscaling technique described previously (section 2.3.1), that renders the climate output relevant to each specific location.

Across Europe sharing of data is not always as easy to undertake, especially across multiple countries, therefore there is a lack of data. In the UK good connections with large heritage organisations, namely English Heritage, The National Trust and Historic Royal Palaces, allows for the sharing of observed data from a number of historic properties. To overcome this the Cartoon Gallery (section 2.2.2) will be imagined to exist at the other European locations researched, as an idealised room. This will allow research into the impact of various climates on future damage, and how specific locations in the future may exhibit characteristics of other locations currently. A similar principle is indicated by the front cover of the ENSEMBLES final report (Van der Linden and Mitchell, 2009), where European cities are relocated to places where the current climate is the same as the projected climate for each city in 2071-2100. For example Barcelona is located on the north coast of Tunisia, and Copenhagen is relocated to Paris approximately. The results should indicate which collections may be at significant risk of damage, and specific areas where the risk may be greater (Lankester and Brimblecombe, 2012a). Projections may also assist future collection managers, by suggesting locations where problems exist currently, and where a solution may be found to a new problem being faced. This also highlights the importance of keeping good records of practices, as this could be far into the future, when current employees are no longer available for consultation.

## 5.2 Sites

The sites that will house the idealised room have been selected to represent different climate regimes across Europe. The Cartoon Gallery from Knole in Sevenoaks, UK is chosen as a typical unheated interior of a historic house. Along with projections for Sevenoaks the Cartoon Gallery will be imagined to exist at six other locations. All the locations are indicated in figure 5.1, and are as follows, Doncaster, UK; Paris, France; Prague, Czech Republic; Oviedo, Leon and Almeria, Spain.



Figure 5.1: Location of the seven European sites where future climate will be projected for the idealised room.

The original location of Sevenoaks, where the Cartoon Gallery actually belongs represents an English climate with maritime influences. This is in contrast to the continental climate of Prague. Doncaster lies to the north of Sevenoaks, and Paris to the

south, an imaginary line could be drawn through the three locations (Lankester and Brimblecombe, 2012a).  Almeria is an example of a dry climate, which falls into the Koppen-Geiger climate classification of BSk. The Koppen-Geiger classification can be broken down, with each letter having a specific meaning, firstly 'B' indicates an arid climate, the 'S' means that it is a steppe climate, defined by the rainfall amount, and the third letter defines the temperature classification, here 'k' is for cold, defined by having an annual temperature below 18°C (Kottek et al., 2006). All four locations of Sevenoaks, Doncaster, Prague and Paris fall into the Cfb classification, with each letter respectively meaning: warm temperate climate (minimum temperature -3-18°C), fully humid and warm summer (maximum temperature <22°C and at least four months with average temperature over 10°C (Kottek et al., 2006).

The final two locations investigated will be Oviedo and Leon, both in Spain, close to the Atlantic coast. These two locations have been specifically chosen to highlight the importance of orography as they are located either side of the Cantabrian Mountains (Lankester and Brimblecombe, 2012a). This should indicate the importance of downscaling the climate output to each individual location. Oviedo lies on the boundary between a Cfb and Csb Koppen-Gieger classification, whilst Leon is Csb, which stands for: warm temperate climate, summer dry and warm summer (Kottek et al., 2006). The climate classifications of the Koppen-Geiger scheme have been interpreted with respect to outdoor heritage by Brimblecombe (2010).

As mentioned in Section 2.2.2, observations of the indoor climate at Knole are regularly undertaken, however outdoors the record is fragmentary, and the local weather station of Gatwick is used. For the other locations data was available for the outdoor climate of each location. This allows for the downscaling of the corresponding grid of Hadley output to each site investigated, as carried out previously for these locations in section 2.3.1.

## 5.3 Idealised room concept

As mentioned the Cartoon Gallery at Knole will be imagined to exist at the other locations. Thus the building simulation aspect of the process will be consistent between all locations, simplifying the matter by having the same building at each site, the transfer function is described previously in section 3.2.7. The coefficients of the transfer function have previously been calculated for the Cartoon Gallery these will be used for all of the locations here, to transfer the downscaled Hadley output indoors.

To statistically compare the results in this chapter, the data of the baseline period, which comprises the years 1961-1990, and the far future 2070-2099, will be tested using the Wilcoxon signed ranks test, with a probability level of 95%.

## 5.4 Results

The results of the indoor projections at the different European locations will be split into two sections, firstly the projected change to the environment, and secondly the application of damage functions to the projected future indoor environment. There are a number of discussion points that arise that could continually be discussed with each point, however these will be dealt with at the end, once raised the first time.

### 5.4.1 Environment

The transfer function for the Cartoon Gallery has been applied to the downscaled climate output for the seven locations discussed, the future projection of temperature and relative humidity are shown in figures 5.2 and 5.3 respectively. Some locations have a shorter time span; this is because the record lengths are different.
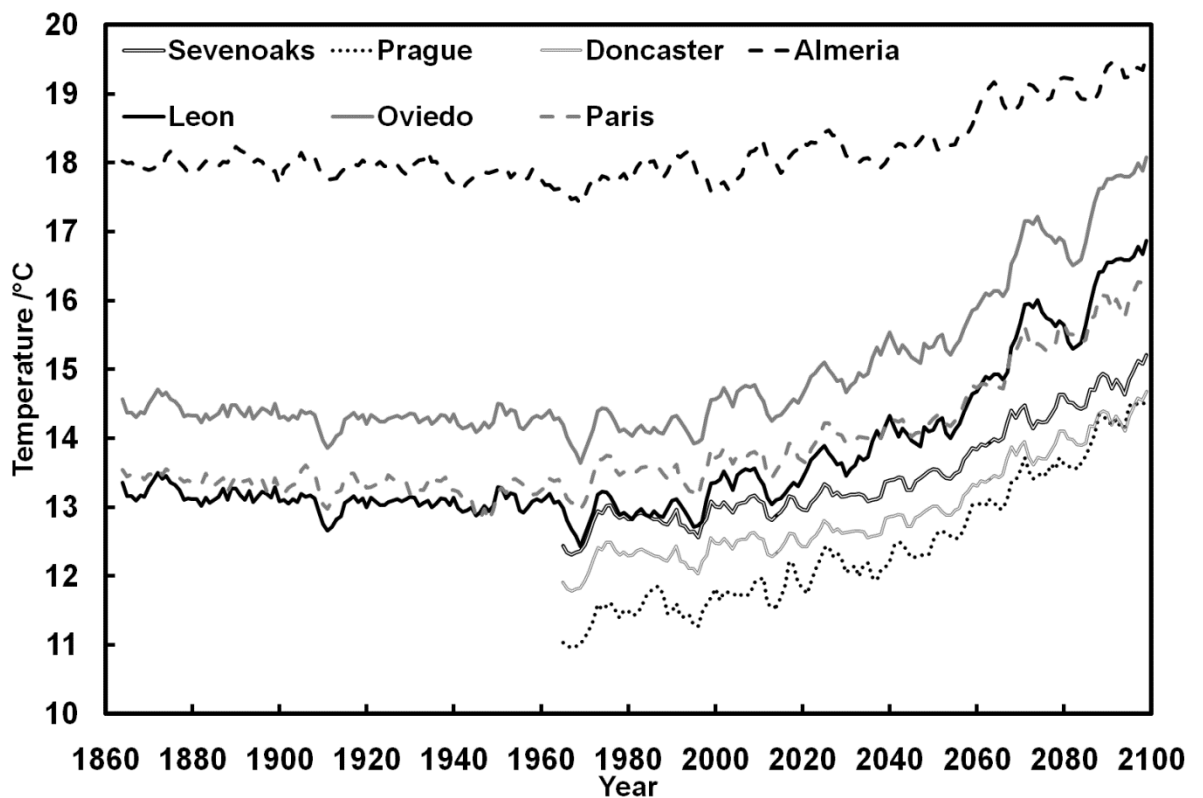


Figure 5.2: Projected indoor temperature of the idealised room across the seven locations, for the period 1860-2100. The data is plotted as a 5 year smoothed average, to help visualise the long term trend.

Figure 5.2 shows that the projected indoor temperature is expected to increase across all locations, but with different magnitudes. For example the temperature in Prague is projected to increase from 11.0°C in 1961 to 14.5°C in 2099. Table 5.1 presents the baseline temperature, projected future temperature and the difference for each of the locations. There are a number of points to note from the results, an example of one location having a similar climate in future to another location can be seen, the interior temperature in Leon is quite similar to the baseline value (1961) in Almeria. Thus current management strategies used in Almeria may be relevant in the future in Leon. It is interesting that Prague and Doncaster are almost a degree apart in 1961, but by 2099 they have very similar indoor temperatures. The opposite is true for Sevenoaks and Leon, they have a similar baseline temperature, 12.4°C and 12.7°C respectively, but by 2099 they have diverged and are quite different, 15.2°C and 17.2°C respectively. The final observation is the difference between the geographically close locations of Leon and Oviedo, highlighting the importance of the application of downscaling.

Table 5.1: Projected temperature of the seven locations, for the baseline (1961), midterm future (2050) and long term future (2099), with the difference from the baseline to the long term future. Results rounded to one decimal place.

| Location | 1961 | 2050 | 2099 | 1961-2099 Difference |
|----------|------|------|------|----------------------|
| Sevenoaks | 12.4 | 13.5 | 15.2 | 2.7 |
| Prague | 11.0 | 13.1 | 14.5 | 3.5 |
| Doncaster | 11.9 | 12.9 | 14.6 | 2.7 |
| Almeria | 17.3 | 18.1 | 19.9 | 2.6 |
| Leon | 12.7 | 13.9 | 17.2 | 4.5 |
| Oviedo | 13.9 | 15.1 | 18.4 | 4.5 |
| Paris | 13.4 | 14.2 | 16.3 | 2.9 |

Figure 5.3 shows the projected indoor relative humidity, it is expected to decrease at six of the locations, but Almeria is likely to experience an increase in relative humidity, of 4% (see table 5.2). This shows the need to assess individual locations, rather than accepting a simple belief that temperature will increase therefore relative humidity will decrease, this suggests that it is not always true (Lankester and Brimblecombe, 2012a). The reason that this is not always true is because it is dependent upon the magnitude of the temperature and specific humidity change. If the temperature increases and specific humidity stays constant then the relative humidity will decrease. However if the specific humidity increases then this will offset some of the relative humidity decrease, caused by the increasing temperature, up until the point where the two cancel each other out, or as in this case goes further, causing an increase in relative humidity. Almeria has the smallest temperature increase in the future, which is not large enough to prevent an increase in relative humidity, because of the relatively greater increase in specific humidity.
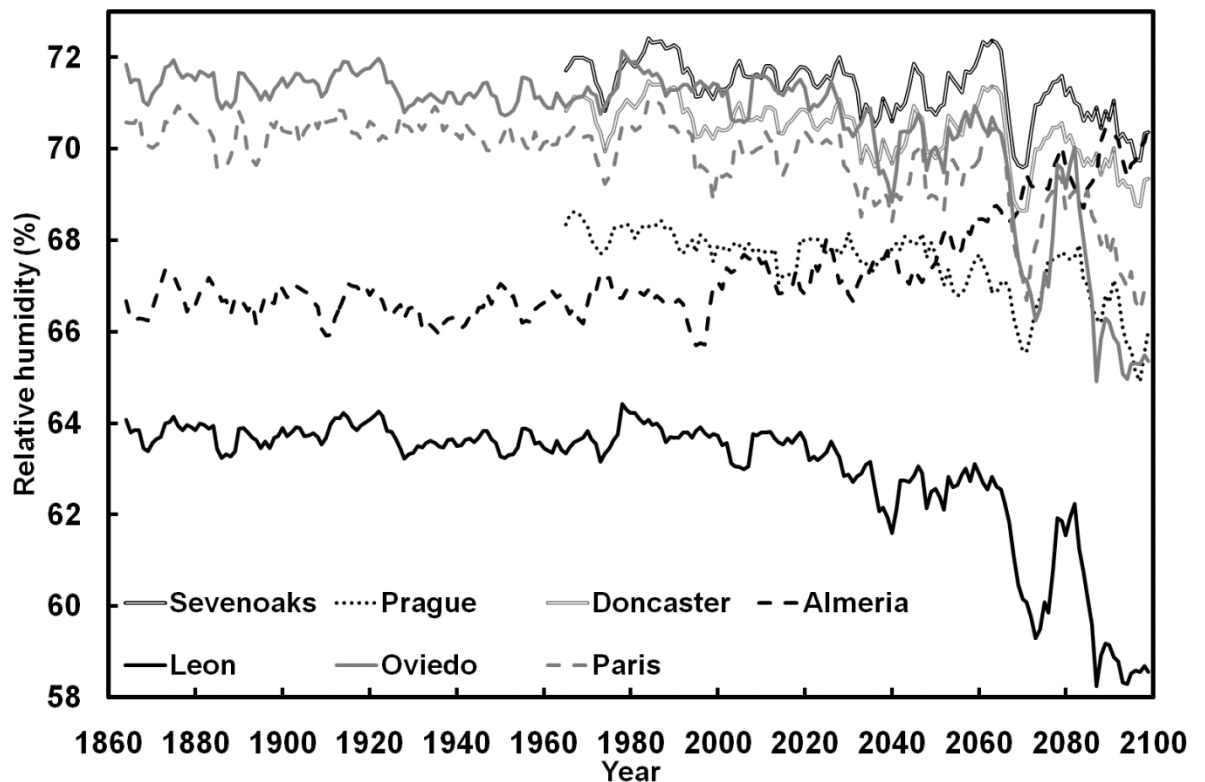


Figure 5.3: Projected indoor relative humidity of the idealised room across the seven locations, for the period 1860-2100. The data is plotted as a 5 year smoothed average.

Table 5.2: Projected relative humidity of the seven locations, for the baseline (1961), midterm future (2050) and long term future (2099), with the difference from the baseline to the long term future.

| Location | 1961 | 2050 | 2099 | 1961-2099 Difference |
|---|---|---|---|---|
| Sevenoaks | 71.7 | 71.7 | 70.9 | -0.8 |
| Prague | 67.8 | 66.8 | 67.1 | -0.7 |
| Doncaster | 70.8 | 70.7 | 69.9 | -0.9 |
| Almeria | 66.5 | 68.9 | 70.6 | 4.1 |
| Leon | 63.3 | 63.1 | 58.7 | -4.6 |
| Oviedo | 70.8 | 70.8 | 65.6 | -5.2 |
| Paris | 70.6 | 70.4 | 67.7 | -2.9 |

As with the temperature projections table 5.2 shows the corresponding relative humidity baseline and future values. Doncaster and Oviedo have a similar baseline relative humidity, however by 2099 they have diverged by approximately 4%. As with the temperature projections the importance of orography is highlighted by Leon and Oviedo. The similarities between locations for relative humidity are different to those of temperature.

### 5.4.2 Damage

Whilst change in the indoor environment is important, the impact this has on damage to collections is also significant, the damage functions discussed in chapter 4 will be used with the projected data for the ideal room across the seven locations. The publication from which this chapter derives (Lankester and Brimblecombe, 2012a) only assessed two damage functions, one for paper and one for salts, in order to highlight the application of the technique. However here all of the damage functions discussed previously will be investigated, with some presented in appendix C, to keep the discussion here concise.

**Daily average temperature >20°C**

This first measure is not a true damage function, and could be in the previous section detailing how the environment will change, but equally it has a place here. Certain damaging events require specific temperatures, maybe not 20°C but this gives an indication of the method. One recent example of specific temperatures being used to detail damage, in relation to climate change, is by Stengaard Hansen et al. (2011), where

the number of days over 20°C is counted as an indication of pest damage. Additionally this is a useful measure to indicate that there may be longer or shorter warm periods in the future, which again could affect insect pest activity (Child, 2007), amongst other things.

Figure 5.4 shows the number of days over 20°C per year, for the majority of locations there is a substantial increase in warm days, with the exception of Almeria. Leon and Oviedo indicate approximately twice as many days over 20°C, and Paris, Prague, Doncaster and Sevenoaks in the region of three times as many warm days. Almeria is an exception, as it is currently a warm location with between 140-150 warm days per year on average, which only increases slightly in the future to approximately 160.
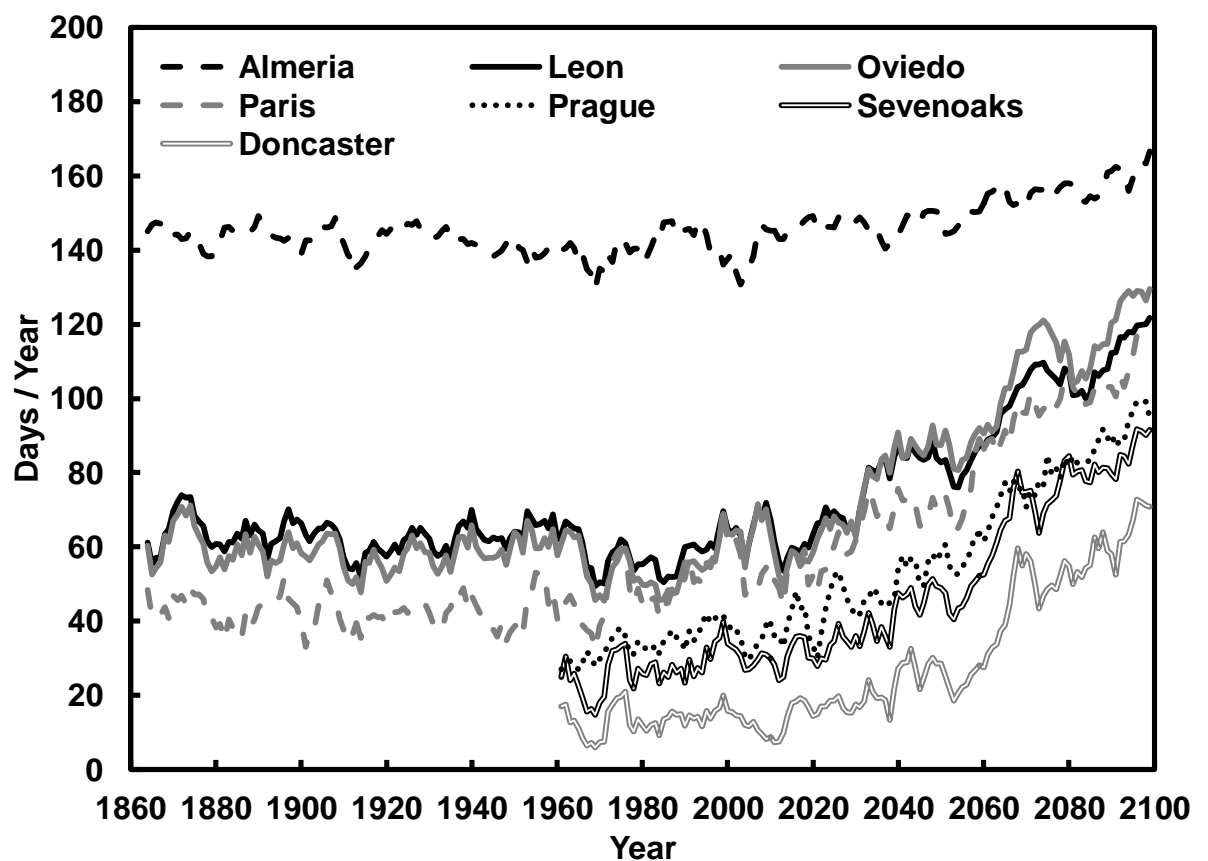


Figure 5.4: The projected number of days, per year, where the average daily temperature indoors exceeds 20°C, across the seven locations. Results are plotted as a five year smoothed average.

In contrast to 20°C, described here as warm days, the number of days per year where the temperature exceeds 25°C has been projected, and will be described as hot days (figure 5.5). These more simple analyses allow for an estimate of damage by those unfamiliar

with the technique, and if there are not the resources available to use a specific damage function. They are especially useful as the temperature and humidity projections shown previously present an average value, thus neglecting the annual cycle of environmental conditions.

The number of hot days, as shown in figure 5.5, increases into the far future. The projections show a worrying situation for Oviedo and Leon, as they present a similar number of hot days in the far future as Almeria, around 75, a substantial increase from the baseline value of less than 10. While there is deviation in the number of hot days, as expected from year to year, even where there are fewest hot days projected (Doncaster and Sevenoaks) there is a shift from none or a couple of hot days per year over the baseline and short term future, to approximately 5-15 per year after 2080.
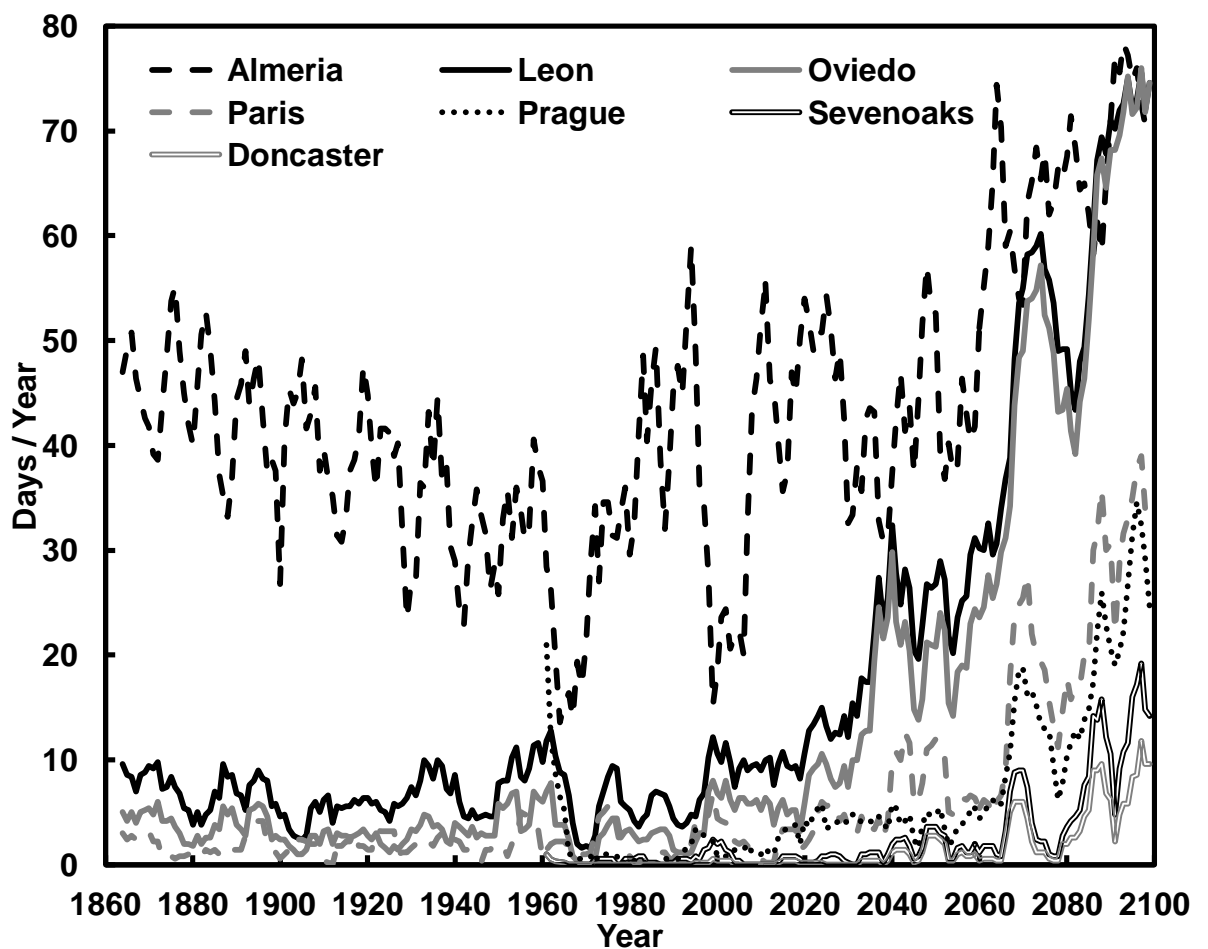


Figure 5.5: The projected number of days, per year, where the average daily temperature indoors exceeds 25°C, for the seven idealised rooms across Europe. Results are plotted as a five year smoothed average.

One specific use of the number of days over 25°C is for the number of flying days of the common furniture beetle, an increase in flying may cause any infestations to spread to other objects (Child, 2007).

*5.4.2.1 Paper*

**Zou**

The results for the locations across Europe for this damage function are shown in figure 5.6. The degradation rate of paper increases across all seven locations, with varying magnitudes. The degradation rate is heavily dependent upon temperature, thus the warmest location of Almeria has the highest rate of degradation. By the end of the century Oviedo has a similar rate of degradation, to the baseline period of Almeria. This replicates what was seen for the temperature projections, further evidencing the importance of temperature in this case.
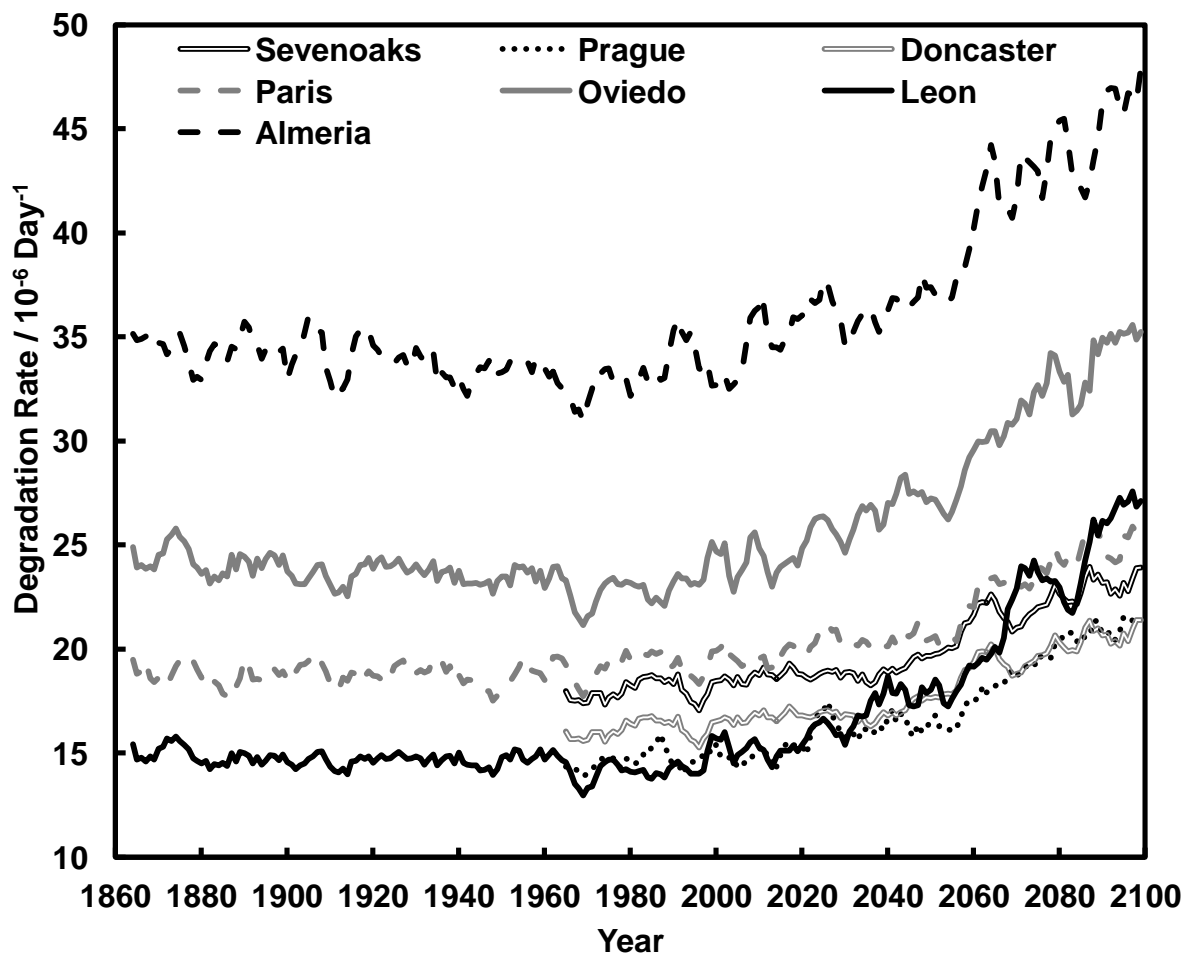


Figure 5.6: The projected chemical degradation rate of bleached bisulfite pulp paper, using the Zou damage function, for the period 1860 to 2100, across the seven locations.

Results are plotted as a five year smoothed average. The baseline period medians of all locations are significantly different to those of the corresponding far future period.

The results of the isoperm and TWPI damage functions can be found in appendix C; they show similar results to this damage function, adding little to the discussion. Unfortunately it is not possible to directly compare the rates of degradation, as discussed earlier. The first function has an absolute degradation rate, compared to the isoperm function which uses a relative degradation rate. An arbitrary rate is attributed to set conditions (T=20°C and RH=50%), and the effect that temperature and humidity have on the rate is determined within each separate function. This allows for comparison within each function, but not between each function. Whilst it is not possible to directly compare between each function, it may be possible to determine the effect of climate change on each one, by determining the rate increase, allowing for comparison of these values between each function. This is carried out in chapter 8.

**Pretzel**

This damage function looks at chemical degradation of paper as described by Pretzel (2005) taking further work introduced by Michalski (2002). This is somewhat different to the other paper damage functions. As with the other functions it uses the Arrhenius equation to determine the dependence of the rate of degradation to temperature. However the dependence on relative humidity, which is less well established (Pretzel, 2005), uses the notion of a power law relationship. The dependence of relative humidity on the degradation rate is stated as $RH^{1.3}$, as described earlier in section 4.2.4.

This is very important as it gives added weight to the humidity; this is shown in the projected impact of climate change, as shown in figure 5.7. In contrast to the other damage functions, where the rate of degradation increases, here the rate decreases across all locations, except Almeria. Previously temperature was the dominating factor, but in this function relative humidity dominates. This is confirmed with the comparison to the projected relative humidity, which has a very similar trend.

The baseline period medians of all locations apart from Paris, Doncaster and Sevenoaks are significantly different to those of the corresponding far future period.

This raises the important question of whether this particular function is correct, that there is a greater dependence on relative humidity as suggested. Alternatively are the other functions correct, or is there some middle ground. This is critical to the future projections

of damage to paper from chemical degradation. Resolution of this question is not a matter to be dealt with here as it is beyond the scope of this thesis.
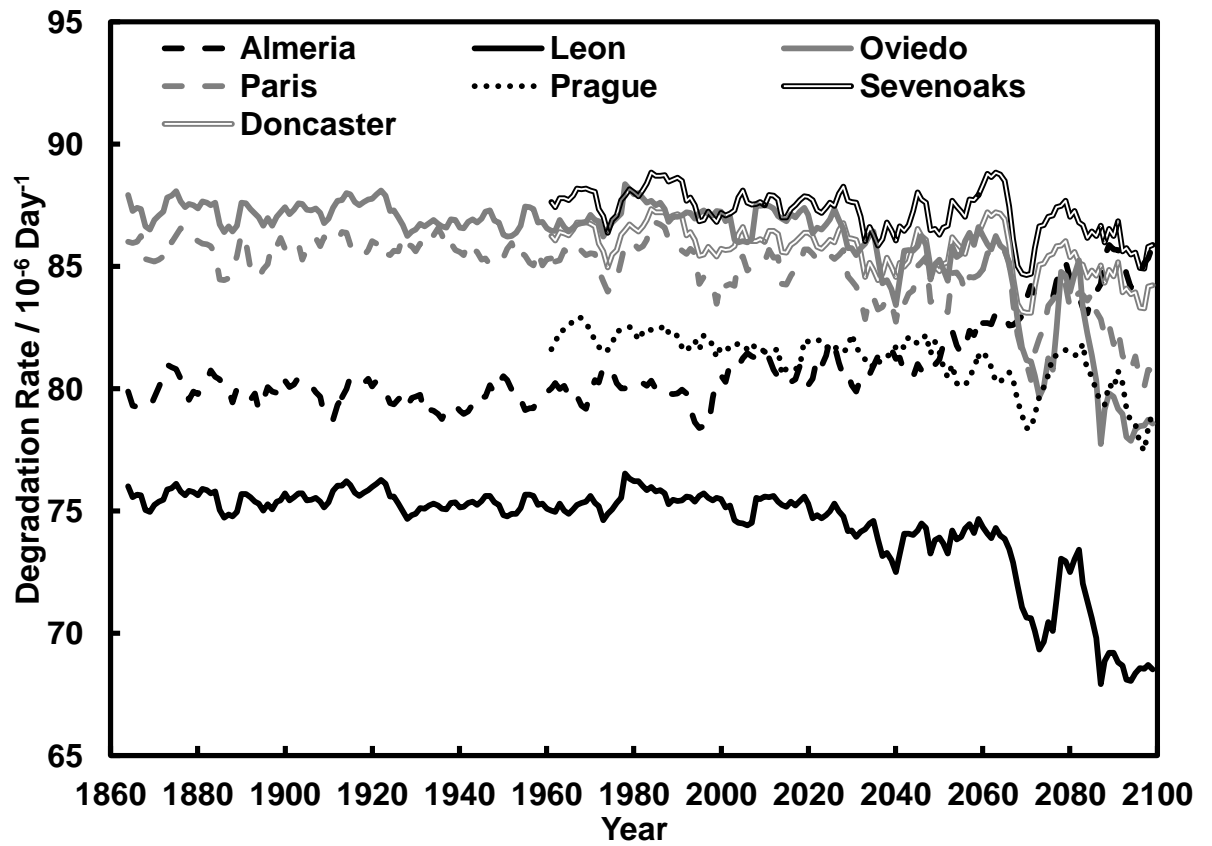


Figure 5.7: The projected relative degradation rate of paper using the Pretzel damage function, from 1860 through to 2100 across the seven locations. The rate is shown as a 5 year smoothed average.

*5.4.2.2 Silk isoperm*

The projected impact that climate change will have upon the degradation rate of silk across the European locations is presented in figure 5.8. It is projected that at all locations the degradation rate will increase, thus reducing the useable lifetime of collections containing silk. Low relative humidity does have the impact of helping reduce the degradation of silk, as shown in figure 4.3; however any slight shift of the relative humidity, as projected here has not outweighed the negative effect of the increase in temperature.
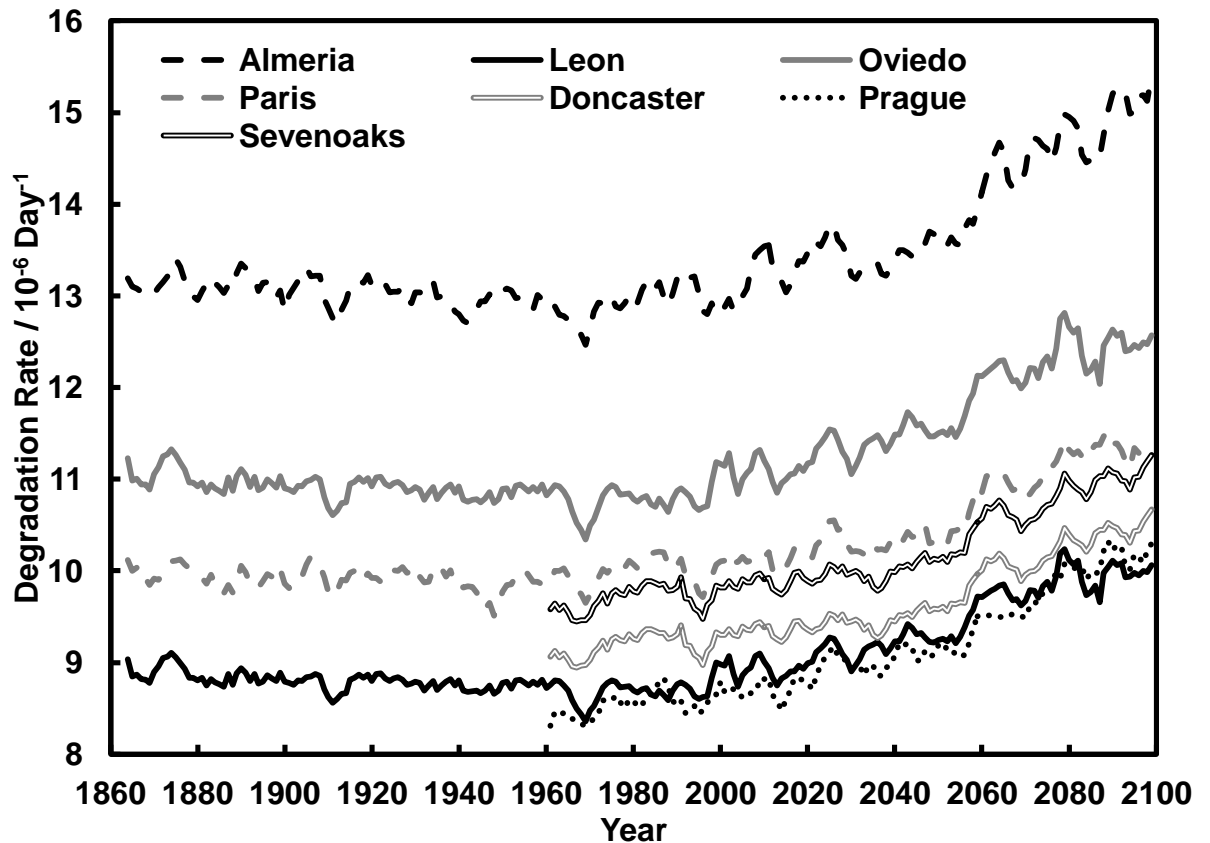


Figure 5.8: The projected effect of climate change on the degradation of silk. The rate is plotted as a smoothed five year average. The baseline period medians of all locations are significantly different to those of the corresponding far future period.

*5.4.2.3 Mould*

**Isaksson**

The results of the function described by Issaksson et al. (2010), for the seven European locations are shown in figure 5.9, where it is shown that risk of mould growth is projected to increase in the future. However, there is only a slight indication of this from this function, and not for all the sites.
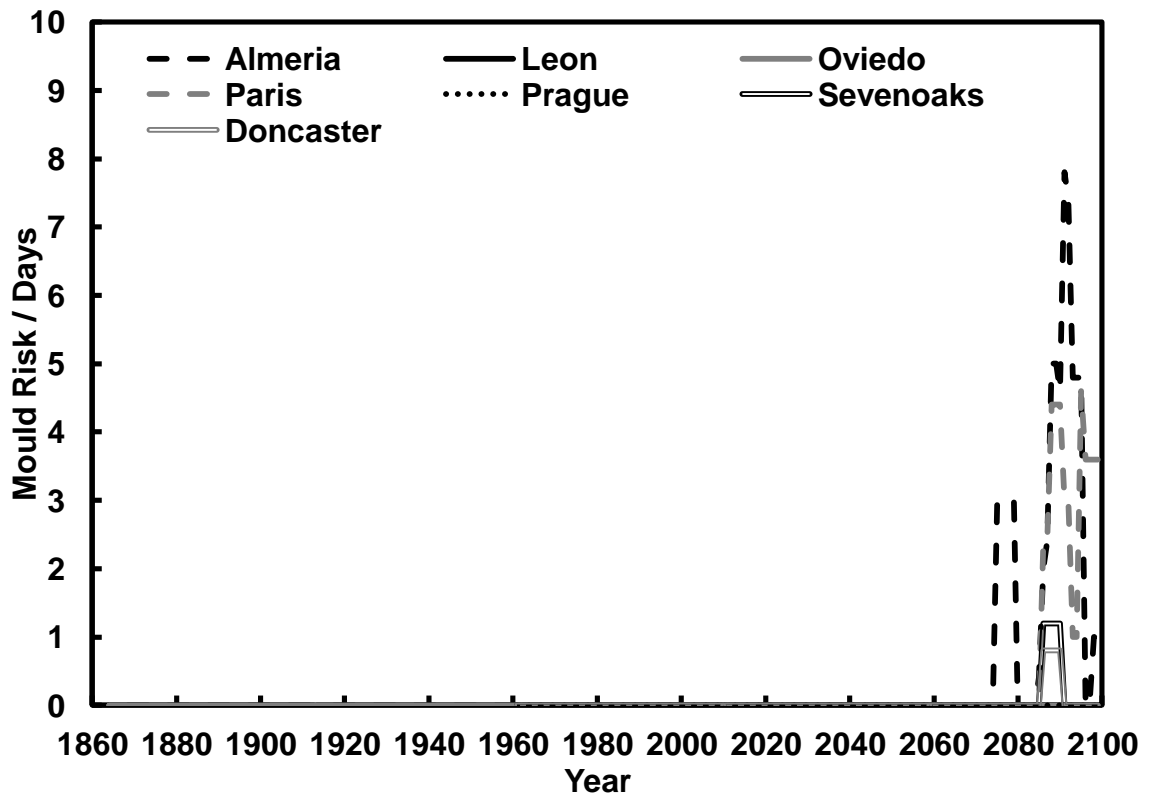


Figure 5.9: The projected impact of climate change on mould growth, as described by the Isaksson function. Results for the seven European locations, from 1860 to 2100. Results are plotted as a five year smoothed average.

However if mould growth starts to become a problem where it hadn't previously it could be quite significant in collection management terms, as this might require resources to solve the problem in comparison to an ongoing issue increasing in severity. It is likely to require more input to minimise this risk, than it would if there is already a problem that may get worse, as current preventive conservation measures may be increased accordingly, rather than implementing new methods.

It is difficult to determine whether the projected mould growth is likely to pose a risk to the collection, or of the significance of the risk. It can be subjective depending upon the

situation, if the idealised room were a store that is not accessed often, where individual objects are even more rarely accessed, even the low levels suggested here could proceed without intervention and become a problem requiring significant input. The same may also be true of a historic house that is closed over the winter, the mould growth, possibly hidden from view could progress before discovered. Alternatively these are quite low levels, which if the early signs are picked up on, in an open building with a good level of staffing then it is less likely that the mould would pose a major problem.

It is important to assess the statistical significance, however the Wilcoxon Signed ranks test requires a minimum number of test pairs, here a large number have a difference between the pairs of zero, ruling them out. Therefore it is not possible to apply this statistical test to any of the locations. It is unlikely that there is a significant difference between the baseline and far future for any of the locations.

**Critical Relative Humidity**

The results for each of the seven locations when using a critical relative humidity (as described previously in section 4.4.2) are presented in figure 5.10 a and b, they have been split for clarity. At all locations an increase in mould risk is projected in the future. This may be unexpected when the projected humidity is considered, the annual average decreased for all locations with the exception of Almeria. This indicates that the annual averages can actually hide the real picture. The seasonal fluctuations are also important, and these results suggest that at some point in the year the humidity increases, above the current level, resulting in the increase in mould growth.

In comparison with the previous mould growth model the critical relative humidity indicates that mould growth is occurring currently and is likely to increase further. The critical humidity is often set at a level to prevent mould growth, which is quite different to the conditions required for mould growth. The critical relative humidity assumes that other variables are at the optimal level and it is also set slightly below the actual humidity required to ensure no mould growth occurs. It is such that this method most likely over estimates mould growth, but still indicates that some of the required conditions are moving towards becoming more favourable in the future.

Mould growth has already been observed at Knole, thus mould growth is possible, something that the first model does not indicate, which could be a problem, as the environment might be assumed to be safe. It is always better that a method fails safe, even if a model predicts mould growth and none could actually occur, this is better than a model that is too conservative and does not predict mould growth when it is possible. This

could lead to situations where mould growth is not predicted, and could actually proceed unhindered, or environmental conditions are not improved to prevent mould growth, due to relying upon a flawed model.
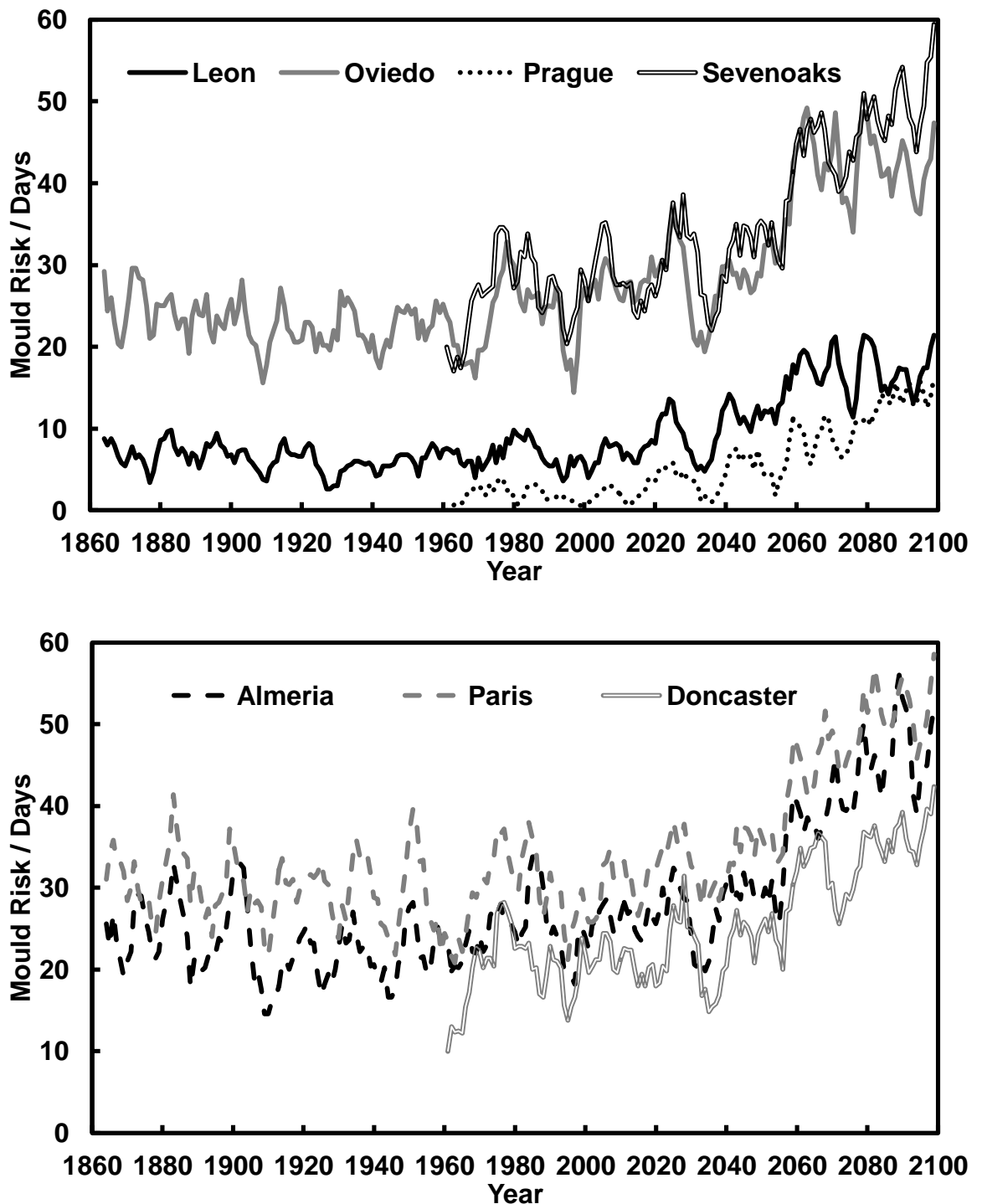




Figure 5.10 a and b: Projected number of days per year where the critical relative humidity is exceeded, resulting in risk of mould growth. (a) four of the European locations and (b) the other three, which have been split for clarity. Results are plotted as a five year smoothed average. The baseline period medians of all locations are significantly different to those of the corresponding far future period.

The mould growth models predict mould growth for specific materials, thus they can only be held true for these materials, and care must be taken as other materials may be more susceptible. This is one advantage of the critical RH method, that whilst mould may not grow, it is very sensitive and unlikely to predict that no mould growth will occur when it is actually possible. One advantage of the Isaksson method is that it can be re-calibrated to other materials, given the number of days taken for mould to grow, at the specific conditions. Thus if there is a known mould problem with a specific material then it can be modelled, helping to prevent future growth by controlling the environment. This can be very useful as environmental control can be difficult, if the model suggests significant ongoing issues it may be easier to relocate the object, but it could be that there is a slow build up to germination, so occasional dehumidification could set back the process, and the length of time required for dehumidification could be estimated using the model.

The results of the Hukka damage function are somewhat similar to those of the Isaksson function, and thus are shown in appendix C. Both the Hukka and the Isaksson models are for mould growth on spruce and pine sapwood, therefore direct comparison between the models should be applicable. While the results of the two functions are somewhat similar, the magnitude is quite different, and growth occurs slightly earlier in the Hukka model. This suggests that the Hukka model has a lower threshold for the requirement of mould growth, and is thus more sensitive than the Isaksson model. Without actual mould growth data to compare to, which isn't possible here, then it is difficult to say which is more accurate.

**Graph method**

This method is calculated in a different way to the previous methods, this uses a graph to describe the ideal conditions, rather than an equation. There are other variables between the models, such as the substrate for mould growth and the mould strain. Where the others models are generic in terms of the mould strain, this is a specific one, relating to *Aspergillus restrictus*. The substrate which it was grown upon is not specified, leading to the assumption that it was grown on an ideal substrate. An ideal substrate is likely to support mould growth more so than spruce and pine sapwood does.

The results shown in figures 5.11a and b, split between the two for clarity, appear to confirm this with mould growth occurring much earlier than previously projected by the Isaksson and Hukka models. Thus this model is not seen as directly comparable to those models. For this model the first observation is that the projected mould growth for Oviedo is substantial in comparison to the other locations, particularly during the baseline period. This is different from the previous two mould functions (excluding the critical RH function,

the potential flaws of which have been discussed) where Oviedo had no projected mould growth. The results of this model, in comparison to the previous two, indicate mould growth becoming an issue earlier, around 2020 compared with 2070, this would suggest that this model is more sensitive, so is possibly more suitable for more susceptible materials. This highlights the uncertainty between damage functions, due to the underlying structural model. This is an important consideration when selecting which damage function is the most representative, which could vary depending on the material considered.

Note that Sevenoaks has small peaks around the current decade that would indicate mould growth was possible, this would correspond to the observed growth, where other models do not. It is not to say that this is the optimal model to use, it is dependent upon the materials in the collection, and their susceptibility, further work is required to determine the actual impact of projections.

The reason for the projected increase in mould germination is because of an increase in relative humidity. However the projected relative humidity, as shown in figure 5.3, does not indicate this. It is a seasonal increase in winter relative humidity that accounts for this. The critical relative humidity method requires at the lowest a humidity of 80%, and thus an increase in risk assumes an increase in humidity above 80%. This value is for a temperature of 20°C, for lower temperatures the critical value increases, as described by equation 4.17 in section 4.4.2. Values of 80% relative humidity only occur in the winter, in the summer the temperature is warmer and has driven the relative humidity down. Thus the projection of these results indicates that the winter relative humidity increases in the future, this would correspond to results in chapter 6. This is to be expected as the long term climate projections used here derive from the same climate model ultimately.
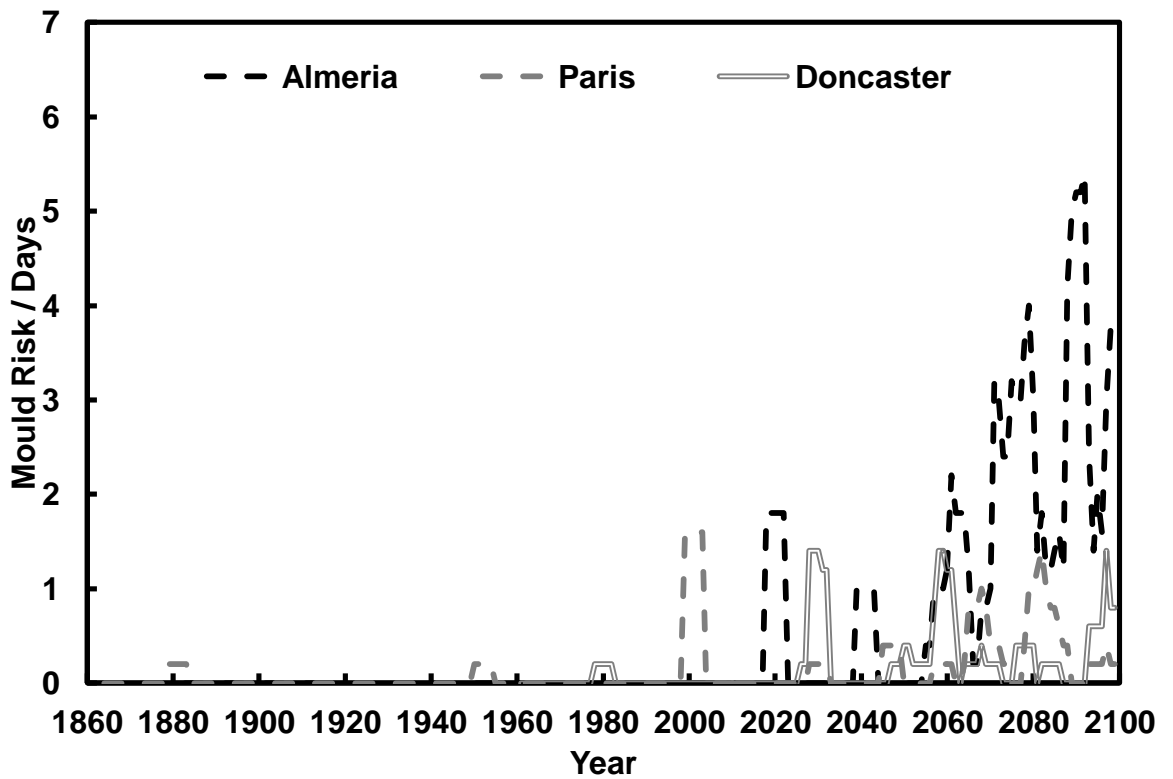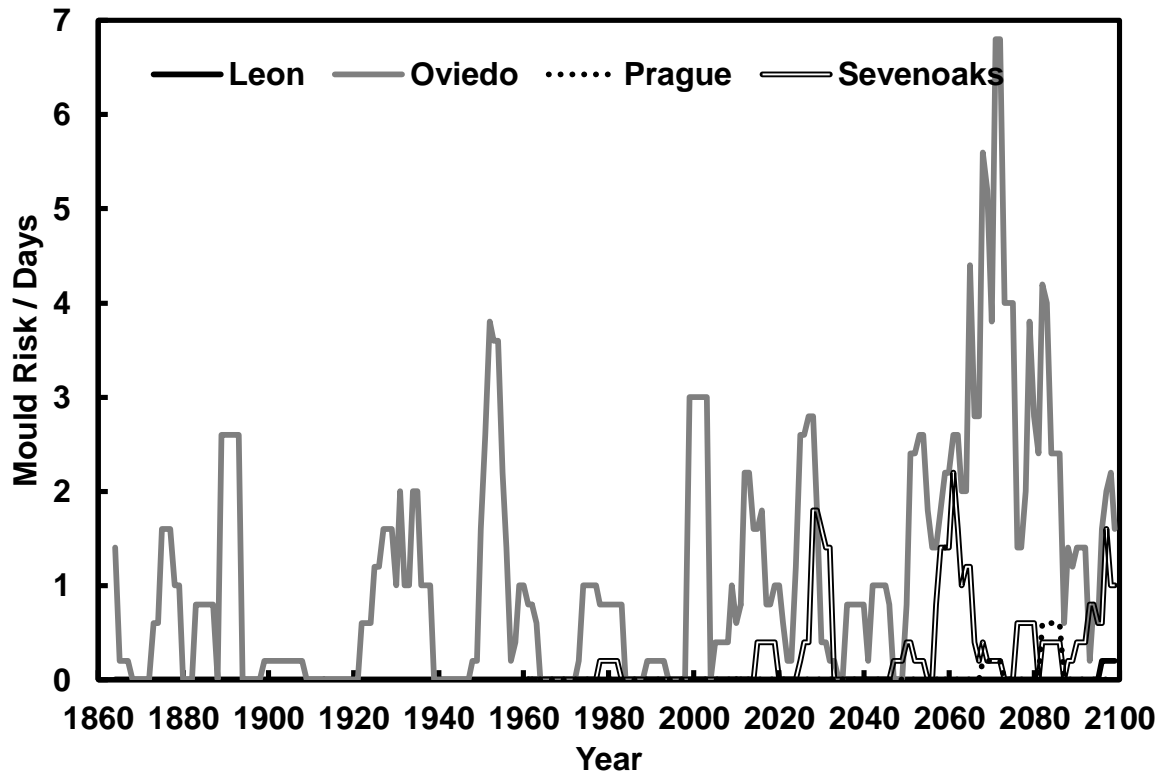
Figure 5.11 a and b: Projected number of days, per year, where mould is expected to grow, for the years 1860-2100. (a) includes four of the seven European locations and (b) the other three, they have been split for clarity. With the exception of Leon and Prague the

baseline median of the other locations is significantly different to that of the far future median.

*5.4.2.4 Degree days*

The results for the degree day method are presented in figure 5.12, as would be expected with projected increases in temperature, the count of degree days over 15°C also increases, across all locations, but with different magnitudes. Again Almeria has a high baseline value, which increases in the latter part of the century, but only by a small proportion of the baseline level. In contrast the other locations, which all have significantly lower baseline levels compared to Almeria, are projected to increase substantially. The increase across the remaining six locations on average shows a twofold rise in degree days. As previously explained conservation measures valid currently in one location may be applicable elsewhere in the future. However, with insect pests, this might not be so straight forward as in different locations the pest species encountered may be different, and although pest management strategies are similar, they are not always transferable. One such example would be the moth pheromone trap which is species specific. This discussion also raises another impact that climate change may have, the spread of insects to locations that exhibit favourable conditions in the future, as briefly mentioned elsewhere (Child, 2007). The significance of this would be important, a new species of insect pest may require considerable input, of both resources and knowledge to solve this problem. Of course this is new to the location, but is likely to have occurred elsewhere, again raising the importance of information dissemination.

This method is another that is not directly linked to damage, but can be used as an indicator. It may be possible that, with other optimal conditions that are neglected here, there is one life cycle per year of a particular insect pest, and in the future this could increase to two life cycles. It may also be the case that the onset of required conditions occurs earlier in the year than previously and possibly continues for longer. This is confirmed to some degree by the number of warm days per year, as shown earlier in figure 5.4.

Increased temperature can also affect other factors related to insect pest damage, for example greater numbers of eggs are produced at warmer temperatures for the webbing clothes moth (*Tineola Bisselliella*) (Child, 2007). It is also possible that mobility is increased, as mentioned earlier the common furniture beetle (*Anobium Punctatum*) does not readily fly at temperatures below 25°C (Child, 2007).

These risks could pose a number of problems, firstly it is possible without good integrated pest management (IPM) that numbers could increase substantially because of the compounding factors described. Also longer periods of activity could have a logistical impact upon management strategies. Often these are organised around the opening of the house, for example deep cleaning would often be carried out when the house is closed to the public, maybe over the winter period. If insects are active for longer this could affect how problems are managed. Additionally pest issues may arise (maybe earlier than before), but cannot be dealt with fully because it requires the closure of the house. This raises another aspect of the impact of climate change, not investigated in this work, but a possible problem. If temperatures are rising, and there are longer warm periods in the future then there could be longer opening times across the season, which again would impact upon when conservation work can be carried out effectively.
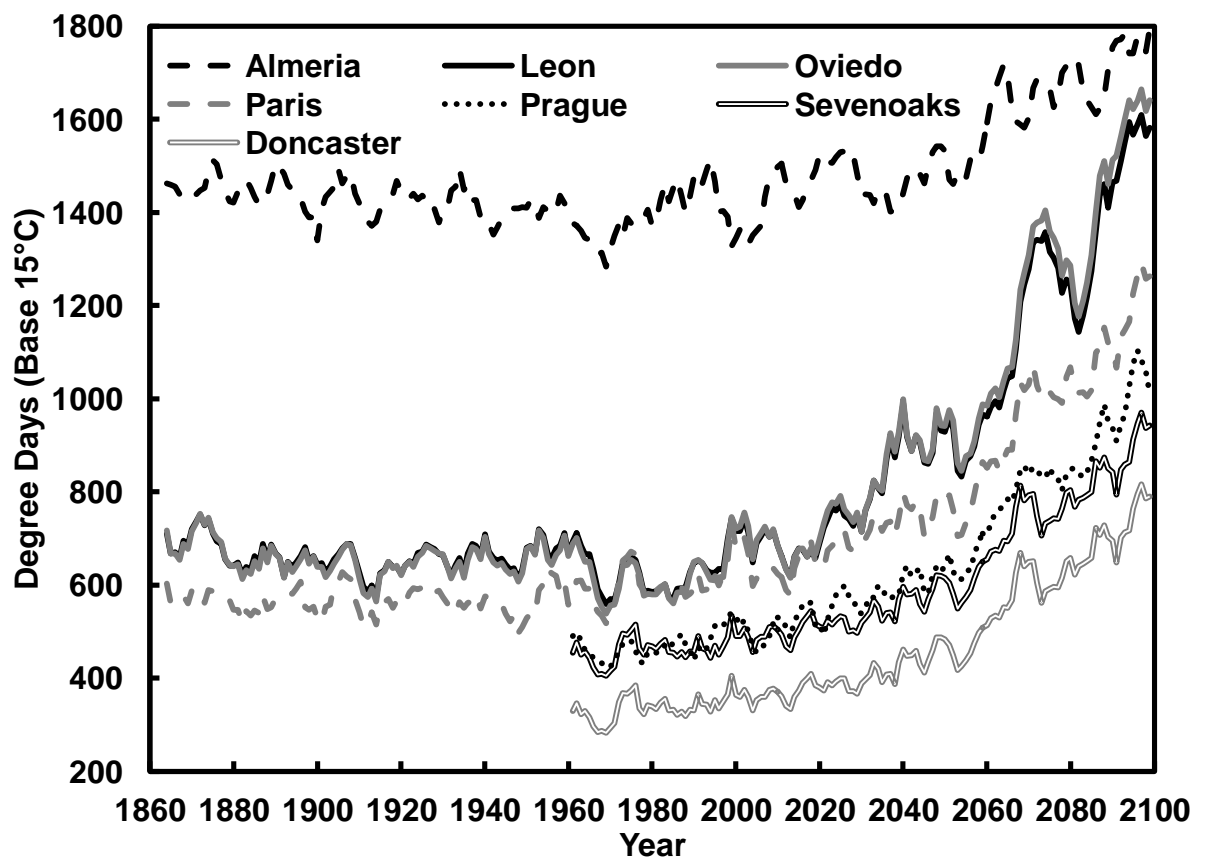


Figure 5.12: The projected impact of climate change on the number of degree days (base 15°C) indoors. Results are presented as five year smoothed averages, from 1860 to 2100, for seven European locations. The baseline period medians of all locations are significantly different to those of the corresponding far future period.

*5.4.2.5 Salts*

**Salt Transitions – thenardite/mirabilite**

The number of salt transitions of thenardite to mirabilite that exceed 10 MPa, thus causing damage, projected over the coming century are shown in figure 5.13 a and b, split for clarity. The results here do not follow a specific trend, Almeria and Paris projections indicate no change in the number of transitions across the century. Oviedo and Prague show a slight increase, although it is difficult to tell the magnitude because of the natural variation year on year. Both the UK locations, Doncaster and Sevenoaks show a slight decrease in damaging salt transitions, although difficult to tell whether this is a true effect, or the natural variation, as it is very slight. The final location, Leon, is projected to have an increased number of transitions, rising from around 12 to 17 in the far future.

The nature of the thenardite/mirabilite salt transition function, with a varying critical humidity dependent upon temperature is the reason for the results at each location being quite unique. This highlights the importance of individual assessments, not only of location but also each individual environment, as this will change from one historic house to the next, and also from each room to another. Thus the idealised room technique is not useful with this damage function, as the critical humidity is dependent upon the individual room environment. Therefore an idea of what may happen at certain locations is not valid, with the exception of Sevenoaks, and more specifically the Cartoon Gallery at Knole, as the real location.

While the actual projections for this function are not valid, the determination of a process that specifically focussed on ease of use, to be readily transferable to other locations was the aim, so that the individual projections can be determined. In a real situation where the model was applied to a location in Europe, where observed data is available then the application of this function would be valid.
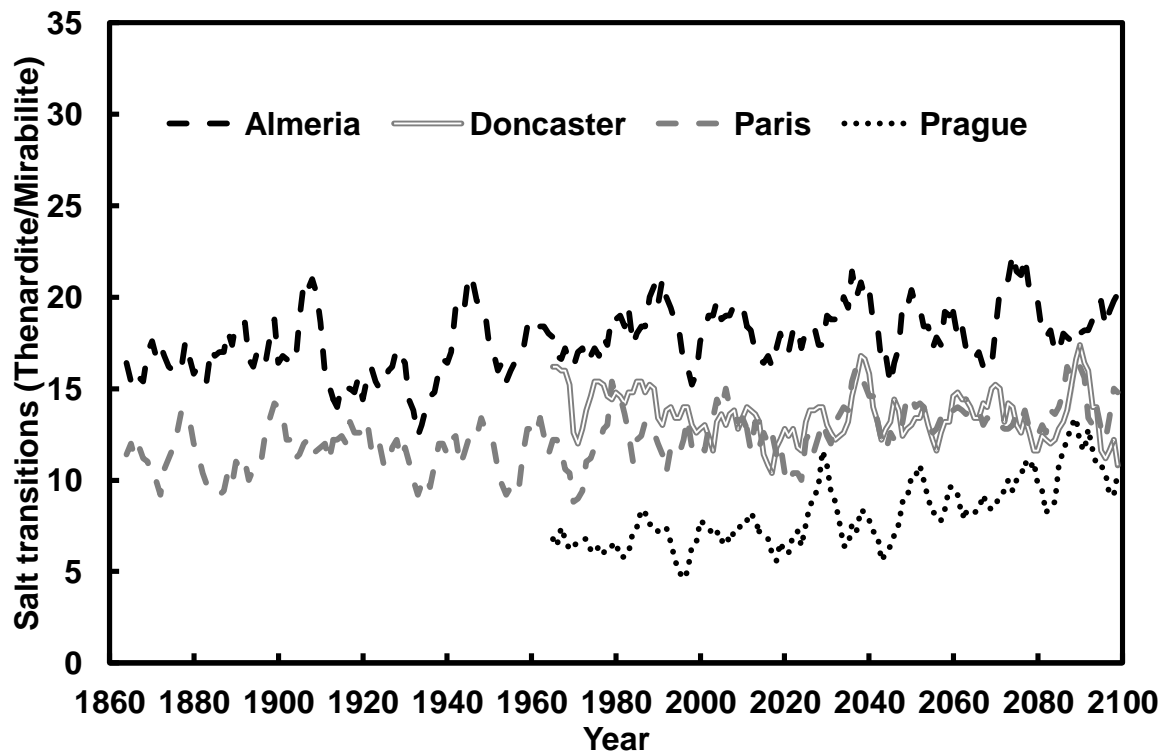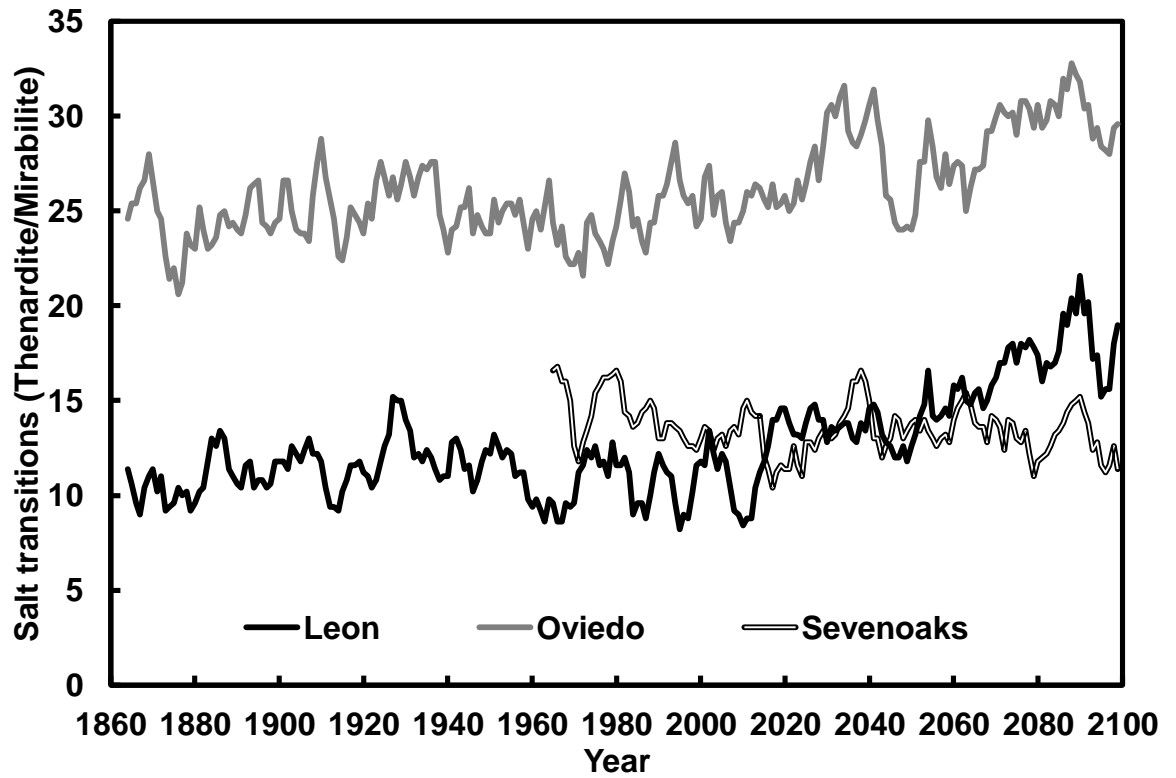
Figure 5.13 a and b: The projected number of transitions exceeding 10 MPa of thenardite to mirabilite. Results are plotted as five year smoothed averages, from 1860 to 2100. (a) includes three of a total seven European locations, and (b) the remaining four, these have been split for clarity. The baseline period medians of all locations are significantly different to those of the corresponding far future period.

**Salt transitions – 75.3%**

The results of the impact that climate change will have on transitions of one of the more common salts, Halite (NaCl) are presented in figures 5.14 a and b. Figure 5.14a shows that transitions for Leon are not projected to change, while Paris is quite similar, but could possibly be interpreted to increase slightly in the far future. The opposite is true for Sevenoaks, a slight decrease in the far future is projected. These slight changes are unlikely to have an impact overall in these locations, when there are 20 a year already, a small shift either side of this are unlikely to affect management strategies employed.

In figure 5.14b, the same principles apply, as only relatively small shifts are projected. One point to note is the difference between Leon and Oviedo, with Oviedo having almost twice the number of transitions on average. There is also a difference in the shift of future projections, Leon with no change and Oviedo with a slight increase in the far future. The results of the other two salt damage functions (60 and 85%) can be found in appendix C.

*5.4.2.6 Dimensional change*

**Michalski**

**5% Humidity shock**

The next set of figures projects damage caused by dimensional change, using a number of different functions. The first, described by Michalski (1996) at the 5% relative humidity fluctuation level describes damage to wooden objects with very high vulnerability, through gradual fatigue fracture. Information on specific types of objects can be found in table 4.5. The projections of the impact of climate change, across the seven locations, to these objects are shown in figures 5.15 a and b, split for clarity. All locations with the exception of Almeria indicate an increase in these damaging fluctuations; no change is projected for Almeria. Gradual fatigue indicates that at a certain threshold value the object will fail to some degree. The projected increase in the number of damaging events would bring about this failure point sooner. This assumes comparison of two identical objects at different points in time, however, the older object would actually be closer to this failure point, but will also be approaching it at a faster rate.

The comparison of Leon, Prague and Sevenoaks here shows that between the years 1960-2000 the projected number of damaging events for Leon and Sevenoaks is similar, and dissimilar to Prague, but by the year 2100 Sevenoaks and Prague are similar, with Leon dissimilar. The 10 and 20% damage functions are shown in appendix C, as is the 40% function.

Figure 5.14 a and b: The projected number of halite transitions at a critical humidity of 75.3%. (a) presents three of seven locations and (b) the other four. Results are presented as five year smoothed averages. The baseline period medians of all locations are significantly different to those of the corresponding far future period.

Figure 5.15 a and b: Projected yearly number of 5% humidity fluctuations, from one day to another, as described for the Michalski damage function for dimensional change. Seven locations are shown across the period 1860-2100, with (a) having four of the seven and (b) three, they have been split for clarity. Results are plotted as five year smoothed averages. The baseline period medians of all locations are significantly different to those of the corresponding far future period.

**30% Humidity shock**

The value of 30% day to day relative humidity fluctuation does not fall into the categories used by Michalski (1996), but follows on from the 5, 10 and 20% values used. However it is used by Jakiela et al. (2008), where it is said that a 30% relative humidity change day to day has considerable damaging potential for wooden objects. Figure 5.16 presents the projection of these damaging events at seven locations. The first comment is that such events are very rare, with the majority of locations having less than one per year, and often none. Obviously it is not possible to have a part of a fluctuation, thus the values here can be thought of as the probability of an event occurring. Such that if it is one then each year there is projected to be one damaging event of this magnitude, if 0.5 then once every two years, 0.2 once every five years and so on. While these are rare events they are almost certainly going to cause damage, thus the general increase that is projected would require some form of mitigation for objects that are likely to be damaged.
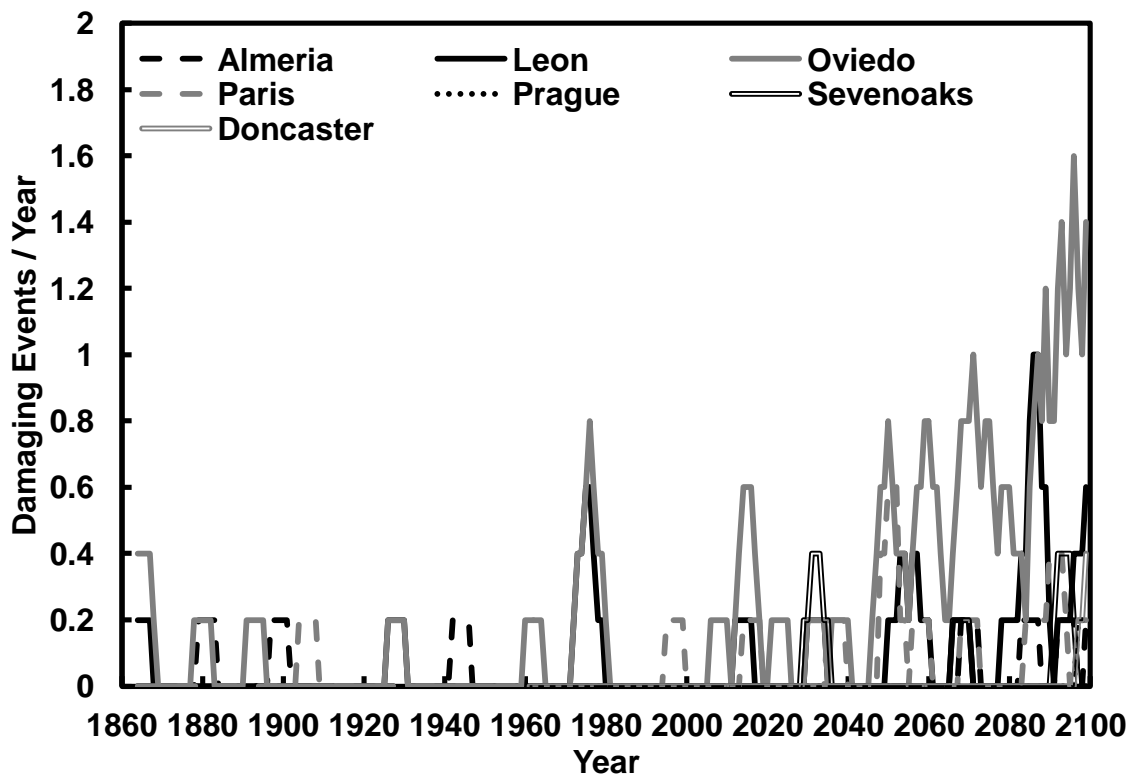


Figure 5.16: The projected yearly number of 30% day to day humidity fluctuations, for the 30% humidity shock damage function. Seven European locations are shown, for the period 1860-2100. The baseline period medians of all locations except Leon and Oviedo are not significantly different to those of the corresponding far future period.

Assessing the impact of the 5, 10, 20 and 30% relative humidity changes it is not initially obvious which is most important. In terms of objects there are often a disproportionate

number of objects with very high vulnerability. This may be because of the age and importance of the object, which has only managed to survive because of previous treatment and repair. Thus the fluctuations that affect the more vulnerable objects may be interpreted as having greater significance. Therefore the increases in transitions projected are likely to require additional resources for preventive conservation in an attempt to stop this damage from occurring. Preventive conservation methods such as protecting these objects by placing them in showcases, and controlling the relative humidity either with a buffer such as silica gel, or using mechanical control would reduce these damaging fluctuations and preserve them for longer periods.

**Mecklenburg**

**Cotton wood**

This damage function also estimates dimensional change of wood, taking a different approach from the previous function. Each change in relative humidity is dependent upon the starting relative humidity. Depending on this a specific amount of change is allowed, determined by the stress caused, before the yield point is reached. Once this is passed it is classed as a damaging event. This is also dependent upon whether the wood is absorbing or desorbing moisture, as there is a hysteresis effect. The results are assessed for both adsorption and desorption events independently, and then the total number of events is evaluated.

The damage function is species specific; the projected number of damaging events due to adsorption of moisture for cotton wood is shown in figure 5.17. All seven locations show an increase in damaging events in the future, due to the impact of climate change. On average the locations show an increase of 10 damaging events per year in the future. If this were a change from zero to ten there would be obvious need for mitigation to prevent damage. However, determining the impact here would depend upon the individual conditions. If damage is observed currently then it will only increase, but this does not help inform whether further conservation measures are required, the current provision may be adequate.
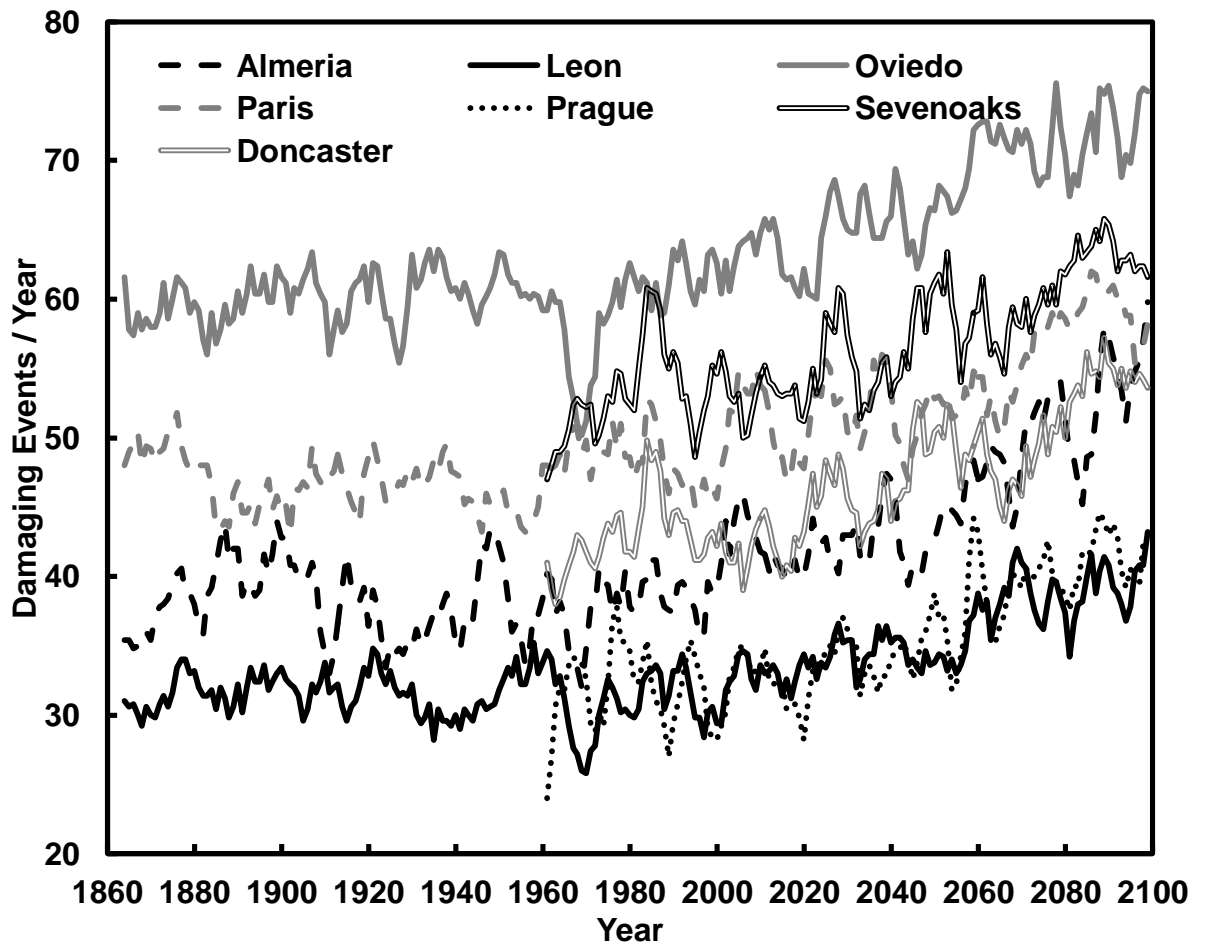
Figure 5.17: Projected number of damaging events to cotton wood per year, due to adsorption of moisture as described by the Mecklenburg damage function. Results for seven locations for the period 1860-2100, plotted as five year smoothed averages. The baseline period medians of all locations are significantly different to those of the corresponding far future period.

The corresponding projection of desorption events are shown in figure 5.18 a and b, split for clarity. Again an increasing number of damaging events is projected at all locations in the future. The corresponding total, of the adsorption and desorption events are shown in figure 5.19, confirming that all locations show an increase in overall damaging events to cotton wood. The previous discussion for the adsorption events relating to the significance is also relevant for the combined results.

Figure 5.18 a and b: The projected impact of climate change on the number of damaging events indoors to cotton wood, caused by desorption of moisture. (a) presents four of seven European locations and (b) the remaining three. Results are plotted as five year smoothed averages. The baseline period medians of all locations are significantly different to those of the corresponding far future period.
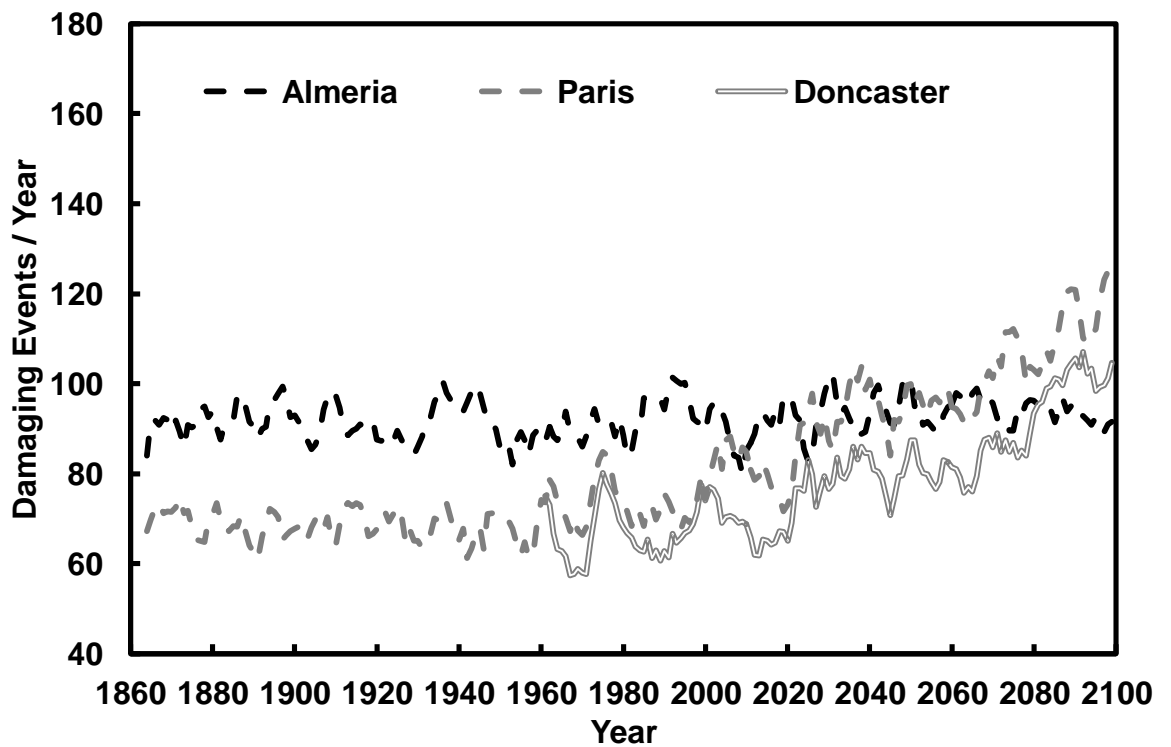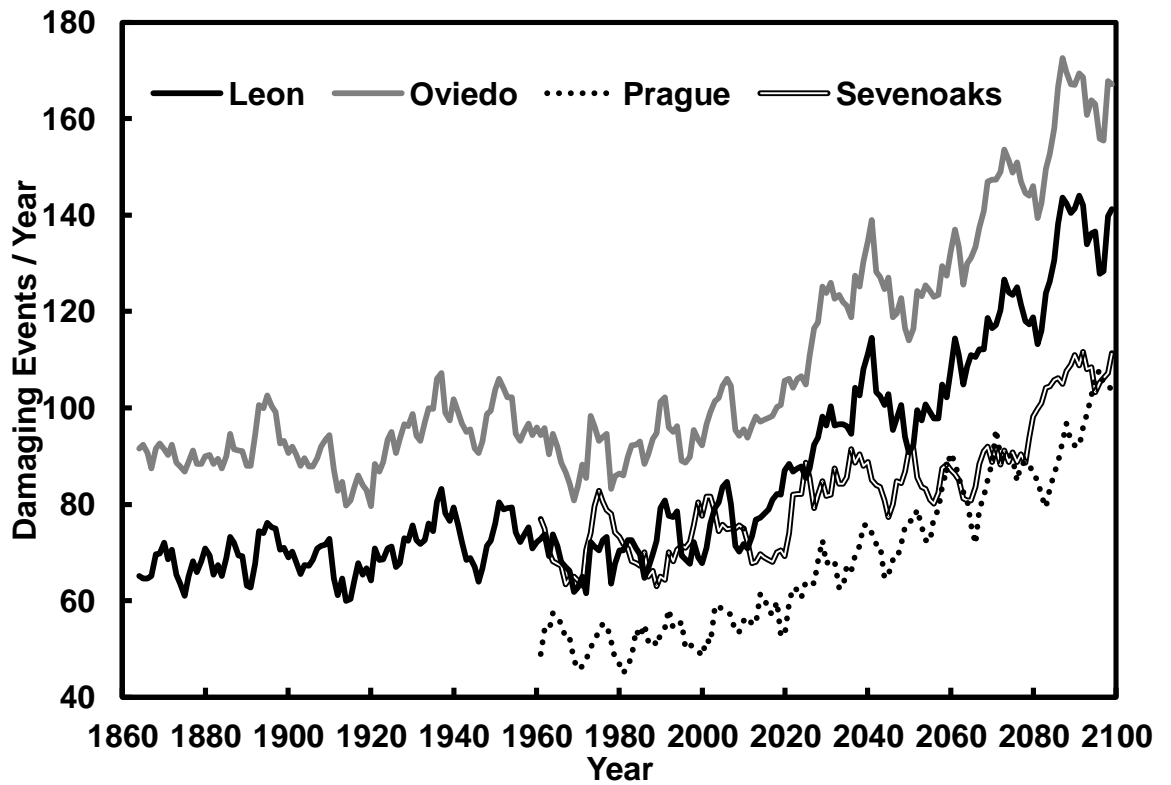
Figure 5.19: The projected number of damaging events to cotton wood from both adsorption and desorption events. Results for seven locations are shown from 1860 to 2100. Results are plotted as five year smoothed averages. The baseline period medians of all locations are significantly different to those of the corresponding far future period.

**White oak**

The damage function described by Mecklenburg et al. (1998) is also defined for the white oak species, so can be applied to objects made from this material. The projected impact of climate change on the adsorption of moisture is shown in figure 5.20. All seven locations are projected to have an increase in the number of damaging events, as is also projected for the number of desorption events, shown in figure 5.21. This is summarised for white oak in figure 5.22, where the total of both adsorption and desorption damaging events are shown.



Figure 5.20: The projected impact of climate change on the number of damaging events per year to white oak by moisture adsorption, as described in the damage function by Mecklenburg. Results for seven locations are presented from 1860 to 2100. Results are plotted as five year smoothed averages. The baseline period medians of all locations are significantly different to those of the corresponding far future period.

Figure 5.21: The projected number of damaging events per year for white oak, caused by moisture desorption. Seven European locations are presented, with results from 1860 to 2100. Results are plotted as five year smoothed averages. The baseline period medians of all locations are significantly different to those of the corresponding far future period.

As with the cotton wood projections of damaging events, those for white oak also increase in the future, for both adsorption and desorption events. For white oak the magnitude of results, 70-130 damaging events, per year, in total across the seven locations is greater than that for cotton wood, which has 50-100 damaging events in total. In both cases the minimum value is for Prague, and the maximum for Oviedo. The difference between the two types of wood indicates that the type of wood under consideration is important, as each has different properties, thus can resist humidity fluctuations more or less effectively. In both cases the order of each location is the same, indicating the future environment in Oviedo has the greatest number of damaging events for this type of damage, but for other types it may be ideal. This highlights the complexity of mixed historic collections, often many materials form one collection. Thus the display conditions are often a compromise between the materials, to minimise the risk to the whole collection, which inevitably means that the ideal conditions for each individual material are not met.
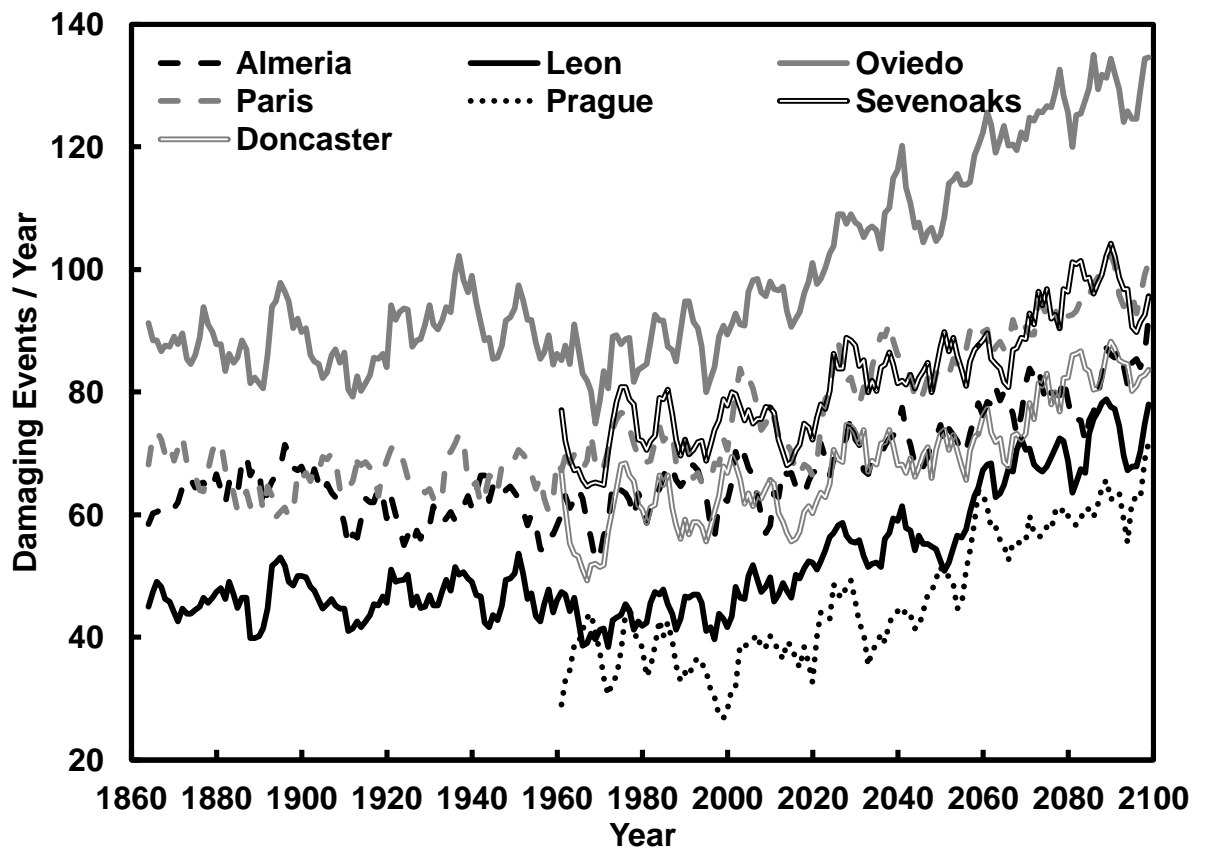
Figure 5.22: The projected number of damaging events per year to white oak, from both adsorption and desorption of moisture. Results from 1860-2100 for seven European locations are shown. Results are plotted as five year smoothed averages. The baseline period medians of all locations are significantly different to those of the corresponding far future period.

In addition to the adsorption and desorption yield points, that are described as causing irreversible damage, there is also a function defined for failure of white oak. The projected impact of climate change on the failure of white oak is shown in figures 5.23 a and b. The results here differ somewhat to the adsorption and desorption events for white oak, with some locations having a sharp increase in the far future (Oviedo, Doncaster, Prague, Paris and Sevenoaks), as opposed to the steady increase seen before. Almeria is projected to have a decreasing number of failure events in future. Leon shows something different altogether, the number of failure events per year increases from about 1960 to 2060, but then drops back to a similar value of the baseline over the period 2070-2100. This is especially unusual as Oviedo, while downscaled to the specific location is still based on the same data from the Hadley model, doesn't follow this pattern, it continues to increase in the future. This suggests that it is the downscaled climate of Leon itself that is causing the reduction. Referring back to the projected change in future relative humidity

(figure 5.3) and the figure detailing the damage function (figure 4.6) it is possible to explain this projection. The relative humidity steadily decreases from an average of 64% to 62%, and then around the year 2060 the humidity drops quite fast, with a final average of 58%. Also important are the seasonal shifts, as discussed previously. An expected seasonal change slowly increases the projected number of damaging events, as winter humidity increases. The damage function allows less variation at higher values of relative humidity before damage occurs, than at modest relative humidity. Thus also explaining the sudden decrease towards the end of the century, when the relative humidity drops to an average of 58%, where the damage function allows a greater range of fluctuation before damage occurs. It is important to remember that these are annual averages, with fluctuation around this value, thus it is not only the average value that is important, but how the full humidity range shifts lower, thus moving towards the safer region of the damage function.

The nature of the white oak failure damage function also helps explain why the number of damaging events increases for the previous cotton wood and white oak functions, and the other locations in this function for failure events. When the humidity is increased, as happens in the winter months, less humidity fluctuation is allowed, therefore increasing the number of damaging events. The summer relative humidity is expected to decrease, however this is in the safe zone, and less likely to have an impact.

Returning back to figures 5.23 a and b, a substantial increase, from less than five events to more than ten, or even 15 is projected for the other locations, with the exception of Almeria where failure events decrease in the future. Results tend to shift from less than five failure events per year to between five and 20 per year, depending on location. If every event causes an irreversible crack then a possible fourfold increase could be quite significant.
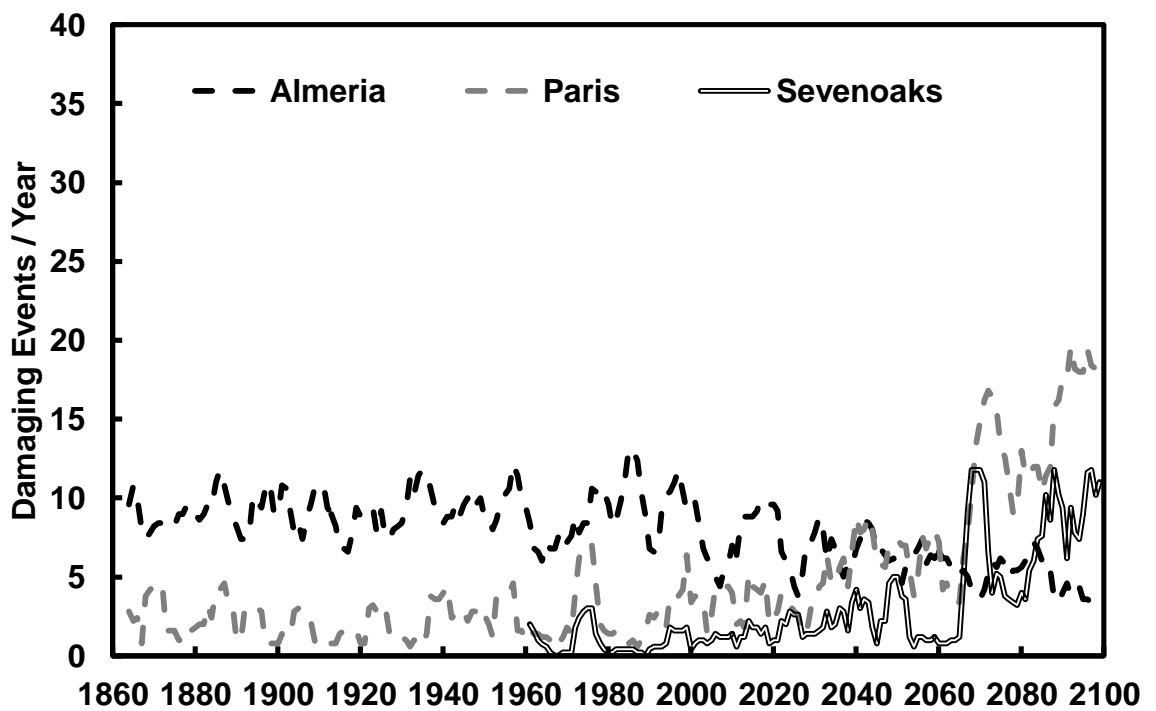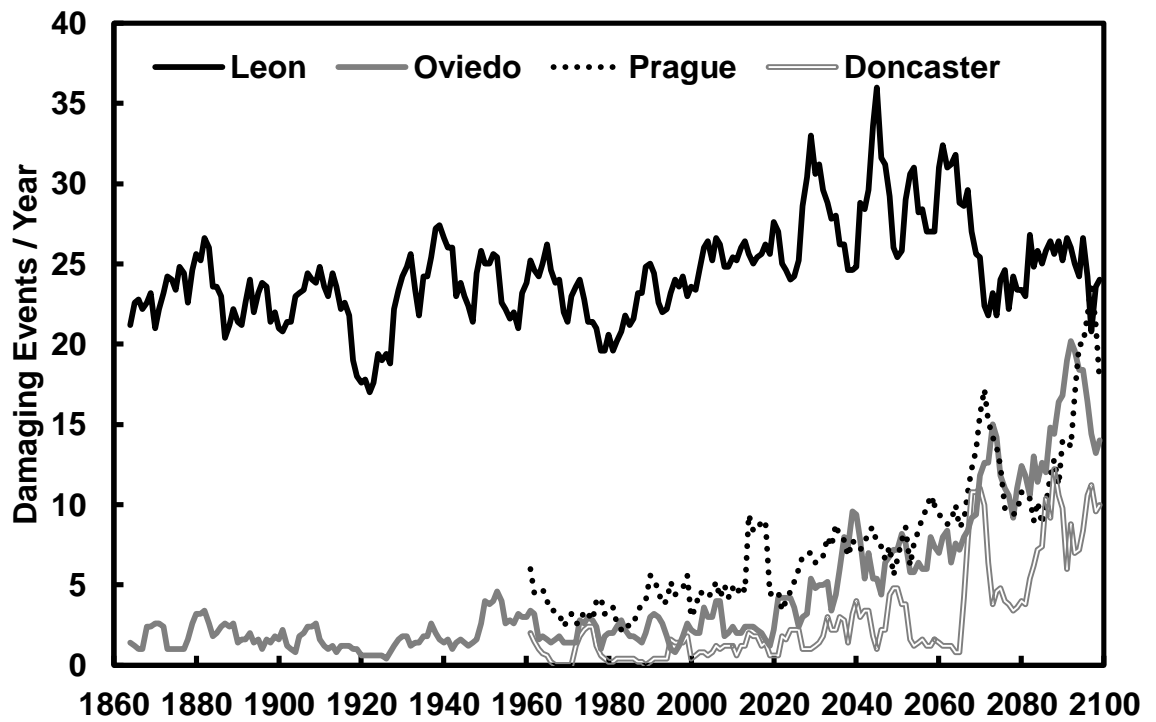
Figure 5.23 a and b: The projected impact of climate change on the yearly number of damaging events to white oak that will cause failure of the material. (a) presents four of seven locations and (b) the remaining three. Results are plotted as five year smoothed averages. The baseline period medians of all locations are significantly different to those of the corresponding far future period.
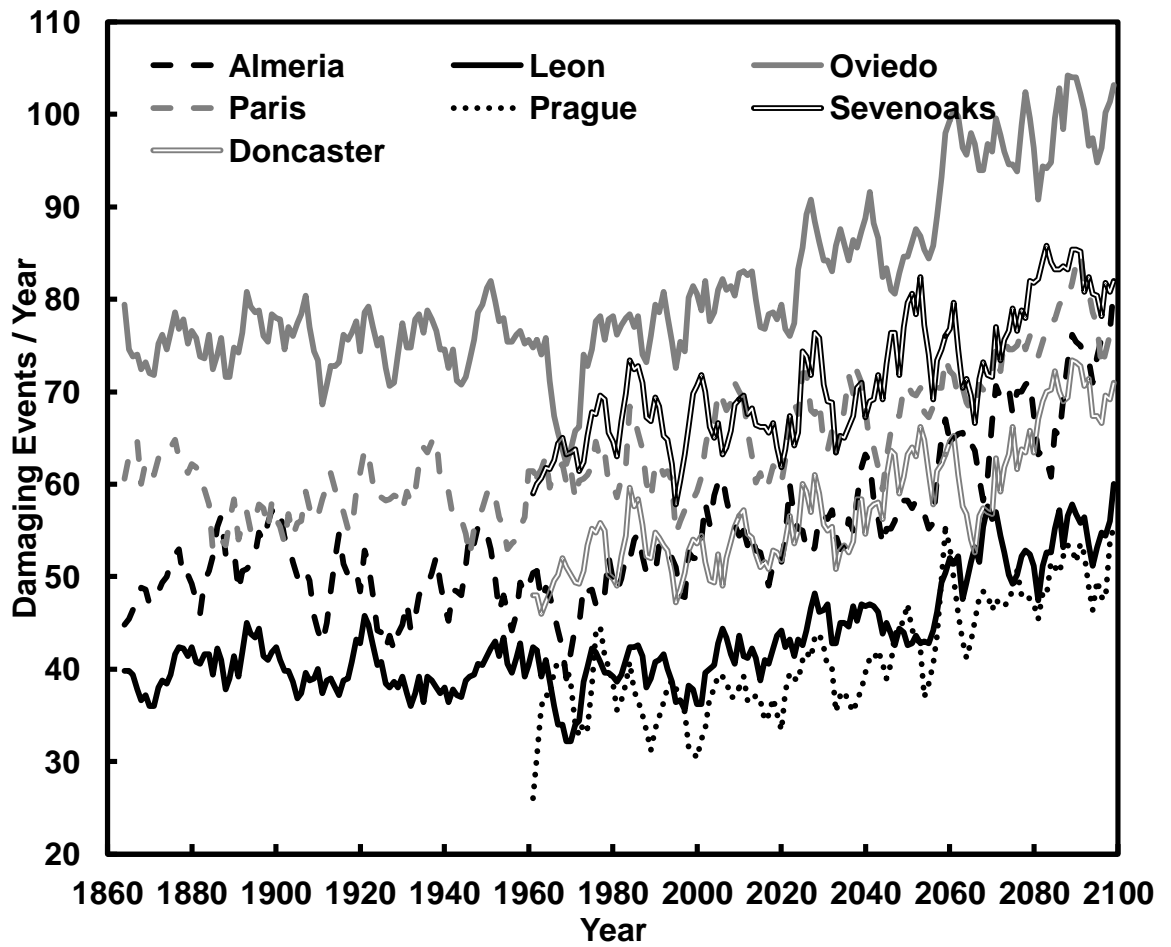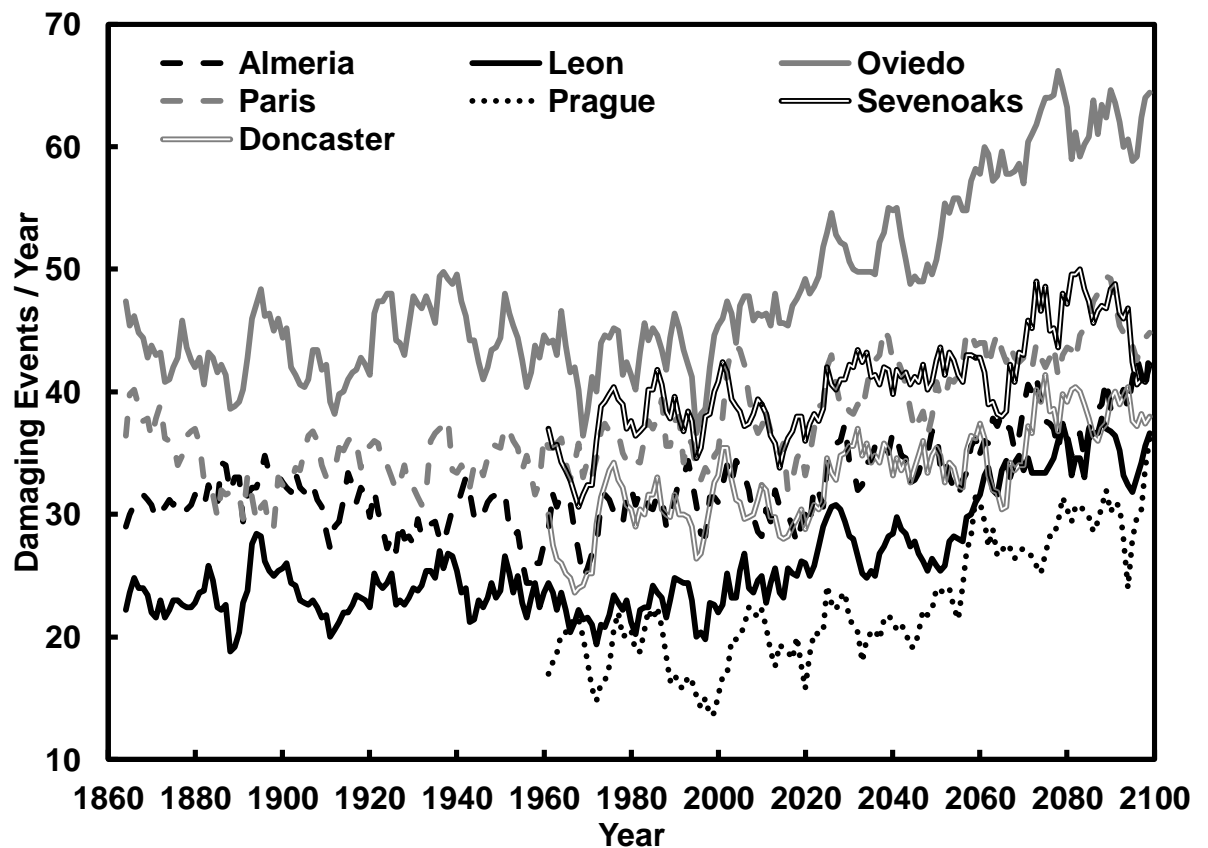
## 5.5 Discussion and Conclusions

A number of points are raised throughout the results, some which could have been on multiple occasions. One of the most important is the significance of a projected change. It is not always immediately obvious whether a change is significant, this work has specifically been generic, to allow a wide application of the developed technique. However this means that there are few examples of damage that relate to the functions used. Where there are examples it appears easier to quantify the projected change, otherwise it is not immediately obvious whether the change is likely to significantly impact upon damage, and techniques to prevent such damage.

This is not always the case though, even with an example some damage functions do not explicitly define damage, for example the thenardite/mirabilite salt transition function explicitly defines that each transition is damaging, however the total extent of damage is not defined. There is confidence that the predictions from this function are important, and each transition has an important effect, but the magnitude of this effect is unknown. Where it is not immediately obvious what the implications of a projected change may be it is not possible to identify measures to prevent this change.

Methods to mitigate damage are typically well known, however it must be apparent whether these are necessary. Take for example conservation heating; this reduces relative humidity and thus damage associated with high relative humidity. It is not a small feat to implement this, therefore it must be certain that this is required before moving forward and using this as a management strategy.

It is also important to remember that the same predicted change could have a varying significance depending upon the specific collection. Two identical objects could have very different values, thus any damage could affect the objects in different ways. The issue of attributing significance to future projections will be discussed in section 6.5, where effort will be made to try and help quantify the significance.

Throughout the results there are various examples of a location having similar damage, or environment in the future compared to another location currently, or in the past. This highlights the importance of dissemination of management strategies, so that knowledge is widely available for those who may require it in the future, to prevent the wheel being invented twice.

The importance of downscaling data from large areas to the specific location is seen on many occasions, with Leon and Oviedo often having differing levels of damage, and on

occasion a different shift of direction. It is expected that the onset of new problems is likely to have greater significance compared to the worsening of current problems.

It has been shown that it is important to assess the impact of climate change on a specific location, rather than assume from general statements. The sensitivity of some damage functions, and variations across environments can result in different projections than the assumed norm. Almeria is a good example, which often bucks the trend of the other locations.

The results of each damage function across the locations are summarised in table 5.3. The majority of results indicate an increase in damage. Chemical degradation is projected to increase across all locations, as is biological damage, with a couple of exceptions, which are projected to remain the same.

Physical damage is not so easily described; salt damage varies widely upon the salt and the location. Dimensional change depends upon the severity, the smaller the change the greater the chance of change for the worse. For example where few transitions occur they have a greater probability of causing damage, as they tend to be for the higher magnitude humidity shocks. Thus a change here has a greater chance of being a change for the worse. A high number of events are likely to be related to fatigue, changes here are important but are less likely to have an impact as soon.

Almeria is the exception to the rule for dimensional change, with the result depending upon the individual damage function. It is important to consider the assumptions made about the damage functions, as described in chapter 4. This summary of course does not indicate the magnitude of such a change, which is of great importance. It is important to remember to take into account all of the underlying assumptions and uncertainties that are associated with this work when assessing the results presented in this chapter.

While there are projections of future damage, care must be taken when interpreting these results. They are there as an indication of the direction in which damage may move in the future, but the projections are sensitive to the building and room under investigation, especially for some of the functions, for example the salt transitions. Therefore if the impact of climate change is to be investigated the specific location must be used with the process, to give results for an individual location.

Table 5.3: Summary of projected results, at the end of the century, for each damage function at all locations. Red indicates changes for the worse, green indicates a change for the better, and yellow no observable change. For temperature and relative humidity which can be interpreted in various ways, red is an increase and green a decrease.

| | | Location | Doncaster | Sevenoaks | Prague | Paris | Oviedo | Leon | Almeria |
|---|---|---|---|---|---|---|---|---|---|
| **Environment** | | Temperature | ↑ | ↑ | ↑ | ↑ | ↑ | ↑ | ↑ |
| | | Relative humidity | ↓ | ↓ | ↓ | ↓ | ↓ | ↓ | ↑ |
| | | T>20°C | ↑ | ↑ | ↑ | ↑ | ↑ | ↑ | ↑ |
| | | T>25°C | ↑ | ↑ | ↑ | ↑ | ↑ | ↑ | ↑ |
| **CHEMICAL** | **Chemical degradation** | Zou | red | red | red | red | red | red | red |
| | | Isoperm | red | red | red | red | red | red | red |
| | | TWPI | red | red | red | red | red | red | red |
| | | Silk isoperm | red | red | red | red | red | red | red |
| **BIOLOGICAL** | **Mould germination** | Isaksson | red | red | yellow | red | yellow | red | red |
| | | Critical RH | red | red | red | red | red | red | red |
| | | Hukka | red | red | yellow | red | yellow | red | red |
| | | Graph method | red | red | red | red | red | red | red |
| | **Pests** | Degree Days | red | red | red | red | red | red | red |
| **PHYSICAL** | **Salt transitions** | Then/Mir | green | green | red | yellow | red | red | yellow |
| | | 60% | yellow | red | red | red | red | red | green |
| | | 75.3% | yellow | green | green | red | red | yellow | yellow |
| | | 85% | red | red | red | red | red | red | red |
| | **Wood dimensional change** | **5%** Humidity shock | red | red | red | red | red | red | yellow |
| | | **10%** Humidity shock | red | red | red | red | red | red | yellow |
| | | **20%** Humidity shock | red | red | red | red | red | red | yellow |
| | | **30%** Humidity shock | red | red | yellow | red | red | red | yellow |
| | | **40%** Humidity shock | yellow | yellow | yellow | yellow | yellow | red | yellow |
| | | Cotton wood | red | red | red | red | red | red | red |
| | | White oak | red | red | red | red | red | red | red |
| | | White oak failure | red | red | red | red | red | yellow | green |

# CHAPTER 6

# DAMAGE FUNCTION RESULTS USING UKCP

## 6.1 Introduction

The impact that climate change will have at various locations around the UK is projected in this chapter. Three historic houses are investigated, Knole, Brodsworth Hall and the Swiss Cottage at Osborne House, as described in section 2.2. At Knole two rooms will be investigated, the Cartoon Gallery and the Leicester Gallery. The transfer function for each room at each of the locations was coupled with future climate data from the UKCP09 weather generator. This allows projection of future indoor environment, and in turn this is used with damage functions to project future damage.

Some of the work presented in this chapter, particularly that at Knole, has formed the main body of a publication (appendix F). The focus of this paper was to project the future environment within the Cartoon Gallery and Leicester Gallery, along with arising damage from mould growth, dimensional change and increased pest activity. Comparison was drawn between the two rooms, and the importance of seasonality was investigated (Lankester and Brimblecombe, 2012b). Here the work is expanded upon significantly, using further damage functions, and additional locations.

There are two ways that the results can be presented, either location by location, addressing the risks at each house. Alternatively it could be presented damage function by damage function, comparing the change at each location. Both are necessary, and important to discuss. This will result in the replication of results, but discussed with relation to different aspects. Firstly each case study location is presented.

## 6.2 Results – Locations

There are four case study locations for which results are presented, for each one the results are split into three distinct areas, firstly the projected change to the internal environment, secondly the projected change in the seasonality of the internal environment, and thirdly the projected change in damage. Each of the damage functions will also include the expected change in seasonality of the specific type of damage.

### 6.2.1 Knole

At Knole two rooms are investigated, to examine whether it is necessary to carry out projections for individual rooms. The Cartoon and Leicester Galleries are presented on the same graphs where possible.

6.2.1.1 Environment

The projected impact of climate change on the annual average temperature in the two galleries is shown in figure 6.1, along with the projection for outdoors at Knole. The indoor temperature is projected to increase, but not by as much as outdoors in the future. The Cartoon Gallery is slightly warmer than the Leicester Gallery, and both experience a similar increase in future temperature, of roughly three degrees by the 2085 period. The rooms indoors are warmer than outdoors, this is attributed to solar gain, given there is no heating in these spaces.
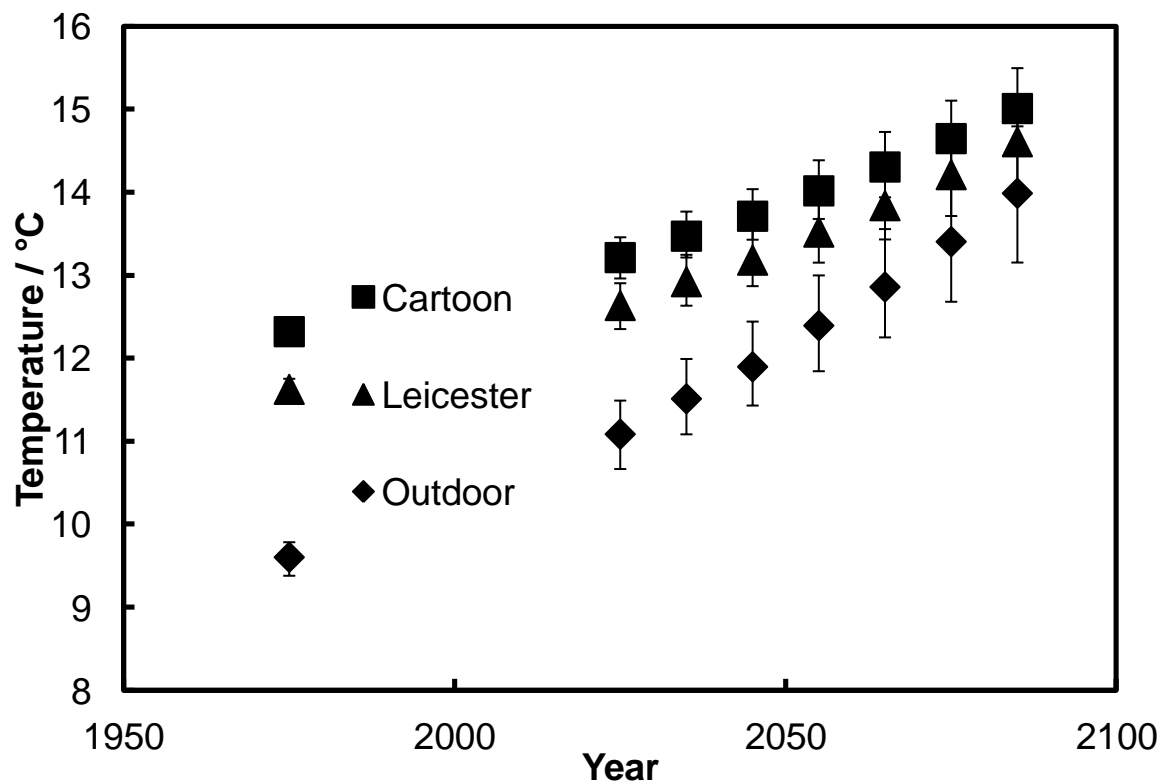


Figure 6.1: The impact of climate change on the annual average temperature at Knole, outdoors and in the two galleries. The error bars represent the interquartile range, with the data point the median value.

Previously the UKCP09 weather generator data used was shown not to be normally distributed; therefore it is necessary to use non-parametric statistics. Here the Wilcoxon

signed ranks test will be used to determine whether the medians of different time periods are significantly different. The null hypothesis is that they are not significantly different from one another, and the level of probability (p) used is 95%.The data shown in figure 6.1, the median of the baseline data (1975) for the Cartoon Gallery is significantly different to that for the 2025 period, and subsequently the 2025 median is significantly different to the 2055 median. Lastly the 2055 median is significantly different to the 2085 median. The four time periods discussed here, 1975, 2025, 2055 and 2085 can be described respectively as the baseline, near future, mid-term future and the far future. The Leicester Gallery has the same statistical relationship between the time periods.

The projected change to the annual average relative humidity in the future, due to climate change, is shown in figure 6.2. Outdoors at Knole it is expected that there will be a decrease in relative humidity, however indoors both the Cartoon and Leicester Galleries indicate no change in the annual average relative humidity. Again both galleries have slightly different averages due to the individual nature of each room. The data has been shown to be non-parametric, therefore the associated error is shown here as the interquartile range. The error increases with time, this is due to the nature of the UKCP09 weather generator output, the further into the future the more uncertain the projections become.
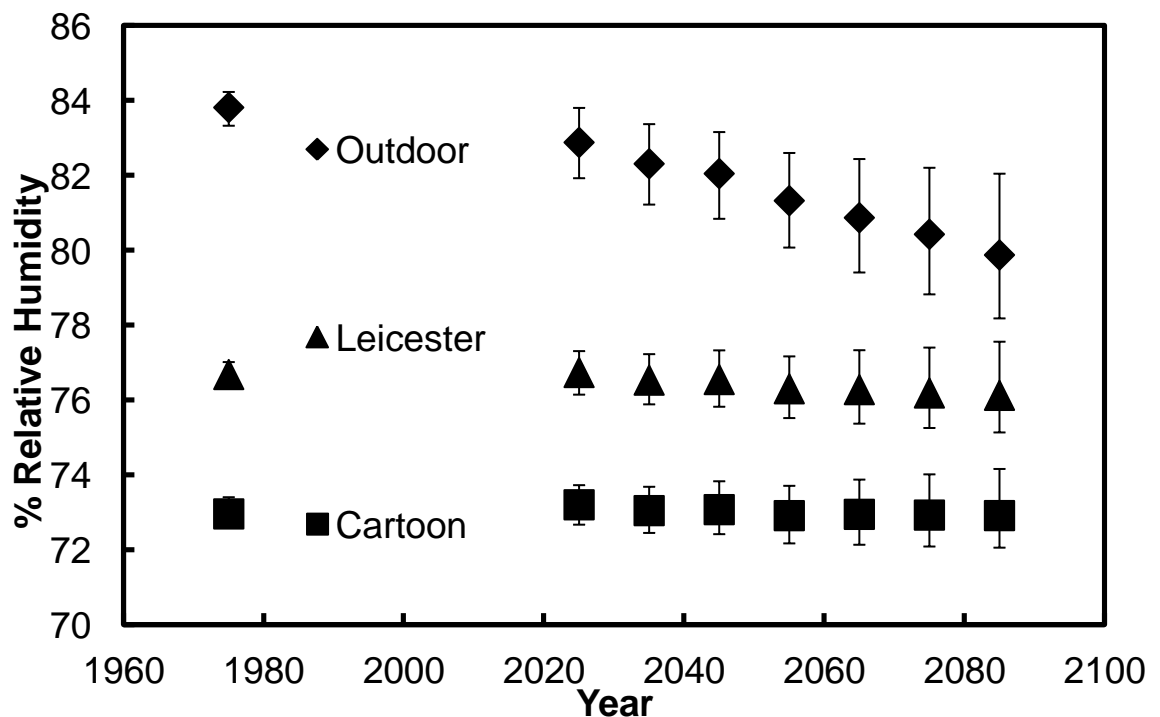


Figure 6.2: The impact of climate change on the annual average relative humidity at Knole, outdoors and in the two galleries. The error bars represent the interquartile range, with the data point the median value.

The reason that the relative humidity outdoors decreases and the relative humidity indoors shows no change is related to the change in specific humidity. Firstly outdoors the temperature increases and the relative humidity decreases, as is expected when the temperature increases. However indoors the same is not true, one explanation is that the specific humidity increases, offsetting the increase in temperature, by the right amount that relative humidity shows no change. The expected increase in specific humidity is confirmed in figure 6.3, for the Cartoon Gallery.

Both the Cartoon and Leicester Galleries median of the baseline period is significantly different to that of the near future, as is the near future to the mid-term future and the mid-term future to the far future. The statistical test is useful to confirm that there is significant difference between the time periods, the graph shows that the data has a wide range of uncertainty in the future, however the medians are significantly different.
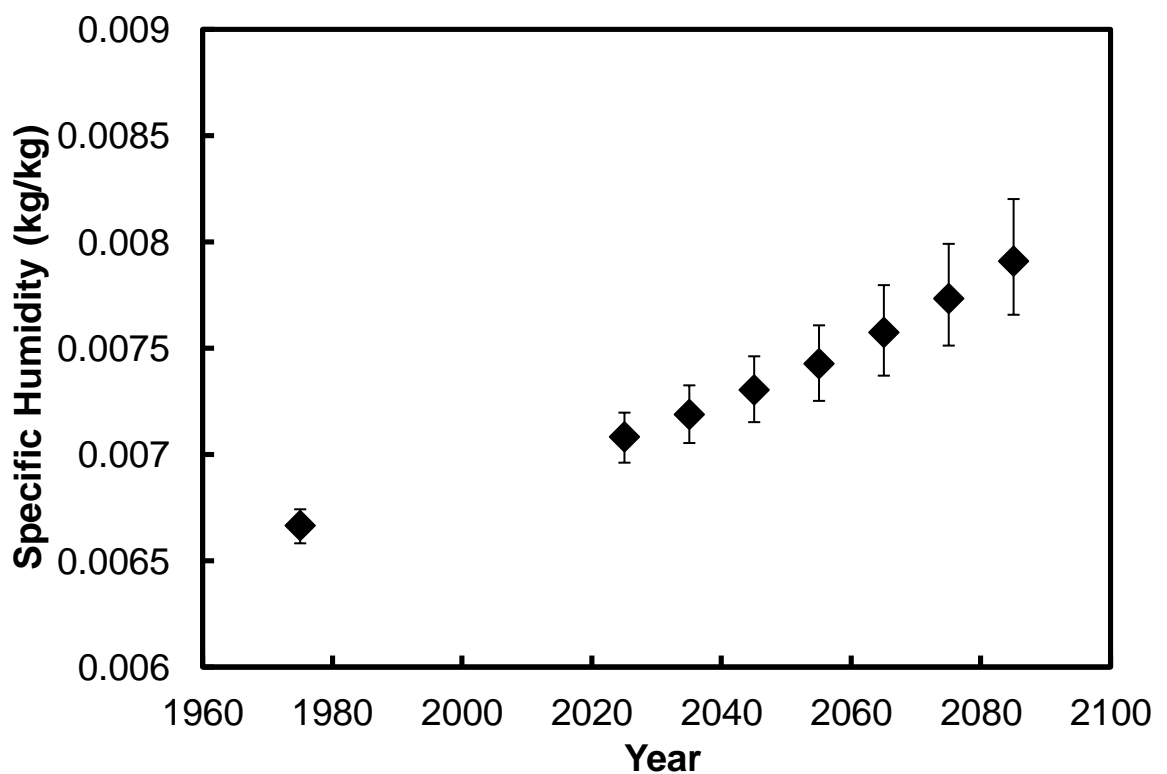


Figure 6.3: The projected rise in specific humidity in the Cartoon Gallery across the coming century. Error bars represent the interquartile range.

The median of the baseline specific humidity (figure 6.3) is significantly different to that of the near future. The same is true for the median of the near future to the mid-term future periods, and the mid-term future to the far future medians.

6.2.1.2 Seasonality

While the annual average values are important, indicating the future trend of temperature and relative humidity, it is also important to assess seasonal changes to the environment. This is of particular importance as a number of management strategies are embedded in the seasonal practices of historic houses, for instance a deep clean is often carried out in the winter, when closed to the public. Thus changes in seasonality could have significant impacts on the preventive conservation measures.

The seasonal change in temperature for the baseline and far future periods, 1975 and 2085 respectively, for the Cartoon Gallery is shown in figure 6.4. The region enclosed by the set of lines is that of the interquartile range. Unlike the previous two figures it is not possible to include all the time periods, thus the baseline and far future are shown, each period until the far future steps closer to this away from the baseline. It is projected that the temperature will increase year round, and that the seasonality stays the same. However the gap between summer and winter temperatures increases in the future. The increase projected in summer is more marked than that in the winter months.
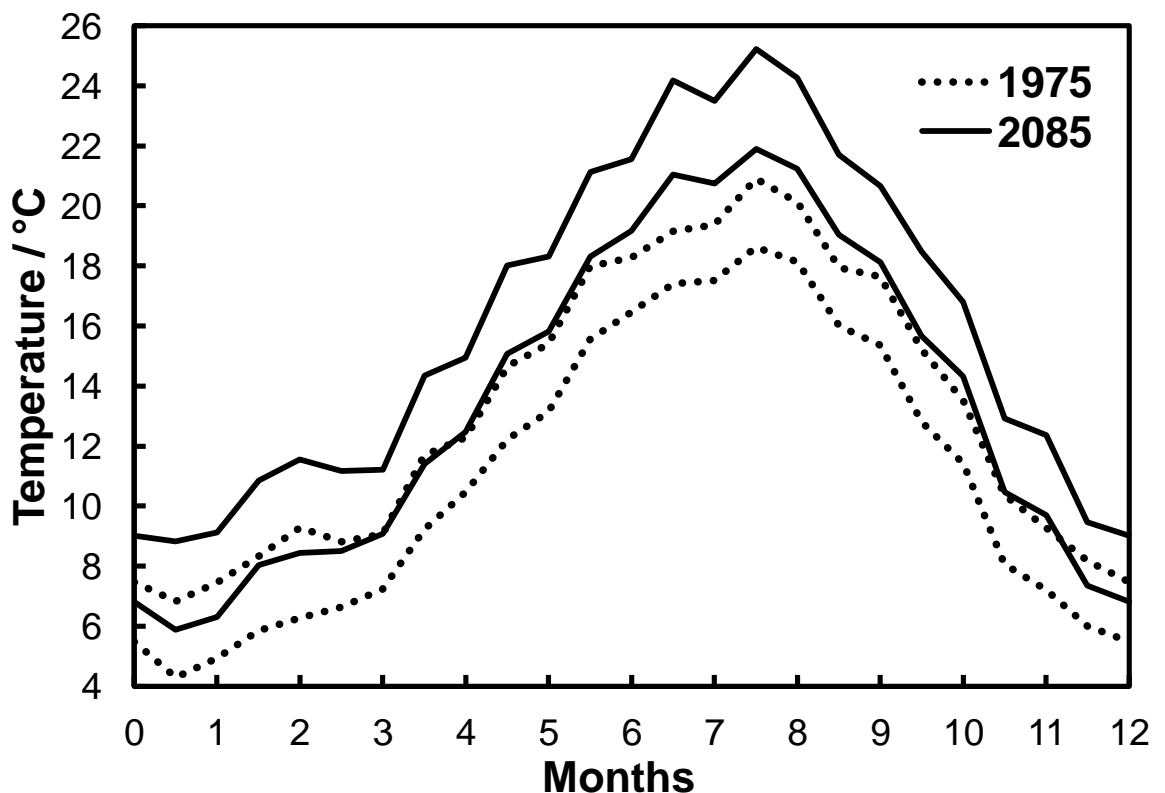


Figure 6.4: The seasonal temperature in the Cartoon Gallery, for the baseline and far future periods. The enclosed region represents the interquartile range of the weather generator outputs.

The seasonal change in relative humidity in the Cartoon Gallery is shown in figure 6.5. Again the baseline and far future periods are shown. It is projected that the summer months will be drier (less humid) in the future, and that winter months will be wetter (more humid) in the future. When combined with the temperature data, winters will be wetter and warmer, and summers will be warmer and drier. This projection of relative humidity shows quite a change rather than stability as expected from the results of the annual average relative humidity projection. With such a change it is likely that this will have a greater impact on damage than the annual average would lead to believe. This change in seasonality has the potential to effect the implementation of management strategies in the future; this will be discussed further as examples arise when assessing each damage function.

The decrease in summer relative humidity is to be expected given the increase in temperature. However an increase in winter relative humidity, also with an increase in temperature, does not follow expectations. Normally the relative humidity would decrease if the temperature rises, this doesn't happen because of the change in specific humidity. Thus the winter specific humidity also increases, increasing relative humidity.
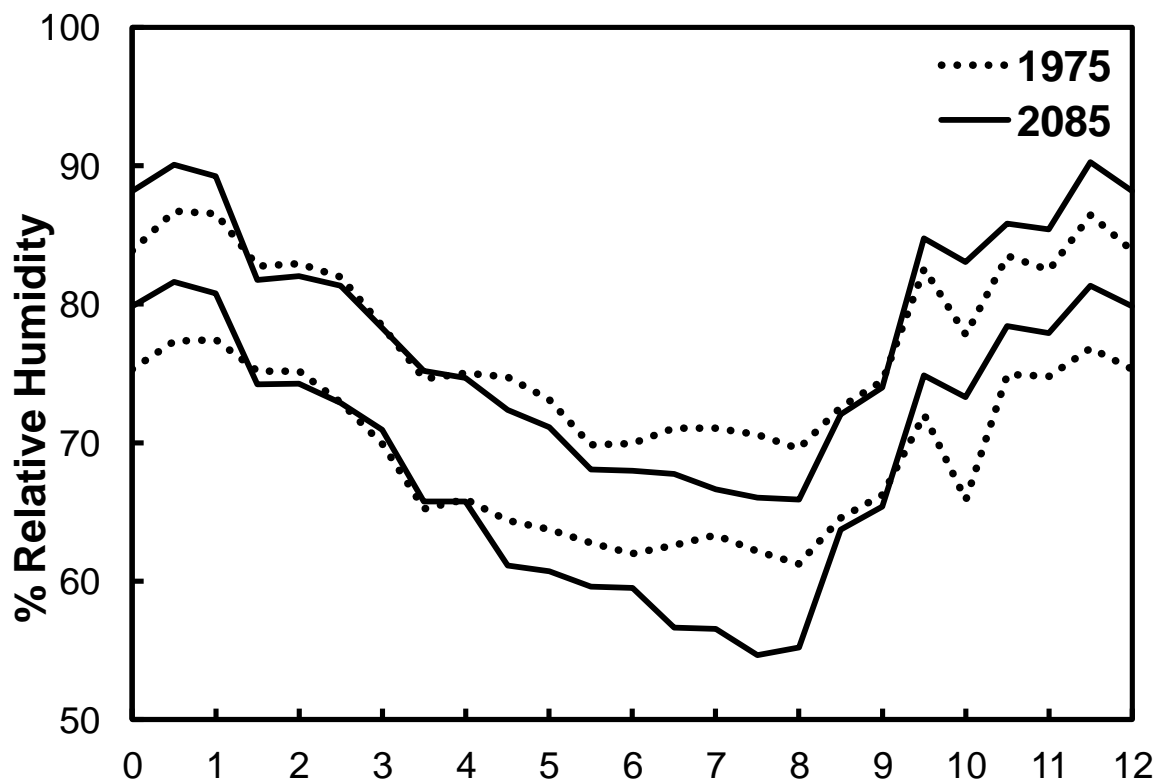


Figure 6.5: The seasonal relative humidity in the Cartoon Gallery, for the baseline and far future periods. The enclosed region represents the interquartile range of the weather generator outputs.

6.2.1.3 Damage

The projected impact that climate change has on the environment within the two galleries at Knole has been shown, but the impact on damage is often more relevant. Here the damage functions that are significant are assessed, the remaining can be found in appendix D, to keep the discussion concise.

**Daily average temperature >20°C**

The number of days where the average temperature exceeds 20°C in the Cartoon and Leicester Galleries is shown in figure 6.6. The impact of climate change is that there is more than four times the number of days exceeding 20°C by the end of the century. Both rooms show a similar number of exceedances, with the Leicester Gallery having a consistently higher number across the coming century. This increase is quite substantial and while this method has no direct impact on damage, warmer temperatures do, one example being that pest activity increases.
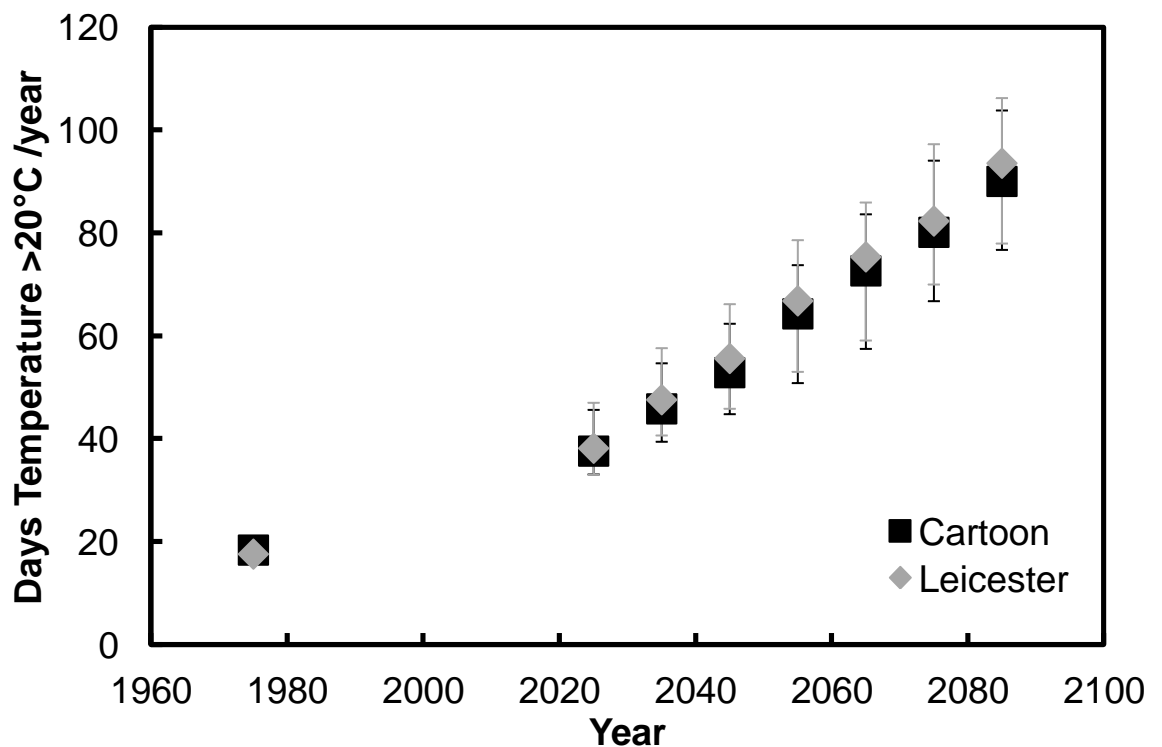


Figure 6.6: The number of days projected per year with an average temperature exceeding 20°C in the Cartoon and Leicester Galleries at Knole. Error bars represent the interquartile range.

Both the Cartoon and Leicester Gallery baseline median is significantly different to that of the 2025 period. This is also true of the 2025 and 2055 medians, and the 2055 and 2085 medians.

The change in the number of days per year with an average temperature exceeding 20°C in the Cartoon Gallery is also shown in figure 6.7, for the baseline and far future periods split into each month. In the past the majority of days over 20°C were during July and August, this is still the case in the future. However, in the future almost every day the average temperature will exceed 20°C compared to approximately 15% and 40% of the time in July and August respectively for the baseline period. Additionally the months surrounding these, June and September show a substantial increase in the future, possibly to a greater level than August of the past, which had the highest percentage of time over 20°C. Therefore the main risk will still be in the summer, but it will be for a longer period, and will be substantially warmer. The number of days where the average temperature exceeds 25°C has also been projected, the results of this can be found in appendix D.
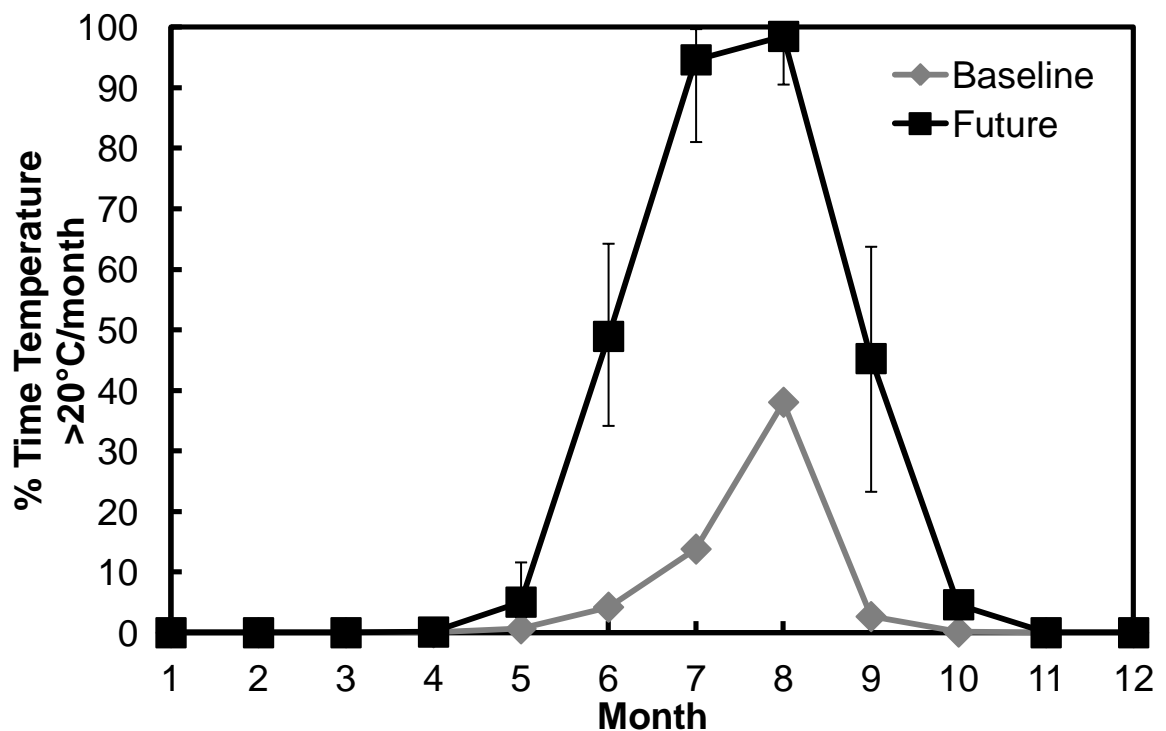


Figure 6.7: The percentage of time projected per month with an average daily temperature exceeding 20°C in the Cartoon Gallery at Knole. Error bars represent the interquartile range.

**Paper**

**Zou**

In figure 6.8 the projected impact of climate change on degradation of paper, as described by the Zou damage function (section 4.2.1) is shown. There is an increase in the degradation rate in both rooms assessed; this is due to the dependence of the function on temperature. By the far future the degradation rate is 1.5 times that of the baseline, a significant increase, potentially reducing the useable life of an object by a third. (If the rate is 0.01, the lifetime is 100 years, if this increases to 0.015 the lifetime is 66.6 years). Both the Cartoon and Leicester Gallery show a similar response in the future.



Figure 6.8: The annual average projected degradation rate of paper derived from the Zou damage function in the Cartoon and Leicester Galleries at Knole. Error bars represent the interquartile range.

The impact of climate change on the seasonality of paper degradation in the Cartoon Gallery is shown in figure 6.9. The summer rate is still greater than the winter rate; this was not expected to change, because of the dependence on temperature. However the expected change from baseline to future is larger during the summer months, this is due to the increased temperatures projected. Paper degradation is usually assessed as a yearly observation, lower winter temperatures (less degradation) offset warmer summer temperatures (more degradation). In the future the summer increase is greater than the

winter increase in rate, resulting overall in the average tending more towards that of the summer. The winter does not offset this as much as previously, especially given the increase in winter temperature. The impact of climate change on the Isoperm and TWPI functions has also been projected, these show similar results to this function, and therefore they are presented in appendix D.



Figure 6.9: The monthly average projected degradation rate of paper derived from the Zou damage function in the Cartoon Gallery at Knole. Error bars represent the interquartile range.

**Pretzel**

The impact of climate change on the paper damage function, as described by Pretzel (section 4.2.4), is shown in figure 6.10. This function gives a greater dependence on relative humidity than the other paper damage functions. As previously there is a sharp increase in rate from the baseline to the 2025 time period. However, after this period the rate only increases slightly, and then begins to plateau. This is in contrast to the previous functions where the rate increases rapidly from one time period to the next. The reason for this not occurring here is shown in figure 6.11, where the data is presented on a month by month basis. The drop in summer humidity has decreased the rate of degradation, thus slowing the increase in rate of degradation. The rate has still increased over that of the baseline period because some other months indicate an increase in the degradation rate,

likely to be related to the increasing temperature. It is quite possible that if there was further future climate data that a greater reduction in summer humidity may reduce the rate. Another possibility is that the temperature and relative humidity are equally affecting the degradation, so an increase in temperature and a decrease in humidity may cancel each other out, resulting in the continuation of the plateau shown here.
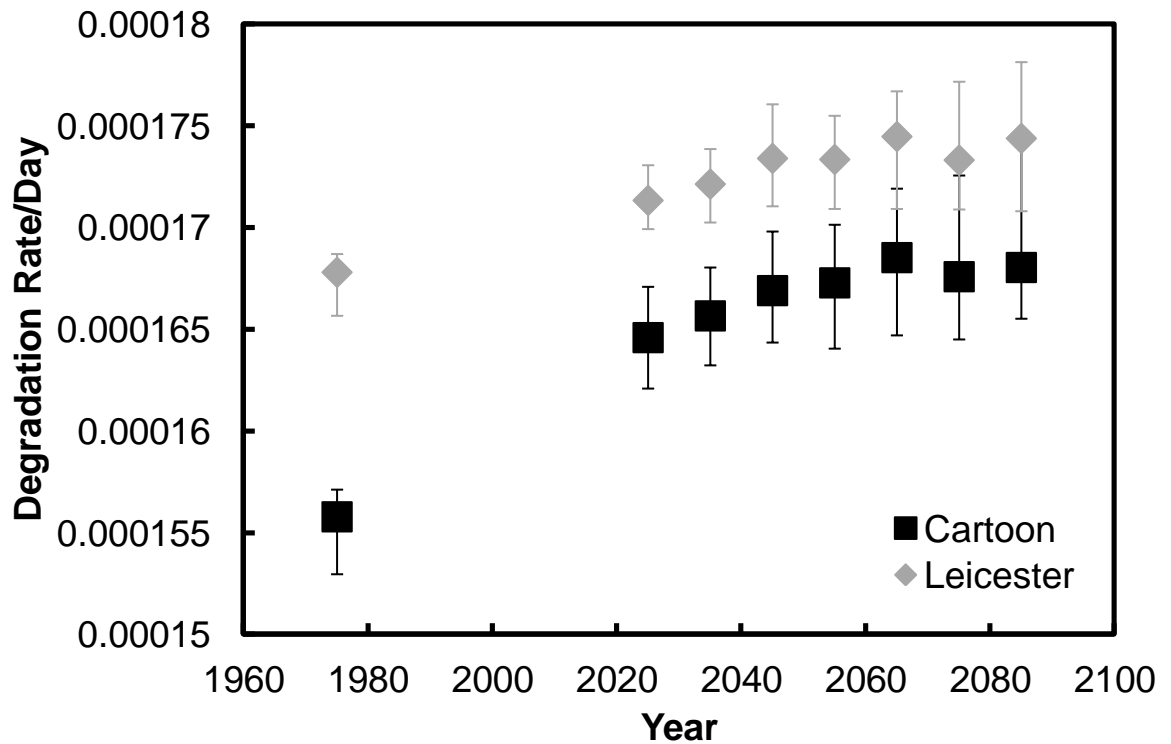


Figure 6.10: The annual average projected degradation rate of paper derived from the Pretzel damage function in the Cartoon and Leicester Galleries at Knole. Error bars represent the interquartile range.

In figure 6.10 the median value of baseline period, for both the Cartoon and Leicester Gallery, is significantly different to the median value of the near future period. The same is also true of the median of the near term future and the mid-term future, as is the mid-term future to the far future.
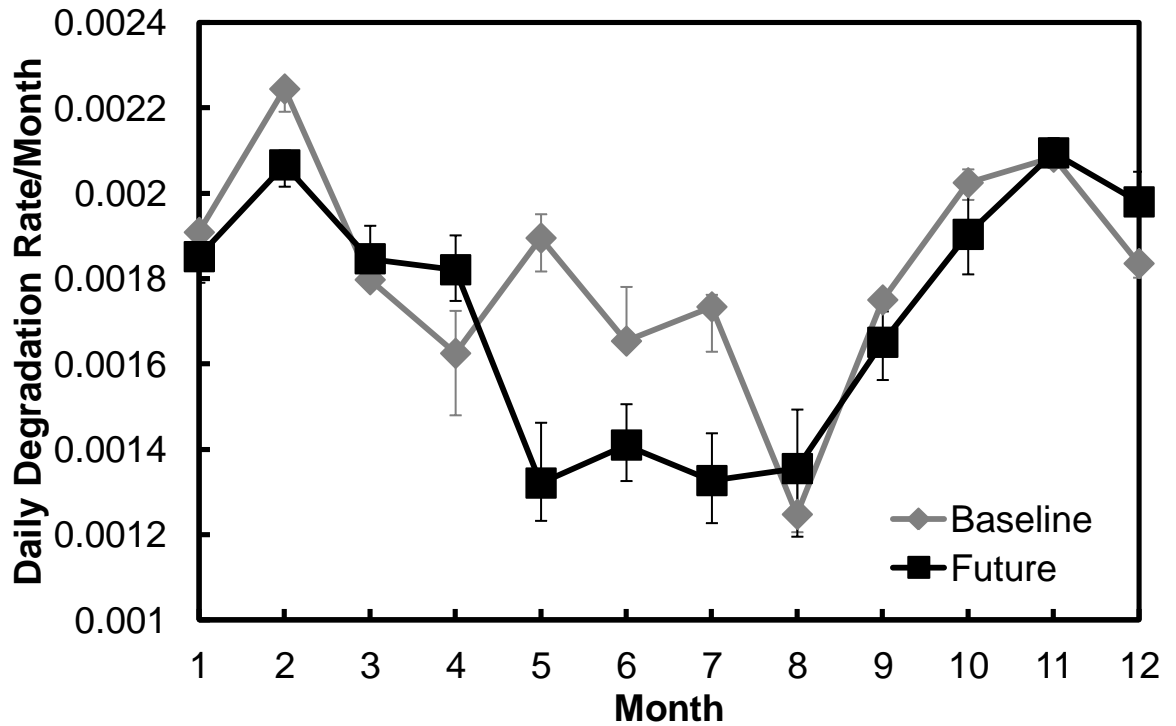
Figure 6.11: The monthly average projected degradation rate of paper derived from the Zou damage function in the Cartoon Gallery at Knole. Error bars represent the interquartile range.

**Silk isoperm**

The projected change in damage to silk over the coming century is shown in figure 6.12. The damage function, as described by Luxford (Section 4.3.1), is an adaptation of the isoperm method. As with the paper isoperm function the rate increases through the century, with both rooms having similar values. The increase in chemical degradation to silk arises because of the increase in temperature that is projected. This is confirmed by the seasonal data shown in figure 6.13, which follows the annual temperature cycle. The median of the baseline period for the Cartoon Gallery is significantly different to that of the near future period. There is also significant difference between the median of the near future and mid-term future, and also between the median of the mid-term and far future. The same is true of the Leicester Gallery.
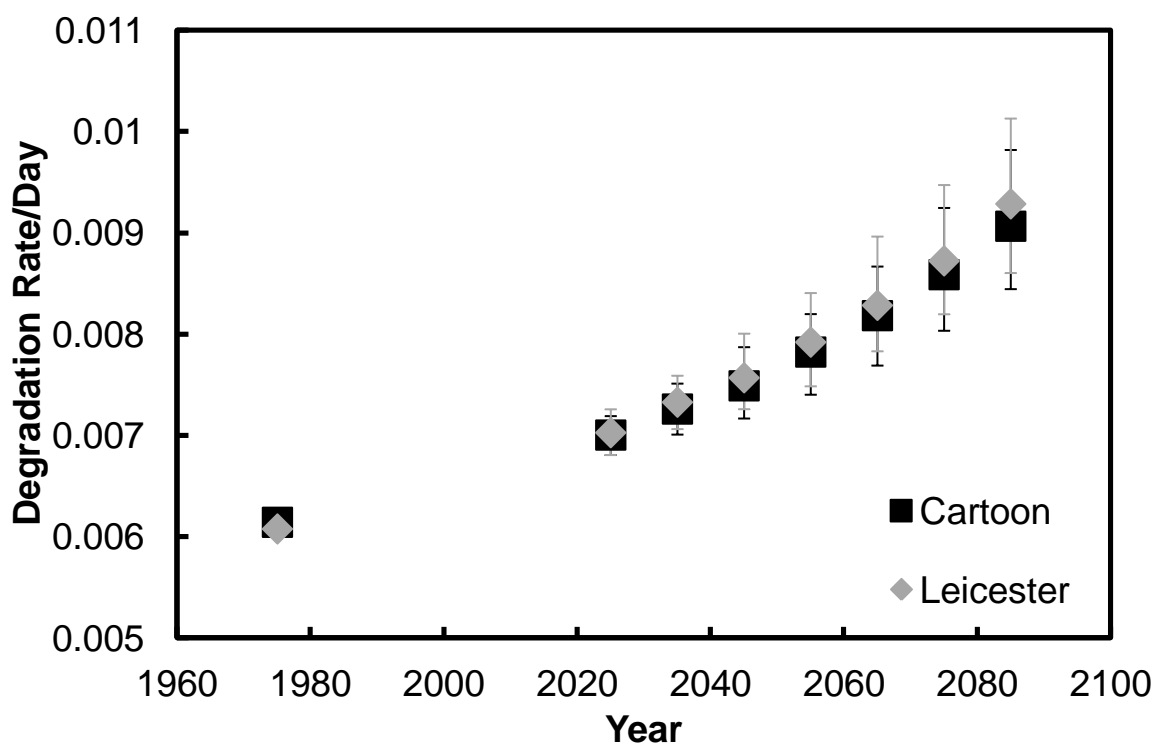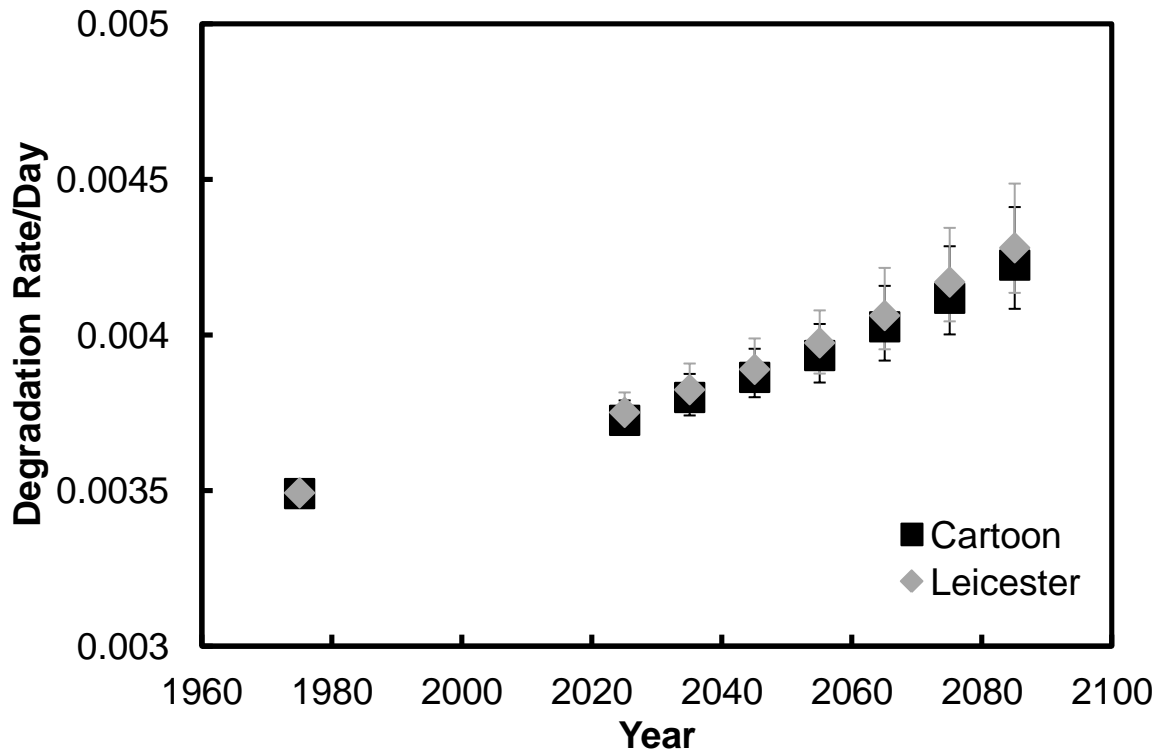
Figure 6.12: The annual average projected degradation rate of silk derived from the silk isoperm damage function in the Cartoon and Leicester Galleries at Knole. Error bars represent the interquartile range.
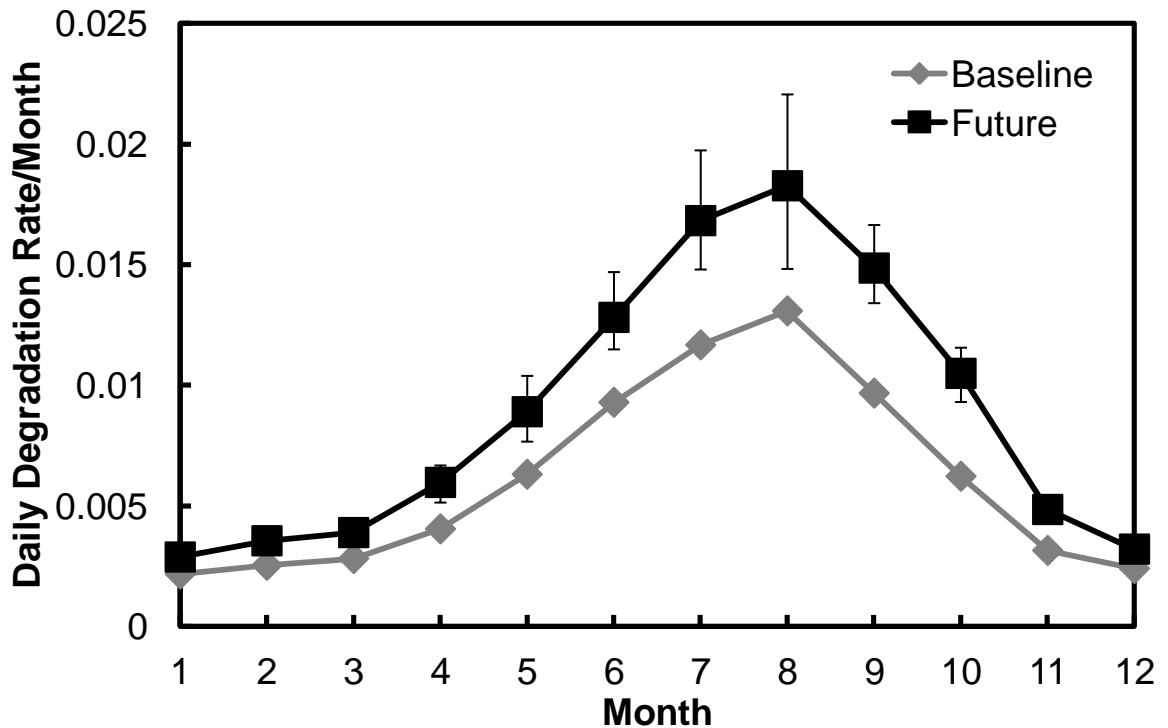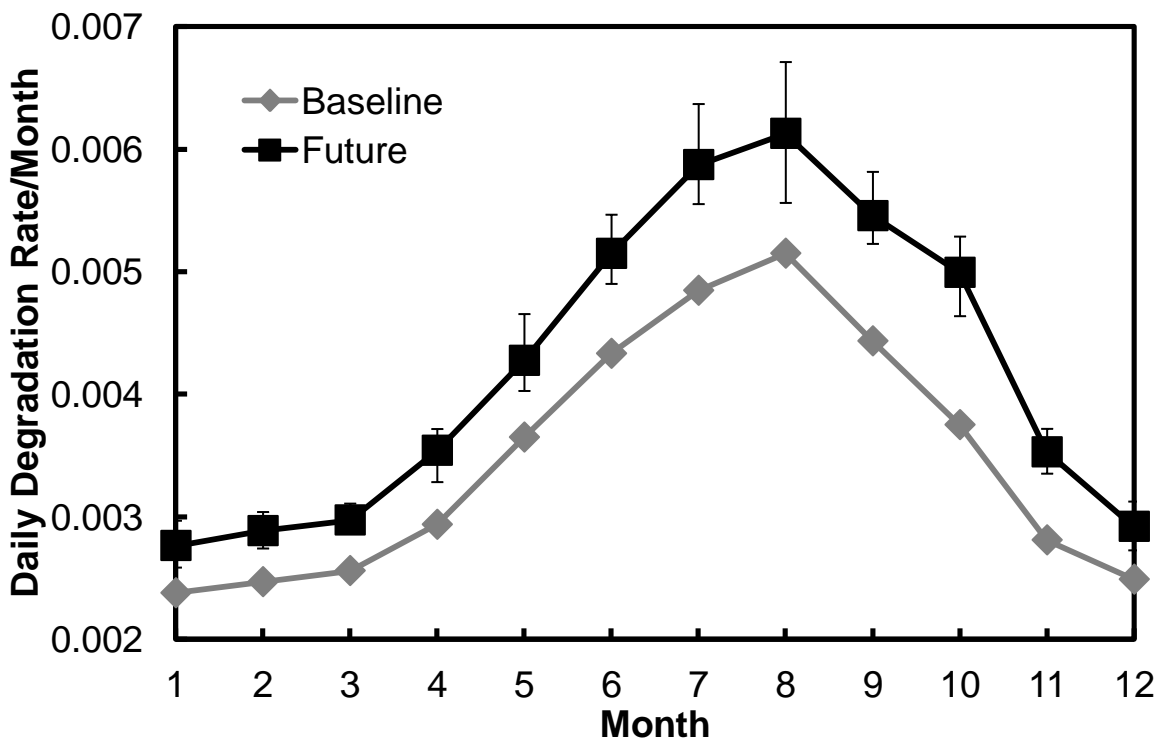


Figure 6.13: The monthly average projected degradation rate of silk derived from the silk isoperm damage function in the Cartoon Gallery at Knole. Error bars represent the interquartile range.

**Mould**

**Isaksson**

The impact of climate change on mould growth in the two rooms at Knole is shown in figure 6.14. An increase in mould growth is projected in both rooms. There is however an obvious difference between the two rooms. The Leicester Gallery has an environment that is ideal for mould growth for most of the year, across all time periods, including the baseline. The Cartoon Gallery however does not have a suitable environment for mould growth over the baseline period, but it becomes more suitable throughout the century. The reason for the risk of mould growth is because of the relative humidity within the two rooms. The Leicester Gallery relative humidity is largely above the critical value required by this function, but the Cartoon Gallery relative humidity falls below this for the baseline period. As the century progresses winter relative humidity increases, thus exceeding the critical relative humidity, allowing the germination and growth of mould to occur, assuming the conditions are ideal for the required time. The associated error of the data for the Cartoon Gallery is large because the value lies close to the critical value. Thus each year can have similar relative humidity but the critical value falls in the middle. This means some years are very good for mould growth and others not so.
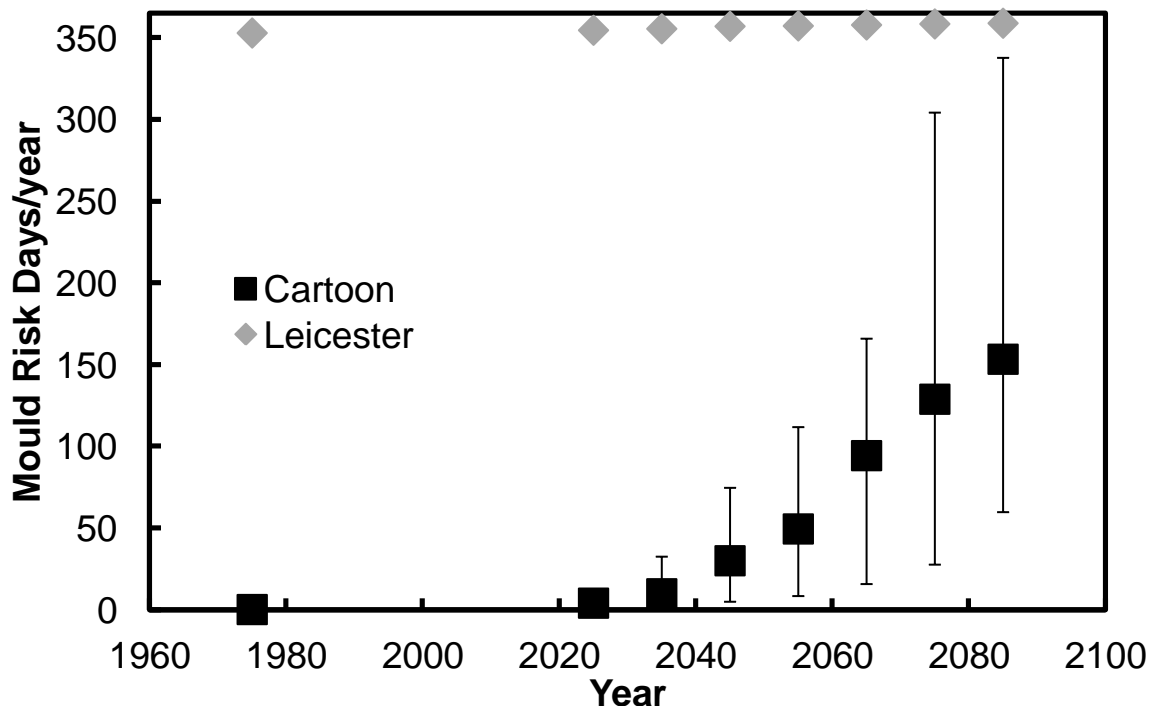


Figure 6.14: The annual average projected number of mould risk days derived from the Isaksson damage function in the Cartoon and Leicester Galleries at Knole. Error bars represent the interquartile range.

Even though there are such large uncertainties, the median values between the baseline and 2025 period, the 2025 and 2055 periods, and 2055 and 2085 periods are all significantly different to each other, for both of the two rooms.

The seasonal analysis of the mould growth is shown in figure 6.15. Initially this may seem unusual, the increase in relative humidity which drives increasing mould risk is in winter months, but the actual time when this becomes apparent is shifted to the first half of the year. The reason for this is that it takes time for mould to germinate, therefore when the conditions are ideal the mould is undertaking the process of germination. The time for this depends upon the conditions; therefore this delay shifts the result as seen here.
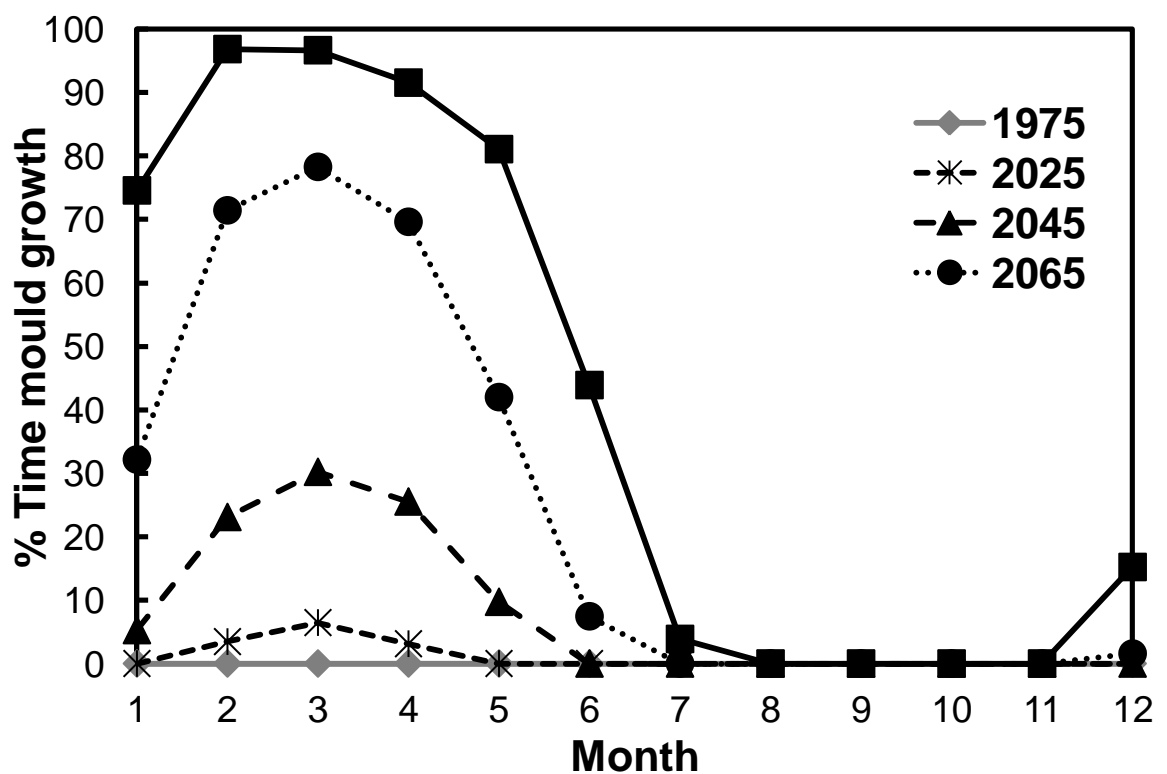


Figure 6.15: The monthly average projected number of mould risk days derived from the Isaksson damage function in the Cartoon Gallery at Knole. All future time periods show the increase over time.

**Critical Relative Humidity**

The effect of climate change on the second mould damage function, the critical relative humidity (section 4.4.2), is shown in figure 6.16. Again the two rooms show differing results, but both are projected to have an increase in the number of days that exceed the critical relative humidity. This damage function is likely to be the most sensitive, because it is based on the conditions to prevent mould growth, rather than the conditions required for

mould growth, two different things. Often the conditions to prevent mould growth are well below that required, thus it is likely to overestimate the mould growth that will occur. However, in comparison to the previous damage function (Isaksson), the results for the Leicester Gallery show the opposite of this, a reduced number of mould risk days. The reason behind this is down to the method used in the Isaksson damage function. A running sum of mould risk is calculated, which when exceeding 1 is taken as germination of mould. This sum is allowed to continue to build above 1 if the conditions are suitable for mould growth. When this occurs, the sum can build to a considerable value, when the relative humidity is suitable for mould growth. Negative feedback is possible when conditions are unfavourable, reducing the running sum. However, because the sum has become so large the negative feedback does not reduce the value to below 1, resulting in the day being reported as a risk day, even though the conditions are not ideal, and may not have been for a number of days.
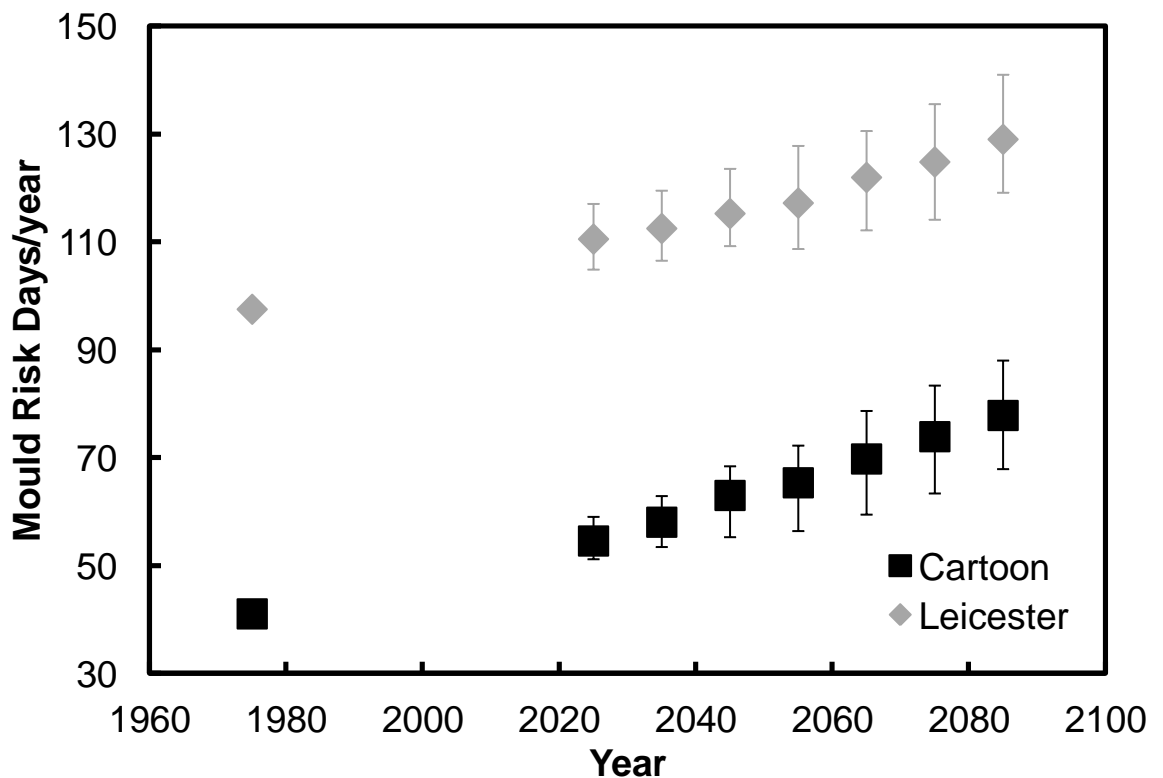


Figure 6.16: The annual average projected number of mould risk days derived from the critical relative humidity damage function in the Cartoon and Leicester Galleries at Knole. Error bars represent the interquartile range.

Returning to discuss the results shown in figure 6.16, the median values for the baseline periods, of both rooms, are significantly different to the corresponding medians of the near

future periods. The same is true of the near to mid-term future medians, and the mid-term to far future medians.

The seasonal analysis of the damage function is shown in figure 6.17, indicating that it is the winter increase in relative humidity that results in the increased risk of mould growth projected in figure 6.16. While this increase in mould risk is mainly driven by relative humidity, the projection of increased winter temperatures also speeds up the time to germination. The decrease in summer humidity reduces the risk of mould growth in the summer months; this is a small change however in comparison to the risk in winter months. The impact of climate change to the Hukka damage function is shown in appendix D.
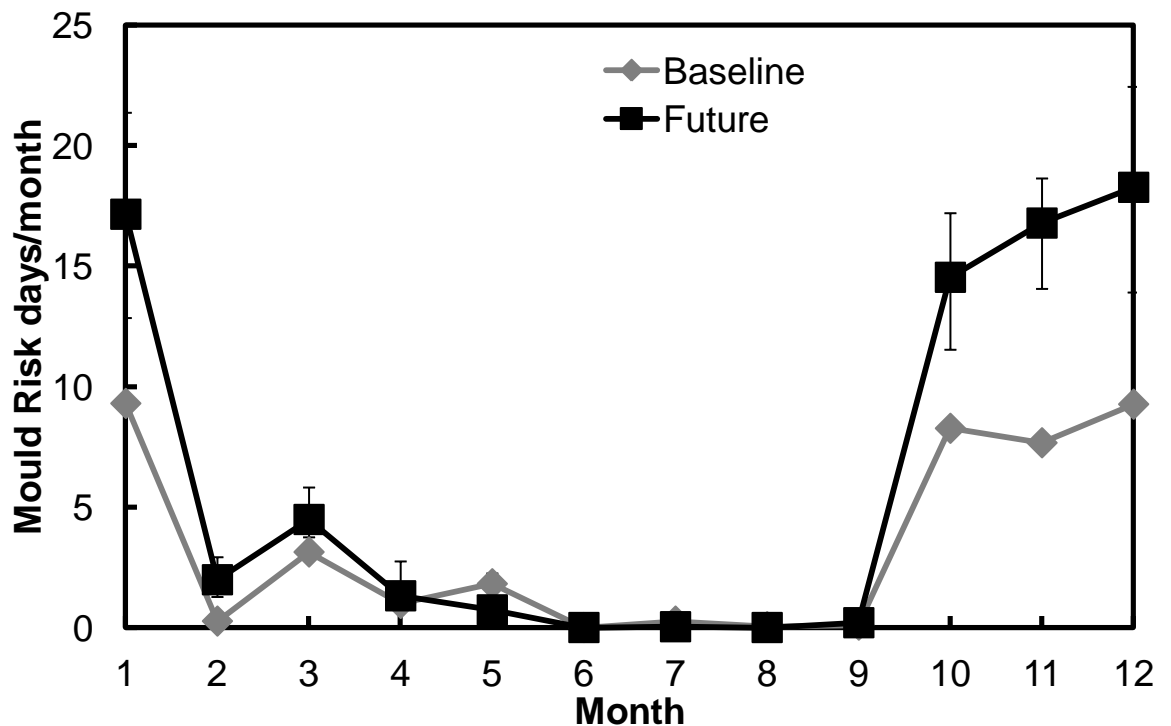


Figure 6.17: The monthly average projected number of mould risk days derived from the critical relative humidity damage function in the Cartoon and Leicester Galleries at Knole. Error bars represent the interquartile range.

**Degree days**

The projected impact of climate change on the number of degree days in the Cartoon and Leicester Gallery is shown in figure 6.18. As with previous functions that are dependent upon temperature the two rooms show a similar projection. Both rooms are projected to have more than double the number of degree days in the future, a significant increase. In this work degree days, with a base temperature of 15°C, are linked to pest activity. While there are no definitive links between degree days and insect life cycles, an increase in the number of degree days indicates that there are greater chances of insect activity in the future, leading to an increased risk of damage. Recent work by Brimblecombe and Lankester (2012) has compared degree days to the life cycle of the biscuit beetle suggesting that one life cycle is the equivalent of 490 degree days. If this is applied at Knole the baseline period falls short by around 100 degree days, and the far future period is close to twice this, such an increase could have a significant effect on insect damage. It is possible that a number of factors will combine to compound the damage caused by insects. Increased temperatures will increase the activity of insects, causing more damage through feeding, and life cycles may complete quicker, providing an additional generation of insects that can cause damage.



Figure 6.18: The annual average projected number of degree days in the Cartoon and Leicester Galleries at Knole. Error bars represent the interquartile range.

The median of the baseline period, for both rooms at Knole is significantly different to the respective median of the near future period. The near future period median is also significantly different to that of the mid-term period, and the mid-term period median is significantly different to that of the far future, for both rooms.

The effect of climate change on degree days on a month by month basis is shown in figure 6.19. This is presented as a cumulative count rather than individually as elsewhere. This helps to show that the total yearly number of degree days of the baseline period is surpassed much earlier in the year in the far future. This occurs at some point during July, even before the warmest month of August.



Figure 6.19: The cumulative monthly average projected number of degree days in the Cartoon Gallery at Knole. Error bars represent the interquartile range.

**Salts**

**Salt transitions – thenardite/mirabilite**

The projected impact of climate change on the number of damaging salt transitions of thenardite to mirabilite is shown in figure 6.20. This function is dependent upon both relative humidity and temperature, with the temperature defining a widely variable critical relative humidity at which the salt crystallises, thus causing damage. It is projected, for both rooms, that there is a small downward trend in the number of transitions. However, this is slight and the medians are not significantly different until 2055 and 2075 for the Leicester and Cartoon Gallery respectively. The small reduction in transitions in the future is likely to occur in the autumn and winter months, as shown in figure 6.21. In addition to this salt phase changes are very sensitive to relative humidity, therefore the uncertainty associated with the projections here, with only small changes that often overlap the seasonal baseline values, may not be accurate in this instance.
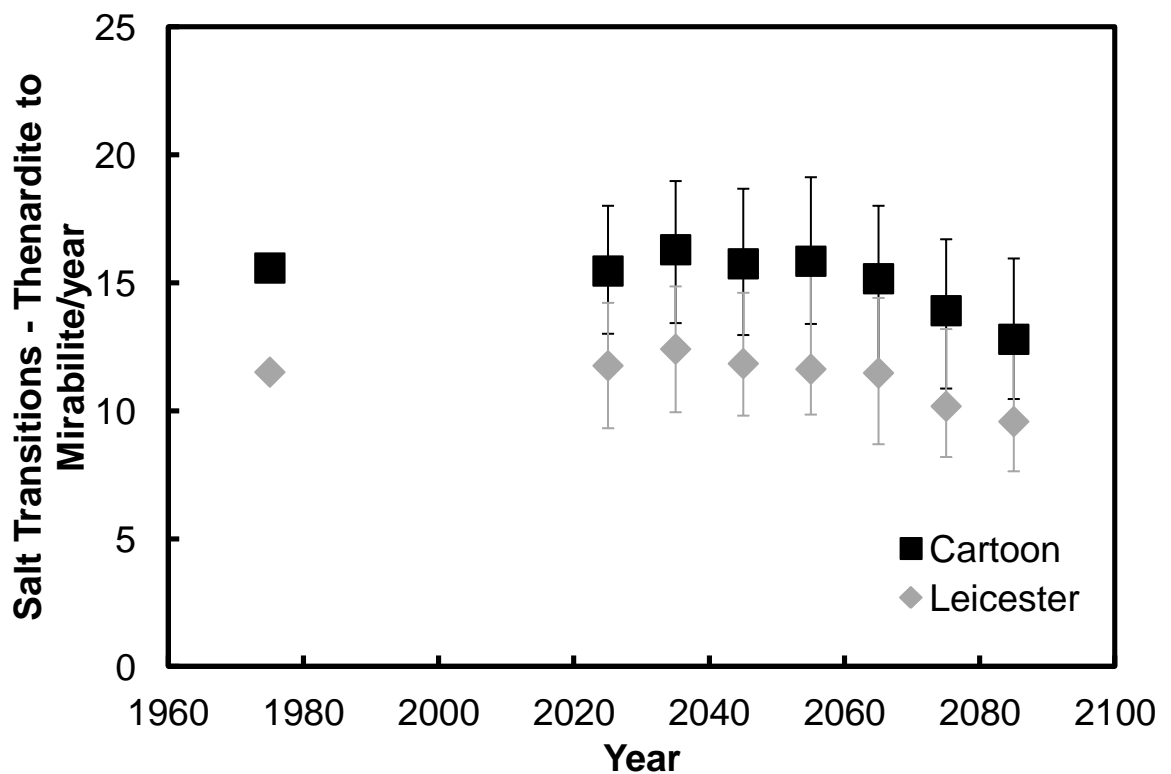


Figure 6.20: The annual average projected number of thenardite mirabilite salt transitions in the Cartoon and Leicester Galleries at Knole. Error bars represent the interquartile range.

Figure 6.21: The monthly average projected number of thenardite mirabilite salt transitions in the Cartoon Gallery at Knole. Error bars represent the interquartile range.

**Salt transitions – 75.3%**

This salt transition damage function is that of Halite, that has a critical humidity at 75.3%, the impact of climate change on these transitions is shown in figure 6.22. Again there is a difference between the two rooms, when a function related to humidity is assessed. Both rooms are projected to have a reduction in the number of salt transitions in the future, by around 15 transitions in each room, a sizeable reduction from the initial 50-55 transitions. This is also driven by the seasonal humidity change, the monthly break down of transitions (figure 6.23) shows that the main reduction comes in the summer months, when humidity is lower in the future. However, the increase in winter humidity is also projected to help reduce the number of transitions.

In both rooms the median of the baseline period is significantly different to that of the near future period. The same is true of the medians of the near future and mid-term future, and also the mid-term future and far future. While the results may be statistically significant it is difficult to determine whether the impact on damage is significant, and whether management practices to prevent damage would need to be changed. The salt transition damage function of 60% relative humidity can be found in appendix D.
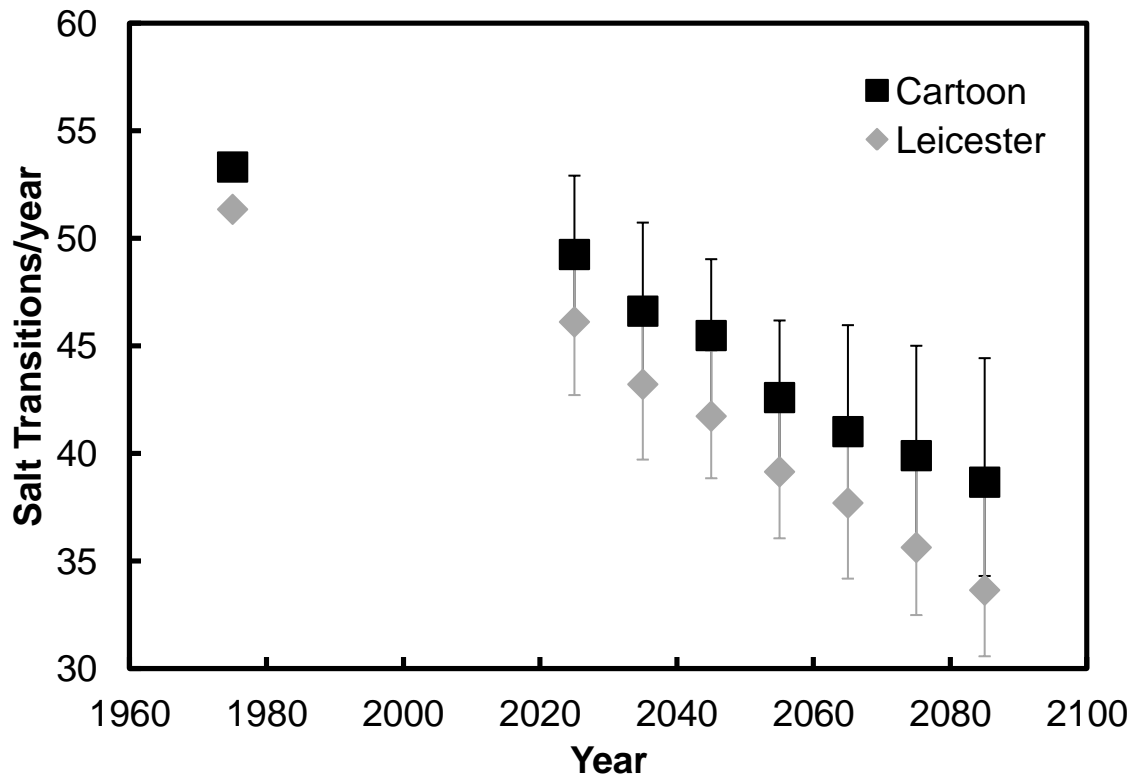
Figure 6.22: The annual average projected number of 75.3% salt transitions in the Cartoon and Leicester Galleries at Knole. Error bars represent the interquartile range.
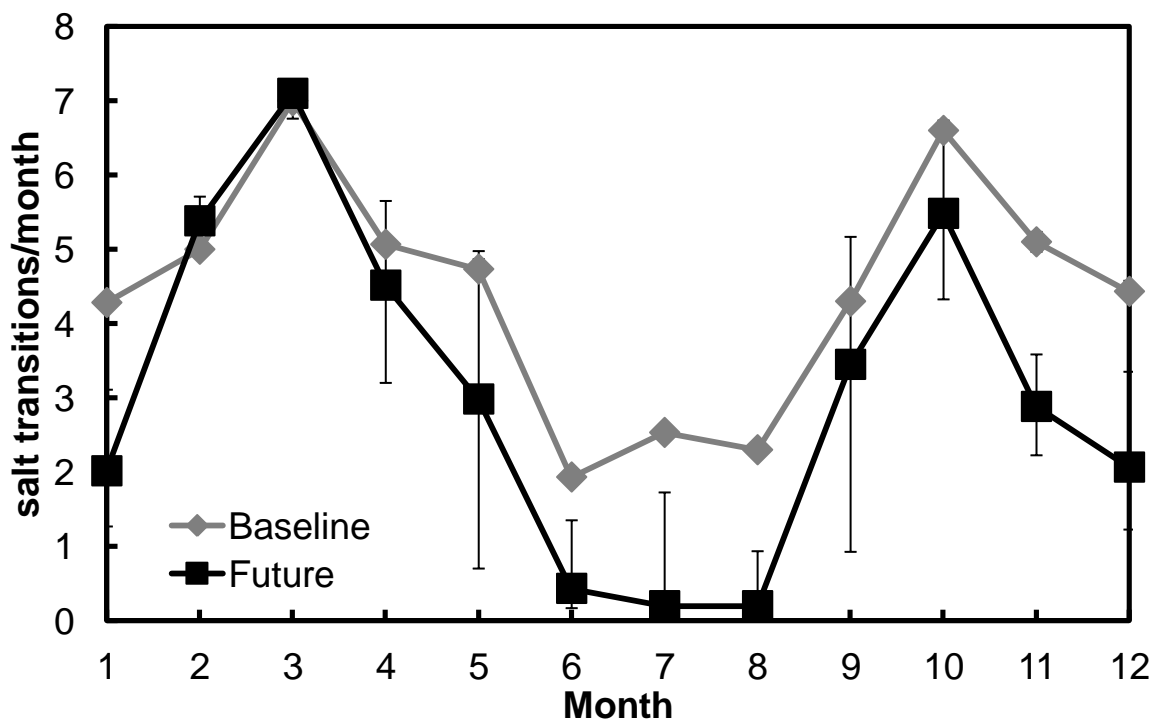


Figure 6.23: The monthly average projected number of 75.3% salt transitions in the Cartoon Gallery at Knole. Error bars represent the interquartile range.

**Salt transitions – 85%**

The projected impact of climate change on the 85% salt transition damage function is shown in figure 6.24. It is expected that a salt mixture with transitions at 85% would have more transitions in the future in the Cartoon Gallery, however in the Leicester Gallery it is projected that there will be less transitions. Initially this appears odd; however it can be explained easily. The transitions in the Cartoon Gallery increase due to the increase in winter humidity, causing more cycling of the humidity around the critical value, as shown by the seasonal analysis in figure 6.25. However, in the Leicester Gallery the humidity is initially higher, and closer to the critical value, thus more transitions occur here than in the Cartoon Gallery. In the future the humidity increases further, moving away from the critical value, and thus resulting in less transitions.
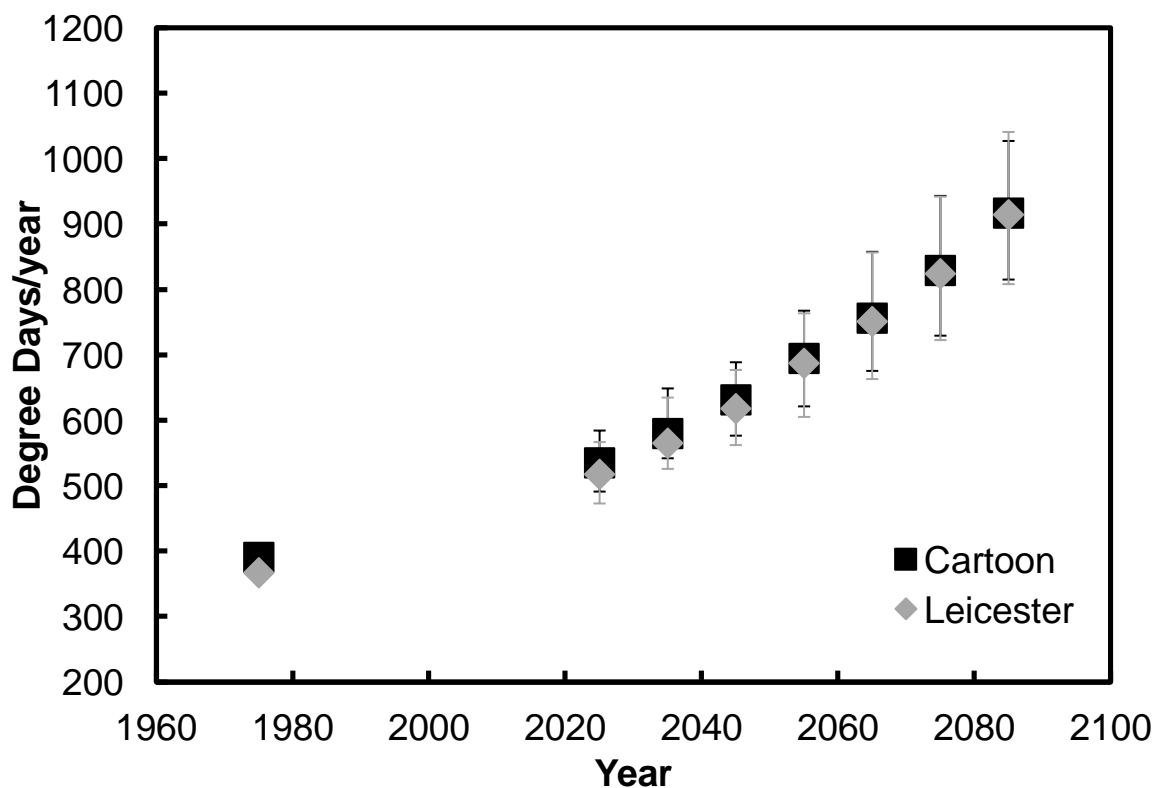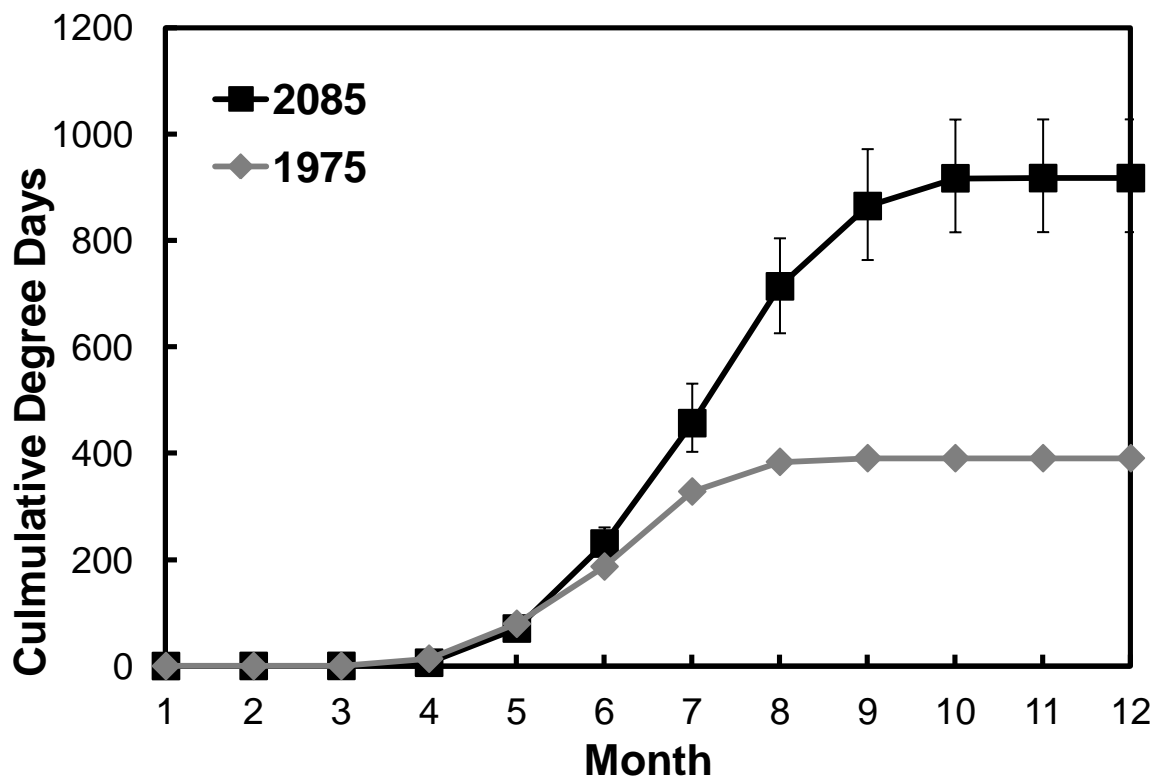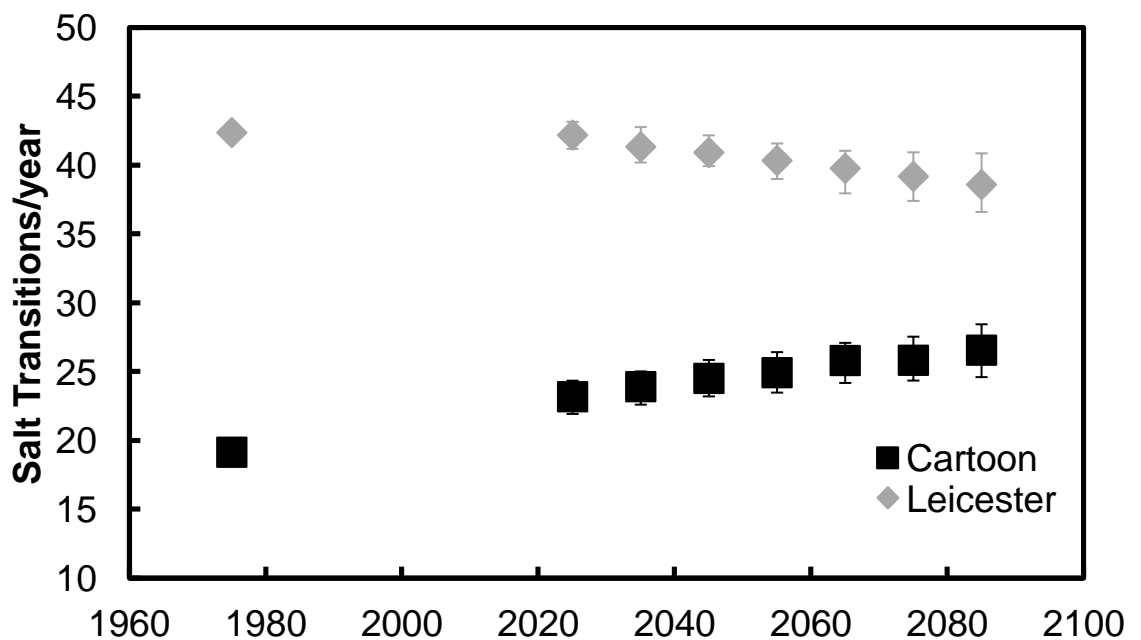


Figure 6.24: The annual average projected number of 85% salt transitions in the Cartoon and Leicester Galleries at Knole. Error bars represent the interquartile range.

In both the rooms the median of the baseline period is significantly different to that of the near future period. The same is true of the median of the near future and mid-term future periods, and the mid-term and far future periods. The point is raised again that the results may be statistically significant, but it is difficult to assess whether the impact on damage will be significant. There is roughly a shift of five transitions in either room. Without knowing the impact of a single transition, and the susceptibility of a collection it is not known how the damage will change.

This overall method has been generically determined to allow it to be applied to a wide range of situations. This does occasionally mean that it is not possible to determine the significance of a projected change. However where there is knowledge of damage occurring the technique will indicate how this will change in future, and in these instances it is easier to determine the significance of a projection.
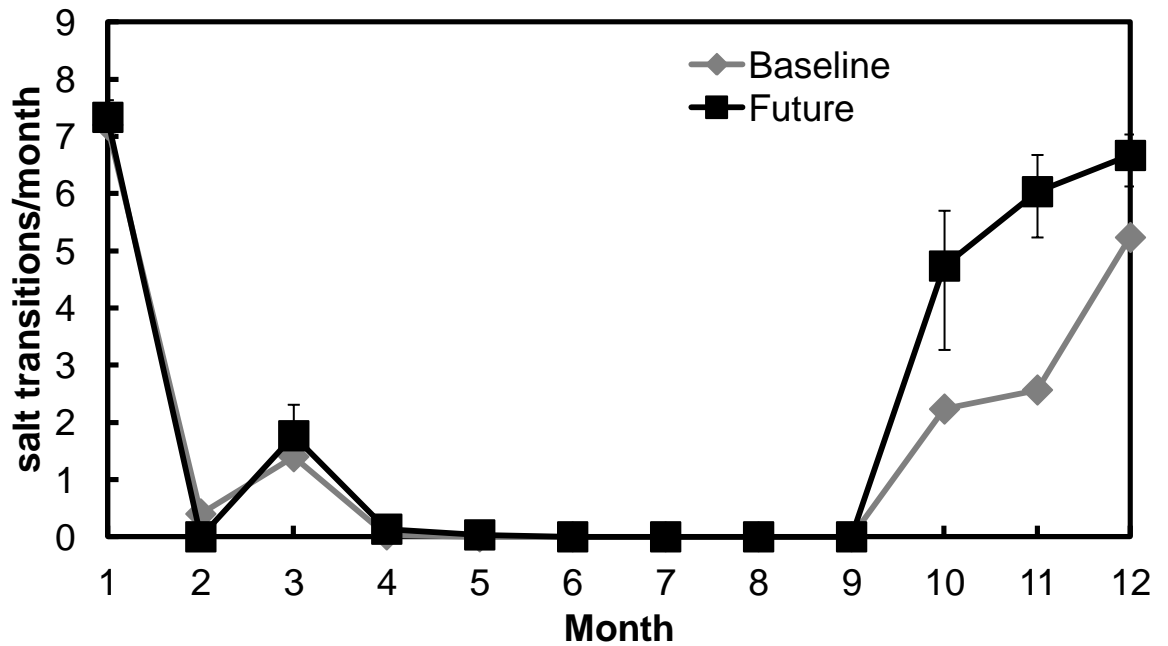


Figure 6.25: The monthly average projected number of 85% salt transitions in the Cartoon Gallery at Knole. Error bars represent the interquartile range.

**Dimensional change**

**Michalski**

**5% Humidity Shock**

The impact of climate change on this dimensional change damage function is shown in figure 6.26. In the Cartoon and Leicester Gallery the number of damaging events arising from 5% humidity changes is projected to decrease. There are a larger number of these events initially, and they are only damaging to the most sensitive of objects, if these are located within either rooms it is likely that damage will have been caused to them already. A reduction such as that seen here, given the magnitude of events is unlikely to be significant in terms of damage; there are still a significant number of events to cause concern. In terms of statistical significance the median of the baseline period is significantly different to that of the near future, for both rooms. The same is true of the median of the near future and mid-term future, and for the mid-term and far future.
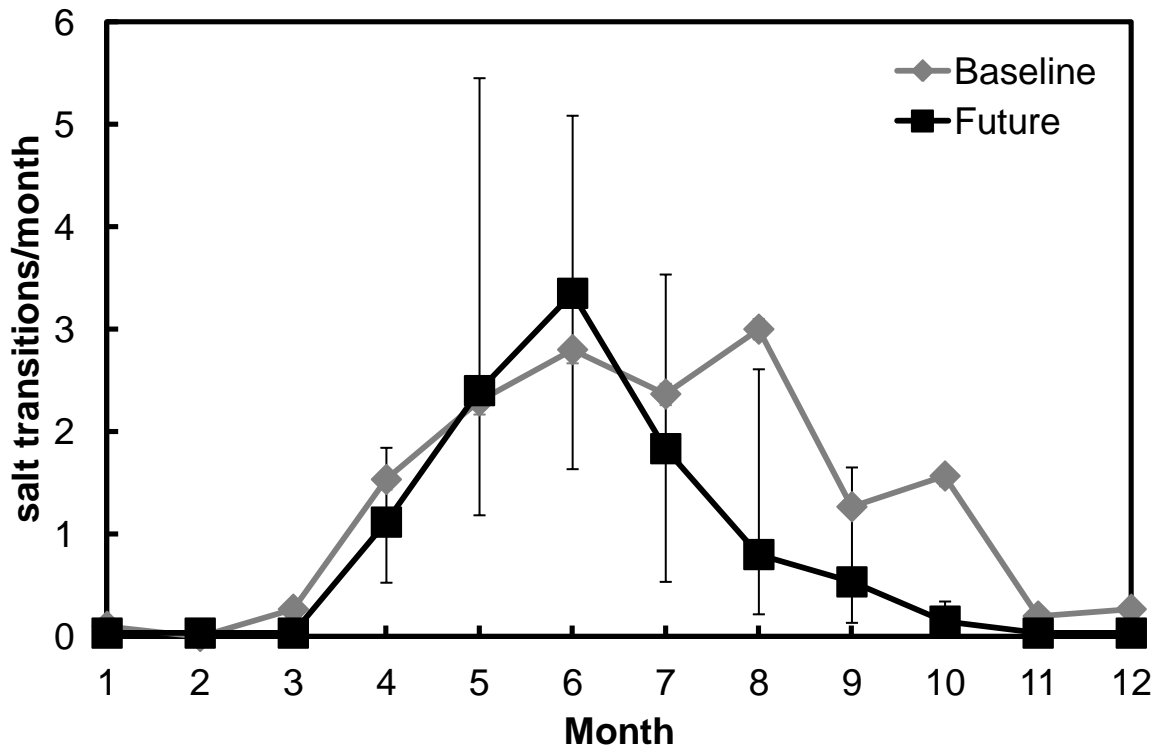


Figure 6.26: The annual average projected number of damaging events arising from a 5% humidity change in the Cartoon and Leicester Galleries at Knole. Error bars represent the interquartile range.

The reason for a reduction in the number of damaging events is unknown; one possible explanation is that the future climate data has fewer occurrences of humidity shifts, which

is then replicated indoors. This has been investigated further, the number of 10% humidity changes from day to day outdoors determined, using the Osborne UKCP09 weather generator data. This also indicates a reduction from the baseline to the future periods. The reduction is not quite as large, 21.5% outdoors compared to 25.1% indoors, but the rest can be attributed to the humidity buffering effect a building has. Therefore the projected reduction in humidity shock events is due to the climate output used, which itself presents a reduction in the fluctuation of humidity.

The seasonal analysis of the impact of climate change on this damage function is shown in figure 6.27. It is expected that there is a reduction in damaging events in all months, with those in summer showing the greatest reduction and driving the reduction seen overall. The damage functions that focus on relative humidity changes of 10 and 20% can be found in appendix D.



Figure 6.27: The monthly average projected number of damaging events arising from a 5% humidity change in the Cartoon Gallery at Knole. Error bars represent the interquartile range.

**30% humidity shock**

The projected impact that climate change will have on dimensional change as described by this damage function is shown in figure 6.28. Again there is a reduction in both rooms in the number of damaging events, which in this case are very likely to cause damage. The results here can be thought of as probabilities. If there is projected to be 0.5 or 0.2 transitions per year, this is equal to one transition every two years or one every five years, respectively. The median of the baseline period and near future period are significantly different to one another, for both rooms here. The same is true of the near future median and mid-term future median, and also the mid-term and far future median. In terms of damage the initial reduction from the baseline to 2025 period is likely to be a significant drop, as each event has a high probability of inflicting damage. Therefore damage to wooden sculpture, which this damage function is linked to, would be expected to reduce. However the smaller reductions between each time period in the future are unlikely to be significant, there would be little difference, if any, in the management practices employed to prevent such damage.



Figure 6.28: The annual average projected number of damaging events arising from a 30% humidity change in the Cartoon and Leicester Galleries at Knole. Error bars represent the interquartile range.

The month by month break down of the results are shown in figure 6.29, this indicates that it is the winter months in future that are most likely to provide a damaging event. It also shows that the main threat from the baseline period was during October, which is significantly reduced in the future.



Figure 6.29: The monthly average projected number of damaging events arising from a 30% humidity change in the Cartoon Gallery at Knole. Error bars represent the interquartile range.

**40% humidity shock**

The projected impact of climate change on the final damage function of this set is shown in figure 6.30. As with the previous functions there is also a reduction in both rooms in the number of damaging events, or the probability of an event occurring within a given year. The seasonal analysis (figure 6.31) indicates that October was also the month where these events were most likely to occur during the baseline period, however in the far future the risk is spread evenly across all months. In both figures 6.29 and 6.31 there is a greater risk of damage during the October baseline period. This may be due to the seasonal increase in relative humidity at this time of the year as shown previously in figure 6.5. It is perhaps surprising that this is not replicated in the future. Elsewhere (6.2.1.3), however, it has been discussed that the UKCP09 weather generator output has a reduction in the relative humidity variation in the future and the absence of an increase in risk during October in future periods may be due to this. In both rooms the median of the baseline is significantly different to that of the near future - the following periods however are not significantly different to one another. With the risk being so small, a once in 10

year event the actual impact on damage or measures to prevent damage the projected change is unlikely to be significant. It is possible that no such measures are in place to mitigate for such a change in relative humidity, therefore a reduction in risk would not change this in future.
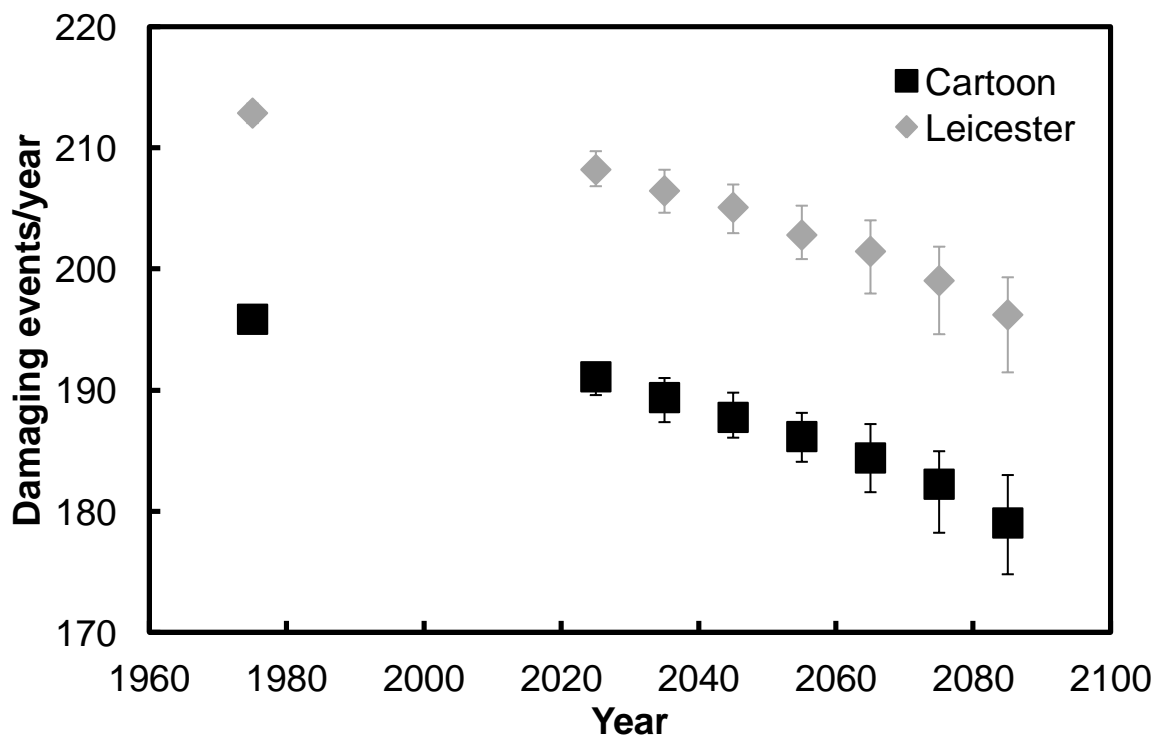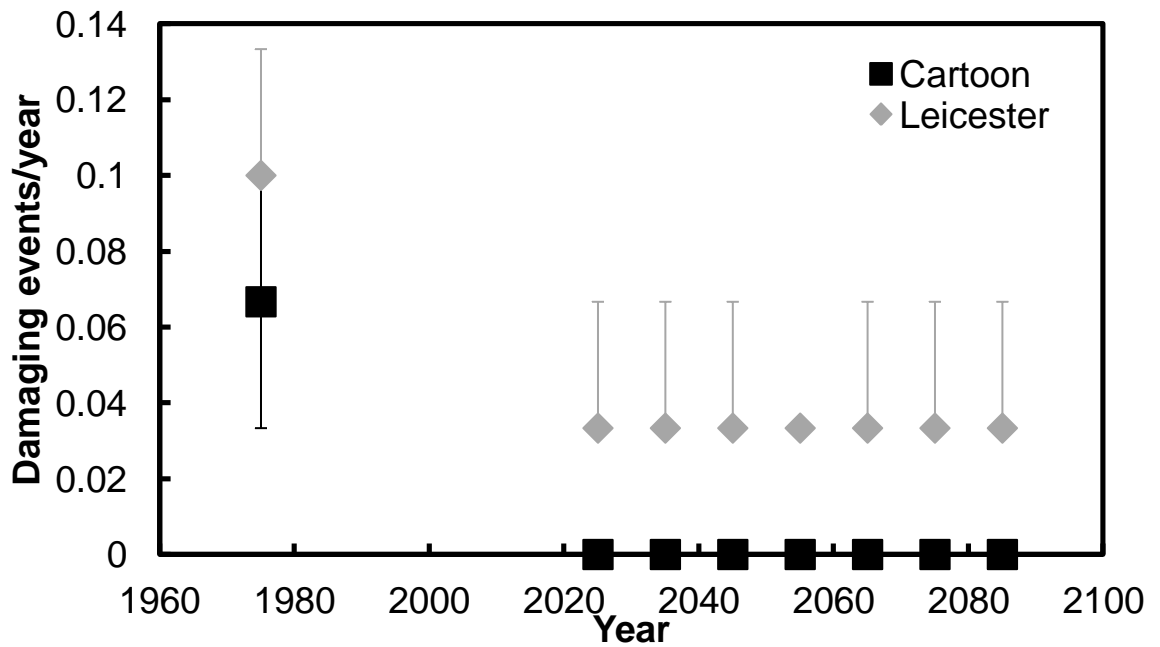


Figure 6.30: The annual average projected number of damaging events arising from a 40% humidity change in the Cartoon and Leicester Galleries at Knole. Error bars represent the interquartile range.
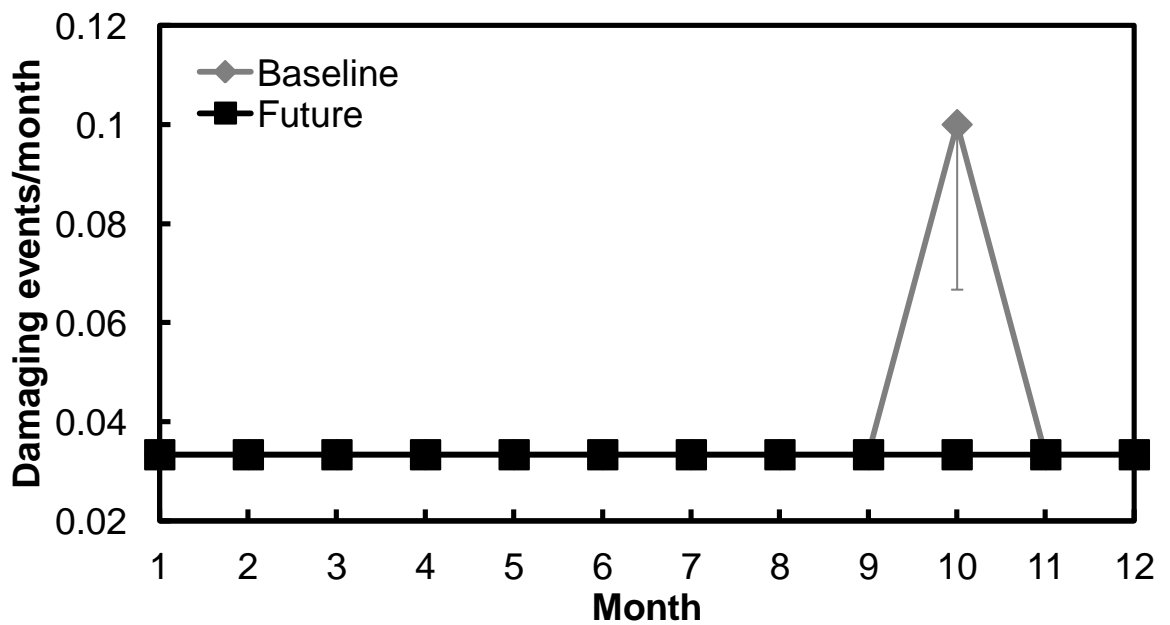


Figure 6.31: The monthly average projected number of damaging events arising from a 40% humidity change in the Cartoon Gallery at Knole. Error bars represent the interquartile range.

**Mecklenburg**

**Cotton wood adsorption**

The projected impact of climate change on damaging adsorption events to cotton wood at Knole is shown in figure 6.32. A decrease in events is projected for both rooms in the future. This damage function allows greater variation in relative humidity in the middle range, therefore the reduced relative humidity of future summers drives the reduction in damaging events projected. This also explains why the Leicester Gallery is projected to have a greater number of damaging events compared to the Cartoon Gallery. The seasonal analysis of the data (figure 6.33) confirms that it is the summer months where the number of damaging events is reduced. The reduction is offset slightly by an increase in winter humidity, as less fluctuation is allowed by the damage function, resulting in increased numbers of damaging events.
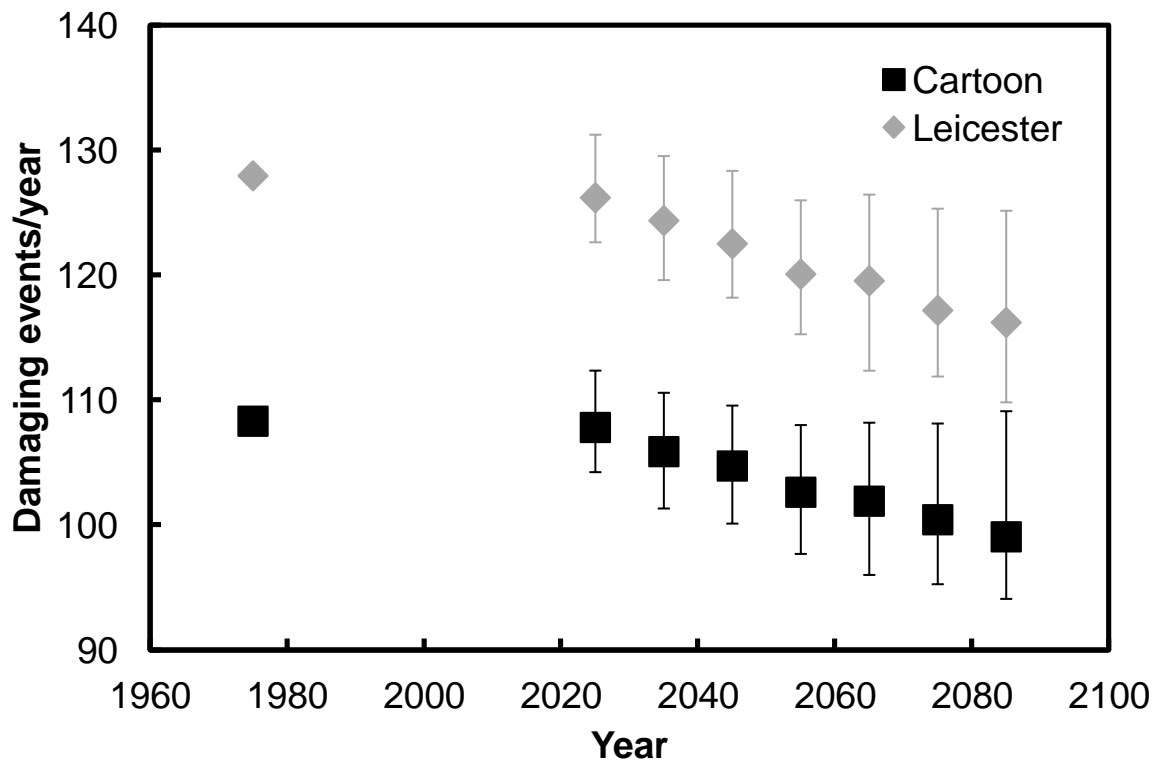


Figure 6.32: The annual average projected number of damaging events arising from adsorption of moisture in the Cartoon and Leicester Galleries at Knole. Error bars represent the interquartile range.
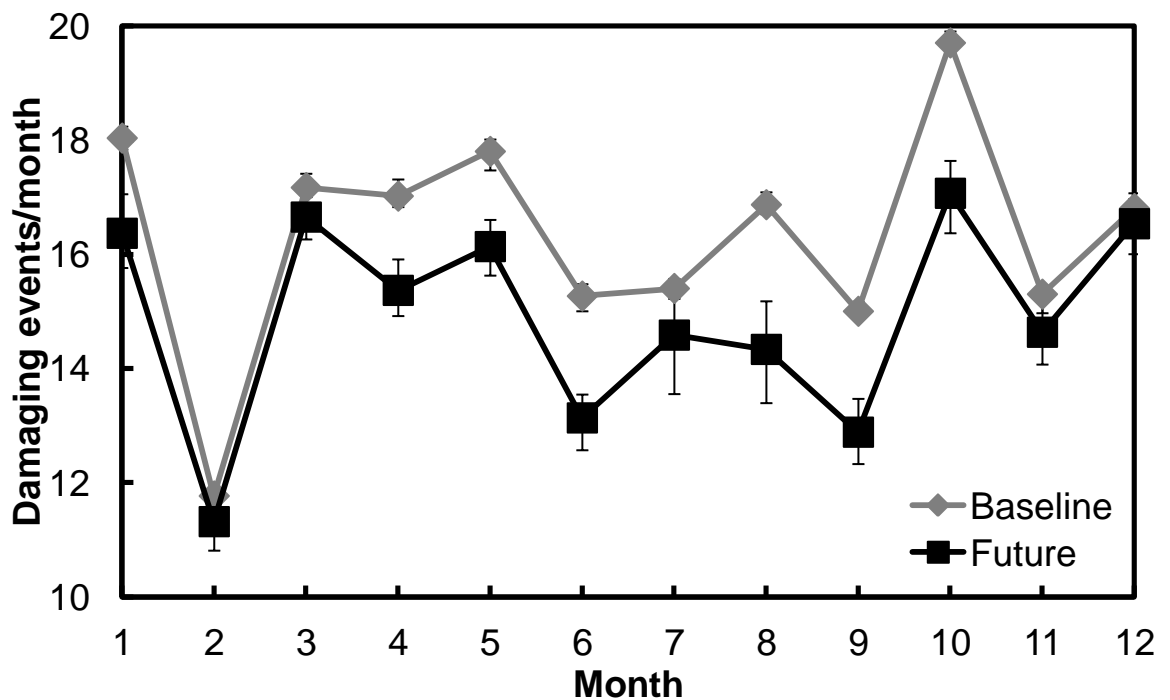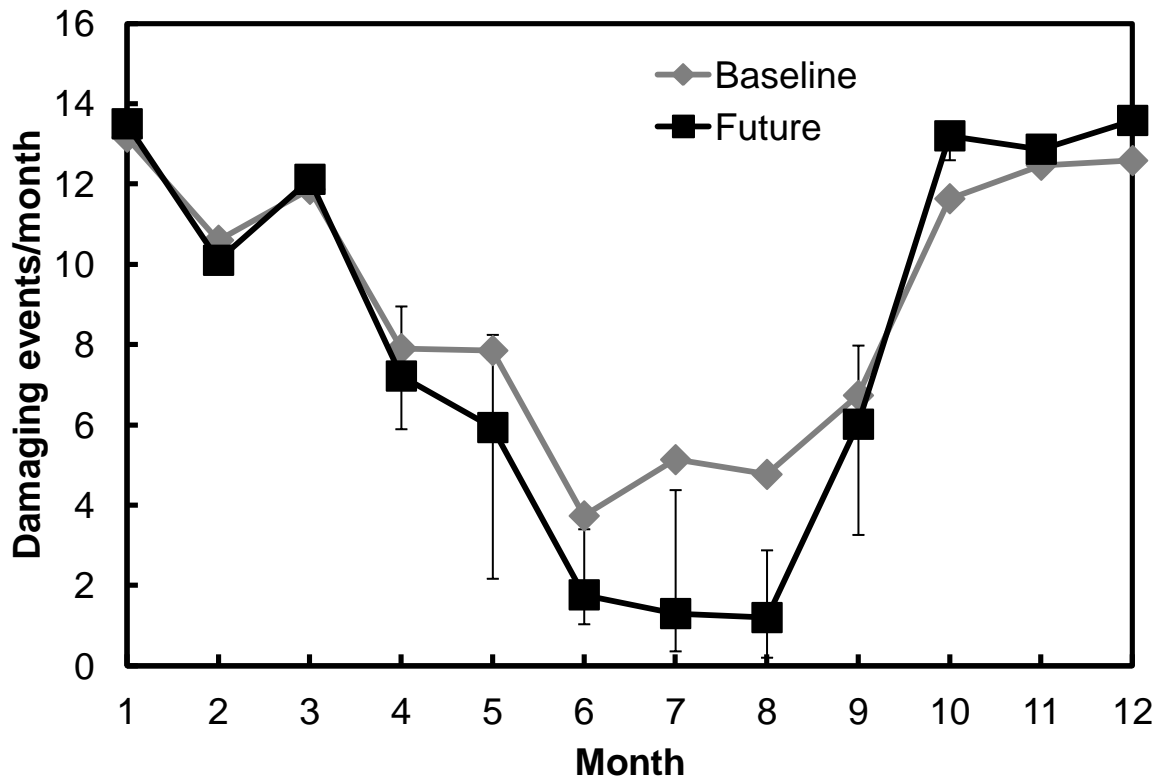
Figure 6.33: The monthly average projected number of damaging events arising from adsorption of moisture in the Cartoon Gallery at Knole. Error bars represent the interquartile range.

The Leicester Gallery median of the baseline period is significantly different to that of the near future period. The same is true of the median of the near future period and the mid-term future period, and also for the mid-term and far future period. However, in the Cartoon Gallery the baseline period median is not significantly different to that of the near future period, but it is significantly different to that of the mid-term future period. The mid-term future median is also significantly different to the far future median. While the results are statistically significant it is not immediately obvious whether the results are significant in terms of damage. It is important to remember the assumptions of the damage functions, here the worst case scenario is predicted, with respect to the direction of the wood, assuming tangential, and also that no previous damage has been caused to the wood. In addition to these, because the daily average values are used there is an assumption about the size of the wood, pieces with a quicker response time could be investigated if hourly averages were used, and this presents further work.

**Cotton wood desorption**

In addition to damaging events from adsorption of moisture there are also potentially damaging events from desorption of moisture, the impact that climate change is projected to have on this type of damage, to cotton wood, is shown in figure 6.34. The results are similar to that for the damaging events caused by adsorption, the two rooms are projected to have a different number of events, which are expected to reduce in the future. The cause of this is again the reduction is summer relative humidity, as shown by the seasonal analysis in figure 6.35. The magnitude of damage from this mechanism is less than that caused by adsorption of moisture.

The projected reduction proceeds at different rates within each room. This is due to the difference in relative humidity. The Leicester Gallery has a higher relative humidity than the Cartoon Gallery, thus is allowed less variation in relative humidity before a damaging event occurs. The same change in relative humidity in both rooms will therefore have a greater impact on the Leicester Gallery, as it moves towards the safer zone, whereas the Cartoon Gallery was already closer to this zone.
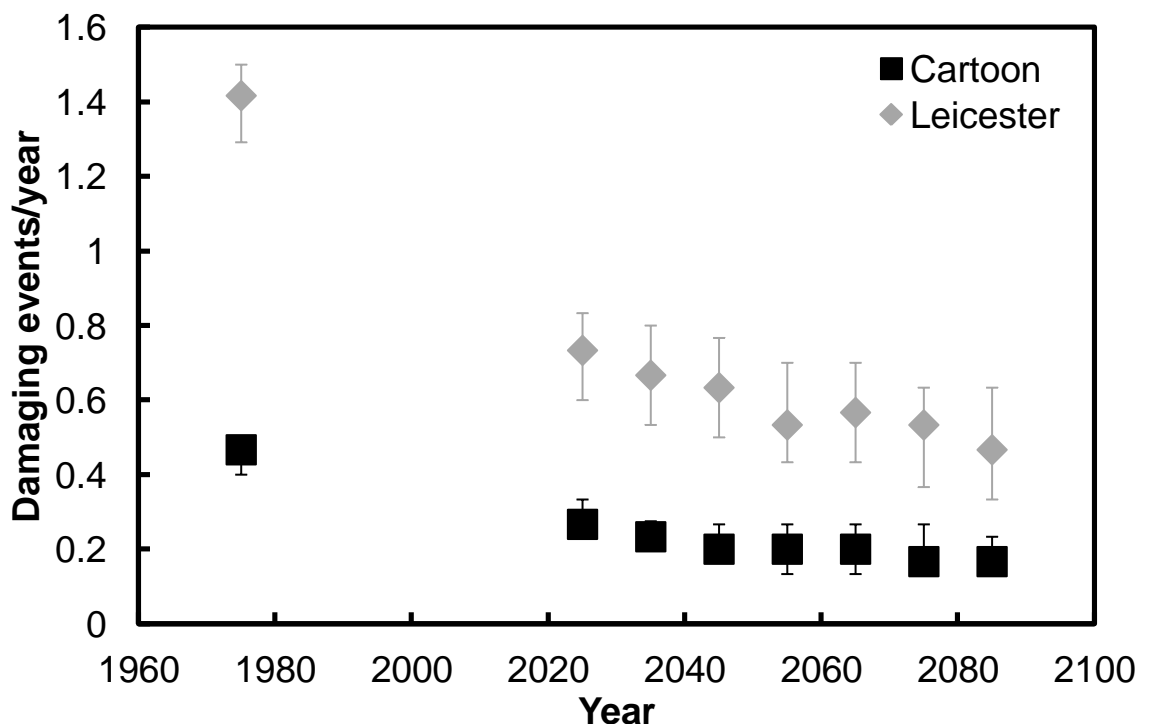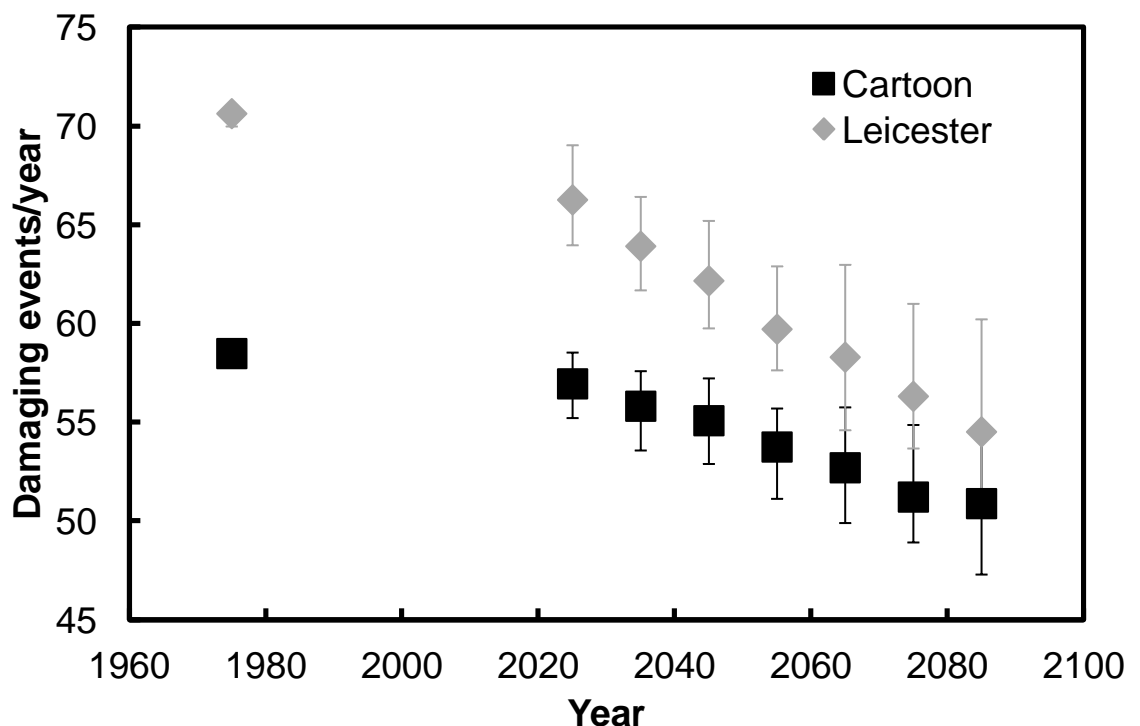


Figure 6.34: The annual average projected number of damaging events arising from desorption of moisture in the Cartoon and Leicester Galleries at Knole. Error bars represent the interquartile range.
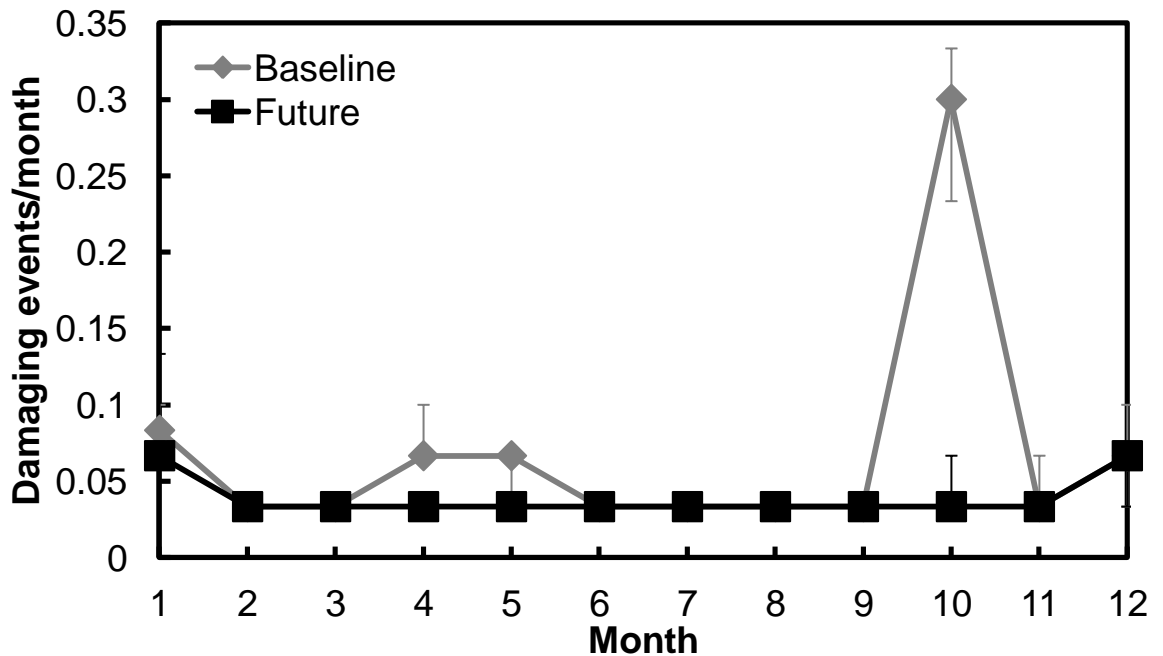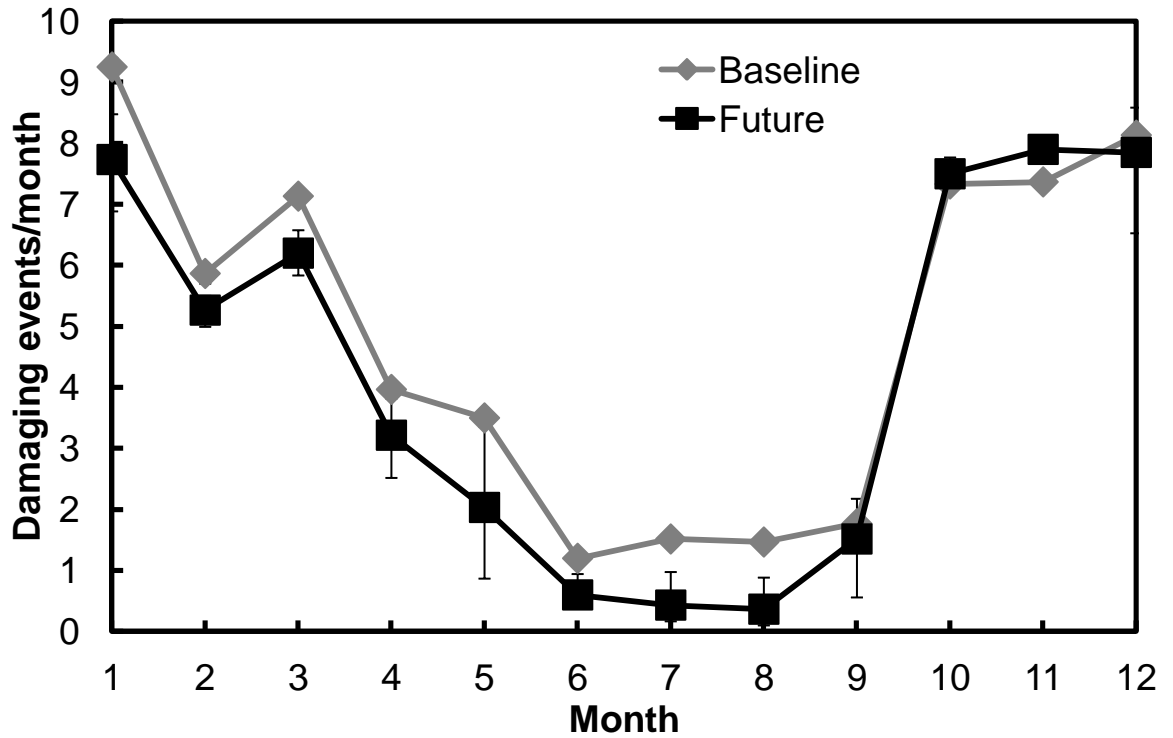
Figure 6.35: The monthly average projected number of damaging events arising from desorption of moisture in the Cartoon Gallery at Knole. Error bars represent the interquartile range.

The median of the baseline period is significantly different to that of the near future period, in both rooms. The same is true of the near future median to the mid-term future median, and also for the mid-term future to far future median. Again the significance of this change to the damage that will occur is difficult to determine.

The impact of climate change on the damage function for the total of the previous two functions can be found in appendix D, with those of the white oak adsorption, desorption and total damage functions. The equilibrium moisture content (EMC) function is also in appendix D.

**White oak failure**

The final damage function from the this set is that of failure events on white oak wood, the impact that climate change has on this is shown in figure 6.36. As shown with previous dimensional change damage functions the number of damaging events, or in this case failure events, is projected to decrease in the future.
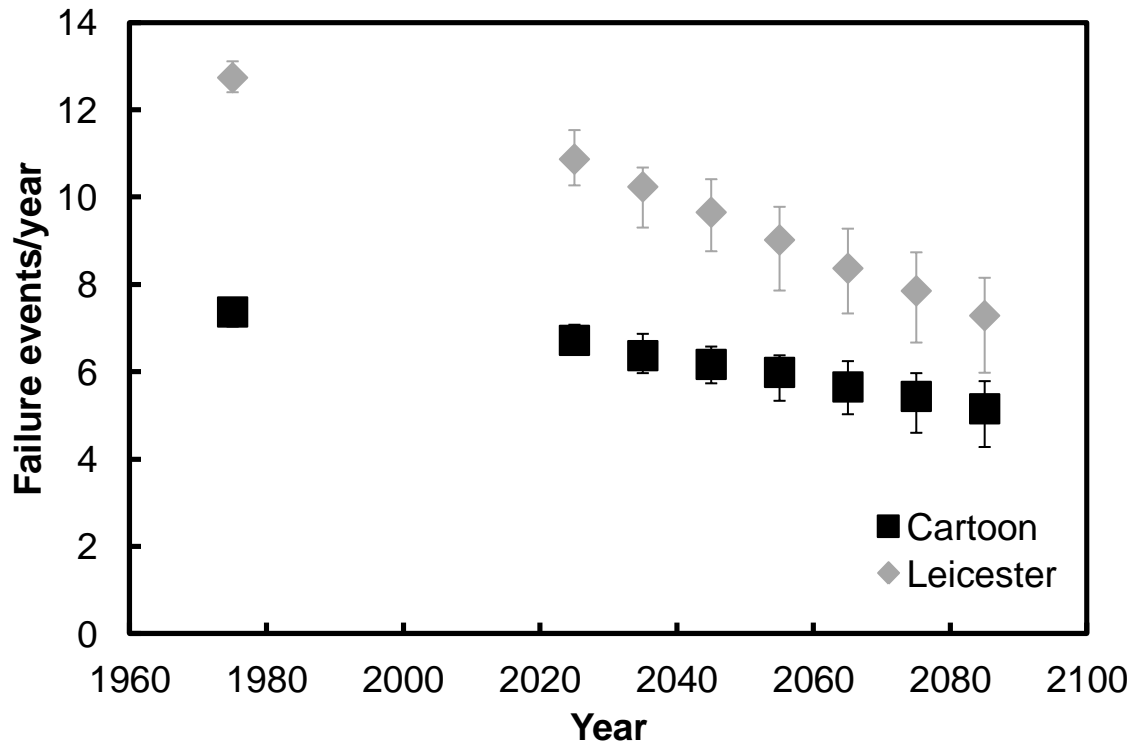


Figure 6.36: The annual average projected number of failure events in the Cartoon and Leicester Galleries at Knole. Error bars represent the interquartile range.

The median of the baseline period, for both rooms, is significantly different to that of the near future period. This is also true of the near future median and the mid-term future median, and also the mid-term and far future median. The results are shown to be statistically significant, and given the impact of one damaging event in this instance it is also likely that the reduction seen here is also significant in terms of the reduction to damage. However it may not be significant in terms of the preventive conservation measures in place. For example if an object were sensitive to these events it may be placed within an enclosure to buffer the humidity change, and thus prevent damage. While there is a reduction in events, there are still projected events occurring, it would require a stop in damaging events in order to be able to remove an object from an enclosure. This assumes that the enclosure is solely used for the purpose of protection from the environment, and not for security.

The seasonal analysis of this damage function is shown in figure 6.37. Unusually the reduction is not driven by the summer months, events in these months were already low, most other months show a clear reduction in the number of failure events.
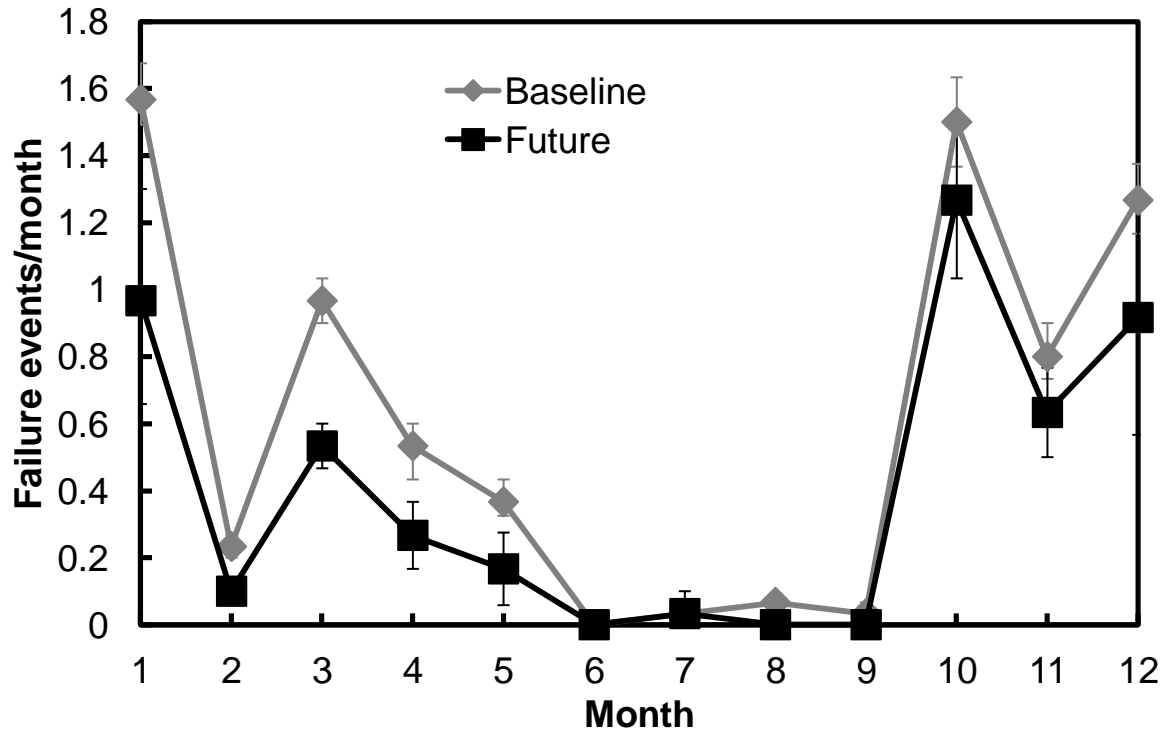


Figure 6.37: The monthly average projected number of failure events in the Cartoon Gallery at Knole. Error bars represent the interquartile range.

### 6.2.2 Brodsworth Hall

6.2.2.1 Environment

The impact that climate change is projected to have on the temperature within the Library at Brodsworth Hall is shown in figure 6.38. It is projected that the temperature will increase by approximately 1.5 degrees across the century, compared to the outdoor projection this is less than half. The impact of this relatively small change upon damage functions will be shown in the following sections. The median of the baseline period is significantly different to that median of the near future period. The same is true for the near future to mid-term future median, and also for the mid-term to far future medians.



Figure 6.38: The annual average projected temperature in the Library at Brodsworth Hall, and outdoors at Brodsworth. Error bars represent the interquartile range.

In figure 6.39 the projected impact of climate change on the relative humidity within the Library is shown. In this instance the relative humidity is projected to increase in the future, albeit only by a few percent. This is in contrary to the projection outdoors which is shown to decrease in the future. This difference in change is due to there being less of a temperature increase indoors. Outdoors the temperature increase outweighs the specific humidity increase, and the relative humidity decreases. However indoors with a lower increase in temperature the specific humidity increase outweighs the temperature increase, and the relative humidity increases.
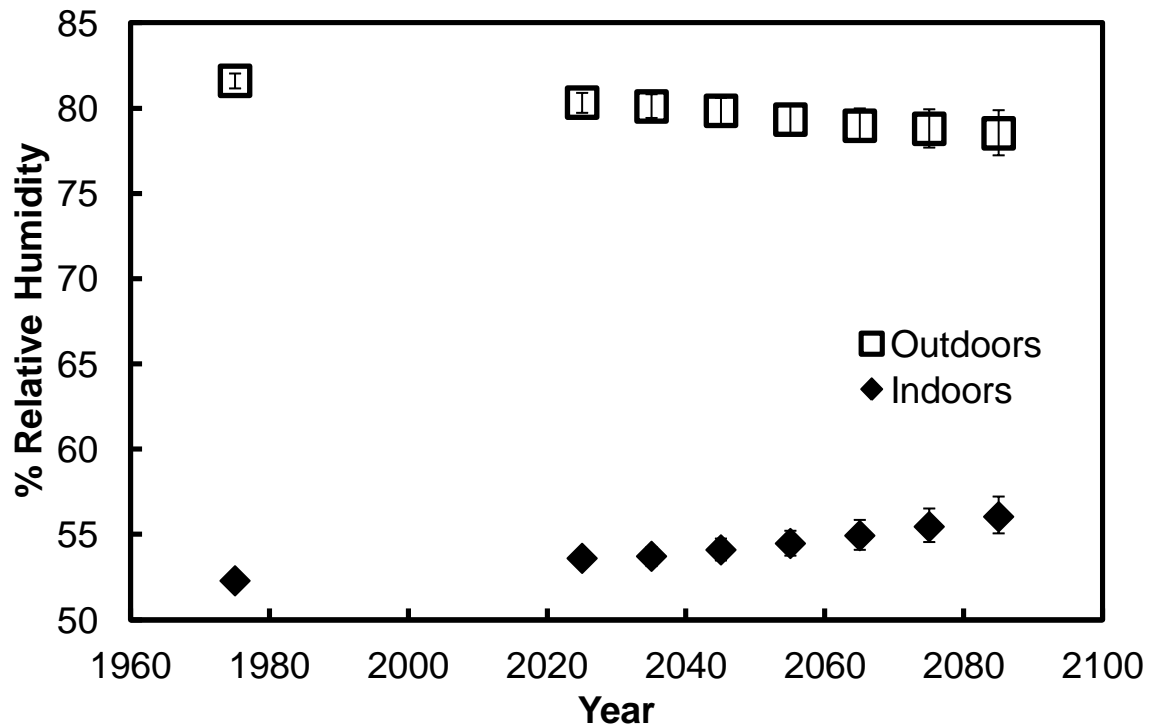
Figure 6.39: The annual average projected % relative humidity in the Library at Brodsworth Hall, and outdoors at Brodsworth. Error bars represent the interquartile range.

For the relative humidity projection in figure 6.39 the projected median of the baseline period is significantly different to that of the near future period. The same is true for the near future to mid-term future median, and also for the mid-term future to far future median.

6.2.2.2 Seasonality

The projected seasonal change in temperature in the Library is shown in figure 6.40. The result here is similar to that of the Cartoon Gallery at Knole. The summer temperature shows a prominent increase in temperature, with a shift of the interquartile range to above that of the baseline period. The winter temperature is also projected to increase, but not as much above the baseline data as the summer temperatures are projected to. The overall temperature range is projected to increase, although this could be due to the increase in uncertainty associated with the far future time period.
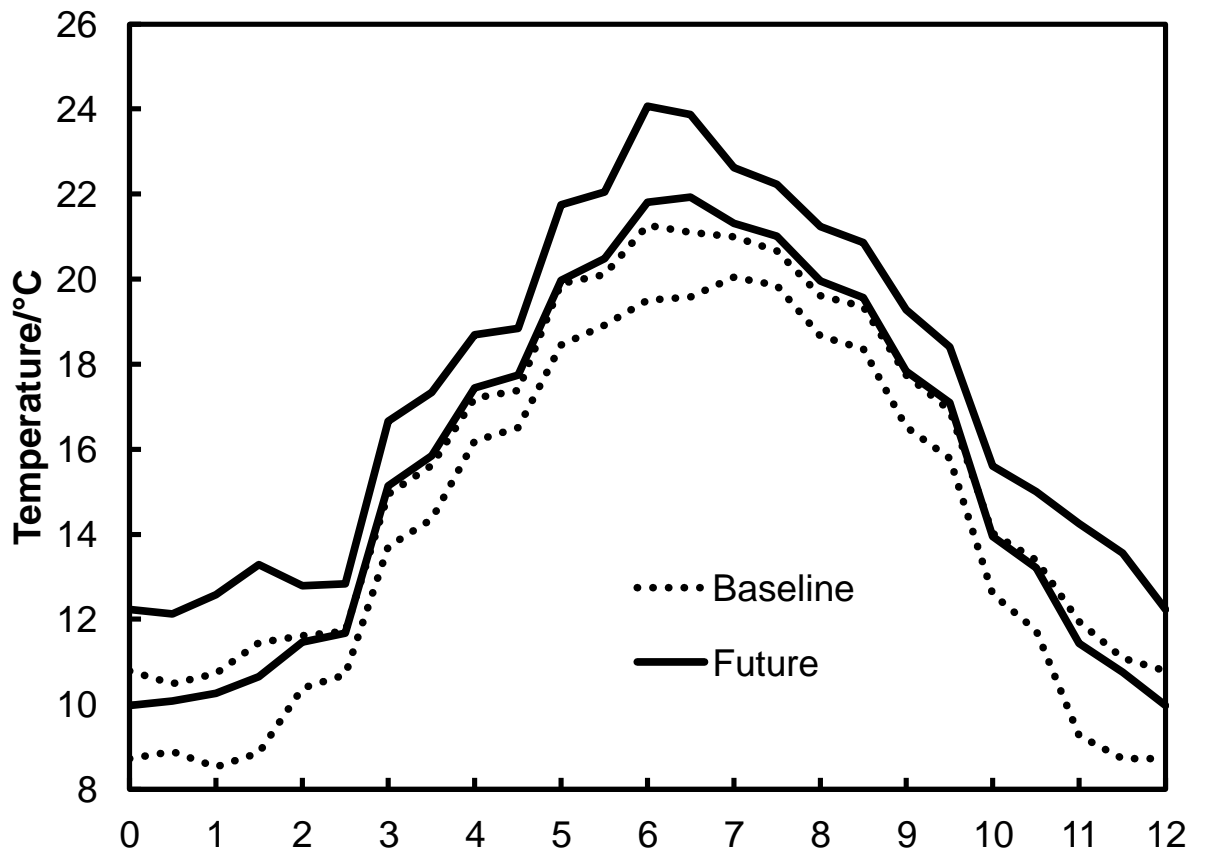


Figure 6.40: The monthly average projected temperature in the Library at Brodsworth Hall, for the baseline and far future periods. The enclosed region represents the interquartile range.

The seasonal projection of relative humidity in the Library at Brodsworth Hall is shown in figure 6.41. Apart from the increase in relative humidity shown previously there is no shift in the seasonal pattern, as has been shown to change at Knole. While there is no significant shift in the seasonality, the increase in future relative humidity is less in the summer months than in other months.
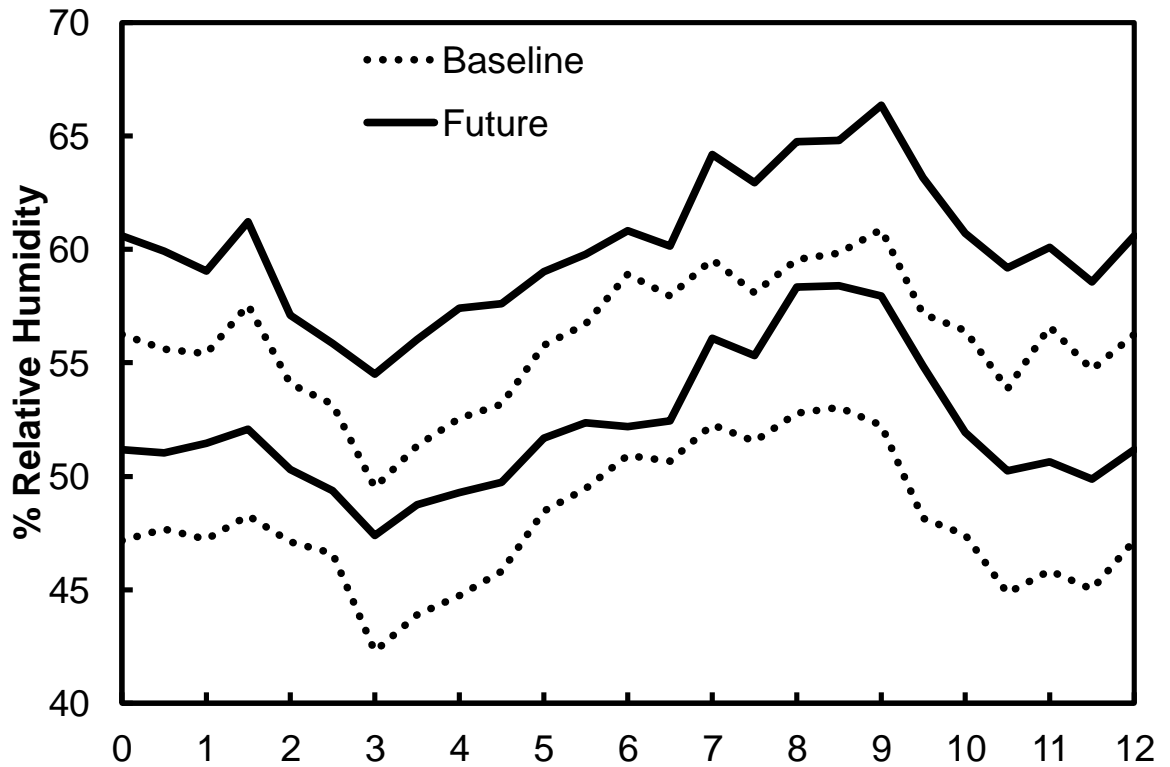


Figure 6.41: The monthly average projected % relative humidity in the Library at Brodsworth Hall, for the baseline and far future periods. The enclosed region represents the interquartile range.

6.2.2.3 Damage

**Daily average temperature >25°C**

The impact that climate change is projected to have on the number of days where the average temperature exceeds 25°C is shown in figure 6.42. During the baseline period it is expected that there are no days where the average temperature within the Library exceeds 25°C, however it is projected that this will begin to occur due to climate change, with an average of 1.5 days per year by the end of the century. The median of the baseline period is significantly different to the median of the near future period. The same is true of the near future and mid-term future median, and also of the mid-term and far future median. The seasonal plot of this damage function (figure 6.43) indicates that it is in

July that drives the increase in the far future. The impact of climate change on the number of days where the average temperature exceeds 20°C can be found in appendix D.
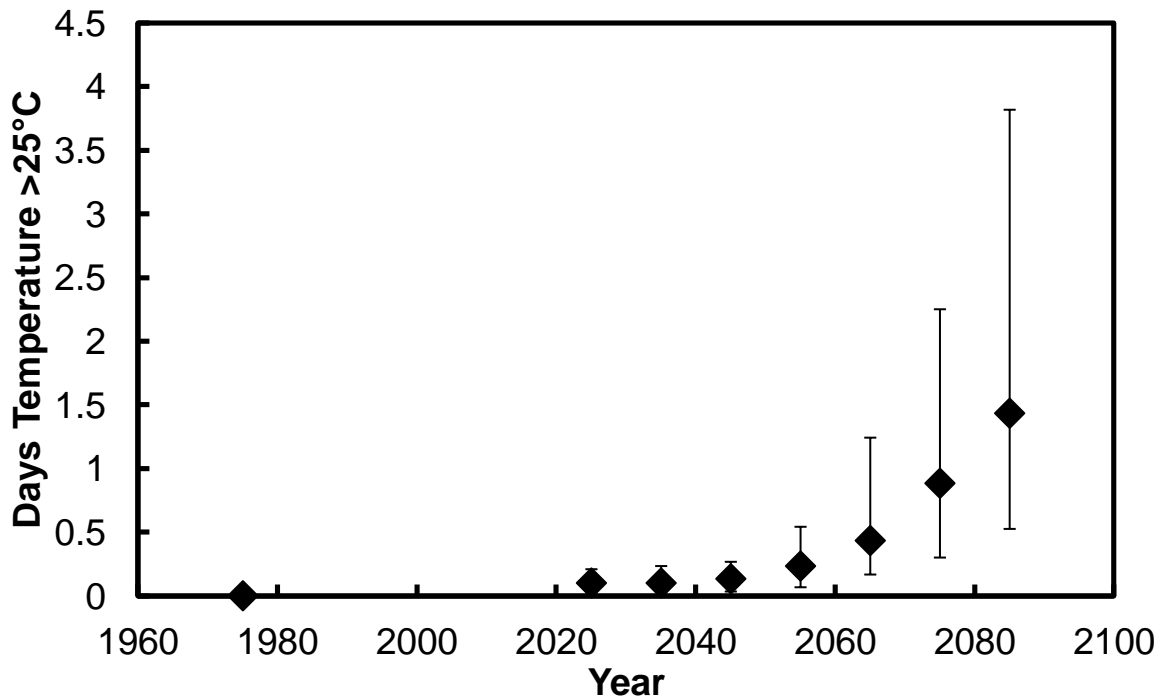


Figure 6.42: The annual average projected number of days where the daily average temperature exceeds 25°C in the Library at Brodsworth Hall. Error bars represent the interquartile range.
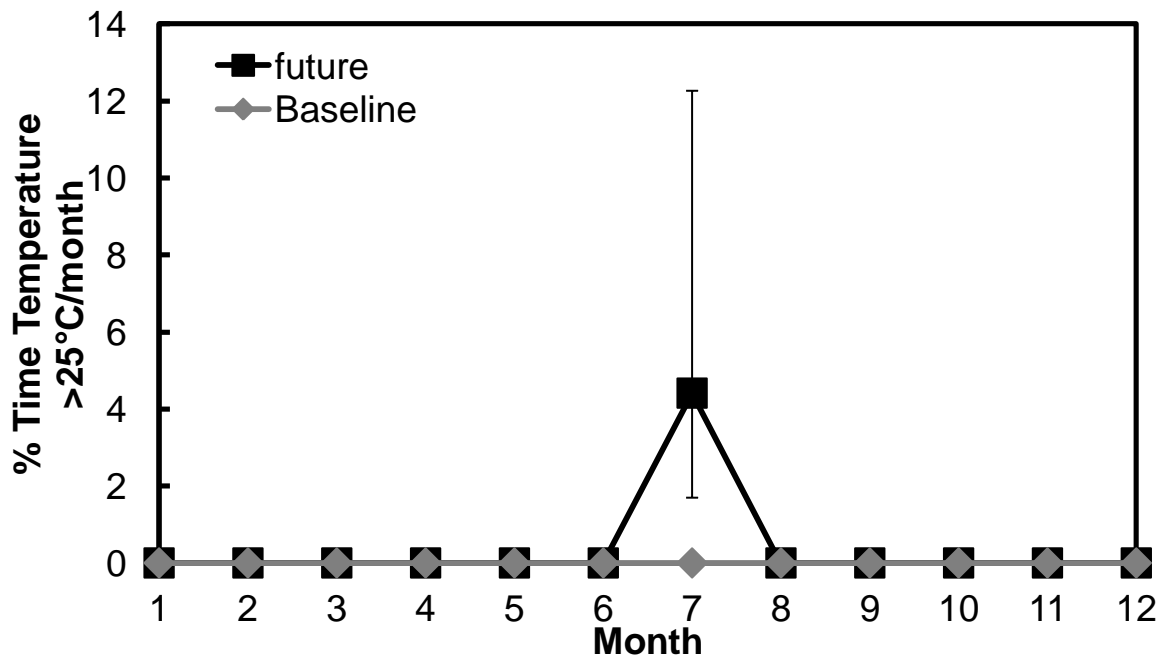


Figure 6.43: The monthly average projected number of days where the daily average temperature exceeds 25°C in the Library at Brodsworth Hall. Error bars represent the interquartile range.

**Paper**

**Isoperm**

The impact that climate change is projected to have on chemical degradation of paper, as described by the isoperm damage function is shown in figure 6.44. Again an increase in the rate is projected; approximately 25% more than the baseline median. This increase in rate is driven by the increase in temperature. The season analysis, as shown in figure 6.45, again shows that it is the summer months that contribute the majority of the rate increase. The median of the baseline period is significantly different to the median of the near future period. The same is also true of the near future and mid-term future median, and also of the mid-term and far future medians.

The impact of climate change on the Zou ,Twpi, Silk and Pretzel damage functions are shown in appendix D. The first three show an increase in damage similar to that at Knole, with a different magnitude. The Pretzel function is also similar to previously.
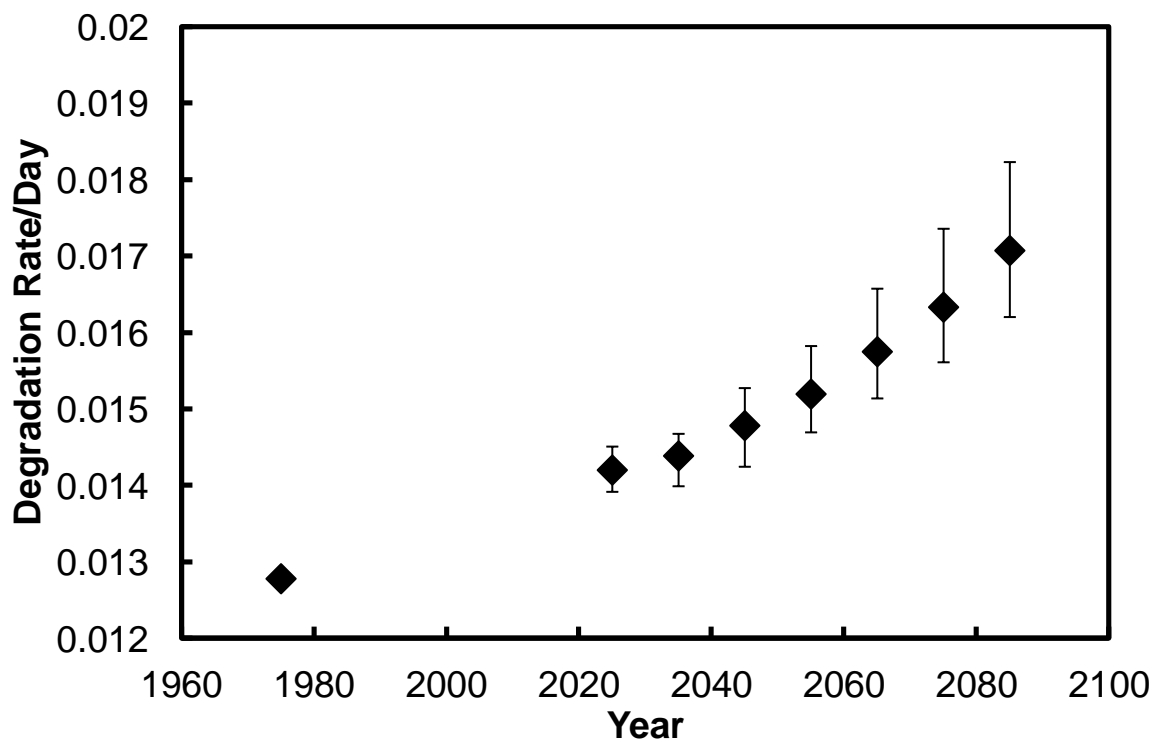


Figure 6.44: The annual average projected degradation rate of paper in the Library at Brodsworth Hall. Error bars represent the interquartile range.
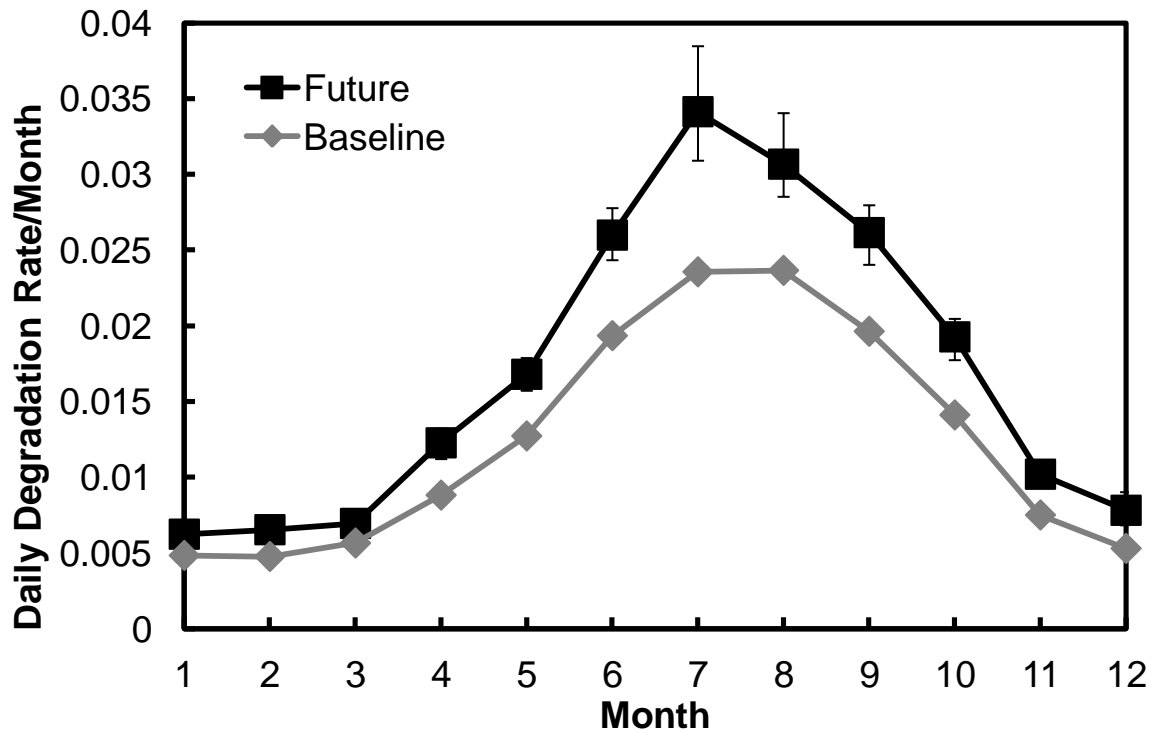
Figure 6.45: The monthly average projected degradation rate of paper in the Library at Brodsworth Hall. Error bars represent the interquartile range.

**Mould**

**Isaksson**

In the Library at Brodsworth Hall the relative humidity is too low for mould to grow, both for the baseline period, and for all of the future periods. This occurs for this damage function and also the critical relative humidity damage function, and the Hukka damage function.

**Degree days**

The impact on the number of degree days that climate change is projected to have in the Library is shown in figure 6.46. It is projected that there will be an increase in the number of degree days, with approximately 1.5 times as many in the far future compared to the baseline. The median of the baseline period is significantly different than the median of the near future period. The same is true of the near future to mid-term future period, and also of the mid-term and far future periods.
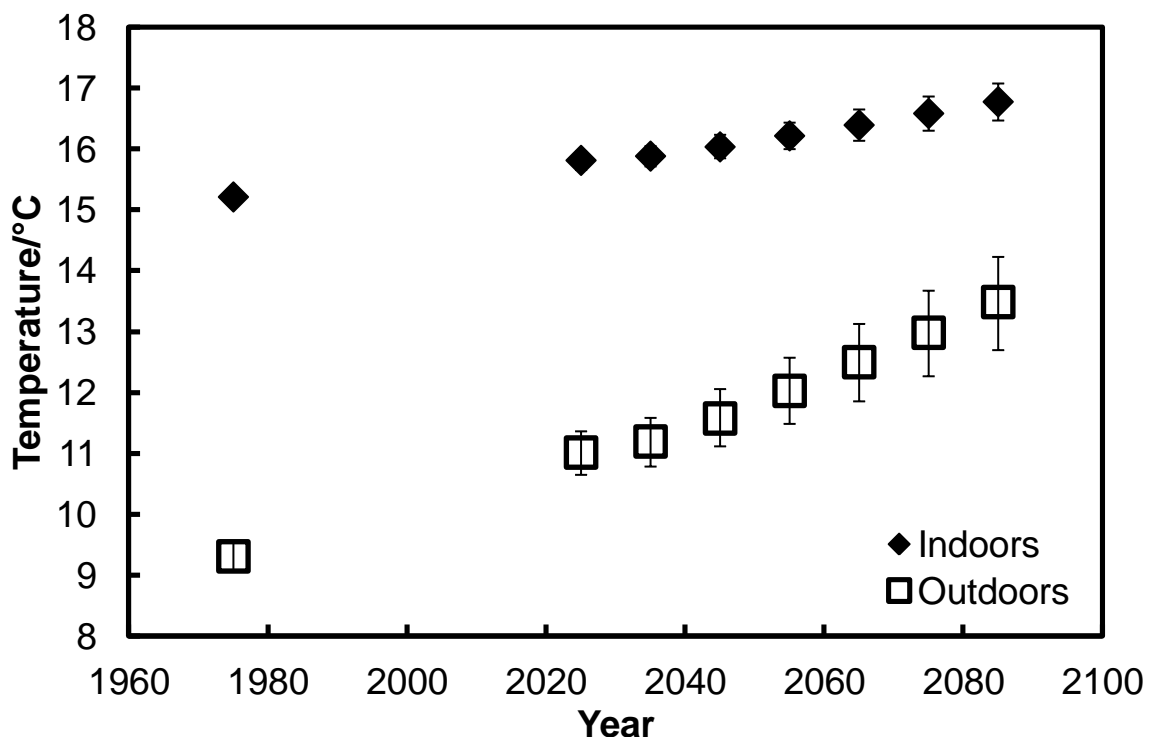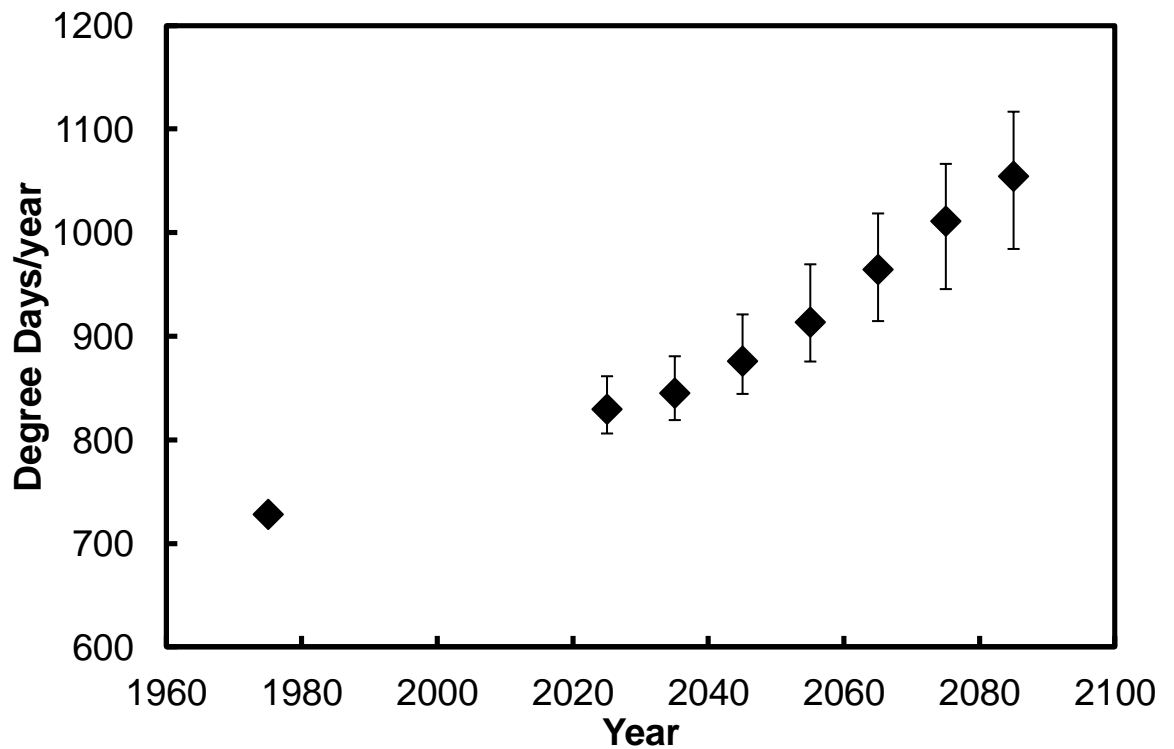


Figure 6.46: The annual average projected number of degree days in the Library at Brodsworth Hall. Error bars represent the interquartile range.

The month by month analysis of this damage function is shown in figure 6.47. It is projected that it is mainly the months that already contribute degree days that continue to in the future. It is only November that did not previously have any degree days, but is projected to in the future. Across the months that had degree days in the past they all fairly evenly increase in the future, with the exception of July. In relation to insects this may indicate that there is a slightly longer period that they can be active for, and during this period they are likely to be more active than in the past, as temperatures are warmer.
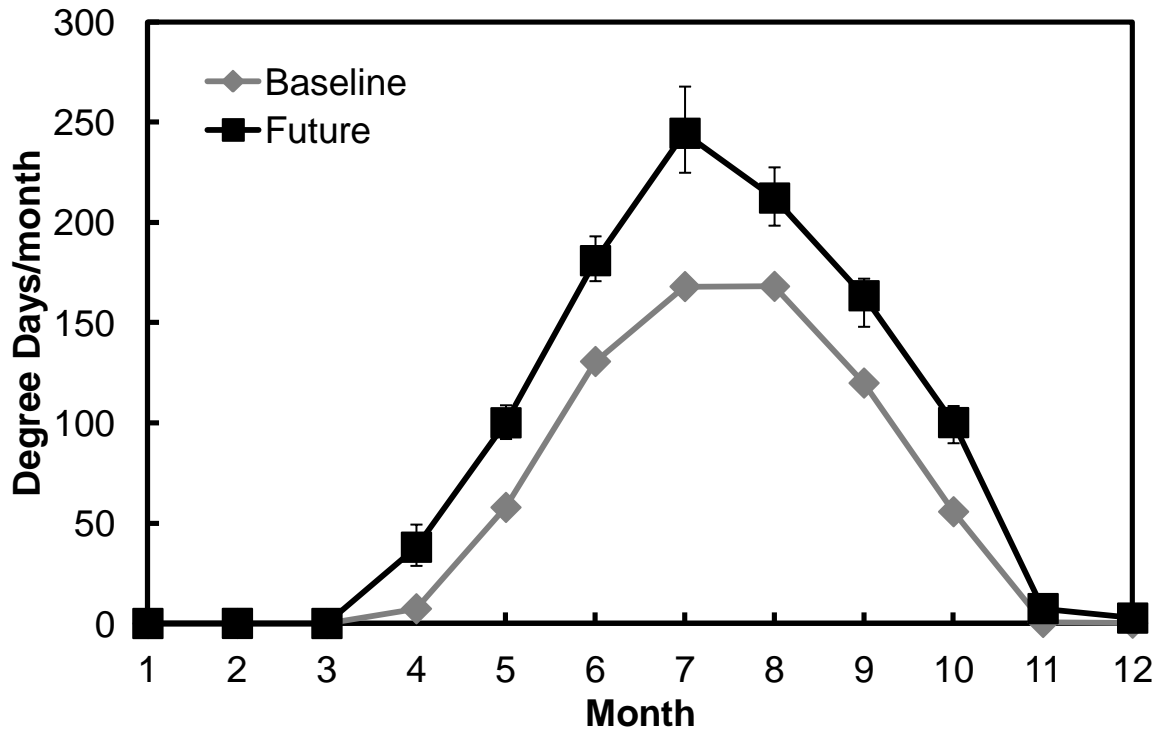


Figure 6.47: The monthly average projected number of degree days in the Library at Brodsworth Hall. Error bars represent the interquartile range.

**Salts**

**Salt transitions – thenardite/mirabilte**

The impact that climate change is projected to have on salt transitions of thenardite to mirabilite are shown in figure 6.48. Assuming that the salt is present it is projected that it will cause more damage in the future, this does come to a plateau however in the far future. This function is dependent on a combination of temperature and relative humidity, and specifically the temperature and relative humidity pair at the same point in time, therefore without further analysis it is not possible to determine which is responsible for the increase in transitions. The median of the baseline period is significantly different to the median of the near future period. This is also true of the near future median to the mid-term future median, and also the mid-term and far future medians.
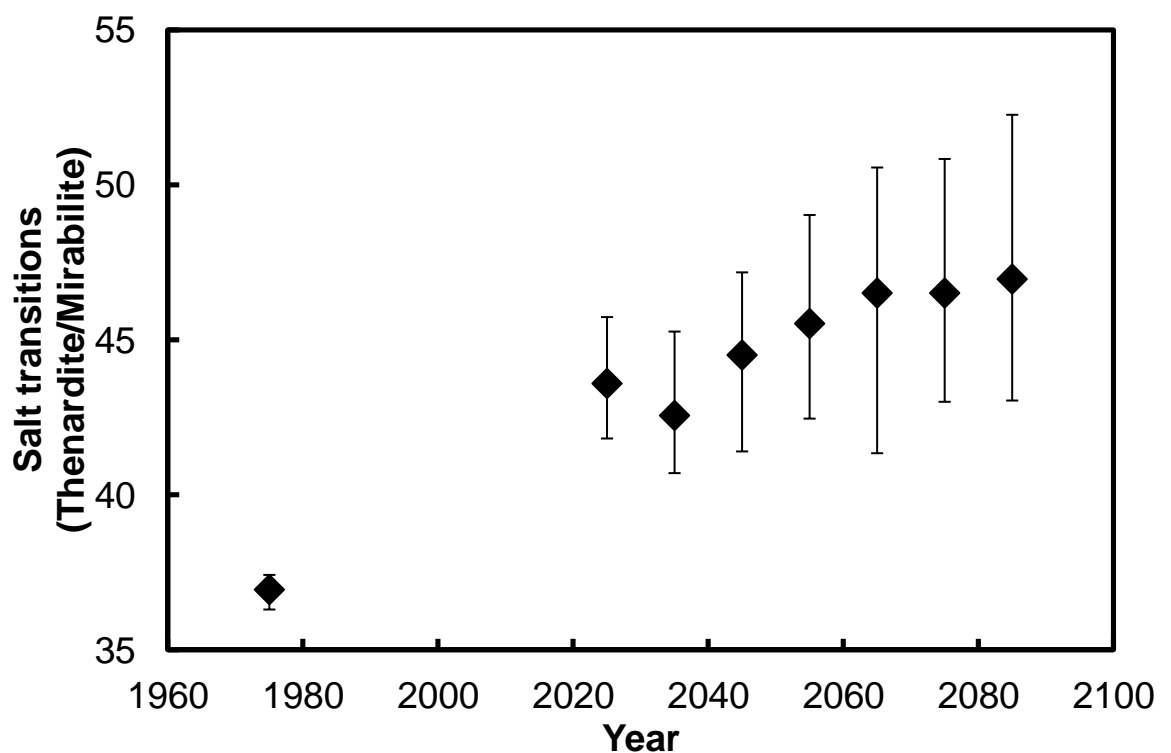


Figure 6.48: The annual average projected number of thenardite mirabilite salt transitions in the Library at Brodsworth Hall. Error bars represent the interquartile range.

The seasonal analysis of this damage function is shown in figure 6.49. This helps to some degree to decipher whether it is the temperature or relative humidity that drives the projected increase. It is projected, for most months, that the number of transitions will increase, however during the summer months the opposite is true, there is a reduction in transitions. In the summer the temperature increases in the future, it would appear that this acts to increase the critical relative humidity, to a level greater than that in the room. In addition to this the function requires the temperature to be below 22.5°C in order to cause a damaging transition, the occurrence of this increases in the future, so will also act to reduce the number of transitions that cause damage.
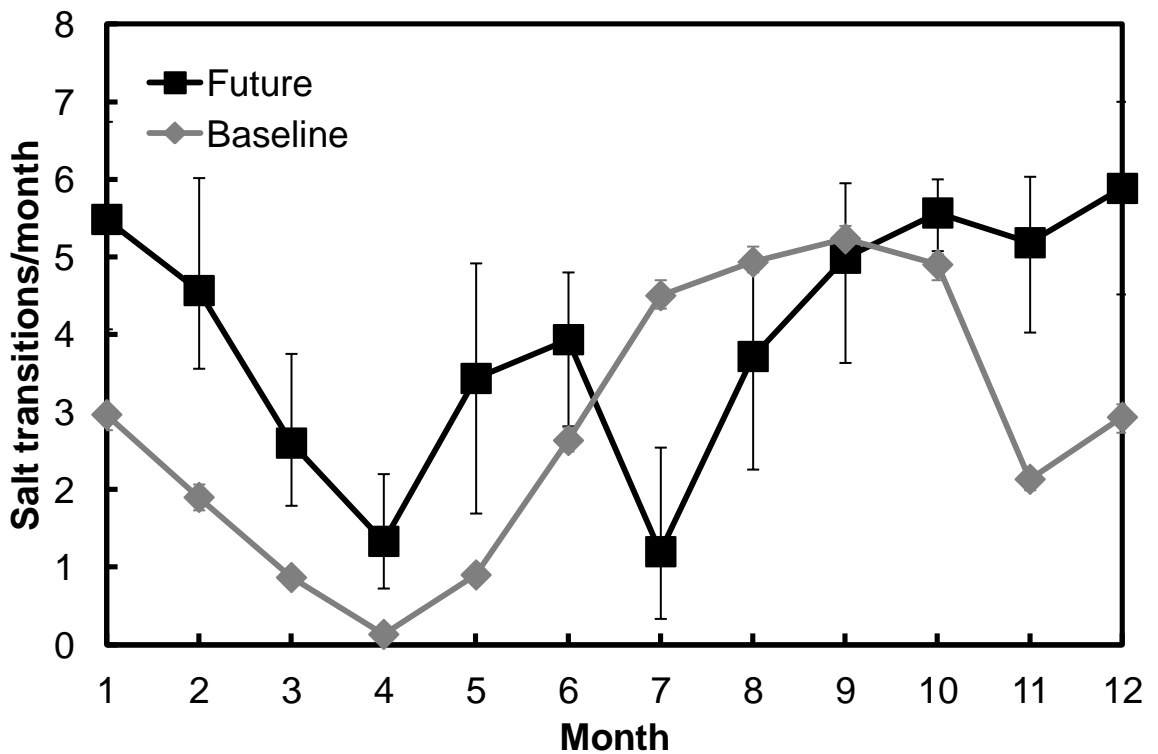


Figure 6.49: The monthly average projected number of thenardite mirabilite salt transitions in the Library at Brodsworth Hall. Error bars represent the interquartile range.

**Salt transitions – 60%**

The impact that climate change is projected to have on salt transitions at a critical relative humidity of 60% is shown in figure 6.50. It is projected that the number of transitions would increase in the Library, this is due to the increase in relative humidity that is projected. The annual trend is an increase towards 60%; therefore the variation around the average increasingly crosses the critical relative humidity.
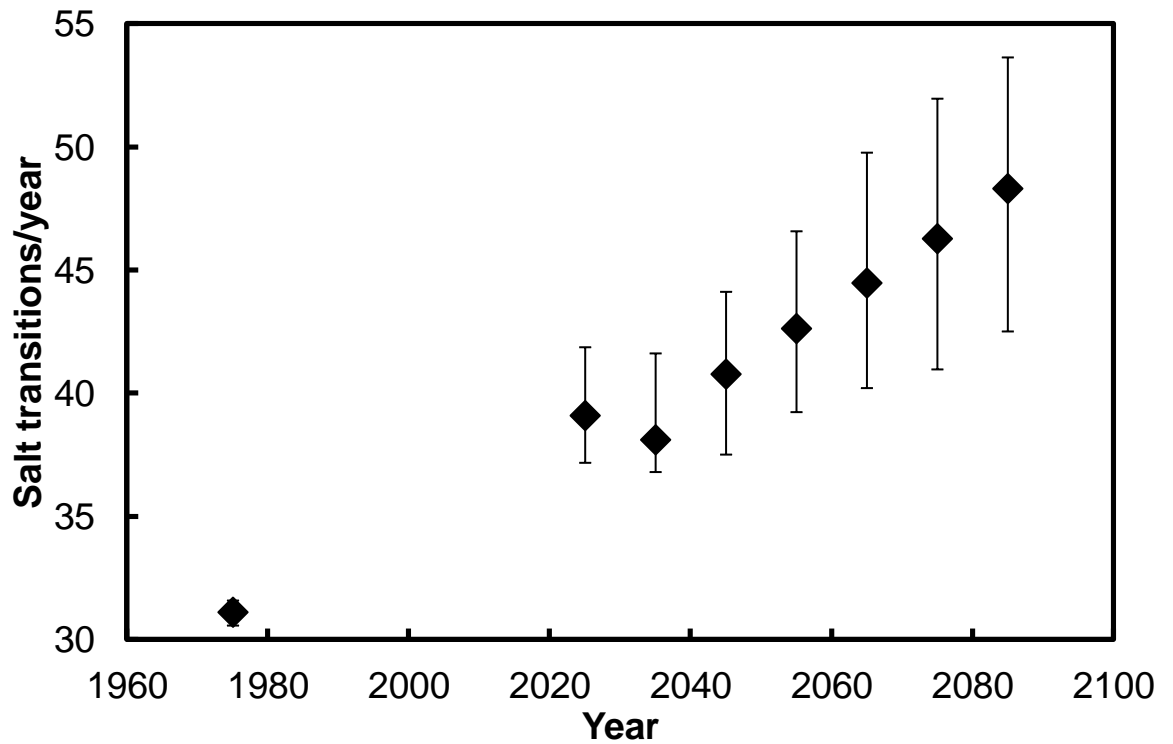


Figure 6.50: The annual average projected number of 60% salt transitions in the Library at Brodsworth Hall. Error bars represent the interquartile range.

The seasonal analysis of this damage function (figure 6.51) indicates that there is projected to be an increase in most months, with a possible exception of the summer months. This correlates to the period where the least increase in relative humidity is projected. The median of the baseline period is significantly different to that of the near future period. The same is true of the near future median and mid-term future median, and also of the mid-term to far future medians. With respect to the significance of the change on damage, it is likely to be significant; the change will raise the number of transitions to in excess of 150% of the baseline value, a large increase. Should this pose a risk enclosing a susceptible object in an enclosure that is humidity controlled or buffered would provide mitigation.

The impact of climate change on salt transitions at 75% can be found in appendix D. The relative humidity within the Library at Brodsworth Hall is too low to cause transitions at the level of 85% relative humidity; this is true of both the baseline and all future periods.
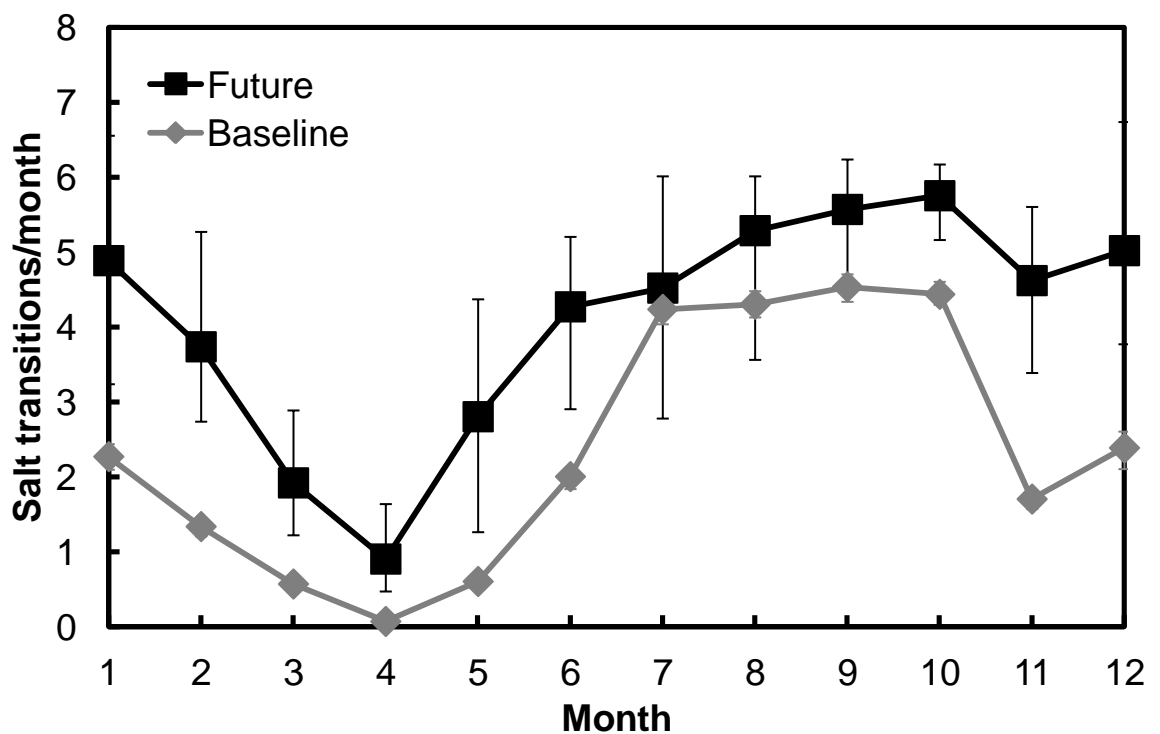


Figure 6.51: The monthly average projected number of 60% salt transitions in the Library at Brodsworth Hall. Error bars represent the interquartile range.

**Dimensional change**

**Michalski**

**20% humidity shock**

The projected impact of climate change on dimensional change as described by this damage function is shown in figure 6.52. A decrease in damaging events is projected as seen previously at Knole. A reduction all year round is projected (figure 6.53), with the winter months more pronounced where there is more damage expected. The reduction projected, of almost 50%, is likely to be significant to any damage that is caused. A shift from almost four to two damaging events per year effectively doubles the lifetime. However if each event is catastrophic then the reduction is not significant; where this is the case for a specific object it would still require preventive conservation measures to prevent damage. Statistically the baseline period median is significantly different to the near future median. The same is true of the near future and mid-term future median, and also of the mid-term and far future medians.



Figure 6.52: The annual average projected number of damaging events due to a 20% change in relative humidity, in the Library at Brodsworth Hall. Error bars represent the interquartile range.

The 5, 10, and 30% relative humidity change functions can be found in appendix D. They show a similar relation to the impact of climate change as shown here and previously for Knole. In the Library at Brodsworth Hall climate change has no impact on dimensional change as described by the 40% change damage function. There are no transitions projected for the baseline period or any of the future periods.
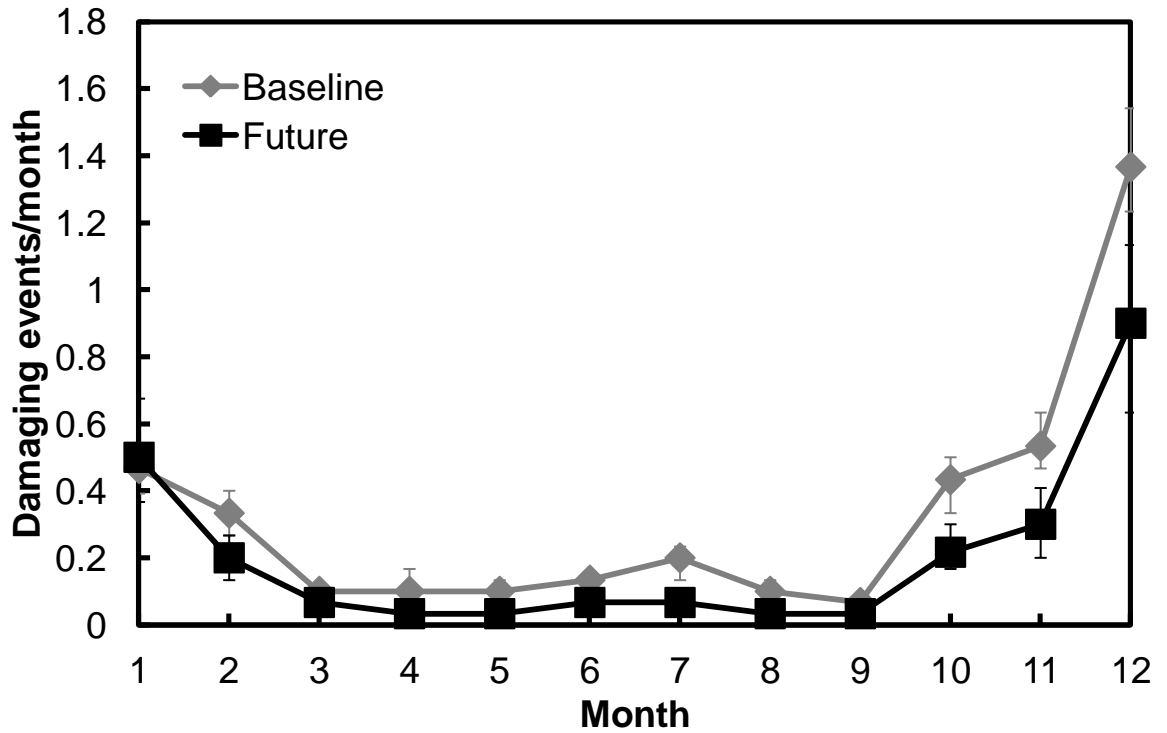


Figure 6.53: The monthly average projected number of damaging events due to a 20% change in relative humidity, in the Library at Brodsworth Hall. Error bars represent the interquartile range.

**Mecklenburg**

**White oak adsorption**

The impact that climate change is projected to have on the number of damaging events to white oak, as caused by adsorption of moisture is shown in figure 6.54. An increase in the number of damaging events is projected, rising from 10 to 15 in the far future, a 50% increase. Most months are projected to have an increasing number of damaging events (figure 6.55); this is more pronounced in the winter months, where the relative humidity is higher. When the relative humidity increases it moves further into the region where less fluctuation is required before a damaging event occurs. The median of the baseline is significantly different to the median of the near future period. The same is also true of the near future median and mid-term future median, and also the mid-term and far future medians. In terms of damage the projected change is likely to be significant, however in terms of conservation measures it is likely to make little difference, and therefore is not significant.
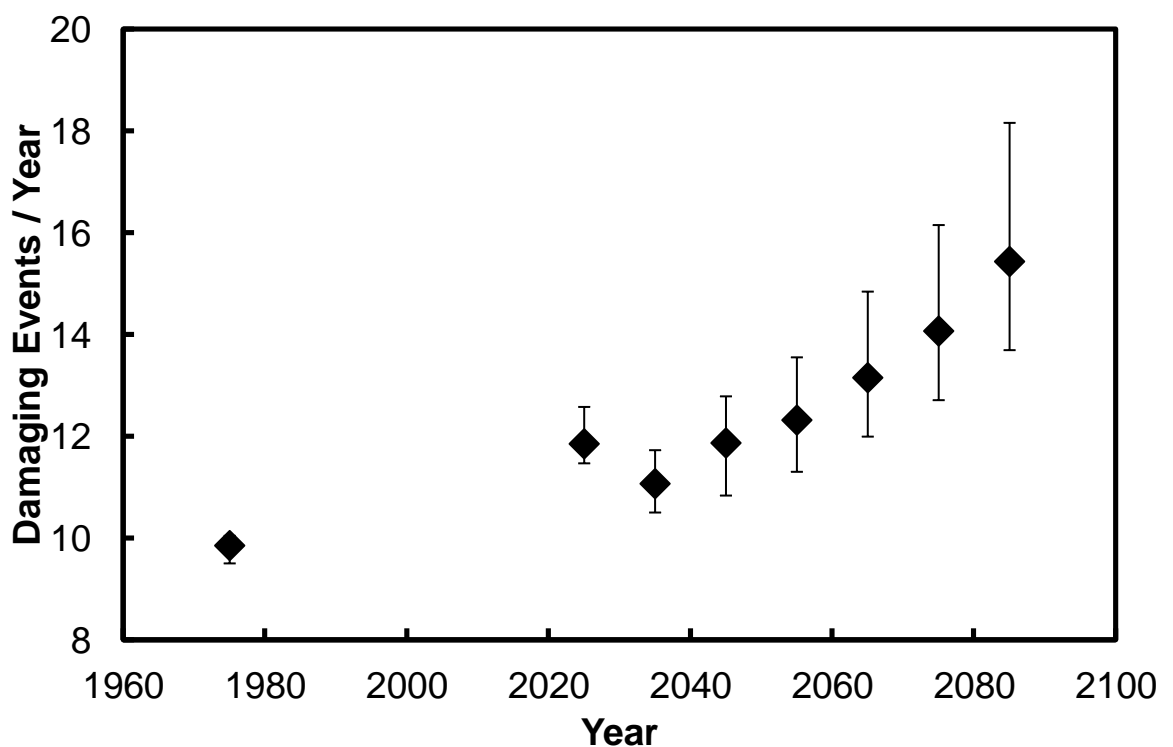


Figure 6.54: The annual average projected number of damaging events to white oak, as caused by adsorption of moisture, in the Library at Brodsworth Hall. Error bars represent the interquartile range.
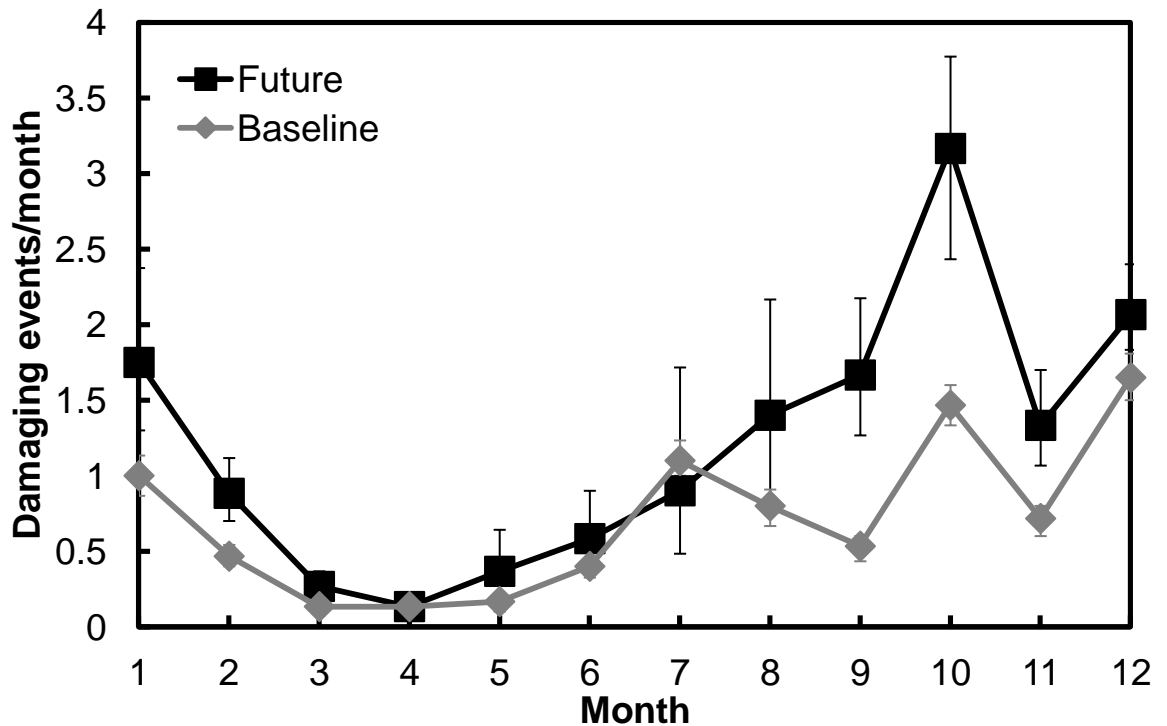
Figure 6.55: The monthly average projected number of damaging events to white oak, as caused by adsorption of moisture, in the Library at Brodsworth Hall. Error bars represent the interquartile range.

Damage from the Michalski dimensional change damage functions is projected to decrease in the future in the Library. However damage from the Mecklenburg dimensional change damage functions is projected to increase. It is possible to determine why the Mecklenburg functions project a decrease in damage, as discussed. The reason behind the decrease in humidity fluctuations has also been discussed previously. This contradiction of damage functions that are essentially for the same thing is a concern. The Michalski function is quite general in its approach, whereas the Mecklenburg function is specific, thus these results are more likely to be relevant, but humidity fluctuations are important.

The remainder of the Mecklenburg damage functions can be found in appendix D, as they add little to the overall discussion.

**Equilibrium Moisture Content**

The impact that climate change is projected to have on equilibrium moisture content in wooden material within the Library at Brodsworth Hall is shown in figure 6.56. This function is highly dependent upon the relative humidity, thus it is no surprise that the EMC is expected to rise in the future. The seasonal analysis (figure 6.57), confirms the correlation with relative humidity, increasing across all months, less so in summer where the increase in relative humidity is smallest. The median of the baseline period is significantly different to the near future period. The same is also true of the near future and mid-term future median, and also the mid-term and far future medians. In terms of damage the increase is relatively small, however it is possible that a critical value is exceeded, and it would be significant. One example would be that particular insect pests require a minimum moisture content of wood, the results here are likely to be too low in this case, but it presents the point that threshold values are important.
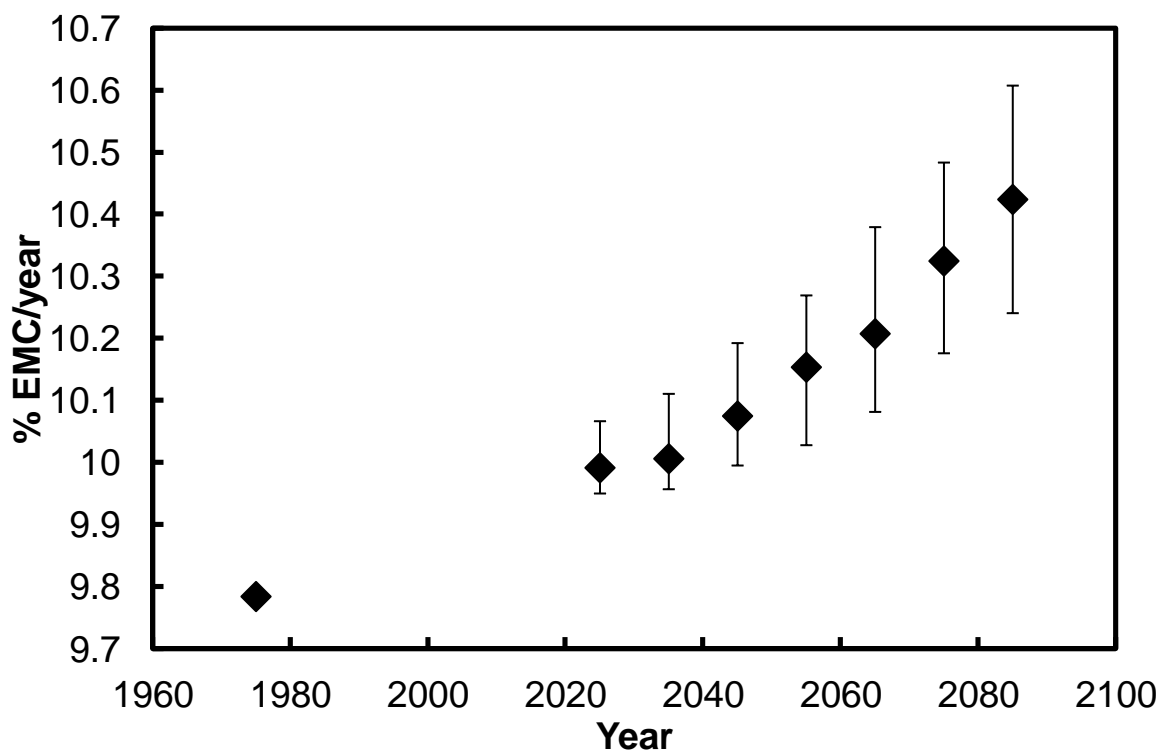


Figure 6.56: The annual average projected % equilibrium moisture content of wood in the Library at Brodsworth Hall. Error bars represent the interquartile range.
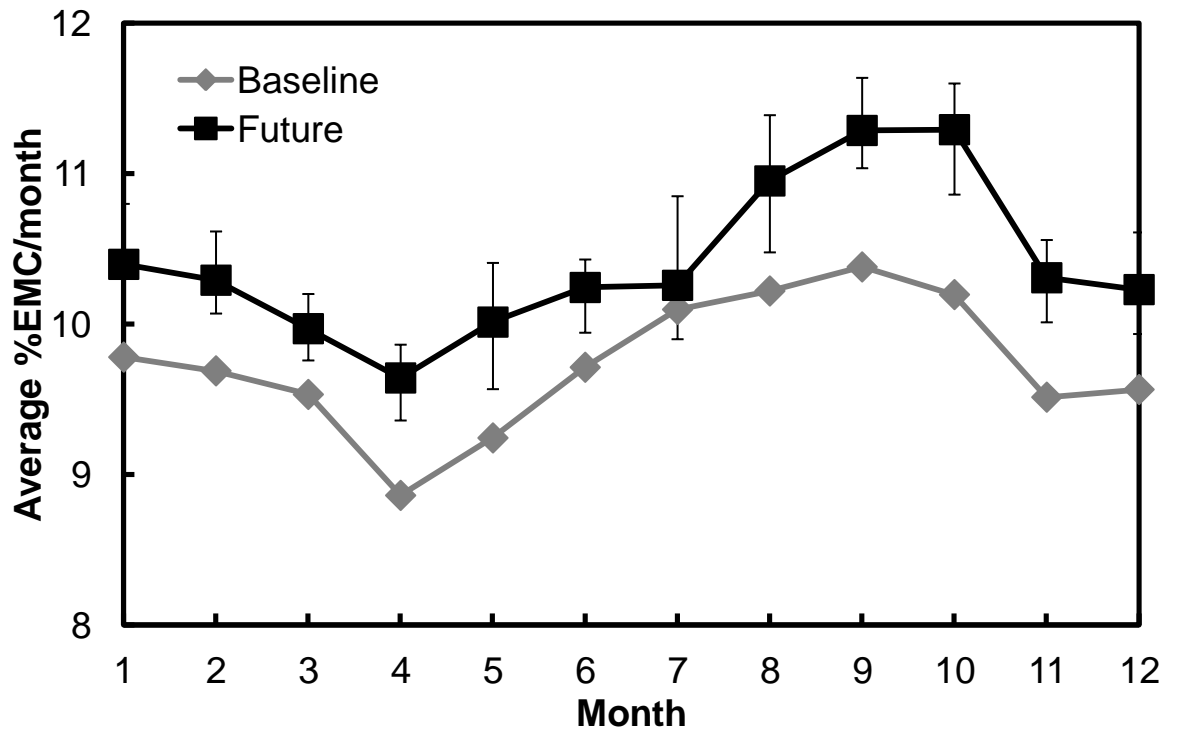
Figure 6.57: The monthly average projected % equilibrium moisture content of wood in the Library at Brodsworth Hall. Error bars represent the interquartile range.

### 6.2.3 Swiss Cottage

The previous two case study locations have looked at all the damage functions described in chapter 4, this was to look at how each may respond to climate change. With this case study location only the damage functions that relate to objects or collections within Swiss Cottage will be investigated.

#### 6.2.3.1 Environment

The impact that climate change is projected to have on the temperature within the Swiss Cottage is shown in figure 6.58 along with the projection outdoors. Both indoor and outdoor temperature is projected to increase, with the indoor temperature less so than that outdoors. The temperature rise indoors is in the region of three degrees, compared to four and a half degrees outdoors. The median of the baseline period, for both indoors and outdoors is significantly different to the median of the near future period. The same is true of the near future median and mid-term future median, and also of the mid-term and far future medians.
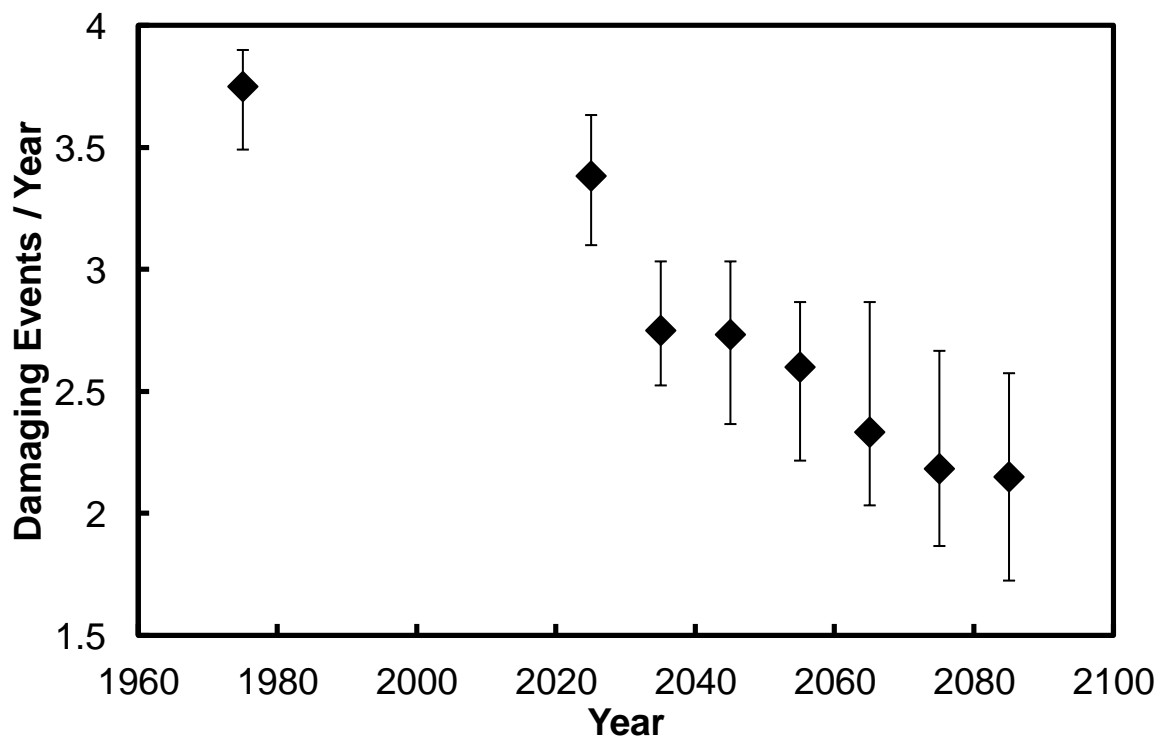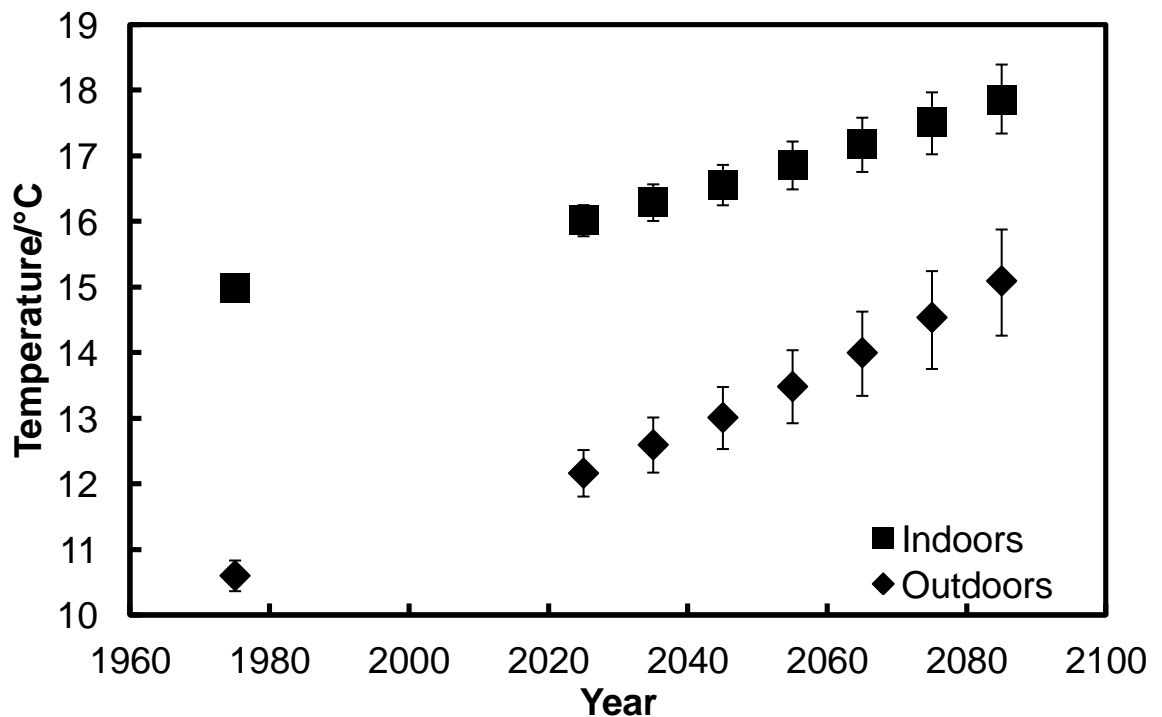


Figure 6.58: The annual average projected temperature in the Swiss Cottage. Error bars represent the interquartile range.

The impact that climate change is projected to have on the relative humidity indoors and out at Swiss Cottage is shown in figure 6.59. Outdoors the relative humidity is projected to decrease in the future, however indoors it is projected to increase. The increase in indoor relative humidity is by 1.7% in the far future. The reason that there is a difference between the direction of change indoors and outdoors is due to the increase in specific humidity, as described previously. The indoor data median of the baseline is significantly different to that of the near future period, however outdoors it is not significantly different. The indoor near future median is significantly different to that of the mid-term future median, and also the mid-term future median is significantly different to the far future median. Outdoors this is not true. The outdoor baseline median is significantly different to that of the mid-term period.
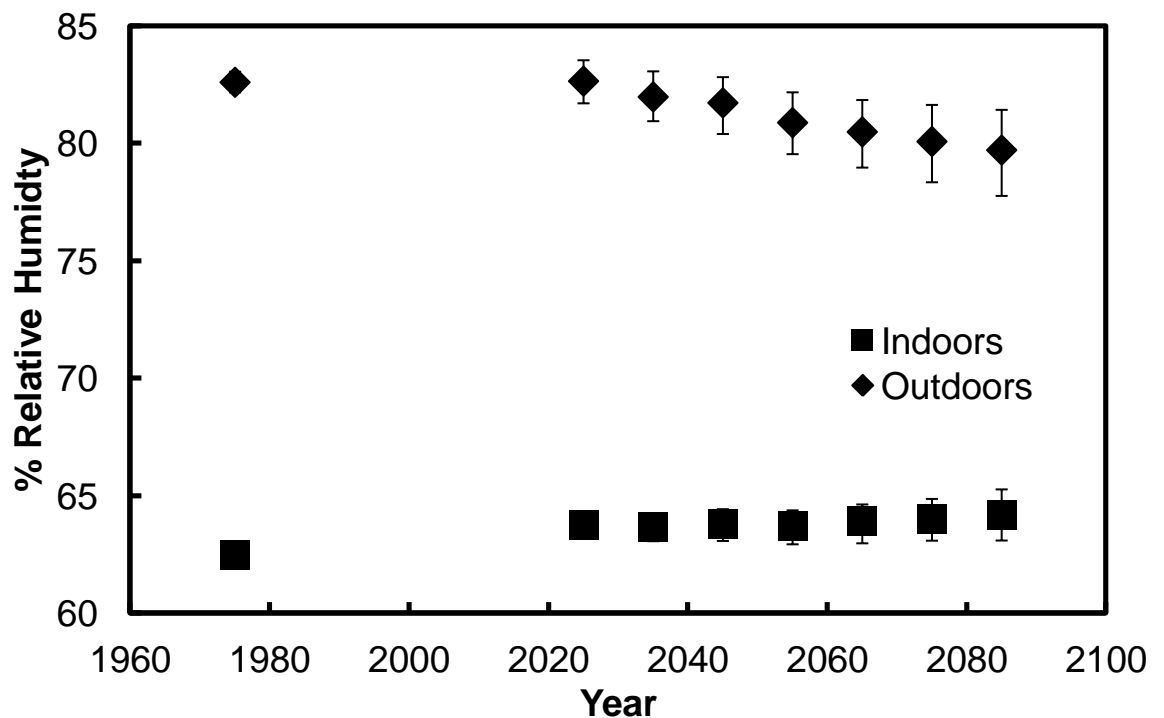


Figure 6.59: The annual average projected % relative humidity in the Swiss Cottage. Error bars represent the interquartile range.

6.2.3.2 Seasonality

The impact that climate change is projected to have on temperature seasonally is shown in figure 6.60. It is projected that there is an increase in temperature in all months in the future. The impact that climate change is projected to have on relative humidity from month to month is shown in figure 6.61. The shifts here are more subtle, with a slight increase in the spring months, and a slightly larger increase in summer months. A slight decrease is projected in the months of November and December.
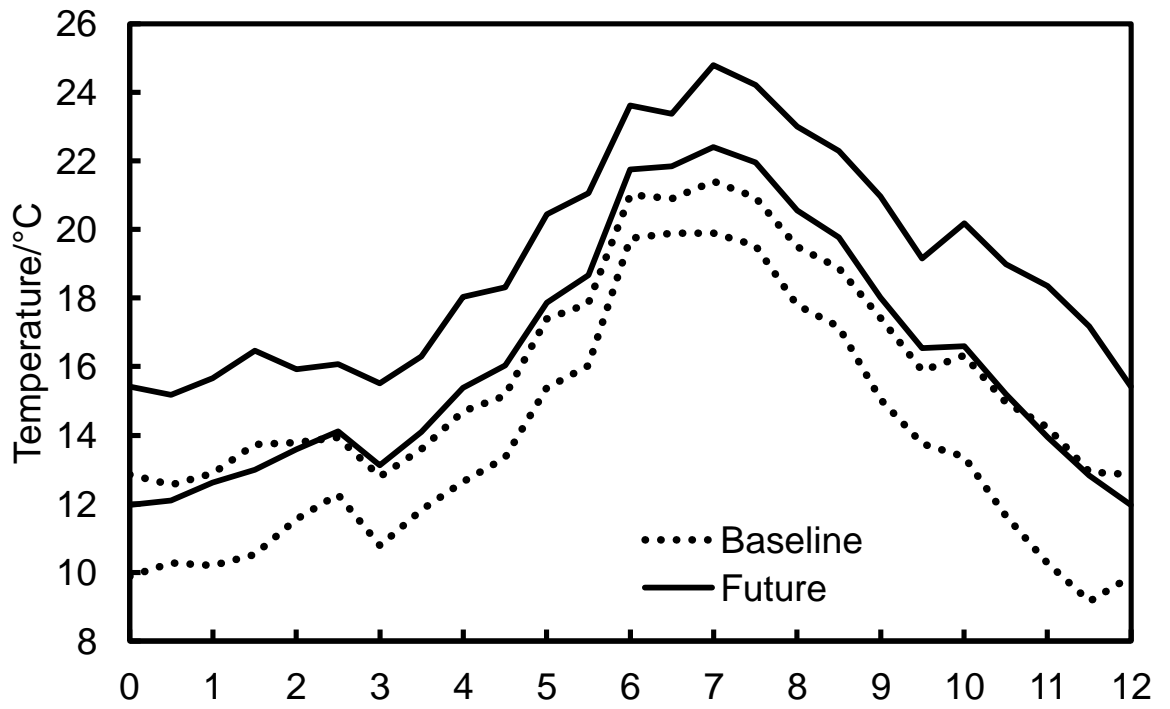
Figure 6.60: The monthly average projected temperature in the Swiss Cottage. The enclosed region represents the interquartile range.
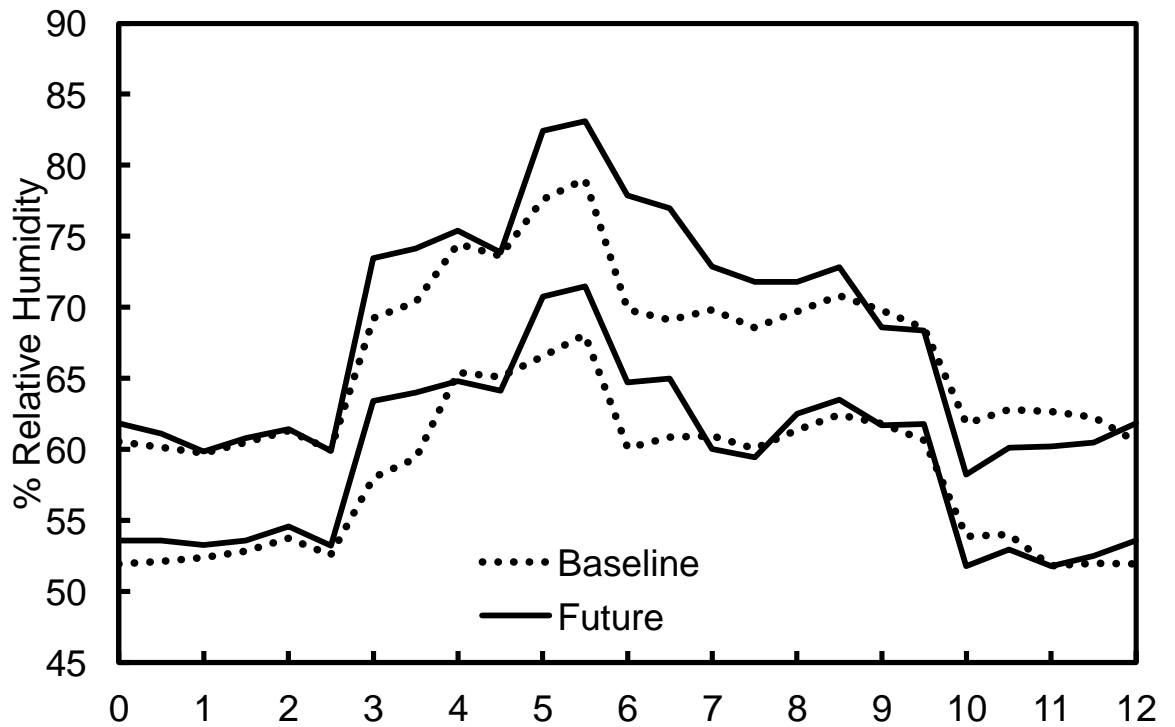


Figure 6.61: The monthly average projected % relative humidity in the Swiss Cottage. The enclosed region represents the interquartile range.

6.2.3.3 Damage

**Daily average temperature >20°C**

The impact that climate change is projected to have on the number of days where the average temperature exceeds 20°C is shown in figure 6.62. It is projected that the number of days exceeding 20°C in the far future is going increase, by more than twice the baseline value. This is a significant increase, and will provide much more heat, that in various ways can act to cause damage. The seasonal analysis of this is shown in figure 6.63. As expected the summer months show an increase in these types of days, but there is also an increase through the months of October, November and December. This is likely to prove significant in terms of damage, as it will prolong the period of activity of insect pests. The median of the baseline period is significantly different to that of the near future period. The same is also true of the near to mid-term future medians, and also of the mid-term to far future medians.

The damage functions of paper and silk used for the Swiss Cottage can be found in appendix D. Again an increase in degradation rate for both is projected.
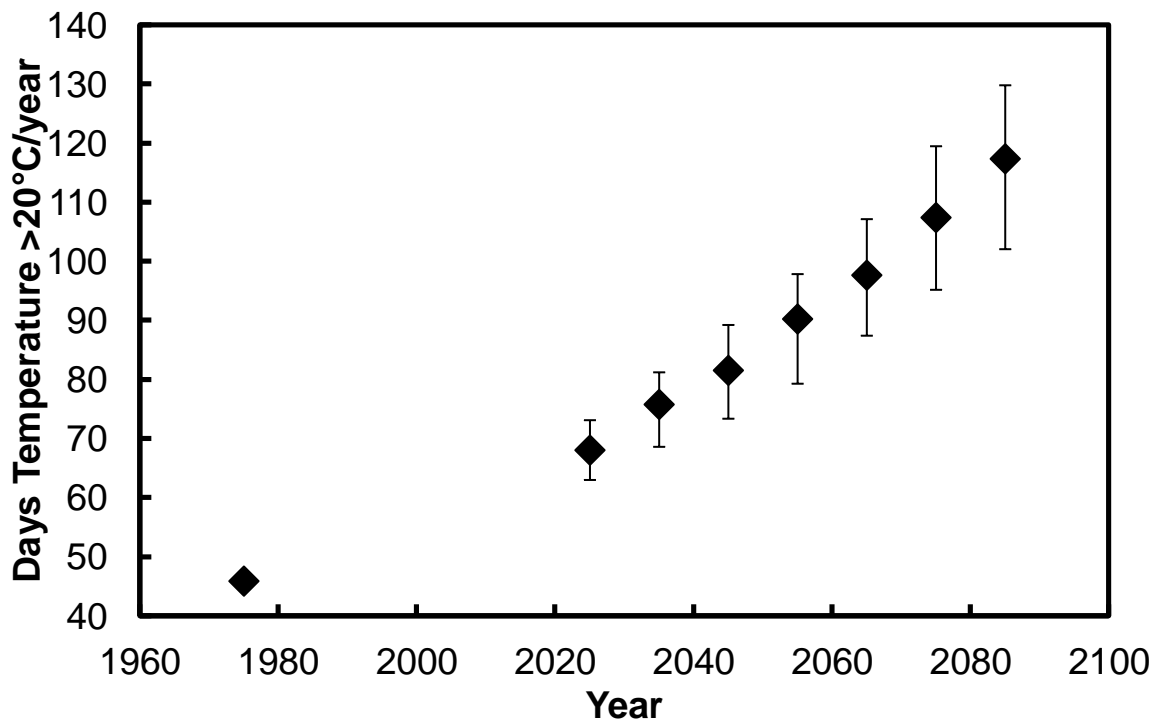


Figure 6.62: The projected annual average number of days exceeding 20°C in the Swiss Cottage. Error bars represent the interquartile range.
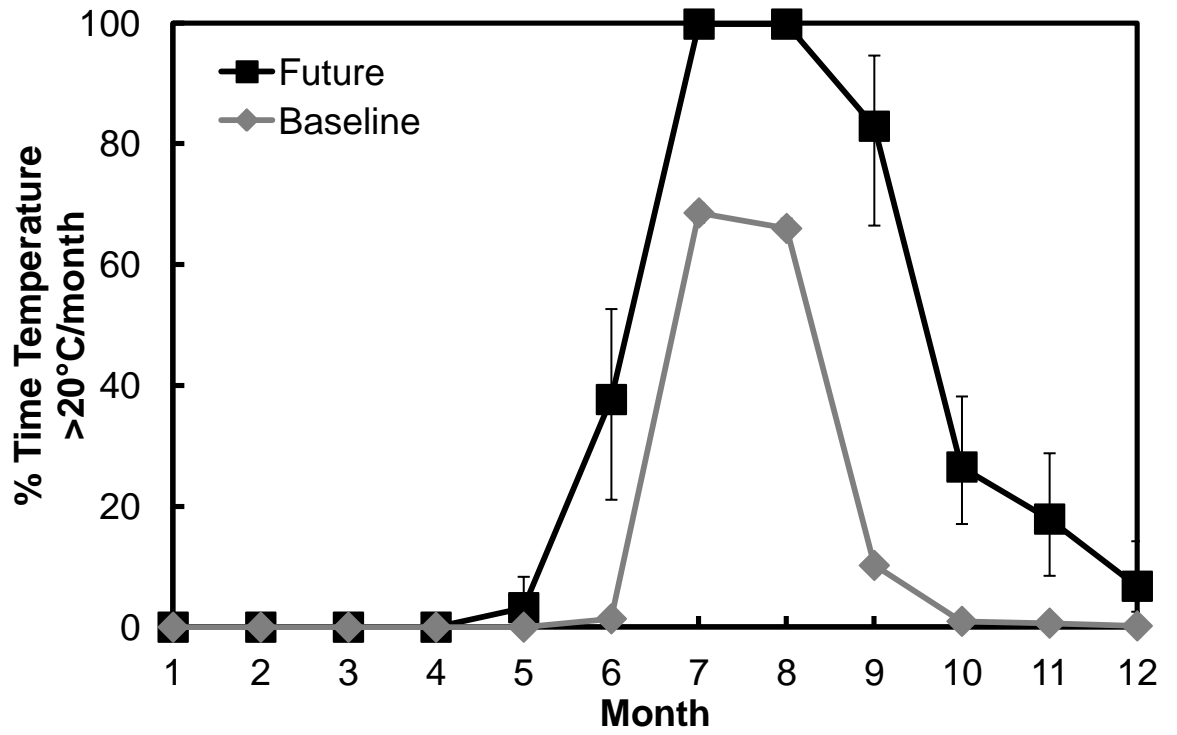
Figure 6.63: The monthly average projected number of days exceeding 20°C in the Swiss Cottage. Error bars represent the interquartile range.

**Dimensional change**

**20% humidity shock**

The impact of climate change on damage to wood caused by dimensional change, as described by this damage function is shown in figure 6.64. It is projected that the number of damaging events will decrease in the far future, resulting in half as many by the end of the century. Given that such a change is likely to cause significant damage to some objects such a reduction will be significant, in terms of damage. However in terms of mitigation of damage it is unlikely to be significant. This is because damage is still occurring; a sensitive object would still need to be protected in an enclosure for example to buffer such humidity changes. Statistically the median of the baseline period is significantly different to that of the near future period. The same is also true of the near future median and mid-term future median, and also the mid-term and far future medians.
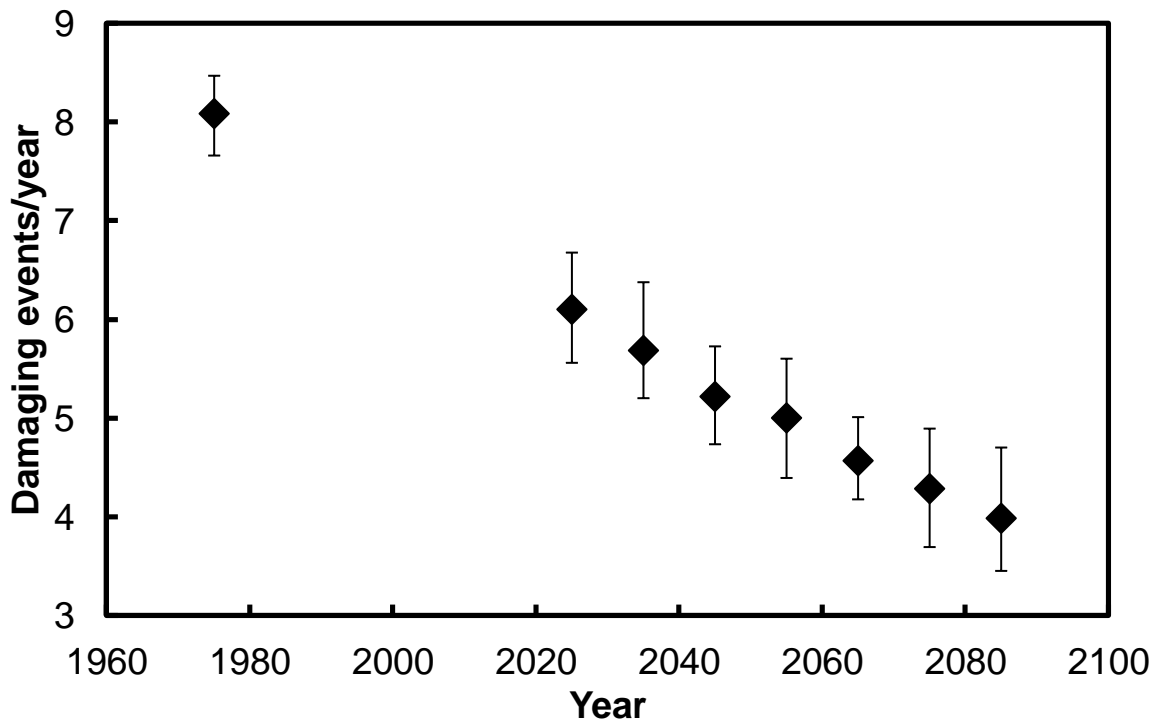


Figure 6.64: The annual projected average number of damaging events due to a 20% humidity change, in the Swiss Cottage. Error bars represent the interquartile range.

**30% humidity shock**

The projected impact of climate change on the dimensional change of wood, as described by this damage function is shown in figure 6.65. A reduction in the risk of a damaging event is projected, this is likely to be significant in terms of preventive conservation measures. The baseline period risk could be considered possible once every two years, but even by the near future this risk has reduced to once every five years. Thus it could be considered possible to remove an object from an enclosure that was there for the purpose of preventing humidity shock, as the risk is considerably lower in the future. Statistically the median of the baseline period is significantly different to that of the near future, the same is true of the near to mid-term future medians. However the mid-term to far future medians are not significantly different, it appears that after the mid-term future period the number of damaging events reaches a plateau. The impact of climate change on the 5 and 10% change functions can be found in appendix D, a reduction in damaging events is projected.



Figure 6.65: The annual average projected number of damaging events due to a 30% humidity change, in the Swiss Cottage. Error bars represent the interquartile range.

**Mould**

**Isaksson**

The projected impact of climate change on mould growth, as described by the Isaksson function, is that there will be no mould growth expected in the future. The baseline period has no expected mould growth, the same is true of all the future periods, the relative humidity within the Swiss Cottage is too low for mould growth to occur.

**Degree days**

The impact that climate change is projected to have on the number of degree days within the Swiss Cottage is shown in figure 6.66. The number of degree days is projected to more than double by the end of the century. This is likely to have a significant impact on damage, one example would be damage caused by insect pests. Statistically the median of the baseline period is significantly different to that of the near future period. The same is also true of the near future median and mid-term future median, and also the mid-term and far future medians. The seasonal analysis of this function has not been carried out, but is likely to be very similar to that in figure 6.47, indicating a prolonged period of months from which degree days arise.
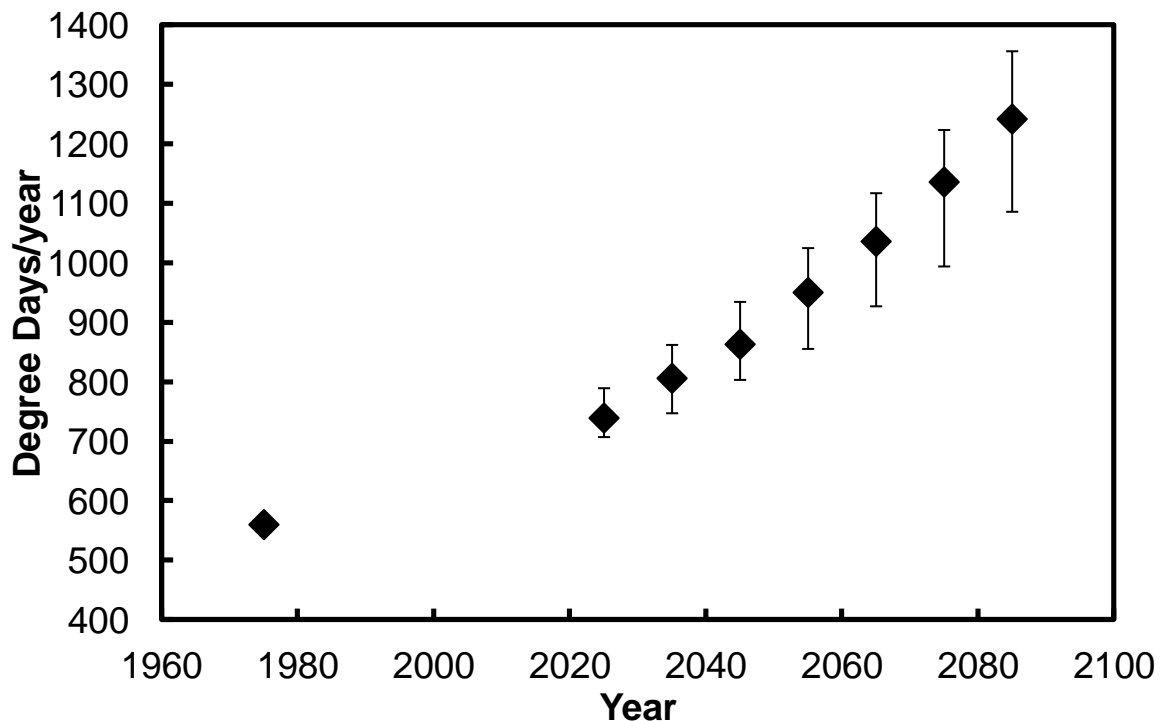


Figure 6.66: The annual average projected number of degree days in the Swiss Cottage. Error bars represent the interquartile range.

## 6.3 Results – Location Comparison

As discussed previously it is also important to compare the results of each damage function between the locations. This may help identify significant risks at certain locations, and how some locations are impacted upon differently to others, and help determine the reasons driving these differences.

### 6.3.1 Environment

Temperature

The comparison of projected temperature across all four locations is shown in figure 6.67. The Swiss Cottage and Brodsworth Hall are considerably warmer than the two rooms at Knole. The projections for the two Knole rooms and the Swiss Cottage tend to follow the same trend in future. Brodsworth however does not, this is likely to be due to the fact that the room has conservation heating, and that this is not taken into account in the transfer function.
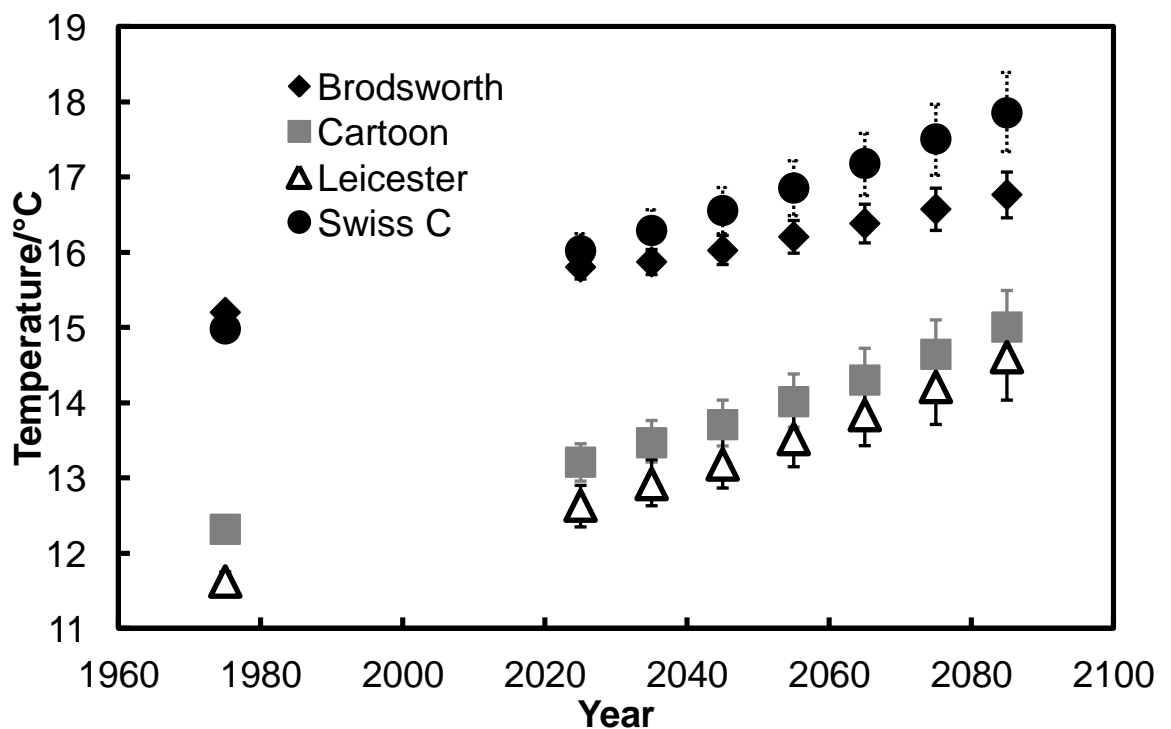
Figure 6.67: The annual average projected temperature across all locations. Error bars represent the interquartile range.

Relative Humidity

The comparison of projected relative humidity at all four locations is shown in figure 6.68. Each location has a different level of relative humidity to the other locations; this may present interesting results for those functions dependent on relative humidity. With the exception of Brodsworth the relative humidity is largely projected to stay the same, as an annual average.
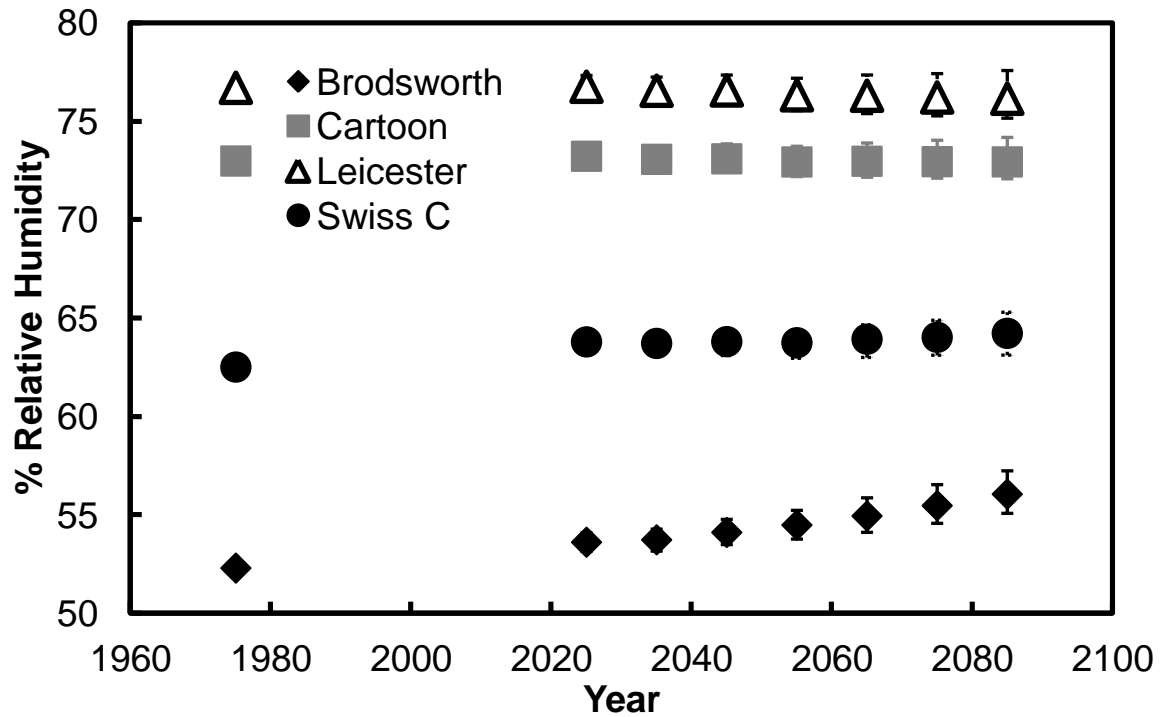


Figure 6.68: The annual average projected % relative humidity across all locations. Error bars represent the interquartile range.

### 6.3.2 Damage

The comparison of projected damage is carried out across the locations. Where the comparison does not add to the discussion it is presented in appendix D. One example is where projections for Brodsworth show no damage, leaving the two Knole rooms which have been compared previously.

**Daily average temperature >25°C**

The comparison of the number of days where the average temperature exceeds 25°C is shown in figure 6.69. Although the Library at Brodsworth has a higher annual average temperature than the two Knole rooms, they are projected to have a greater number of days with a temperature exceeding 25°C, although the opposite is true for days over 20°C. The reason for this is due to the nature of the annual average, the Knole rooms have a larger range of temperature than the Library at Brodsworth Hall, as the two seasonal analysis figures show. The summer temperatures of the two Knole rooms exceed 25°C, and the Library does not, explaining the result here.
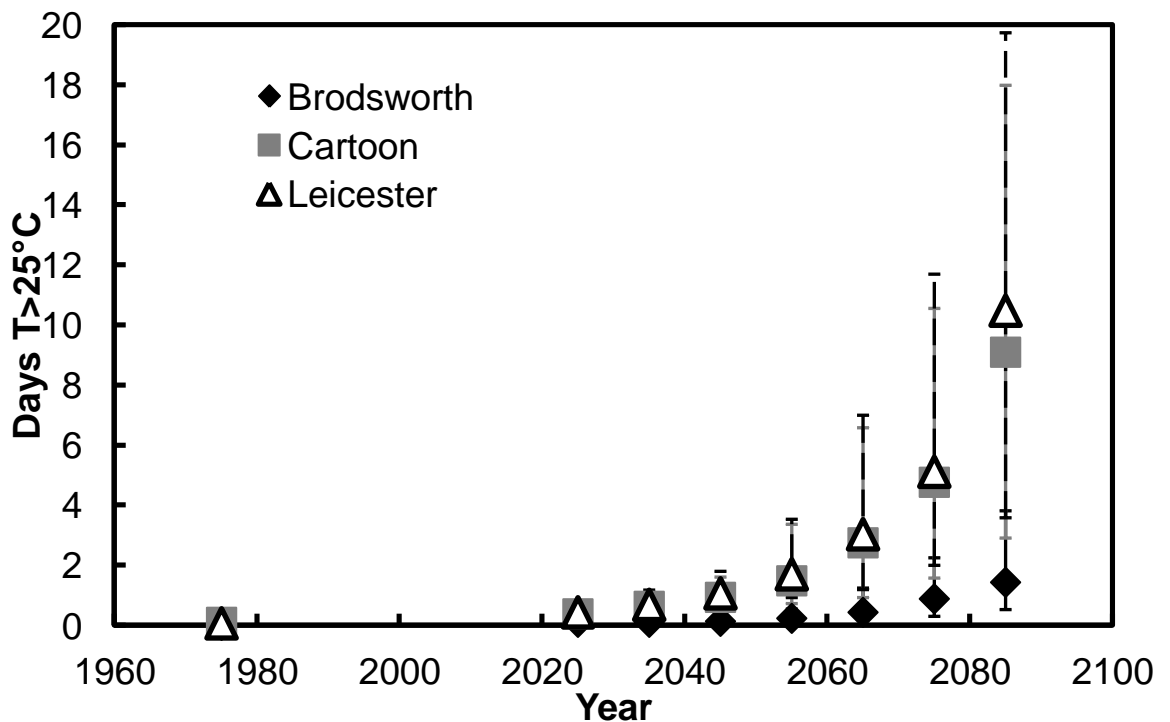


Figure 6.69: The annual average projected number of days where the daily average temperature exceeds 25°C, across all locations. Error bars represent the interquartile range.

**Zou**

Comparison of the results from the Zou damage function for paper is shown in figure 6.70. A similar increase in rate is projected at all locations. While temperature is a dominant factor in this function relative humidity also is important, this is why the projection for the Library at Brodsworth Hall is lower than the other locations although its temperature is similar to that in the Swiss Cottage.
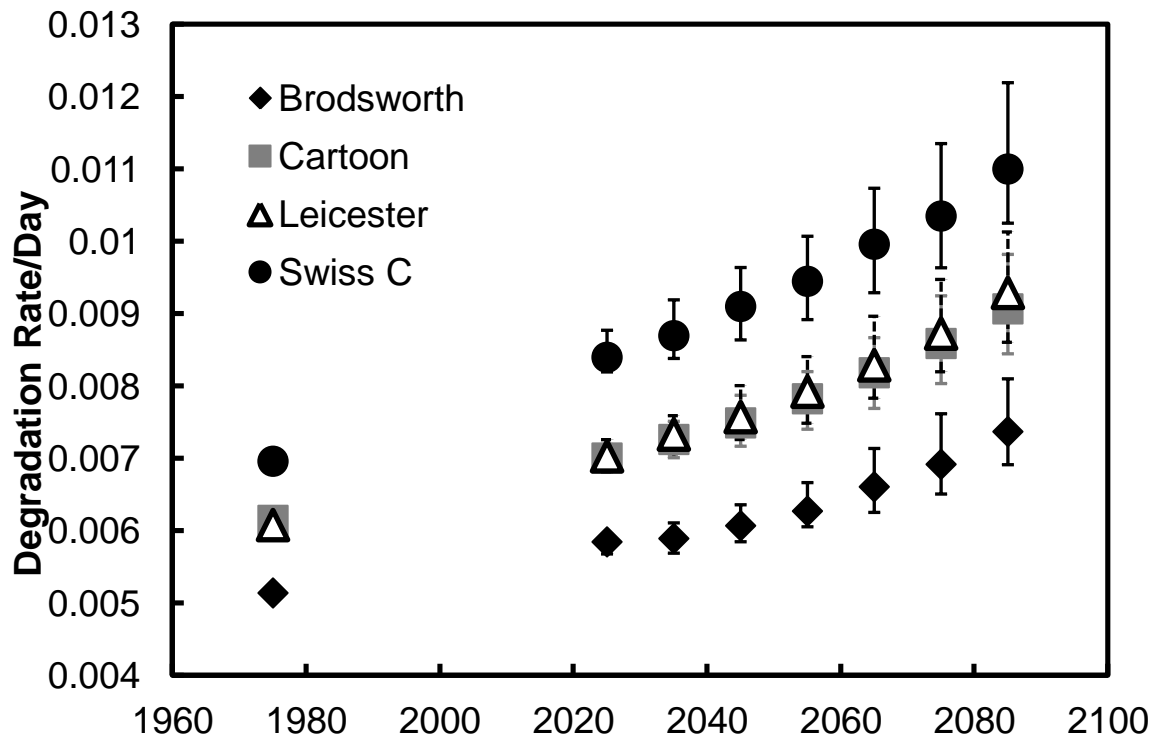


Figure 6.70: The annual average projected chemical degradation rate of paper across all locations, using the Zou function. Error bars represent the interquartile range.

**Pretzel**

The comparison of the results of this paper damage function is shown in figure 6.71. The results at Brodsworth Hall are considerably lower than those in the two Knole rooms; this is further evidence of the importance of relative humidity for this function. Comparing the temperature the Library is significantly warmer; however the relative humidity is significantly lower. This function weights relative humidity as the dominant factor, in contrast to the other paper damage functions, thus resulting in the lower level of degradation projected here.
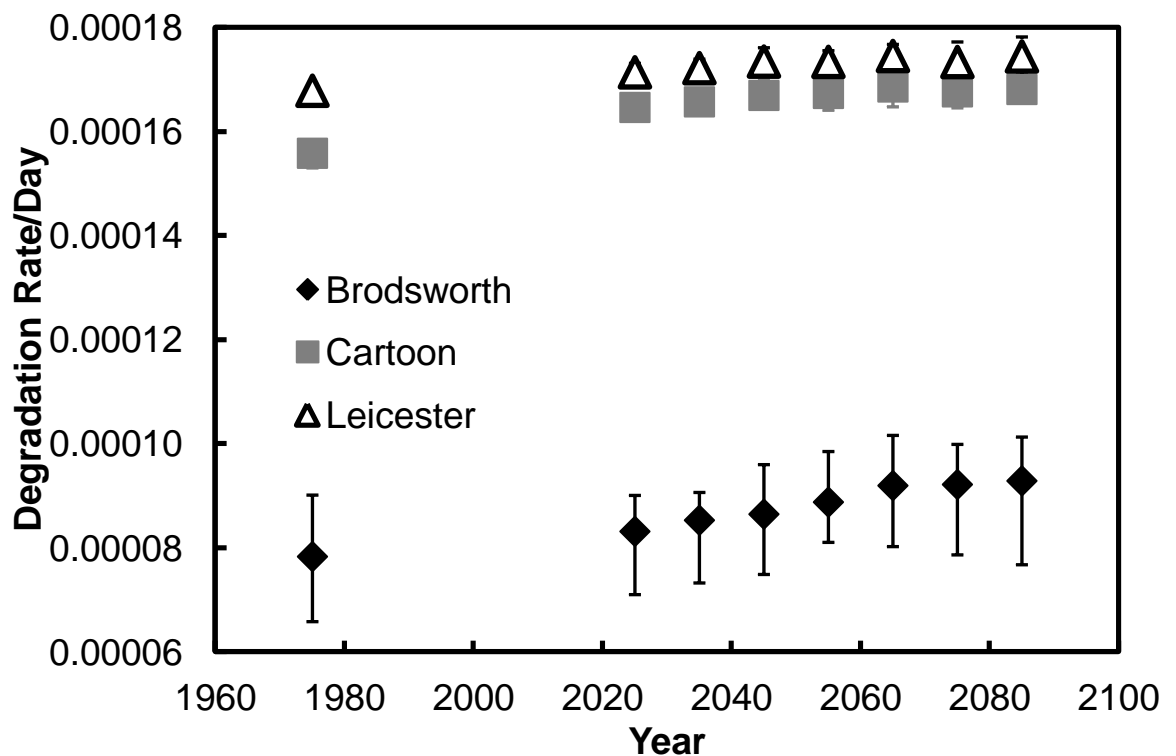


Figure 6.71: The annual average projected chemical degradation rate of paper across all locations, using the Pretzel function. Error bars represent the interquartile range.

**Silk isoperm**

The results of the silk damage function across four locations are compared in figure 6.72. All locations indicate an increase in the degradation rate, as expected with the increase in temperature expected. There is a similar response of the projected rate here compared to that for paper as described by the Zou function for Brodsworth, where the rate there is lower than other locations, because of the lower relative humidity in the Library.
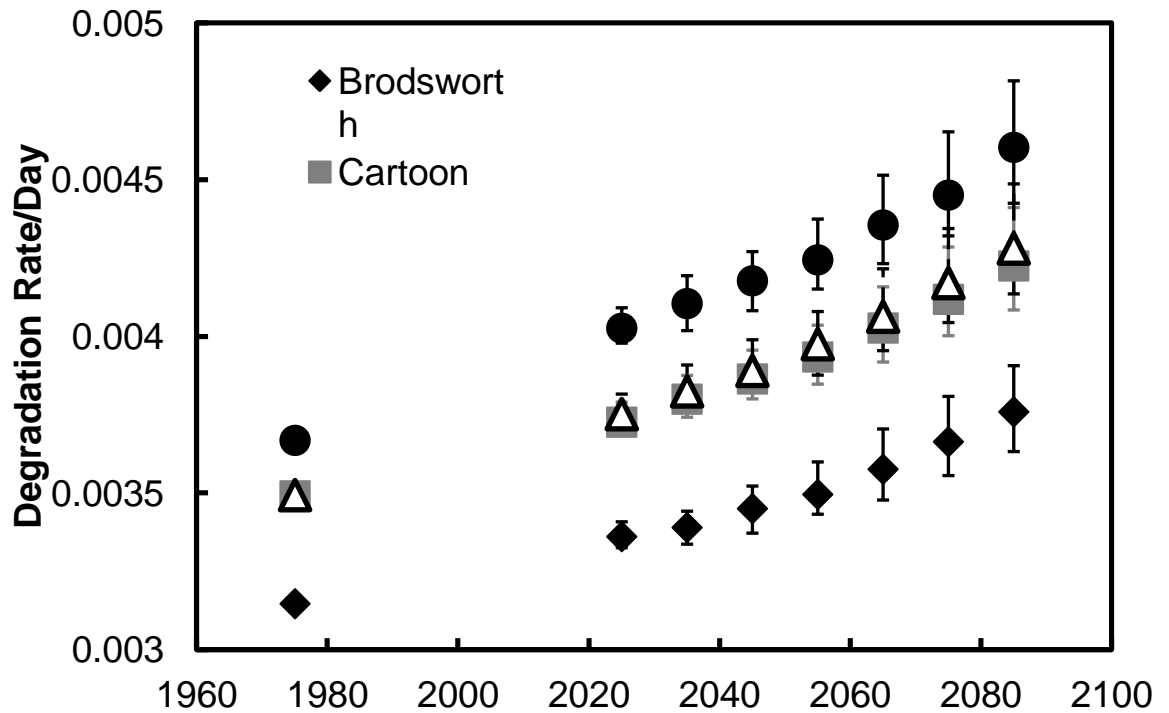


Figure 6.72: The annual average projected silk chemical degradation rate across all locations. Error bars represent the interquartile range.

**Salt transitions – thenardite/mirabilite**

The comparison of the results from this function is shown in figure 6.73. The projected changes appear subtle, the two Knole rooms are projected to decrease slightly, and Brodsworth is projected to increase. The difference in results, both magnitude and direction of change can be described by the damage function, which is determined by temperature and relative humidity.
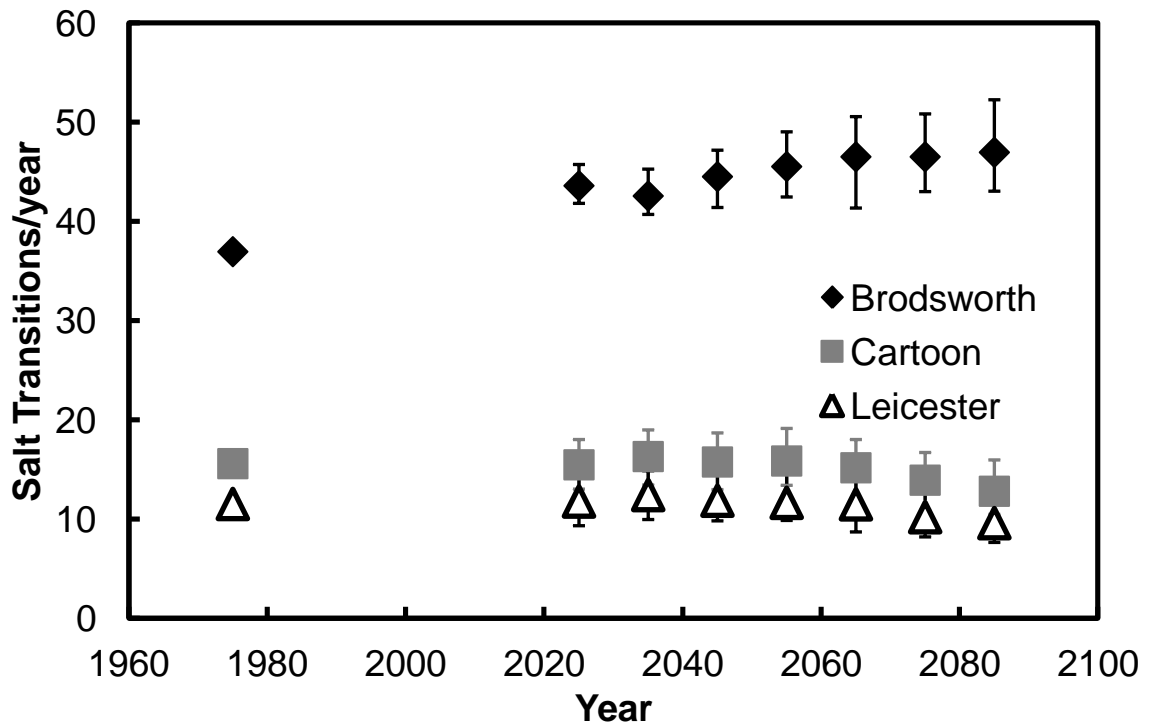


Figure 6.73: The annual average projected number thenerdite mirabilite salt transitions across all locations. Error bars represent the interquartile range.

**20% Humidity Shock**

The comparison of the results for this function is shown in figure 6.74. The Leicester Gallery at Knole is projected to have more damaging events than the other locations. The reason for this is unknown, one possibility is that the air tightness (or air exchange rate) of the building is poor, and thus does not buffer the environment as well as other rooms. There is evidence of this in the Leicester Gallery, how this compares to the other locations is unknown.
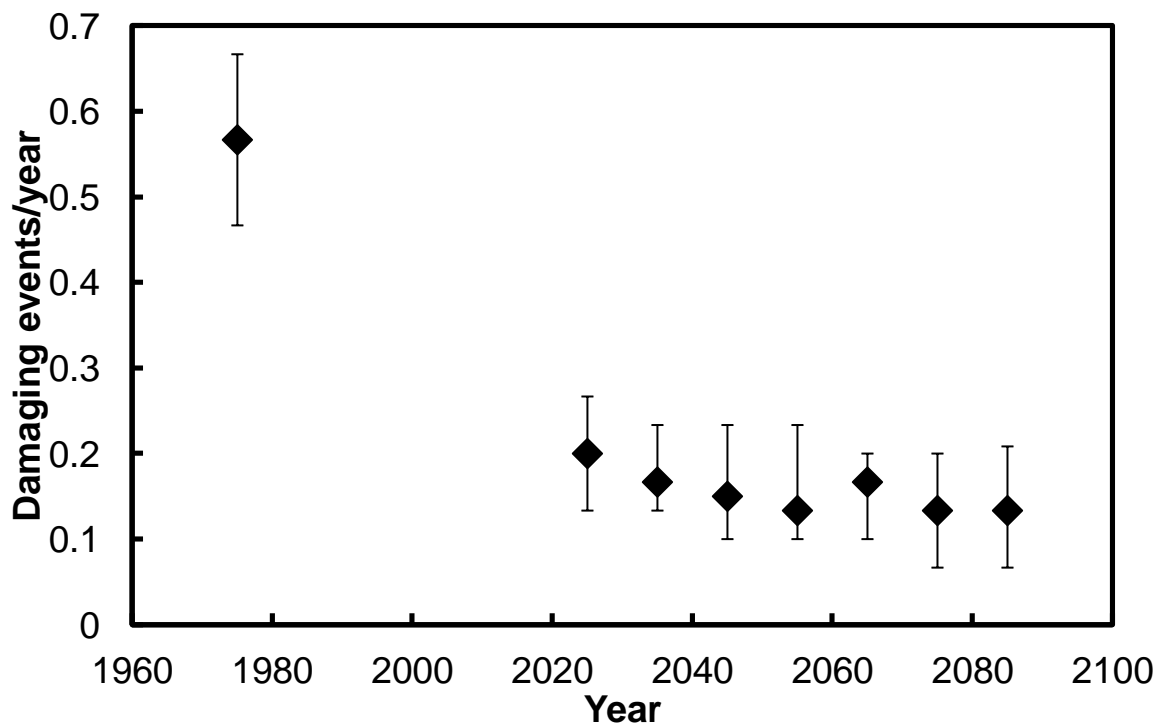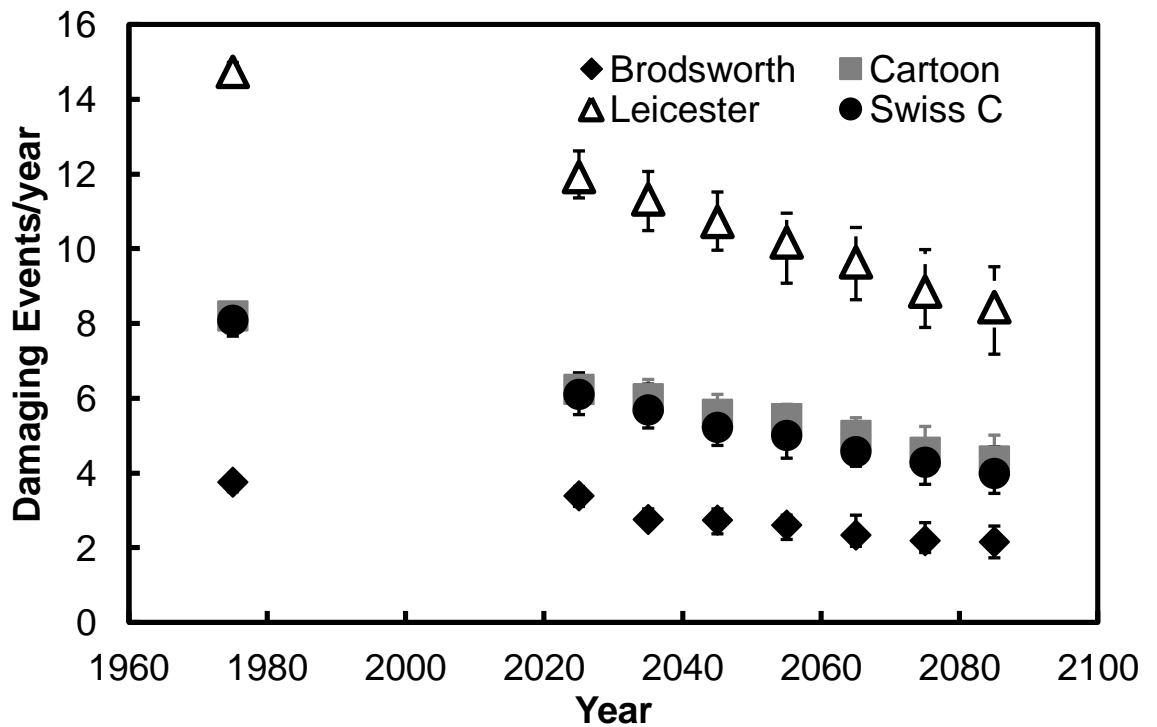


Figure 6.74: The annual average projected number of damaging events, due to a 20% humidity change, across all locations. Error bars represent the interquartile range.

**White oak total**

The total number of damaging events to white oak for three locations is shown in figure 6.75. Brodsworth is projected to have a significantly lower number of damaging events, across the whole data period. This is due to the relative humidity of the Library being considerably lower than that in the other rooms. This helps show how damage can be reduced significantly, by a shift in relative humidity. The application of conservation heating at Knole is likely to reduce the high number of damaging events projected here. Chapter 7 presents the theoretical application of conservation heating at Knole, and how its effectiveness may change in the future due to climate change.
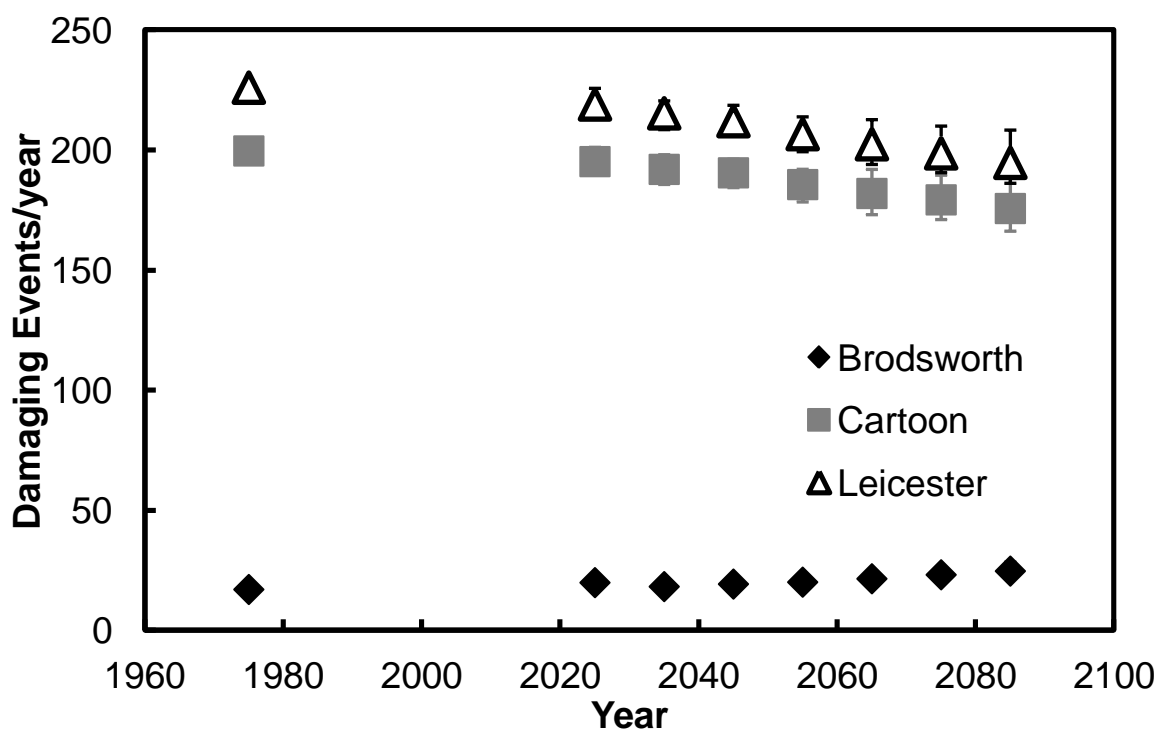


Figure 6.75: The annual average projected number of damaging events to white oak across all locations. Error bars represent the interquartile range.

**Degree days**

The comparison of degree days across the four locations investigated is shown in figure 6.76. The results are similar to those for temperature described previously, all show a substantial increase.
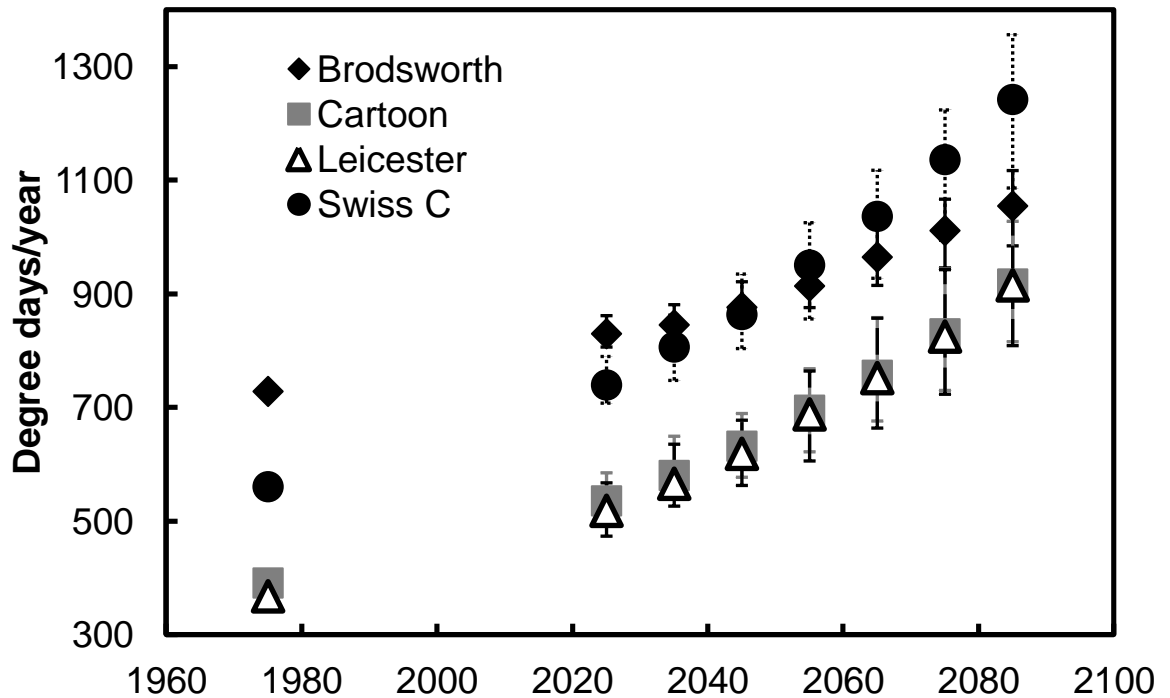


Figure 6.76: The annual average projected number of degree days across all locations. Error bars represent the interquartile range.

## 6.4 Discussion

Throughout the results some discussion points arise on a number of occasions, also similarities can be drawn with the discussion in the previous chapter (5.5). Thus the first point of discussion is the significance of projected changes with respect to damage or management strategies. Again this has not been straightforward, it was not as challenging as in the previous chapter, and on occasions it is possible to determine whether a change is significant, for instance the onset of mould growth is clearly a significant change. It has clearly been beneficial to be able to relate to specific examples at the locations presented. However, it has not always been possible to determine the significance of a projected change. This has been discussed in greater detail in the previous chapter, and is an issue with future projections. Another aspect that is not immediately obvious to understand is

the difference between relative change and absolute change. Further analysis will be carried out in section 6.5 to try and help determine the significance of future projections, and to try and help understand the difference between relative and absolute change.

The importance of treating each room individually has been clearly shown. This is most important when assessing damage that is driven by relative humidity. The Cartoon and Leicester Galleries are a prime example, each are only a couple of percent relative humidity different, with respect to annual averages, but the projected mould growth in particular, amongst other damage, is very different. Thus where threshold values are important it is a necessity to look at individual rooms, as it is possible that damage can be amplified. The comparison between rooms also provides evidence that this is important. In general, most changes projected are in the same direction at the properties, with the exception of salt transitions and dimensional change, both humidity driven damage mechanisms.

A possible problem has been identified with the Isaksson damage function. The sum to germination of mould growth is allowed to continue to grow over the critical value of one. This can grow significantly, so that the negative feedback, when conditions are not ideal, has little effect, resulting in an over prediction of days where mould growth is possible. Perhaps this is why Hukka and Viitanen (1999) include a maximum mould growth value in their damage function.

It is important to remember the limitations and assumptions of the damage functions used in this work, which are described in chapter 4. The mould functions for example are for specific mould species, and the Mecklenburg functions assume a tangential direction of restraint. Investigation of other species, or directions of restraint could form further work. The limitations of the climate output and building simulation technique are also important considerations.

For the Cartoon Gallery at Knole two separate projections of future change have been produced, one using the Hadley output and one with the UKCP09 weather generator output. These will be briefly compared here, although it must be remembered that the two climate outputs use a different emission scenario, which may account for some difference, thus only the change of direction will be compared. In general most projections are similar, as temperature is projected to increase and the relative humidity projections are similar also. All of the functions related to chemical degradation are projected to increase in the future, as are the mould damage function projections. The projections of salt transitions tend to agree but sometimes the changes are slight and have been shown as no change. Although they could be interpreted as either increase or decrease, these match with the

UKCP09 weather generator projections. For the dimensional change of wood projections, however, there is a significant difference. The UKCP09 weather generator projections suggest a decrease in damaging events, whereas the Hadley output projections suggest an increase in damaging events. This could be related to the decrease in relative humidity fluctuations associated with the UKCP09 weather generator output. Further work is required to understand whether this is a robust change or an artefact of these particular projections.

## 6.5 Significance

This chapter and the previous discuss the significance of the projected impacts of climate change. Occasionally it is straightforward; some changes when in context are obviously significant, in terms of damage. This work has taken a generic approach so there are not always examples to relate the projected changes to, thus determining the significance can be difficult. This can also relate to the damage function itself, some are easy to understand, the Lipfert damage function of stone recession outdoors (Lipfert, 1989), describes precisely the loss in millimetres that is expected, however with salt transitions for example it isn't known exactly how damaging one transition may be, and it is not always certain that damage is actually caused. The changes can also be significant with respect to different aspects, for example a change may significantly affect the damage caused to a collection, and thus it is a significant change. However, the management strategy in place may also mitigate against the projected change in damage, therefore it would not be a significant change with respect to the management strategy. Work in this chapter will help to clarify the issue of significance, and quantify some of the previous results.

Another important point to address is the difference between absolute and relative change. The Lipfert function is an example of an absolute change, it predicts recession of stone in millimetres. None of the damage functions used in this work present an absolute change of damage in this way, the absolute number of transitions or events are determined, but in relation to damage this is a relative change, i.e. the damage will increase by 20% of the baseline value. Assessing some of the damage functions and trying to relate a relative change to an absolute change may help in determining the significance of the predicted change.

One approach that could help attribute significance of predicted changes is the back casting of the environment and damage, which can then be related to projected future changes. This will be discussed here.

A variety of different projections have been determined at different properties, but in relation to each type of damage it is not immediately apparent which poses the greatest risk. It is important to understand which types of damage will be the most important in the future, therefore informing future priorities. There are some important questions such as is there likely to be a shift from current pressures, which would likely have a significant impact on overall management strategies.

### 6.5.1 Relative and absolute change

A number of damage functions, mainly those dealing with chemical degradation, utilise a relative change. Here some of the projected changes are investigated to try determine the absolute change in damage that climate change is projected to have.

Four different paper damage functions have been used, three of which in general project an increase in damage in the future. By normalising the estimated damage from each function it is possible to compare the projected relative degradation rates from each separate function. Each of the damage functions is compared, for the Cartoon Gallery and Leicester Gallery at Knole, in figures 6.77 and 6.78 respectively. The baseline value for each function was taken as 1, and the change relative to this is shown.

In the Cartoon Gallery the three similar functions, Zou, TWPI and Isoperm all show a similar increase in future, the normalised rate increases to approximately 1.5 times that of the baseline period in the far future. The Zou damage function is projected to increase by 1.48 times the baseline value, the TWPI function projects an increase by 1.45 times the baseline, and the Isoperm function projects a 1.51 increase in the rate of chemical degradation. These are all somewhat similar, taking into account the interquartile range, each of the functions overlap, for each of the time periods. The Pretzel damage function is not considered as it takes a different approach to the other three.

The result of this analysis is that future degradation of paper will be approximately 1.5 times faster by 2085. The rate increase of the damage functions for each time period is shown in table 6.1.

The normalisation of the results has changed the relative rate into an absolute change in rate. Even though the degradation rates used are relative the rate change determined is absolute. This is because the relative baseline and relative future rate are both linked by the underlying damage function. There is also an unknown baseline absolute rate, and an unknown future absolute rate, also linked by the same damage function. Therefore an

increase of the baseline by 1.5 times is an absolute rate change, because the absolute rate also increases by the same amount.
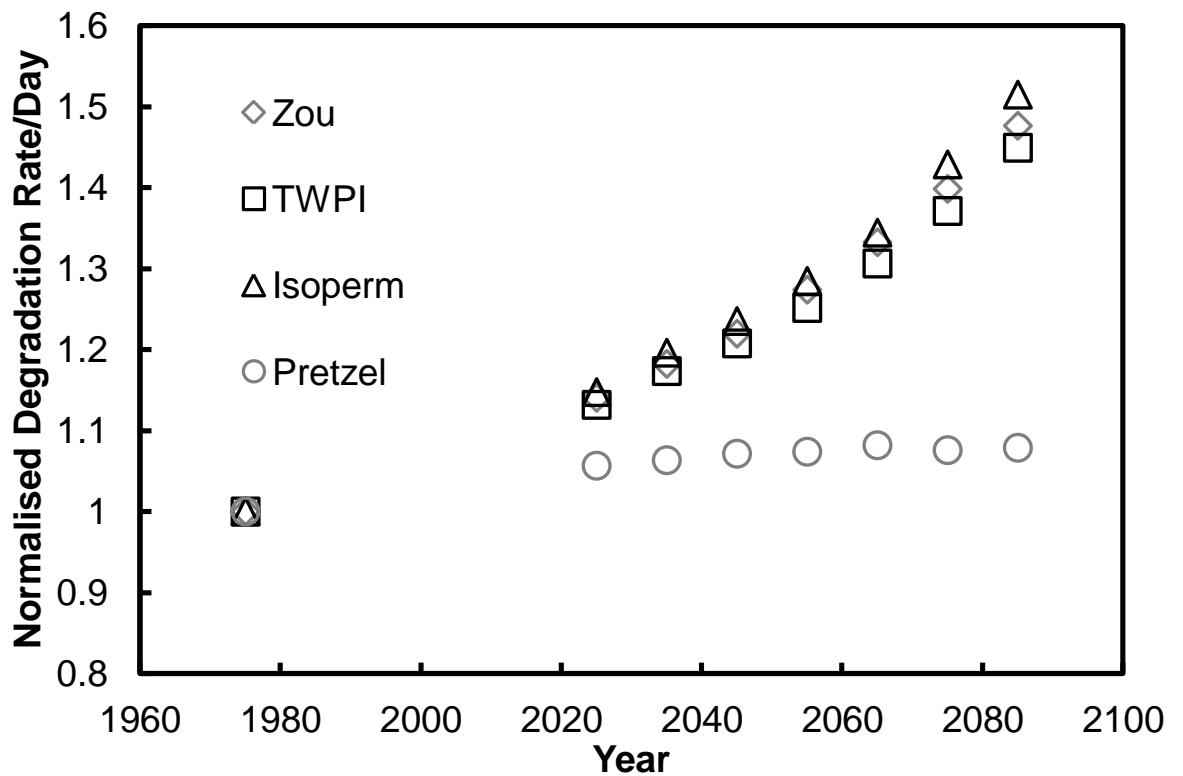


Figure 6.77: Comparison of the paper damage functions for the Cartoon Gallery. Error bars are excluded for clarity.

Table 6.1: Normalised degradation rates of paper

|  | Zou | TWPI | Isoperm | Pretzel |
|---|---|---|---|---|
| **1975** | 1.00 | 1.00 | 1.00 | 1.00 |
| **2025** | 1.14 | 1.13 | 1.15 | 1.06 |
| **2035** | 1.18 | 1.17 | 1.20 | 1.06 |
| **2045** | 1.22 | 1.21 | 1.24 | 1.07 |
| **2055** | 1.27 | 1.25 | 1.28 | 1.07 |
| **2065** | 1.33 | 1.31 | 1.34 | 1.08 |
| **2075** | 1.40 | 1.37 | 1.43 | 1.08 |
| **2085** | 1.48 | 1.45 | 1.51 | 1.08 |

In the Leicester Gallery (figure 6.78) there is a similar  increase in the projected degradation rate of paper, this time with just over a 1.5 times increase of the baseline value. While this is a similar result to that of the Cartoon Gallery it is not directly comparable. The normalisation procedure is based on the baseline value of each individual damage function. As the baseline value changes between each room a comparison between rooms is not applicable. This must be carried out on a room by room basis, when assessing multiple functions. It is possible to assess the same function at different locations. The three main functions are similar; therefore only one will be normalised and compared across locations, to compare the projected change.
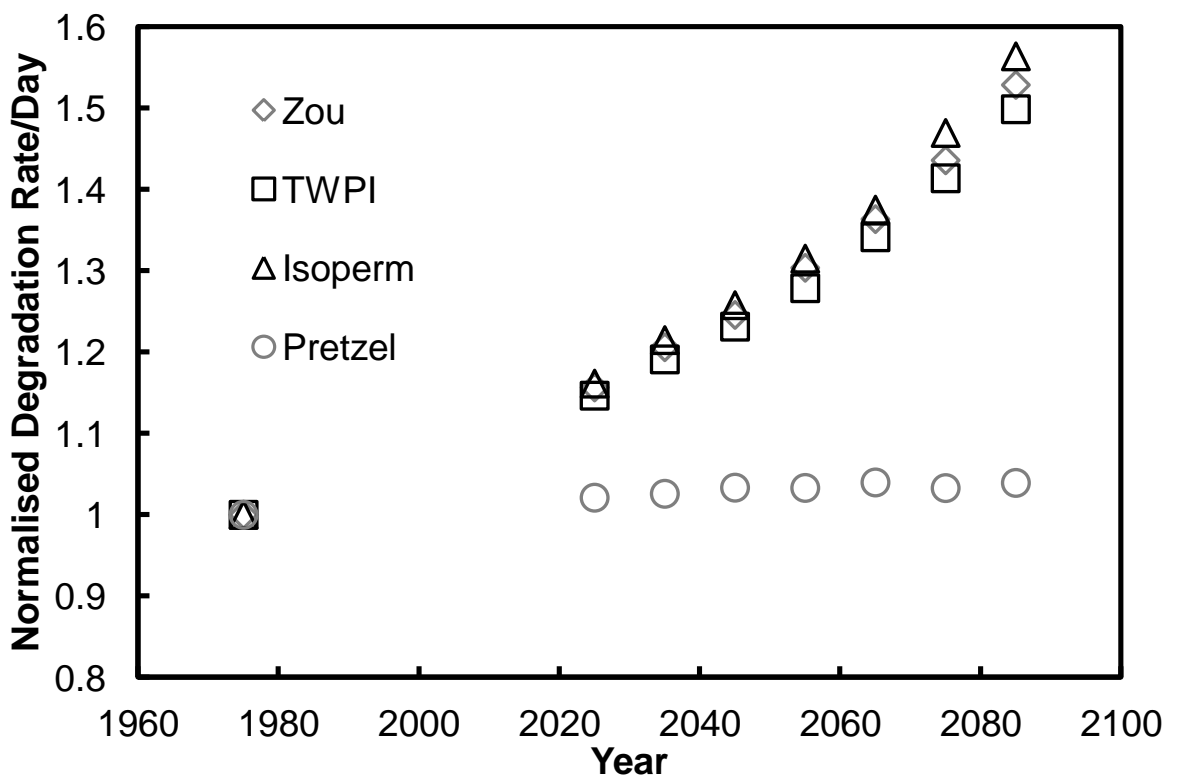


Figure 6.78: Normalised paper damage function results, in the Leicester Gallery at Knole.

The Zou damage function is chosen as the function to compare across the different locations, as it is the only function utilised for the Swiss Cottage. Each location is normalised to its own baseline, to determine which location has the greatest increase, normalisation across the whole data set would present the same as the comparison between locations shown previously. The comparison between the normalised results is shown in figure 6.79. Swiss Cottage is projected to have the greatest increase in degradation rate compared to the other locations. However there is little difference between the locations, such that it can be approximated in the future (2085) the increase in rate of paper degradation is projected to be 1.5 times that of the baseline value. This

assumes similar conditions to those investigated, if the temperature was 25°C for example this would not hold true. In this instance the damage is largely influenced by the increase in temperature, where relative humidity dominates it is less likely that a general statement such as this is applicable. Damage that is largely dependent upon relative humidity generally has critical threshold values, thus slight differences in room environments can have a significant impact, occasionally resulting in the amplification of damage.
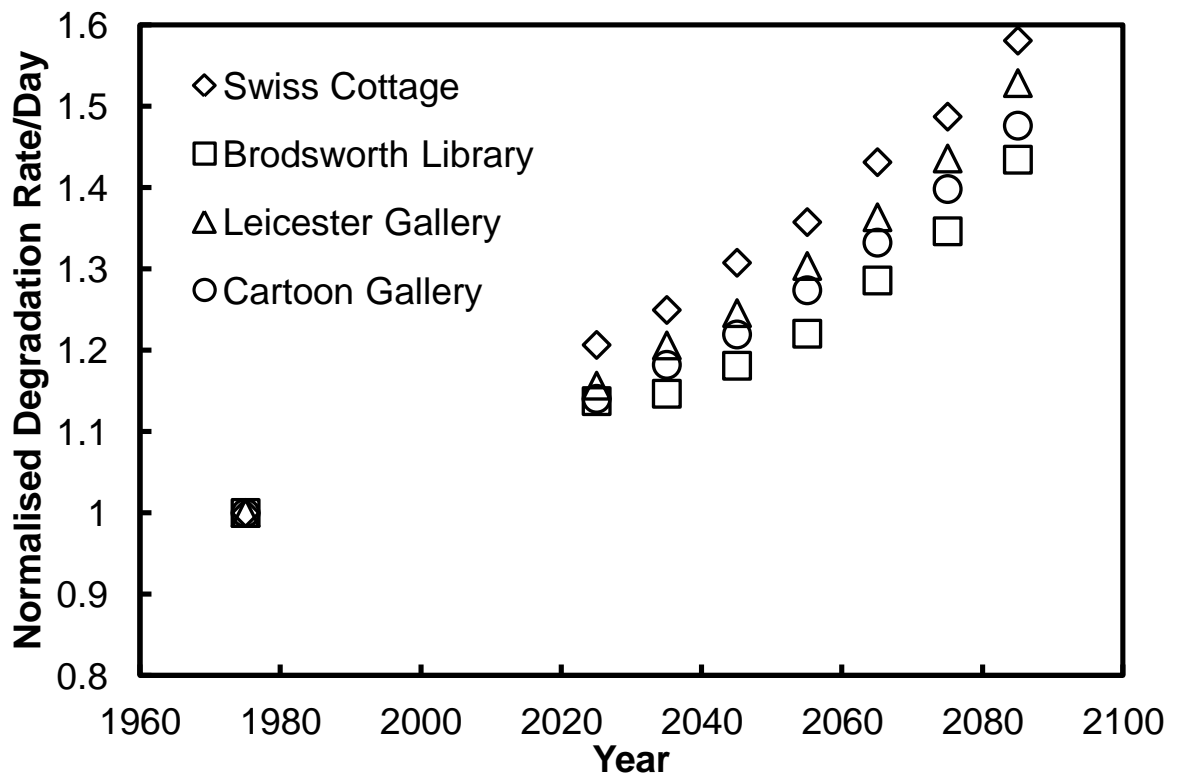


Figure 6.79: Normalised Zou paper damage function results, across four different locations.

In summary the normalisation technique has allowed for a more general statement of the impact of climate change on the degradation of paper. Where an actual rate of paper degradation has been measured how this will change in future can be projected. If it were in the Cartoon Gallery for example it may increase by 1.5 times. The normalisation has also helped show that the three damage functions predict similar results. As the silk damage function follows a similar principle to the paper damage functions it is also possible to determine the absolute change in rate.

The absolute rate change also helps with significance, an increase such as 1.5 times the baseline is likely to be deemed significant, but that projected by the Pretzel function in the Cartoon Gallery, 1.08 is not likely to be significant. When related to an example the specific conditions will also help determine the significance. If the degradation rate was

low anyway an increase by 1.5 times may be an acceptable rate of degradation. In this instance the notion of lifetimes may be beneficial to relate the rate to a lifetime, which may be easier to attribute significance to.

### 6.5.2 Damaging events

One of the issues relating to significance that is raised on multiple occasions is the importance, or significance of a single event or transition. Some damage functions explicitly define the damage that a single event will cause, others however are not defined so well. Take for example the Lipfert damage function, not used in this work, this determines the surface loss of stone, and the result is a specific value, for example that 2mm of the stone surface will be lost in a year. There is only one way to interpret this, a specific loss is defined. When this is related to a specific example it is then possible to determine the significance, if 2mm of loss will lead to the carved detail being lost then this is significant damage. The Lipfert function is somewhat different to those considered here, the Lipfert function is based on the accumulation of damage (dose × time), but the functions considered here describe damage caused by events.

The Lipfert function is an example of a damage function that is quantitative, or could be called a true damage function. There are examples in other work as well as here, of relationships that are called damage functions when in reality they do not define damage. There are some examples of semi-quantitative damage functions, the thenardite/mirabilite salt transition function used in this work can be described as such. The function determines whether a transition occurs that has the strength to physically break the stone, therefore each transition is known to have the potential to cause damage, however the amount of damage is unknown. Therefore a change in the magnitude of this damage function is important, but without knowing how much damage this causes it is difficult to determine whether this is significant in terms of damage.

It has been mentioned that significance can relate to different aspects, statistically significant, significant in terms of damage, and significant in terms of management strategies or preventive conservation measures. There is an order here; a change must be statistically significant before it can be significant in terms of damage. The same is true for significance with respect to management strategies; it first must be significant with respect to damage.

There are also examples of qualitative damage functions, where the risk of damage can be described as changing either positively or negatively, but the actual damage caused is

unknown. These can also be referred to as risk functions. An example of one of these used here is the Halite salt transition function.

Each of the functions used in this work are classified into the three defined categories in table 6.2. This helps when determining the significance of a result from each function. In addition to this there is another factor that can confuse the situation, in cultural heritage not all deterioration is classified as damage. If a change or deterioration can be repaired then it is not always termed damage. An example would be the lifting of a veneer, technically there is likely to have been deterioration of glue that holds the veneer in place. However this change would not necessarily be classed as damage, should the veneer be able to be reapplied. A loss of a piece of veneer would be classed as damage, but a damage function cannot determine when a veneer lifts whether it is subsequently lost.

Another example that highlights damage, caused by fatigue, is that of acoustic emission. Acoustic emission is the sound produced when small amounts of deterioration occur within a material, due to stresses. This can be measured, and there will be a specific number of these acoustic emission events. Each event is a very small amount of deterioration, at some point, the end point, this will manifest as damage. However this end point is unknown, so in relation to the work in this thesis, an increase in 5% humidity shocks (or 10 and 20%) is difficult to quantify because the endpoint, when damage is caused is unknown. It is true that should the number increase then the end point will approach faster, but it may be that even though the number of events increases the end point is so far away that actually causing damage is unrealistic. This helps explain why these have been classified as qualitative damage functions. The 30% and 40% functions are classified as semi-quantitative because the work of Jakiela et al. (2008) has shown that a humidity shock exceeding 30% can cause damage, but not exactly how much. 20% humidity shocks have been classified as both semi-quantitative, and qualitative, this is because the damage caused depends upon the object, if it is of very high vulnerability a fracture is caused, but for other vulnerabilities the result is not as severe.

There is a current research project covering the question of deterioration and when this becomes damage. The project is titled 'Change or Damage? Effect of Climate on Decorative Furniture Surfaces in Historic Properties', (Luxford, 2012).

Other recent research has investigated determining an endpoint, where the fatigue process will cause damage (Bratasz et al., 2011). The work looks very promising, and could be very useful. It does raise the question, where on the journey to the endpoint is the object in question. However, knowing the end point is very useful as it can help attribute significance to predictions. For instance the number of damaging events can be

considered and the overall time taken to reach the endpoint determined, from the start point. An assessment of the time taken to reach the endpoint can help determine the significance of a predicted change.

Not a single indoor damage function has been classified in the top category, as being quantitative. None can be compared to functions similar to the Lipfert function, which explicitly defines the extent of the damage caused. Some of the semi-quantitative functions are well defined, and are useful, but do not quite reach the 'gold standard' level. The mould functions describe how much mould will grow, but it doesn't say that this will cause a specific amount of damage to the substrate. The dimensional change functions are similar also, a crack may form because of the humidity shock, but how long is this crack? The paper functions are also not perfect, they describe the rate of degradation, but again this does not specifically define when the paper will be unusable, i.e. it is falling apart.

Ultimately the problem with determining significance is because not all damage functions define the actual damage that is caused. To be of the greatest use a damage function needs to explicitly define the damage caused. Therefore improved indoor damage functions are required in order to make a better assessment of the significance of the impact of climate change on future damage. Some effort has been made to determine the significance, but without a truly quantitative damage function the significance is difficult to determine fully. Educated guesses can be made using alternative evidence, but these may not be precise. This is not to say damage functions in their current form are not useful, in their own applications they can be very good. However, for application in this work improvement would be beneficial.

Table 6.2: Classification of damage functions

| Quantitative | Semi-quantitative | Qualitative |
|---|---|---|
| | Thenardite/mirabilite salt transitions | 60/75/85% salt transitions |
| | Isaksson | Degree days |
| | Hukka | Critical relative humidity |
| | Cotton wood adsorption and desorption | Equilibrium moisture content |
| | White oak adsorption and desorption | Days temperature exceeds X°C |
| | White oak failure | 5% Humidity Shock |
| | 20% Humidity Shock | 10% Humidity Shock |
| | 30% Humidity Shock | 20% Humidity Shock |
| | 40% Humidity Shock | |
| | Zou | |
| | TWPI | |
| | Isoperm | |
| | Pretzel | |
| | Silk | |

Climate change is normally a relatively slow process, as time passes it gives an opportunity to advance our knowledge, and carry out further research into some aspects of the work presented in this thesis, such as that of significance, to gain a better understanding of the impact of climate change on historic collections. However, if thresholds or amplification are important then climate change may not proceed slowly, thus it is important to assess the impact of climate change, which could be refined when knowledge advances. In addition it is important to identify where there are thresholds, and prioritise these to understand how fast the change may occur.

### 6.5.3 Backcasting

One method that may help relate damage to environmental conditions is backcasting of the indoor climate. The principle is the same as projecting the future, but carried out for the past. The same transfer functions can be used, assuming there has not been a change of use as this would alter the relationship between indoor and outdoor climate. The transfer functions can then be coupled with historic records of climate, such as the central England temperature record (HadCET) which has daily temperature observations from the late 18th century. This process has been carried out by Brimblecombe and

Lankester (2012)[2], for the Cartoon Gallery at Knole. As with the current process the historic climate predictions can then be associated with damage functions.

What makes this technique particularly useful here is the ability to then relate these historic damage predictions to the actual damage that has taken place over this time. Documentation such as condition reports of objects are often kept, and updated, therefore any deterioration has been recorded over time. Determining the relationship between observed damage and that predicted from a damage function can help validate future projections. This would help attribute significance to future projections.

In the Cartoon Gallery the temperature from 1780 to 1980 hasn't changed significantly, but since 1980 there has been a slight upwards trend. There is historic evidence of insect pests at Knole, and recently there is evidence that some pests are again a problem (Brimblecombe and Lankester, 2012). This helps provide evidence that the predicted historic temperature has been associated with insect pest damage, although there may be other contributory factors. The recent resurgence could be driven by the increase in temperature that is apparent. However there may also be other contributory factors here, such as the ban on insecticides that were very effective. It is likely that both these factors contribute in some way. This discussion only relates to temperature and not relative humidity, which is important for insect pests, although some are not dependent upon the relative humidity, such as the webbing clothes moth, a significant problem in recent years (Pinniger, 2011).

The projected increase in future temperature, a significant change compared to the historic average is likely to impact significantly on the activity of insect pests, and thus increase the risk of damage. Evidence shows that at the lower temperatures in the past insect pests were a problem at Knole, and future temperatures are likely to exacerbate this problem.

## 6.6 Conclusions

It can be concluded that climate change is projected to have a varied impact on damage, as described by the damage functions applied in this chapter. Whether climate change is viewed as a negative or positive change by an organisation depends on the collections, an archive for example is likely to view climate change as a negative change, due to the projected increase in degradation of paper. The relationship between temperature and

---

[2] The implementation of backcasting in the Cartoon Gallery was carried out by P.Brimblecombe, and therefore is not presented here as part of this thesis.

specific humidity is critical in transfer of the environment indoors, and whether the change in relative humidity increases or decreases.

In general across all locations assessed the temperature is projected to increase, leading to a higher rate of chemical degradation of paper and silk. This also results in an increase number of days over 20 and 25°C, and a significant increase in degree days.

The annual average relative humidity is not projected to change significantly over the coming century, with the exception of Brodsworth Hall, where there is a slight increase. However the seasonal analysis performed indicates a shift in seasonal relative humidity, particularly in the two rooms at Knole. The projected changes in relative humidity in both rooms at Knole indicate an increased risk from mould growth; other locations fall below the required relative humidity. The seasonal analyses have proved crucial in determining the driving factors of change in damage, and in assisting decisions on suitable conservation measures. For example the high winter relative humidity in the Cartoon Gallery drives the increase in projected mould growth; this helps target preventive conservation strategies towards this time of the year and the specific threat of high humidity. The seasonal analyses have also highlighted that the annual averages can hide some impacts of climate change, as shown with the relative humidity changes and the number of days over specific temperatures.

The change in salt transitions is dependent upon the individual location and salt. This is quite different to the outdoor projections from NOAH'S ARK where there is a clear increase in transitions.

Dimensional change damage is projected to decrease using the Michalski damage function. The Mecklenburg function projects an increase in the two Knole rooms, and a decrease in the Library, this is linked to the respective relative humidity in each room. A summary of the projections of each damage function is shown in table 6.3.

Comparison of the two rooms at Knole indicates similar results for temperature based damage functions; however those that depend heavily on relative humidity tend to show different results. This is due to the difference in relative humidity between the two rooms, and the sensitive nature of the functions based on relative humidity. Thus the individual analysis of each room is crucial, even the slightest difference in relative humidity has been shown to impact on the results of damage functions. This raises the opportunity to compare the preservation quality of rooms to one another in the future. One management option may be moving objects to a different room to help preserve it for longer. There are a variety of issues surrounding this option, for instance objects can have an association

with a specific room, thus they belong in that room, and have a greater historical significance in a specific room, moving the object to another room would result in a loss of value, and would be seen as inappropriate. With functions such as the paper damage functions it is possible to determine an average increase in degradation rate.

In general the projected changes to damage tend to be relatively small, it is not often that a large change, such as a 50% increase in damage is projected, and when this does occur it is when there are a small number of events. Therefore it is likely that current problems will either get slightly better or worse, rather than experience catastrophic changes. The exception to this is the onset of mould growth which has been projected. Small changes in current damage are more likely to be easier to manage than the onset of a different type of damage. Therefore although this is a less common occurrence it is more likely to have a significant impact.

The significance of change is discussed, it is easier to determine the significance of a change when there is a specific example to refer to, and when the impact of a single event is known. The significance also relates to one of three things. Firstly statistical significance, this is the first thing to consider, if a result is not statistically significant then it can't be considered a change. However, even if a change is certain to occur it may not be significant in terms of damage, or management strategies. Each of these is independent, and must be taken into consideration when deciding where resources should be focused to mitigate future risks. Investigation into significance is also carried out, highlighting the lack of quantitative damage functions, making it difficult to determine significance. Back casting is discussed as a method for understanding the significance of future projections.

Careful consideration must be used when interpreting the results presented for the Library at Brodsworth Hall, due to the complications discussed earlier. Conservation heating is employed here, and the standard transfer function is unlikely to hold true in the future for this scenario, if the relative humidity changes significantly. The change in relative humidity is projected to be less than 5%, however the impact that this would have is unknown, and thus caution must be taken.

The results presented in this chapter will allow for collection managers at the individual properties to make an assessment of future pressures and whether they may be different to current pressures. This should help with long term planning. Further work on significance of future changes would help put these projections into perspective, although individual collection managers will be able to do this for certain projections, as they have an excellent understanding of the collections and its current issues. Thus knowing how these may change in the future (increase or decrease for example) would be beneficial.

Table 6.3: Summary of the damage function projections. Red indicates a change for the worse, green a change for the better, yellow no change and white no result.

| | | | Cartoon Gallery | Leicester Gallery | Library | Swiss Cottage |
|---|---|---|---|---|---|---|
| | **Environment** | Temperature | ↑ | ↑ | ↑ | ↑ |
| | | relative humidity | ↔ | ↔ | ↑ | ↔ |
| | | T>20°C | ↑ | ↑ | ↑ | ↑ |
| | | T>25°C | ↑ | ↑ | ↑ | ↑ |
| **CHEMICAL** | **Chemical degradation** | Zou | red | red | red | red |
| | | Isoperm | red | red | red | white |
| | | TWPI | red | red | red | white |
| | | Pretzel | red | red | red | white |
| | | Silk isoperm | red | red | red | red |
| **BIOLOGICAL** | **Mould germination** | Isaksson | red | red | yellow | yellow |
| | | Critical RH | red | red | yellow | white |
| | | Hukka | red | red | yellow | white |
| | **Pests** | Degree Days | red | red | red | red |
| **PHYSICAL** | **Salt transitions** | Then/Mir | green | green | red | white |
| | | 60% | red | red | red | white |
| | | 75.3% | green | green | red | white |
| | | 85% | red | green | yellow | white |
| | **Wood dimensional change** | **5%** Humidity shock | green | green | green | green |
| | | **10%** Humidity shock | green | green | green | green |
| | | **20%** Humidity shock | green | green | green | green |
| | | **30%** Humidity shock | green | green | green | green |
| | | **40%** Humidity shock | green | green | green | green |
| | | Cotton wood | green | green | red | white |
| | | White oak | green | green | red | white |
| | | White oak failure | green | green | red | white |

# CHAPTER 7

# APPLICATION OF CONSERVATION HEATING AS A MANAGEMENT TOOL

## 7.1 Introduction

While it is important to understand the possible impact that climate change may have in the future it is also important to think about how we could prevent damage from occurring. It is possible that climate change may also have an impact on the effectiveness of these mitigation strategies, or on the resources required to implement them.

One strategy currently used in historic houses to prevent damage is conservation heating; instead of a thermostat controlling heating a humidistat is used. Some collections are more susceptible to damage from humidity, as discussed in chapter 4, thus controlling relative humidity rather than temperature can help prevent damage associated with incorrect humidity.

To control the relative humidity heating is used, if the humidity is above the maximum set point heating will increase to reduce the relative humidity. This relationship can be seen on the psychrometric chart in figure 1.1, if the humidity ratio is kept constant (along the horizontal blue lines) an increase in temperature (a shift to the right) will decrease the relative humidity (red curved lines). This can lead to a requirement of heating in the summer, and not heating in the winter (Neuhaus and Schellen, 2007), to prevent humidity dropping too low, but leading to discomfort of visitors. Typically though in the UK humidity is higher in the winter when temperatures are lower, and vice versa in the summer, although at its lowest the humidity may still fall above the permitted range of relative humidity, requiring heating to reduce this further.

Conservation heating will be applied in theory to determine the effectiveness of the technique in the future. The transfer equation will be applied as normal, and additionally conservation heating will be applied so that it can be compared against the environment with no conservation heating.

There are various set points that control the application of conservation heating, these can vary depending upon the building or standard practices implemented by various heritage organisations. One example of the set points used is (Neuhaus and Schellen, 2007):

- Minimum temperature ($Tmin$) = 10°C

- Maximum temperature ($Tmax$) = 25°C

- Minimum relative humidity ($RHmin$) = 45%

- Maximum relative humidity ($RHmax$) = 55%

The humidity set points are designed so that the indoor climate is kept within the desired conditions of 40-60% relative humidity (Neuhaus and Schellen, 2007). A minimum temperature can be used to prevent damage that could occur from events such as burst water pipes from freezing (ASHRAE, 2003). The maximum temperature prevents damage that accelerates at higher temperatures such as chemical deterioration of paper, see chapter 4.

The set points vary between historic houses (Staniforth et al., 2010). In this specification the maximum relative humidity set point should be adjustable for each room, normally somewhere between 50-65%, in order to keep conditions between 40-65% for 90% of the time (Staniforth et al., 2010). While it is adjustable an indication of maximum relative humidity is given at 58%, and a minimum relative humidity set point of 40%, it states that heating should be turned off if this is reached, but no other measures are required (Staniforth et al., 2010). With regard to temperature set points, a minimum of 5°C should be used, for the reason stated previously, and a maximum of 22°C is used, as an energy conservation measure (Staniforth et al., 2010), but also this prevents temperature increasing to levels that can rapidly damage some collections. The maximum temperature limit is specified for the summer, with 18°C specified for winter. However in the research here the winter temperature is very unlikely to rise this high, and it is only set for energy conservation measures (Staniforth et al., 2010) which are not of direct importance here. Although these limits are significant in the larger picture, such as mitigation of climate change by reducing emissions.

Upper temperature limits can prove problematic as they result in the loss of control of humidity. Particularly in the summer it can prevent the relative humidity being reduced below the set point. It may be expected that these episodes increase in the future because of the higher temperatures associated with climate change.

In the future it may be possible that conservation heating requires less energy to operate. Less heat will be required from conservation heating to reach the desired level of relative humidity, because of the increased temperatures associated with climate change, thus reducing energy costs of these systems.

Given the importance of conservation heating, as a widely applied method of environmental control, it is worth considering briefly here.

## 7.2 Method

Conservation heating is modelled using an AWK program. This was achieved by applying the transfer function then assessing this data. If the humidity is above 58% then the humidity is reset to 58%, and the temperature increased by the correct amount corresponding to the humidity change, as would happen if the heating was turned on to reduce humidity. If this would increase the temperature above the maximum value of 22°C the temperature is set to this, and the relative humidity increased according to the amount of heating that can be applied. Thus on some occasions no heating can take place as the temperature is naturally above 22°C, which is not reset, and sometimes the humidity can be decreased but not fully as the temperature limit is reached.

Conservation heating was applied in theory to the Cartoon Gallery at Knole, currently an unheated room, with high humidity. It has also been shown to have an increased risk to humidity related damage problems, such as insect pests and mould growth in the future. As mentioned previously climate change may reduce the energy costs of heating, due to temperature increases.

Some of the work presented in this chapter has been published by the author (Lankester and Brimblecombe, 2012b). The AWK program that applies conservation heating to a room can be found in appendix E.

## 7.3 Results

Conservation heating has been modelled in the Cartoon Gallery at Knole. Here results of this on the impact to the indoor environment, the effectiveness of conservation heating and the impact on damage, in a changing climate are shown. Finally a simplified energy costing of conservation heating is applied, to determine how the energy cost is projected to change.

### 7.3.1 Environment

The projected impact of climate change on temperature in the Cartoon Gallery, with and without the application of conservation heating is shown in figure 7.1. The baseline and future data are replicated from the previous chapter, and the work here adds the scenario with conservation heating applied. The first thing to assess is the difference between the

baselines with and without conservation heating. During the summer there is a similar increase over the months, where relative humidity is close to the required set point, but needs a little additional heating to reduce it to an acceptable level. In the winter there is a substantial rise in temperature, due to the very high winter humidity in the Cartoon Gallery. If the annual average temperature for the baseline with conservation heating is compared to that of the future without conservation heating they are very similar. Thus the application of conservation heating results in a similar increase in the temperature as that associated with the impact of climate change, by the end of the century. This is a substantial increase, and could be important for damage driven by temperature.
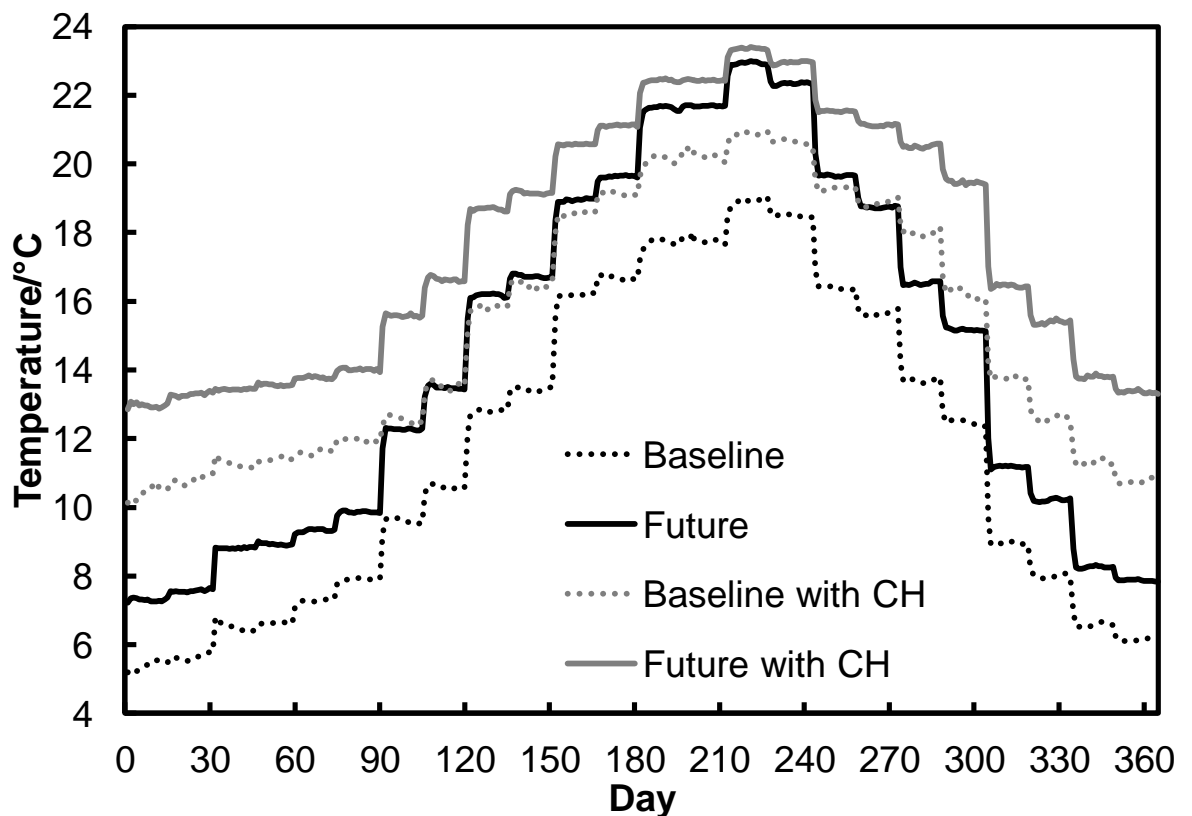
Figure 7.1: The impact of climate change on the application of conservation heating in the Cartoon Gallery at Knole. Each line represents the median value, which is presented for each day across the year, from the 100 runs of the weather generator.

The increase in temperature is of course offset by the decrease in relative humidity, but extreme caution must be taken, as this increase in temperature could bring about alternative problems to those solved by conservation heating. The types of collections that are displayed within a room will be very important; those that are temperature sensitive, such as paper and silk will degrade much faster. Additionally insect pests that are not

sensitive to relative humidity, such as the webbing clothes moth and biscuit beetle are likely to thrive if the temperature increases by such a degree.

A similar comparison to previously applies in the future also, to how the application of conservation heating impacts upon the temperature. Starting with the winter months, there is a similar trend, a considerable amount of heating is required, to reduce the relative humidity which is projected to increase in the future. In the summer there is a smaller increase in temperature, because of the top limit of temperature, of 22°C. This prevents additional heating, and results in the loss of control of the relative humidity, as shown in figure 7.3.

The increase in future winter relative humidity enhances the need for conservation heating in the winter, in comparison to the baseline. However in the summer this need reduces, driven by two factors, the reduction in relative humidity, and the already increased temperature, which allows for less heating due to the upper limit. This relationship can be linked to the required energy of conservation heating, explored in section 7.3.4.

The impact of climate change on the application of conservation heating in the Cartoon Gallery, with relation to relative humidity is shown in figure 7.2. The results for the relative humidity with conservation heating applied are somewhat artificial. They produce a straight line, because the theoretical application uses the value of 58%. There is no fluctuation around this as there is likely to be in a real world situation.

With the exception of the summer the relative humidity is controlled all year round. For the baseline period there is occasional loss of control of the relative humidity, with the most occurring in the warmest months of July and August. In the future however the temperature increases and the top temperature limit is reached more often, resulting in the increase in relative humidity on many more occasions.
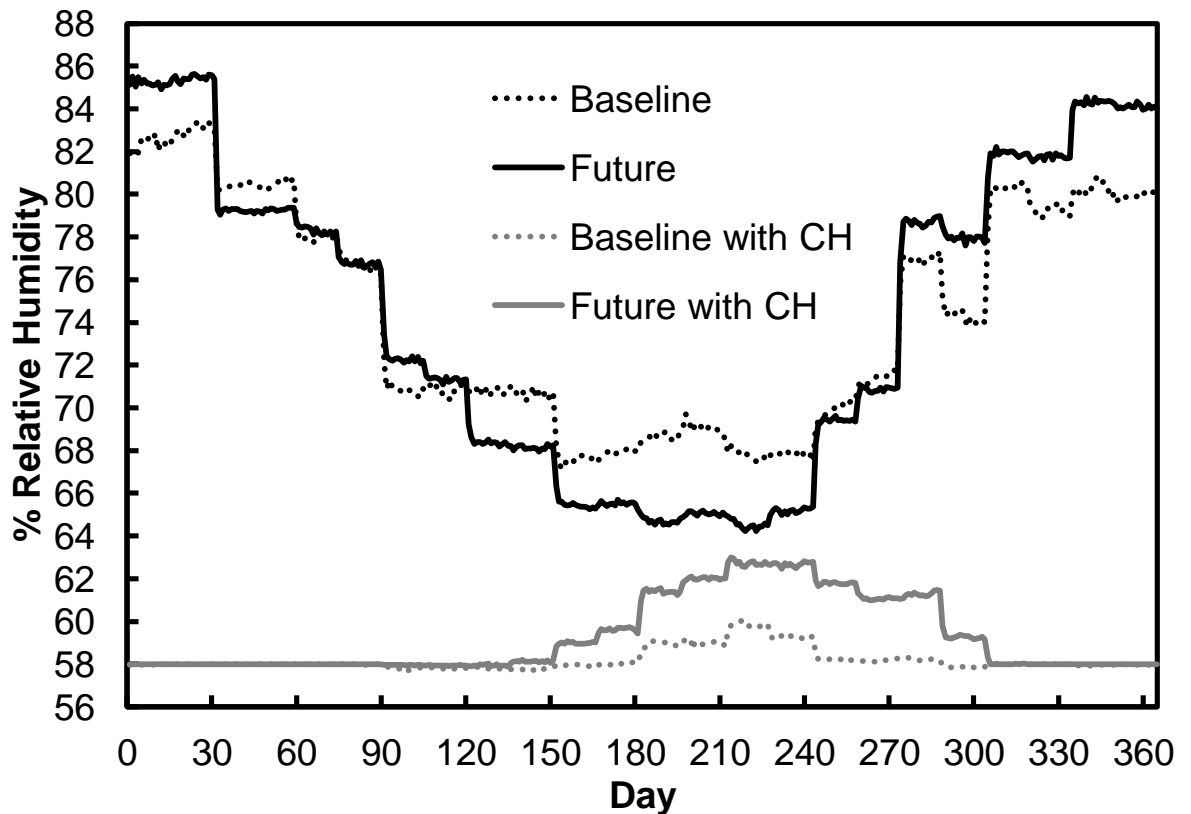
Figure 7.2: the impact of climate change on the application of conservation heating on relative humidity in the Cartoon Gallery. Each line represents the median value, which is presented for each day across the year, from the 100 runs of the weather generator.

### 7.3.2 Loss of control

Conservation heating is applied with the desire to control relative humidity within a set range, here that is said to be below 65%. This allows for some loss of control, above the set point of 58%. In figure 7.3 the percentage of time where the ideal conditions are lost, i.e. loss of control, is shown. This is presented for both the baseline and future, with and without conservation heating applied.

Without the application of conservation heating there is a significant reduction in the projected time over 65% in the future. This is due to the reduction of summer relative humidity. Comparing the baseline and future periods where conservation heating is applied, an increase in loss of control is projected, from 1.7% to 9% of the time across the year over 65% relative humidity. Although loss of control is more frequent in the future, conservation heating would still reduce the number of high humidity events, from 76% to 9% of the time (Lankester and Brimblecombe, 2012b).

Typically conservation heating is not used in summer months, as shown by the shaded region in figure 7.3. Therefore the lower summer humidity projected in the future would result in less time outside of the desired relative humidity.

The reduction in effectiveness of conservation heating in the future may affect damage. However, results suggest the application of conservation heating would be an effective method of humidity control in the future, although slightly less effective than currently.
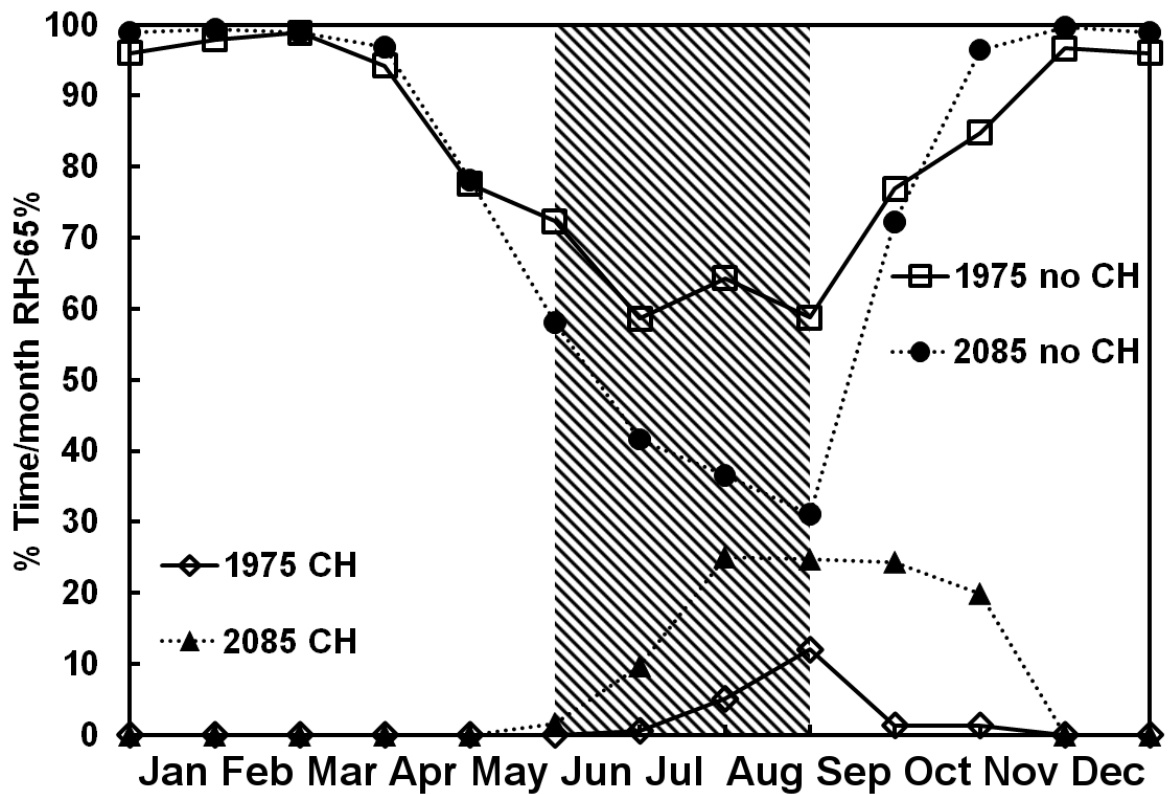


Figure 7.3: The impact of climate change on the loss of control of relative humidity, with and without conservation heating (CH) for the baseline and far future periods. Projected for the Cartoon Gallery at Knole.

### 7.3.3 Damage

Here the application of conservation heating and the projected change in effectiveness of conservation heating in the future is discussed with relation to damage.

**Mould growth**

It is not necessary to present results from any of the damage functions here as they will show no risk of mould growth. The application of conservation heating reduces the relative humidity to below that required for mould growth. Therefore it is an excellent management

strategy. While the loss of control increases in the future, the relative humidity does not rise to a level where mould growth is possible. There is no reduction in effectiveness of conservation heating, with regard to mould growth.

Currently at Knole mould growth is an ongoing issue, the application of conservation heating would be expected to remove this risk.

**Damaging dimensional change to wood**

The projected change in damaging events to white oak across the century, with and without conservation heating is shown in figure 7.4. The results where conservation heating is not applied have been discussed previously, the number of damaging events decrease, because of the summer reduction in relative humidity, thus moving away from the zone where only a small change in humidity is allowed before damage occurs. Applying conservation heating reduces the number of damaging events significantly, again the reason for this is that the relative humidity is then within the safe range where greater humidity fluctuation is allowed before damage occurs. The number of damaging events where conservation heating is applied increases in the future, due to the loss of control in the summer months. In comparison to not having conservation heating this small increase is not significant. However, in comparison to the baseline value it may be significant, as the number of damaging events doubles. So as mentioned previously, conservation heating is still an effective management strategy overall, however its effectiveness will reduce in future.

Figure 7.4: The impact of climate change on the application of conservation heating, with respect to the total number of damaging events to white oak, resulting from both adsorption and desorption events. Error bars represent the interquartile range.

**Paper and Silk**

There is a significant increase in temperature when conservation heating is applied, so this is likely to be of importance to collections that are sensitive to temperature, such as paper and silk. The chemical degradation of these materials is dependent upon temperature, and the increase of that seen here will result in a significant increase in degradation rate. For the baseline period, the application of conservation heating raises the temperature by a similar amount to that of climate change projections in the far future. The result of this on degradation rate has been shown previously. Damage can only then increase further as time moves through the coming century and the impact of climate change is ever more present. It would not be expected to increase by the same amount again, because of the upper temperature limit, but there is still a large increase in temperature of the other months.

**Degree days**

The impact that climate change is projected to have on the application of conservation heating, with respect to degree days is shown in figure 7.5. It is projected that the application of conservation heating will increase the number of degree days significantly, from 296 to 733 for the baseline period without and with conservation heating respectively. The projected value of 733 for the baseline period with conservation heating is almost as much as the projected value (789) in the future without conservation heating. The far future period (2085) where conservation heating is applied has 1258 degree days, more than four times that of the baseline period without conservation heating. Taking the example mentioned previously of 490 degree days for one life cycle of the biscuit beetle (Brimblecombe and Lankester, 2012) an increase such as this is huge. This results in the insect pest potentially completing (approximately) five life cycles every two years, compared to one every two years previously. In addition to the biscuit beetle the webbing clothes moth also does not require moisture from the environment, and such a change is likely to positively impact on this insect pest also, resulting in increased damage levels. The webbing clothes moth is currently presenting major problems across the heritage sector, thus this would only be expected to increase (Brimblecombe and Lankester, 2012).
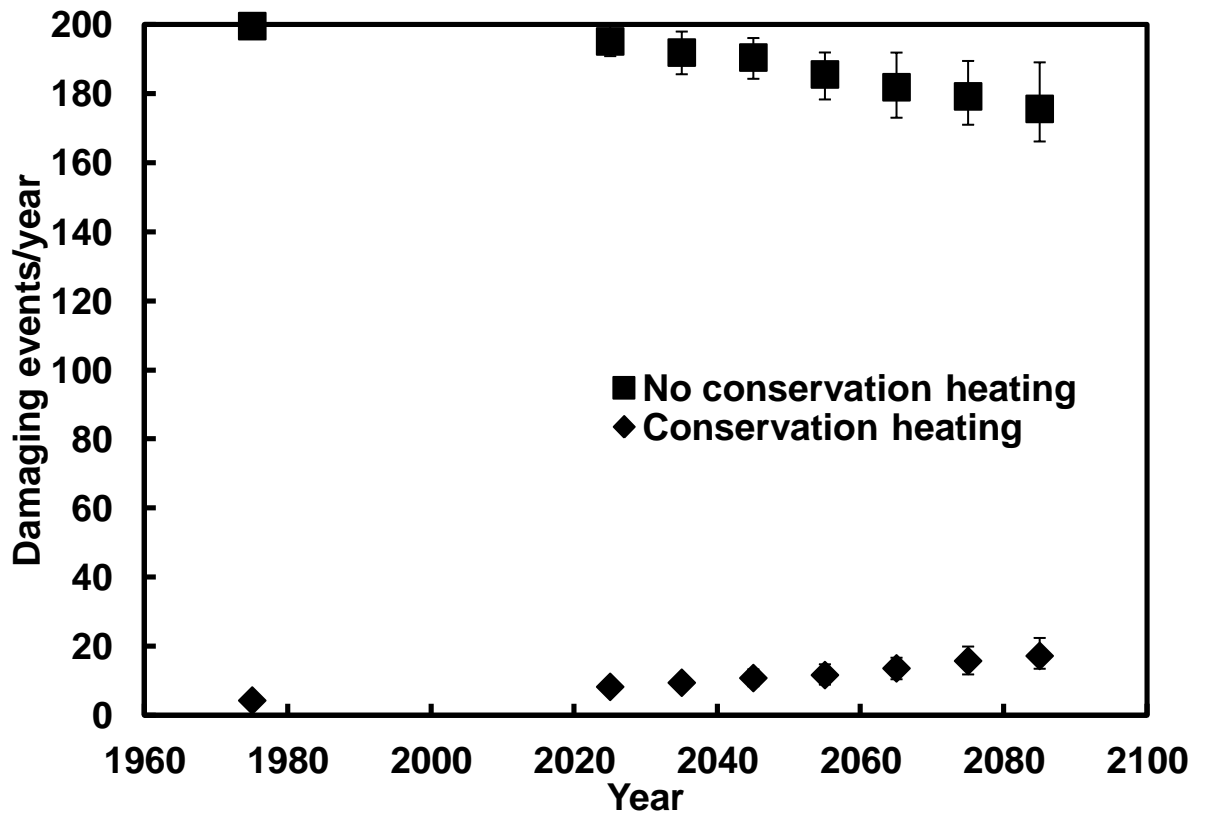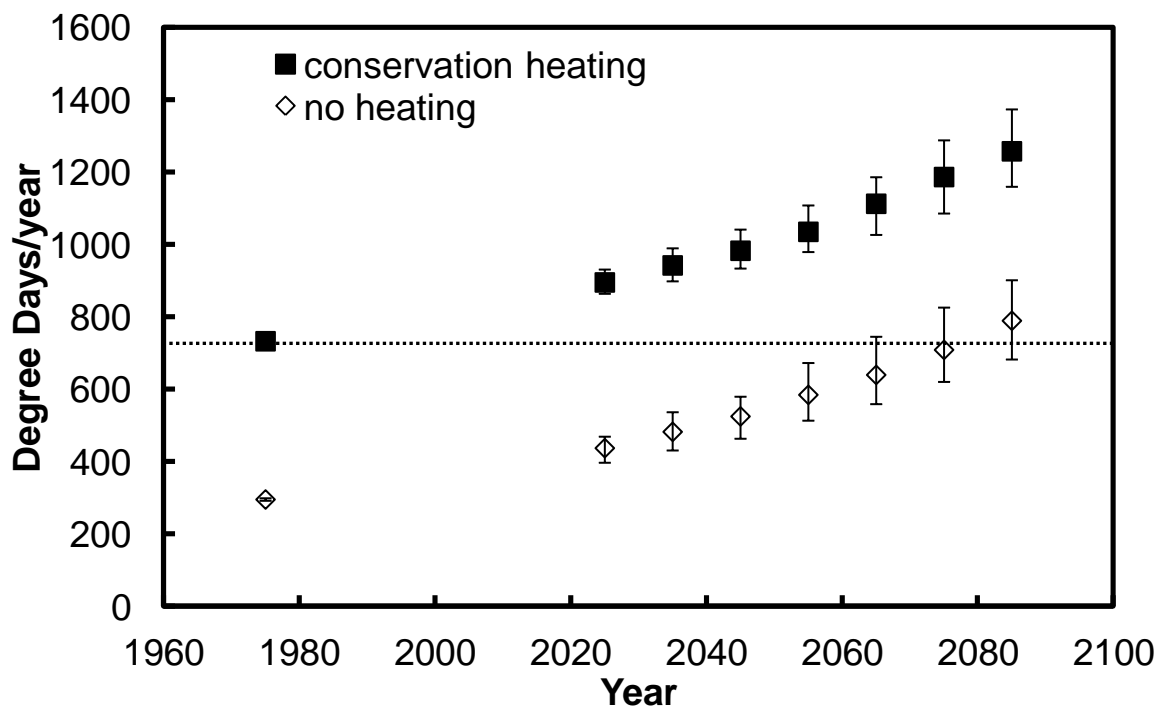


Figure 7.5: The impact of climate change on the application of conservation heating, with respect to the total number of degree days. Error bars represent the interquartile range. The dotted line helps compare the baseline value of degree days where conservation heating is applied to the future periods where conservation heating is not applied.

A good integrated pest management (IPM) program can help reduce risk of damage from insect pests, it would be expected that increased resources for this would be required in future to prevent infestation from the two pests described here. While this is the case for these two insect pests, the application of conservation heating may reduce the risk of damage from other insect pests. Relative humidity is important to a number of insect pests that cause damage to historic interiors, such as the common furniture beetle and death watch beetle. A reduction in relative humidity, such as that from conservation heating, would be expected to reduce damage from these pests.

### 7.3.4 Energy

Conservation heating works by increasing the temperature to reduce the relative humidity. As mentioned earlier it could be possible that the projected increase in future temperature may reduce the heating required to lower the relative humidity to within the required conditions. The difference between the temperature of the baseline period with and without conservation heating is shown in figure 7.6, also shown is the difference between the temperature of the future period with and without conservation heating. This indicates the increase in temperature that has been added by conservation heating, to reduce the relative humidity. There is some similarity to the trend in figure 7.6 compared to the seasonal relative humidity, with a reduction in summer relative humidity, and an increase in winter relative humidity, given the principle of conservation heating this would be expected.

The sum of the baseline temperature, using the method of incremental degree days (base of 0°C), can be compared to that of the future period to determine whether there is a change in the temperature required to reduce the relative humidity. The total number of degrees Celsius that have been added by conservation heating over the baseline totals 1317, where the total number for the future period totals 1219, a reduction in the added temperature. Thus there would be a reduction in the energy required to implement this temperature increase.
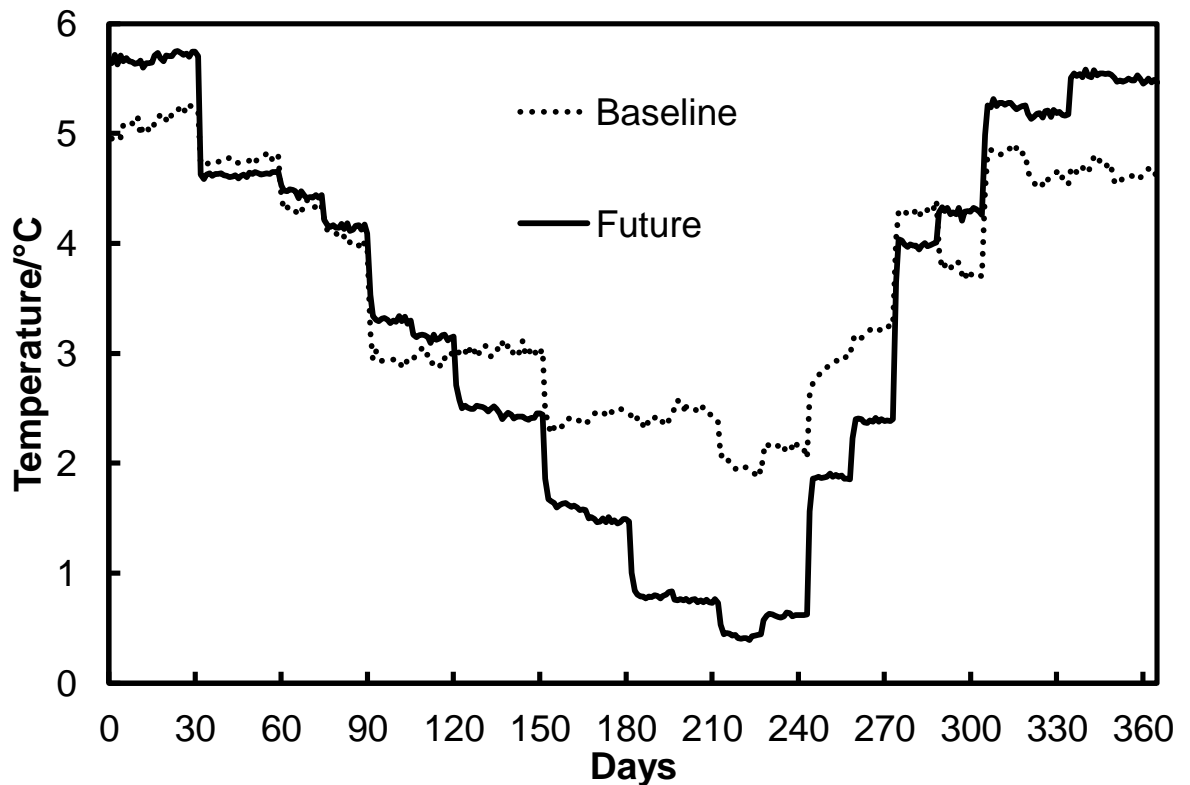
Figure 7.6: The average temperature added daily by conservation heating to reduce the relative humidity, for the baseline and future periods.

It is possible to estimate the amount of energy required to implement conservation heating, and thus the difference between the baseline and future periods, which would represent the impact of climate change. This can also be linked to the cost of energy to see whether this would result in a decrease in the future, as expected from the results.

It has been stated elsewhere (Lloyd et al., 2007) that the cost of conservation heating averaged at £100 per room per year. This figure will be used here; however there are a number of assumptions about the physical properties of each room that this makes. For example the air exchange rate, the type of system used and the material construction.

If the annual energy cost is taken to be £100 the energy consumption in kilowatt hours (kWh) can be calculated by dividing by the cost of one kWh. Because English Heritage is a non-governmental organisation (NGO) it purchases energy with other government departments together, demanding a better price, on average nine pence per kWh, for electricity. On top of this there is a climate change levy of 0.485 pence per kWh. To bring this in line with the wider business market the total rate used here will be 11.5 pence per kWh.

This results in 870 kWh per year of electricity. The number of degrees which are required, for the baseline period, to reduce the relative humidity is 1317. Dividing the total energy use by the number of degrees heating required gives the energy required to raise the temperature by one degree. This gives a value of 0.66 kWh/°C.

It is also possible to determine how long an appliance would need to be on for daily to implement a specific change. The wattage of the appliance used is required, which is typically 2kW. Using equation 7.1 the daily kilowatt hours (KWh) can be calculated.

$$\text{Wattage x hours used} = \text{daily kWh consumption} \qquad \textbf{(Eq. 7.1)}$$

For example a required rise in temperature of 5°C would consume 3.3 kWh of electricity. This value divided by the appliance wattage results in the number of hours used, here 1.65 or 1 hour 39 minutes. This equates to 0.33 hours per degree, or almost 20 minutes.

Using the value of kWh required per degree increase (0.66) the future cost can be calculated. The required increase in degrees across the year on average is projected to be 1219. This results in a total of 805 kWh per year. This equates to a projected cost of £92.56 in the far future, a saving of £7.44 per room per year, on average.

A large number of assumptions have been made here, so it is better to use the % saving between the baseline and far future periods, which should stay constant. The result is a 7.44% saving of energy cost. This is valid per room per year, but would also relate to the total energy cost of conservation heating.

English Heritage has roughly 80 rooms (with 70 of these at Brodsworth Hall and Audley End House) that employ conservation heating, the National Trust have considerably more. At English heritage if the saving were £7.44 per room per year a total saving of £595 per year would be made.

This has been calculated on the assumption that conservation heating is on all year round. Previously it has been stated that conservation heating is switched off in summer months. In some locations this is true, but for many English Heritage properties this is not the case, and it is just limited by the upper temperature set point. If conservation heating was turned off, it is possible that there would be a small increase in energy use. Whether energy use increases or decreases is of little importance in the larger picture.

It is of very little significance as it is likely to be a fraction of a percent of the current total energy cost across English Heritage properties. In comparison to the relative costs presented by Lloyd et al. (2007), cleaning far outweighs the total cost of energy to control

the temperature and relative humidity. Taking an estimate from the diagram presented by Lloyd et al. attributes 80% of the housekeeping budget to cleaning cost; and approximately 7% as fuel cost. A 7.44% saving here equates to less than a 1% saving of the cleaning cost and just over half a percent of the total household budget, which itself is only part of the total budget of running a historic house.

This approximation includes assumptions, but they are likely to cancel out between the baseline and future periods. Importantly the change in direction is determined, and the relative change is projected.

There is also an assumption that the energy cost will stay constant over the coming century, which is highly unlikely; however it is the only way to compare like for like the impact of climate change on the energy cost of conservation heating. Additionally as a percentage of the total energy use it would remain the same

## 7.4 Conclusions

Conservation heating is projected to be a less effective management strategy in the future, because of the impact of climate change. There is more time in the future when humidity control is lost. However conservation heating still represents an effective strategy for reducing the risk of humidity driven damage. The application of conservation heating increases the temperature by a similar amount to climate change, imposing risks to collections where damage is driven by temperature. Examples of these are the chemical degradation of paper and silk, or the insect pest activity of species that do not require moisture from the environment. Where this is an issue dehumidification may be an alternative solution. Thus the application of conservation heating should be carefully considered, whether it will help reduce damage is dependent on the types of collections.

It is important to consider the uncertainties associated with each stage of this work when assessing these results. Specifically here the average cost estimates are important. It is possible that other costs that represent the total costs could change, and therefore the conservation heating costs could become more or less significant.

It is projected in future that less heating will be required to bring humidity under control. This results in less energy usage and a reduction in cost. Given the projected future temperature and relative humidity it would be expected that the energy use of conservation heating would reduce, this work has confirmed this and determined the magnitude of the change. The reduction in cost is unlikely to be significant, as conservation heating is relatively inexpensive to run, especially in comparison to other

conservation costs. This confirms that conservation heating will continue to be a sustainable strategy for collection managers for mitigation of poor environmental conditions.

# CHAPTER 8

# CONCLUSIONS

## 8.1 Conclusions

This thesis proposes a method to project the impact of climate change on future damage to historic interiors. There are three aspects of the method, the first is a simple yet novel transfer function for predicting the indoor temperature and relative humidity in the cultural heritage field. The second couples the transfer function with future climate projections. The last projects the potential damage that arises from future indoor environments.

The transfer function allows for the prediction of the indoor environment within unheated interiors. The method has advantages and disadvantages in comparison with the traditional approach. The technique has been designed for simplicity and to be rapidly applicable, so that it can be utilised widely within the cultural heritage field. The transfer function predicts the temperature, specific humidity and relative humidity. It is calibrated over a period of observations of indoor and outdoor conditions, and this is required for each room and location. Transfer functions have been defined for two rooms at Knole, the Library at Brodsworth and the Swiss Cottage Museum at Osborne House.

The relationship described between indoor and outdoor climate by the transfer function has been coupled with climate output to project the indoor environment in the future. Two models have been used, the Hadley Centre HadCM3 and the UKCP09 weather generator. The first has been applied across Europe, and some of its spatial and temporal limitations have been overcome for this work. The UKCP09 weather generator has been applied around the UK, taking advantage of the weather generator to standardise downscaling methods.

It has been shown that the output from the UKCP09 weather generator is not normally distributed, therefore non-parametric statistics must be used. Investigation of the three emission scenarios available for the UKCP09 weather generator has shown that until 2045 there is little difference between the climate projections from each scenario.

Future damage has been assessed using the indoor climate projections with a number of damage functions. A range of damage functions are presented, and where necessary modified for use in this work. Typically this required careful consideration of reporting methods that allowed comparisons between baseline and future data. The future

projections of both damage and indoor environment are a worst case scenario (using the greatest projected climate change within the IPCC scenarios), thus highlighting the potential for significant problems. Should emissions fall below those of the high emission scenarios used here it may take longer for projections shown here to occur. Alternatively if methods such as geoengineering or emission reduction were successful they may not occur, however the effects of climate change until 2045 are irreversible now.

The uncertainties and underlying assumptions associated with all stages of this work must be taken into account when considering the impacts projected here. This includes the future climate projections, the transfer function and the damage functions. There are a number of similar issues associated with the use, validation and interpolation of these models. There are additional uncertainties associated with the use of statistical models, such as the transfer function. While the transfer function has been shown to be reliable with current observations, it may not be reliable with extrapolation to future environmental conditions, particularly if these fall outside of the range that the function was calibrated within. It is not expected that this will be the norm, and even so the system does not appear to be non-linear, thus serious problems with extrapolation would not be expected. It is believed that the transfer function will work well in a changed climate.

In general a rise in future indoor temperature is projected, somewhat less than that outdoors. Projections of future relative humidity vary depending on location, but generally there is not a significant change in terms of the annual average. Consideration of seasonal changes to relative humidity is important, as this can impact significantly on damage, even where the annual relative humidity shows no change. In general results indicate that winter months will be warmer and slightly wetter (higher relative humidity), and summer months will be warmer and drier (lower relative humidity).

Projections of damage across Europe indicate an increased risk of paper degradation through chemical deterioration, an increased risk of mould growth, and damage from insect pests. Projections indicate a likely increase in damage to wood caused by dimensional change. Salt damage projections vary by location and the specific salt. The difference in projected damage between Leon and Oviedo indicates the importance of downscaling.

The projected increase in temperature across the UK locations results in an increase in paper and silk degradation rates, and a greater number of warmer days. It also results in an increased number of degree days, increasing the risk of damage by pests.

Mould risk is projected to increase in the two rooms at Knole, due to increased winter relative humidity, the humidity is too low at other locations for mould growth. Again salt damage is dependent upon the specific location. A decrease in humidity fluctuations is projected, but there is an increased risk of damage to wood through dimensional change in the rooms at Knole, using the Mecklenburg functions, again due to the rise in winter relative humidity. The comparison between the Cartoon Gallery and Leicester Gallery at Knole indicates the need to assess the impact of climate change on a room by room basis.

Whether climate change is viewed as a negative or positive change by an organisation depends on the collections, an archive for example is likely to view climate change as a negative change, due to the projected increase in degradation of paper.

In general the projected changes to damage tend to be relatively small, it is not often that a large change, such as a 50% increase in damage is projected, and if this does occur it is when there are a small number of events. Therefore it is likely that current problems will either get slightly better or worse, rather than experience catastrophic changes. The exception to this is the onset of mould growth which has been projected. Small changes in current damage are more likely to be easier to manage than the onset of a different type of damage. Therefore although this is a less common occurrence it is more likely to have a significant impact.

Conservation heating should still be an effective management strategy in the future for reducing the risk of humidity driven damage. However, it is expected that its effectiveness will reduce somewhat, as there are increased periods of loss of control, where the temperature exceeds the maximum set point. One positive result of this is a reduction in the energy use of conservation heating, although in the larger picture of conservation costs and energy use this is a negligible financial saving. Conservation heating will need to be carefully chosen for individual collections, specifically those that are sensitive to damage driven by temperature. There is projected to be a dramatic rise in future temperature, in addition to the higher temperatures associated with conservation heating. This could increase damage, especially where there are thresholds, such as with insect pests. Alternative methods may be more suitable in the future, such as dehumidification.

Overall the methodology presented is sufficient. It requires application at other locations, and further work could improve some areas, specifically the significance of the projected changes. Work has been initiated on this, but there is still only a basic understanding. It should also be possible to develop the model for heated buildings, however it is more important to determine the significance of projections first. One significant problem

appears to be the lack of quantitative damage functions. If there were more defined functions, such as the Lipfert function, which states the loss of surface in millimetres, it would be easier to determine the significance of the change. Determining the significance of changes is important, as this informs whether a change poses a risk, and helps inform whether mitigation is required, and potentially the appropriate strategy. The method is in place to link future climate to damage, but appears to fall at the final hurdle, through the absence of quantitatively convincing damage functions.

The simple technique provides a fast method to gain an idea of how climate change will affect individual locations in the future. This can provide information on where current problems may disappear, or new problems may arise, in the future, so can be useful for long term strategic planning.

It is important to balance the threat of climate change to other future threats to heritage, and maybe the balance between this and other important threats, environmental pollution, financial stringency, changing population etc. In a world where climate change could have a significant impact, the loss of land in low lying areas for instance, the impact of climate change to heritage could fall low down on this list.

However, there are some areas where the impact of climate change is starting to be felt. There is a drive towards energy efficiency, as mitigation of climate change. Light bulbs are a good example in heritage, some types of bulbs/lighting methods are being banned by the EU, and thus it will not be possible to purchase these in the future. This presents significant problems to those in the heritage field, as lighting within historic showcases is not straightforward to adapt. While it may appear simple to replace the lighting, these extra costs are unlikely to have been anticipated. Undertaking such replacements at hundreds of sites across a country is a significant exercise and is likely to require extra financing.

Accepting the idea of global change, which encompasses climate change, and includes practical changes, such as energy reduction measures, it is likely that these will be a more immediate issue in the short term future than climate change itself.

In summary future projections tend towards increased damage. The generic method to produce these results allows collection managers ample time to determine the risk towards their own collections, and plan ahead to have preventive conservation measures in place. This helps to ensure that historic collections on open display are preserved for future generations.

## 8.2 Further work

The research carried out in this thesis has brought about questions that future research may be able to answer. Some of these are outlined here:

- What is the significance of projected changes?
- How will climate change impact heated or controlled historic interiors?
- Is it possible to improve the transfer function, and are they applicable further afield?
- How do future projections using the transfer function compare those of a more complex model?
- How are other environmental parameters, such as air pollution, projected to change indoors?
- How will climate change impact other damage, for example by insect pests?
- How will climate change indirectly have an impact on damage, for example through visitor numbers?

Some further work has already looked into the impact of climate change on damage caused by insect pests (Brimblecombe and Lankester, 2012). This looked at specific factors related to insect pests and determined how the future indoor environment would impact upon these. The degree day measure was also related to the number of life cycles of the biscuit beetle. Additional work in this direction is seeking to develop a population model for the webbing clothes moth, currently seen as the biggest threat to historic collections. This model can then be used to determine the impact of climate change on the population of webbing clothes moth, and thus the possible risk of damage.

The work in this thesis has focused upon unheated historic interiors; future work could look to the impact of climate change on heated historic interiors, again some thought has been given to this area also. Additionally, taking the transfer function and applying it to further historic interiors is one possibility for future work. However it would be better if people could carry this out themselves for interiors that they are responsible for, some effort will be made to present the process of determining and applying the transfer function, allowing others to project future damage, and therefore helping preserve collections for future generations.

While the current transfer function is acceptable it is possible that with further work it could be improved. Very recently there has been one of the first outputs from a large European project, Climate for Culture, this has used the Hambase building simulation model to predict indoor environments, and then future climate (Huijbregts et al., 2012). Initial

comparisons would appear to show a good correlation between the accuracy of the transfer function and Hambase. Further work comparing the two model outputs at the same location would be useful, as would comparison of the future damage projections, although the other work uses a different climate model. Comparison with other building simulation models would be useful, although it is important to remember that some of these models are in excess of the standard required. It is important to consider the accuracy of the climate model. It would be appropriate to consider the use of ensembles of climate models to gain a better understanding of future climate projections. This may also be the case for the building simulation models.

Presented results have used daily averages of projected climate, a method has been presented to downscale daily averages of temperature and humidity, although it was not utilised, additionally hourly average data is available from the UKCP09 weather generator. Further work could make use of either technique, although where possible the weather generator should be used for consistency with other weather variables. It is possible that the use of daily averages instead of hourly averages could underestimate some damage, for example where the response time of wood is less than a day. Thus further work here would help project future damage for such collections, and determine whether hourly data is necessary.

There is a need for improved damage functions as discussed, and also indoor damage functions for other materials of interest to cultural heritage. If new functions become available it would be simple to implement these and project the impact of climate change. Another area that may be considered is the prediction of pollutants indoors, which could then be projected into the future - some work has already been undertaken on this (Brimblecombe and Grossi, 2012). This then allows for the use of damage functions that utilise pollution data. The work of the MEMORI project aims to determine the effect of organic acids on some organic materials, thus functions from this project could be utilised. Some investigation has projected the emission of organic acids from wood under a changing climate; these organic acids can cause damage to collections if concentrated within enclosures (Lankester et al., 2012).

The addition of projections of indoor pollution would be of great benefit. There is also scope to investigate how light levels may change in the future, which would complete the main factors of the environment which can cause damage to collections.

Further work is required to determine the significance of changes predicted from damage functions. The results presented in this work are difficult to interpret with regards to actual damage caused to interiors, and how this may affect visitor perceptions, and loss of value.

It would also be useful to determine which projections pose the greatest threat, and therefore require prioritisation. This would help collection managers direct their limited resources towards the greatest threats. A risk analysis of the threats posed by each type of damage to certain materials, in relation to specific collections could be one method of determining which projections pose the greatest threat. It is important to link the projections to specific collections as there may be only small changes to an object of international significance, but greater changes may be projected to items with less associated value. A risk analysis would help determine which mitigation options pose the greatest benefit.

A number of problems arose from incomplete data sets; further work in the monitoring field is required to improve the reliability of the monitoring equipment, usually with respect to the radio signals. Although this will not prevent staff turning everything off when they go home for Christmas.

Some initial work, although not presented, was carried out to classify indoor environments with regards to heritage, similar to the outdoor heritage climatology idea (Brimblecombe, 2010). Further work in this area would be beneficial. Also investigation of other management strategies may be beneficial, for instance pest traps. An increased temperature allows for greater mobility, therefore it is possible that there may be an increased number of pests caught. This could wrongly be interpreted as an increase in pest population.

Another important area of consideration is how climate change will impact on visitor numbers. Visitors are another key factor in damage to historic collections, with dust being one example. A changing climate is likely to impact on visitor numbers, if it is warm it is possible that some people would prefer to visit the garden of a property and not the house itself, there may be other examples which may drive people inside. Some work on this has been undertaken already (Grossi et al., 2010).

Most projections of the future, with respect to heritage, both indoors and out appear to be focussed within Europe, expansion of this to the rest of the world, beyond this narrow range of climate types, is crucial.

# REFERENCES

ASAE STANDARDS (1998) Psychrometric data. Available online: http://www.ecaa.ntu.edu.tw/weifang/ebook/psy-data1998.pdf.

ASHLEY-SMITH, J. (1999) Risk Assessment for Object Conservation, Oxford, Butterworth-Heinemann.

ASHRAE (2003) Museums, Libraries, and Archives. Chapter 21. IN ASHRAE (Ed.) *ASHRAE Handbook: Heating, Ventilating, and Air-Conditioning Applications.* Atlanta, ASHRAE.

AUGENBROE, G. (2002) Trends in building simulation. *Building and Environment,* 37**,** 891-902.

AYERST, G. (1969) The Effects of Moisture and Temperature on Growth and Spore Germination in some Fungi. Journal of Stored Products Research, 5, 127-141.

BELL, N. (2008) Defining the benchmark for measuring physical change to buildings, collections and sites - characterising the condition of materials and assemblages. http://www.heritagescience.ac.uk/index.php?section=19.

BENAVENTE, D., BRIMBLECOMBE, P. & GROSSI, C. (2008) Salt weathering and climate change. IN PERLA COLOMBINI, M. & TASSI, L. (Eds.) *New trends in Analytical, Environmental and Cultural Heritage Chemistry.* Kerala, India, Transworld Research Network.

BENAVENTE, D., SANCHEZ-MORAL, S., FERNANDEZ-CORTES, A., CANAVERAS, J., ELEZ, J. & SAIZ-JIMENEZ, C. (2011) Salt damage and microclimate in the Postumius Tomb, Roman Necropolis of Carmona, Spain. Environmental Earth Sciences, 63, 1529-1543.

BIERMANN, C. (1996) Handbook of pulping and papermaking, San Diego, California, Academic Press.

BIONDA, D. (2004) Salt deterioration and microclimate in historical buildings. Zurich, institut fur Denkmalpflege, Forschungsstelle Technologie and Konservierung.

BIONDA, D. (2006) Modelling Indoor Climate and Salt Behaviour in Historic Buildings: A Case Study. *Swiss Federal Institute of Technology Zurich.* Zurich, Swiss Federal Institute of Technology Zurich.

BLADES, N., CASSAR, M. & BIDDULPH, P. (2008) Optimizing Drying Strategies to Reduce Down Times for Actively-Used Flood Damaged Historic Buildings. 104-108.

BOWDEN, D. & BRIMBLECOMBE, P. (2005) Monitoring dust at Ickworth House with the Dust-Bug. *Views,* 42**,** 25-27.

BRATASZ, L., KOZLOWSKI, R., LASYK, L., LUKOMSKI, M. & RACHWAL, B. (2011) Allowable microclimatic variations for painted wood: numerical modelling and direct tracing of the fatigue damage. *ICOM CC 16th Triennial Conference.* Lisbon.

BRIMBLECOMBE, P. (1994) The Balance of Environmental Factors Attacking Artifacts. IN KRUMBEIN, W. E., BRIMBLECOMBE, P., COSGRAVE, D. E. & STANIFORTH, S. (Eds.) *Durability and Change: The Science, Responsibility, and Cost of Sustaining Cultural Heritage.* Chichester, John Wiley and Sons.

BRIMBLECOMBE, P. (2008) Understanding How the Environment Causes Physical Change. http://www.heritagescience.ac.uk/index.php?section=19.

BRIMBLECOMBE, P. (2010) Heritage Climatology. IN LEFEVRE, R. & SABBIONI, C. (Eds.) *Climate Change and Cultural Heritage.* Bari, Italy, Edipuglia.

BRIMBLECOMBE, P. & GROSSI, C. M. (2005) Aesthetic thresholds and blackening of stone buildings. *Science of The Total Environment,* 349**,** 175-189.

BRIMBLECOMBE, P. & GROSSI, C. M. (2008) Millennium-long recession of limestone facades in London. *Environmental Geology,* 56**,** 463-471.

BRIMBLECOMBE, P. & GROSSI, C. M. (2012) Carbonyl compounds indoors in a changing climate. *Chemistry Central,* 6.

BRIMBLECOMBE, P., GROSSI, C. M. & HARRIS, I. (2006a) Climate change critical to cultural heritage. IN GOMEZ-HERAS, M. & VAZQUEZ-CALVO, C. (Eds.) *Heritage, Weathering and Conservation: Proceedings of the International Heritage.* Taylor and Francis, The Netherlands.

BRIMBLECOMBE, P., GROSSI, C. & HARRIS, I. (2006b) The effect of long-term trends in dampness on historic buildings. *Weather,* 61**,** 278-281.

BRIMBLECOMBE, P., GROSSI, C. & HARRIS, I. (2007) Future trends in surface wetness and relative humidity and potential impact on materials. *Pollution atmosphérique numéro spécial,* special**,** 95-100.

BRIMBLECOMBE, P. & LANKESTER, P. (2012) Long term changes in climate and insect damage in historic houses. Studies in Conservation, IN PRESS.

BRIMBLECOMBE, P., THICKETT, D. & HUN YOON, Y. (2009) The Cementation of coarse dust to indoor surfaces. *Journal of Cultural Heritage,* 10**,** 410-414.

BROOKER, D. B. (1967) Mathematical model of the psychrometric chart. *Transactions of the American Society of Agricultural Engineers,* 10**,** 558-563.

CAMUFFO, D. (1998) *Microclimate for Cultural Heritage,* Amsterdam, Elselvier Science.

CASSAR, M. & TAYLOR, J. (2004) A Cross-disciplinary Approach to the Use of Archives as Evidence of Past Indoor Environments in Historic Buildings. *Journal of the Society of Archivists,* 25**,** 157-172.

CHILD, R. (2007) Insect Damage as a Function of Climate. IN PADFIELD, T. & BORCHERSEN, K. (Eds.) Museum Microclimates. Copenhagen, National Museum of Denmark.

COLEY, D. & KERSHAW, T. (2010) Changes in internal temperatures within the built environment as a response to a changing climate. *Building and Environment,* 45**,** 89-93.

CRAWLEY, D., HAND, J., KUMMERT, M. & GRIFFITH, B. (2005a) Contrasting the Capabilities of building Energy Performance Simulation Programs. *Building Simulation, Ninth International IBPSA Conference.* Montreal, Canada.

CRAWLEY, D., HAND, J., KUMMERT, M. & GRIFFITH, B. (2005b) Contrasting the Capabilities of building Energy Performance Simulation Programs. Washington, Glasgow, Madison and Golden, US Department of Energy, University of Strathclyde, University of Wisconsin-Madison, National Renewable Energy Laboratory.

CRAWLEY, D., HAND, J. & LAWRIE, L. (1999) Improving the weather information available to simulation programs. *Proceedings of Building Simulation '99.* Kyoto, Japan, IBPSA.

CRAWLEY, D., LAWRIE, L., PEDERSEN, C. & WINKELMANN, F. (2000) EnergyPlus: Energy Simulation Program. *ASHRAE,* 42**,** 49-56.

DWAN, A. (1987) Paper Complexity and the Interpretation of Conservation Research. Journal of the American Institute for Conservation, 26, 1-17.

ENGLISH HERITAGE (2007) *Brodsworth Hall and Gardens,* London, English Heritage.

ENGLISH HERITAGE (2008) Climate Change and the Historic Environment. London, English Heritage.

ERHARDT, D., MECKLENBURG, M., TUMOSA, C. & MCCORMICK-GOODHART, M. (1995) The Determination of Allowable RH Fluctuations. *WAAC Newsletter,* 17**,** 19-23.

FLORIAN, M. (2002) Fungal Facts solving fungal problems in heritage collections, London, Archetype Publications.

GINELL, G. (1994) The Nature of Changes Caused by Physical Factors. IN KRUMBEIN, W. E., BRIMBLECOMBE, P., COSGRAVE, D. E. & STANIFORTH, S. (Eds.) *Durability and Change: The Science, Responsibility, and Cost of Sustaining Cultural Heritage.* Chichester, John Wiley and Sons.

GOODESS, C.M., HALL, J., BEST, M., BETTS, R., CABANTOUS, L., JONES, P.D., KILSBY, C.G, PEARMAN, A. & WALLACE, C.J. (2007) Climate scenarios and decision making under uncertainty. *Built Environment*, 33, 1,10-30.

GROSSI, C. M., BONAZZA, A., BRIMBLECOMBE, P., HARRIS, I. & SABBIONI, C. (2008a) Predicting twenty-first century recession of architectural limestone in European cities. *Environmental Geology,* 56**,** 455-461.

GROSSI, C. M. & BRIMBLECOMBE, P. (2004) Aesthetics of simulated soiling patterns on architecture. *Environmental Science & Technology,* 38**,** 3971-3976.

GROSSI, C. M., BRIMBLECOMBE, P. & HARRIS, I. (2007) Predicting long term freeze-thaw risks on Europe built heritage and archaeological sites in a changing climate. *Science of The Total Environment,* 377**,** 273-281.

GROSSI, C. M., BRIMBLECOMBE, P. & LLOYD, H. (2010) The effect of weather on visits to historic properties. *Views,* 47**,** 69-70.

GROSSI, C. M., BRIMBLECOMBE, P., MENENDEZ, B., BENAVENTE, D. & HARRIS, I. (2008b) Long term change in salt weathering of stone monuments in north-west France. IN LUKASZEWICZ, J. & NIEMCEWICZ, P. (Eds.) *11th International Congress on Deterioration and Conservation of Stone.* Torun, Nicolaus Copernicus University Press.

GROSSI, C., BRIMBLECOMBE, P., MENENDEZ, B., BENAVENTE, D., HARRIS, I. & DEQUE, M. (2011) Climatology of salt transitions and implications for stone weathering. Science of The Total Environment, 409, 2577-2585.

HALL, M. (Ed.) (2010) *Materials for energy efficiency and thermal comfort in buildings,* Cambridge, Woodhead Publishing.

HOWATSON, C. (Ed.) (2007) *Osborne,* London, English Heritage.

HUIJBREGTS, Z., KRAMER, R. P., MARTENS, M., VAN SCHIJNDEL, A. & SCHELLEN, H. (2012) A proposed method to assess the damage risk of future climate change to museum objects in historic buildings. *Building and Environment,* IN PRESS**,** 1-14.

HUKKA, A. & VIITANEN, H. (1999) A mathematical model of mould growth on wooden material. Wood Science and Technology, 33, 475-485.

HULME, M., JENKINS, G. J., LU, X., TURNPENNY, J., R., MITCHELL, T. D., JONES, R. G., LOWE, J., MURPHY, J. M., HASSEL, D., BOORMAN, P., MCDONALD, R. & HILL, S. (2002a) Climate Change Scenarios for the United Kingdom: The UKCIP02 Scientific Report. Tyndall Centre for Climate Change Research, School of Environmental Sciences, University of East Anglia, Norwich, UK.

HULME, M., TURNPENNY, J. & GENKINS, G. (2002b) Climate Change Scenarios for the United Kingdom: The UKCIP02 Briefing Report. Tyndall Centre for Climate Change Research, School of Environmental Sciences, University of East Anglia, Norwich, UK.

IMAGE PERMANENCE INSTITUTE (2005) Step-by-Step Workbook: Achieving a Preservation Environment for Collections. Rochester, New York, Image Permanence Institute.

INM. Publicación D25.4 del, 2a Edición. Guía resumida del clima de España, 1971–2000. Plan Estadístico Nacional, 2001–2004. Ministerio de Medio Ambiente; 2004.

IPCC (2000) IPCC Special Report Emission Scenarios: Summary for Policymakers. Intergovernmental Panel on Climate Change.

IPCC (2007a) *Climate Change 2007: The Physical Science Basis. Contribution of Working Group I to the Fourth Assessment Report of the Intergovernmental Panel on Climate Change [Solomon, S., D. Qin, M. Manning, Z. Chen, M. Marquis, K.B. Averyt, M. Tignor and H.L. Miller (eds.)].* Cambridge University Press, Cambridge, United Kingdom and New York, NY, USA.

IPCC (2007b) Summary for Policymakers. IN PARRY, M. L., CANZIANI, O. F., PALUTIKOF, J. P., VAN DER LINDEN, P. J. & HANSON, C. E. (Eds.) Climate Change 2007: Impacts, Adaptation and Vulnerability. Contribution of Working Group II to the Fourth Assessment Report of the Intergovernmental Panel on Climate Change. Cambridge, UK, Cambridge University Press.

ISAKSSON, T., THELANDERSSON, S., EKSTRAND-TOBIN, A. & JOHANSSON, P. (2010) Critical conditions for onset of mould growth under varying climate conditions. Building and Environment, 45, 1712-1721.

JAKIELA, S., BRATASZ, L. & KOZLOWSKI, R. (2008) Numerical modelling of moisture movement and related stress field in lime wood subjected to changing climate conditions. Wood Science and Technology, 42, 21-37.

JENKINS, G. J., MURPHY, J. M., SEXTON, D. M. H., LOWE, J. A., JONES, P. & KILSBY, C.G. (2009) UK climate projections briefing report. Met Office Hadley Centre, Exeter, UK.

JOHNS, T. C., GREGORY, J. M., INGRAM, W. J., JOHNSON, C. E., JONES, A., LOWE, J. A., MITCHELL, J. F. B., ROBERTS, D. L., SEXTON, D. M. H., STEVENSON, D. S., TETT, S. F. B. & WOODAGE, M. J. (2003) Anthropogenic climate change for 1860 to 2100 simulated with the HadCM3 model under updated emissions scenarios. *Climate Dynamics,* 20**,** 583-612.

JONES, P. D., KILSBY, C. G., HARPHAM, C., GLENIS, V. & BURTON, A. (2009) *UK Climate Projections science report: Projections of future daily climate for the UK from the Weather Generator.* University of Newcastle, UK.

KEENAN, J. H. & KEYES, F. G. (1936) *Thermodynamic properties of steam,* New York, John Wiley and Sons.

KILIAN, R., LEISSNER, J., ANTRETTER, F., HOLL, K. & HOLM, A. (2010) Modelling climate change impact on cultural heritage - The European project Climate for Culture. IN BUNNIK, T., DE CLERCQ, H., VAN HEES, R. P. J., SCHELLEN, H. & SCHUEREMANS, L. (Eds.) *Effect of Climate Change on Built Heritage.* Pfaffenhofen, WTA Publications.

KNELL (1994) *Care of collections,* London, Routledge.

KOESTLER, R., BRIMBLECOMBE, P., CAMUFFO, D., GINELL, G., GRAEDEL, T., LEAVENGOOD, P., PETUSHKOVA, J., STEIGER, M., URZI, C., VERGES-BELMIN, V. & WARSCHEID, T. (1994) Group Report: How do External Environmental Factors Accelerate Change? IN KRUMBEIN, W. E., BRIMBLECOMBE, P., COSGRAVE, D. E. & STANIFORTH, S. (Eds.) *Durability and Change: The Science, Responsibility , and Cost of Sustaining Cultural Heritage.* Chichester, John Wiley and Sons.

KOTTEK, M., GRISER, J., BECK, C., RUDOLF, B. & RUBEL, F. (2006) World map of the Koppen-Gieger climate classification updated. *Meteorologische Zeitschrift,* 15**,** 259-263.

KUNZEL, H. (1995) Simultaneous heat and moisture transport in building components: one and two dimensional calculation using simple parameters. Fraunhofer Institute of Building Physics.

LA GENNUSA, M., LASCARI, G., RIZZO, G. & SCACCIANOCE, G. (2008) Conflicting needs of the thermal indoor environment of museums: In search of a practical compromise. *Journal of Cultural Heritage,* 9**,** 125-134.

LANKESTER, P. & BRIMBLECOMBE, P. (2012a) Future thermohygrometric climate within historic houses. Journal of Cultural Heritage, 13, 1-6.

LANKESTER, P. & BRIMBLECOMBE, P. (2012b) The impact of future climate on historic interiors. Science of The Total Environment, 417-418, 248-254.

LANKESTER, P., THICKETT, D. & BRIMBLECOMBE, P. (2012) The impact of climate change on historic interiors and display enclosures. IN DAHLIN, E. (Ed.) *Proceedings of the 2nd European Workshop on Cultural Heritage Preservation.* Norway 24-26th September 2012, 131-139.

LAWRENCE, M. (2005) The relationship between relative humidity and the dewpoint temperature in moist air: a simple conversion and applications. *Bulletin of the American Meteorological Society,* 86**,** 225-233.

LIPFERT, F. (1989) Atmospheric Damage to Calcareous Stones: Comparison and Reconciliation of Recent Experimental Findings. *Atmospheric Environment,* 23**,** 415-429.

LLOYD, H., BRIMBLECOMBE, P. & LITHGOW, K. (2007) Economics of Dust. *Studies in Conservation, 52***,** 135-146.

LUXFORD, N. (2009) Reducing the Risk of Open Display: Optimising the Preventive Conservation of Historic Silks. School of Art. Southampton, University of Southampton.

LUXFORD, N. (2012) www.bartlett.ucl.ac.uk/graduate/csh/research/changeordamage.

MAY, E. & JONES, M. (2006) Conservation Science Heritage Materials, Cambridge, The Royal Society of Chemistry.

MECKLENBURG, M., TUMOSA, C. & ERHARDT, D. (1998) Structural response of painted wood surfaces to changes in ambient relative humidity. Painted Wood: history and conservation (Part 6: Scientific Research). The Getty Conservation Institute.

MENART, E., DE BRUIN, G. & STRLIC, M. (2011) Dose-response functions for historic paper. Polymer Degradation and Stability, 96, 2029-2039.

MICHALSKI, S. (1990) An overall framework for preventive conservation and remedial conservation. IN GRIMSTAD, K. (Ed.) *ICOM CC 9th Triennial Meeting.* Dresden, Germany, 26-31 August.

MICHALSKI, S. (1996) Quantified Risk Reduction in the Humidity Dilemma. APT Bulletin, 27, 25-29.

MICHALSKI, S. (2002) Double the life for each five-degree drop, more than double the life for each halving of relative humidity. IN CONSERVATION, I. C. F. & VONTOBEL, R. (Eds.) 13th triennial meeting, Rio de Janeiro, 22-27 September 2002: Preprints., James & James, London.

MICHALSKI, S. (2007) The ideal climate, risk management, the ASHRAE chapter, proofed fluctuations, and towards a full risk analysis model. IN BOERSMA, F. (Ed. *Proceedings of Experts' Roundtable on Sustainable Climate Management Strategies.* Tenerife, Getty Conservation Institute, Los Angeles.

MONFET, D., ZMEUREANU, R., CHARNEUX, R. & LEMIRE, N. (2007) Computer Model of a University Building using the EnergyPlus Program. *Building Simulation.*

MOON, H. J. & AUGENBROE, G. (2003) Evaluation of Hygrothermal Models for Mold Growth Avoidance Prediction. Eighth International IBPSA Conference. Eindhoven, Netherlands.

NEUHAUS, E. & SCHELLEN, H. (2007) Conservation Heating for a Museum Environment in a Monumental Building. *Proceedings of the 10th Conference on the thermal performance of the exterior envelopes of whole buildings.* Florida, USA.

NISHIMURA, D. (2009) Understanding Preservation Metrics. Image Permanence Institute.

PAS 198, (2012) Specification for managing environmental conditions for cultural collections.

PAVLOGEORGATOS, G. (2003) Environmental parameters in museums. *Building and Environment,* 38**,** 1457-1462.

PRETZEL, B. (2005) The RIBA project: a climate strategy for paper based archives at the V&A. IN VERGER', I. (Ed. *ICOM 14th Triennial Meeting.* The Hague ICOM.

PADFIELD, T. (2011) Conservation Physics.

PAVLOGEORGATOS, G. (2003) Environmental parameters in museums. Building and Environment, 38, 1457-1462.

PINNIGER, D. (2001) Pest Management in Museums, Archives and Historic Houses, Archetype Publications, London.

PINNIGER, D. (2011) Ten years on - from vodka beetles to risk zones. *A Pest Odyssey, 10 years later.* London, English Heritage.

PRETZEL, B. (2005) The RIBA project: a climate strategy for paper based archives at the V&A. IN VERGER', I. (Ed. ICOM 14th Triennial Meeting. The Hague ICOM.

PRICE, C. (2000) An Expert Chemical Model for Determining the Environmental Conditions Needed to Prevent Salt Damage in Porous Materials, London, Archetype Publications Ltd London.

REILLY, J. (2005) IPI's Climate Notebook Software for Environmental Analysis. *Archiving 2005* Washington DC.

REILLY, J., NISHIMURA, D. & ZINN, E. (1995) New Tools for Preservation: Assessing Long-Term Environmental Effects on Library and Archives Collections. Washington DC, Commission on Preservation and Access.

RICHARD, M., MECKLENBURG, M. & TUMOSA, C. (1995) Technical Considerations for the Transport of Panel Paintings. IN DARDES, K. & ROTHE, A. (Eds.) The Structural Conservation of Panel Paintings: Proceedings of a symposium at the J. Paul Getty Museum. Los Angeles, The Getty Conservation Institute.

RIDOUT, B. (2000) Timber Decay in Buildings: The conservation approach to treatment, London, E & FN Spon.

SABBIONI, C., BRIMBLECOMBE, P. & CASSAR, M. (2010) *The Atlas of Climate Change Impact on European Cultural Heritage: Scientific Analysis and Management Strategies,* London, Anthem Press.

SABBIONI, C., CASSAR, M., BRIMBLECOMBE, P. & LEFEVRE, R. (2008) Vulnerability of Cultural Heritage to Climate Change. Strasbourg, European and Mediterranean Major Hazards Agreement  (EUR-OPA).

SABBIONI, C., CASSAR, M., BRIMBLECOMBE, P., TIDBLAD, J., KOZLOWSKI, R., DRDÁCKY, M., SAIZ-JIMENEZ, C., GRØNTOFT, T., WAINWRIGHT, I. & ARINO, X. (2006) Global climate change impact on built heritage and cultural landscapes. IN GOMEZ-HERAS, M. & VAZQUEZ-CALVO, C. (Eds.) *Heritage, Weathering and Conservation: Proceedings of the International Heritage, Weathering and Conservation Conference* Madrid Spain, Taylor & Francis.

SACKVILLE-WEST, R. (1998) *Guidebook - Knole*, The National Trust.

SEBERA, D. (1994) Isoperms An Environmental Management Tool. Washington DC, Commission on the Preservation and Access.

SEDLBAUER, K., KRUS, M. & BREUER, K. (2003) Mould growth prediction with a new biohygrothermal method and its application in practice. Materials. Lodz, Poland.

SIMPSON, W. & TENWOLDE, A. (1999) Physical Properties and Moisture Relations of Wood. IN LABORATORY, F. P. (Ed.) Wood Handbook - Wood as an engineering material. Madison, U.S. Department of Agriculture, Forest Service, Forest Products Laboratory.

SOLOMON, S., QIN, D., MANNING, M., ALLEY, R. B., BERNTSEN, T., BINDOFF, N. L., CHEN, Z., CHIDTHAISONG, A., GREGORY, J. M., HEGERL, G. C., HEIMANN, M., HEWITSON, B., HOSKINS, B. J., JOOS, F., JOUZEL, J., KATTSOV, V., LOHMANN, U., MATSUNO, T., MOLINA, M., NICHOLLS, N., OVERPECK, J., RAGA, G., RAMASWAMY, V., REN, J., RUSTICUCCI, M., SOMERVILLE, R., STOCKER, T. F., WHETTON, P., WOOD, R. A. & WRATT, D. (2007) Technical Summary. IN SOLOMON, S., QIN, D., MANNING, M., CHEN, Z., MARQUIS, M., AVERRYT, K. B., TIGNOR, M. & MILLER, H. L. (Eds.) *Climate Change 2007: The Physical Science Basis. Contribution of Working group I to the Fourth Assessment Report of the Intergovernmental Panel on Climate Change.* Cambridge, United Kingdom and New York, NY, USA., Cambridge University Press.

STANIFORTH, S., BLADES, N. & LITHGOW, K. (2010) Conservators Manual - Specification for environmental control. The National Trust.

STENGAARD HANSEN, L., AKERLUND, M., GRONTOFT, T., RHYL-SVENDSEN, M., SCHMIDT, A., BERGH, J. & VAGN JENSEN, K. (2012) Future pest status of an insect pest in museums, *Attagenus smirnovi*: Distribution and food consumption in relation to climate change. Journal of Cultural Heritage, 13, 22-27.

STRANG, T. & GRATTAN, D. (2009) Temperature and Humidity Considerations for the Preservation of Organic Collections - The Isoperm Revisited. e-Preservation Science, 6, 122-128.

TAYLOR, J., BLADES, N., CASSAR, M. & RIDLEY, I. (2005) Reviewing past environments in a historic house library using building simulation IN VERGER, I.

(Ed. *ICOM - Committee for Conservation 14th Triennial Meeting.* The Hague, James and James LONDON.

THE NATIONAL TRUST (2006) *Manual of Housekeeping: The care of collections in historic houses open to the public,* Oxford, Butterworth - Heinemann.

THICKETT, D. (2005) Print Frame Microclimates. IN RAYNER, J., KOSEK, J. & CHRISTENSEN, B. (Eds.) Mounting and Housing, Art on Paper for storage and display, history, science and present-day practice. London, ARCHETYPE BOOKS

THICKETT, D., RHEE, S.-J. & LAMBARTH, S. (2007) Libraries and Archives in Historic Buildings. IN PADFIELD, T. & BORCHERSEN, K. (Eds.) *Museum Microclimates.* Copenhagen, The National Museum of Denmark.

THOMSON, G. (1999) *The Museum Environment,* Oxford, Butterworth-Heinemann.

UK METEOROLOGICAL OFFICE (2006) MIDAS Land Surface Stations data (1853-current). NCAS British Atmospheric Data Centre.

VAN DER LINDEN, P. J. & MITCHELL, J. F. B. (Eds.) (2009) *ENSEMBLES: Climate Change and its Impacts: Summary of research and results from the ENSEMBLES project,* Exeter, UK, Met Office Hadley Centre.

ZOU, X., UESAKA, T. & GURNAGUL, N. (1996a) Prediction of paper permanence by accelerated aging I. Kinetic analysis of the aging process. Cellulose, 3, 243-267.

ZOU, X., UESAKA, T. & GURNAGUL, N. (1996b) Prediction of paper permanence by accelerated aging II. Comparison of the predictions with natural aging results. Cellulose, 3, 269-279.